

**CRACKING AND CHLORIDE CONTENTS IN  
REINFORCED CONCRETE BRIDGE DECKS**

**By**

**Will D. Lindquist**

**David Darwin**

**JoAnn P. Browning**

**A Report on Research Sponsored by  
THE KANSAS DEPARTMENT OF TRANSPORTATION  
K-TRAN PROJECT NO. KU-01-09**

**Structural Engineering and Engineering Materials  
SM Report No. 78**

**THE UNIVERSITY OF KANSAS CENTER FOR RESEARCH, INC.  
LAWRENCE, KANSAS**

**February 2005**

**ABSTRACT**

The effects of material properties, design specifications, construction practices, and environmental site conditions on the performance of reinforced concrete bridge decks are evaluated. Field surveys were performed on 59 bridges to measure deck cracking, chloride ingress, and delaminated area. The surveys were limited to steel girder bridges – bridges that are generally agreed to exhibit the greatest amount of cracking in the concrete decks. The study includes two bridge deck types with silica fume overlays, one in which 5% of the cement is replaced by silica fume (19 bridges) and the other in which 7% of the cement is replaced by silica fume (11 bridges), plus decks with conventional overlays (16 bridges) and monolithic bridge decks (13 bridges). Information from the current study is combined with data from two earlier studies. In total, 27 variables are evaluated, covering bridge age, construction practices, material properties, site conditions, bridge design, and traffic volume. The performance of silica fume overlay decks relative to conventional overlay and monolithic decks is of particular interest due to the widespread use of silica fume overlays in the state of Kansas.

The results of the study indicate that chloride contents increase with the age of the bridge deck, regardless of deck type. In addition, concrete for all bridge deck types sampled in the same age range exhibit similar chloride contents for samples taken both at and away from cracks, regardless of deck type. For bridges within the same age range, the average chloride concentration taken away from cracks at the level of the top transverse reinforcement rarely exceeds even the most conservative estimates of the corrosion threshold for conventional reinforcement. Chloride concentrations taken at crack locations, however, can exceed the corrosion threshold in as little as nine months. Based on these observations, it appears clear that attention

should be focused on minimizing bridge deck cracking rather than concrete permeability.

The study demonstrates that crack density increases with increases in the volume of cement paste and that neither higher compressive strengths nor higher concrete slumps are beneficial to bridge deck performance. In addition, crack density is higher in the end regions of decks that are integral with the abutments than decks with pin-ended girders. The results of the crack surveys indicate that cracking increases with age, although a large percentage of the cracking is established early in the life of the deck. Even with the increase in crack density over time, however, both monolithic and conventional overlay bridges cast in the 1980s exhibit less cracking than those cast in the 1990s. The differences are attributed to changes in material properties and construction procedures over the past 20 years. The trend in cracking for decks with silica fume overlays cast in the 1990s (containing 5% silica fume), however, is quite the opposite. A decrease in crack density is observed for 5% silica fume overlay decks, which appears to be the result of increased efforts to limit evaporation prior to the initiation of wet curing. Recently constructed 7% silica fume overlay decks, however, have not shown continued improvement.

In light of the chloride and cracking observations, conventional high-density overlays are recommended in lieu of silica fume overlays, and full-depth monolithic decks are recommended for new deck construction.

**Keywords:** bridge decks, chloride content, concrete bridge construction, concrete mix design, cracking, durability, diffusion coefficient, overlay, permeability, shrinkage, silica fume

## **ACKNOWLEDGEMENTS**

This report is based on research performed by Will D. Lindquist in partial fulfillment of the requirements for the MSCE degree from the University of Kansas. Funding for this research was provided by the Kansas Department of Transportation under K-Tran Project No. KU-01-09.

Oversight of this project was provided by Dan Scherschligt of the Kansas Department of Transportation. Bridge deck construction data and traffic control for the bridge surveys was provided by KDOT personnel. Personnel from the KDOT Bureau of Materials and Research obtained the concrete samples and performed the chloride content tests. The efforts of all those who participated are gratefully acknowledged, with special thanks to Mark Walker from the KDOT Bureau of Materials and Research.

## TABLE OF CONTENTS

	<u>Page</u>
<b>ABSTRACT</b> .....	ii
<b>ACKNOWLEDGEMENTS</b> .....	iv
<b>LIST OF TABLES</b> .....	x
<b>LIST OF FIGURES</b> .....	xiv
<b>CHAPTER 1:INTRODUCTION</b> .....	1
1.1 General.....	1
1.2 Significance of Bridge Deck Cracking .....	1
1.3 Types of Bridge Deck Deterioration.....	2
1.3.1 Crack Classification Based on Causes of Cracking.....	2
1.3.2 Crack Classification Based on Orientation.....	4
1.4 Corrosion.....	6
1.5 Silica Fume .....	6
1.6 Chloride Concentrations .....	7
1.7 Bridge Deck Overlay Specifications.....	9
1.8 Previous Work .....	13
1.8.1 Literature Review.....	13
1.8.2 Primary Factors Affecting Cracking.....	45
1.9 Object and Scope .....	45
<b>CHAPTER 2:DATA COLLECTION</b> .....	46
2.1 General.....	46
2.2 Bridge Selection.....	46
2.3 Data Sources .....	48
2.4 Survey Techniques.....	49
2.5 Chloride Content Test.....	51
2.6 Crack Density Determination .....	52
<b>CHAPTER 3:CHLORIDE DATA AND DIFFUSION PROPERTIES</b> .....	54
3.1 General.....	54

3.2	KDOT District 1 Salt Usage .....	56
3.3	On and Off Crack Chloride Concentrations.....	57
3.3.1	Off Crack Chloride Concentrations .....	59
3.3.1	On Crack Chloride Concentrations .....	60
3.4	Fick’s Equation Modeling.....	61
3.4.1	Surface Concentrations .....	62
3.4.2	Diffusion Coefficients.....	65
3.4.2.1	Monolithic Decks.....	65
3.4.2.2	Conventional Overlay Decks .....	66
3.4.2.3	Silica Fume Overlay Decks .....	68
3.4.3	Diffusion Coefficient Age-Correction .....	69
3.4.4	Comparison of Deck Diffusion Coefficients .....	71
3.5	Diffusion Coefficients Versus Silica Fume Overlay Specifications..	73
3.6	Effects of Concrete Properties on Diffusivity.....	75
3.6.1	Slump .....	78
3.6.2	Air Content.....	79
3.6.3	Water-Cementitious Material Ratio.....	81
3.6.4	Percent Volume of Water and Cementitious Material .....	83
3.6.5	Water and Cement Content.....	84
3.6.6	Compressive Strength .....	84
<b>CHAPTER 4: TIME AS A VARIABLE IN BRIDGE DECK</b>		
<b>CRACKING</b>	.....	86
4.1	General.....	86
4.2	Inclusion of Data from Previous Studies in Kansas.....	87
4.3	Bridge Deck Cracking Versus Time .....	89
4.4	Crack Density Versus Construction Era .....	91
4.5	Crack Density Versus Silica Fume Overlay Specification .....	93
4.6	Material Properties Versus Construction Date .....	95
4.6.1	Slump .....	96

4.6.2 Air Content.....	97
4.6.3 Percent Volume of Water and Cementitious Materials .....	97
4.6.4 Water Content .....	98
4.6.5 Cementitious Material Content .....	99
4.6.6 Water-Cementitious Material Ratio .....	99
4.6.7 Compressive Strength .....	100
4.7 Site Conditions Versus Construction Date .....	100
4.7.1 Minimum Daily Air Temperature .....	101
4.7.2 Maximum Daily Air Temperature .....	102
4.7.3 Average Daily Air Temperature .....	103
4.7.4 Daily Air Temperature Range.....	103
4.8 Bridge Design Versus Construction Date .....	104
4.8.1 Structure Type.....	104
4.8.2 Deck Thickness.....	105
4.8.3 Transverse Bar Spacing .....	105
4.8.4 Top Reinforcing Bar Cover .....	105
4.8.5 Transverse Bar Size .....	105
<b>CHAPTER 5: CRACK SURVEY EVALUATION AND RESULTS .....</b>	<b>107</b>
5.1 General.....	107
5.2 Influence of Deck Type .....	109
5.3 Influence of Material Properties .....	110
5.3.1 Water Content .....	112
5.3.2 Cementitious Material Content.....	113
5.3.3 Percent Volume of Water and Cement .....	114
5.3.4 Water-Cement Ratio .....	115
5.3.5 Slump .....	116
5.3.6 Air Content.....	118
5.3.7 Compressive Strength .....	119
5.4 Influence of Site Conditions .....	120

5.4.1 Average Daily Air Temperature .....	122
5.4.2 Minimum Daily Air Temperature .....	123
5.4.3 Maximum Daily Air Temperature .....	123
5.4.4 Daily Air Temperature Range.....	124
5.5 Influence of Design Parameters .....	125
5.5.1 Structure Type.....	126
5.5.2 Transverse Reinforcing Bar Size .....	127
5.5.3 Transverse Reinforcing Bar Spacing .....	128
5.5.4 Deck Thickness.....	130
5.5.5 Top Cover .....	130
5.5.6 Girder End Condition.....	132
5.5.7 Span Type .....	134
5.5.8 Bridge Skew.....	135
5.5.9 Span Length .....	135
5.5.10 Bridge Length .....	136
5.6 Influence of Bridge Contractor .....	137
5.7 Influence of Traffic .....	138
5.7.1 Average Annual Daily Traffic (AADT) .....	139
5.7.2 Load Cycles .....	140
<b>CHAPTER 6:SUMMARY, CONCLUSIONS, AND</b>	
<b>RECOMMENDATIONS.....</b>	<b>142</b>
6.1 Summary .....	142
6.2 Conclusions.....	143
6.2.1 Chloride Data and Diffusion Properties.....	143
6.2.2 Time as a Variable in Deck Cracking.....	145
6.3.3 Crack Survey and Evaluation and Results.....	146
6.3 Recommendations.....	148
<b>REFERENCES.....</b>	<b>150</b>
<b>APPENDIX A: BRIDGE DECK DATA.....</b>	<b>285</b>

<b>APPENDIX B: BRIDGE DECK SURVEY SPECIFICATION .....</b>	<b>291</b>
<b>APPENDIX C: CRACK DENSITY CALCULATION PROGRAM</b>	
<b>LISTING .....</b>	<b>293</b>
<b>APPENDIX D: BRIDGE DECK CHLORIDE CONTENTS AND</b>	
<b>DIFFUSION DATA .....</b>	<b>320</b>
<b>APPENDIX E: FIELD SURVEY RESULTS AND AGE-CORRECTED</b>	
<b>CRACK DENSITIES .....</b>	<b>355</b>

## LIST OF TABLES

<u>Table</u>	<u>Page</u>
1.1 Bridge deck cracking studies included in the review of literature.....	154
1.2 Factors affecting bridge deck cracking (Krauss and Rogalla 1996).....	155
1.3 Primary factors found to increase cracking based on previous research .....	156
2.1 Bridge deck types included in the current study and the studies by Schmitt and Darwin (1995, 1999) and Miller and Darwin (2000) .....	157
3.1 KDOT District One Salt Usage History.....	157
3.2 Time to corrosion threshold for uncracked concrete based on data from Figs. 3.1 through 3.4 .....	158
3.3a Average apparent surface concentration build-up rates [kg/m <sup>3</sup> /month (kg/m <sup>3</sup> /year)] and standard deviations for all bridge types.....	158
3.3b Average apparent surface concentration build-up rates [lb/yd <sup>3</sup> /month (lb/yd <sup>3</sup> /year)] and standard deviations for all bridge types.....	158
3.4 Student's t-test for mean effective diffusion coefficients $D_{eff}$ versus placement age.....	159
3.5 Average rate of change for effective diffusion coefficients $D_{eff}$ obtained from dummy variable regression analysis .....	160
3.6 Student's t-test for mean adjusted effective diffusion coefficients $D_{eff}^*$ versus placement age .....	160
3.7 The time (years) to reach corrosion threshold levels at a depth of 76 mm (3 in.) based on adjusted effective diffusion coefficients $D_{eff}^*$ calculated from data obtained within the first 48 months of deck construction using Fick's Second Law of Diffusion [Eq. (1.2)] .....	161
3.8 The time (years) to reach corrosion threshold levels at a depth of 76 mm (3 in.) based on adjusted effective diffusion coefficients $D_{eff}^*$ calculated from data obtained between 48 and 96 months of deck construction using Fick's Second Law of Diffusion [Eq. (1.2)].....	161

3.9	Student's t-test for mean adjusted effective diffusion coefficients $D_{eff}^*$ versus special provision number .....	162
3.10	Student's t-test for mean adjusted effective diffusion coefficients $D_{eff}^*$ versus concrete slump .....	163
3.11	Student's t-test for mean adjusted effective diffusion coefficients $D_{eff}^*$ versus air content .....	165
3.12	Student's t-test for mean adjusted effective diffusion coefficients $D_{eff}^*$ versus water-cementitious material ratio .....	167
3.13	Student's t-test for mean adjusted effective diffusion coefficients $D_{eff}^*$ versus percent volume of water and cement .....	168
3.14	Student's t-test for mean adjusted effective diffusion coefficients $D_{eff}^*$ versus water content.....	168
3.15	Student's t-test for mean adjusted effective diffusion coefficients $D_{eff}^*$ versus cement content .....	168
3.16	Student's t-test for mean adjusted effective diffusion coefficients $D_{eff}^*$ versus concrete compressive strength.....	169
4.1	Cracking rates obtained from dummy variable regression analysis .....	171
4.2	Student's t-test for mean crack diversity versus date of construction for individual bridge decks.....	171
4.3	Student's t-test for mean crack density corrected to an age of 78 months versus silica fume special provision number for individual bridge decks .....	173
5.1	Student's t-test for mean crack density versus bridge deck type .....	174
5.2	Student's t-test for mean crack density versus water content.....	174
5.3	Student's t-test for mean crack density versus cement content.....	175
5.4	Student's t-test for mean crack density versus percent volume of water and cementitious materials.....	176
5.5	Student's t-test for mean crack density versus water-cement ratio .....	177

5.6	Student's t-test for mean crack density versus concrete slump.....	178
5.7	Influence of slump on crack density corrected for water content for monolithic placements obtained using a dummy variable analysis.....	179
5.8	Student's t-test for mean crack density versus percent air content.....	180
5.9	Student's t-test for mean crack density versus compressive strength.....	181
5.10	Student's t-test for mean crack density versus average air temperature .....	182
5.11	Student's t-test for mean crack density versus minimum air temperature .....	183
5.12	Student's t-test for mean crack density versus maximum air temperature .....	184
5.13	Student's t-test for mean crack density versus daily air temperature range.....	185
5.14	Student's t-test for mean crack density versus structure type .....	186
5.15	Student's t-test for mean crack density versus top transverse bar size.....	187
5.16	Student's t-test for mean crack density versus top transverse bar spacing .....	188
5.17	Influence of top transverse bar spacing on crack density corrected for bar size for overlay decks obtained using dummy variable analyses.....	188
5.18	Student's t-test for mean crack density versus deck thickness.....	189
5.19	Student's t-test for mean crack density versus top cover.....	189
5.20	Probability of subsidence (settlement) cracking of fresh concrete based on cover depth, transverse bar size, and concrete slump (Dakhil, Cady, and Carrier 1975) .....	190
5.21	Cracking rates for end sections of silica fume and conventional overlays obtained from a dummy variable regression analysis .....	190
5.22	Student's t-test for mean crack density versus girder end condition .....	191

5.23	Student's t-test for mean crack density versus span type .....	192
5.24	Student's t-test for mean crack density versus bridge skew .....	193
5.25	Student's t-test for mean crack density versus span length .....	194
5.26	Student's t-test for mean crack density versus bridge length .....	195
5.27	Student's t-test for mean crack density versus bridge contractor .....	196
5.28	Student's t-test for mean crack density versus average annual daily traffic (AADT) .....	197
5.29	Average rate of change of crack density as a function of load cycles obtained from dummy variable regression analyses .....	198
5.30	Average rate of change of age-corrected crack density as a function of load cycles obtained from dummy variable regression analyses .....	198
A.1	Bridge data and deck properties for 7% Silica Fume Overlays .....	286
A.2	Mix design information for 7% silica fume overlay bridge placements .....	287
A.3	Field information and site conditions for 7% silica fume overlay bridge placements .....	289
D.1	Chloride concentration data .....	321
D.2	Calculated surface concentrations and diffusion coefficients .....	348
E.1	Field survey results and age-corrected crack densities for all bridge decks .....	356
E.2	Crack densities for individual bridge placements .....	361
E.3	Crack densities for end sections .....	370
E.4	Crack densities and data for individual spans .....	375
E.5	Bridge traffic data .....	389

## LIST OF FIGURES

<u>Figure</u>	<u>Page</u>
2.1 Breakdown of the number of bridges selected from each county.....	199
3.1 Chloride content taken away from cracks interpolated at a depth of 25.4 mm (1.0 in.) versus placement age .....	200
3.2 Chloride content taken away from cracks interpolated at a depth of 50.8 mm (2.0 in.) versus placement age .....	201
3.3 Chloride content taken away from cracks interpolated at a depth of 63.5 mm (2.5 in.) versus placement age .....	202
3.4 Chloride content taken away from cracks interpolated at a depth of 76.2 mm (3.0 in.) versus placement age .....	203
3.5 Chloride content taken on cracks interpolated at a depth of 25.4 mm (1.0 in.) versus placement age.....	204
3.6 Chloride content taken on cracks interpolated at a depth of 50.8 mm (2.0 in.) versus placement age.....	205
3.7 Chloride content taken on cracks interpolated at a depth of 63.5 mm (2.5 in.) versus placement age.....	206
3.8 Chloride content taken on cracks interpolated at a depth of 76.2 mm (3.0 in.) versus placement age.....	207
3.9 Linear trend lines for interpolated chloride data taken on and off of cracks at four depths .....	208
3.10 Box-and-whisker plot of the base level chloride contents for all Bridge deck types.....	209
3.11 Box-and whisker plot of the difference between the maximum and Minimum apparent surface concentration and the top sample taken from off-crack locations for each placement .....	209
3.12 Apparent surface concentration $C_o$ calculated from Fick's Second Law versus the measured chloride content away from cracks at 9.5 mm for monolithic bridge decks .....	210

3.13	Apparent surface concentration $C_o$ calculated from Fick's Second Law versus the measured chloride content away from cracks at 9.5 mm for conventional overlays .....	210
3.14	Apparent surface concentration $C_o$ calculated from Fick's Second Law versus the measured chloride content away from cracks at 9.5 mm for silica fume overlays .....	211
3.15	Average apparent surface concentration $C_o$ calculated from Fick's Second Law versus bridge deck placement age at the time of sampling.....	211
3.16	Average apparent surface concentration $C_o$ calculated from Fick's Second Law for the current study versus the results based on data obtained by Miller and Darwin 2000 .....	212
3.17	Average apparent surface concentration $C_o$ calculated from Fick's Second Law versus age of placement for monolithic deck placements.....	212
3.18	Average apparent surface concentration $C_o$ calculated from Fick's Second Law versus age of placement for conventional overlay deck placements .....	213
3.19	Average apparent surface concentration $C_o$ calculated from Fick's Second Law versus age of placement for silica fume overlay deck placements .....	213
3.20	Effective diffusion coefficient $D_{eff}$ versus age of placement .....	214
3.21	Effective diffusion coefficient $D_{eff}$ versus age for monolithic bridge placements.....	215
3.22	Mean effective diffusion coefficient $D_{eff}$ versus placement age for monolithic bridge placements .....	215
3.23	Box-and-whiskers plot of effective diffusion coefficients $D_{eff}$ for monolithic placements sampled at an age of 96 months or greater .....	216
3.24	Effective diffusion coefficient $D_{eff}$ versus age for conventional overlay bridge placements .....	216

3.25	Mean effective diffusion coefficient $D_{eff}$ versus placement age range for conventional overlay bridge placements .....	217
3.26	Box-and-whiskers plot of effective diffusion coefficients $D_{eff}$ for conventional overlay bridge placements in three age ranges.....	217
3.27	Effective diffusion coefficient $D_{eff}$ versus age for silica fume overlay bridge placements .....	218
3.28	Mean effective diffusion coefficient $D_{eff}$ versus placement age range for silica fume overlay bridge placements .....	218
3.29	Box-and-whiskers plot of effective diffusion coefficients $D_{eff}$ for silica fume overlay bridge placements in two age ranges.....	219
3.30	Mean effective diffusion coefficient $D_{eff}$ and adjusted mean effective diffusion coefficient $D_{eff}^*$ versus bridge deck type for individual placements between 0 and 48 months old.....	219
3.31	Mean effective diffusion coefficient $D_{eff}$ and adjusted mean effective diffusion coefficient $D_{eff}^*$ versus bridge deck type for individual placements between 48 and 96 months old.....	220
3.32	Adjusted mean effective diffusion coefficient $D_{eff}^*$ of individual placements versus special provision number for silica fume overlay placements between 0 and 48 months and 48 and 96 months old .....	220
3.33	Adjusted mean effective diffusion coefficient $D_{eff}^*$ of individual placements versus concrete slump for 5% silica fume overlay placements between 0 and 48 months and 48 and 96 months old .....	221
3.34	Adjusted mean effective diffusion coefficient $D_{eff}^*$ of individual placements versus concrete slump for 5% and 7% silica fume overlay placements between 0 and 48 months old.....	221
3.35	Adjusted mean effective diffusion coefficient $D_{eff}^*$ of individual placements versus concrete slump for conventional overlay placements between 48 and 96 months and 96 and 144 months old .....	222
3.36	Adjusted mean effective diffusion coefficient $D_{eff}^*$ of individual placements versus concrete slump for monolithic placements older than 120 months.....	222

3.37	Adjusted mean effective diffusion coefficient $D_{eff}^*$ of individual placements versus air content for 5% silica fume overlay placements between 0 and 48 months and 48 and 96 months old .....	223
3.38	Adjusted mean effective diffusion coefficient $D_{eff}^*$ of individual placements versus air content for 5% and 7% silica fume overlay placements between 0 and 48 months old.....	223
3.39	Adjusted mean effective diffusion coefficient $D_{eff}^*$ of individual placements versus air content for conventional overlay placements between 48 and 96 months and 96 and 144 months old .....	224
3.40	Adjusted mean effective diffusion coefficient $D_{eff}^*$ of individual placements versus air content for monolithic bridge placements older than 120 months.....	224
3.41	Adjusted mean effective diffusion coefficient $D_{eff}^*$ of individual placements versus water-cementitious material ratio for silica fume overlay placements.....	225
3.42	Adjusted mean effective diffusion coefficient $D_{eff}^*$ of individual placements versus water-cement ratio for conventional overlay placements.....	225
3.43	Adjusted mean effective diffusion coefficient $D_{eff}^*$ of individual placements versus water-cement ratio for monolithic bridge placements older than 120 months.....	226
3.44	Adjusted mean effective diffusion coefficient $D_{eff}^*$ of individual placements versus concrete slump for monolithic bridge placements older than 120 months.....	226
3.45	Adjusted mean effective diffusion coefficient $D_{eff}^*$ of individual placements versus water content for monolithic bridge placements older than 120 months.....	227
3.46	Adjusted mean effective diffusion coefficient $D_{eff}^*$ of individual placements versus cement content for monolithic bridge placements older than 120 months.....	227
3.47	Adjusted mean effective diffusion coefficient $D_{eff}^*$ of individual placements versus concrete compressive strength for 5% silica fume overlay placements between 0 and 48 months and 48 and 96 months old .....	228

3.48	Adjusted mean effective diffusion coefficient $D_{eff}^*$ of individual placements versus concrete compressive strength for 5% silica fume and 7% silica fume overlay placements between 0 and 48 months old .....	228
3.49	Adjusted mean effective diffusion coefficient $D_{eff}^*$ of individual placements versus concrete compressive strength for conventional overlay placements between 48 and 96 months and 96 and 144 month old .....	229
3.50	Adjusted mean effective diffusion coefficient $D_{eff}^*$ of individual placements versus concrete compressive strength for monolithic bridge placements older than 120 months. ....	229
4.1	Crack density of entire monolithic bridge decks evaluated in the current study and by Schmitt and Darwin (1995) and/or Miller and Darwin (2000).....	230
4.2	Crack density of entire conventional overlay bridge decks evaluated in the current study and by Schmitt and Darwin (1995) and/or Miller and Darwin (2000) .....	231
4.3	Crack density of entire silica fume overlay bridge decks evaluated in the current study and by Schmitt and Darwin (1995) and/or Miller and Darwin (2000).....	232
4.4	Correlation of crack density of entire bridge decks for bridges evaluated in the current study and by Schmitt and Darwin (1995).....	233
4.5	Correlation of crack density of entire bridge decks for bridges evaluated in the current study and by Miller and Darwin (2000).....	233
4.6	Correlation of crack density of entire bridge decks for bridge evaluated by Miller and Darwin (2000) and by Schmitt and Darwin (1995).....	234
4.7	Crack density of entire bridge decks versus bridge age for all monolithic decks included in the analysis .....	234
4.8	Crack density of entire bridge decks versus bridge age for all conventional overlays included in the analysis.....	235

4.9	Crack density of entire bridge decks versus bridge age for all silica fume overlays included in the analysis .....	235
4.10	Mean crack density of entire bridge decks versus date of construction for all monolithic decks included in the analysis.....	236
4.11	Mean crack density of entire bridge decks versus date of construction for all conventional overlays included in the analysis.....	236
4.12	Mean crack density of entire bridge decks versus date of construction for all silica fume overlays included in the analysis.....	237
4.13	Mean crack density of entire bridge decks corrected to an age of 78 months versus special provision revision number for silica fume overlay bridge decks .....	237
4.14	Average concrete slump versus placement date for monolithic decks and overlay subdecks .....	238
4.15	Average concrete slump versus placement date for overlay placements.....	238
4.16	Average air content versus placement date for monolithic decks and overlay subdecks.....	239
4.17	Average concrete air content versus placement date for overlay placements.....	239
4.18	Percent volume of water and cement versus placement date for monolithic decks and overlay subdecks.....	240
4.19	Percent volume of water and cementitious materials versus placement date for overlay placements .....	240
4.20	Water content versus placement date for monolithic decks and overlay subdecks.....	241
4.21	Water content versus placement date for overlay placements .....	241
4.22	Cement content versus placement date for monolithic decks and overlay subdecks.....	242
4.23	Water/cement ratio versus placement date for monolithic decks and overlay subdecks.....	242

4.24	Water/cementitious material ratio versus placement date for overlay placements.....	243
4.25	Average concrete compressive strength versus placement date for monolithic decks and overlay subdecks.....	243
4.26	Average concrete compressive strength versus placement date for overlay placements.....	244
4.27	Minimum daily temperature versus placement date for monolithic deck and overlay subdecks.....	244
4.28	Minimum daily temperature versus placement date for overlay placements.....	245
4.29	Maximum daily temperature versus placement date for monolithic deck and overlay subdecks.....	245
4.30	Maximum daily temperature versus placement date for overlay placements.....	246
4.31	Average temperature versus placement date for monolithic deck and overlay subdecks.....	246
4.32	Average temperature versus placement date for overlay placements.....	247
4.33	Daily air temperature range versus placement date for monolithic deck and overlay subdecks.....	247
4.34	Daily air temperature range versus placement date for overlay placements.....	248
4.35	Bridge deck superstructure type versus date of placement for all bridge deck types .....	248
4.36	Deck thickness versus the last day of concrete placement .....	249
4.37	Transverse bar spacing versus the last day of concrete placement.....	249
4.38	Top cover versus the last day of concrete placement .....	250
4.39	Transverse bar spacing versus the last day of concrete placement.....	250

5.1	Mean crack density for individual placements corrected to an age of 78 months versus bridge deck type.....	251
5.2	Mean crack density for individual placements corrected to an age of 78 months versus water content for 5% and 7% silica fume overlay placements.....	251
5.3	Mean crack density for individual placements corrected to an age of 78 months versus water content for conventional overlay placements....	252
5.4	Mean crack density for individual placements corrected to an age of 78 months versus water content for overlay subdeck placements .....	252
5.5	Mean crack density for individual placements corrected to an age of 78 months versus water content for monolithic placements.....	253
5.6	Mean crack density for individual placements corrected to an age of 78 months versus cement content for overlay subdeck placements .....	253
5.7	Mean crack density for individual placements corrected to an age of 78 months versus cement content for monolithic placements .....	254
5.8	Mean crack density for individual placements corrected to an age of 78 months versus percent volume of water and cement for overlay subdeck placements .....	254
5.9	Mean crack density for individual placements corrected to an age of 78 months versus percent volume of water and cement for monolithic placements.....	255
5.10	Mean crack density for individual placements corrected to an age of 78 months versus water-cement ratio for overlay subdeck placements...	255
5.11	Mean crack density for individual placements corrected to an age of 78 months versus water-cement ratio for monolithic placements .....	256
5.12	Mean crack density for individual placements corrected to an age of 78 months versus concrete slump for 5% and 7% silica fume overlay placements.....	256
5.13	Mean crack density for individual placements corrected to an age of 78 months versus concrete slump for conventional overlay placements .	257

5.14	Mean crack density for individual placements corrected to an age of 78 months versus concrete slump for subdeck placements .....	257
5.15	Mean crack density for individual placements corrected to an age of 78 months versus percent concrete slump for monolithic placements ....	258
5.16	Mean crack density for individual placements corrected to an age of 78 months versus air content for 5% and 7% silica fume overlay and conventional overlay placements .....	258
5.17	Mean crack density for individual placements corrected to an age of 78 months versus air content for overlay subdeck placements.....	259
5.18	Mean crack density for individual placements corrected to an age of 78 months versus air content for monolithic placements.....	259
5.19	Mean crack density for individual placements corrected to an age of 78 months versus compressive strength for 5% and 7% silica fume overlay placements.....	260
5.20	Mean crack density for individual placements corrected to an age of 78 months versus compressive strength for conventional overlay placements.....	260
5.21	Mean crack density for individual placements corrected to an age of 78 months versus compressive strength for subdeck placements.....	261
5.22	Mean crack density for individual placements corrected to an age of 78 months versus compressive strength for monolithic placements.....	261
5.23	Mean crack density for individual placements corrected to an age of 78 months versus average air temperature for 5% and 7% silica fume overlay and conventional overlay placements .....	262
5.24	Mean crack density for individual placements corrected to an age of 78 months versus average air temperature for overlay subdeck placements.....	262
5.25	Mean crack density for individual placements corrected to an age of 78 months versus average air temperature for monolithic placements....	263
5.26	Mean crack density for individual placements corrected to an age of 78 months versus minimum air temperature for 5% and 7% silica fume overlay and conventional overlay placements.....	263

5.27	Mean crack density for individual bridge decks corrected to an age of 78 months versus minimum air temperature for overlay subdeck placements.....	264
5.28	Mean crack density for individual placements corrected to an age of 78 months versus minimum air temperature for monolithic bridge placements.....	264
5.29	Mean crack density for individual placements corrected to an age of 78 months versus maximum air temperature for 5% and 7% silica fume overlay and conventional overlay placements.....	265
5.30	Mean crack density for individual bridge decks corrected to an age of 78 months versus maximum air temperature for overlay subdeck placements.....	265
5.31	Mean crack density for individual placements corrected to an age of 78 months versus maximum air temperature for monolithic placements.....	266
5.32	Mean crack density for individual placements corrected to an age of 78 months versus daily air temperature range for 5% and 7% silica fume overlay and conventional overlay placements.....	266
5.33	Mean crack density for individual bridge decks corrected to an age of 78 months versus daily air temperature range for overlay subdeck placements.....	267
5.34	Mean crack density for individual placements corrected to an age of 78 months versus daily air temperature range for monolithic bridge placements.....	267
5.35	Mean crack density for entire bridge decks corrected to an age of 78 months versus structure type, based on deck type, for all bridge deck types .....	268
5.36	Mean crack density for entire bridge decks corrected to an age of 78 months versus structure type for all bridge deck types.....	268
5.37	Mean crack density for entire bridge decks corrected to an age of 78 months versus top transverse reinforcing bar size for 5% and 7% silica fume overlay bridges.....	269

5.38	Mean crack density for entire bridge decks corrected to an age of 78 months versus top transverse reinforcing bar size for conventional overlay bridges.....	269
5.39	Mean crack density for entire bridge decks corrected to an age of 78 months versus top transverse reinforcing bar size for monolithic bridges.....	270
5.40	Mean crack density for entire bridge decks corrected to an age of 78 months versus top transverse reinforcing bar size for all bridge deck types .....	270
5.41	Mean crack density for entire bridge decks corrected to an age of 78 months versus top transverse bar spacing for 5% and 7% silica fume and conventional overlay bridges .....	271
5.42	Top transverse bar spacing versus top transverse bar size for 5% and 7% silica fume and conventional overlay bridges .....	271
5.43	Mean crack density for entire bridge decks corrected to an age of 78 months versus deck thickness for 5% and 7% silica fume overlay bridges.....	272
5.44	Mean crack density for entire bridge decks corrected to an age of 78 months versus deck thickness for conventional overlay bridges .....	272
5.45	Mean crack density for entire bridge decks corrected to an age of 78 months versus deck thickness for monolithic bridges .....	273
5.46	Mean crack density for entire bridge decks corrected to an age of 78 months versus top cover for monolithic bridges.....	273
5.47	Mean crack density of end sections corrected to an age of 78 months versus girder end condition for 5% and 7% silica fume overlay and conventional overlay bridges .....	274
5.48	Ratio of end section crack density to the crack density of the entire deck versus girder end condition for 5% and 7% silica fume overlay and conventional overlay bridges .....	274
5.49	Mean crack density for individual spans corrected to an age of 78 months versus span type for 5% and 7% silica fume overlay and conventional overlay bridges .....	275

5.50	Mean crack density for individual spans corrected to an age of 78 months versus span type for monolithic bridges.....	275
5.51	Mean crack density for entire bridge decks corrected to an age of 78 months versus bridge skew for 5% and 7% silica fume overlay and conventional overlay bridges .....	276
5.52	Mean crack density for entire bridge decks corrected to an age of 78 months versus bridge skew for monolithic bridges .....	276
5.53	Mean crack density for individual spans corrected to an age of 78 months versus span length for 5% and 7% silica fume overlay bridges.....	277
5.54	Mean crack density for individual spans corrected to an age of 78 months versus span length for conventional overlay bridges .....	277
5.55	Mean crack density for individual spans corrected to an age of 78 months versus span length for monolithic bridges .....	278
5.56	Mean crack density for entire bridge decks corrected to an age of 78 months versus bridge length for 5% and 7% silica fume overlay, conventional overlay, and monolithic bridges.....	278
5.57	Mean crack density for individual placements corrected to an age of 78 months versus bridge contractor (names withheld) for 5% and 7% silica fume overlay placements.....	279
5.58	Mean crack density for individual placements corrected to an age of 78 months versus bridge contractor (names withheld) for conventional overlay placements.....	279
5.59	Mean crack density for individual placements corrected to an age of 78 months versus bridge contractor (names withheld) for monolithic placements.....	280
5.60	Mean crack density for entire bridge decks corrected to an age of 78 months versus traffic volume for 5% and 7% silica fume overlay and conventional overlay bridges .....	280
5.61	Mean crack density for entire bridge decks corrected to an age of 78 months versus traffic volume for monolithic bridges.....	281

5.62	Crack density and dummy variable analysis results for entire bridge decks versus total number of load cycles for 5% and 7% silica fume overlay bridges.....	281
5.63	Crack density and dummy variable analysis results for entire bridge decks versus total number of load cycles for conventional overlay bridges.....	282
5.64	Crack density and dummy variable analysis results for entire bridge decks versus total number of load cycles for monolithic bridges.....	282
5.65	Crack density and dummy variable analysis results for entire bridge decks corrected to an age of 78 months versus total number of load cycles for 5% and 7% silica fume overlay bridges.....	283
5.66	Crack density and dummy variable analysis results for entire bridge decks corrected to an age of 78 months versus total number of load cycles for conventional overlay bridges .....	283
5.67	Crack density and dummy variable analysis results for entire bridge decks corrected to an age of 78 months versus total number of load cycles for monolithic bridges.....	284
E.1	Legend for Bridge Deck Cracking Patterns .....	394
E.2	Bridge Number 30-93 (7% Silica Fume Overlay) .....	395
E.3	Bridge Number 40-92 (7% Silica Fume Overlay) .....	396
E.4	Bridge Number 40-93 (7% Silica Fume Overlay) .....	397
E.5	Bridge Number 46-332 (7% Silica Fume Overlay) .....	398
E.6	Bridge Number 81-53 (7% Silica Fume Overlay) .....	399
E.7	Bridge Number 85-148 (7% Silica Fume Overlay) .....	400
E.8	Bridge Number 85-149 (7% Silica Fume Overlay) .....	401
E.9	Bridge Number 89-269 (7% Silica Fume Overlay) .....	402
E.10	Bridge Number 89-272 (7% Silica Fume Overlay) .....	403
E.11	Bridge Number 103-56 (7% Silica Fume Overlay) .....	404

E.12	Bridge Number 23-85 (5% Silica Fume Overlay) .....	405
E.13	Bridge Number 46-302 (5% Silica Fume Overlay) .....	406
E.14	Bridge Number 46-309 (5% Silica Fume Overlay) .....	407
E.15	Bridge Number 46-317, Unit 1 (5% Silica Fume Overlay) .....	408
E.16	Bridge Number 81-50, Unit 2 (5% Silica Fume Overlay) .....	409
E.17	Bridge Number 87-453 (5% Silica Fume Overlay) .....	410
E.18	Bridge Number 87-454 (5% Silica Fume Overlay) .....	411
E.19	Bridge Number 89-184 (7% Silica Fume Overlay) .....	412
E.20	Bridge Number 89-187 (5% Silica Fume Overlay) .....	413
E.21	Bridge Number 89-206 (5% Silica Fume Overlay) .....	414
E.22	Bridge Number 89-207 (5% Silica Fume Overlay) .....	415
E.23	Bridge Number 89-210 (5% Silica Fume Overlay) .....	416
E.24	Bridge Number 89-234 (5% Silica Fume Overlay) .....	417
E.25	Bridge Number 89-235 (5% Silica Fume Overlay) .....	418
E.26	Bridge Number 89-240 (5% Silica Fume Overlay) .....	419
E.27	Bridge Number 89-244 (5% Silica Fume Overlay) .....	420
E.28	Bridge Number 89-245 (5% Silica Fume Overlay) .....	421
E.29	Bridge Number 89-246 (5% Silica Fume Overlay) .....	422
E.30	Bridge Number 89-247 (5% Silica Fume Overlay) .....	423
E.31	Bridge Number 89-248 (5% Silica Fume Overlay) .....	424
E.32	Bridge Number 46-289 (Conventional Overlay) .....	425
E.33	Bridge Number 46-290 (Conventional Overlay) .....	426

E.34	Bridge Number 46-299 (Conventional Overlay) .....	427
E.35	Bridge Number 46-300 (Conventional Overlay) .....	428
E.36	Bridge Number 46-301 (Conventional Overlay) .....	429
E.37	Bridge Number 75-01 (Conventional Overlay) .....	430
E.38	Bridge Number 75-49 (Conventional Overlay) .....	431
E.39	Bridge Number 81-49 (Conventional Overlay) .....	432
E.40	Bridge Number 89-183 (Conventional Overlay) .....	433
E.41	Bridge Number 89-185 (Conventional Overlay) .....	434
E.42	Bridge Number 89-186 (Conventional Overlay) .....	435
E.43	Bridge Number 89-196 (Conventional Overlay) .....	436
E.44	Bridge Number 89-198 (Conventional Overlay) .....	437
E.45	Bridge Number 89-199 (Conventional Overlay) .....	438
E.46	Bridge Number 89-200 (Conventional Overlay) .....	439
E.47	Bridge Number 89-201 (Conventional Overlay) .....	440
E.48	Bridge Number 3-45 (Monolithic).....	441
E.49	Bridge Number 3-46 (Monolithic).....	442
E.50	Bridge Number 56-142 (Monolithic).....	443
E.51	Bridge Number 56-148 (Monolithic).....	444
E.52	Bridge Number 70-95 (Monolithic).....	445
E.53	Bridge Number 70-103 (Monolithic).....	446
E.54	Bridge Number 70-104 (Monolithic).....	447
E.55	Bridge Number 70-107 (Monolithic).....	448

E.56	Bridge Number 75-44 (Monolithic).....	449
E.57	Bridge Number 75-45 (Monolithic).....	450
E.58	Bridge Number 89-204 (Monolithic).....	451
E.59	Bridge Number 89-208 (Monolithic).....	452
E.60	Bridge Number 99-76 (Monolithic).....	453

## **CHAPTER 1: INTRODUCTION**

### **1.1 GENERAL**

The corrosion of reinforcing steel in bridge decks is a significant financial and safety problem that is exacerbated by bridge deck cracking and deicing chemicals, primarily sodium chloride and calcium chloride. Since the early 1960s, transportation agencies have worked to identify the primary factors contributing to bridge deck cracking. Many recommendations have been made that have resulted in material and design specification changes, more stringent weather limitations on concrete placement, and improved construction procedures. Bridge deck cracking has, however, remained a significant problem warranting continued attention. At the same time, efforts to limit the corrosion of reinforcing steel through the use of epoxy coatings, increased cover, and high-density concrete overlays have become widely accepted. Another method that has become increasingly popular, especially in the state of Kansas, is the use of concrete overlays containing silica fume. The use of silica fume slows the ingress of chlorides due to greatly reduced permeability and, in some cases, concretes containing silica fume have performed well. As with other technological innovations, however, questions regarding both short and long-term field performance exist. Silica fume concrete, especially in bridge deck applications, is certainly not an exception.

### **1.2 SIGNIFICANCE OF BRIDGE DECK CRACKING**

Cracks in bridge decks provide the principal path for deicing chemicals to reach reinforcing steel and accelerate freeze-thaw damage. Cracks may also extend through the full thickness of a deck and cause accelerated corrosion of the supporting girders. A 2002 estimate places the direct cost associated with corrosion of highway bridges at \$8.3 billion annually, with indirect user costs as much as ten times that

amount (Yunovich et al. 2002). Information gathered by the Federal Highway Administration (FHWA) for the state of Kansas indicates that in 2002 approximately 25 percent of the bridges were classified as structurally deficient or functionally obsolete. Although these classifications are not based exclusively on the condition of bridge decks, the bridge decks are primary factors affecting this rating. According to Virmani and Clemeña (1998), the corrosion of bridge deck reinforcing steel is a significant contributor to superstructure deterioration.

### **1.3 TYPES OF BRIDGE DECK DETERIORATION**

Bridge deck deterioration can be classified by either the causes of the deterioration or by the physical description and orientation. The most predominant form of bridge deck deterioration is cracking. Bridge deck cracking is also commonly categorized by the cause or the orientation and physical characteristics of the cracks.

#### **1.3.1 Crack Classification Based on Causes of Cracking**

Bridge deck cracking is the result of a complex interaction of multiple factors that are not yet fully understood. Cracks are typically categorized into two main groups: cracks that occur while the concrete is still plastic and cracks that occur after the concrete has hardened. Plastic shrinkage cracking and subsidence cracking have been identified and occur in plastic concrete, while thermal shrinkage cracking, drying shrinkage cracking, and flexural cracking are believed to be the primary causes of cracking in hardened concrete.

The causes of and remedies for plastic shrinkage cracking are well known. Plastic shrinkage cracks occur in fresh concrete when the rate of surface evaporation exceeds the rate at which concrete bleed water reaches the surface. As water from the surface of the deck is removed by evaporation, negative capillary pressures form and

cause the paste to shrink. Since this occurs predominately at the surface of the deck, differential shrinkage between the top layer and the underlying layer create tensile stresses that are likely to create surface cracks. The concrete bleeding rate, a primary factor in plastic shrinkage cracking, can be reduced for a number of reasons. The use of fine pozzolans and other mineral admixtures or finely ground cements reduces bleeding. In addition, increasing the rate of cement hydration, the use of air entrained air, and a reduction of the water content of the concrete reduces bleeding and makes concrete more susceptible to plastic shrinkage cracking (Mindess, Young, and Darwin 2003). Many methods have been successfully employed to mitigate plastic shrinkage cracking during concrete placement. Admixtures that increase the bleeding rate, evaporation retarders, windbreaks, curing compounds, cooling the concrete or its constituents, and the early application of wet burlap and polyethylene have all been used in various combinations to successfully eliminate plastic shrinkage cracking.

Subsidence or settlement cracking occurs as fresh concrete settles around reinforcing bars near the surface of the deck. Since these cracks occur directly above and parallel to the deck reinforcement, settlement cracks provide a direct path for deicing chemicals to reach the reinforcing steel. Settlement cracks are caused by a local tensile stress concentration resulting from fresh concrete subsiding on either side of the reinforcing steel. The probability of settlement cracks occurring increases with increasing bar size, increasing slump, and decreasing concrete cover (Dakhil, Cady, and Carrier 1975). In addition to forming visually observable cracks, weakened planes in the concrete above the reinforcing bars may also increase the probability of cracking after the concrete has hardened (Babaei and Fouladgar 1997).

Thermal bridge deck cracking results from thermally-induced shrinkage and restraint provided by girders, deck reinforcement, shear studs, and abutments. As concrete cures, hydration results in increasing concrete temperatures and expansion. This initial expansion during hydration causes little or no stress in the plastic

concrete. The concrete hardens in a “stress-free” condition by the time it reaches its peak temperature. As the concrete begins cooling to the ambient temperature, it shrinks; girders and other structural elements, however, restrict the shrinkage and induce tensile stresses. These tensile stresses can result in cracks if the thermally-induced stress exceeds the tensile capacity of the deck. These stresses may also leave the deck more susceptible to cracking caused by other factors (Babaei and Purvis 1996).

Drying shrinkage results from water loss in the cement paste and causes cracking in a manner similar to thermal shrinkage. Water contained in capillary pores, hardened calcium silicate gel (calcium silicate hydrate or C–S–H), and solid surfaces is lost causing shrinkage. In bridge decks, the shrinkage is restrained. Drying shrinkage, however, occurs over a much longer period than other types of shrinkage and allows concrete creep to alleviate a portion of the tensile stress. Although many factors affect drying shrinkage, shrinkage caused by water loss from the C–S–H gel is the most significant. By maximizing the aggregate content (the concrete constituent that resists shrinkage) and minimizing the paste content, overall shrinkage can be reduced. Other mix design factors, such as cement type and fineness, aggregate type and size, admixtures, and member geometry, also affect the amount of drying shrinkage (Mindess, Young, and Darwin 2003).

In addition to cracks caused by the restraint of volume changes, directly applied loads are also responsible for bridge deck cracking. Flexural cracks typically occur in negative moment regions as a result of dead and live loads. Finally, the placing sequence during construction can affect the tensile stresses induced in a bridge deck, both during and after construction.

### **1.3.2 Crack Classification Based on Orientation**

In a 1970 study, the Portland Cement Association categorized bridge deck

cracks into five distinct groups: transverse, longitudinal, diagonal, pattern or map, and random cracking (*Durability* 1970). A sixth category, D-cracking, was defined but not found on any of the decks examined. The following observations and definitions were developed as part of that extensive study (described in Section 1.8).

**Transverse cracks** are fairly straight and occur perpendicular to the roadway centerline. Transverse cracks have been the focus of many studies because they are generally recognized as both the most common and the most detrimental form of cracking (*Durability* 1970, Krauss and Rogalla 1996, Eppers and French 1998, Le and French 1998). Transverse cracks frequently occur directly above transverse reinforcement and can extend completely through the deck (*Durability* 1970).

**Longitudinal cracking** is primarily found in slab bridges. These cracks are typically straight and run parallel to the roadway centerline above the void tubes in hollow-slab bridges and above the longitudinal reinforcement in solid-slab bridges. Like transverse cracks, these cracks frequently occur before the bridge is open to traffic and can extend completely through the deck (*Durability* 1970, Eppers and French 1998).

**Diagonal cracking** typically occurs near the ends of skewed bridges and over single-column piers. Generally, these cracks are parallel and occur at an angle other than 90 degrees with respect to the roadway centerline (*Durability* 1970). Diagonal cracks are typically shallow in depth and do not follow any distinct pattern. The likely causes of these cracks are inadequate design details near abutments, resulting in flexural cracking and drying shrinkage induced cracking.

**Pattern or map cracking** consists of interconnected cracks of any size. They are generally shallow in depth and are not believed to significantly affect bridge performance (*Durability* 1970). Both drying shrinkage and plastic shrinkage are thought to be the primary causes. Finally, **random cracks** are irregularly shaped cracks that do not fit into any of the other classifications. These cracks occur

frequently, but there is no clear relationship between their occurrence and bridge deck characteristics (*Durability* 1970).

#### **1.4 CORROSION**

Corrosion of reinforcing steel is caused by a number of factors that can lead to cracking and more detrimental forms of deterioration, such as surface spalling and delamination. These latter forms of deterioration are principally caused by the volume expansion that accompanies the corrosion of reinforcing steel. Cracks over reinforcing steel, inadequate concrete cover, chloride diffusion through concrete, and the use of deicing chemicals containing chlorides all play an important factor in reinforcing steel corrosion (*Durability* 1970).

The high alkalinity of the concrete pore water creates a tightly adhering film that passivates the steel and provides protection in addition to the physical properties of the concrete. Unfortunately, this passivating layer can be penetrated by chloride ions, applied as deicing salts, and leave the deck reinforcing steel vulnerable to corrosion. The typical wetting and drying cycles experienced by bridge decks aggravates this problem. The corrosion rate and the time until concrete repairs are needed are influenced by the amount of concrete cover protecting the steel, the application rate of deicing salts, and the concrete permeability (ACI Committee 222 1998). For corrosion to occur, both oxygen and water must be present.

#### **1.5 SILICA FUME**

To create durable and less permeable concrete, silica fume is used as a partial replacement of portland cement. Silica fume is produced as a by-product during the production of silicon metal or ferrosilicon alloys and consists of very small spherical particles. During cement hydration, silica fume reacts with calcium hydroxide (CH) and forms calcium-silicate hydrate (C-S-H) through the pozzolanic reaction. In

addition to the supplementary C–S–H produced, the fine spherical particles act as filler between cement and aggregate particles and within the cement paste matrix (Whiting, Detwiler, and Lagergren 2000). The addition of silica fume in concrete results in a stronger, denser, and less permeable concrete. Research has shown that in hardened concrete, although the total porosity is not reduced, the number of large capillary pores is reduced, thus increasing the likelihood of a discontinuous pore system (ACI Committee 234 1996).

Although silica fume is also associated with improved durability, high strength, high early-strength, and abrasion resistance, the primary use of silica fume in bridge decks is to provide corrosion protection through the use of a low permeability bridge deck. There is, however, concern with the use of silica fume in concrete bridge decks. Silica fume is approximately 100 times finer than portland cement and has a correspondingly high surface area (Detwiler, Whiting, and Lagergren 1999). This high surface area results in a cohesive mix with a substantially increased water demand. Typically, this increase in water demand is offset through the use of a high-range water reducer and selecting a target slump approximately 50 mm (2 in.) more than would be used for conventional concretes. The high surface area of silica-fume, however, reduces the total amount and rate of bleeding, leaving the concrete especially susceptible to plastic shrinkage cracking (ACI Committee 234 1996).

## **1.6 CHLORIDE CONCENTRATIONS**

Although the transport of chloride ions in hardened concrete is controlled in part by absorption and capillary action or wicking, the predominant mechanism is “ionic diffusion through the water-filled pore system” (Whiting and Mitchell 1992). Fick’s Second Law of Diffusion is frequently used to model chloride migration through concrete and is shown in Eq. (1.1).

$$\frac{\partial C}{\partial t} = D \left( \frac{\partial^2 C}{\partial x^2} \right) \quad (1.1)$$

where

- $x$  = depth
- $t$  = time
- $C$  = chloride concentration
- $D$  = diffusion coefficient

Although this equation generally models chloride migration through concrete well, there are three principal problems with its application to concrete. First, Fick's Second Law assumes that the material, concrete in this case, is both permeable and homogeneous. Concrete is permeable, but it is certainly not homogeneous. Second, the diffusion properties of the material cannot change with respect to time or concentration of the diffusant. Generally concrete becomes less permeable as hydration progresses and as chloride concentrations within the concrete increase. Lastly, Fick's Second Law assumes that no chemical reactions or binding between the material and the diffusant occur. Young concrete violates this assumption because aluminates generated during the hydration process can chemically bind with chloride ions and prevent further ingress into the concrete (Whiting and Detwiler 1998).

To solve Eq. (1.1) and arrive at the form of the equation that is most commonly used, two additional assumptions must be made; these are applied as an initial condition and a boundary condition for the differential equation. First, the initial chloride content is assumed to be zero throughout the sample, and second, the surface concentration is assumed to be constant throughout the life of the sample. Both of these additional assumptions are again violated by concrete exposed to deicers. Chlorides are contained in aggregates and admixtures and are commonly found in concrete before any deicing salts are applied. Secondly, chlorides are

applied to bridge decks seasonally and are subject to rain, traffic, and other conditions that increase and then decrease the surface concentration throughout the year. Despite these shortcomings, Fick's Second Law is commonly used and serves as a useful tool to measure relative differences between different bridge decks. With the application of the two assumptions, an error-based function can be obtained and readily applied to experimental data (Suryavanshi, Swamy, and Cordew 2002).

$$C(x, t, C_o, D_{eff}) = C_o \cdot \left[ 1 - \operatorname{erf} \left( \frac{x}{2 \cdot \sqrt{t \cdot D_{eff}}} \right) \right] \quad (1.2)$$

where

- $x$  = depth
- $t$  = time
- $C_o$  = apparent surface concentration
- $D_{eff}$  = effective diffusion coefficient
- $\operatorname{erf}$  = error function

Typically, because of the assumptions made in solving the differential equation, terms such as “apparent” and “effective” are used to describe the surface concentration and diffusion coefficient obtained through the use of this technique.

## 1.7 BRIDGE DECK OVERLAY SPECIFICATIONS

Two types of rigid overlays were examined in this study: conventional high-density concrete overlays and silica fume modified overlays. The 59 bridges included in this study were constructed between 1984 and 2002. Because of this wide range in construction dates, these bridges represent a variety of construction procedures and specifications. During this period, one of the most significant revisions to standard construction practices for deck overlays has been the use of silica fume to modify the

concrete. Additional requirements that are included in the specifications covering silica fume outline curing procedures, placing and finishing equipment, concrete mix designs, and temperature restrictions. The specifications usually provide a range of acceptable values and procedures. For this reason most of the individual factors (e.g., cement content and air temperature) and their effect on deck cracking and permeability are examined in Chapters 3, 4, and 5. It is important, however, to begin with the general requirements used for the design and construction of each bridge deck, especially for individual factors that are not typically recorded in construction records.

The conventional overlay specifications applicable to this study (section 720 of the Standard Specifications) are Special Provisions 90P-95, 90P-95-R1, and 90P-95-R2. They require the use of Type II or Type I/II portland cement and a minimum cement content of  $371 \text{ kg/m}^3$  ( $625 \text{ lb/yd}^3$ ). In addition, the maximum water-cement ratio is specified as 0.38, the required entrained air content is  $6.0 \pm 2.0$  percent, and the maximum slump is 19 mm ( $\frac{3}{4}$  in.). The maximum aggregate size is 12.5 mm ( $\frac{1}{2}$  in.), and the ratio of coarse aggregate to fine aggregate is specified as 50:50 by weight. At least one oscillating screed is required to finish the deck, and drum roller finishing equipment is not allowed. These provisions do not require fogging. Application of a liquid membrane forming curing compound followed by wet burlap and polyethylene for a minimum of 72 hours is required.

The current conventional overlay specification (90M-95-R4) requires an air content of  $6.5 \pm 1.5$  percent and allows the use of Type IP cement in addition to Type II and Type I/II cement. The slump can be chosen by the contractor and set between 50 and 125 mm (2 and 5 in.) with a tolerance of 25 percent or 18 mm (0.7 in.), whichever is larger. To begin placement, the estimated evaporation rate must be below 1.0 kg per square meter per hour (0.2 lb per square foot per hour). If the evaporation rate is estimated to exceed  $1.0 \text{ kg/m}^2/\text{hr}$  ( $0.2 \text{ lb/ft}^2/\text{hr}$ ) at anytime during

placement, additional measures such as windbreaks, fogging, cooling the concrete or its constituents must be used to create and maintain satisfactory environmental conditions. A drum roller may be used in lieu of an oscillating screed. In addition to the liquid membrane, a precure material is required immediately after the surface is struck off and the final cure with wet burlap and polyethylene is extended to at least seven days. Any additional measures taken during placement to reduce the evaporation rate must be continued during the finishing operation until the wet burlap is in place.

The silica fume overlay specifications applicable to this study represent two primary groups of specifications. The first group, special provisions 90P-158-R1 through 90P-158-R6 require Type II or Type I/II portland cement with a minimum cement content of  $354 \text{ kg/m}^3$  ( $595 \text{ lb/yd}^3$ ) and a minimum silica fume content of  $18 \text{ kg/m}^3$  ( $30 \text{ lb/yd}^3$ ), equal to 5 percent by weight of cement and 4.8 percent by weight of cementitious materials. The maximum water to cementitious material ratio is 0.40; the required air content is  $6.0 \pm 2.0$  percent; and the target slump can be selected by the contractor and set between 50 mm and 125 mm (2 and 5 in.). The maximum aggregate size is 12.5 mm ( $\frac{1}{2}$  in.), and the ratio of coarse aggregate to fine aggregate is specified as 50:50 by weight. Prior to placing the overlay, a portland cement grout with a water-cement ratio of 0.60 must be brushed on to the dry subdeck. At least one oscillating screed is required to finish the deck, and drum roller finishing equipment is not allowed. The allowable tolerance for the chosen slump changed from 25 mm (1 in.) for special provisions 90P-158-R1 through 90P-158-R4 to the larger of 25 percent of the chosen slump or 18 mm ( $\frac{3}{4}$  in.) beginning with special provision 90P-158-R5.

The second group of overlay specifications (90M-95-R8, 90M-95-R9, 90M-95-R10) added the option of using Type IP cement and decreased the minimum cement content to  $346 \text{ kg/m}^3$  ( $583 \text{ lb/yd}^3$ ) while increasing the minimum silica fume

content to  $26 \text{ kg/m}^3$  ( $44 \text{ lb/yd}^3$ ), equal to a 7 percent replacement of portland cement by weight of cementitious materials. The maximum water to cementitious material ratio is 0.37, down from 0.40. Air content, slump, and aggregate content have the same requirements as the most recent conventional overlay provision.

The finishing and curing requirements have changed significantly since the first silica fume overlay special provision (90P-158). For provisions 90P-158 through 90P-158-R2, curing is achieved with wet burlap covered with white polyethylene sheeting for at a minimum of 72 hours. An onsite silica fume technical representative from the silica fume manufacturer is required to be on the job site during the initial placements. The technical representative may require a precure material and/or fogging after the surface is struck-off with an oscillating screed. Special provision 90P-158-R3 requires the use of a Type 1-D liquid curing compound immediately after finishing in addition to a curing period of seven days. This provision (90P-158-R3) also requires fogging and/or the application of a precure material during the finishing operation.

The requirements for special provisions 90P-158-R4 through 90P-158-R6 have become increasing stringent. The estimated evaporation rate must be below  $1.0 \text{ kg per square meter per hour}$  ( $0.2 \text{ lb per square foot per hour}$ ). If the evaporation rate is estimated to exceed  $1.0 \text{ kg/m}^2/\text{hr}$  ( $0.2 \text{ lb/ft}^2/\text{hr}$ ) at anytime during placement, additional measures such as windbreaks, fogging, cooling the concrete or its constituents must be used to create and maintain satisfactory environmental conditions. These provisions also require the use of both fogging and a precure material during the finishing operation. The Type 1-D membrane must be applied immediately behind the tining operation, and measures must be taken to ensure that the burlap remains wet for the entire curing period. An important change was implemented in special provision 90M-158-R7. The grout previously used to cover the surface of the subdeck prior to overlay placement is no longer required. Instead,

the surface must be thoroughly wetted at least two hours prior to placement and the damp surface must be maintained until the overlay is placed.

Only minor changes have occurred since the development of the first 7 percent silica fume overlay special provision (90M-95-R8). The curing requirements have not changed. In addition to the requirements set forth in 90M-158-R7, rather than continuous fogging throughout the finishing operation, these provisions allow intermittent fogging during finishing if the estimated evaporation rate is below 1.0 kg/m<sup>2</sup>/hr (0.2 lb/ft<sup>2</sup>/hr). This change helps to ensure that water does not begin to pond on the overlay surface during periods of low evaporation. If the evaporation rate is above 1.0 kg/m<sup>2</sup>/hr (0.2 lb/ft<sup>2</sup>/hr), continuous fogging is still required until the wet burlap is in place.

## **1.8 PREVIOUS WORK**

Several studies have been undertaken to ascertain the principal causes and remedies for bridge deck cracking. Ten studies are summarized in this section including two studies of bridge decks in Kansas (Schmitt and Darwin 1995, Miller and Darwin 2000) that serve as a basis and template for this research. The studies range from large multi-state bridge examinations (*Durability* 1970) to smaller laboratory projects (Dakhil, Cady, and Carrier 1975). Each study selected for review represents a unique perspective, substantial advance, or significant body of research on the causes and remedies of bridge deck cracking. The ten studies are summarized in Table 1.1.

### **1.8.1 Literature Review**

*Schmitt and Darwin 1995.* In 1995, Schmitt and Darwin completed a study of steel girder bridges located primarily in northeastern Kansas. This study was the first of three in Kansas with the goal of determining the primary factors that lead to bridge

deck cracking. The study included recommendations for alternate design and construction methods to improve bridge deck performance based on field surveys of 37 composite bridge decks [15 monolithic, 20 high-density (conventional) concrete overlay, 2 silica fume overlay], and 3 monolithic non-composite bridge decks.

Information obtained from the field surveys was compared with thirty-one variables compiled from construction diaries, weather logs, mix designs, and bridge plans to determine and quantify the primary factors affecting bridge deck durability. The field surveys were performed by marking all of the cracks on the bridge deck and transferring these marks to a scale drawing of the deck. The drawings were scanned, and crack densities, in linear meters of crack per square meter of bridge deck, were calculated for each deck from the crack maps through the use of computer programs. In addition to the entire bridge deck, crack densities were also calculated for individual spans, individual placements, and the first and last 3 m (10 ft) of each bridge deck. Due to the inherent differences in the bridge deck types included in the study, most of the variables were analyzed separately for each deck type.

Based on the analysis, Schmitt and Darwin (1995, 1999) reached several conclusions. With respect to monolithic, conventional overlay, and silica-fume overlay bridge decks, they found that the deck type had little influence on the amount of cracking. Bridges with integral abutments showed increased cracking when compared to pin-ended girders (approximately 2 to 3 times). Of the bridges examined with integral abutments, as the attached length of the deck along the abutment increases, the amount of cracking in the end sections of the deck increases. Cracking also appeared to increase with the average annual daily traffic (AADT). Finally, for the bridges included in the study, those built before 1988, on average, exhibited less cracking than those built after 1988.

For monolithic bridge decks, Schmitt and Darwin observed that crack density increases with increasing concrete slump, percent of concrete volume occupied by

water and cement, water content, cement content, and compressive strength. Cracking was also found to increase with an increase in water-cement ratio, although it was noted that this trend was only established for the water-cement ratios used in the bridge decks, 0.40, 0.42, and 0.44. Crack density was found to decrease with increasing amounts of entrained air, with significant decreases observed when the air content exceeded 6.0 percent. Of the environmental factors examined, the researchers found that increases in the maximum air temperature and daily air temperature range on the day of casting correlated with an increase in crack density.

Several conclusions were also drawn with respect to decks with overlays. Crack density was found to increase with increases in placement length and bridge length, and to some extent bridge skew. As for monolithic bridge decks, crack density was found to increase with an increase in maximum daily air temperature on the day of casting, although the trend was not as clear. In addition, crack density was found to increase with increases in the average air temperature and the daily air temperature range. Of the design factors examined, cracking was more severe in decks that contained No. 19 (No. 6) top transverse bars than for decks containing No. 16 (No. 5) bars or a combination of No. 13 and No. 16 (No. 4 and No. 5) bars. Crack density was also more severe in bridge decks with top transverse bar spacing greater than 150 mm (6.0 in.) and for decks with overlays that were placed with zero slump concrete.

Based on their study, Schmitt and Darwin (1995, 1999) made three primary recommendations to reduce cracking in concrete bridge decks. First, the volume of water and cement should not exceed 27.0 percent of the concrete for monolithic bridge deck placements or for the subdeck of two-layer bridge decks. Second, the minimum air content for monolithic bridge decks should be 6.0 percent, and finally concrete used for overlays should not be placed with zero slump. In addition to the three primary recommendations, Schmitt and Darwin (1995) recommended several

additional practices to consider before designing and placing concrete bridge decks. First, designers should be made aware that increased cracking occurs for fixed-ended girders compared to pin-ended girders. Second, closer consideration should be given to the high air temperature and the average daily air temperature when scheduling deck placements. Third, for monolithic bridge decks, the lowest possible slump that still allows reasonable and proper placement and consolidation should be used, with a maximum of 50 mm (2.0 in.). Additionally, shorter placement lengths, especially for overlays, and limiting the top transverse reinforcement to No. 13 or No. 16 (No. 4 or No. 5) bars spaced at 150 mm (6.0 in.) or less should be considered when designing bridge decks. Lastly, fog sprays should be specified for silica-fume overlays to prevent the possibility of extensive plastic shrinkage cracking.

*Miller and Darwin 2000.* In 2000, Miller and Darwin completed a follow-up study to the previous Kansas Department of Transportation sponsored research (Schmitt and Darwin 1995, 1999). In addition to gathering information with respect to the primary factors that contribute to bridge deck cracking, the performance of bridge decks containing silica fume overlays was compared with conventional high-density concrete overlay bridge decks. Forty composite continuous steel girder bridges, 11 of which were included in the previous study by Schmitt and Darwin (1995, 1999), were surveyed and studied using the same procedures and sources previously outlined. The new study included three bridge deck types: 20 silica fume overlay, 16 conventional overlay, and 4 monolithic bridge decks. For the two types of overlay decks, comparisons were made to both the overlay properties and the properties of the bridge subdecks. In addition to the crack density surveys, each bridge deck was evaluated for pavement roughness, chloride content, and performance in rapid chloride permeability test (RCPT) to provide additional points of comparison.

Chloride samples were taken from nearly all of the bridge deck placements included in the study at 19 mm ( $\frac{3}{4}$  in.) increments to a depth of 95 mm ( $3\frac{3}{4}$  in.). Three locations on-cracks and three locations off-cracks were sampled for each placement. The samples were tested for chloride content, and Fick's equation was fitted to the resulting profiles using a least-squares technique. An equivalent surface concentration and effective diffusion coefficient [see Eq. (1.2)] were calculated for each placement and used to evaluate the ability of the concrete to resist chloride ingress. In addition to chloride sampling, concrete cores were taken to perform the rapid chloride permeability test in accordance with ASTM C 1202 (AASHTO T 277) "Standard Test Method for Electrical Indication of Concrete's Ability to Resist Chloride Ion Penetration," except that the cores were only 38 mm (1.5 in.) thick rather than the standard 51 mm (2 in.). This was done because the majority of the silica fume overlays sampled were only 38 mm (1.5 in.) thick. The rapid chloride permeability test (RCPT) measures the electrical conductance of concrete by imposing an electrical potential across a sample and measuring the total charge that passed through the sample in a specified time. The results of the chloride diffusion analyses and rapid chloride permeability tests (RCPT) were compared with the material properties and field data of the deck placements.

For ages between 500 and 1500 days, the effective diffusion coefficients for the silica fume and conventional overlays were found to be similar. Silica fume overlay bridge decks, however, had much lower RCPT values than either the conventional overlay or monolithic bridge decks, possibly highlighting the deficiencies of this method for evaluating permeability when mixes with mineral admixtures are compared to mixes without mineral admixtures. The researchers also concluded that there was no correlation between either the effective diffusion coefficients or the RCPT values and concrete slump for overlay bridges. For silica fume overlays, the effective diffusion coefficient was found to increase slightly as the

air content increased. For conventional overlays, RCPT values increased as air content increased. Chloride contents were found to increase with age, regardless of the bridge deck type. Additionally, at similar ages, both silica fume and conventional overlay decks had similar chloride contents. At a depth of 75 mm (3 in.), these values exceeded the corrosion threshold of conventional steel in less than 500 days for samples taken directly on cracks. Most of the silica fume overlay and conventional overlay decks, however, were not in the same age ranges, limiting the ability to provide accurate comparisons.

Several conclusions were made with respect to cracking tendency. Silica fume overlay decks constructed in 1997 and 1998 were found to have lower crack densities than older silica fume overlay decks. Monolithic and conventional overlay decks built between 1989 and 1995, however, had higher crack densities than bridges of the same type constructed earlier. It was also found that conventional and silica fume overlay decks of approximately the same age had similar levels of cracking. Although the level of cracking in the newer silica fume overlay bridge decks decreased compared to the older silica fume overlays, they exhibited crack densities that were similar to conventional overlay bridge decks.

With respect to the causes of bridge deck cracking, several observations were made. Increases in slump, compressive strength, water content, cement content, and percent volume of water and cement in monolithic bridges and bridge subdecks correlated with increased deck cracking, regardless of the overlay type. Presumably, any cracks formed in the subdeck reflected through into the overlay. In addition to subdecks, conventional overlays placed with zero slump and silica fume overlays placed with slumps greater than 90 mm (3.5 in.) showed high crack densities. For monolithic decks, as the water-cement ratio increased, the crack density increased. This trend was not observed for deck overlays or subdecks. Finally, for monolithic

bridge decks, crack density was significantly lower for decks with over 6 percent entrained air than for decks with less air.

Several environmental conditions were associated with an increase in crack density. Although not all of the trends were found in all three bridge types, an increase in crack density was found to coincide with increases in the average air temperature, low air temperature, maximum air temperature, and daily air temperature range for the date of concrete placement. For silica fume overlays in particular, as the relative humidity increased, crack density decreased. In addition, silica fume overlays that were treated with a precure material and fogged during and after finishing exhibited less cracking.

Several design related factors were found to affect cracking. In general, Miller and Darwin concluded that crack density was not affected by bridge length, span length, span type (interior or exterior), bridge skew, or steel girder type. Crack density was, however, found to increase with increasing sizes of transverse reinforcement and bar spacing. As observed by Schmitt and Darwin (1995), the girder end condition was also found to have a significant effect on the crack density of the first and last 3 m (10 ft) of the bridge deck. Bridges constructed with fixed-ended girders had crack densities nearly three times higher than bridges built with pinned-ended girders. Finally, the pavement roughness indices for monolithic, conventional overlay, and silica fume overlay bridges were found to be nearly identical.

Based on the results of the study, Miller and Darwin made three primary recommendations with respect to the performance of Kansas bridge decks. First, the data obtained in the study indicated that silica fume overlays provide no advantage over conventional overlays in terms of crack density, effective diffusion coefficient, or chloride content, either on or off cracks. Miller and Darwin, however, recommended a reexamination of the silica fume overlay decks when they were in the

same age range as the conventional overlay decks. Second, a maximum cementitious material content and/or compressive strength should be added to the specifications for both subdecks and overlays. Third, fogging should be used immediately after finishing and the use of a precure material with fogging should be expanded to cover conventional overlays, monolithic decks, and bridge subdecks.

*Portland Cement Association 1970.* The Portland Cement Association (PCA) completed one of the earliest studies intended to both characterize and investigate the causes of bridge deck deterioration in 1970 (*Durability 1970*). The cooperative study began in 1961 with the goal of gaining a better understanding of both the causes of and remedies for concrete bridge deck deterioration. The study had four specific objectives: to determine the types and extent of durability problems, to determine the causes of different types of deterioration, to improve the durability of future bridge decks, and to develop methods to mitigate the deterioration of existing bridge decks. To meet these objectives, the study included a detailed investigation of 70 bridge decks in four states, random surveys of over 1000 bridge decks in eight states, and an analytical study of the vibration characteristics of 46 bridge decks.

The random surveys of over 1000 bridges built from 1940 to 1962 included a summary of the deterioration observed and the span in which the deterioration occurred. The primary purpose of the random surveys was to determine the types and extent of bridge deck deterioration. The types of deterioration recorded (on standard data sheets) included scaling, various types of cracking, rusting, surface spalls, joint spalls, and popouts. In addition to quantifying the types and relative levels of deterioration, the data also permitted general relationships and observations to be made as functions of deck age, bridge type, traffic volume, use of air-entrained concrete, etc.

The data from the random surveys indicated that the most severe instances of scaling occurred in decks cast with non-air-entrained concrete. Cracking occurred in

approximately two-thirds of the bridge decks, with transverse cracking being the most prevalent. Transverse cracking appeared to increase with age and span length and had a higher incidence for continuous spans and decks supported by steel girders.

The detailed investigations made on the 70 bridge decks from four states included sketches of the observed deterioration for each deck, the collection of concrete cores for laboratory study, and an examination of related construction and design documentation. The 70 bridges included in the investigation represented a wide range of ages, locations, structure types, and degrees of deterioration. The primary purpose of these detailed investigations was to determine the causes of bridge deck deterioration. Several types of bridge deck deterioration observed from both the detailed field investigations and the laboratory tests were categorized into three groups: scaling, cracking, and surface spalling.

As with the results from the random surveys, in the detailed investigations, scaling was found to be most severe on bridge decks cast with non-air-entrained concrete, although some isolated areas of scaling were found on air-entrained concrete decks. Based on laboratory measurements of the air content and air void distribution in these decks, scaling was found to be caused by localized deficiencies in the air content. In addition to deficiencies in air content, scaling was also found on some decks with a high water-cement ratio paste at the deck surface. Chloride tests performed on samples of air-entrained concrete showed no correlation with scaling.

Cracking was categorized by orientation (described in Section 1.2), with transverse cracking occurring most frequently. The laboratory analysis of cores taken from cracked sections indicated that transverse cracks typically occurred directly above the reinforcing steel. Steel girder bridges had transverse cracks at regularly spaced intervals over the entire length of the deck and, in some instances, had closely spaced transverse cracks in negative moment regions that typically occurred over the top reinforcement. Transverse cracking for decks on steel girders was found to be the

result of many factors, the most important of which were thought to be the restraint provided by the girders on the slab and the local tensile stress concentration caused by subsiding plastic concrete around the top transverse reinforcement. In a similar manner, longitudinal cracks were typically caused by top longitudinal reinforcement or void tubes in hollow-slab bridges.

Diagonal cracking was typically found at the corners of skewed bridges and was considered to be the result of structural deformations caused by loading. Pattern cracking was generally found to be shallow and most likely caused by drying shrinkage. Finally, random cracking, although not the source of major deck deterioration, was found on most bridge decks. The report identified a number of likely factors for random cracking, the most significant of which were wheel loads, shrinkage, temperature stresses, reactive aggregates, and small imperfections in the concrete.

Surface spalls were often observed on decks with inadequate cover and were found to be caused most often by the increase in volume of the reinforcing steel caused by corrosion. In addition to the corrosion products, another factor suggested by the PCA was the pressure generated by freezing liquids in cracks around reinforcing bars.

The final phase of the study included the calculation of the vibrational characteristics for each bridge. The theoretical vibrational characteristics of 46 out of the 70 bridges included in the detailed investigation were calculated using empirical equations developed by Nieto-Ramirez and Veletsos (1966) that compared very well to the actual measured values. The fundamental natural frequency, speed parameter, and impact value were calculated for each bridge and compared with the level of deck deterioration and structure type. The speed parameter quantifies the dynamic response of a bridge as a function of vehicle velocities. The impact value, or dynamic increment of moment, describes the bridge oscillation caused by a smoothly rolling

vehicle. Based on these calculations, it was concluded that the vibration characteristics of the bridge superstructure was not a primary factor contributing to the deterioration of concrete bridge decks. Because the bridges included in this part of the study were built between 1940 and 1960, the designs were relatively conservative, in terms of strength and stiffness, when compared with designs after 1960. It was noted that the added flexibility in bridges built after 1960 could prove to be detrimental to bridge deck durability.

Based primarily on the results of the detailed investigation, the Portland Cement Association made several recommendations with regard to concrete mix design, bridge design, and construction practices. To limit the amount of shrinkage that occurred in the deck, the largest maximum size aggregate should be used to minimize the concrete's paste content. The recommended slump should be between 50 and 75 mm (2 and 3 in.) to reduce the effects of excess bleeding, drying shrinkage, and cracking noted in the detailed investigation. The concrete cover should be at least 50 mm (2 in.) over the top reinforcement in areas where deicers are used and at least 38 mm (1.5 in.) in all other areas. In addition to the cover requirements, the report recommended that adequate deck drainage be emphasized during the design phase to reduce surface scaling in gutter areas. Lastly, during deck construction, cover should be checked to ensure that the design specifications are being met.

*Dakhil, Cady, and Carrier 1975.* Because of the concern that cracks directly over the top reinforcement lead to corrosion and subsequent spalling, Dakhil, Cady, and Carrier (1975) set out to quantify the effects of three variables on the tendency to produce subsidence (settlement) cracking in fresh concrete. The three variables examined in the study were depth of cover, concrete slump, and reinforcing bar size. In addition to the examination of these three variables, a photoelastic study to ascertain the magnitudes of tensile stresses above the reinforcement, and a corrosion study to verify the effects of cracks on corrosion activity were performed.

To determine the relative importance of these variables, a complete test matrix was designed with four depths of cover [19 mm (0.75 in.), 25 mm (1 in.), 38 mm (1.5 in.), and 51 mm (2 in.)], three slumps [51 mm (2 in.), 76 mm (3 in.), and 102 mm (4 in.)], and three reinforcing bar sizes [No. 13 (No. 4), No. 16 (No. 5), No. 19 (No. 6)]. A total of 108 specimens were examined 4 hours after each placement for any signs of cracking that were apparent to the unaided eye. The data indicated that both the occurrence and the severity of cracking decreased with increasing covers, lower slumps, and smaller bar sizes. Depth of cover was found to be the most important factor affecting cracking, with no cracks developing with 51 mm (2 in.) cover except in combination with the highest slump and the two largest bar sizes. Based on the results of the cracking data, the following regression equation was developed to predict the probability of subsidence cracking based on the bar cover, bar size, and concrete slump:

$$p = \frac{1.5e^y - 0.5}{1 + e^y} \quad (1.3)$$

where

$$y = 1.37 - 0.58x_1 - 0.56x_2 + 0.27x_3 \quad (1.4)$$

$p$  = probability of a crack to occur

$x_1$  = concrete cover, in.

$x_2$  = concrete cover divided by nominal bar size

$x_3$  = concrete slump, in.

Limitations of this study, as they pertain to subsidence cracking, include the absence of admixtures and only monitoring plastic concrete for cracking. Although subsidence cracking in plastic concrete occurs regularly, the PCA study (*Durability* 1970) indicated that 46 out of 60 cores taken on cracks over reinforcement had cracks

intersecting aggregate. This indicated that the cracks most likely occurred after the concrete had hardened.

In the photoelastic portion of the study, concrete cover, modeled using a photoelastic gelatin, was the only variable examined. The cover ranged from 19 mm ( $\frac{3}{4}$  in.) to 51 mm (2 in.) over a single No. 16 (No. 5) reinforcing bar. The gelatin models revealed that the maximum tensile stress was located directly over the reinforcement and increased four fold (from 0.3 to 1.2 psi in the model) as the cover decreased from 51 to 19 mm (2 to  $\frac{3}{4}$  in.).

The corrosion study examined 18 specimens (13 cracked and 5 uncracked) that contained No. 16 (No. 5) bars with 19 mm ( $\frac{3}{4}$  in.) or 38 mm (1.5 in.) cover. The specimens were exposed to salt solutions, and the corrosion potential of the reinforcing steel was measured to determine corrosion activity. All of the cracked specimens showed more negative corrosion potentials than the uncracked specimens, corresponding to higher corrosion activity of the embedded bars. This portion of the study helped to validate the research and quantify the importance of maintaining uncracked concrete.

*Poppe 1981.* In an effort to determine the factors that affect the durability of concrete bridge decks, Poppe (1981) examined the effect of variables involving design, construction, and material properties that were thought to influence durability (specifically deck cracking). Bridges were constructed during the study to determine the effect of each variable. Individual parameters were varied between bridges and placements and compared with control bridge decks and placements.

The bridge decks and placements were compared using a cracking index calculated from the crack surveys. Crack surveys were performed by first dividing the bridge into a grid delineated using the girder lines and 3 m (10 ft) longitudinal stations. Within each section of the grid, cracks were marked and sized according to their width. The cracking index was calculated by dividing the total number of cracks

by the total number of grids. In addition to counting the cracks, wider cracks were given more weight, under the assumption that wide cracks are more harmful. The resulting weighted average was used to compare control bridge decks with modified bridge decks.

Based on the data obtained in this study, several conclusions were made. Increasing the thickness of concrete bridge decks above the common thickness (in California at the time of the study) of 159 mm (6.25 in.) resulted in reduced cracking. Reinforcing steel placement and formwork had little effect on deck cracking. Unfavorable weather conditions, including wind, heat, and low humidity had the biggest effect on deck cracking out of all of the construction practices considered. During the curing process, the use of membrane curing compounds was recommended when wind or low humidity was encountered during placement. None of the other placing and finishing variables studied had a significant effect on deck cracking. Under favorable environmental conditions, the use of shrinkage compensating cement reduced deck cracking by about 25 percent when compared to bridge decks built with Type II cement. Finally, the use of differing amounts of entrained air appeared to have no effect on deck cracking.

*North Carolina State 1985.* In 1985, investigators at North Carolina State completed a two volume study examining the effects of construction, material related, and structural parameters on transverse cracking of bridge decks (Cheng and Johnston 1985, Perfetti, Johnston, and Bingham 1985). A total of 72 bridges constructed between 1972 and 1981 were evaluated in the study. Of the 72 bridges, 52 had steel girders and 20 had prestressed concrete girders; 35 had simple spans, while 37 had both continuous and simple spans or continuous spans only.

In the first volume of the study (Cheng and Johnston 1985), data obtained from plans, construction diaries, and weather and test records were compared with transverse cracking observed in field surveys. The second volume of the study

(Perfetti, Johnston, and Bingham 1985) sought to relate the field survey results with the superstructure type, deck casting sequence, and vibrational characteristics of the superstructure. During the field surveys, the number of major and minor transverse cracks were recorded and used to quantify the number of cracks per linear foot of bridge deck (CLF) using the following expression:

$$\text{CLF} = [\text{MACR} + (\text{MICR} / 4)] / \text{LENGTH} \quad (1.5)$$

where

- MACR = the number of Major Transverse Cracks, defined as cracks that could be followed completely across the bridge deck, or cracks that extended from one edge of the deck to the roadway centerline
- MICR = the number of Minor Transverse Cracks, defined as shorter transverse cracks that typically occurred close to the edge of the deck, at parapet joints, or at intersecting vertical drain pipes
- LENGTH = appropriate span or bridge length inspected

The field surveys showed that, as observed in the PCA study (*Durability* 1970), transverse cracks occurred most often above the top reinforcing bars. The surveys also indicated, again corroborating with the PCA study, that transverse cracking was more severe on continuous spans than on simple spans and on steel girder bridges than on prestressed concrete girder bridges. The average crack spacings, organized by the span/girder type, were:

Continuous Steel	3.0 m (10 ft)
Continuous Prestressed	4.3 m (14 ft)
Simple Steel	27.4 m (90 ft)

Simple Prestressed

129.2 m (424 ft)

Based on the results of the field surveys, several conclusions were drawn in the first volume of the study. Conditions during placement in which the relative humidity was less than 60 percent and the ambient air temperature was below 7° C (45° F) were found to increase the incidence of transverse cracking. The researchers suggested that low ambient temperatures may aggravate surface evaporation rates, and low temperatures may increase the effects of thermal shrinkage due to a large temperature difference between the cool girders and warm concrete. In addition, concrete bridge decks cast with 7.5 percent air showed lower amounts of transverse cracking than decks with lower quantities of entrained air. Other than air content, however, no clear relationships were found between transverse cracking and mix design parameters. Alternating casting sequences for continuous girder bridges to reduce flexural tension by placing the positive moment regions followed by the negative moment regions were recommended. For steel girder bridges, as the girder yield strength increased, the incidence of transverse cracking increased. Bridge decks placed with slumps below 75 mm (3 in.) with concrete strengths at the extremes of the strength range [24-52 MPa (3500-7500 psi)] had a slight tendency towards increased cracking.

The second volume of the study was designed to compare observed transverse cracking with calculated vibration characteristics and to model and calculate deck stresses induced by different deck casting sequences. Comparisons were made using a theoretical vibration analysis and finite element models of the deck casting sequence. The vibration analysis was performed using the same equations used in the PCA study (*Durability* 1970). Like the 1970 PCA study, Perfetti et al. (1985) concluded that there were no consistent relationships between the incidence of cracking and the calculated vibration characteristics of the bridges examined. Finite element analysis

was used to evaluate bridge decks under dead and live loads both during and after construction. No correlation was found between transverse cracking and the residual maximum dead load stresses in the deck induced during the casting sequence alone; a relationship was found to exist, however, between the total tensile stresses in the deck developed by the dead load stresses in addition to the live load stress envelopes. The cracking stress threshold was found to be approximately 1.7 MPa (250 psi). Stresses above this level, which are due to the combined effects of dead and live loads plus the effects of other environmental and material properties, appear to cause increased cracking. Alternating casting sequences that help lower the total tensile stresses in the deck by placing positive moment regions followed by negative moment regions were recommended.

Based on both the theoretical vibration analysis and the finite element model, three primary observations were made with respect to structural considerations. First, based on the field surveys, bridges with simple spans and prestressed concrete girders will exhibit the least amount of transverse cracking. Second, based on the finite element analysis, the maximum concrete tensile stress induced by dead load plus live load should be limited to 1.7 MPa (250 psi). Finally, alternating placement sequences, as opposed to continuous placing sequences, were recommended to minimize dead loads and help limit the total tensile stresses in the deck.

*Babaei and Purvis 1996.* In a 1996 study by Babaei and Purvis for the Pennsylvania Department of Transportation (PennDOT), the causes and methods to mitigate premature cracking were investigated. The project was completed in three phases. The first phase included a “walk-by” survey of 111 Pennsylvania bridge decks and an in-depth study of 12 decks with the goal of determining the types, significance, and causes of premature cracking in bridge decks. The second phase consisted of field tests and the observation of eight bridge deck construction projects with the intent of identifying any construction or design procedures that may lead to

cracking. The third phase consisted of laboratory work to substantiate the findings from the first two phases. In addition to the three primary phases, two supplementary research studies were completed to test Type K cement and the effectiveness of an “inverted bar” detail, which places the longitudinal reinforcement above the transverse reinforcement, in reducing crack widths.

Of the 111 bridges surveyed, 51 were prestressed concrete girder bridges, 41 were prestressed concrete spread box-beam bridges, and 19 were steel girder bridges, all built within 5 years of the study. The surveys indicated that transverse cracking occurred more frequently than other types of cracking and occurred in both positive and negative moment regions. Simply supported bridges were found to perform better than continuous span bridges, presumably because of the negative moments present in continuous bridges. The in-depth surveys of 12 simply supported bridges included crack mapping, crack width measurements, top reinforcement cover and location measurements, and concrete coring.

Based on the data obtained from the in-depth surveys and comparisons with design and construction records, Babaei and Purvis observed that most of the transverse cracks were directly above the top transverse reinforcing bars and extended down at least to the level of the bars. In addition, based on concrete cores, the transverse cracks typically intersected the coarse aggregate particles, indicating that the cracks formed after the concrete had hardened. Thermal shrinkage and drying shrinkage were thought to largely control cracking in these decks.

Phase two of the study included field tests, and the observation of eight bridge decks under construction. During the construction of the eight bridge decks, concrete temperature was recorded throughout the curing process and concrete samples were taken to determine thermal and drying shrinkage, respectively. Based on observations of construction procedures, two practices were identified for their

potential to cause cracking: delaying curing the concrete in hot weather and adjusting the water content of the mix after the truck had left the ready-mix plant.

Temperature measurements were taken at the construction site to estimate the amount of thermal shrinkage. Field samples were tested in the laboratory to measure the amount of drying shrinkage. Thermal shrinkage was estimated using the maximum difference between the concrete temperature during a period up to 8.5 hours after casting and the ambient air temperature. The ambient temperature was assumed to be the temperature of the underlying girders since no artificial heating was employed during the construction of the decks. The difference between the maximum concrete temperature and the corresponding ambient air temperature was assumed to contribute to thermal shrinkage at a rate of 9.9 microstrain per degree C (5.5 microstrain per degree F). Deck drying shrinkage was estimated from free-shrinkage specimens cured for 7 days, the same as the bridge decks, and measured for up to 112 days after casting. The drying shrinkage measured from the  $76 \times 76 \times 254$  mm ( $3 \times 3 \times 10$  in.) free-shrinkage specimens was divided by 2.5 to account for the lower volume-to-surface ratio of the specimen compared to the deck. Thermal stresses ranged from 0 to 170 microstrain and drying shrinkage ranged from 192 to 580 microstrain.

Based on analytical work, the authors found that a thermal shrinkage of 228 microstrain may initiate cracking in only a few days. Unlike thermal shrinkage, drying shrinkage occurs over a much longer period of time, allowing concrete creep properties to help diminish cracking. The cracking threshold, based on the sum of thermal and drying shrinkage, was found to be 400 microstrain. Average crack spacings were calculated for each bridge deck based on the total long-term shrinkage displacement of the deck and an average crack width of 0.25 mm (0.01 in.). The results of the shrinkage study correlated very well with the observations in the field. The only four bridges that showed cracking were also predicted to crack from the

thermal and drying shrinkage results. The authors concluded that, to limit the average crack spacing to a minimum of 9 m (30 ft), two conditions had to be met: the 28-day drying shrinkage must be limited to 400 microstrain (corresponding to a long-term shrinkage of 700 microstrain), and the maximum temperature differential between the concrete and the girders must be limited to 12° C (22° F), corresponding to a thermal shrinkage of 121 microstrain, “for at least 24 hours after placement.”

The final phase of the study examined the effects of aggregate type, cement source, and fly ash on shrinkage. In total, thirty 76 × 76 × 254 mm (3 × 3 × 10 in.) free-shrinkage specimens were produced, with three specimens for each concrete mix tested. The study indicated that “soft” aggregates, typically with high absorption and a low specific gravity, undergo higher amounts of drying shrinkage than “hard.” They proposed limiting fine aggregate absorption to a maximum of 1.5 percent and coarse aggregate absorption to a maximum of 0.5 percent.

The investigation of the effect of cement source was conducted for three Type I cements supplied by different sources, and one Type II cement. The study showed that drying shrinkage can vary significantly (as much as 108 percent) depending on the cement supplier. Fly ash was found to increase the drying shrinkage when used as a partial replacement for cement, although it was noted that very few specimens were used and that the fly ash results should not yet be generalized.

In addition to the three primary phases of the study, two additional supplemental research projects were completed. The use of Type K cement in bridge decks and placing the longitudinal reinforcing steel above the transverse reinforcement (“inverted bar” detail) were examined as possible methods to reduce deck cracking. Several problems were encountered in the five bridge deck placements with Type K cement. Two of the bridges developed extensive cracking. They contained a “soft” coarse aggregate (sandstone) and did not provide useful information with regard to Type K cement. Based on a limited number of restrained

shrinkage tests (ASTM C 878) performed in conjunction with these five bridge deck placements, the researchers recommended 200 microstrain as the maximum allowable 28-day restrained shrinkage. The “inverted bar” detail was used on two bridge decks; it was found to have no effect on the number of cracks and did not control crack widths. The researchers concluded that the potential benefits of the “inverted bar” detail were overshadowed by the large bar cover depths. The cover depths were 70 and 76 mm (2.75 and 3.00 in.) and, although the longitudinal bar was closer to the surface with the “inverted bar” detail, the bars were embedded too deep in the concrete for the benefits to be observed.

*Krauss and Rogalla 1996.* In 1996, Krauss and Rogalla completed a multipart study to determine the major factors that contribute to early transverse cracking of bridge decks. The extensive study included a literature review, a survey of multiple transportation agencies, laboratory testing, bridge deck instrumentation, and an analytical study of the stresses resulting from different combinations of variables thought to influence bridge deck cracking. The primary focus of the project was to identify and rank, in order of importance, the factors thought to contribute to cracking from variables in three categories: bridge design, materials, and construction procedures. The results of their study are presented in Table 1.2 and described below.

The survey was intended to get a more comprehensive understanding of current design practices and construction techniques and their perceived contribution to cracking. Fifty-two transportation agencies responded to the survey. Of the 52 respondents, 62 percent believed early transverse cracking to be a significant problem. Even the agencies that did not believe early transverse cracking to be a problem reported extensive cracking. Although the results varied, the primary construction factors thought to contribute to cracking were improper curing, thermal effects, wind, and air temperature. The bridge deck concrete mix design and resulting concrete shrinkage were thought to be the primary material-related factors, while

bridge deck deflections were thought to be the primary design-related factors leading to increased cracking.

The field study involved the instrumentation of the Portland-Columbia Bridge between Pennsylvania and New Jersey. A system was installed to monitor the strains and temperatures of the girders and deck, beginning during the deck replacement and continuing for several months. Although the results obtained from this specific bridge could not be generalized to include all bridges, the results were helpful in confirming the theoretical analysis and providing a general understanding of early transverse cracking.

A series of equations were derived in the analytical study to calculate the stresses developed in a composite reinforced bridge deck subjected to temperature and shrinkage conditions. The stresses measured in the Portland-Columbia Bridge were very similar to the stresses predicted from the derived equations. Shrinkage and thermal stresses were calculated for more than 18,000 additional combinations of bridge geometry and material properties. Shrinkage stresses were found to be affected primarily by material properties rather than design parameters. Some of the design factors found to increase shrinkage stresses were girder depth, deck thickness, and narrower girder spacings. In addition, steel studs or channels and stay-in-place steel forms were found to increase deck stresses. In particular, stay-in-place forms were found to create non-uniform shrinkage that has the tendency to produce large tensile stresses at the deck surface.

Laboratory testing included the development of a restrained ring test to measure cracking tendency of different deck mixes. In addition, free-shrinkage specimens and strength cylinders were made to help relate cracking tendency with shrinkage, strength, modulus of elasticity, and creep characteristics. Thirty-nine concrete mixtures were investigated using the restrained ring test. The effects of water-cement ratio, cement content, aggregate size and type, high-range water

reducers, silica fume, set accelerators and retarders, air entrainment, freeze-thaw cycles, evaporation rate, curing, and shrinkage-compensating cement were examined and ranked by importance.

Based on the laboratory study, several trends with respect to cracking tendency were observed. Cracking tendency was found to increase with increasing cement content and decreasing water-cement ratios. Free shrinkage but not necessarily cracking tendency, was found to be directly proportional to the concrete paste content. Cracking tendency generally decreased the most with a low cement content mix. Typically slump was not found to influence cracking in the restrained shrinkage test; however, the researchers recommended a slump of at least 75 mm (3 in.) to avoid problems with consolidation. Silica fume was found to increase cracking tendency, while the addition of a high-range water reducer and type F fly ash was found to slightly decrease the cracking tendency. Set accelerators were found to have a minimal effect on cracking tendency, and the addition of set retarders produced mixed results. The researchers cautioned that concrete mixtures with retarders require attentive curing to avoid plastic shrinkage cracking. The use of air entraining agents was not found to have an effect on cracking tendency. Both the diffusion properties and Poisson's Ratio were found to only have a minor effect on cracking. Above all else, Krauss and Rogalla found that aggregate type had the most significant material-related effect on cracking. Restrained ring specimens with hard trap rock aggregate cracked relatively late, as did other angular aggregates when compared with round aggregates. Aggregate shrinkage characteristics were also found to be an important factor affecting cracking tendency. The researchers recommended that aggregates should be selected based on the results of the restrained ring test.

Several recommendations were made with respect to material and environmental aspects to minimize thermal stresses. Effort should be made to

minimize paste contents and cements with a high heat of hydration. Lower cement contents should be specified in addition to 28-day compressive strengths between 21 and 28 MPa (3000 and 4000 psi). Krauss and Rogalla suggest a maximum cement content  $306 \text{ kg/m}^3$  ( $517 \text{ lb/yd}^3$ ) used in conjunction with a 38 mm (1.5 in.) maximum size aggregate. In addition, they suggested that bridge deck concrete should be specified based on 56 or 90 day compressive strength to encourage lower heat of hydration concrete mixes. High water contents, although they result in higher paste contents, were not found to increase cracking tendency. [This is in contrast to the field observations of Babaei and Purvis (1996).] Krauss and Rogalla suggest that the increased water content may result in increased creep and consequently decreased cracking tendency. Both the creep characteristics and the modulus of elasticity of the concrete were found to have a major effect on bridge deck cracking. In an effort to reduce concrete temperatures and solar radiation effects, concrete should be cast in the late afternoon or evening, and cast with a temperature below  $27^\circ \text{ C}$  ( $80^\circ \text{ F}$ ). The coefficient of thermal expansion, although limited in range, was found to have a moderate effect on cracking. Krauss and Rogalla (1996) found that the time of casting and weather conditions can have a major effect on bridge deck cracking.

Based on the results of the literature review, field instrumentation, theoretical analysis, and laboratory study, several additional recommendations were made. Based on both the literature review and the transportation agency surveys, cracking was found to be most prevalent on continuous steel girder bridges. Thinner decks were found to have higher stresses and should be at least 200 to 230 mm (8 to 9 in.) thick; the analysis also showed, however, that both the span and girder size could complicate the relationship between deck thickness and cracking. In addition, the use of epoxy-coated bars was found to likely increase the number and width of deck cracks, although Krauss and Rogalla recommended that bridges subjected to deicing chemicals should contain some type of corrosion-resistant reinforcement. A

minimum cover of 50 mm (2 in.) should be used to avoid the likelihood of settlement cracking; furthermore, the top and bottom bars should be offset to avoid the likelihood of full depth cracking. Traffic-induced vibrations were found not to effect deck cracking. In fact, reducing the deck flexibility (and increasing the likelihood of traffic-induced vibrations) was found to decrease early transverse cracking. The transportation agency survey gave mixed results with respect to the effect of traffic volume on cracking although Krauss and Rogalla (1996) found no correlation. Additional design-related factors including quantity of reinforcement in the deck, reinforcing bar size, stud spacing, and skew were found to only have a minor effect on bridge deck cracking.

Inadequate curing was the most common construction related concern with respect to early transverse cracking expressed by transportation agencies, and this concern was verified in the laboratory portion of the study. Decks should be cast with the aforementioned temperature condition with windbreaks and immediate water fogging when the evaporation rate exceeds  $1.0 \text{ kg/m}^2/\text{hr}$  ( $0.2 \text{ lb/ft}^2/\text{hr}$ ). Misting or the use of a monomolecular film immediately after screeding, applying two coats of a curing compound before the concrete surface dries, moist curing with wet burlap for at least 7 days, using a curing membrane following the wet cure, and grooving the deck after the curing period with a diamond saw to avoid delays caused by tining the fresh concrete should be required. Construction-induced stresses were typically found to be below the amount required to create deck cracking. Alternate placing sequences as opposed to continuous placing sequences were found to reduce negative bending stresses in continuous bridges; negative bending stresses, however, were found to only have a minor effect on bridge deck cracking. The type and number of reinforcement ties, construction loads, and the number of revolutions in the concrete truck prior to placement were found to have no effect on bridge deck cracking.

*University of Minnesota 1998.* Researchers at the University of Minnesota completed a two-phase study on transverse cracking in bridge decks (Eppers, French, and Hajjar 1998, Le, French, and Hajjar 1998). The first phase consisted of field observations and a review of documentation for 72 bridge decks in Minnesota. The bridges included 34 simply supported prestressed girder bridges, 34 continuous steel plate-girder bridges, and 4 continuous steel, wide-flange girder bridges. The results of the field investigation were compared with design, material, and construction data. The second phase of the study consisted of both a shrinkage study and a parametric study. For the shrinkage study, two concrete bridge deck mixes were tested under field conditions and their free-shrinkage characteristics were measured with respect to time. The parametric study consisted of a nonlinear finite element analysis of different bridge decks using the shrinkage characteristics obtained from the shrinkage study. The goal of the parametric study was to isolate the influence of individual parameters on transverse cracking, a task that was difficult to perform in the field study.

The field investigation of the 72 bridges included crack surveys and the assignment of bridge-deck-condition ratings. The rating scale ranged from 9, for areas with no cracks, to 5, for areas with a high crack density and large crack widths. Based on these ratings, the dominant design factors found to influence deck cracking were the girder type, end support condition, depth, and spacing, the deck thickness, and the top transverse bar size. In addition, continuous steel girder bridges showed increased amounts of cracking when compared with simply supported prestressed girder bridges. Based on the survey results, several recommendations were made with respect to bridge design, with the goal of reducing longitudinal restraint, believed to be the primary cause of tensile deck stresses. These included reducing deck continuity over interior supports by using expansion joints, using larger girder spacings, and using fewer and smaller shear studs. In addition, for steel girder

bridges, it was found that the use of No. 16 (No. 5) bars resulted in less cracking than No. 19 (No. 6) bars. Bar size was not found to be a significant factor for prestressed girder bridges.

In addition to bridge design related recommendations, several concrete mix design and construction related recommendations were made. These recommendations were based on the comparison of field survey results with mix proportions and concrete properties for 21 bridges. First, Eppers et al. (1998) recommended a maximum cement content between 386 and 392 kg/m<sup>3</sup> (650 and 660 lb/yd<sup>3</sup>), in conjunction with a low water-cement ratio. Coarse and fine aggregate contents should be maximized to reduce the volume of paste. Bridge deck concrete mixes that performed well contained between 1068 and 1098 kg/m<sup>3</sup> (1800 and 1850 lb/yd<sup>3</sup>) of coarse aggregate and approximately 712 kg/m<sup>3</sup> (1200 lb/yd<sup>3</sup>) of fine aggregate. Finally, the minimum air content for bridge deck mixes should be between 5.5 and 6.0 percent.

In an effort to reduce the peak hydration temperature and the temperature differential between the ambient air temperature and core concrete temperature, several other recommendations were made. These recommendations were based on the field investigation and rating of 18 decks supported by prestressed and steel girders. Concrete decks should only be placed when the low ambient air temperature is above 4 to 7° C (40 to 45° F), and the maximum temperature is below 29 to 32° C (85 to 90° F). In addition, the daily temperature range should be less than 28° C (50° F). The best results were found to occur when the high ambient air temperature was between 18 to 21° C (65 and 70° F), and the low ambient air temperature was between approximately 7 to 10° C (45 and 50° F).

To overcome some of the limitations of the field study, namely, the inability to isolate individual parameters and determine their effect on bridge deck cracking, a nonlinear finite element analysis was performed. A shrinkage study performed using

the current Minnesota Department of Transportation (MnDOT) concrete deck mix (at the time of the report) and a previous MnDOT mix was performed to gain information about the shrinkage characteristics with respect to time. The results of the shrinkage study, combined with the ACI 209 recommended shrinkage curve, were then used in a finite element model to more accurately represent the shrinkage characteristics of bridge decks. The ACI 209 shrinkage curve model is a standard equation used to predict concrete shrinkage strain over time. Curing time, relative humidity, member thickness, slump, fine aggregate content, cement content, and air content are used in the model. Two bridges, a simply supported prestressed concrete bridge and a two-span continuous steel girder bridge, were selected for the parametric study from the 72 bridges investigated in the field study as the base cases for the parametric study. In the analysis, individual parameters, such as construction timelines, shrinkage properties, end conditions, deck modulus, and temperature differentials, were changed to determine their effects on transverse cracking.

The analysis showed that over a period of 10,000 days, a prestressed girder bridge with a typical construction timeline, including strand tensioning, girder casting, strand release, and deck casting, showed no signs of transverse cracking. The researchers concluded that this was due to the lack of restraint offered by the simple supports and the tendency of the concrete girders to shrink with the deck. In addition to new bridge construction, a redecking scenario was also modeled with an initial girder age of 20 years. In this situation, the model showed deck cracking, presumably due to the additional restraint provided by girders that had already undergone shrinkage. In all situations, the results obtained in the parametric study generally agreed with behavior observed in the field. To further corroborate the results of the parametric study with a continuous steel girder bridge with three or more spans, a third bridge was also investigated. Again, the results of the parametric study corroborated observations from the field investigation

Based on the results of the parametric study, the primary cause of deck cracking was found to be the differential shrinkage between the concrete deck and supporting girders. The deck modulus was found to have an impact on deck cracking. As the modulus decreased, the tensile stress in the deck dropped and the girder was able to shrink more before cracking occurred. The initial shrinkage rate, rather than the ultimate shrinkage, was found to have the most significant effect on transverse deck cracking. It was concluded that creep probably offset the tensile stresses at later ages. The degree to which the end conditions were restrained was also found to have a significant effect on transverse cracking: although girder stiffness, cross-frames, and splice locations dictated crack locations, the fixed-fixed end restraint case resulted in the most severe cases of transverse cracking.

*Whiting and Detwiler 1998.* In a study completed in 1998, Whiting and Detwiler examined the use of silica fume in concrete bridge decks. The study had several objectives, ranging from evaluating the cracking tendency of silica fume concrete to determining the bond properties of silica fume overlay concrete. Two primary mixes were developed: an “overlay” mix and a “full-depth” mix. Concrete mixes for each of these applications were made with a number of silica fume contents and water-cementitious ratios. Both the full-depth and the overlay mixes were tested for their ability to resist chloride ingress, to determine the amount of drying shrinkage, and to determine the optimum mix design parameters for silica fume concrete.

The cracking tendency and drying shrinkage portion of the study evaluated full-depth mixes with a cementitious material content of approximately  $370 \text{ kg/m}^3$  ( $620 \text{ lb/yd}^3$ ) and overlay mixes with a cementitious material content of approximately  $415 \text{ kg/m}^3$  ( $700 \text{ lb/yd}^3$ ). The water-cementitious material ratio (w/cm) varied from 0.35 to 0.45 for full-depth mixes and from 0.30 to 0.40 for overlay mixes. The silica fume content was varied from 0 to 12 percent by mass of total cementitious material

content. The slump for both mixtures was greater than 75 mm (3 in.), obtained through the use of a high-range water reducer, and the air contents of full-depth and overlay mixes were  $6 \pm 1.5$  and  $7.5 \pm 1.5$  percent, respectively. Unrestrained drying shrinkage specimens measured  $75 \times 75 \times 254$  mm ( $3 \times 3 \times 10$  in.); restrained ring test specimens, developed by Krauss and Rogalla (1996), measured 150 mm (5.9 in.) high and 75 mm (3 in.) thick and were cast around a 19 mm (0.75 in.) thick steel ring with an outside diameter of 300 mm (11.8 in.). Before testing began, the specimens made from the full-depth mix and the specimens made with the overlay mix were cured for 7 and 3 days, respectively. These curing times were selected to simulate typical best practices for full-depth decks and deck overlays.

The drying shrinkage results, measured over a period of 64 weeks, indicated that both the overlay and full-depth mixes with lower water-cementitious material ratios had the least amount of shrinkage. Drying shrinkage for the overlay mixes was generally larger, even with the lower water-cementitious material ratios, presumably due to higher paste contents and shorter moist curing periods. As the silica fume content was increased from 0 to 12 percent, less of an increase in the w/cm ratio was required to increase total shrinkage. For a fixed w/cm ratio, the researchers found that the total shrinkage increased with increases in silica fume content primarily at the extremes of the w/cm ratio range (0.35 and 0.45 for full-depth mixes and 0.30 and 0.40 for overlay mixes). Mixes with w/cm ratios near the median (0.40 for full-depth mixes and 0.35 for overlay mixes) exhibited virtually no change in long-term drying shrinkage as the silica fume content increased, even to 12 percent. The tests indicated that at early ages (four days), the rate of shrinkage increased significantly as silica fume contents increased for all water-cementitious material ratios.

The results of the cracking tendency tests, reported in terms of time-to-cracking, revealed that cracking tendency was highly sensitive to the length of the curing period. Curing periods of 1 and 7 days were used on the full-depth mixes to

determine the effect of curing on cracking tendency. An increased quantity of silica fume was found to increase cracking when the concrete was cured for only 1 day, while, that same amount of silica fume had little effect on cracking when the concrete was moist cured for 7 days. Additionally, the mixes that contained higher cementitious material contents were also found to have an increased tendency to crack, although the effects were not as great as decreasing the length of curing from 7 to 1 day.

The ability of silica fume concrete to delay chloride ingress was also tested with the primary objective of determining an optimum silica fume content and w/cm ratio. The specimens were prepared and tested in general accordance with AASHTO T 259. The curing period was reduced from 14 days to 7 days for full-depth mixes and to 3 days for overlay mixes, a more precise sampling technique was used, and the ponding period was extended to 180 days. Following ponding, 1 mm (0.04 in.) layers of concrete were milled from a 100 mm (4 in.) diameter core and tested for chloride content. The apparent diffusion coefficient was calculated by fitting the observed chloride profile with Fick's Second Law of Diffusion using a least-squares technique. Results of the study indicated that the optimum silica fume content was approximately 6 percent. Little additional benefit was obtained by increasing the silica fume content above 6 percent. Although decreasing the w/cm ratio improved diffusion properties, the benefits became less significant as silica fume contents were increased, especially to 6 percent.

In addition to the shrinkage, permeability, and cracking properties of the mixes, the compressive strength, modulus of elasticity, overlay bond properties, and thermal expansion properties were tested. The compressive strength increased by as much as 10 MPa (1450 psi) when silica fume was increased from 0 to 6 percent by mass; additional increases in silica fume content did not appear to effect strength. Although silica fume increased strength, the mixes with the lowest w/cm ratios

consistently produced the highest strengths. The modulus of elasticity, measured in compression tests at 28 and 90 days, was also found to increase as the silica fume content increased. The researchers concluded that the increases in elastic modulus and compressive strength observed for the silica fume concretes most likely does not result in increased cracking. This assertion was later verified by the cracking tendency tests. This observation disagrees with findings by Krauss and Rogalla (1996).

The bond strength of silica fume overlays to the subdeck was tested using the procedures outlined in ACI 503R-93. The specimens were mixed and cast at 35° C (95° F) to simulate field conditions that have been known to cause problems with overlay placements. The results indicated that bond strength only slightly increased with silica fume contents over 6 percent by mass; these differences, however, were statistically insignificant. The bond strength was not improved for overlays containing less than 6 percent silica fume by mass. Because of concern that thermal shrinkage could be aggravated by silica fume in concretes, the coefficient of thermal expansion was determined for various full-depth and overlay mixes. The results indicated very little difference in thermal expansion for full-depth mixes, regardless of the silica fume content, and a slight decrease for overlay mixes with increasing silica fume contents, but the coefficients were still within the typical range of conventional concretes.

Based on all aspects of the study, two primary recommendations were made. The discussion of the results indicated that 6 percent was the optimum percentage of silica fume, although the researchers recommended a silica fume content between 6 and 8 percent by mass of cementitious material. Additional silica fume did not provide significant added reinforcing steel protection given the high cost. The researchers also recommended a moist curing period of at least seven days.

### **1.8.2 Primary Factors Affecting Cracking**

Although bridge deck cracking is clearly the result of a complex combination of variables, several factors are thought to be more significant than others. Based on the reports reviewed in Section 1.8.1, the primary factors thought to contribute to bridge deck cracking are summarized in Table 1.3. This table only includes factors that were found to significantly affect bridge deck cracking.

## **1.9 OBJECT AND SCOPE**

Since the publication of the PCA report (*Durability* 1970), many analytical and field studies have been conducted, with varying results, to determine the primary factors that affect bridge deck cracking and methods to mitigate them. Few field studies, however, have been performed that include the reexamination of bridge decks over a period of several years to evaluate performance, in terms of cracking and permeability, as a function of age. In three Kansas studies, including that reported here, 86 bridges have been surveyed, 49 of which have been surveyed two or more times.

This report reviews the 59 field surveys performed for this study in conjunction with 76 additional surveys performed over the past 10 years. The 59 surveys cover 30 silica fume overlay, 16 conventional overlay, and 13 monolithic bridge decks. Crack densities, reported in linear meters of crack per square meter of bridge deck, are calculated for each bridge, concrete placement, and span based on the survey data. Chloride samples are taken from each concrete placement and used to determine effective diffusion coefficients, surface concentrations, and the time to reach the chloride corrosion threshold. Plans, information from construction diaries, mix designs, and weather conditions are compiled and compared to crack density and chloride data to identify the principal factors that contribute to bridge deck cracking and elevated chloride contents in both cracked and intact concrete.

## **CHAPTER 2: DATA COLLECTION**

### **2.1 GENERAL**

Field surveys were performed on 59 bridge decks to determine the amount of deck cracking, chloride ingress, and delaminated area. Bridges with both monolithic and overlay decks supported by steel girders were included in the evaluation. The overlay bridge decks included decks with conventional high-density or silica fume overlays on concrete subdecks. The silica fume decks were constructed under a number of specifications that include two principal overlay types, one in which 5% of the cement is replaced by silica fume and the other in which 7% is replaced by silica fume. The three types of bridge decks were evaluated to determine their relative effectiveness in limiting cracking and chloride ingress.

Previous work by Schmitt and Darwin (1995, 1999) and Miller and Darwin (2000) has shown that several variables contribute to bridge deck cracking and concrete permeability. Based primarily on this work, multiple variables from four categories were compiled for comparison with observed bridge deck performance. The four categories included material properties, design specifications, construction practices, and environmental site conditions. Data for these categories was available from Schmitt and Darwin (1995, 1999) and Miller and Darwin (2000) for 49 out of the 59 bridge decks. Information for the other ten bridges was obtained from KDOT records.

### **2.2 BRIDGE SELECTION**

Of the 59 bridges selected for this study, 49 had been investigated by Schmitt and Darwin (1995, 1999), Miller and Darwin (2000), or both. This provided the opportunity to re-examine bridges and allowed cracking to be measured over time for individual bridges and similar groups of bridges. As in the earlier studies, the current

study was limited to composite steel girder bridges. This type of bridge not only represents a significant percentage of the bridges in Kansas, but is also generally acknowledged as providing the most deck restraint and having the highest levels of cracking (*Durability* 1970, Cheng and Johnston 1985, Perfetti, Johnston, and Bingham 1985, Krauss and Rogalla 1996, Eppers, French, and Hajjar 1998, Le, French, and Hajjar 1998).

Of the 59 bridges evaluated in this study, 30 bridges had silica fume overlay decks, 16 had conventional overlay decks, and 13 had monolithic decks. Twenty of the silica fume overlay decks had been previously examined by Miller and Darwin (2000); these decks were made with concrete containing a 5% silica fume replacement of cement by weight. The ten silica fume overlays unique to this study were made with concrete containing a 7% silica fume replacement of cementitious materials by weight.

Table 2.1 summarizes the bridge decks examined in this and the two earlier studies. Several of the bridges have been surveyed on more than one occasion. The numbers in parentheses indicate the number of bridges that have been surveyed in previous studies. For instance, this study includes 13 monolithic decks, 12 of which were previously examined by Schmitt and Darwin (1995, 1999) and 4 of which were previously examined by Miller and Darwin (2000). The bridge deck surveys performed as a part of the previous studies all included a crack survey. Schmitt and Darwin (1995, 1999) did not perform chloride sampling, and neither of the previous studies checked deck delamination.

The ten 7% silica fume overlay bridges added to this study reflect the most recent special provisions to the standard construction specifications in Kansas. At the time these bridges were selected for the study, only 13 steel girder bridges of this type had been constructed in Kansas. Since all of these bridges were relatively new, the construction and design documentation needed to complete the evaluation was readily

available from KDOT district offices. Location and the ability to safely perform a field survey determined which of the 13 bridges were selected for the study.

The 49 bridges from the previous reports were selected for a variety of reasons. Originally, bridges were chosen by Schmitt and Darwin (1995, 1999), aside from deck type, based on the type of steel girder used, the ability to safely survey the bridge, the availability of relevant bridge documentation, and the bridge location. In Kansas they found that, of steel girder bridges, 39 percent were SMCC (steel beam, composite continuous), 31 percent were SWCC (steel welded plate girder, composite continuous), and 11 percent were SWCH (steel welded plate girder, composite continuous and haunched). Nine other types accounted for the remaining 19 percent, with no single type more than 4 percent of the total. Bridges were selected to approximate these percentages. After analysis of the results, Schmitt and Darwin (1995, 1999) found no correlation between steel girder type and cracking tendency. In light of this determination, Miller and Darwin (2000) used similar guidelines, with the exception of girder type.

In total, 77 bridges located primarily in northeastern Kansas have been surveyed. The bridges are located in 15 counties, as shown in Figure 2.1. Overall, the surveys have included 17 monolithic, 30 conventional high-density overlay, and 30 silica fume modified concrete overlay decks representing 161 individual concrete placements. Of these bridges, 13 monolithic, 16 conventional overlay, and 20 silica fume overlay bridge decks have been surveyed two or more times.

### **2.3 DATA SOURCES**

Information for the bridges unique to this study was collected from a variety of sources. The bridge design plans were obtained from the Kansas Department of Transportation (KDOT) Bureau of Design, located in Topeka, Kansas. Information obtained from these plans includes, deck width, bridge length, span lengths,

number of spans, bridge skew, deck thickness, top cover thickness, overlay thickness, reinforcing bar size, bar spacing, and barrier type. Average annual daily traffic (AADT) and bridge location were obtained from the KDOT Bridge Log. Additional information acquired through the Construction Management System (CMS) database included the concrete mix design, air content, slump, compressive strength, and bridge contractor. Concrete placement date, length, and width and the environmental site conditions on the date of concrete placement were gathered from construction diaries available from KDOT district offices. The environmental site conditions included in the construction diaries were daily high and low temperatures. Information for previously surveyed bridge decks was taken from the respective reports (Schmitt and Darwin 1995, Miller and Darwin 2000). Information obtained for the remaining 7% silica fume overlay decks is presented in Appendix A.

Although the amount and availability of data for bridges has improved markedly compared to that available for the first two studies, there are still areas that need improvement. Evaporation rates, for instance, are required to be checked for silica fume overlays to ensure they are below  $1.0 \text{ kg/m}^2/\text{hr}$ ; they are, however, rarely found in any construction diaries or notes. Similarly, the concrete temperature, relative humidity, and wind speed during placement are typically not found, but are required elements to estimate the evaporation rate. Additionally, placement start and finish time were rarely mentioned. This data would be especially beneficial when evaluating the performance of silica fume modified concrete with low water-cement ratios.

## **2.4 SURVEY TECHNIQUES**

An on-site survey was performed for each of the 59 bridges included in this study. The surveys included a detailed crack survey, overlay sounding, and chloride sampling. The sounding was performed by dragging chains over the deck and

identifying areas where the overlay had separated from the subdeck. A distinct “hollow” sound can be heard when the chains are dragged over debonded areas. Chloride surveys were performed by KDOT personnel and did not necessarily occur on the same date that the crack survey and sounding was performed.

Prior to arriving at a bridge, a drawing of the bridge deck, including all boundary areas, was made at a scale of 1 inch equals 10 feet (the required scale for the image analysis programs). Several guidelines were followed for each survey with the intent of minimizing any differences that may result from changing personnel. Three to six inspectors performed each survey on days that were at least partly sunny with a minimum temperature of 16° C (60° F). In addition, the entire deck surface was required to be completely dry before beginning the survey. Traffic control was maintained to ensure that at least one lane was clear of traffic and available to the surveyors. Prior to identifying and marking cracks, a 5 × 5 ft (1.52 × 1.52 m) grid was marked on the available surface of the deck. Inspectors then began to mark cracks that were visible while bending at the waist. Once a crack was identified, the entire crack was marked, even if parts of the crack were not initially visible while bending at the waist. The cracks were marked with lumber crayons and then transferred to the scale drawing using the grids on the deck and the drawing as a guide. The consistent use of these guidelines allowed the results from the two previous studies to be incorporated into this research with confidence that the results were not biased by the survey technique. In addition, and unique to this project, following the crack survey, unbonded areas were located by dragging chains over the entire surface of the deck and recorded on the scale drawing. A draft specification describing the crack survey techniques is presented in Appendix B.

In addition to the crack survey, KDOT personnel took concrete samples from the decks and tested them for chloride content. Three locations on cracks and three locations away from cracks were sampled for each concrete placement. At each of

these locations, powdered concrete samples were obtained using a hammer drill fitted with a hollow 19 mm ( $\frac{3}{4}$  in.) bit attached to a vacuum. Five powdered samples were taken at the following 19 mm ( $\frac{3}{4}$  in.) increments: 0–19 mm (0–0.75 in.), 19–38 mm (0.75–1.5 in.), 38–57 mm (1.5–2.25 in.), 57–76 mm (2.25–3 in.), and 76–95 mm (3–3.75 in.). For decks that had been sampled previously (Miller and Darwin 2000), new samples were taken within 150 mm (6 in.) of the earlier sampling points.

## **2.5 CHLORIDE CONTENT TEST**

Each of the powdered samples was tested for water-soluble chloride content using a method similar to that described in ASTM C 1218. The powdered samples were obtained with a plastic cup and filter attached to the vacuum drill. The chloride testing procedure, outlined by KDOT Method 601 involved following twelve steps: (1) Place a 400 ml beaker onto a top loading balance and then tare the balance. (2) Retrieve the filter paper from the sample cup, and using scissors cut the filter paper into at least 3 pieces and place the pieces into the beaker. (3) Add the remaining material from the sample cup into the beaker. (4) Note and record the mass of the sample to 0.01 grams. (5) Add approximately 150 ml of distilled water to the beaker. (6) Place a lid on the beaker and place the beaker on a hot plate, set to high heat, and allow the solution to boil for approximately 20 minutes. (7) Remove the beaker from the hot plate and allow it to cool to near room temperature. (8) Vacuum filter the solution through No. 1 Whatman filter paper in a two-piece Buchner filter funnel catching the filtrate in a 500 ml vacuum flask. Police and rinse the beaker with hot distilled water, placing the rinse fluids into the funnel. (9) Pour the contents of the vacuum flask into a 250 ml plastic Mettler titration beaker. Again, rinse the flask using hot distilled water and pour the rinse fluids into the plastic beaker. (10) Add approximately 5 ml of concentrated nitric acid and then distilled water until the volume is approximately 300 ml. (11) Titrate the sample on the Mettler DL70

Automatic Titrator (KDOT Method 2120) using a chloride ion specific electrode in combination with a silver/silver chloride reference electrode and 1.0N standardized silver nitrate titrant solution (KDOT Method 2005). The chloride content ( $\text{kg/m}^3$ ) can then be calculated by dividing the product of the volume of silver nitrate titrant (ml), normal concentration of the silver nitrate titrant solution (mmol/ml), and the constant  $81.27 \text{ kg}\cdot\text{g/m}^3\cdot\text{mmol}$  by the difference of the mass of concrete sample and filter paper (g) and the mass of filter paper (g).

## **2.6 CRACK DENSITY DETERMINATION**

To compare the relative degrees of cracking for different bridges as a function of material, construction, design, and environmental factors, a quantitative measure was calculated for each bridge, placement, span, and end section. The crack density, in linear meters of crack per square meter of bridge deck, was determined directly from field surveys using several computer programs.

Multiple steps were required to prepare the field crack maps for crack analysis. The first step was to digitally scan the crack maps at 100 dots per inch (dpi) as grayscale tagged image file format (TIFF) files with 256 shades of gray. Since the ultimate goal was to calculate crack lengths from scaled drawings, it was important that the crack map scale and scanned image resolution be exactly 1 in. equals 10 ft and 100 dpi, respectively. Equally as important, if the crack map included more than one page (which was often the case), the individual scanned files were combined into one TIFF image of the entire uninterrupted bridge deck surface; every effort was made to accurately align the images. A black line one pixel in width was added from the top edge of the image down to the top left corner of the bridge deck. This line indicated the starting point for the program to begin looking for cracks. All other boundary lines and other markings or notes that did not represent cracks were removed from the image to ensure that extraneous lines were not counted as cracks.

Finally, any cracks that bent by more than 15° or that intersected other cracks were separated into single straight lines to ensure that the program accurately calculated the distance between crack end points. The file was then saved as an uncompressed TIFF image.

The TIFF images were then converted to ASCII files containing image data using two programs created by Dr. John Gauch of the University of Kansas. These Linux-based programs create an ASCII file with the gray scale of each pixel recorded as a number between zero and 255 (zero for black and 255 for white). After removing unrelated information from the beginning and end of each ASCII file, the files were ready for analysis. In the two previous studies, Schmitt and Darwin (1995, 1999) and Miller and Darwin (2000) used a FORTRAN program to calculate crack lengths from the ASCII file. The FORTRAN program groups “dark” pixels together and, by finding the end points of the groups, calculates the distance between those points.

This FORTRAN program was used not only because it was available, but also to ensure that consistent procedures and methods were used for each of the three studies. Any pixels that were darker than a gray level of 200 were classified as “dark” and were assumed to represent part of a crack. These “dark” pixels were grouped together and the straight-line distance between the end points was calculated. Finally, the crack density was calculated as the sum of all crack lengths (m) divided by the appropriate deck surface area (m<sup>2</sup>). In addition, it was also possible to calculate the total length of cracks with a specified angle or within a specified range of angles. A listing of the crack measurement program, as modified for this study, appears in Appendix C.

## CHAPTER 3: CHLORIDE DATA AND DIFFUSION PROPERTIES

### 3.1 GENERAL

The chloride contents of samples taken at varying depths from uncracked concrete and at crack locations are plotted versus time. Regardless of bridge deck type, at all depths, chloride contents taken at cracks can exceed the corrosion threshold of conventional steel within a few months. At a depth of 76.2 mm (3.0 in.), chloride contents taken from uncracked concrete rarely exceed the corrosion threshold of conventional steel. Based on the samples taken from uncracked concrete, an effective diffusion coefficient and apparent chloride surface concentrations are calculated for each deck placement. These diffusion properties are compared with the age of the placement at the time of sampling and concrete properties and mix design parameters to determine their relative influence on deck performance. The diffusion characteristics represent an average diffusivity over the life of the bridge deck and generally decrease over time as the hydration products and salt fill the concrete pore system.

Several methods are used to describe the findings of the analyses of chloride data and the diffusion properties of the decks sampled in this study. These are described next.

“Box-and-whisker” plots, beginning with Fig. 3.10, are used to characterize the variability within a specific group of data. The minimum, 25<sup>th</sup> percentile, median, 75<sup>th</sup> percentile, and maximum values are presented in each plot and follow a standard format. The minimum and maximum values are represented by dashed lines and are located at the extremes of the data range. The 25<sup>th</sup> and 75<sup>th</sup> percentile values form a box representing the middle 50% of the data. A line through the middle of each box represents the median value for the data range.

Plots of effective diffusion coefficients for each deck type versus the age of the placement at the time of sampling, concrete mix design, and material properties show a significant amount of scatter. To facilitate the analysis, histograms, beginning with Fig. 3.22, are used to provide a clear illustration of the trends. Each bar, or category, represents a range of values for the variable under consideration and is defined by the midpoint. The size of the range is equal to the difference between the midpoints of consecutive categories. In many cases, the sample sizes and the differences between the means of categories are small. The Student's t-test is used to determine whether the differences between two samples represent significant differences between the populations.

The Student's t-test is a parametric test that is frequently used when samples are small and the true population characteristics are unknown. The t-test relies on the means of the two sample groups, the size of the samples, and the standard deviation of each group to determine statistical significance. Specifically, the test is used to determine whether differences in the sample means,  $X_1$  and  $X_2$ , represent differences in the population means,  $\mu_1$  and  $\mu_2$ , at a specified level of significance  $\alpha$ . For example,  $\alpha = 0.05$  indicates a five percent chance that the test will incorrectly identify (or a 95% chance of correctly identifying) a statistically significant difference in sample means when, in fact, there is no difference. A two-side test is used in the analyses performed, meaning that there is a probability of  $\alpha/2$  that  $\mu_1 > \mu_2$  and  $\alpha/2$  that  $\mu_1 < \mu_2$  when in fact,  $\mu_1$  and  $\mu_2$  are equal.

The results of the statistical evaluation for each histogram are presented in Tables 3.4, 3.6 and 3.9 through 3.16. The tables follow a standard format. Each group of data is compared with the other groups for each histogram. These differences are tested at four  $\alpha$  levels: 0.20, 0.10, 0.05, and 0.02. Differences between samples that are statistically significant at the given level of  $\alpha$  are followed by a "Y"

and differences that are not statistically significant at the given level of  $\alpha$  are followed by an “N” in Tables 3.4 through 3.16.

Three silica fume bridges (89-184, 89-187, and 30-93) are included in the evaluation of chloride contents, bridge age, construction date, and deck type, but are not included in the analysis of any other material-related variables. Bridges 89-184 and 89-187 were constructed in 1990 as experimental decks before the first silica fume special provision (90P-158) was written. In addition, both of these decks have a 57 mm (2.25 in.) overlay rather than a standard 38 mm (1.5 in.) overlay currently in use. More importantly, these decks have erratic diffusion properties and do not accurately reflect the performance of current silica fume overlays. The more recently constructed 7% silica fume overlay bridge (30-93) is excluded from the material analysis because in addition to the silica fume, this bridge deck contains a 33% replacement of cement with slag cement (ground granulated blast furnace slag) by weight of cementitious materials.

Except for these three bridges, all of the samples taken from bridge decks in this study and by Miller and Darwin (2000) are included in the comparisons. Diffusion properties for all bridge decks, regardless of the originating study, are calculated using the methods described in Section 3.4. As discussed in Section 2.2, Schmitt and Darwin (1995, 1999) did not collect chloride data.

### **3.2 KDOT DISTRICT 1 SALT USAGE**

Deicing salts are applied to roads to improve driving conditions before, during, and after winter precipitation. Typical salt application rates range from between 28 to 85 kilograms per kilometer of driving lane (100 to 300 lbs. per single lane-mile). KDOT District 1 applies rock salt at a rate of 85 kg/lane·km (300 lb/lane·mile). In addition, KDOT applies a salt brine pretreatment consisting of 23% salt to bridge decks when frost is expected and the temperature is between  $-9^{\circ}$  and  $0^{\circ}$

C (15° and 32° F). The salt brine pretreatment is applied at a rate of 94 to 118 liters per kilometer of driving lane (40 to 50 gallons per single lane-mile).

Ninety percent of the samples included in this study and the previous study (Miller and Darwin 2000) are from KDOT District 1. District 1 encompasses 17 counties in northeast Kansas. The total centerline length of roads treated in District 1 is 2,889 km (1,795 mi.), and the total length of all driving lanes is 7,313 km (4,544 mi.). Rock salt usage, including the salt used in the pretreatment, for District 1 over the past seven years is presented in Table 3.1. With an average lane width of 3.7 m (12 ft), the average surface application rate per year over the past seven years is 1.24 kg/m<sup>2</sup> (2.28 lb/yd<sup>2</sup>). This approximation is below the actual value for bridge decks because they are often treated more frequently than other driving surfaces.

### **3.3 ON AND OFF CRACK CHLORIDE CONCENTRATIONS**

Bridge deck chloride contents taken from uncracked concrete are plotted as a function of the age of the deck placement at the time of sampling in Figs. 3.1 through 3.4 for varying depths and are described in Section 3.3.1. Chloride contents taken at crack locations are plotted as a function of age in Figs. 3.5 through 3.8 for varying depths and are described in Section 3.3.2. Each plot includes data corresponding to one of four depths, 25.4 mm (1.0 in.), 50.8 mm (2.0 in.), 63.5 mm (2.5 in.), and 76.2 mm (3.0 in.). The five 19 mm ( $\frac{3}{4}$  in.) powdered samples taken at three locations, on and off cracks, (as described in Section 2.4) are used to generate these plots. The mean depths for the 19 mm ( $\frac{3}{4}$  in.) samples are 9.5 mm (0.375 in.), 28.6 mm (1.125 in.), 47.6 mm (1.875 in.), 66.7 mm (2.625 in.), and 85.7 mm (3.375 in.). These depths represent the midpoints of the five samples taken at each of the six locations; these depths, however, are not of particular interest because reinforcement is not placed at these levels. The on and off-crack chloride concentrations found in Figs. 3.1 through 3.8 are linearly interpolated from the raw data using the midpoints of

each sample. The raw chloride content data are tabulated in Table D.1 of Appendix D.

Each of the on-crack and off-crack plots includes a linear trend line, prediction intervals, and for comparison, a line representing the lower limit of accepted values for the corrosion threshold of conventional reinforcing steel [ $0.60 \text{ kg/m}^3$  ( $1.0 \text{ lb/yd}^3$ )]. The upper prediction interval, labeled as 20% U, indicates the concentration of chloride as a function of time that has a 20% probability of being exceeded. Conversely, the lower prediction interval, labeled as 20% L, indicates the concentration of chloride as a function of time that has an 80% probability of being exceeded. Figure 3.9 is a summary plot of the linear trend lines, both on and off cracks, for each of the four depths examined.

Although the data points in Figs. 3.1 through 3.8 are identified by bridge deck type, the linear trend lines and prediction intervals are generated using all of the data presented for each plot, both with the exception of the oldest monolithic decks. This is done based on two observations. First, the off-crack chloride concentrations rarely exceed the corrosion threshold of conventional steel for any bridge deck type at 63.5 mm (2.5 in.) and 76.2 mm (3.0 in.). Second, the on-crack chloride concentration data appear to be independent of bridge deck type. Differences in diffusion properties as a function of deck type will be examined in Section 3.4.

Based on the data in Figs. 3.1 through 3.8, it is apparent that attention should be focused on minimizing bridge deck cracking. Adequate reinforcing steel protection is provided by uncracked concrete, and the protection is independent of deck type. This assertion is discussed further in the diffusion analysis presented in Section 3.4.

Many factors affect the chloride corrosion threshold level for conventional reinforcing steel. Commonly accepted values for the corrosion threshold fall between  $0.60$  and  $1.20 \text{ kg/m}^3$  ( $1.0$  and  $2.0 \text{ lb/yd}^3$ ). McDonald, Pfeifer, and Sherman (1998)

report that the corrosion threshold for damaged ECR is similar to that of conventional reinforcement.

### 3.3.1 Off Crack Chloride Concentrations

Figures 3.1 through 3.4 compare the chloride contents for uncracked concrete plotted versus the age of the deck placement at the time of sampling. The figures show a nearly linear increase in chloride content with age. Typically, chloride contents for silica fume (5% and 7%) overlay, conventional overlay, and monolithic bridge decks in the same age range [ $< 156$  months (13 years)] taken away from cracks at a depth of 76.2 mm (3.0 in.) are below even the most conservative estimates of the corrosion threshold for conventional reinforcement [ $0.6 \text{ kg/m}^3$  ( $1.0 \text{ lb/yd}^3$ )]. In contrast, for the oldest decks included in this study [limited to monolithic decks older than 168 months (14 years)], 42% of the samples exceed the corrosion threshold; based on trends in the data for bridges just below 156 months, however, this does not represent the expected behavior of the more recently constructed decks. As a summary of Figs. 3.1 through 3.4, Fig. 3.9 shows the linear trend lines for chloride contents both on and off cracks versus age at each depth for all bridge decks. Based on the regression equations for the trend lines, as well as the upper and lower 20% prediction intervals, times to reach the corrosion threshold are calculated for each depth and shown in Table 3.2. These calculations do not take into account the differences in diffusion properties between deck types; differences that will be addressed in Section 3.4.

As indicated in Table 3.2, at the standard top reinforcement cover depth now used in Kansas of 76.2 mm (3.0 in.), 20% of the chloride samples taken off cracks from randomly selected bridge decks can be expected to exceed  $0.6 \text{ kg/m}^3$  ( $1.0 \text{ lb/yd}^3$ ) in 160 months (13.3 years), 50% in 254 months (21.2 years), and 80% in 349 months (29.1 years). For a corrosion threshold of  $1.2 \text{ kg/m}^3$  ( $2.0 \text{ lb/yd}^3$ ), these numbers

increase to 410 months (34.2 years), 504 months (42.0 years), and 599 months (49.9 years), respectively. At either corrosion threshold level and for all types of bridge decks, the benefits of using a 76.2 mm (3.0 in.) cover and uncracked concrete are unmistakable.

### **3.3.2 On Crack Chloride Concentrations**

Figures 3.5 through 3.8 show chloride contents taken on cracks plotted against the age of the placement at the time of sampling. As for the off-crack data, the chloride concentrations increase nearly linearly with age. The values, however, are markedly higher than for the samples taken away from cracks. At cracks, the average chloride concentration at a depth of 76.2 mm (3.0 in.) can exceed the corrosion threshold of conventional reinforcement in as little as nine months, regardless of deck type. By 24 months, the chloride content at cracks exceeds 0.6 kg/m<sup>3</sup> (1.0 lb/yd<sup>3</sup>) in the majority of the decks surveyed. Chloride concentrations increase steadily as the sample depth decreases, regardless of the placement age.

There appears to be no correlation between deck type and chloride concentration, reaffirming the decision to combine the chloride concentration data for all of the bridge deck types. At depths of 63.5 mm (2.5 in.) and 76.2 mm (3.0 in.), a disproportionate number of samples taken from monolithic decks fall below the 20% L. In fact, over 60% of the samples taken from monolithic decks older than 144 months fall below the lower 20% prediction intervals at those depths. This observation is likely due to the fact that the monolithic decks included in this study have lower traffic volumes than the overlay decks. Lower traffic volume roads are treated with deicing chemicals less often than the higher volume roads.

### 3.4 FICK'S EQUATION MODELING

Despite some of the shortcomings inherent to modeling chloride ingress through uncracked concrete using Fick's Second Law of Diffusion, Eq. (1.1), it provides a useful method to compare concrete permeabilities based on measured chloride ion concentrations. The chloride concentrations of the samples taken from three crack free locations for each placement are used to calculate an effective diffusion coefficient ( $D_{eff}$ ) and apparent chloride surface concentrations ( $C_o$ ). The solution to Fick's Second Law, Eq. (1.2), has four degrees of freedom, depth  $d$ , time  $t$ , surface concentration  $C_o$ , and the effective diffusion coefficient  $D_{eff}$ .

$$C(x,t,C_o,D_{eff}) = C_o \cdot \left[ 1 - \operatorname{erf} \left( \frac{x}{2 \cdot \sqrt{t \cdot D_{eff}}} \right) \right] \quad (1.2)$$

The apparent surface concentration  $C_o$  and the effective diffusion coefficient  $D_{eff}$  are unknown, but can be estimated using an iterative least-squares curve fitting technique. The age of the sample is used as the total time  $t$  and is calculated as the difference between sample date and placement date. Since each sample represents a region with a depth of 19 mm ( $3/4$  in.), the concentration  $C$  from Eq. (1.2) is numerically integrated between the end points of the samples and divided by the total depth of the samples, 19 mm ( $3/4$  in.), to obtain average chloride concentration for each sample according to Fick's Second Law. This process is performed for each sample (five samples for each location) during each iteration of the minimization process. To begin the calculation, three apparent surface concentrations (one for each sample location) and one effective diffusion coefficient are assumed as initial values for each placement. The minimization solver in Microsoft Excel 2000 modifies the surface concentrations and diffusion coefficient to minimize the sum of the squared differences between the measured chloride concentrations and the average chloride

concentrations predicted by Fick's Second Law. This process is performed for each placement and the results are used to estimate bridge deck performance. The calculated diffusion data are tabulated in Table D.2 of Appendix D.

In many cases, bridge deck concrete contains chlorides from sources other than deicing salts. Water, aggregates, and admixtures can contain chlorides (base level chlorides) that must be subtracted from the measured chloride concentrations prior to the diffusion analysis. One base level chloride content is estimated for each placement by examining the chloride contents taken from uncracked concrete at all depths and sample locations for that placement. Chloride concentrations that do not differ by more than  $0.05 \text{ kg/m}^3$  ( $0.08 \text{ lb/yd}^3$ ) from the measured chloride concentration at the deepest level of each sample are considered to be the base level chlorides. These base levels are averaged for each placement and subtracted from the measured chloride concentrations for that placement. The "box-and-whiskers" plot in Fig. 3.10 shows the variability in base levels for all bridge deck types. Average base levels range between 0 and  $0.37 \text{ kg/m}^3$  (0 and  $0.62 \text{ lb/yd}^3$ ), but fifty percent of the base level concentrations fall between  $0.02$  and  $0.17 \text{ kg/m}^3$  ( $0.03$  and  $0.29 \text{ lb/yd}^3$ ), with a median concentration of  $0.11 \text{ kg/m}^3$  ( $0.19 \text{ lb/yd}^3$ ). Further analysis reveals that there is no discernable difference between base levels taken from different deck types.

### **3.4.1 Surface Concentrations**

Due to the variable nature of applying deicing chemicals to bridge decks, an apparent surface concentration is calculated for each off-crack sample location, (three apparent surface concentrations for each placement). This improves the chloride diffusion model by more accurately depicting field conditions. The median difference between the calculated maximum and minimum apparent surface concentration for each placement is  $2.68 \text{ kg/m}^3$  ( $4.52 \text{ lb/yd}^3$ ). By way of comparison,

the median difference between the maximum and minimum chloride concentrations at the shallowest sample depth for an individual placement is  $1.55 \text{ kg/m}^3$  ( $2.61 \text{ lb/yd}^3$ ). It is obvious that there is a large variation in surface concentration for each placement.

The variability of the apparent surface concentrations is summarized in Fig. 3.11. The maximum difference between the calculated maximum and minimum apparent chloride concentration for a placement is  $10.08 \text{ kg/m}^3$  ( $16.99 \text{ lb/yd}^3$ ). The corresponding 75<sup>th</sup> percentile value is  $4.16 \text{ kg/m}^3$  ( $7.01 \text{ lb/yd}^3$ ). The variability of the chloride concentrations taken at the shallowest sample depth is also shown in Fig. 3.11. The maximum difference between the minimum and maximum chloride concentration for each placement is  $5.72 \text{ kg/m}^3$  ( $9.64 \text{ lb/yd}^3$ ), and the 75<sup>th</sup> percentile value is  $2.28 \text{ kg/m}^3$  ( $3.84 \text{ lb/yd}^3$ ). The large difference in variability between apparent surface concentrations taken from the same placement justifies the use of three apparent surface concentrations for each placement (one for each sample location). In addition, this information highlights the importance of calculating an apparent surface concentration rather than estimating a concentration based on samples taken near the surface of the deck. There is a large chloride concentration gradient near the deck's surface that must be taken into account.

The calculated apparent surface concentration is compared with the measured chloride content at the shallowest depth [centered at  $9.5 \text{ mm}$  ( $0.375 \text{ in.}$ )] at each location for monolithic (MONO), conventional overlay (CO), and silica fume overlay (5% SFO, 7% SFO) bridge decks in Figs. 3.12, 3.13, and 3.14, respectively. For each figure, the data are identified based on the originating study. A linear regression line forced through the origin is included in the plots, and in all cases, lies above the 45-degree line. The slope of these regression lines can be interpreted as a relative measure of the performance of the three deck types over time. Higher slopes indicate a greater differential between apparent surface concentrations and actual chloride

contents taken from just under the surface. The greater the differential, the greater the gradient of the chloride content profile near the deck's surface. These unit-less slopes for monolithic, conventional overlay, and silica fume overlay decks are 1.28, 1.54, and 1.75, respectively.

As would be expected, the apparent surface concentrations increase with deck age, as indicated in Fig. 3.15. In Fig. 3.16, the apparent surface concentrations calculated using data from this study are compared with the values calculated based on the data gathered earlier by Miller and Darwin (2000) for decks that were surveyed in both studies. Eighty-one percent of the points lie above the 45-degree line, indicating generally increasing surface concentrations over time. The greatest differential between concentrations occurs for placements with a low calculated surface concentration based on data from the earlier study. The trend line, for the range of data included, indicates a decrease in the rate of chloride build-up as surface concentrations (and therefore time) increase. Figures 3.17, 3.18, and 3.19 show the average apparent surface concentration versus placement age at the time of sampling for monolithic, conventional overlay, and silica fume overlay bridge placements, respectively. Lines connect data for placements surveyed both by Miller and Darwin (2000) and in the current study. The average apparent surface concentration build-up rates, calculated as the average slopes of these lines, are presented in Tables 3.3 a and b for each deck type. The build-up rate for monolithic, conventional overlay, and silica fume overlay bridges are 0.504, 0.204, and 0.660 kg/m<sup>3</sup>/year (0.850, 0.344, and 1.112 lb/yd<sup>3</sup>/year), respectively. The average build-up rate for all bridge deck types is 0.456 kg/m<sup>3</sup>/year (0.769 lb/yd<sup>3</sup>/year). The standard deviations are high relative to the average build-up rates, indicating the high variability in surface concentrations found in the field.

### 3.4.2 Diffusion Coefficients

The effective diffusion coefficients ( $D_{eff}$ ) calculated using Fick's Second Law of Diffusion provide a useful tool to compare the permeabilities of different bridge deck concretes. A lower diffusion coefficient indicates a higher resistance to chloride ion penetration. Figure 3.20 shows the diffusion coefficients calculated for all bridge placements surveyed in this study and by Miller and Darwin (2000) as a function of age at the time of sampling. In general, the diffusion coefficients appear to decrease over time, and particularly for the overlay decks, show much less variation over time. Continued hydration and the deposition of salt in the concrete pores over time may partially account for the decrease in diffusion coefficients. In addition, modeling chloride diffusion in bridge decks as if the chloride surface concentrations are constant (as done here), rather than increasing underestimates the diffusion coefficients.

Miller and Darwin (2000) expressed concern over the accuracy in determining diffusion coefficients for bridges under 500 days old. Their concern was that younger bridges may not have been exposed to the quantity of deicing salts required to develop a profile that can be accurately modeled by Fick's Second Law.

Because the calculated effective diffusion coefficients appear to be highly dependent on age, the bridges are divided based on the age of the deck at the time of sampling. The effective diffusion coefficients for each bridge deck type are compared in three age categories: (1) 0 to 48 months, (2) 48 to 96 months, and (3) over 96 months.

#### 3.4.2.1 Monolithic Decks

Figure 3.21 shows the effective diffusion coefficients versus time for monolithic bridge deck placements. Lines connect the data for placements that have been sampled two times; for monolithic decks, only the four youngest placements

have been sampled twice. For three of the four placements surveyed on two occasions, the diffusion coefficients decreased with time. Figure 3.22 shows the mean effective diffusion coefficients for the monolithic placements in three age categories: 0 to 48 months, 48 to 96 months, and greater than 96 months. The mean effective diffusion coefficients for these categories are 0.09, 0.17, and 0.16 mm<sup>2</sup>/day. Only one placement falls into the first category (and is therefore ineligible for statistical comparisons), and there is no statistical difference in the diffusion properties for the remaining two age categories (Table 3.4).

The variability of diffusion coefficients for monolithic placements older than 96 months is shown in Fig. 3.23. This is the only age category for monolithic placements with enough data to construct a box-and-whiskers plot. Substantial variation exists between the diffusion coefficients taken for the 15 placements older than 96 months. The  $D_{eff}$  ranges from 0.06 to 0.29 mm<sup>2</sup>/day. Fifty percent of the values fall between 0.11 and 0.22 mm<sup>2</sup>/day, with a median of 0.15 mm<sup>2</sup>/day.

#### **3.4.2.2 Conventional Overlay Decks**

The effective diffusion coefficients for the conventional overlay deck placements are plotted versus time in Fig. 3.24. Thirty-six individual placements are shown, 35 of which were surveyed twice. Of the 35 placements sampled by Miller and Darwin (2000) and as part of this study, 23 exhibit diffusion coefficients that have decreased with time. The values of  $D_{eff}$  for the remaining 12 placements increased, but at an average rate of less than half the absolute value of  $D_{eff}$  for the 23 decks with decreasing effective diffusion coefficients. The diffusion coefficients for the conventional overlay decks are highly dependent on the age of sampling (Fig. 3.24). Figure 3.25 presents the mean effective diffusion coefficients for three age groups: 0 to 48 months, 48 to 96 months, and greater the 96 months. Six of the placements surveyed as a part of this study and by Miller and Darwin (2000) fall into

the 48 to 96 month category two times. They were first surveyed shortly after 48 months and surveyed again just before they reached 96 months. For these placements, the results of the first study are included in the first age category, 0 to 48 months. The mean effective diffusion coefficient decreased from 0.15 mm<sup>2</sup>/day for the first age category to 0.08 mm<sup>2</sup>/day for the remaining two age categories. The differences between the first age category and the two remaining categories are statistically significant at  $\alpha = 0.02$  (Table 3.4).

The variability of diffusion coefficients for conventional overlay placements for each age category is shown in Fig. 3.26. There is virtually no difference in effective diffusion coefficients in terms of variability or performance for decks sampled between 48 and 96 months and decks sampled between 96 and 144 months. The 33 conventional overlay placements in the 48 to 96 month category have diffusion coefficients that range from 0.03 to 0.26 mm<sup>2</sup>/day with a median of 0.07 mm<sup>2</sup>/day. Fifty percent of the values fall between 0.05 and 0.10 mm<sup>2</sup>/day. The 28 conventional overlay placements in the 96 to 144 month category also have diffusion coefficients that range from 0.03 to 0.26 mm<sup>2</sup>/day with a median of 0.07 mm<sup>2</sup>/day. Fifty percent of the values fall between 0.04 and 0.09 mm<sup>2</sup>/day, only slightly lower than the previous age group. Substantial differences exist, however, between the diffusion coefficients taken for the 8 placements in the first age group, 0 to 48 months. These placements have diffusion coefficients that range from 0.05 to 0.22 mm<sup>2</sup>/day, with a median of 0.16 mm<sup>2</sup>/day. This information (Figs. 3.25 and 3.26) clearly identifies the importance and advantage of sampling bridge placements older than 48 months to identify the long-term diffusion properties of concrete in bridge decks.

### 3.4.2.3 Silica Fume Overlay Decks

Two types of silica fume decks are included in this study. These include decks built under special provisions 90M-150-R1 through R7 containing 5% silica fume and decks built under special provisions 90M-150-R8 and R9 containing 7% silica fume. All of the bridge decks containing 5% silica fume were sampled by both Miller and Darwin (2000) and as a part of this study. The effective diffusion coefficients are plotted as a function of age in Fig. 3.27. Data points connected by lines indicate bridges that have been surveyed twice. As with the conventional overlay decks, the diffusion coefficients generally decrease over time (Fig 3.27). Of the 42 placements surveyed twice, the effective diffusion coefficients decreased for 31 placements and increased for 11 placements. As before, the average rate of increase is half the rate of the absolute value of decrease. Figure 3.28 presents the mean effective diffusion coefficients for the three age categories: 0 to 48 months, 48 to 96 months, and greater than 96 months. The mean effective diffusion coefficient decreases significantly ( $0.13 \text{ mm}^2/\text{day}$  to  $0.07 \text{ mm}^2/\text{day}$ ) for the 5% silica fume decks as the age range increases from between 0 and 48 months to between 48 and 96 months. The mean effective diffusion coefficient increases to  $0.11 \text{ mm}^2/\text{day}$  in the last age category (Fig. 3.28); this category, however, contains only four placements from bridges 89-187 and 89-184, which were constructed prior to the first silica fume special provision.

The variability of  $D_{eff}$  for the silica fume overlay decks is shown in Fig. 3.29. There is a wider range in diffusion coefficients for the 7% silica fume overlays than for the 5% silica fume overlays sampled between the ages of 0 and 48 months.  $D_{eff}$  for the 7% silica fume overlay decks ranges from  $0.02 \text{ mm}^2/\text{day}$  to  $0.38 \text{ mm}^2/\text{day}$ , with a median of  $0.11 \text{ mm}^2/\text{day}$ . Fifty percent of these coefficients fall between  $0.09$  and  $0.27 \text{ mm}^2/\text{day}$ . For the 5% silica fume overlays, diffusion coefficients range from  $0.02 \text{ mm}^2/\text{day}$  to  $0.32 \text{ mm}^2/\text{day}$ , with a median of  $0.10 \text{ mm}^2/\text{day}$ . Fifty percent of

these coefficients fall between 0.07 and 0.18 mm<sup>2</sup>/day. The variability in the effective diffusion coefficients decreases even further for the 5% silica fume overlays sampled between the ages of 48 and 96 months. Although the diffusion coefficients range from 0.02 mm<sup>2</sup>/day to 0.27 mm<sup>2</sup>/day, the median is 0.06 mm<sup>2</sup>/day and half of the values fall between 0.04 and 0.09 mm<sup>2</sup>/day. Figure 3.29, like Fig 3.26 for the conventional overlay data, again highlights the importance of analyzing placements older than 48 months.

The difference, in terms of bridge deck performance, between a 5% and a 7% silica fume overlay is of particular interest. The comparison between silica fume overlay types is restricted to bridges with ages between 0 and 48 months due to the limited age range of the available 7% silica fume overlays. The mean effective diffusion coefficient decreases (0.17 mm<sup>2</sup>/day to 0.13 mm<sup>2</sup>/day) with decreasing silica fume contents (Fig. 3.28). This observation appears to contradict the laboratory findings by Whiting and Detwiler (1998). This difference, however, is only statistically significant at  $\alpha = 0.20$  (Table 3.4), and should be reevaluated when the 7% silica fume overlays are at least four years old.

### **3.4.3 Diffusion Coefficient Age-Correction**

Bridge deck age at the time of sampling (for diffusion analysis) has a significant effect on the diffusion properties of concrete. Because of the salient trends observed for the effective diffusion coefficients over time, significant age-dependent differences can exist for bridges in the same age category with similar diffusion properties. To eliminate bridge age at the time of sampling as a variable and allow bridges to be compared on an equal-age basis, the technique of dummy variables (Draper and Smith 1981) is used to determine the mean rate of decrease in the effective diffusion coefficient for each of the three bridge deck types. This multiple linear regression method assumes that the actual decrease in diffusion coefficients

over time is linear and independent of the initial diffusion coefficient of the bridge deck. Multiple surveys of the same bridge at different ages lends itself very well to the application of this technique.

The results of the dummy variable analysis for monolithic, conventional overlay, and silica fume overlay decks are presented in Table 3.5. The rate of decrease in  $D_{eff}$  obtained for monolithic decks is the least (-0.0003613 mm<sup>2</sup>/day/month), about that of the conventional overlay decks (-0.0005182 mm<sup>2</sup>/day/month), and about one-third the rate of decrease for silica fume overlay decks (-0.001035 mm<sup>2</sup>/day/month). The rate of decrease for monolithic decks is based on just four placements (eight surveys) with an average age of 94.3 months, the only placements that have been surveyed two times.

It is recognized that effective diffusion coefficients represent an average diffusivity for each placement at the time of sampling, and that the relationship between  $D_{eff}$  and bridge age is nonlinear. For these reasons, the effective diffusion coefficients are adjusted using the results in Table 3.5 only within each of the age categories, reducing differences for decks sampled at different ages. The diffusion coefficients are adjusted linearly to the average age of all bridge decks at the time of sampling within each age category. The average ages for all bridge decks sampled between 0 and 48 months, 48 and 96 months, and 96 and 144 months are 20.5 months, 72.9 months, and 120.8 months, respectively. Monolithic bridges encompass only one age category, those older than 120 months, with an average age of 176.3 months. For comparison, both the mean and the adjusted effective diffusion coefficients are presented in Figs. 3.30 and 3.31; although the changes in the average values are small, the age-adjusted effective diffusion coefficients  $D_{eff}^*$  will be referenced in the balance of this report.

### 3.4.4 Comparison of Deck Diffusion Coefficients

The data obtained in this study allows the diffusion coefficients for monolithic, conventional overlay, and silica fume overlay bridge placements to be compared over the first eight years (96 months) after construction. For purposes of comparison, the coefficients are divided into two 48-month age groups: (1) 0 to 48 months, and (2) 48 to 96 months. The mean and age-adjusted (as described in Section 3.3.3) effective diffusion coefficients are presented in Figs. 3.30 and 3.31.

Figure 3.30 shows the mean and adjusted effective diffusion coefficients for each bridge deck type sampled during the first 48 months after construction. The largest difference between the mean and adjusted effective diffusion coefficients is 0.01 mm<sup>2</sup>/day and occurs for conventional overlays. The adjustment changes the remaining coefficients by less than 0.01 mm<sup>2</sup>/day. Only one monolithic deck fell within this age range and is included for comparison purposes only. The only statistically significant ( $\alpha = 0.20$ ) difference is between the 5% silica fume overlays and the 7% silica fume overlays (Table 3.6). The mean adjusted effective diffusion coefficient is 0.17 mm<sup>2</sup>/day for the 7% silica fume overlays and 0.13 mm<sup>2</sup>/day for the 5% silica fume overlays. The mean adjusted effective diffusion coefficient is 0.16 mm<sup>2</sup>/day for conventional overlays and 0.09 mm<sup>2</sup>/day for the single monolithic deck sampled between 0 and 48 months.

Using Fick's Second Law, the average time required for the chloride content to reach the corrosion threshold in uncracked concrete can be determined for any depth using these diffusion coefficients (Fig 3.30) and the mean surface concentration (for this age range), 6.0 kg/m<sup>3</sup> (10.1 lb/yd<sup>3</sup>). The times for the chloride content to reach the corrosion threshold at a depth of 76.2 mm (3.0 in.), as a function of deck type, are presented in Table 3.7. The single monolithic deck is excluded from the analysis.

The time to reach a chloride content of  $0.60 \text{ kg/m}^3$  ( $1.0 \text{ lb/yd}^3$ ) ranges from 17.6 years for the 7% silica fume overlays to 23.4 years for the 5% silica fume overlays. For the chloride content of  $1.20 \text{ kg/m}^3$  ( $2.0 \text{ lb/yd}^3$ ), the times increase to 28.3 years for the 7% silica fume overlays and 37.0 years for the 5% silica fume overlays. The times required for the chloride concentration to reach the corrosion threshold in conventional overlays are 18 years and 30.1 years for  $0.60 \text{ kg/m}^3$  ( $1.0 \text{ lb/yd}^3$ ) and  $1.20 \text{ kg/m}^3$  ( $2.0 \text{ lb/yd}^3$ ), respectively.

The mean effective diffusion coefficients for placements with ages between 48 and 96 months old are shown in Fig. 3.31. Although none of the 7% silica fume overlays fall within this range, a distinct trend for the remaining decks emerges. As observed for Fig. 3.30, the linear age-adjustment has only a small effect, with the largest change of just under  $0.01 \text{ mm}^2/\text{day}$  for any deck type. While the 5% silica fume and conventional overlays within this age range are not statistically different at any  $\alpha$  level, monolithic decks have diffusion coefficients that are over two times higher than the other overlay deck types, a result that is statistically significant at  $\alpha = 0.02$  (Table 3.6). Based on Fick's Second Law, using the diffusion coefficients from this age range and the mean surface concentration (for this age range) of  $10.0 \text{ kg/m}^3$  ( $16.1 \text{ lb/yd}^3$ ), the times calculated for the chloride ion concentration to reach the corrosion threshold at a depth of 76.2 mm (3.0 in.) are presented in Table 3.8.

For a chloride content at 76.2 mm (3.0 in.) of  $0.60 \text{ kg/m}^3$  ( $1.0 \text{ lb/yd}^3$ ), the times range from 13.6 years for the monolithic placements to 33.4 years for the 5% silica fume overlays. For a chloride content of  $1.20 \text{ kg/m}^3$  ( $2.0 \text{ lb/yd}^3$ ), the times increase to 19.2 years for the monolithic placements and 46.7 years for the 5% silica fume overlays. The times required for chloride concentrations to reach the corrosion threshold in conventional overlays are 25.0 years and 36.3 years for values of  $0.60 \text{ kg/m}^3$  ( $1.0 \text{ lb/yd}^3$ ) and  $1.20 \text{ kg/m}^3$  ( $2.0 \text{ lb/yd}^3$ ), respectively.

Overall, the diffusion coefficients calculated based on Fick's Second Law appear to be more reliable and consistent for samples taken from bridge decks when they are at least four years old (48 months). For bridges in this category in the current study, chloride ion concentrations reach the corrosion threshold in monolithic decks in less than half of the time required for either 5% silica fume or conventional overlays. Statistically, there is no difference between the diffusion performance for the 5% silica fume overlays and the conventional high-density overlays.

As shown in Section 3.3.2, regardless of the bridge deck type, the time for the chloride concentration to reach the corrosion threshold in cracked concrete can be measured in months rather than years, as it is for uncracked concrete.

### **3.5 DIFFUSION COEFFICIENTS VERSUS SILICA FUME OVERLAY SPECIFICATIONS**

Many of the requirements outlined in construction specifications affect the performance of the concrete used in bridge decks. These requirements include factors that must be monitored during construction. Some of these factors, however, have not been recorded in construction diaries or reports. Most notably, while the concrete temperature during placement is monitored for compliance with the specifications, it has typically not been recorded in Kansas. The average daily wind speed and relative humidity are additional site conditions not included in construction records. The inability to correlate weather conditions with measured bridge deck diffusivity represents a weakness in the evaluation of programs developed specifically to improve deck diffusivity.

Many changes related to the construction of silica fume overlay bridges have occurred since the first silica fume overlay placements. Since 1990, eleven revisions to the standard specifications have been made. Eight of those revisions [90P(M)-158-R1, R2, R3, R4, R5, R6, R8, R9] are represented by the silica fume overlays selected

for this study. The eight revisions are divided into five groups based on the type, quantity, and scope of changes specified by the special provisions. As discussed previously, four silica fume overlay placements were cast prior to the first special provision, 90P-158. No significant changes were made in Revisions 1 or 2. Revision 3 increased the curing period from 72 hours to 7 days and required treatment with a precure material or fogging of the struck-off surface. Revision 3 included provisions to monitor and maintain evaporation rates below  $1.0 \text{ kg/m}^2/\text{hr}$  ( $0.2 \text{ lb/ft}^2/\text{hr}$ ) or the application of a precure material immediately after overlay placement. Revision 4 required both fogging and the use of a precure material. Revisions 5 and 6 did not include significant changes and are grouped together with Revision 4. Finally, Revisions 7 through 9 are grouped together and represent a fourth category. Most notably, these special provisions increased the required silica fume content from 5 to 7% by mass of cement. A more detailed explanation of the differences between the special provisions is provided in Section 1.7.

The mean adjusted effective diffusion coefficients for the silica fume overlay placements are presented in Fig. 3.32 based on the special provision in effect during construction. The results are further separated by the age of the placement at the time of sampling. Contrary to the expected behavior, the diffusivity has increased with subsequent provision releases for bridges sampled between 0 and 48 months. The mean adjusted effective diffusion coefficients obtained for bridges sampled between 0 and 48 months increases from  $0.08 \text{ mm}^2/\text{day}$  for bridges constructed under special provisions 90P-158-R1 and R2 to  $0.11 \text{ mm}^2/\text{day}$  for bridges constructed under 90P-158-R3. The mean effective diffusion coefficient continues to increase (to  $0.15 \text{ mm}^2/\text{day}$ ) for bridges constructed under special provisions 90P-158-R4 through R6. While statistically no different from Revisions 3–6 (Table 3.9), the mean effective diffusion coefficient slightly increases to  $0.17 \text{ mm}^2/\text{day}$  for bridges constructed under the most recent special provisions (90M-158-R8 and R9). The remaining differences

between categories are statistically significant at least at  $\alpha = 0.20$  (Table 3.9). The increase in  $D_{eff}^*$  with changes in the special provisions, while contrary to the expected behavior, is clearly identifiable and at the very least represents largely ineffectual attempts to improve diffusivity.

In contrast to the results for bridges sampled at ages below 48 months, the values of mean effective diffusion coefficients obtained for placements sampled between 48 and 96 months remain nearly constant.  $D_{eff}^*$  only increases from 0.06 mm<sup>2</sup>/day for bridges constructed without special provisions to 0.07 mm<sup>2</sup>/day for bridges constructed under the most recent special provisions. None of the differences between categories are statistically significant (Table 3.9). Figure 3.32 clearly indicates that the additional curing requirements and placement procedures introduced with the new revisions of the special provisions have not helped to improve the diffusivity characteristics of silica fume overlays.

### **3.6 EFFECTS OF CONCRETE PROPERTIES ON DIFFUSIVITY**

The material properties analyzed include slump, air content, water-cementitious material ratio, percent volume of water and cementitious materials, water content, cement content, and compressive strength. Construction techniques and practices can also have a large effect on concrete permeability. Ineffective or incomplete consolidation, interruptions in the curing process, and placing concrete during periods of high evaporation increase concrete diffusivity. While these variables may dominate the performance for some of the bridges included in this study, other than the basic guidelines required in the special provisions, this information is largely unavailable.

The bridges are divided into four groups for analysis: 5% silica fume overlays, 7% silica fume overlays, conventional overlays, and monolithic bridge decks. The 5% percent silica fume overlays are further divided into two age categories: decks

sampled between 0 and 48 months and decks sampled between 48 and 96 months. All of the 7% silica fume overlays fall within the 0 to 48 month age group. Conventional overlays are divided into groups with ages of 48 to 96 months and 96 to 144 months, and monolithic decks are grouped together as placements older than 120 months. The four monolithic bridges significantly younger than 120 months (see Fig. 3.21), two silica fume overlay bridges cast before the first special provision, and one silica fume overlay bridge containing slag cement (ground granulated blast furnace slag) are excluded from the analysis.

In addition to dividing the data into groups based on the age of the bridge at the time of sampling, all of the data presented in this section has been adjusted to account for age differences within each age category (as described in Section 3.4.3 and presented in Table 3.5) are used to linearly adjust the effective diffusion coefficients to the average age of all bridge placements within a specified age group.

The analysis of the effects of material properties includes 38 silica fume overlay placements and 35 conventional overlay placements, all of which have been sampled as a part of this study and by Miller and Darwin (2000). The analysis also includes 16 monolithic placements of which 4 were also sampled by Miller and Darwin (2000). The number of placements used in the analysis of each material property varies due to limitations in the availability of data for some bridge placements. For the overlay bridges surveyed in this study, there is virtually no variation in the quantity of cement used in the concrete mixes. This leads to relationships between the (1) water-cementitious material ratio, (2) percent volume of water and cementitious materials, and (3) water content and the mean adjusted effective diffusion coefficient that are nearly identical. As a result, the mean adjusted effective diffusion coefficient will not be compared to the percent volume of water and cementitious materials, water content, or cement content for overlays.

More detailed evaluations of the effect of material properties on diffusion coefficients are presented in the balance of this section. The key observations from these analyses can be summarized as follows:

For **silica fume overlays** sampled between 0 and 48 months and 48 and 96 months, there is no significant correlation between the mean adjusted effective diffusion coefficients and concrete slump. Diffusivity increases significantly with increasing air contents for 5% silica fume overlay decks sampled between 0 and 48 months, although no correlation is apparent for bridges sampled between 48 and 96 months. Diffusivity consistently decreases as the water-cementitious material ratio  $w/cm$  increases. This observation does not follow the expected trend and is in all likelihood due to the small range in the  $w/cm$  ratio (0.37 to 0.40). There is no apparent correlation between diffusivity and compressive strength within the range of 38 to 59 MPa (5500 to 8500 psi).

For **conventional overlays** sampled between 48 and 96 months and 96 and 144 months, there is no significant correlation between the mean adjusted effective diffusion coefficient and concrete slump. For both age ranges, diffusivity significantly increases with increasing air contents. For bridges sampled between 96 and 144 months, as the air content increases from 4.375 to 6.625%, the diffusivity increases by more than three times (0.04 mm<sup>2</sup>/day to 0.13 mm<sup>2</sup>/day). No trend with diffusion properties is apparent as the water-cement ratio increases from 0.36 to 0.40 and for compressive strengths between 38 and 52 MPa (5500 and 7500 psi).

For **monolithic placements** older than 120 months, there is no apparent correlation between the mean adjusted effective diffusion coefficient and concrete slump. Diffusivity appears to increase with air content although two placements with the highest air contents have low diffusion coefficients.

The mean adjusted effective diffusion coefficient increases as the (1) water-cement ratio, (2) water content, and (3) cement content increase. The mean adjusted effective diffusion coefficient appears to be insensitive to compressive strength within the range of 31 to 45 MPa (4500 to 6500 psi).

### 3.6.1 Slump

For the 5% silica fume overlays, the overlay slump varies from 19 to 127 mm (0.75 to 5.0 in.). For the 7% silica fume overlays, the slump varies from 57 to 102 mm (2.25 to 4.0 in.). Categories for both types range from a mean of 38 to greater than 100 mm (1.5 in. to greater than 4.0 in.). For conventional overlays, the overlay slump varies from 0 to 160 mm (0 to 6.25 in.), with categories ranging from 0 to 19 mm (0 to 0.75 in.). For monolithic bridge decks, the slump ranges from 44 to 76 mm (1.75 to 3.0 in.), with categories ranging from 44 to 70 mm (1.75 to 2.75 in.).

The mean adjusted effective diffusion coefficients are shown as a function of concrete slump for the silica fume overlays in Figs. 3.33 and 3.34. For bridges sampled between 0 and 48 months, the mean adjusted effective diffusion coefficients range from 0.11 to 0.15 mm<sup>2</sup>/day for 5% silica fume overlays and from 0.15 to 0.23 mm<sup>2</sup>/day for 7% silica fume overlays with no clear trend identifiable, as shown in Fig 3.34. None of these differences are statistically significant at any  $\alpha$  level (Table 3.10). For 5% silica fume overlays sampled between 48 and 96 months (Fig. 3.33), the mean adjusted effective diffusion coefficient increases slightly, from 0.06 mm<sup>2</sup>/day to 0.08 mm<sup>2</sup>/day, as the slump increases from 38 mm (1.5 in.) to greater than 100 mm (4.0 in.), although the increase is not statistically significant (Table 3.10).

The mean adjusted effective diffusion coefficients are shown as a function of concrete slump for conventional overlays in Fig. 3.35. The mean adjusted effective diffusion coefficient for conventional overlays with a slump of 0 mm (0 in.) sampled

between 48 and 96 months old is significantly lower than the remaining categories (Table 3.10). This is not observed for placements sampled between 96 and 144 months, where the mean adjusted effective diffusion coefficients decrease from 0.10 mm<sup>2</sup>/day to 0.06 mm<sup>2</sup>/day with an increase in slump from 0 mm (0 in.) to 19 mm (0.75 in.). Similar to the silica fume overlays, however, none of these differences is statistically significant at any  $\alpha$  level (Table 3.10).

The mean adjusted effective diffusion coefficients are shown as a function of concrete slump for monolithic placements in Fig. 3.36. The diffusion coefficients vary from between 0.13 mm<sup>2</sup>/day to 0.20 mm<sup>2</sup>/day, with no apparent trend or significant differences between categories (Table 3.10).

### 3.6.2 Air Content

For silica fume overlay placements, the air content varies from 3.5 to 8.0%, with the categories ranging from 4.5 to 6.5%. For conventional overlay placements, the air content varies from 2.0 to 7.1%, and the categories ranging from 4.375 to 6.625%, and for monolithic bridge placements, the air content varies from 5.0 to 6.5%, with the categories ranging from 4.875 to 6.375%.

The mean adjusted effective diffusion coefficients for silica fume placements are shown as a function of air content in Figs. 3.37 and 3.38. For the 5% silica fume overlays sampled during the first 48 months after construction, the mean adjusted effective diffusion coefficient increases, as expected, from 0.11 mm<sup>2</sup>/day to 0.20 mm<sup>2</sup>/day as the air content increases from 4.5 to 6.5%, a difference that is statistically significant at  $\alpha = 0.10$  (Table 3.11). This trend becomes non-monotonic however, when the same samples are analyzed between 48 and 96 months. The mean adjusted effective diffusion coefficient for placements with an air content of 4.5% is 0.06 mm<sup>2</sup>/day. There is a slight increase, to 0.07 mm<sup>2</sup>/day, as the air content increases from 4.5 to 5.5%, but this difference is not statistically significant (Table 3.11). The

mean adjusted effective diffusion coefficient decreases to  $0.04 \text{ mm}^2/\text{day}$  as the air content is increased to 6.5%, although only three placements fall into this category. Samples taken between 48 and 96 months tend to indicate that, over time, diffusivity may be significantly less sensitive to changes in air content. The 5 and 7% silica fume overlays sampled during the first 48 months after construction are compared in Fig. 3.38. There is only one 7% silica fume deck in the 4.5% air content category. In the other two categories, the effective diffusion coefficients for the 7% silica fume placements are approximately the same as for the 5% silica fume placements. None of the differences is statistically significant (Table 3.11).

The mean adjusted effective diffusion coefficients for the conventional overlay placements are shown as a function of air content in Fig. 3.39. The diffusion coefficients for conventional overlays in both age ranges (48 to 96 months old and 96 to 144 months old) increase with increases in air content. Mean effective diffusion coefficients for conventional overlays between the ages of 48 and 96 months increase from  $0.08 \text{ mm}^2/\text{day}$  to  $0.15 \text{ mm}^2/\text{day}$  for an increase in air content from 4.375 to 6.625%, although in most cases, the differences between categories are not statistically significant (Table 3.11). The only two statistically significant differences ( $\alpha = 0.20$ ) occur when the highest air content category (6.625%) is considered. The trend is more pronounced for conventional overlays sampled between 96 and 144 months old. The mean adjusted effective diffusion coefficient increases from  $0.04 \text{ mm}^2/\text{day}$  to  $0.13 \text{ mm}^2/\text{day}$  with an increase in air content from 4.375 to 6.625%, a difference that is statistically significant at  $\alpha = 0.20$  (Table 3.11).

The mean adjusted effective diffusion coefficients for monolithic placements older than 120 months are shown as a function of air content in Fig. 3.40. The mean adjusted effective diffusion coefficients increase from  $0.12 \text{ mm}^2/\text{day}$  to  $0.20 \text{ mm}^2/\text{day}$  as the air content increases from 4.875 to 5.625%, a difference that is statistically significant at  $\alpha = 0.20$  (Table 3.11). The mean adjusted effective diffusion coefficient

decreases to  $0.10 \text{ mm}^2/\text{day}$  as the air content category continues to increase to 6.375%, a statistically significant difference at  $\alpha = 0.20$  (Table 3.11), even though only two placements are included in the last category. The small data set, however, limits the usefulness of this comparison.

### 3.6.3 Water-Cementitious Material Ratio

The water-cementitious material ratio should have the single largest effect on concrete diffusivity properties. In a controlled laboratory setting, lower water-cement ratios will result in lower diffusion coefficients. For example, some of the best diffusion results for overlay mixes obtained by Whiting and Detwiler (1998) had a water-cementitious material ratio of 0.30 and a silica fume content of 6%. The small ranges and small samples in the current study, however, mean that the trends are not always as expected.

Two water-cementitious material ratios, 0.38 and 0.40, were used for the 5% silica fume overlay placements compared to a single value, 0.37, for the 7% silica fume overlay placements. Water-cement ratios of 0.36, 0.38, and 0.40 were used for the conventional overlay placements, while water-cement ratios of 0.40 and 0.42 were used for the monolithic bridge decks. Due to small variations in the cement contents for silica fume and conventional overlays, the water-cementitious material ratios are almost exclusively a function of water content.

Two water contents were used for the 5% silica fume overlays in this study,  $141 \text{ kg/m}^3$  ( $238 \text{ lb/yd}^3$ ) and  $148 \text{ kg/m}^3$  ( $250 \text{ lb/yd}^3$ ). The 7% silica fume overlays had a water content for all bridge deck placements of  $138 \text{ kg/m}^3$  ( $232 \text{ lb/yd}^3$ ). For the conventional overlays, water contents were  $133 \text{ kg/m}^3$  ( $225 \text{ lb/yd}^3$ ),  $141 \text{ kg/m}^3$  ( $238 \text{ lb/yd}^3$ ), and  $148 \text{ kg/m}^3$  ( $250 \text{ lb/yd}^3$ ). The cementitious material content was  $370 \text{ kg/m}^3$  ( $623 \text{ lb/yd}^3$ ) or  $371 \text{ kg/m}^3$  ( $625 \text{ lb/yd}^3$ ) for the 5% silica fume overlays and  $371 \text{ kg/m}^3$  ( $625 \text{ lb/yd}^3$ ) or  $372 \text{ kg/m}^3$  ( $627 \text{ lb/yd}^3$ ) for the 7% silica fume overlays. The

cement content used for all of the conventional overlay bridge placements included in this study was  $371 \text{ kg/m}^3$  ( $625 \text{ lb/yd}^3$ ). For the monolithic decks, cement contents included  $357 \text{ kg/m}^3$  ( $602 \text{ lb/yd}^3$ ),  $359 \text{ kg/m}^3$  ( $605 \text{ lb/yd}^3$ ),  $379 \text{ kg/m}^3$  ( $639 \text{ lb/yd}^3$ ), and  $390 \text{ kg/m}^3$  ( $657 \text{ lb/yd}^3$ ). Only one bridge deck (bridge 89-204), however, was designed with a cement content of  $390 \text{ kg/m}^3$  ( $657 \text{ lb/yd}^3$ ).

The mean adjusted effective diffusion coefficients for silica fume placements are shown as a function of water-cementitious material ratio in Fig. 3.41. For the 5% silica fume overlays sampled within the first 48 months after construction, as the water/cementitious material ratio increases from 0.38 to 0.40 [water content increases from  $141 \text{ kg/m}^3$  ( $238 \text{ lb/yd}^3$ ) to  $148 \text{ kg/m}^3$  ( $250 \text{ lb/yd}^3$ )], the diffusion coefficient decreases from  $0.14 \text{ mm}^2/\text{day}$  to  $0.12 \text{ mm}^2/\text{day}$ . This decrease, however, is not statistically significant at any level of  $\alpha$  (Table 3.12). For 7% silica fume overlays with a water-cementitious material ratio of 0.37, the mean adjusted effective diffusion coefficient is  $0.18 \text{ mm}^2/\text{day}$ . For the 5% silica fume overlays sampled 48 to 96 months after construction, the trend is very similar. The diffusion coefficient decreases from  $0.11$  to  $0.07 \text{ mm}^2/\text{day}$  with an increase in the water-cementitious material ratio from 0.38 to 0.40. This difference is statistically significant at  $\alpha = 0.05$  (Table 3.12). This trend likely indicates problems during the finishing or curing processes at the lower water-cementitious material ratios. Under ideal conditions a decrease in the water-cementitious material ratio will result in a decrease in the diffusivity of the concrete.

The mean adjusted effective diffusion coefficients for conventional overlay placements are shown as a function of water-cement ratio in Fig. 3.42. For conventional overlays sampled 48 to 96 months after construction, as the water-cement ratio increases from 0.36 to 0.38 [water content increases from  $133 \text{ kg/m}^3$  ( $225 \text{ lb/yd}^3$ ) to  $141 \text{ kg/m}^3$  ( $238 \text{ lb/yd}^3$ )] the mean adjusted effective diffusion coefficient decreases from  $0.09$  to  $0.05 \text{ mm}^2/\text{day}$ , a difference that is statistically

significant at  $\alpha = 0.10$  (Table 3.12). For conventional overlays sampled 96 to 144 months after construction, as the water-cement ratio increases from 0.36 to 0.38 the mean effective diffusion coefficient decreases from 0.09 to 0.04 mm<sup>2</sup>/day. This difference is statistically significant at the highest level,  $\alpha = 0.02$  (Table 3.12). The trend for conventional overlays, however, reverses as the water-cement ratio increases to 0.40, with the diffusivity increasing significantly in both age categories. The mean adjusted effective diffusion coefficient for overlays with a water-cement ratio of 0.40 is 0.14 mm<sup>2</sup>/day for placements sampled between 48 and 96 months old and 0.12 mm<sup>2</sup>/day for placements sampled between 96 and 144 months old.

The mean adjusted effective diffusion coefficients for monolithic placements are shown as a function of water-cement ratio in Fig. 3.43. The mean adjusted effective diffusion coefficient increases from 0.13 mm<sup>2</sup>/day to 0.20 mm<sup>2</sup>/day as the water-cement ratio increases from 0.42 to 0.44, a difference that is statistically significant at  $\alpha = 0.20$  (Table 3.12).

#### **3.6.4 Percent Volume of Water and Cementitious Material**

The cement content of the overlay bridges included in this study is nearly identical for each overlay type. For this reason, any comparisons made between diffusion coefficients and water-cementitious material ratio, percent volume of water and cementitious material, and water content for these decks show similar trends. The mean adjusted effective diffusion coefficients as a function of the percent volume of water and cement for monolithic decks older than 120 months are presented in Fig. 3.44. For monolithic bridge decks, the volume of water and cement, determined from the initial mix design, ranges from 26.5% to 28.8% with categories of 27, 28, and 29%. The mean adjusted effective diffusion coefficients increase from 0.15 mm<sup>2</sup>/day to 0.20 mm<sup>2</sup>/day as the cement paste content increases from 27 to 29%. Due to the

small sample sizes, none of the results are statistically significant at  $\alpha = 0.20$  (Table 3.13), although the trend is clear.

### 3.6.5 Water and Cement Content

The mean adjusted effective diffusion coefficients as a function of water content for monolithic decks older than 120 months are shown in Fig. 3.45. The water contents for these placements range from  $147 \text{ kg/m}^3$  ( $248 \text{ lb/yd}^3$ ) to  $165 \text{ kg/m}^3$  ( $278 \text{ kg/m}^3$ ), corresponding to an increase in diffusivity from  $0.07 \text{ mm}^2/\text{day}$  to  $0.19 \text{ mm}^2/\text{day}$ , an increase that is statistically significant at  $\alpha = 0.20$  (Table 3.14).

The mean adjusted effective diffusion coefficients as a function of cement content for monolithic decks older than 120 months are shown in Fig. 3.46. The cement contents used in these placements include  $357 \text{ kg/m}^3$  ( $602 \text{ lb/yd}^3$ ),  $359 \text{ kg/m}^3$  ( $605 \text{ lb/yd}^3$ ),  $379 \text{ kg/m}^3$  ( $639 \text{ lb/yd}^3$ ), and  $390 \text{ kg/m}^3$  ( $657 \text{ lb/yd}^3$ ). Only one bridge deck (bridge 89-204), however, has a cement content of  $390 \text{ kg/m}^3$  ( $657 \text{ lb/yd}^3$ ) and is not included in Fig. 3.46. Because of the small difference, the monolithic decks with cement contents of  $357 \text{ kg/m}^3$  ( $602 \text{ lb/yd}^3$ ) and  $359 \text{ kg/m}^3$  ( $605 \text{ lb/yd}^3$ ) are included together as one category. The diffusivity increases from  $0.15 \text{ mm}^2/\text{day}$  to  $0.19 \text{ mm}^2/\text{day}$  as the cement content increases from  $357 \text{ kg/m}^3$  ( $602 \text{ lb/yd}^3$ ) to  $379 \text{ kg/m}^3$  ( $639 \text{ lb/yd}^3$ ), although this difference is not statistically significant (Table 3.15).

### 3.6.6 Compressive Strength

For the silica fume overlay placements, the concrete compressive strength varies from 36 to 62 MPa (5200 to 9000 psi) for the 5% silica fume overlays and from 43 to 63 MPa (6300 to 9100 psi) for the 7% silica fume overlays. For the conventional overlay placements, the compressive strength varies from 34 to 50 MPa (4900 to 7300 psi). For the monolithic overlay placements, the concrete compressive strength varies from 29 to 51 MPa (4200 to 7400 psi). The categories for all bridge

deck types range from 31 to 59 MPa (4500 to 8500 psi). In all cases, concrete diffusivity would be expected to drop with increasing compressive strengths due to lower water-cement ratios and concrete maturation.

The mean adjusted effective diffusion coefficients for the silica fume overlays are shown as a function of concrete compressive strength in Figs. 3.47 and 3.48. For the 5% silica fume overlays sampled 0 to 48 months after construction, there is a slight, but nonmonotonic increase in the diffusivity as the compressive strength increases from 38 to 59 MPa (5500 to 8500 psi). The only difference statistically significant difference ( $\alpha = 0.10$ ) occurs as the compressive strength increases from 45 to 52 MPa (6500 to 7500 psi) (Table 3.16). When 5% silica fume overlays sampled 48 to 96 months after construction are considered, diffusivity drops off as the compressive strength increases above 38 MPa (5500 psi). Very few 7% silica fume overlays are available, and no clear correlation between the mean adjusted effective diffusion coefficient and concrete compressive strength is apparent for these decks.

The mean adjusted effective diffusion coefficients for the conventional overlays and monolithic placements are shown as a function of concrete compressive strength in Figs. 3.49 and 3.50. For the conventional overlays in both age ranges, the mean adjusted effective diffusion coefficient only varies slightly with compressive strength. The same is true for the monolithic placements, and none of the differences is statistically significant (Table 3.16).

## **CHAPTER 4: TIME AS A VARIABLE IN BRIDGE DECK CRACKING**

### **4.1 GENERAL**

In this chapter, bridge deck cracking is evaluated based on age and the date of construction. The results show that deck cracking increases slowly as the deck ages, and for most decks, the majority of cracking is established early on in the life of the bridge. To aid in later comparisons, an age correction term is determined for each bridge deck type using crack density data obtained for bridges surveyed on more than one occasion as a part of multiple studies (Schmitt and Darwin 1995, Miller and Darwin 2000). A cracking rate is determined for each bridge deck type and applied to the raw crack density data to aid in isolating particular variables by eliminating the influence that age may have on the comparisons. These age-corrected crack densities are the basis for the performance evaluations in Chapter 5.

When crack density is plotted versus date of construction, two distinct trends emerge. First, more recently constructed monolithic and conventional overlay decks exhibit higher crack densities than older bridges of the same type. Second, the converse is true for silica fume overlay decks, with bridges built 15 years ago exhibiting higher crack densities than more recently built bridges, even when age is taken into account. Changes in construction techniques, concrete mix designs, and environmental site conditions appear to be responsible for both trends. To help determine which of these changes plays a role in bridge deck cracking, construction, design, and environmental variables are plotted versus the date of construction. Since the characteristics of the concrete used in subdecks and monolithic decks differ from those of the concrete used for overlays, these two materials are evaluated separately.

## 4.2 INCLUSION OF DATA FROM PREVIOUS STUDIES IN KANSAS

Bridge deck survey data gathered by Schmitt and Darwin (1995) and Miller and Darwin (2000) are included with the data obtained in this study to increase the sample size and the range of ages and construction dates used in the analysis. A high percentage of the bridges surveyed as a part of this study (49 out of 59) have been surveyed previously (see Table 2.1). The only bridges included in this study that have not previously been surveyed are the newest silica fume overlay bridges, those containing 7% silica fume by weight of cementitious material.

Although effort is made to keep bridge survey methods consistent, the observations are inherently subjective, and the results must be scrutinized to determine if a reasonable correlation exists between studies. Figures 4.1, 4.2, and 4.3 present a bridge-by-bridge comparison of crack densities for bridges surveyed in more than one study for monolithic bridge decks, conventional high-density overlay decks, and silica fume overlay decks, respectively.

The results for the monolithic decks (MONO) are shown in Fig. 4.1. Crack densities for 12 of the 13 bridge decks from the current study are greater than the densities measured by Schmitt and Darwin (1995). The crack density of the one remaining deck differs by  $0.06 \text{ m/m}^2$ , or about 12%. The crack densities for the monolithic decks surveyed by Miller and Darwin (2000) are greater than the crack densities obtained by Schmitt and Darwin (1995) for the three bridges included in both studies.

The results for the conventional overlay decks (CO) are presented in Fig. 4.2. Crack densities for 12 of the 16 bridge decks from the current study are higher than crack densities obtained by Miller and Darwin (2000). Of the four remaining bridges, the crack densities are the same for one, and lower by  $0.05 \text{ m/m}^2$  (11%),  $0.07 \text{ m/m}^2$  (8%), and  $0.23 \text{ m/m}^2$  (26%) for the other three. The crack densities measured by Miller and Darwin (2000) are greater than those measured by Schmitt and Darwin

(1995) for only two out of the six bridges included in both studies. Three of the other four decks, however, differ by  $0.04 \text{ m/m}^2$  or less (maximum of 6%), and the remaining deck differs by  $0.15 \text{ m/m}^2$  (28%).

The results for silica fume overlay decks (SFO) are presented in Fig. 4.3. Crack densities for 16 out of the 20 bridge decks surveyed in the current study are greater than those obtained by Miller and Darwin (2000). Two of the remaining bridges, 89-184 and 89-187, are also part of the study by Schmitt and Darwin (1995). The crack density results for bridge 89-187 decreased with each successive survey. The crack density results from Miller and Darwin (2000) for bridge 89-184 increased by  $0.32 \text{ m/m}^2$  (46%) compared to the results obtained by Schmitt and Darwin (1999) and then decreased by  $0.13 \text{ m/m}^2$  (13%) for the current study. These bridges were constructed prior to the development of special provisions and have areas of significant plastic shrinkage cracking and excessive fine-width transverse cracks. For these reasons, these silica fume overlays are only included in the bridge age and construction date analysis and not included in the comparisons presented in Chapter 5.

For the majority of bridge decks, crack density increases with age (successive surveys). That is, with all else being equal, a bridge surveyed 10 years after construction will have a higher crack density than a bridge surveyed one year after construction. Figures 4.4, 4.5, and 4.6 present comparisons of the crack densities obtained for bridges surveyed in multiple studies. In the figures, results from the more recent study are plotted versus the results from an earlier study. In the three plots, the vast majority of the data points fall above the 45-degree line, indicating an increase in crack density with time. Data points that fall below the 45-degree line, indicating a decrease in cracking versus time, may occur as the result of increased relaxation (creep) in the bridge deck or may be due to differences inherent in processes that require human judgment, even though the survey methods (described

in Section 2.4, with a draft specification provided in Appendix B) are designed to provide consistent results. The balance of this chapter will focus on the [rate](#) at which cracking occurs for different bridge deck types, the amount of cracking observed for bridges constructed in different construction eras, and changes in bridge designs, construction techniques, concrete mix designs, or environmental conditions that may account for these observations.

### **4.3 BRIDGE DECK CRACKING VERSUS TIME**

Bridge deck age is equal to the difference between the survey date and the date of the last concrete placement. The monolithic decks evaluated as a part of this study range in age from 12 to 240 months (Fig. 4.7). The conventional overlay decks range in age from 20 to 145 months (Fig. 4.8), and the silica fume overlay decks range in age from 4 to 142 months (Fig. 4.9). Only two silica fume overlay decks, 89-184 and 89-187, are older than 97 months. The average age for all 59 bridge decks at the time of survey is 78 months.

Data points connected by lines in Figs. 4.7 through 4.9 represent bridges surveyed on more than one occasion as a part of separate studies. Although crack density appears to only increase gradually over time, it is clear that crack density is dependant on deck age.

There is substantial scatter between the initial crack density values for all bridge deck types, presumably due to the myriad of variables that contribute to deck cracking. The crack density for most bridges, however, appears to increase at a similar rate for each bridge deck type. To eliminate bridge age as a variable and allow bridges to be compared on an equal-age basis, the technique of dummy variables (Draper and Smith 1981) is used to determine the mean rate of increase in crack density for each of the three bridge deck types. This multiple linear regression method assumes that the actual increase in crack density over time is linear and

independent of the initial crack density of the bridge deck. Multiple surveys of the same bridge at different ages lends itself very well to the application of this technique.

The results of the dummy variable analysis for monolithic, conventional overlay, and silica fume overlay decks are presented in Table 4.1. The cracking rate for conventional overlay decks is the least ( $0.0008 \text{ m/m}^2/\text{month}$ ), while the cracking rate for silica fume overlay decks is over three times that level ( $0.0028 \text{ m/m}^2/\text{month}$ ). The mean age at the time of the surveys for all 5% silica fume overlay decks is 53 months, 34 months younger than the conventional overlay decks and 62 months younger than the average age for monolithic decks.

According to Le, French, and Hajjar (1998), the initial shrinkage rate has a greater effect on cracking than the total shrinkage and so it comes as no surprise that silica fume decks, with the lowest average age, have the highest cracking rate. In addition, for all deck types, the greatest percentage of crack density is established early on in the life of the decks. Based on these observations, it appears that the key to minimizing total crack density is to limit initial cracking.

The cracking rates obtained from the dummy variable analyses are used to adjust the raw crack density data obtained from the surveys of each bridge. These adjustments represent an age correction that helps to isolate individual parameters by eliminating differences in deck performance due to age. All of the raw crack density data is adjusted to an age of 78 months, the average age at the time of the survey for all bridge deck types. For bridges that were surveyed in more than one study, the age-corrected crack density is calculated by averaging the individual age-corrected crack densities obtained for the bridge in each study. The results of the field surveys from all three studies in addition to the age-corrected crack densities for each bridge deck surveyed are tabulated in Table E.1 of Appendix E.

#### 4.4 CRACK DENSITY VERSUS CONSTRUCTION ERA

Many changes related to bridge deck design, construction procedures, and material specifications have occurred since the first bridge in this study was built in 1983. Figures 4.10 through 4.12 show average crack density plotted versus construction date for each bridge deck type. Two distinct trends emerge. First, the crack densities (and age-corrected crack densities) for both monolithic and conventional overlay decks are higher for the newer bridge decks (Figs. 4.10 and 4.11). Conversely, the crack density of the silica fume overlay decks is generally lower for the newer decks (Fig. 4.12), although the most recently constructed 7% silica fume overlay decks have not shown continued improvement.

The age correction adjustment has the greatest effect on both the oldest and newest bridges included in the study. The greatest difference between the average measured crack densities and the age-corrected crack densities is  $0.16 \text{ m/m}^2$  and occurs for the most recently constructed silica fume overlay decks (Fig. 4.12). Since none of the 7% silica fume overlay decks have been surveyed on more than one occasion, the cracking rate calculated for the 5% silica fume decks is applied to the 7% silica fume overlay decks. In no case, however, does the age correction adjustment change the trends observed in the raw data. The age-corrected crack density will be referenced in the balance of this report.

As a variable, the date of construction (and the associated aspects of construction procedures and materials) has had a measurable impact on cracking in bridge decks. In Fig. 4.10, monolithic bridge decks are placed in two groups based on casting date, 1984–1987 and 1990–1993. Monolithic decks constructed between 1990 and 1993 have an average age-corrected crack density,  $0.50 \text{ m/m}^2$ , that is more than three times the age-corrected crack density,  $0.16 \text{ m/m}^2$ , of monolithic decks constructed between 1984 and 1987 (Fig. 4.10). The difference in age-corrected

crack density for these two age groups is statistically significant at  $\alpha = 0.02$  (Table 4.2).

Similar results are shown for bridges with conventional overlays, which are placed in three groups: 1985–1987, 1990–1992, and 1993–1995. Conventional overlay decks constructed between 1993 and 1995 have an average age-corrected crack density of  $0.81 \text{ m/m}^2$  (Fig. 4.11). Conventional overlay decks constructed between 1990 and 1992 have an average age-corrected crack density,  $0.53 \text{ m/m}^2$ , more than two times the age-corrected crack density,  $0.24 \text{ m/m}^2$ , of conventional overlay decks constructed between 1985 and 1987 (Fig. 4.11). All of the differences in the average age-corrected crack density for each of these age categories is statistically significant at  $\alpha = 0.02$  (Table 4.2).

The crack density results for monolithic and conventional overlay decks stand in sharp contrast to the results for silica fume overlay decks. For the periods 1990–1991, 1995–1996, and 1997–1998, the age-corrected crack density dropped from  $0.87$  to  $0.42 \text{ m/m}^2$  between the first and third time period. The trend is not entirely monotonic, however, and for the most recent time period, 2000–2002, the mean age-corrected crack density increased to  $0.48 \text{ m/m}^2$ . Although most of the differences in the age-corrected crack densities between these groups are not statistically significant (Table 4.2), it is clear that improvement has been made since the first silica fume decks were built in 1990.

A number of changes in concrete materials and construction procedures over the past 20 years may explain the observations found in Figs. 4.10 through 4.12. During this period, cement has become progressively finer, as producers have chosen to develop higher early strength cements. Finer cements lead to greater shrinkage (Chariton and Weiss 2002).

Concrete placement, which used to involve cranes and buckets, is now almost universally performed by pump. Concretes that are pumped generally require higher

paste contents for the efficient use of the equipment than concretes that are not. In addition, any trend toward the use of higher slump concretes for use with pumping would be expected to increase settlement cracking and, thus, total crack density. Finishing machines have also changed during this period. In the early 1980s, bridge decks in Kansas were finished primarily with vibrating screeds. Over the intervening years, the screeds changed, first to single roller drum screeds and, more recently, to double drum roller screeds. Roller screeds move more paste to the surface than vibrating screeds, which tends to increase plastic shrinkage cracking.

The trend for silica fume overlay decks built between 1990 and 1998 shown in Fig. 4.12 reflects a major effort to limit the evaporation of water during concrete placement, finishing, and before the initiation of wet curing. As discussed previously, the most recently constructed silica fume overlay decks, those built between 2000 and 2002, have a silica fume content of 7 percent. The recent increase in cracking indicates that the additional silica fume, even with the careful attention to evaporation that had previously decreased cracking (Fig. 4.12), has directly translated into increased cracking.

#### **4.5 CRACK DENSITY VERSUS SILICA FUME OVERLAY SPECIFICATION**

Many of the changes that have likely resulted in decreased cracking for silica fume overlay decks since 1990 can be attributed to modifications made to the standard specifications. Since 1990, there have been 11 such revisions regarding the design and construction of silica fume overlays. For conventional overlays, five revisions have been made since 1990, although only Special Provisions 90P-95, 90P-95-R1, and 90P-95-R2 were used to construct the bridges in this study built after 1990. No significant changes thought to affect bridge deck cracking were made during these revisions.

Eight of the 11 silica fume overlay revisions (90P-158-R1, R2, R3, R4, R5, R6, and 90M-158-R8 and R9) were used to construct the 30 silica fume overlay decks examined in this study. The mean age-corrected crack density is plotted versus the special provision number used during construction in Fig. 4.13. It is clear that progress has been made since the first silica fume overlay decks were constructed prior to the first special provision. With the implementation of provisions 1 and 2, fogging and/or the use of a precure material were required after finishing the surface. Upon implementation, the mean age-corrected crack density decreased from 0.87  $\text{m}/\text{m}^2$  to 0.58  $\text{m}/\text{m}^2$ , of a difference statistically significant at  $\alpha = 0.20$  (Table 4.3). Special Provision 90P-158-R3 increased the curing period from 72 hours to 7 days, although it was not entirely clear whether the burlap used during the curing period had to be kept continuously moist for the duration of the curing period. Consequently, the mean age-corrected crack density increased slightly from 0.58  $\text{m}/\text{m}^2$  for bridges constructed using 90P-158-R1 and R2 to 0.61  $\text{m}/\text{m}^2$ , although this difference is statistically insignificant (Table 4.3). The mean age-corrected crack densities for bridges constructed using Special Provisions 90P-158-R1 through R3 are, however, statistically different than the mean age-corrected crack density obtained for decks built before the first special provision.

Special Provisions 90P-158-R4, R5, and R6 require the contractor to monitor and maintain an evaporation rate below 1.0  $\text{kg}/\text{m}^2/\text{hr}$  (0.2  $\text{lb}/\text{ft}^2/\text{hr}$ ) in addition to fogging and the application of a precure material immediately after placement. Unlike Provision R3, Provisions R4, R5, and R6 also require the contractor to keep the burlap “wet 100 percent of the time during the [seven day] cure period.” The mean age-corrected crack density for bridges built using these provisions decreased from 0.61  $\text{m}/\text{m}^2$  to 0.39  $\text{m}/\text{m}^2$ , a statistically significant difference at  $\alpha = 0.05$  (Table 4.3). For Special Provisions 90M-158-R7 through R10, the most notable change is the increase in silica fume content from 5% by mass of cement to 7% by mass of

cementitious materials. In addition to increasing the required silica fume content, the use of drum roller screeds is allowed in lieu of oscillating screeds, required under the earlier special provisions. The mean age-corrected crack density for these bridges increased from  $0.39 \text{ m/m}^2$  for bridges constructed under provisions 4, 5, and 6 to  $0.48 \text{ m/m}^2$ , although this increase is not statistically significant at any level of  $\alpha$ .

The balance of the chapter identifies specific changes in bridge deck concrete mix designs, environmental conditions at the time of placement, and bridge deck designs.

#### **4.6 MATERIAL PROPERTIES VERSUS CONSTRUCTION DATE**

Based on the observations presented in Section 4.4, it is important to identify the changes that may have resulted in increased cracking for more recently constructed monolithic and conventional overlay decks (Fig. 4.10 and 4.11) and generally decreased cracking for more recently constructed silica fume overlay decks (Fig. 4.12). The balance of the chapter examines different material, environmental, and design-related changes since the first bridge in this study was constructed in 1983.

The analysis of these changes is broken into two main categories: (1) monolithic and subdeck placements and (2) overlay placements. Monolithic and overlay subdecks are plotted together, as are the different overlay types. This analysis includes all bridges in the current study (and by Miller and Darwin 2000) and all relevant bridges evaluated by Schmitt and Darwin (1995, 1999). In total, 42 5% silica fume overlay placements, 14 7% silica fume overlay placements, 58 conventional overlay placements, 36 monolithic bridge deck placements, and 60 subdeck placements are included in the comparisons. There are substantial differences between the different bridge deck types and high scatter with a low linear coefficient of determination  $R^2$  in all cases.

More detailed evaluations of the changes in material properties are presented in the balance of this section. The key observations from these analyses can be summarized as follows:

For **monolithic** deck and **overlay subdeck** placements, there is a clear trend towards increasing slump for more recently constructed bridges, particularly for monolithic deck placements. There is no correlation between air content, percent volume of water and cement, cement content, water content, or water/cement ratio with construction date. There is a tendency towards higher compressive strengths for the most recently constructed monolithic decks, but no correlation exists between compressive strength and construction date for overlay subdeck placements. In either case, the compressive strengths are well above the strengths required by design.

For **conventional** and **silica fume overlay** placements, there is no correlation between slump and concrete placement date. The slump for conventional overlay placements is below 25 mm (1.0 in.), while the slump for all silica fume overlay placements is at least 20 mm (0.8 in.). There is a slight tendency towards increasing air contents for more recently constructed overlays. There is no correlation between the percent volume of water and cementitious material, water content, cementitious material content, and water/cementitious material ratio and placement date. There is a tendency towards increasing compressive strength over the past 20 years, although this increase has also been accompanied by an increase in the range of compressive strengths of bridge decks.

#### **4.6.1 Slump**

Average concrete slump versus construction date for monolithic and overlay subdeck placements is presented in Fig. 4.14. The slumps range from 38 mm (1½ in.)

to 89 mm (3½ in.). There is substantial scatter, although the slump of monolithic and overlay subdeck placements exhibit a clear upward trend with time. The placement slump versus construction date for overlays is presented in Fig. 4.15. The slumps of the overlay placements range from 0 mm (0 in.) to 160 mm (6.3 in.), and represent two entirely different schools of thought. All but one of the conventional overlays are placed with a slump below 25 mm (1.0 in.), while the subsequent silica fume overlays are all placed with a minimum slump of 20 mm (0.8 in.) and an average slump of 60 mm (2.4 in.). This increase in slump for the silica fume overlays is based on a change in the special provisions that increases the target slump from the maximum specified for conventional overlays, 19 mm (¾ in.), to between 50 (2 in.) and 125 mm (5 in.) for silica fume overlays.

#### **4.6.2 Air Content**

The air content of monolithic decks and overlay subdecks is presented in Fig. 4.16. For these decks, the average air content is nearly constant over time. Of the 114 monolithic and overlay subdeck placements, only three do not have an air content between 4 and 7%. The average air content for these placements is 5.5%. The average air content versus construction date for overlay placements is presented in Fig. 4.17. There is a slight increase in air content over time, accompanied by an increase in the range of air contents. The average air content for the conventional overlays is 5.3% with a standard deviation of 0.8%. The average air content for 5% silica fume overlays is also 5.3%, but with a standard deviation of 1.0%. The average air content for the 7% silica fume overlay is 6.2% with a standard deviation of 1.1%.

#### **4.6.3 Percent Volume of Water and Cementitious Materials**

The volume of water and cement (cement paste) as a percentage of concrete volume for monolithic decks and overlay subdecks is plotted versus construction date

in Fig. 4.18. With only one exception (bridge 30-93), portland cement is the only cementitious material used in the monolithic and overlay subdeck placements. Silica fume is only used in overlays.

As shown in Fig. 4.18, there is substantial variation between the different bridge deck types, although the trend line is nearly horizontal. The percent volume of water and cement for the majority of the oldest monolithic decks (constructed before 1988) and the newest silica fume overlay subdecks (7%, constructed after 1998) is less than the values for the conventional and 5% silica fume overlay subdecks, constructed after the monolithic decks and before the 7% silica fume overlay subdecks. For silica fume and conventional overlay subdecks, these observations are largely attributable to changes in the water content. For monolithic decks, changes in the percent volume of cement paste are a result of changes in both the water and cement content of the placements.

The percent volume of water and cementitious materials for the overlays is plotted versus construction date in Fig. 4.19. The values for conventional overlays range between 25.1 and 26.6%. Thirty-five out of the 43 5% silica fume overlay placements contain very close to 26.8 percent cement paste, while the rest contain between 26.0 and 26.2% cement paste. All 16 of the 7% silica fume overlay placements contain between 25.8 and 26.0% paste.

#### **4.6.4 Water Content**

The water contents of monolithic decks and overlay subdecks are plotted versus date of construction in Fig. 4.20. The water contents range from 143 kg/m<sup>3</sup> (241 lb/yd<sup>3</sup>) to 173 kg/m<sup>3</sup> (292 lb/yd<sup>3</sup>). The water contents for overlays range from 133 kg/m<sup>3</sup> (224 lb/yd<sup>3</sup>) to 148 kg/m<sup>3</sup> (250 lb/yd<sup>3</sup>), as shown in Fig. 4.21. No consistent correlation exists between water content and construction date. Because of the minimal variation in cementitious material contents for these placements, the

trends observed for water content are nearly identical to the trends observed for percent volume of water and cementitious material (Section 4.5.3).

#### **4.6.5 Cementitious Material Content**

The cement content of monolithic decks and overlay subdecks versus date of construction is presented in Fig. 4.22. There are three primary cement contents used in the mix designs for monolithic and subdeck placements. Only six out of the 91 placements have cement contents other than  $357 \text{ kg/m}^3$  ( $602 \text{ lb/yd}^3$ ),  $359 \text{ kg/m}^3$  ( $605 \text{ lb/yd}^3$ ), or  $379 \text{ kg/m}^3$  ( $639 \text{ lb/yd}^3$ ). The majority of the monolithic and overlays subdeck data falls into the  $357 \text{ kg/m}^3$  ( $602 \text{ lb/yd}^3$ ) category, and 8 out of 40 silica fume overlay subdeck placements have cement contents other than  $357 \text{ kg/m}^3$  ( $602 \text{ lb/yd}^3$ ). The cementitious material content for overlays is constant and depends only on the overlay type. The cement content of all conventional overlays is  $371 \text{ kg/m}^3$ , and the cementitious material content for all silica fume overlays have values between  $370 \text{ kg/m}^3$  ( $623 \text{ lb/yd}^3$ ) and  $372 \text{ kg/m}^3$  ( $627 \text{ lb/yd}^3$ ).

#### **4.6.6 Water-Cementitious Material Ratio**

Only the silica fume overlays and a single subdeck contain cementitious materials other than portland cement. The one subdeck (bridge 30-93) contains a 33% replacement of cement with ground granulated blast furnace slag, and the silica fume overlays contain either 5% or 7% silica fume. The water/cement ratio for the monolithic decks and subdeck placements is plotted versus construction date in Fig. 4.23. The water/cement ratios range from between 0.40 to 0.45. The water/cementitious material ratio for the overlay placements is plotted versus construction date in Fig. 4.24. The water/cementitious material ratios range from between 0.36 and 0.40. There are no distinct trends with construction date for water/cement or water/cementitious material ratio.

#### **4.6.7 Compressive Strength**

Compressive strength is plotted versus construction date for monolithic and overlay subdecks in Fig. 4.25. There is a clear trend towards increasing compressive strengths when plotted versus placement date for the monolithic decks. This trend towards increasing compressive strengths does not exist for the overlay subdeck placements. The average compressive strength for all monolithic and overlay subdecks is 40 MPa (5800 psi). This is well above the typical strength requirements and indicates an effort to produce concretes with high early strengths. The trend for overlays is pronounced (Fig. 4.26), with the average strength of overlays increasing over time. The compressive strength for all overlays ranges from 34 MPa (4900 psi) to 63 MPa (9100 psi). Average compressive strengths increase from 44 MPa (6400 psi) for conventional overlays to 49 MPa (7100 psi) for 5% silica fume overlays to 51 MPa (7400 psi) for 7% silica fume overlays.

#### **4.7 SITE CONDITIONS VERSUS CONSTRUCTION DATE**

Environmental conditions can be key indicators of the potential for bridge deck cracking to occur as a result of thermally induced loads (Babaei and Purvis 1996). Additionally, plastic shrinkage cracking is aggravated by high evaporation rates that can be a result of high air temperatures. It is important to determine, even if in part, whether bridge decks are being constructed during periods of increasingly demanding environmental conditions. The environmental conditions under consideration are high and low air temperature, average temperature, and daily air temperature range. These data are available directly from the bridge construction records. A substantial amount of scatter is expected due to the changes in temperature for different seasons, which in all cases, results in a very low coefficient of determination  $R^2$ . As in the previous section, the placements are divided into (1) monolithic and overlay subdeck placements and (2) overlay placements.

More detailed evaluations of the changes in material properties are presented in the balance of this section. The key observations from these analyses can be summarized as follows:

In general, the average, minimum, and maximum daily air temperatures for **monolithic** placements constructed between 1984 and 1995 are lower than for **overlay subdecks** constructed between 1990 and 2002. The average daily temperature for all monolithic placements, on average, is 7° C lower than for the more recently constructed overlay subdecks. The minimum and maximum daily air temperatures, on average, are, respectively, 7° and 5° C higher for overlay subdeck placements than for monolithic placements. There is no correlation between the daily air temperature range and placement date for monolithic or overlay subdeck placements.

**Silica fume overlays** placed between 1990 and 2002 were generally cast at lower air temperatures than the **conventional overlay** placements constructed between 1990 and 1995. The average daily temperature for all silica fume placements, on average, is 4° C lower than the conventional overlays. The minimum and maximum daily air temperatures, on average, are 5° and 10° C lower for silica fume overlay placement than for conventional overlay placements. There is no correlation between the daily air temperature range and placement date for the overlay decks.

#### **4.7.1 Minimum Daily Air Temperature**

The minimum daily air temperature for the day of placement is plotted versus construction date for monolithic and overlay subdeck placements in Fig. 4.27. The temperatures range from -7° to 24° C. There is a significant difference between the average daily minimum temperature for monolithic placements cast between 1984 and 1990 and subdeck placements cast between 1990 and 2002. The minimum daily

air temperature for monolithic placements cast between 1984 and 1990 ranges from  $-3^{\circ}$  to  $12^{\circ}$  C with an average of  $6^{\circ}$  C. In contrast, the minimum daily air temperature for subdeck placements cast after 1990 ranges from  $-7^{\circ}$  to  $24^{\circ}$  C, with an average of  $13^{\circ}$  C.

The minimum daily air temperature for the day of placement is plotted versus construction date for overlay bridges in Fig. 4.28. The values range from  $-4^{\circ}$  to  $24^{\circ}$  C. There does not appear to be a correlation between minimum daily air temperature and placement date for either overlay types cast after 1992. Overlays cast between 1983 and 1992, however, are consistently placed with higher minimum daily air temperatures. The minimum daily temperature for overlay decks cast between 1983 and 1992 ranges from  $3^{\circ}$  to  $24^{\circ}$  C with an average of  $14^{\circ}$  C. In contrast, the minimum daily air temperature for overlays cast after 1992 range from  $-4^{\circ}$  to  $24^{\circ}$  C, with an average of  $9^{\circ}$  C.

#### **4.7.2 Maximum Daily Air Temperature**

The maximum daily air temperature is plotted versus construction date for monolithic and overlay subdeck placements in Fig. 4.29. The values range from  $6^{\circ}$  to  $39^{\circ}$  C. Similar to the minimum daily air temperature, the maximum daily temperature for the monolithic decks cast between 1984 and 1990 is consistently lower than that of the more recently placed overlay subdecks. The maximum daily air temperature for monolithic placements cast between 1984 and 1990 ranges from  $6^{\circ}$  to  $31^{\circ}$  C with an average of  $19^{\circ}$  C. In contrast, the maximum daily air temperature for subdeck placements cast after 1990 ranges from  $10^{\circ}$  to  $39^{\circ}$  C with an average of  $24^{\circ}$  C.

The maximum daily air temperature for overlay placements is plotted versus construction date in Fig. 4.30. The values range from  $7^{\circ}$  to  $37^{\circ}$  C. There is a slight trend towards decreasing high daily air temperatures, although this trend is primarily a product of generally higher daily temperatures for conventional overlay decks cast

before 1995. The average maximum daily air temperature is 29° C for conventional overlay placements, while the average is only 19° C for silica fume overlays.

#### **4.7.3 Average Daily Air Temperature**

Average air temperature, equal to the average of the high and low daily temperatures, is plotted versus construction date for monolithic and overlay subdeck placements in Fig. 4.31. Because the average daily air temperature is directly related to the high and low daily air temperatures, the trends are similar. Monolithic decks cast between 1984 and 1990 were frequently placed at lower air temperatures than the overlay subdecks cast since 1990. The average air temperature during placement is 13° C for monolithic decks and 20° C for overlay subdecks.

The average air temperature is plotted versus construction date for overlays in Fig. 4.32. The values range from 30° to 4° C. There is a slight trend towards decreasing average temperatures, although this trend is again, primarily a product of generally higher average temperatures for the conventional overlay decks. The average temperature has decreased from 21° C for the conventional overlays to 17° C for the silica fume overlays.

#### **4.7.4 Daily Air Temperature Range**

The daily air temperature range is defined as the difference between the high and low daily temperatures. The daily air temperature range is plotted versus construction date for monolithic and overlay subdeck placements in Fig. 4.33. The values vary between 22° and 2° C, and the average daily air temperature range is 13° C for both monolithic and overlay subdeck placements. For overlay placements, the daily air temperature range varies from 27° to 3° C (Fig. 4.34). In spite of the positive slope shown in Fig. 4.33 and 4.34, no real trend is apparent. The average daily air

temperature range increases slightly from 13° C for conventional overlays to 14° C for silica fume overlays.

#### **4.8 BRIDGE DESIGN VERSUS CONSTRUCTION DATE**

To gain a better understanding of the bridge design factors that may contribute to bridge deck cracking, it is desirable to gain an historical perspective on what changes have occurred as a matter of preference for the bridges included in this study. Although variables such as span length and bridge length and their relation to bridge deck cracking will be examined in Chapter 5, they are dependant on the particular bridge site and do not represent a construction trend.

Five design-related variables will be considered for each bridge deck type: the type of steel superstructure, deck thickness, transverse bar spacing, top cover, and transverse bar size are plotted versus the last day of concrete placement for each bridge deck type. One data point is plotted for each bridge. The results indicate that no correlation exists between these variables and the date of concrete placement for any of the bridge deck types.

##### **4.8.1 Structure Type**

Three types of steel superstructures are examined: SMCC (steel beam, composite continuous), SWCC (steel welded plate girder, composite continuous), and SWCH (steel welded plate girder, composite continuous and haunched). The steel structure type is plotted versus construction date for all bridge deck types in Fig. 4.35. In total, 25 SMCC, 44 SWCC, and 13 SWCH bridges were included in the study. No bias is apparent towards any of the three bridge types.

#### **4.8.2 Deck Thickness**

Deck thickness is plotted versus construction date for all bridge deck types in Fig. 4.36. The decks range in thickness from 203 mm (8.0 in.) to 229 mm (9.0 in.). The majority of bridge decks are constructed with a deck thickness of 216 mm (8.5 in.) or 229 mm (9.0 in.); however, the newest silica fume decks are primarily 220 mm (8.7 in.) thick.

#### **4.8.3 Transverse Bar Spacing**

Transverse bar spacing is plotted versus construction date for all bridge decks in Fig. 4.37. The transverse bar spacing ranges from 100 mm (4.0 in.) to 300 mm (11.8 in.), although most of the bridge decks have bar spacings between 150 mm (6.0 in.) and 200 mm (8.0 in.). While some conventional overlay decks have bar spacings less than 150 mm (6.0 in.), only two out of thirty silica fume overlay bridges have bar spacing less than 150 mm (6.0 in.).

#### **4.8.4 Top Reinforcing Bar Cover**

Top reinforcing bar cover is plotted versus construction date for all bridge deck types in Fig. 4.38. Forty-six of the overlay bridges collected in this study have a top bar cover of 75 mm (3.0 in.), while one silica fume overlay has a top reinforcing bar cover of 80 mm (3.1 in.). In addition, five monolithic decks have a top cover of 75 mm (3.0 in.), while the remaining bridges have a top bar cover of 64 mm (2.5 in.).

#### **4.8.5 Transverse Bar Size**

The top transverse bar size is plotted versus construction date for all bridge deck types in Fig. 4.39. Four bar size combinations are used in the bridges included in this study: No. 13 and No. 16 (No. 4 and No. 5), No. 16 (No. 5), No. 16 and No. 19 (No. 5 and No. 6), and No. 19 (No. 6). Only one monolithic deck, bridge 105-046,

has top bars greater than No. 16 (No. 5), while a significant portion of conventional overlays and 5% silica fume overlays have larger top transverse bars.

## CHAPTER 5: CRACK SURVEY EVALUATION AND RESULTS

### 5.1 GENERAL

Bridge deck performance is evaluated based on crack densities corrected to an age of 78 months (6½ years), the average age of all bridge decks at the time of sampling. This age-related analysis is explained in Chapter 4. The influence of individual variables related to the deck type, material properties of the concrete, construction site conditions during placement, bridge design parameters, bridge contractor, and traffic are analyzed by directly comparing variables from these categories with measured crack densities. Data collected from these categories is compared with data obtained from the four bridge deck types evaluated in this study: 5% and 7% silica fume overlays, conventional overlays, and monolithic placements.

It is clear from the analysis that many factors contribute to bridge deck cracking, although material-related factors generally appear to have the greatest effect. In addition, trends observed for monolithic decks are clearer than trends observed for overlay decks, presumably due to the additional variables associated with the overlays. For this reason, the effect of material properties and site conditions on crack density is expanded to include overlay subdecks.

The properties of overlay bridge subdecks play a large role in the overall performance of bridge decks. Cracks originating in the subdeck presumably “reflect” into the overlay and adversely influence performance. Due to the presence of overlays, however, the subdecks are not directly observable. For this reason, crack densities obtained on the overlays above a subdeck are used to gauge performance. Typically the crack density for the full bridge deck is used to represent the crack density of the subdeck because the subdeck was cast on one or two days and the location of each subdeck placement was not permanently recorded. In three cases

(bridges 46-317, 81-50, and 89-245) however, the subdeck placement locations were available and the crack density obtained for the portion of the bridge deck corresponding to the subdeck placement is used in the analysis.

The results indicate that age-corrected crack densities for silica fume overlays containing 5% and 7% silica fume are nearly identical (see Section 5.2). In light of this observation, and because of the relatively small number of 7% silica fume overlay bridges (10), the results for 5% and 7% silica fume overlays are combined for the analyses presented in sections 5.3 through 5.7. In addition, three silica fume overlay bridges (30-93, 89-184, and 89-187) are not included in the analysis because they were constructed using significantly different construction and material specifications. Except for these three bridges, all of the results obtained from surveys performed by Miller and Darwin (2000) and Schmitt and Darwin (1995) are included in the analysis (as described in Section 4.2). In total, the analysis includes data from 86 bridges, representing 173 individual concrete placements. Of the bridges surveyed, 13 monolithic, 16 conventional overlay, and 20 silica fume overlay bridge decks have been surveyed two or more times. The cracking patterns, bridge crack density data, and bridge data used as the basis for the comparisons that follow are presented in Appendix E.

In addition to the crack survey, each onsite field survey of overlay decks included “sounding” to locate areas where the overlay had delaminated (debonded) from the subdeck. The total delaminated area for each deck, reported in square meters, is provided in Table E.1 of Appendix E. Only 12 bridges were found to have any delamination, and in each case, the area was a small percentage of the total deck area (maximum 0.5%).

Due to the myriad of variables contributing to bridge deck cracking, the results generally show large amounts of scatter. To facilitate the analysis, histograms, beginning with Fig. 5.1, are used to show any trends. Each bar, or category,

represents a range of values for the variable under consideration and is defined by the midpoint. In many cases, the sample sizes and the differences between the means of categories are small. The Student's t-test (described in Section 3.1) is used to determine whether the differences between two samples represent differences between populations.

## 5.2 INFLUENCE OF DECK TYPE

Mean age-corrected crack densities for bridge decks are shown as a function of bridge deck type in Fig. 5.1. Four deck types are examined: 7% silica fume overlays (7% SFO), 5% silica fume overlays (5% SFO), conventional overlays (CO), and monolithic bridge decks (MONO). The 7% and 5% silica fume overlay decks have nearly the same mean crack density ( $0.51 \text{ m/m}^2$  for 7% SFO and  $0.49 \text{ m/m}^2$  for 5% SFO). The age-corrected crack density results for the 5% silica fume overlays, excluding bridges 89-184 and 89-187, are statistically indistinguishable from the results obtained for the 7% silica fume overlays, excluding bridge 30-93 (Table 5.1). In light of this observation, the decision to consider all silica fume overlays as a single deck type for the remainder of the analysis is justified.

The mean age-corrected crack density for conventional overlays,  $0.44 \text{ m/m}^2$ , is slightly lower than the crack densities obtained for silica fume overlays, although the difference is not statistically significant (Table 5.1). The mean age-corrected crack density for monolithic decks,  $0.33 \text{ m/m}^2$ , is significantly lower than that for both silica fume overlay types ( $\alpha = 0.20$  for 7% SFO,  $\alpha = 0.10$  for 5% SFO) and conventional overlays ( $\alpha = 0.20$ ). In general, when the effect of cracking on corrosion initiation is considered, the use of overlays to improve bridge deck performance is not supported by this data obtained in this study.

### 5.3 INFLUENCE OF MATERIAL PROPERTIES

In this section, the influence of seven material-related variables on bridge deck cracking is quantified. The variables include the water content, cementitious material content, percent volume of water and cementitious material, water-cementitious material ratio, slump, air content, and compressive strength. Separate analyses are performed for silica fume overlays, conventional overlays, overlay subdecks, and monolithic bridges. Material properties for bridges in each of these categories are compared with age-corrected crack densities and the results are tested for statistical significance.

The analyses of the effects of material properties that are presented in the balance of this section largely corroborate the findings by Schmitt and Darwin (1995) and Miller and Darwin (2000). In general, the influence of material properties on cracking is greater than that of the site conditions or design parameters and is more clearly identifiable for the overlay subdecks and monolithic decks than for overlays. The key observations from these analyses can be summarized as follows:

For bridges with **silica fume overlays**, there is no apparent correlation between age-corrected crack density and the water and air contents of the overlays. The cement content for each overlay type (5% and 7%) is constant and eliminates the possibility of evaluating the effects of cement content, paste volume, and water-cementitious material ratio. Cracking is the highest for overlays placed at the extremes of the slump range [26 mm (1.0 in.) and  $\geq 90$  mm ( $\geq 3.5$  in.)]. There is no apparent influence of compressive strength on cracking for silica fume overlays.

For bridges with **conventional overlays**, there is no apparent correlation between age-corrected crack density and the air content of the overlay. Mean age-corrected crack density is the highest for overlays placed with zero slump. Crack density decreases by more than half as the water

content increases from 133 to 145 kg/m<sup>3</sup> (225 to 245 lb/yd<sup>3</sup>). This trend is contrary to the expected behavior, and for the most part, highlights the importance of avoiding overlays with zero slump. Crack density is highest for overlays with a mean compressive strength of 52 MPa (7500 psi), 36% (on average) greater than crack densities obtained for overlays with mean compressive strengths between 38 and 45 MPa (5500 and 6500 psi).

Analyses of overlay bridges based on the properties of **subdecks**, show that crack density increases with increases in (1) water content, (2) cement content, and (3) percent cement paste. These trends indicate that concrete shrinkage is a major contributor to bridge deck cracking. The mean age-corrected crack density decreases as the water-cement ratio increases. The lowest levels of cracking were observed for subdecks cast with a water-cement ratio of 0.45, and the highest levels of cracking were observed for subdecks cast with a water-cement ratio of 0.40 and 0.41. Mean air contents between 4.5 and 6.5% did not affect the level of cracking. Slight increases in crack density were observed for increasing slump and compressive strengths, although the differences were not statistically significant.

The results for **monolithic** bridge decks are very similar to the results for overlay subdecks. Crack density increases with increases in (1) water content, (2) cement content, (3) percent paste and (4) compressive strength. There was no statistical difference for bridges cast with water-cement ratios of 0.42 or 0.44. Crack density decreases by 66% (on average) as the air content drops from 6.5% to 4.5 or 5.5%. Increasing concrete slump has only a minor influence on increased crack density.

### 5.3.1 Water Content

For silica fume overlays, the water content values are  $138 \text{ kg/m}^3$  ( $232 \text{ lb/yd}^3$ ) for overlays containing 7% silica fume and  $141 \text{ kg/m}^3$  ( $238 \text{ lb/yd}^3$ ) and  $148 \text{ kg/m}^3$  ( $250 \text{ lb/yd}^3$ ) for overlays containing 5% silica fume. For conventional overlays, the water content values are  $133 \text{ kg/m}^3$  ( $224 \text{ lb/yd}^3$ ),  $139 \text{ kg/m}^3$  ( $235 \text{ lb/yd}^3$ ), and  $145 \text{ kg/yd}^3$  ( $245 \text{ lb/yd}^3$ ). For overlay subdecks, water contents range from 143 to  $173 \text{ kg/m}^3$  ( $241$  to  $292 \text{ lb/yd}^3$ ), with categories ranging from  $147$  to  $174 \text{ kg/m}^3$  ( $248$  to  $293 \text{ lb/yd}^3$ ). For monolithic decks, water contents range from 143 to  $167 \text{ kg/m}^3$  ( $241$  to  $281 \text{ lb/yd}^3$ ), with categories ranging from  $147$  to  $165 \text{ kg/m}^3$  ( $248$  to  $278 \text{ lb/yd}^3$ ).

The mean age-corrected crack density for individual placements is shown as a function of water content for silica fume and conventional overlay placements in Figs. 5.2 and 5.3. The effect of water content on crack density for silica fume overlays is not entirely clear, with mean age-corrected crack densities ranging from  $0.47$  to  $0.60 \text{ m/m}^2$ . For conventional overlay decks, however, there is a clear trend towards lower levels of cracking with increasing water contents (Fig. 5.3), as crack density decreases from  $0.62$  to  $0.30 \text{ m/m}^2$  with an increase in mean water content from  $133$  to  $145 \text{ kg/m}^3$  ( $225$  to  $245 \text{ lb/yd}^3$ ). This increase in crack density can largely be attributed to difficulties in placing overlays with zero slump overlays (see Section 5.3.5).

The mean age-corrected crack density for individual placements is shown as a function of water content for overlay subdeck and monolithic placements in Figs. 5.4 and 5.5. Unlike the observations for overlays, the trend for subdecks and monolithic decks is clear: an increase in water content results in an increase in crack density. For overlay subdecks (Fig. 5.4), the crack density increases from  $0.54$  to  $0.78 \text{ m/m}^2$  as the mean water content increases from  $147$  to  $174 \text{ kg/m}^3$  ( $248$  to  $293 \text{ lb/yd}^3$ ). The subdeck properties clearly play an integral role in the performance of bridge decks with overlays. The contrast is even clearer for monolithic placements, where the

crack density increases from 0.14 to 0.73 m/m<sup>2</sup> as the water content increases from 147 to 165 kg/m<sup>3</sup> (248 to 278 lb/yd<sup>3</sup>), which is a statistically significant increase at  $\alpha = 0.02$  (Table 5.2).

### 5.3.2 Cementitious Material Content

The cementitious material content for the overlays included in this study is nearly constant. For silica fume overlays, the cementitious material content consists of cement and silica fume. Cement is the only cementitious material used in conventional overlays. The cement content of all conventional overlays is 371 kg/m<sup>3</sup>, and the cementitious material content for all silica fume overlays is between 370 and 372 kg/m<sup>3</sup> (623 and 627 lb/yd<sup>3</sup>). For this reason, the influence of overlay cementitious material content on crack density is not evaluated for either overlay type.

For overlay subdecks, cement contents include 357 kg/m<sup>3</sup> (602 lb/yd<sup>3</sup>), 379 kg/m<sup>3</sup> (639 lb/yd<sup>3</sup>), and 413 kg/m<sup>3</sup> (696 lb/yd<sup>3</sup>). For monolithic placements, cement contents include 357 kg/m<sup>3</sup> (602 lb/yd<sup>3</sup>), 359 kg/m<sup>3</sup> (605 lb/yd<sup>3</sup>), 379 kg/m<sup>3</sup> (639 lb/yd<sup>3</sup>), and 390 kg/m<sup>3</sup> (657 lb/yd<sup>3</sup>). Only one bridge is included in the last category and is subsequently excluded from the analysis, while decks with cement contents of 357 and 359 kg/m<sup>3</sup> (602 and 605 lb/yd<sup>3</sup>) are grouped together [357 kg/m<sup>3</sup> (603 lb/yd<sup>3</sup>)].

The mean age-corrected crack density for individual placements is shown as a function of cement content for overlay subdecks and monolithic placements in Figs. 5.6 and 5.7. In both cases, an increase in cement content results in an increase in crack density. For overlay decks, the age-corrected crack density increases from 0.53 to 0.78 m/m<sup>2</sup> as the cement content increases from 357 to 413 kg/m<sup>3</sup> (602 to 696 lb/yd<sup>3</sup>), which is statistically significant at  $\alpha = 0.05$  (Table 5.3). The increase is even more pronounced for monolithic decks, where crack density increases from 0.18 to

0.69 m/m<sup>2</sup> as the cement content increases from 358 to 379 kg/m<sup>3</sup> (603 to 639 lb/yd<sup>3</sup>), which is statistically significant at  $\alpha = 0.02$  (Table 5.3).

Numerous other researchers have found that increasing cement contents result in increased levels of cracking (Schmitt and Darwin 1995, 1999, Miller and Darwin 2000, Cheng and Johnston 1985, Babaei and Purvis 1996, Krauss and Rogalla 1996 Eppers, French, and Hajjar 1998, Whiting and Detwiler 1998). Eppers, French, and Hajjar (1998) recommend a maximum cement content of 392 kg/m<sup>3</sup> (660 lb/yd<sup>3</sup>). In the laboratory study by Krauss and Rogalla (1996), concretes with a low water-cement ratio, low cement factor, and low slump performed the best.

### **5.3.3 Percent Volume of Water and Cement**

The percentage volume of water and cementitious materials in the initial mix design provides a close approximation of the paste volume of the concrete. The volume of cement paste has a strong influence on crack density since cement paste largely controls concrete shrinkage. For the overlay bridges in this study, the cementitious material content is nearly identical for the overlays [approximately 371 kg/m<sup>3</sup> (625 lb/yd<sup>3</sup>)]. As a result, any differences in the paste volume of the overlays are attributable to changes only in the water content of the mix. For this reason, overlay properties are excluded from the analysis.

Mean age-corrected crack density is shown as a function of paste volume in Figs. 5.8 and 5.9 for overlay subdecks and monolithic bridge decks, respectively. For overlay bridge subdecks, the volume of water and cement ranges from 25.7 to 30.5%, with categories ranging from 26 to 30%. For monolithic bridge decks, the volume of water and cement ranges from 26.5 to 28.8% with categories of 27, 28, and 29%. For the overlay subdecks, crack density varies from between 0.51 m/m<sup>2</sup> to 0.56 m/m<sup>2</sup> for paste volumes between 26 and 28%; as the paste volume increases to 29 and 30%, the crack density increases to 0.63 and 0.78 m/m<sup>2</sup>, respectively. The trend is even clearer

for monolithic decks, where the mean age-corrected crack density is 0.19 and 0.16  $\text{m/m}^2$  for paste volumes of 26 and 27%, increasing sharply to 0.68 and 0.73  $\text{m/m}^2$  for paste volumes of 28 and 29%, respectively. The results of the statistical analysis are presented in Table 5.4. Limiting the paste volume of concrete has long been recognized as a key to minimizing bridge deck cracking (Schmitt and Darwin 1995, 1999, Miller and Darwin 2000, Krauss and Rogalla 1996). Based on the observations presented in Figs. 5.8 and 5.9, the level of cracking can be significantly reduced by using paste contents less of 27% or less for both overlay subdeck and monolithic bridge decks.

#### **5.3.4 Water-Cement Ratio**

Due to the use of nearly identical cement contents for overlays, the influence of water-cement ratio on cracking is identical to the trends observed in Section 5.3.1 for water content, and not repeated here.

Mean age-corrected crack densities are shown as a function of the water-cement ratio for overlay subdecks and monolithic placements in Figs. 5.10 and 5.11. The water-cement material ratio ranges from 0.40 to 0.45 for subdeck placements. For monolithic placements, water-cement ratios include 0.40, 0.42, and 0.44. Only one monolithic bridge was placed with a water-cement ratio of 0.40 and is, therefore, excluded from the analysis. In addition, due to nearly identical cement contents for all overlay placements, the influence of water-cement ratio on cracking is identical to the trends observed in Section 5.3.1.

For overlay subdeck placements (Fig. 5.10), the age-corrected crack density generally decreases with increasing water-cement ratios. The highest age-corrected crack density (0.73  $\text{m/m}^2$ ) occurs for placements with a water-cement ratio of 0.41, and the lowest crack density (0.45  $\text{m/m}^2$ ) occurs for placements with a water-cement ratio of 0.45. The difference between these categories is statistically significant at  $\alpha =$

0.05 (Table 5.5). This observation may be the result of a lower modulus of elasticity and higher levels of creep associated with concretes with higher water-cement ratios. For monolithic placements (Fig. 5.11), the age-corrected crack density increases slightly as the water-cement ratio increases from 0.42 to 0.44. This small increase in crack density is not statistically significant (Table 5.5).

### 5.3.5 Slump

For the silica fume overlays, the concrete slump varies from 19 to 127 mm (0.75 to 5.0 in.), with categories ranging from 26 to greater than 90 mm (1.0 to  $\geq 3.5$  in.). Thirty-seven 5% silica fume overlays and 13 7% silica fume overlays are included in this analysis. The mean slump for the silica fume overlays is 67.7 mm (2.7 in.). For conventional overlays, the overlay slump varies from 0 to 160 mm (0 to 6.25 in.), with categories ranging from 0 to 19 mm (0 to 0.75 in.). The mean slump for the conventional overlays is 15.9 mm (0.63 in.). For overlay subdecks, the concrete slump varies from 6.4 to 160 mm (0.25 to 6.3 in.), with categories ranging from 38 to greater than 76 mm (1.5 to  $\geq 3.0$  in.). The mean concrete slump for overlay subdeck placements is 63.7 mm (2.5 in.). For monolithic bridge decks, the slump ranges from 44 to 76 mm (1.75 to 3.0 in.), with categories ranging from 44 to 70 mm (1.75 to 2.75 in.). The mean slump for the monolithic placements is 53.9 mm (2.1 in.).

The mean age-corrected crack density for silica fume overlays is shown as a function of concrete slump in Fig. 5.12. No distinct trend is apparent, although the highest levels of cracking occur at the extremes of the slump range investigated [26 and  $\geq 90$  mm (1.0 and  $\geq 3.5$  in.)]. These observations are based on small sample sizes and are, in most cases, statistically insignificant (Table 5.6). The mean age-corrected crack density for conventional overlays is shown as a function of concrete slump in Fig. 5.13. Similar to observations made by both Schmitt and Darwin (1995, 1999)

and Miller and Darwin (2000), the highest levels of cracking occur for overlays placed with zero slump. Only two placements are available in the 3 mm (0.125 in.) category, and no apparent correlation exists between the remaining categories [encompassing slumps from 6 to 19 mm (0.25 to 0.75 in.)]. Problems encountered during consolidation, finishing, and curing operations likely account for the difficulties in placing overlays with zero slump. None of the overlays in this study have reinforcement, thereby eliminating subsidence (settlement) cracking initiated in the overlay as a cause of increased cracking.

Concrete slump, in addition to bar size and top cover depth, has long been recognized as a key controller of subsidence cracking (Dakhil, Cady, and Carrier 1975). At the same time, it is also recognized that subsidence cracking is primarily a result of poor construction practices (Krauss and Rogalla 1996) that can exacerbate cracking on bridges cast with high slump concrete. The mean age-corrected crack density for overlay subdecks is shown in Fig. 5.14. There is a slight, nonmonotonic trend towards increased cracking in conjunction with increasing subdeck slump, although none of the categories are statistically different from each other (Table 5.6). The mean age-corrected crack density for monolithic placements is shown in Fig. 5.15. For these placements, the results are presented in two ways. Based on the raw data, the results appear to indicate that crack density increases sharply, from 0.18 to 0.87  $\text{m}/\text{m}^2$ , as concrete slump increases from 38 to 76 mm (1.5 to 3.0 in.). These results, however, include the influence of water content. For the monolithic decks in this study (almost exclusively cast without water reducers), there is a strong correlation between water content and concrete slump.

To separate the influence of slump from water content on concrete cracking, a dummy variable analysis (Draper and Smith 1981) was performed. For the analysis, the monolithic placements were divided into five categories based on water content. The water content categories ranged from 143 to 169  $\text{kg}/\text{m}^3$  (241 to 281  $\text{lb}/\text{yd}^3$ ). The

results of the dummy variable analysis are summarized in Table 5.7 and show that increasing slump results in an average increase in crack density at a rate of 0.0029  $\text{m/m}^2/\text{mm}$ . While slump still affects the total crack density of monolithic placements, the trend is much less salient. Once this effect is applied to the raw data, the mean crack density is found to increase from 0.11 to 0.22  $\text{m/m}^2$  as the slump increases from 38 to 76 mm (1.5 to 3.0 in.), as shown in Fig. 5.15. Thus, slump appears to have a measurable but relatively small influence on bridge deck cracking.

### 5.3.6 Air Content

Mean age-corrected crack density for individual placements is shown as a function of air content for silica fume and conventional overlays in Fig. 5.16. Air contents range from 3.5 to 7.25%, with categories ranging from 4.5 to 6.5%. Mean age-corrected crack density is shown as a function of air content for overlay subdeck placements and monolithic placements in Figs. 5.17 and 5.18. Air contents range from 4.5 to 6.5% for monolithic bridge decks and from 2.25 to 7.5% for subdecks with categories for both deck types ranging from 4.5 to 6.5%.

For the silica fume and conventional overlays (Fig. 5.16), the level of cracking remains nearly constant with increasing air contents. For bridge subdecks (Fig. 5.17), there is a slight (at best) decrease in crack density from 0.54 to 0.50  $\text{m/m}^2$  as the air content category increases from 4.5 to 6.5%; this decrease, however, is not statistically significant (Table 5.8). For monolithic bridge placements (Fig. 5.18), crack density remains nearly constant (0.37 and 0.38  $\text{m/m}^2$  for 4.5 and 5.5%, respectively) for air contents less than 5.5%, but drops to 0.13  $\text{m/m}^2$  as the air content increases from 5.5 to 6.5%, a decrease in crack density that is statistically significant at  $\alpha = 0.10$  (Table 5.8).

Both Schmitt and Darwin (1995, 1999) and Miller and Darwin (2000) found similar results. Monolithic placements with air contents less than 6% were found to

have increased levels of cracking. No correlation with cracking was found in overlays with air contents between 4 and 7%. Reports by Cheng and Johnston (1985) and Eppers, French, and Hajjar (1998) also found that air contents above 5.5% reduced transverse cracking. Observations on the positive effects of higher air contents on cracking, however, have not been universal. Poppe (1981) concluded that air content has a neutral effect on cracking, and in a laboratory investigation, Krauss and Rogalla (1996) found no correlation between cracking tendency and air entrainment for concretes with a constant paste content.

### **5.3.7 Compressive Strength**

The mean age-corrected crack density for individual placements is shown as a function of compressive strength for silica fume overlays, conventional overlays, overlay subdecks, and monolithic bridge decks in Figs. 5.19 through 5.22. For silica fume overlays (Fig. 5.19), compressive strength varies from 36 to 62 MPa (5200 to 9000 psi), with categories ranging from 38 to 59 MPa (5500 to 8500 psi). For conventional overlays (Fig. 5.20), compressive strength varies from 34 to 57 MPa (4900 to 8200 psi), with categories ranging from 38 to 52 MPa (5500 to 7500 psi). For overlay bridge subdecks (Fig. 5.21), compressive strength varies from 30 to 52 MPa (4400 to 7500 psi), with categories ranging from 31 to 52 MPa (4500 to 7500 psi). For monolithic bridge decks (Fig. 5.22), compressive strength varies from 29 to 51 MPa (4200 to 7400 psi), with categories ranging from 31 to 45 MPa (4500 to 6500 psi).

The relationship between cracking and compressive strength for bridge deck overlays is not entirely clear. For silica fume overlay decks (Fig. 5.19), the mean age-corrected crack density for placements within the first category [38 MPa (5500 psi)] is the highest ( $0.75 \text{ m/m}^2$ ), but drops sharply to  $0.42 \text{ m/m}^2$  for bridges in the second category [45 MPa (6500)]. As the mean compressive strength increases from

45 to 59 MPa (6500 to 8500 psi), crack density increases from 0.42 to 0.62 m/m<sup>2</sup>. For conventional overlays (Fig. 5.20), the mean age-corrected crack density increases from 0.43 m/m<sup>2</sup> to 0.57 m/m<sup>2</sup> as compressive strengths increase from 38 to 52 MPa (5500 to 7500 psi). Neither of the increases observed for overlay decks is statistically significant at any confidence level  $\alpha$  (Table 5.9).

For overlay subdecks (Fig. 5.21), there is a slight increase in age-corrected crack density, from 0.50 m/m<sup>2</sup> to 0.56 m/m<sup>2</sup>, as the compressive strength increases from 31 to 52 MPa (4500 to 7500 psi). The impact of compressive strength is, however, very clear when the comparison is made for monolithic bridge decks, with crack densities increasing from 0.16 m/m<sup>2</sup> to 0.49 m/m<sup>2</sup> as compressive strength increases from 31 to 45 MPa (4500 to 6500 psi) (Fig. 5.22).

Schmitt and Darwin (1995, 1999) and Miller and Darwin (2000) identified the same trend for monolithic decks and largely attributed the increased cracking to higher cement contents. Krauss and Rogalla (1996) recommend concretes with low cement contents and a specification that includes a provision for a maximum compressive strength in addition to the traditionally specified minimum compressive strength.

#### **5.4 INFLUENCE OF SITE CONDITIONS**

Maintaining adequate site conditions during concrete placement has long been recognized by transportation agencies as critical to limiting both thermal cracking and plastic shrinkage cracking. While not all environmental conditions affecting deck cracking are considered, the influences of four site conditions on the date of concrete placement are analyzed in this study. These conditions include average air temperature, low air temperature, high air temperature, and daily air temperature range.

Air temperature, wind speed, relative humidity, and concrete temperature contribute to the evaporation rate of water on the concrete surface. High daily air temperatures, low relative humidity, and wind increase the number and severity of cracks, especially for overlays with little or no bleed water. Unfortunately, the wind speed, relative humidity, and concrete temperature were not regularly recorded in the daily journals or project files, making evaporation rate calculations impossible. Schmitt and Darwin (1995) and Miller and Darwin (2000) estimated the wind speed and relative humidity for each placement during construction with data obtained from the closest available weather station. This information likely does not represent actual conditions on the bridge deck, and no identifiable trends were observed using the data.

Mean age-corrected crack density is compared with the available site conditions for silica fume overlays, conventional overlays, overlay subdecks, and monolithic decks in the balance of this section. The effects of site conditions on cracking varied significantly and few correlations are obtained. This is especially true for overlay subdecks, where no trends are identified. The key observations for silica fume overlays, conventional overlays, and monolithic decks can be summarized as follows:

For **silica fume overlays**, mean age-corrected crack density increases by 45%, on average, as the daily air temperature range increases from 4° C to 12° and 20° C.

For **conventional overlays**, mean age-corrected crack density increases as the daily low, high, and average temperatures increase. The level of cracking increases 49% as the low daily temperature increases from 0° to 20° C. Cracking increases 60%, on average, as the maximum air temperature increases from 15° C to 25° and 35° C, and 27% as the average daily air temperature increases from 5° to 25° C. An increase in the daily air

temperature range from 4° to 20° C results in a small increase (13%) in crack density.

For **monolithic bridge** placements, mean age-corrected crack density increases 132% as the daily maximum air temperature increases from 5° to 25° C and 214% as the air temperature range increases from 4° to 20° C.

#### 5.4.1 Average Daily Air Temperature

Mean age-corrected crack density is shown as a function of average daily temperature in Figs. 5.23, 5.24, and 5.25 for bridge deck overlays, overlay subdecks, and monolithic bridge decks, respectively. The average daily temperature ranges from 3° to 30° C for silica fume overlays, 5° to 30° C for conventional overlays, 3° to 31° C for overlay subdecks, and 2° to 30° for monolithic bridge placements. The average air temperature categories range from 5° to 25° C for all bridge deck types.

For silica fume and conventional overlays (Fig. 5.23), there is a slight tendency towards increased cracking with increasing average daily temperatures. This trend is clearest for conventional overlays for which the crack density increases from 0.41 m/m<sup>2</sup> to 0.52 m/m<sup>2</sup> as the mean average air temperature increases from 5° to 25° C. Contrary to the results obtained for the overlay placements, the mean age-corrected crack density decreases slightly with increasing average daily temperatures for both overlay subdeck (Fig. 5.24) and monolithic placements (Fig. 5.25). In no case, however, are any of the differences observed between crack density and average air temperature statistically significant (Table 5.10).

The effect of average air temperature on cracking appears inconsistent. In 1981, Poppe found that high air temperatures lead to increased cracking, while Cheng and Johnston (1985) reported that cracking tended to increase as average temperatures decreased (most significantly below 7° C). Both Schmitt and Darwin (1995) and Miller and Darwin (2000) observed increased levels of cracking with

increasing average temperatures for conventional overlay placements, although no trend was observed for silica fume overlays or monolithic bridge decks.

#### **5.4.2 Minimum Daily Air Temperature**

Mean age-corrected crack density is shown as a function of minimum daily temperature in Figs. 5.26, 5.27, and 5.28 for bridge deck overlays, overlay subdecks, and monolithic bridge decks, respectively. The minimum daily temperature ranges from  $-3^{\circ}$  to  $24^{\circ}$  C for silica fume overlays,  $-4^{\circ}$  to  $24^{\circ}$  C for conventional overlays,  $-3^{\circ}$  to  $23^{\circ}$  C for overlay subdecks, and  $-3^{\circ}$  to  $23^{\circ}$  for monolithic bridge placements. The minimum daily air temperature categories range from  $0^{\circ}$  to  $20^{\circ}$  C. It should be noted that, although not consistently recorded, most of the bridge decks cast during cold weather were protected using insulating blankets and/or heated enclosures.

For silica fume overlays (Fig. 5.26), no trend is apparent between the level of cracking and the minimum air temperature. Conversely, the crack density for conventional overlays (Fig. 5.26) increases from  $0.41 \text{ m/m}^2$  to  $0.61 \text{ m/m}^2$  [statistically significant at  $\alpha = 0.20$  (Table 5.11)] as the average minimum temperature increases from  $0^{\circ}$  to  $20^{\circ}$  C. The influence of minimum air temperature on both overlay subdeck (Fig. 5.27) and monolithic (Fig. 5.28) placements appears insignificant. Crack densities for subdeck placements are between  $0.53$  and  $0.57 \text{ m/m}^2$  for subdeck placements and between  $0.29$  and  $0.38 \text{ m/m}^2$  for monolithic placements, differences that are both statistically insignificant (Table 5.11). Based on field surveys, Eppers, French, and Hajjar (1998) observed a reduced incidence of cracking when the minimum daily temperature was between  $7^{\circ}$  and  $10^{\circ}$  C.

#### **5.4.3 Maximum Daily Air Temperature**

Mean age-corrected crack density is shown as a function of maximum daily temperature in Figs. 5.29, 5.30, and 5.31 for bridge deck overlays, overlay subdecks,

and monolithic bridge decks, respectively. The maximum daily temperature ranges from 7° to 34° C for silica fume overlays, 9° to 37° C for conventional overlays, 7° to 39° C for overlay subdecks, and 6° to 36° C for monolithic bridge placements. The maximum daily air temperature categories range from 15° to 35° C for subdeck and overlay placements and from 5° to 35° C for monolithic placements.

For 5% and 7% silica fume overlays (Fig. 5.29) and overlay subdeck placements (Fig. 5.30), no trend between crack density and high daily air temperature is apparent. For conventional overlays, the mean crack density increases substantially from 0.33 m/m<sup>2</sup> to 0.57 m/m<sup>2</sup> as the maximum daily air temperature increases from 15° to 25° C, a statistically significant increase at  $\alpha = 0.02$  (Table 5.12). As the average maximum temperature increases to 35° C, the mean crack density decreases slightly to 0.49 m/m<sup>2</sup>, although statistically there is no difference between the results for placements cast with an average temperature of 25° and 35° C (Table 5.12). For monolithic decks (Fig. 5.31), crack density increases sharply from 0.19 m/m<sup>2</sup> to 0.44 m/m<sup>2</sup> as the average maximum daily temperature increases from 5° to 35° C, which is a statistically significant change at  $\alpha = 0.20$ . The results for monolithic decks, however, are in most cases statistically insignificant due primarily to small sample sizes at the extremes of the temperature ranges (Table 5.12).

#### **5.4.4 Daily Air Temperature Range**

Mean age-corrected crack density is shown as a function of daily air temperature range in Figs. 5.32, 5.33, and 5.34 for bridge deck overlays, overlay subdecks, and monolithic bridge decks, respectively. The daily air temperature range, calculated as the difference between maximum and minimum daily temperatures, varies from 4° to 24° C for silica fume overlays, 4° to 20° C for conventional overlays, 3° to 31° C for overlay subdecks, and 2° to 30° for monolithic bridge

placements. The daily air temperature range categories range from 4° to 20° C for all bridge deck types.

For both overlay types (Fig. 5.32), the mean age-corrected crack density increases slightly as the daily air temperature range increases. The trend is clearest for silica fume overlays with a daily air temperature range greater than 8° C, where the average crack density increases from 0.35 m/m<sup>2</sup> to an average of 0.52 m/m<sup>2</sup>. Crack density drops slightly with an increasing daily air temperature range for bridge subdecks (Fig. 5.33). The crack density for monolithic placements (Fig. 5.34), however, increases sharply from 0.14 m/m<sup>2</sup> to 0.44 m/m<sup>2</sup> as the average daily temperature range increases from 4° to 20° C. With the exception of the silica fume overlays, the differences observed between cracking and daily air temperature range are not statistically significant (Table 5.13). The trends observed, however, largely corroborate research by Eppers, French, and Hajjar (1998) that showed increased levels of cracking when the daily air temperature range exceeds 10° C.

## **5.5 INFLUENCE OF DESIGN PARAMETERS**

Evaluation of design parameters for silica fume overlay, conventional overlay, and monolithic bridges revealed correlations between cracking and several of the design parameters under consideration. In large part, however, design parameters were not found to significantly influence bridge deck cracking. The following ten variables are considered in the analysis: structure type, transverse reinforcing bar size, transverse reinforcing bar spacing, deck thickness, top bar cover, girder end condition, span type, skew, span length, and bridge length.

The analyses of the influence of design parameters are presented in the balance of this section. For monolithic decks, eight variables were considered and none of the variables analyzed were found to influence deck cracking. The effects of transverse reinforcing bar spacing and girder end condition on crack density were not

included in the analysis of monolithic decks. For bridges with overlays, the effect of top cover on crack density was not included in the analysis.

The key observations for **overlay bridges** can be summarized as follows:

The top transverse bar size significantly increases bridge deck cracking (57%) when No. 19 (No. 6) bars are used as the only top transverse reinforcement. In addition to bar size, crack density increases, on average, 57% for both overlay types, with a transverse reinforcing bar spacing greater than 153 mm (6.0 in.) compared to a bar spacing less than 153 mm (6.0 in.). Age-corrected crack density appears to increase slightly with increasing bridge length. Finally, crack density is significantly higher for the end sections of fix-ended girders than for pin-ended girders. This increase in crack density for fix-ended girders, while significant (nearly three times the value for pin-ended girders), is limited to the first and last 3 m (10 ft) of the bridge deck.

### 5.5.1 Structure Type

Mean age-corrected crack density for bridge decks is shown as a function of steel superstructure type for silica fume overlays, conventional overlays, and monolithic bridge decks in Fig. 5.35. Three types of steel superstructures are examined: SMCC (steel beam, composite continuous), SWCC (steel welded plate girder, composite continuous), and SWCH (steel welded plate girder, composite continuous and haunched). For silica fume overlays, SWCH structures exhibit the highest levels of cracking ( $0.63 \text{ m/m}^2$  compared to  $0.54 \text{ m/m}^2$  for SMCC structures and  $0.45 \text{ m/m}^2$  for SWCC structures); however, none of the differences between the structure types are statistically significant (Table 5.14). For conventional overlays, SWCC structures exhibit the highest levels of cracking ( $0.55 \text{ m/m}^2$  compared to  $0.38 \text{ m/m}^2$  for SMCC structures and  $0.26 \text{ m/m}^2$  for SWCH structures), a statistically

significant difference from both SMCC ( $\alpha = 0.20$ ) and SWCH ( $\alpha = 0.02$ ) structures (Table 5.14). For monolithic decks, SWCH structures exhibit the highest levels of cracking ( $0.40 \text{ m/m}^2$  compared to  $0.35 \text{ m/m}^2$  for SMCC structures and  $0.40 \text{ m/m}^2$  for SWCC structures) although, similar to the results for silica fume overlays, none of these differences are statistically significant (Table 5.14).

Mean age-corrected crack density is shown as a function of structure type for all bridges in Fig. 5.36 without distinction of deck type. Differences in crack density between the different structure types are minimal and statistically insignificant (Table 5.14). Structure type does not appear to have a measurable effect on bridge deck cracking, an observation corroborated by both Schmitt and Darwin (1995) and Miller and Darwin (2000).

### **5.5.2 Transverse Reinforcing Bar Size**

Mean age-corrected crack density for bridge decks is shown as a function of transverse reinforcing bar size for silica fume overlays, conventional overlays, and monolithic decks in Figs. 5.37, 5.38, 5.39, respectively. The comparison for silica fume overlay decks includes No. 16 (No.5), No. 16 and No. 19 (No. 5 and No. 6) combined, and No. 19 (No. 6). The comparison for conventional overlay decks includes No. 13 and No. 16 (No. 4 and No. 5) combined, No. 16 (No. 5), and No. 19 (No. 6). The comparison for monolithic decks includes No. 13 and No. 16 (No. 4 and No. 5) combined and No. 16 (No. 5).

The crack density for both overlay types (silica fume and conventional) is the highest with the largest top transverse reinforcing bar size (Figs. 5.37 and 5.38), although the relationship for silica fume overlays is not entirely clear. For silica fume overlay decks, the mean age-corrected crack is greatest for decks with No. 19 (No. 6) bars ( $0.56 \text{ m/m}^2$ ) and the least for bridges with No. 16 and No. 19 (No. 5 and No. 6) bars combined ( $0.42 \text{ m/m}^2$ ). For conventional overlays, the mean age-corrected crack

density increases from  $0.35 \text{ m/m}^2$  to  $0.60 \text{ m/m}^2$  for conventional overlays as the bar size increases from No. 16 (No. 5) to No. 19 (No. 6). While this difference is not statistically significant for silica fume overlays, it is significant at the highest level ( $\alpha = 0.02$ ) for conventional overlays (Table 5.15). For monolithic bridge decks (Fig. 5.39), the crack density is lower for decks constructed with No. 16 (No. 5) bars as opposed to bridges constructed with both No. 13 and No. 16 (No. 4 and No. 5) bars combined ( $0.40 \text{ m/m}^2$  compared to  $0.26 \text{ m/m}^2$ ). As expected, this difference is not statistically significant and indicates parity between the bar size categories.

Mean age-corrected crack density is shown as a function of transverse reinforcing bar size in Fig. 5.40 without distinction of deck type. Two monolithic decks and one silica fume overlay deck that were previously excluded (individual decks are typically excluded from analyses if they contain only one bridge in a particular category) have been added to the data set. The two monolithic decks excluded (89-208 and 105-46) have crack densities of  $0.10$  and  $0.67 \text{ m/m}^2$ , and the silica fume overlay deck (89-248) has a crack density of  $0.40 \text{ m/m}^2$ . Bridge decks with transverse bar sizes smaller than No. 19 (No. 6) bars, including the combination of No. 16 and No. 19 (No. 5 and No. 6) bars have significantly ( $\alpha = 0.02$ ) less cracking than decks constructed with No. 19 (No. 6) bars (Table 5.15). With mean crack densities increasing from between only  $0.36$  and  $0.39 \text{ m/m}^2$  to  $0.59 \text{ m/m}^2$ . Increasing the top transverse bar size has long been known to increase deck cracking (Dakhil, Cady, and Carrier 1975, Schmitt and Darwin 1995, Eppers, French, and Hajjar 1998, Miller and Darwin 2000).

### **5.5.3 Transverse Reinforcing Bar Spacing**

Mean age-corrected crack density for bridge decks as a function of transverse reinforcing bar spacing for silica fume and conventional overlays is shown in Fig. 5.41. For silica fume overlays, the bar spacing varies from 102 to 229 mm (4 to 9

in.), and for conventional overlays, the bar spacing varies from 127 to 305 mm (5 to 12 in.). Bar spacing is divided into two categories: less than or equal to 153 mm (6 in.), and greater than 153 mm (6 in.). The monolithic decks included in this study, with the exception of one deck, have a bar spacing of 153 mm (6 in.) and are therefore not included in the analysis. The results for silica fume and conventional overlays are similar. The mean age-corrected crack density for spacings less than or equal to 153 mm (6 in.) is  $0.42 \text{ m/m}^2$  for silica fume overlays and  $0.34 \text{ m/m}^2$  for conventional overlays. For spacings greater than 153 mm (6 in.), the mean crack density increases to  $0.60 \text{ m/m}^2$  for silica fume overlays and to  $0.63 \text{ m/m}^2$  for conventional overlays, both of which are statistically significant changes ( $\alpha = 0.05$  for silica fume overlays and  $\alpha = 0.02$  for conventional overlays) (Table 5.16).

For the overlay bridges included in this study, it appears to be clear that bridge decks with a transverse bar spacing greater than 153 mm (6 in.) have a higher incidence of cracking. It is important to note that in many cases transverse bar spacing increases with increasing bar sizes. For the overlay bridges in this study, the relationship between transverse bar spacing and bar size is presented in Fig. 5.42. Transverse bar spacing appears to increase slightly with bar size although a large amount scatter exists.

To separate the influence of bar spacing from bar size on deck cracking, a dummy variable analysis (Draper and Smith 1981) was performed for both silica fume and conventional overlays. For the analysis, the overlays were divided into four categories based on the top transverse bar size: No. 13 and No. 16 (No. 4 and No. 5) combined, No. 16 (No.5), No. 16 and No. 19 (No. 5 and No. 6) combined, and No. 19 (No. 6). The results of the dummy variable analyses are summarized in Table 5.17. The results indicate that for a given bar size, an increase in bar spacing results in an average increase in crack density of  $0.0045 \text{ m/m}^2/\text{mm}$  for silica fume overlays and  $0.0025 \text{ m/m}^2/\text{mm}$  for conventional overlays. Based on these cracking rates, an

increase in bar spacing of 25.4 mm (1.0 in.) increases the crack density by 0.11 m/m<sup>2</sup> for silica fume overlays and by 0.06 m/m<sup>2</sup> for conventional overlays. The R<sup>2</sup> value is low in both cases, indicating large amounts of scatter within bar-size categories.

#### **5.5.4 Deck Thickness**

Mean age-corrected crack density for bridge decks as a function of deck thickness for silica fume overlays, conventional overlays, and monolithic decks is shown in Figs. 5.43, 5.44, and 5.45. Deck thickness varies from 216 to 229 mm (8.5 to 9.0 in.) for overlay decks and from 203 to 229 mm (8.0 to 9.0 in.) for monolithic decks. No identifiable trend is evident for these small changes in thickness and none of the differences between categories is statistically significant (Table 5.18). Krauss and Rogalla (1996) recommend a deck thickness no less than 203 mm (8 in.), equal to the thinnest decks included in this study.

Several studies have found that thin decks tend to have increased levels of cracking due to increased deck stresses. Eppers, French, and Hajjar (1998) and Poppe (1981) completed two such studies. These studies included deck thicknesses of 159 mm (6.25 in.), which are thinner than any of the decks in the current study. A change in deck thickness from 203 to 229 mm (8.0 to 9.0 in.) does not appear to influence deck cracking.

#### **5.5.5 Top Cover**

Mean age-corrected crack density for bridge decks is shown as a function of top reinforcing bar cover for monolithic bridge decks in Fig. 5.46. All of the silica fume and conventional overlay bridge decks have a cover of 76 mm (3 in.), and consequently, no evaluation of the effect of top cover is possible for those decks. Monolithic decks included in this study have a top cover of either 64 mm (2.5 in.) or 76 mm (3.0 in.). Contrary to the expected behavior, bridge decks with a top cover of

64 mm (2.5 in.) have a lower crack density ( $0.24 \text{ m/m}^2$ ) than bridges with a top cover of 76 mm (3.0 in.) ( $0.46 \text{ m/m}^2$ ). A difference that is statistically significant at  $\alpha = 0.20$  (Table 5.19). Two bridges built with a 76 mm (3 in.) cover, however, were also cast with the highest percentages of cement paste (28.8%) and have the two highest values of crack density. When these two decks are removed, the mean crack density for decks with a 76 mm top cover depth decreases to  $0.24 \text{ m/m}^2$  (Fig. 5.46). Based on this observation, a change in top cover from 64 to 76 mm (2.5 to 3.0 in.) does not appear to influence bridge deck cracking for monolithic decks.

In terms of corrosion protection, the overlay bridges included in this study have a top cover depth of 76 mm (3.0 in.). Before the overlay is placed, however, the top cover depth ranges from as little as 19 mm (0.75 in.) for conventional overlays to 38 mm (1.5 in.) for the silica fume overlays. Based on Eq. (1.3), developed by Dakhil, Cady, and Carrier (1975), the probability of subsidence cracking can be determined as a function of concrete cover, bar size, and concrete slump.

$$p = \frac{1.5e^y - 0.5}{1 + e^y} \quad (1.3)$$

where

$$y = 1.37 - 0.58x_1 - 0.56x_2 + 0.27x_3 \quad (1.4)$$

$p$  = probability of a crack to occur

$x_1$  = concrete cover, in.

$x_2$  = concrete cover divided by nominal bar size

$x_3$  = concrete slump, in.

Based on the cover depths used in the bridges in this study [19 mm (0.75 in.) for conventional overlays and 38 mm (1.5 in.) for silica fume overlays] the probability of subsidence cracking to occur is presented in Table 5.20 for slumps ranging between 51 and 102 mm (2.0 to 4.0 in.) and three bar sizes: No. 13, No. 16,

and No. 19 (No. 4, No. 5, and No. 6). In addition, the probability of subsidence cracking with a 51 mm (2.0 in.) cover depth (the largest cover depth used in the Dakhil et al. report) is also presented in Table 5.20 for purposes of comparison. As expected, the probability of cracking increases with decreasing cover, increasing slump, and increasing bar size. In particular, with a slump of 102 mm (4.0 in.) and a cover of 19 mm (0.75 in.), the probability of cracking is 100% and is independent of bar size. When Eq. (1.3) is extrapolated to include a cover depth of 76 mm (3.0 in.), the probability of subsidence cracking drops to zero for all combinations of slump and bar sizes. The probability of cracking is clearly influenced the most by increasing the cover to 51 mm (2.0 in.) or more.

#### **5.5.6 Girder End Condition**

As a general rule, highway agencies prefer bridge decks that are integral with the abutments because of difficulties in maintaining pinned connections. In addition, bridges with pinned ends, as compared to those with fixed ends, often require deeper sections or have larger deflections. To evaluate the effect of the girder end condition on deck performance, the crack densities for the first and last 3 m (10 ft) of each bridge deck are calculated and compared as a function of the end condition. The girder end conditions are either fixed or pinned.

It is recognized that the age-correction used to adjust the crack density for full bridge decks (presented and detailed in Section 4.3) does not represent the rate of cracking in the highly restrained (in the case of fixed-ended girders) or relatively unrestrained (in the case of pin-ended girders) end sections of the deck. For this reason, the cracking rate is recalculated using the technique of dummy variables (Draper and Smith 1981) for the end sections of the decks. Separate dummy variable analyses are performed for bridges with fixed and pinned ends in addition to the two overlay deck types.

The results of the dummy variable analysis are presented in Table 5.21. Because only two monolithic bridge decks in this study have pinned girders, monolithic bridges are not included in this analysis. In addition, the newest 7% silica fume overlay bridges are not included because they have only been surveyed one time each. The end-section cracking rate for fix-ended decks is 0.0054 m/m<sup>2</sup>/month for silica fume overlays and 0.0018 m/m<sup>2</sup>/month for conventional overlays. The end-section cracking rate for pin-ended decks is substantially less for silica fume overlays (0.0032 m/m<sup>2</sup>/month) and remains nearly constant for conventional overlays (0.0019 m/m<sup>2</sup>/month). These cracking rates are used to linearly adjust the raw end section crack density data for each end section to an age of 78 months (6½ years), the average age of all bridges. The raw age-corrected end-section crack densities are tabulated in Table E.3 of Appendix E.

The mean age-corrected crack density for end sections is shown as a function of girder end condition for silica fume and conventional overlay bridges in Fig. 5.47. The mean age-corrected crack density in the end regions of bridge decks with fixed supports for both silica fume and conventional overlay decks is nearly three times the value observed for pin-ended decks, as shown in Fig. 5.47. These differences are statistically significant at the highest level,  $\alpha = 0.02$  (Table 5.22). In an effort to isolate cracking as a result of the girder end condition as opposed to other factors, Fig. 5.48 presents the ratio of the crack density in the end section to the crack density in the entire bridge deck. Because of the additional restraint provided by fixed-ended girders, this ratio is greater than 1.0. Conversely, the lack of restraint provided by pinned girders results in a crack density ratio less than 1.0. The mean crack density ratios for silica fume overlay and conventional overlay decks with fix-ended girders are 1.76 and 3.08, respectively. For silica fume overlay and conventional overlay decks with pin-ended girders, the mean crack density ratios are 0.72 and 0.68, respectively. For either bridge deck type, it is clear that the benefits of bridges with

fixed ends must be weighed against potential problems that may arise due to increased cracking in the end sections of the deck.

### 5.5.7 Span Type

The mean age-corrected crack density for individual spans is shown as a function of span type for silica fume and conventional overlays in Fig. 5.49 and for monolithic bridge decks in Fig. 5.50. Three types of spans are included in the analysis: fixed connection end spans [End (F)], pinned connection end spans [End (P)], and continuous interior spans [Interior (F)]. The raw crack density data for individual spans are tabulated in Table E.4 of Appendix E.

For silica fume overlays, the crack density is the lowest for pinned connection end spans (Fig. 5.49). There is a slight increase in crack density for both continuous interior spans and fixed end spans. For conventional overlays, the crack density is the highest for pinned connection end spans and is slightly lower for the fixed end spans and interior spans (Fig. 5.49). None of the differences observed for either overlay type is statistically significant (Table 5.23). Only two monolithic bridges (56-142 and 99-76) have pin-ended girders, and for this reason have been excluded from the analysis. No difference in crack density is observed between continuous interior spans and fix-ended exterior spans for monolithic bridges (Fig. 5.50).

The type of span does not appear to influence the level of cracking observed on the bridge deck. The effect of the end condition on crack density, described in Section 5.5.6, appears to be limited to approximately the first and last 3 m (10 ft) of the bridge deck and has no significant effect on the average crack density of the full bridge deck.

### 5.5.8 Bridge Skew

The mean age-corrected crack density of entire bridge decks is shown as a function of deck skew for silica fume overlays and conventional overlays in Fig. 5.51 and monolithic decks in Fig. 5.52. Skew is defined as the acute angle between the abutment and a line normal to the centerline of the roadway and ranges from 0 to 55 degrees, with categories ranging from 0 to 50 degrees for the bridges included in this study.

The effect of bridge skew on crack density is not well defined (Figs. 5.51 and 5.52). Some statistical significance is observed between categories for the overlay bridge decks (Table 5.24), although none of the differences follows a defined trend and is likely a result of other factors. In this study, silica fume overlay bridges falling into the 30-degree category were found to have statistically less (at least at  $\alpha = 0.20$ ) cracking than decks falling into the other categories (Table 5.24). Similarly, conventional overlay decks in the 30-degree category had the least amount of cracking, but only had statistically less ( $\alpha = 0.20$ ) cracking than bridges falling into the highest category, 50 degrees (Table 5.24). In an analytical study, Krauss and Rogalla (1996) found that skew does not significantly affect transverse cracking, although bridge skew can create slightly higher stresses near the corners of the deck that causes cracks. Cracks at the corners of decks were noted during the field surveys, but they were not significant enough to measurably increase crack density in the end sections or, much less, the entire bridge deck.

### 5.5.9 Span Length

The mean age-corrected crack density for individual spans is shown as a function of span length for silica fume overlays, conventional overlays, and monolithic bridge decks in Figs. 5.53, 5.54, and 5.55. For silica fume overlays, span lengths range from 6.1 to 61.6 m (20 to 202 ft), with span length categories ranging

from 5 to 55 m (16 to 180 ft). For conventional overlays, span lengths range from 12.2 to 48.8 m (40 to 160 ft), with span length categories ranging from 15 to 45 m (49 to 148 ft). For monolithic bridge decks, span lengths range from 11.3 to 36.6 m (37 to 120 ft), with span length categories ranging from 15 to 35 m (49 to 115 ft).

For silica fume overlay bridges (Fig. 5.53), the level of cracking ranges from 0.38 to 0.45  $\text{m/m}^2$  for spans with a mean length between 5 and 35 m (16 and 115 ft), but increases to 0.51 and 0.62  $\text{m/m}^2$  for spans with a mean length of 45 and 55 m (148 and 180 ft), respectively. Differences between spans with the highest and the lowest levels of cracking are statistically significant (Table 5.25). Crack density decreases slightly with increasing span lengths for conventional overlays (Fig. 5.54), although none of the differences are statistically significant (Table 5.25). No trend between span length and crack density for monolithic bridges is apparent (Fig. 5.55). In general, span length does not appear to significantly affect the level of cracking on bridge decks. Some tendency towards increased cracking may exist for spans over 50 m (164 ft) long, although it is recognized that this observation is based on a small sample size.

#### **5.5.10 Bridge Length**

The mean age-corrected crack density for bridge decks is shown as a function of bridge length in Fig. 5.56. For silica fume overlays, bridge length ranges from 37.8 to 432.2 m (123.9 to 1388.5 ft). For conventional overlays, bridge length ranges from 40.4 to 134.1 m (132.5 to 439.8 ft). For monolithic bridge decks, bridge length ranges from 37.2 to 303.5 m (122.0 to 995.7 ft). Bridge length categories for all deck types range from 50 to 130 m (164 to 427 ft).

For silica fume overlays, the relationship between bridge length and cracking is unclear. There is a slight tendency towards increased cracking for bridge lengths over 90 m (295 ft) in overlay decks, although this trend is not observed for monolithic

decks. For silica fume overlays, the crack density is greatest for bridges in the 90 m (295 ft) category ( $0.58 \text{ m/m}^2$ ) and the least for bridges in the 50 m (164 ft) category ( $0.33 \text{ m/m}^2$ ). For conventional overlays, crack density increases from  $0.36 \text{ m/m}^2$  to  $0.53 \text{ m/m}^2$  as the bridge length category increases from 50 m (164 ft) to 130 m (427 ft), although this difference is not statistically significant (Table 5.26). For monolithic decks, the crack density is nearly constant for all bridge length categories, with no statistically significant differences (Table 5.26).

In general, bridge length appears, at most, to have a small effect on crack density.

## 5.6 INFLUENCE OF BRIDGE CONTRACTOR

In addition to the multiple design, material, and environmental related variables affecting bridge deck cracking, the bridge contractor responsible for construction ultimately determines the quality of the bridge deck. Cheng and Johnston (1985) report that under identical circumstances, “different contractors produce decks of widely different qualities.” It is important to note that, while age is taken into account, the circumstances for the bridges included as a part of this study are by no means identical. Mean age-corrected crack density for individual placements is shown as a function of the bridge contractor for silica fume overlays, conventional overlays, and monolithic bridges in Figs. 5.57, 5.58, and 5.59, respectively. Five contractors responsible for casting only one or two placements (usually representing one bridge) are excluded from the analysis. A single letter (A through I) represents each of the remaining nine contractors included in the analysis.

For silica fume overlays (Fig. 5.57), crack density varies from  $0.27 \text{ m/m}^2$  for contractor H to  $0.57 \text{ m/m}^2$  for contractors A and D. The statistical analysis provided in Table 5.27 indicates a large degree of indifference, with one exception, between contractor performances. Of the five contractors having more than two placements,

contractor H is statistically lower [at  $\alpha = 0.05$  or better (Table 5.27)] than the other contractors. For conventional overlays (Fig. 5.58), a much wider range of contractor performance is observed. The mean age-corrected crack density varies from 0.23  $\text{m/m}^2$  for contractor B to 0.80  $\text{m/m}^2$  for contractor E. The mean crack density for conventional overlay placements cast by contractor B is a significant improvement over the results obtained for silica fume overlays (0.23  $\text{m/m}^2$  for conventional overlays compared to 0.46  $\text{m/m}^2$  for silica fume overlays), and may indicate difficulties with the placement of silica fume overlays. For both conventional overlays and silica fume overlays, bridges built by contractors H and B have a consistently lower crack density. For monolithic decks (Fig. 5.59), only three contractors have cast more than two placements. The mean age-corrected crack density for placements cast by contractors A and C are low (0.13 and 0.19  $\text{m/m}^2$ ) and stand in sharp contrast to the mean crack density (0.81  $\text{m/m}^2$ ) for contractor I. The six placements cast by contractor I are from the same bridge, however, and may not represent performance on other projects.

In general, the contractor responsible for constructing the bridge deck can play a significant role in the overall performance of a bridge deck. A comprehensive solution to bridge deck cracking may ultimately require strict provisions regarding the selection of a contractor.

## **5.7 INFLUENCE OF TRAFFIC**

In this section, the influence of traffic-related variables on bridge deck cracking is quantified. The variables include average annual daily traffic (AADT) and the total number of load cycles. The total number of load cycles each bridge has been subjected to is taken as the average AADT at the time of the surveys multiplied by the bridge age. Separate analyses are performed for silica fume overlays, conventional overlays, overlay subdecks, and monolithic bridges and the results are

tested for statistical significance. In addition, dummy variable analyses are performed for each bridge deck type to determine the effect of load cycles on cracking. The raw crack density and traffic data are presented in Table E.5 of Appendix E.

Generally, there is a tendency for increased cracking with increases in AADT, although these trends are largely statistically insignificant and should be treated as such. Based on the dummy variable analysis, however, bridges subjected to a greater number of load cycles appear to show greater levels of cracking.

### **5.7.1 Average Annual Daily Traffic (AADT)**

Mean age-corrected crack density for entire bridge decks is shown as a function of the average annual daily traffic (AADT) for silica fume overlays and conventional overlays in Fig. 5.60, and monolithic bridge decks in Fig. 5.61. For bridges that were surveyed one time, the reported AADT at the time of the bridge survey is used in the analysis. For bridges that have been surveyed on more than one occasion, the average AADT for all surveys is used. This adjustment, however, is of little consequence and does not change the AADT category for any of the bridge decks. The AADT ranges from 150 to 14705 for silica fume overlays, from 245 to 17690 for conventional overlays, and from 0\* to 11990 for monolithic decks.

For silica fume overlays, no clear trend is identifiable (Fig. 5.60). With the exception of the first category (AADT = 2500), crack density appears to increase slightly with increasing traffic volume. The mean crack density for bridges in the first category, however, is statistically different from that of bridges in the second category (AADT = 7500) at  $\alpha = 0.02$  (Table 5.28). For conventional overlays (Fig. 5.60), the mean age-corrected crack density increases slightly from 0.35 to 0.51 m/m<sup>2</sup> as the AADT category increases from 2500 to 12500, although this increase in crack

---

\* Reported as such in the Kansas Department of Transportation Bridge Log.

density is not statistically significant (Table 5.28). For monolithic bridge decks (Fig. 5.61), the bridges in the first category (AADT = 1000) have the lowest level of cracking ( $0.13 \text{ m/m}^2$ ). The crack density increases sharply to  $0.48 \text{ m/m}^2$  for the second category (AADT = 3000), but decreases to  $0.36 \text{ m/m}^2$  for the last category (AADT = 5000). The difference in mean crack density for bridges in the last category (AADT = 5000) is statistically significant from the two other categories ( $\alpha = 0.02$  for AADT = 3000 and  $\alpha = 0.20$  for AADT = 5000) (Table 5.28).

### 5.7.2 Load Cycles

The AADT only quantifies the average amount of traffic on a bridge deck each day. For this reason, the total number of load cycles a bridge has experienced likely gives a more accurate representation of the effect of traffic on crack density. The uncorrected crack density is shown as a function of the total number of load cycles in Figs. 5.62, 5.63, and 5.64 for silica fume overlays, conventional overlays, and monolithic bridge decks, respectively. The total number of load cycles range from  $0.2 \times 10^6$  to  $31.4 \times 10^6$  for silica fume overlays,  $0.4 \times 10^6$  to  $48.2 \times 10^6$  for conventional overlays, and 0 to  $44.0 \times 10^6$  for monolithic decks. Initially, the crack density age-correction is not applied because this adjustment at least partially accounts for the effect of traffic on cracking over time. For this reason, the technique of dummy variables (Draper and Smith 1981) is used to determine the rate of increase in crack density as a function of load cycles for each of the three bridge deck types. These cracking rates (shown in each of the figures) include the combined effect of traffic and bridge deck age.

The results of the dummy variable analysis for monolithic, conventional overlay, and silica fume overlay decks are presented in Table 5.29. The linear regression lines shown in Figs. 5.62, 5.63, and 5.64 are plotted using the weighted average intercept and cracking rates obtained in the dummy variable analysis (Table

5.29). Similar to the results of the age-correction dummy variable analyses presented in Table 4.1, the cracking rate for conventional overlays is the lowest ( $0.0019 \text{ m/m}^2/1 \times 10^6$  cycles), and the cracking rate for silica fume overlays is the highest ( $0.0164 \text{ m/m}^2/1 \times 10^6$  cycles). The cracking rate for monolithic decks is  $0.0078 \text{ m/m}^2/1 \times 10^6$  cycles. In each case, the coefficient of determination is slightly less than for the age-correction analysis presented in Table 4.1. Based on this analysis, it appears that bridges subjected to a greater number of load cycles show greater levels of cracking, but it cannot be discerned whether this difference is due to loading or time.

In an effort to determine whether cracking increases with the number of load cycles, a separate dummy variable analysis is performed using the age-corrected crack density for each bridge deck, thereby eliminating bridge age as a variable. The results of the dummy variable analysis for each bridge deck type are presented in Table 5.30. The age-corrected crack densities, in addition to the results of the dummy variable analyses, are shown as a function of the total number of load cycles in Figs. 5.65, 5.66, and 5.67 for silica fume overlays, conventional overlays, and monolithic bridge decks, respectively.

For all deck types, the cracking rate for the age-corrected crack densities (Table 5.30) is substantially less than the cracking rate for the uncorrected crack densities (Table 5.29). This is expected because the influence of age (and some influence of load cycles) is removed. The cracking rate for conventional overlays is the least ( $0.0003 \text{ m/m}^2/1 \times 10^6$  cycles), and the cracking rate for silica fume overlays is the highest ( $0.0045 \text{ m/m}^2/1 \times 10^6$  cycles). The cracking rate for monolithic decks is  $0.0025 \text{ m/m}^2/1 \times 10^6$  cycles. Generally, load cycles appear to have a measurable but relatively small influence on deck cracking compared to other variables.

## CHAPTER 6: SUMMARY, CONCLUSIONS, AND RECOMMENDATIONS

### 6.1 SUMMARY

The purpose of this study is to identify the causes of cracking, to determine the diffusion properties and chloride contents of concrete bridge decks, and to gage the performance of silica fume overlay decks relative to conventional overlay and monolithic decks. The silica fume overlay decks were constructed under a number of specifications that require concrete in which 5 and 7% of the cement is replaced by silica fume. Field surveys are performed on 59 bridge decks, primarily in northeast Kansas, to determine the crack density, chloride ingress, concrete diffusivity, and delaminated area. Crack density is measured in terms of length per unit area ( $m/m^2$ ) and concrete diffusivity is estimated in terms of effective diffusion coefficients  $D_{eff}$  ( $mm^2/day$ ). Both the crack densities and diffusion coefficients are adjusted to account for differences in age. The study includes four deck types: 5% silica fume overlays (19 bridges), 7% silica fume overlays (11 bridges), conventional overlays (16 bridges), and monolithic bridge decks (13 bridges). Of the 59 bridges selected for this study, 49 had been investigated by Schmitt and Darwin (1995, 1999), Miller and Darwin (2000), or both.

Bridge deck performance is evaluated as a function of material properties, design specifications, construction practices, and environmental site conditions using the data obtained in this study, along with that obtained by Schmitt and Darwin (1995) and Miller and Darwin (2000). The monolithic decks evaluated as a part of this study range in age from 12 to 240 months. The conventional overlay decks range in age from 20 to 145 months, and the silica fume overlay decks range in age from 4 to 142 months, although only two of the bridges are older than 97 months. The average age for all 59 bridge decks at the time of survey is 78 months.

## 6.2 CONCLUSIONS

The following conclusions are based on the data and analyses presented in this report. Conclusions regarding bridge subdecks are based on the material properties or construction conditions of the subdecks. Conclusions regarding overlays are based on the material or construction conditions of the overlays only. In all cases, the conclusions are based on age-adjusted effective diffusion coefficients (as described in Chapter 3) and age-corrected crack densities (as described in Chapter 4).

### 6.2.1 Chloride Data and Diffusion Properties

1. Chloride content increases with the age of the bridge deck, regardless of bridge deck type.
2. Silica fume (both 5% and 7%) overlay, conventional overlay, and monolithic bridge decks in the same age range [ $< 156$  months (13 years)] exhibit similar chloride contents for samples taken both at and away from cracks.
3. Typically, chloride contents for silica fume (5% and 7%) overlay, conventional overlay, and monolithic bridge decks in the same age range [ $< 156$  months (13 years)] taken away from cracks at a depth of 76.2 mm (3.0 in.) are below even the most conservative estimate of the corrosion threshold for conventional reinforcement [ $0.6 \text{ kg/m}^3$  ( $1.0 \text{ lb/yd}^3$ )]. In contrast, for the oldest decks included in this study [limited to monolithic decks older than 168 months (14 years)], 42% of the samples exceed the corrosion threshold; based on trends in the data for bridges just below 156 months, however, this does not represent the expected behavior of the more recently constructed decks.
4. At cracks, the average chloride concentration at a depth of 76.2 mm (3.0 in.) can exceed the corrosion threshold of conventional reinforcement in as little

as nine months, regardless of deck type. By 24 months, the chloride content at cracks exceeds  $0.6 \text{ kg/m}^3$  ( $1.0 \text{ lb/yd}^3$ ) in the majority of the decks surveyed.

5. In general, the effective diffusion coefficient in uncracked regions  $D_{eff}^*$  appears to decrease with age (successive surveys). This observation is likely due to continued hydration and deposition of salt in the concrete pores, as well as shortcomings in the modeling process. Modeling chloride diffusion in bridge decks as if the chloride surface concentrations are constant (as done here), rather than increasing over time, tends to underestimate the diffusion coefficient at later ages.
6. Within the age ranges of 0 to 48 months and 48 to 96 months, all overlay bridge deck types exhibit similar diffusion properties.
7. For bridge decks sampled between 0 and 48 months,  $D_{eff}^*$  is lower for the single monolithic deck in this age range than for the overlay decks.
8. For bridge decks sampled between 48 and 96 months,  $D_{eff}^*$  is higher for monolithic decks than for overlay bridge decks.
9. Attempts to improve silica fume overlay decks through the use of special provisions have not decreased diffusivity.
10. For all bridge deck types, there is no correlation between  $D_{eff}^*$  and concrete slump.
11. For conventional overlays,  $D_{eff}^*$  increases as air content increases.
12. For monolithic bridge decks,  $D_{eff}^*$  increases as the (1) water-cement ratio, (2) water content, and (3) cement content increase.
13. For all bridge deck types, there is no apparent correlation between  $D_{eff}^*$  and compressive strength.

### **6.2.2 Time as a Variable in Bridge Deck Cracking**

1. Bridge deck crack density increases with age.
2. For the 49 bridges included in this study and one or both of the earlier studies (Schmitt and Darwin 1995, Miller and Darwin 2000), the crack densities obtained in the different studies show close agreement. Generally, the crack densities measured in this study are similar or greater than those obtained in the previous studies.
3. For all bridge deck types, a large percentage of the crack density is established early in the life of the deck.
4. The age-corrected crack densities for monolithic bridge decks constructed between 1984 and 1987 are lower than those of bridges constructed between 1990 and 1993.
5. The age-corrected crack densities for conventional overlay bridges are the lowest for bridges constructed between 1985 and 1987 and continue to increase for bridges constructed between the periods 1990–1992 and 1993–1995.
6. For silica fume overlay bridges constructed during the periods 1990–1991, 1995–1996, and 1997–1998 (containing 5% silica fume), the age-corrected crack densities decrease between the first and third time period. The newest silica fume overlays (containing 7% silica fume), constructed between 2000 and 2002, have slightly higher crack densities than silica fume overlays constructed between 1997 and 1998. The decrease in crack density appears to be the result of increased efforts to limit evaporation prior to the initiation of wet curing.
7. For silica fume and conventional overlays, both the average compressive strength and the range of compressive strengths have increased over the past 20 years.

### 6.2.3 Crack Survey Evaluation and Results

1. The crack densities of overlay bridges are generally higher than the crack densities of monolithic bridges. In addition, the crack densities of silica fume overlay decks appear to be independent of silica fume content and are slightly higher than the crack densities for conventional overlay decks.
2. The crack densities of monolithic bridge decks and overlay decks increase with increases in the water content, cement content, and percent volume of water and cement of the deck and subdeck, respectively. In general, increased paste contents in bridge subdecks result in increased cracking in decks with overlays, regardless of the overlay type or quality.
3. For silica fume overlays, the use of both fogging and precure material during and after finishing decreases the crack density.
4. For conventional overlay bridges, the highest crack densities are obtained for overlays placed with zero slump concrete.
5. For monolithic bridge decks, crack density increases slightly as concrete slump increases.
6. For monolithic bridge decks and overlay subdecks, the least amount of cracking is observed in decks with air contents greater than 6%. This trend is especially clear for monolithic bridge decks.
7. There is no correlation between the crack density and the air content of overlays.
8. For conventional overlay and monolithic bridge decks, crack density increases with increasing concrete compressive strength.
9. For conventional overlays, crack density increases as the average and minimum air temperatures on the date of placement increases.

10. For conventional overlay and monolithic bridge decks, crack density increases as the maximum air temperature on the date of placement increases.
11. For overlay bridges and monolithic bridge decks, crack density increases as the daily air temperature range on the date of concrete placement increases.
12. Monolithic placements (constructed between 1984 and 1995) were generally cast at lower air temperatures than overlay subdecks (constructed between 1990 and 2002).
13. The steel structure type appears to have no effect on bridge deck cracking.
14. For overlay bridges, cracking is more severe for those decks containing No. 19 (No. 6) top transverse reinforcing bars than for those containing a combination of No. 13 and No. 16 (No. 4 and No. 5) bars or No. 16 (No. 5) bars. The monolithic decks included in this study have either a combination of No. 13 and No. 16 (No. 4 and No. 5) bars or No. 16 (No. 5) bars and no tendency towards increased cracking is observed.
15. For overlay bridges, cracking is more severe for decks with top reinforcing bar spacings greater than 152 mm (6.0 in.). No analysis is possible for monolithic decks because all of the decks in this study have a top reinforcing bar spacing of 152 mm (6.0 in.).
16. In general, increased fixity, such as obtained with bridge decks that are integral with abutments, results in increased crack density near the supports. Although an analysis of the effect of end restraint on monolithic decks is not possible based on the current data set, the results for overlay bridges indicate a strong correlation between increased fixity and increased end-section cracking.
17. In general, the span type (interior and exterior), bridge skew, and bridge length do not appear to affect crack density.

18. Some contractors consistently cast bridge decks with low crack densities, while others consistently cast bridge decks with high crack densities.
19. For all bridge deck types, bridges subjected to a greater number of load cycles show greater levels of cracking.
20. For the overlay bridges, delamination of the overlay from the subdeck is not significant.

### **6.3 RECOMMENDATIONS**

Based on the results of this study, the following recommendations are made to improve bridge deck performance:

1. Conventional high-density overlays should be used in lieu of silica fume overlays containing either 5% or 7% silica fume. Conventional overlays, on average, have lower crack densities than silica fume overlays, and both types have similar diffusion properties and chloride contents, both at and away from cracks. These observations indicate that silica fume overlays provide no advantage over conventional overlays.
2. The use of high-density concrete overlays should be limited to resurfacing applications. This recommendation is based on two observations: (1) cracking is more severe in overlay decks than monolithic decks, and (2) adequate reinforcing steel protection from chloride ingress can be provided by uncracked concrete. The average chloride concentration at crack locations exceeds the corrosion threshold by the end of the first winter season after construction. The higher level of cracking in overlay decks represents a liability that can be addressed through the exclusive use of monolithic decks for full-depth construction.

3. When developing mix designs for overlay subdecks and monolithic decks, the total cement-paste volume should be less than 27% of the total volume of concrete.
4. Concrete for monolithic and overlay subdecks should be placed at the lowest slump that will allow for proper placement and consolidation.
5. When appropriate, the use of pin-ended girders should be considered, as an alternative to fix-ended girders, to significantly reduce cracking near the bridge abutments [3 m (10 ft)].
6. A contractor selection process should be implemented based on the quality of previous work. It is clear that some contractors consistently produce bridge decks with severe cracking, while others consistently produce bridges with low cracking.

As noted in Chapter 2, although the amount and availability of data for bridges has improved markedly compared to that available for the first two studies, there are still areas that need improvement. Evaporation rates, for instance, are required to be checked for silica fume overlays to ensure they are below  $1.0 \text{ kg/m}^2/\text{hr}$ ; this information, however, is rarely found in construction diaries or notes. Similarly, the concrete temperature, relative humidity, and wind speed during placement are required to estimate the evaporation rate but are typically not recorded. Additionally, start and finish times for the individual bridge placements and curing regimes are rarely mentioned. Recording this information was recommended by both Schmitt and Darwin (1995) and Miller and Darwin (2000). The availability of this information would have been invaluable to this study and will be invaluable in future investigations of the factors that control bridge deck quality.

## REFERENCES

- AASHTO T 259-80. (1980). "Resistance of Concrete to Chloride Ion Penetration," *1995 Standard Specifications for Transportation Materials and Methods of Sampling and Testing*, Part II Tests, American Association of State Highway and Transportation Officials, Washington, D.C., pp. 648-649.
- ACI Committee 222. (1996). "Corrosion of Metals in Concrete (ACI 222R-96)," *Manual of Concrete Practice*, Part 1, American Concrete Institute, Farmington Hills, MI, 30 pp.
- ACI Committee 234. (1996). "Guide for the Use of Silica Fume in Concrete (ACI 234R-96)," *Manual of Concrete Practice*, Part 1, American Concrete Institute, Farmington Hills, MI, 51 pp.
- ASTM C 1202-97. (1997). "Electrical Indication of Concrete's Ability to Resist Chloride Ion Penetration," *1999 Annual Book of ASTM Standards*, Vol. 4.02, American Society for Testing and Materials, West Conshohocken, PA, 1999, pp. 618-623.
- Babaei, K. and Fouladgar, A. M. (1997). "Solutions to Concrete Bridge Deck Cracking," *Concrete International*, Vol.15, No.7, July, pp. 34-37.
- Babaei, K. and Purvis, R. L. (1996). "Prevention of Cracks in Concrete Bridge Decks Summary Report," *Report No. 233*, Wilbur Smith Associates, Falls Church, VA, 30 pp.
- Chariton, T. and Weiss, W. J. (2002). "Using Acoustic Emission to Monitor Damage Development in Mortars Restrained from Volumetric Changes," *Concrete: Material Science to Application*, A Tribute to Surendra P. Shah, SP-206, American Concrete Institute, Farmington Hills, MI, pp. 205-219.
- Cheng, T. T.-H. and Johnston, D. W. (1985). "Incidence Assessment of Transverse Cracking in Concrete Bridge Decks: Construction and Material Considerations," *Report No. FHWA/NC/85-002 Vol. 1*, North Carolina State University, Raleigh, Department of Civil Engineering, 232 pp.
- Dakhil, F. H., Cady, P. D., and Carrier, R. E. (1975). "Cracking of Fresh Concrete as Related to Reinforcement," *ACI Journal, Proc.* Vol. 72, No. 8, Aug., pp. 421-428.
- Detwiler, R. J., Whiting, D. A., and Lagergren, E. S. (1999). "Statistical Approach to Ingress of Chloride Ions in Silica Fume Concrete for Bridge Decks," *ACI Materials Journal*, Vol. 96, No. 6, Jan.-Feb., pp. 670-695.

*Durability of Concrete Bridge Decks-A Cooperative Study, Final Report*, (1970). The state highway departments of California, Illinois, Kansas, Michigan, Minnesota, Missouri, New Jersey, Ohio, Texas, and Virginia; the Bureau of Public Roads; and Portland Cement Association, 35 pp.

Eppers, L., French, C., and Hajjar, J. F. (1998). "Transverse Cracking in Bridge Decks: Field Study," Minnesota Department of Transportation, Saint Paul, MN, 195 pp.

Federal Highway Administration (FHWA) (2002). "FHWA Bridge Programs NBI Data," FHWA website: [www.fhwa.dot.gov/bridge/britab.htm](http://www.fhwa.dot.gov/bridge/britab.htm)

Kansas Department of Transportation. (1990). *Standard Specifications for State Road and Bridge Construction*, Topeka, KS, 1154 pp.

Kansas Department of Transportation. (1993). *Special Provision to the Standard Specifications Edition of 1990*, 90P-158-R1, Topeka, KS, 9 pp.

Kansas Department of Transportation. (1994). *Special Provision to the Standard Specifications Edition of 1990*, 90P-158-R2, Topeka, KS, 10 pp.

Kansas Department of Transportation. (1994). *Special Provision to the Standard Specifications Edition of 1990*, 90P-158-R3, Topeka, KS, 10 pp.

Kansas Department of Transportation. (1995). *Special Provision to the Standard Specifications Edition of 1990*, 90P-158-R4, Topeka, KS, 12 pp.

Kansas Department of Transportation. (1995). *Special Provision to the Standard Specifications Edition of 1990*, 90M-158-R5, Topeka, KS, 12 pp.

Kansas Department of Transportation. (1996). *Special Provision to the Standard Specifications Edition of 1990*, 90P-158-R6, Topeka, KS, 12 pp.

Kansas Department of Transportation. (1996). *Special Provision to the Standard Specifications Edition of 1990*, 90M-158-R6, Topeka, KS, 12 pp.

Kansas Department of Transportation. (1997). *Special Provision to the Standard Specifications Edition of 1990*, 90M-158-R7, Topeka, KS, 11 pp.

Kansas Department of Transportation. (1997). *Special Provision to the Standard Specifications Edition of 1990*, 90M-158-R8, Topeka, KS, 11 pp.

Kansas Department of Transportation. (1997). *Special Provision to the Standard Specifications Edition of 1990*, 90M-158-R9, Topeka, KS, 11 pp.

Kansas Department of Transportation. (1997). *Special Provision to the Standard Specifications Edition of 1990*, 90M-158-R10, Topeka, KS, 11 pp.

Kansas Department of Transportation. (1998). *Special Provision to the Standard Specifications Edition of 1990*, 90M-95-R4, Topeka, KS, 9 pp.

Krauss, P. D., and Rogalla, E. A. (1996). "Transverse Cracking in Newly Constructed Bridge Decks," *National Cooperative Highway Research Program Report 380*, Transportation Research Board, Washington, D.C., 126 pp.

Le, Q. T. C., French, C., and Hajjar, J. F. (1998). "Transverse Cracking in Bridge Decks: Parametric Study," Minnesota Department of Transportation, Saint Paul, MN, 195 pp.

McDonald, D.B., Pfeifer, D.W., and Sherman, M.R. (1998). "Corrosion Evaluation of Epoxy-Coated Metallic-Clad and Solid Metallic Reinforcing Bars in Concrete," *Report No. FHWA-RD-98-153, Federal Highway Administration*, McLean, VA, 127 pp.

Mindess, S., Young, F., and Darwin, D. (2003). *Concrete*, Prentice-Hall, Inc., Englewood Cliffs, New Jersey, pp. 417-420.

Perfetti, G. R.; Johnston, D. W.; and Bingham, W. L. (1985). "Incidence Assessment of Transverse Cracking in Concrete Bridge Decks: Structural Considerations," *Report No. FHWA/NC/88002 Vol. 2*, North Carolina State University, Raleigh, Dept. of Civil Engineering, 201 pp.

Poppe, J. B. (1981). "Factors Affecting the Durability of Concrete Bridge Decks: Summary Final Report," *Report No. FHWA/CA/SD-81/2*, California Department of Transportation, Division of Transportation Facilities Design, Sacramento, CA, 61 pp.

Schmitt, T. R., and Darwin, D. (1995). "Cracking in Concrete Bridge Decks," *SM Report No. 39*, The University of Kansas Center for Research, Inc., Lawrence, Kansas, 151 pp.

Schmitt, T. R., and Darwin, D. (1999). "Effect of Material Properties on Cracking in Bridge Decks," *Journal of Bridge Engineering*, ASCE, Feb., Vol. 4, No. 1, pp. 8-13.

Suryavanshi, A. K., Swamy, R. N., and Cordew, G. E. (2002). "Estimation of Diffusion Coefficients for Chloride Ion Penetration into Structural Concrete," *ACI Materials Journal*, Vol. 99, No. 5, Sept.-Oct., pp. 441-449.

Virmani, Y. P., and Clemeña, G. G. (1998). "Corrosion Protection-Concrete Bridges," *Report* No. FHWA-RD-98-088, Federal Highway Administration, Washington, D.C.

Whiting, D. A., and Detwiler, R. (1998). "Silica Fume Concrete for Bridge Decks," *National Cooperative Highway Research Program Report* 410, Transportation Research Board, Washington, D.C., 180 pp.

Whiting, D. A., Detwiler, R. J., and Lagergen, E. S. (2000). "Cracking Tendency and Drying Shrinkage of Silica Fume Concrete For Bridge Decks," *ACI Materials Journal*, Vol. 97, No. 1, Nov.-Dec., pp. 71-77.

Whiting, David, and Michell, Terry M. (1992). "History of the Rapid Chloride Permeability Test," *Transportation Research Record*, Transportation Research Board, Washington, D.C., No. 1335, pp. 55-62.

Yunovich, M., Thompson, N. G., Balvanyos, T., and Lave, L. (2002). "Highway Bridges," Appendix D, *Corrosion Cost and Preventive Strategies in the United States*, by G. H. Koch, M. PO, H. Broongers, N. G. Thompson, Y. P. Virmani, and J. H. Payer, *Report* No. FHWA-RD-01-156, Federal Highway Administration, McLean, VA, 773 pp.

**Table 1.1 – Bridge deck cracking studies included in the review of literature**

<b>Author(s) / Title</b>	<b>Date</b>	<b>Primary Sponsor</b>
Schmitt and Darwin	1995	Kansas Department of Transportation
Miller and Darwin	2000	Kansas Department of Transportation
Portland Cement Association	1970	Multi-State Cooperative
Dakhil, Cady, and Carrier	1975	Pennsylvania State University
Poppe	1981	California Department of Transportation
Volume I: Cheng and Johnston Volume II: Perfetti, Johnston, and Bingham	1985	North Carolina Department of Transportation
Babaei and Purvis	1996	Pennsylvania Department of Transportation
Krauss and Rogalla	1996	NCHRP 380
Part I: Eppers, French, and Hajjar Part II: Le, French, and Hajjar	1998	Minnesota Department of Transportation
Whiting and Detwiler	1998	NCHRP 410

**Table 1.2 – Factors affecting bridge deck cracking (Krauss and Rogalla 1996)**

FACTORS	EFFECT			
	MAJOR	MODERATE	MINOR	NONE
<b>DESIGN</b>				
Restraint	✓			
Continuous/simple span		✓		
Deck thickness		✓		
Girder type		✓		
Alignment of reinforcement bars		✓		
Form type		✓		
Concrete cover			✓	
Girder spacing			✓	
Quantity of reinforcement			✓	
Reinforcement bar sizes			✓	
Dead-load deflections during casting			✓	
Stud spacing			✓	
Bar type – epoxy coated			✓	
Skew			✓	
Traffic volume				✓
Frequency of traffic-induced vibrations				✓
<b>MATERIALS</b>				
Modulus of elasticity	✓			
Creep	✓			
Heat of hydration	✓			
Aggregate type	✓			
Cement content and type	✓			
Coefficient of thermal expansion		✓		
Paste volume – free shrinkage		✓		
Water-cement ratio		✓		
Shrinkage-compensating cement		✓		
Silica fume admixture		✓		
Early compressive strength			✓	
HRWRAs			✓	
Accelerating admixtures			✓	
Retarding admixtures			✓	
Aggregate size			✓	
Diffusivity			✓	
Poisson's Ratio			✓	
Fly ash				✓
Air content				✓
Slump				✓
Water content				✓
<b>CONSTRUCTION</b>				
Weather	✓			
Time of casting	✓			
Curing period and method		✓		
Finishing procedures		✓		
Vibration of fresh concrete			✓	
Pour length and sequence			✓	
Reinforcement ties				✓
Construction loads				✓
Traffic-induced vibrations				✓
Revolutions in concrete truck				✓

**Table 1.3 – Primary factors found to increase cracking based on previous research**

<b>Material Considerations</b>	<b>Primary Factor</b>	<b>Design and Construction Factors</b>	<b>Primary Factor</b>
<b>Cement Content</b>	K1, K2, M2, N380, N410, P, NC1	<b>Fixed Girders</b>	K1, K2, M1, M2
<b>Cement Type</b>	N380, P	<b>Reinforcing Bar Size</b>	K1, K2, M2, PSU
<b>Water Content</b>	K1, K2, P	<b>Ambient Air Temperature</b>	K1, K2, NC1, M2, N410, C
<b>Paste Volume</b>	K1, K2, N380	<b>Time of Casting</b>	N380
<b>Aggregate Type</b>	N380, P	<b>Finishing Procedures</b>	N410, M2
<b>Air Content</b>	NC1, K1, K2	<b>Girder Type</b>	N410, NC1, NC2, PCA, N380, M1, M2, C
<b>Compressive Strength</b>	NC1, K1, K2	<b>Curing Practices</b>	N380, N410, M2, K2, C
<b>Creep</b>	N380		
<b>Heat of Hydration</b>	N380		
<b>Modulus of Elasticity</b>	N380		
<b>Mineral Admixtures</b>	N410		
<b>Initial Shrinkage Rate</b>	M2		
K1 – Kansas DOT, Schmitt and Darwin (1995, 1999)		NC1 – North Carolina DOT, Cheng and Johnston (1985)	
K2 – Kansas DOT, Miller and Darwin (2000)		NC2 – North Carolina DOT, Perfetti et al. (1985)	
PCA – <i>Durability</i> (1970)		P – Pennsylvania DOT, Babaei and Purvis (1996)	
PSU – Penn. State University, Dakhil et al. (1975)		N380 – NCHRP 380, Krauss and Rogalla (1996)	
C – California DOT, Poppe (1981)		N410 – NCHRP 410, Whiting and Detwiler (1998)	
M1 – Minnesota DOT, Le et al. (1998)		M2 – Minnesota DOT, Eppers et al. (1998)	

**Table 2.1 – Bridge deck types included in the current study and the studies by Schmitt and Darwin (1995, 1999) and Miller and Darwin (2000)**

	<b>Monolithic</b>	<b>Conventional Overlay</b>	<b>Silica Fume Overlay</b>	<b>Total</b>
<b>Schmitt and Darwin (S&amp;D)</b>	<b>15</b>	<b>20</b>	<b>2</b>	<b>37<sup>†</sup></b>
<b>Miller and Darwin (M&amp;D)</b>	<b>4</b> (3 S&D)	<b>16</b> (6 S&D)	<b>20</b> (2 S&D)	<b>40</b>
<b>Current Study</b>	<b>13</b> (12 S&D) (4 M&D)	<b>16</b> (6 S&D) (16 M&D)	<b>30</b> (2 S&D) (20 M&D)	<b>59</b>

<sup>†</sup>Study also included 3 non-composite bridge decks that are not included in the data evaluated in this study.

**Table 3.1 – KDOT District One Salt Usage History**

<b>Fiscal Year</b>	<b>Rock Salt Totals</b>		<b>Average Application Rate<sup>†</sup></b>	
	<b>(kg × 1000)</b>	<b>(Tons)</b>	<b>(kg/m<sup>2</sup>)</b>	<b>(lb/yd<sup>2</sup>)</b>
<b>1998</b>	34,443	37,967	1.29	2.38
<b>1999</b>	30,956	34,123	1.16	2.14
<b>2000</b>	28,519	31,437	1.07	1.97
<b>2001</b>	43,906	48,398	1.65	3.04
<b>2002</b>	29,544	32,567	1.10	2.04
<b>2003</b>	23,903	26,348	0.89	1.65
<b>2004</b>	39,639	43,695	1.48	2.73
<b>Average</b>	32,987	36,362	1.24	2.28

<sup>†</sup>The average application rate is calculated using the total lane miles reported annually by KDOT which has increased slightly from 7,281 km (4,524 mi.) in 1998 to 7,313 km (4,544 mi.) in 2004.

**Table 3.2 – Time to corrosion threshold for uncracked concrete based on data from Figs. 3.1 through 3.4**

Depth	Time (months) to reach 0.6 kg/m <sup>3</sup> (1.0 lb/yd <sup>3</sup> )			Time (months) to reach 1.2 kg/m <sup>3</sup> (2.0 lb/yd <sup>3</sup> )		
	20% U <sup>†</sup>	Trend Line	20% L <sup>‡</sup>	20% U <sup>†</sup>	Trend Line	20% L <sup>‡</sup>
25.4 mm (1.0 in.)	0	23	65	3	44	86
50.8 mm (2.0 in.)	20	91	163	81	152	222
63.5 mm (2.5 in.)	69	143	218	186	261	335
76.2 mm (3.0 in.)	160	254	349	410	504	599

<sup>†</sup>The upper 20% prediction interval category (20% U) indicates the time at which only 20% of the decks are expected to reach the corrosion threshold more quickly.

<sup>‡</sup>The lower 20% prediction interval category (20% L) indicates the time at which 80% of the decks are expected to reach the corrosion threshold more quickly.

**Table 3.3a – Average apparent surface concentration build-up rates [kg/m<sup>3</sup>/month (kg/m<sup>3</sup>/year)] and standard deviations for all bridge types**

	All	Monolithic	Conventional Overlay	Silica Fume Overlay
Average	0.038 (0.456)	0.042 (0.504)	0.017 (0.204)	0.055 (0.660)
Standard Deviation	0.032 (0.384)	0.011 (0.132)	0.034 (0.408)	0.050 (0.600)
Age Range [months (years)]	4 – 145	36 – 133	36 – 145	4 – 142

**Table 3.3b – Average apparent surface concentration build-up rates [lb/yd<sup>3</sup>/month (lb/yd<sup>3</sup>/year)] and standard deviations for all bridge types**

	All	Monolithic	Conventional Overlay	Silica Fume Overlay
Average	0.064 (0.769)	0.071 (0.849)	0.029 (0.344)	0.093 (1.112)
Standard Deviation	0.054 (0.647)	0.019 (0.222)	0.057 (0.688)	0.084 (1.011)
Age Range [months (years)]	4 – 145	36 – 133	36 – 145	4 – 142

**Table 3.4 – Student's t-test for mean effective diffusion coefficients  $D_{eff}$  versus placement age (Figs. 3.22, 3.25, 3.28)**

				80%	90%	95%	98%				
<b>Monolithic Decks</b>				<b>Confidence Level <math>\alpha</math></b>							
<b>(months)</b>		<b>d.o.f.</b>	<b>t calc</b>	<b>0.20</b>	<b>0.10</b>	<b>0.05</b>	<b>0.02</b>				
48 to 96	over 96	17	0.291	1.333	N	1.740	N	2.110	N	2.567	N
<b>Conventional Overlays</b>				<b>Confidence Level <math>\alpha</math></b>							
<b>(months)</b>		<b>d.o.f.</b>	<b>t calc</b>	<b>0.20</b>	<b>0.10</b>	<b>0.05</b>	<b>0.02</b>				
0 to 48	48 to 96	39	3.061	1.304	Y	1.685	Y	2.023	Y	2.426	Y
0 to 48	over 96	34	3.459	1.307	Y	1.691	Y	2.032	Y	2.441	Y
48 to 96	over 96	59	0.653	1.296	N	1.671	N	2.001	N	2.391	N
<b>Silica Fume Overlays</b>				<b>Confidence Level <math>\alpha</math></b>							
<b>(months)</b>		<b>d.o.f.</b>	<b>t calc</b>	<b>0.20</b>	<b>0.10</b>	<b>0.05</b>	<b>0.02</b>				
0 to 48 (7%)	0 to 48 (5%)	49	1.587	1.299	Y	1.677	N	2.010	N	2.405	N
0 to 48 (7%)	48 to 96 (5%)	51	4.550	1.298	Y	1.675	Y	2.008	Y	2.402	Y
0 to 48 (7%)	96+ (5%)	15	0.891	1.341	N	1.753	N	2.132	N	2.603	N
0 to 48 (5%)	48 to 96 (5%)	76	4.254	1.293	Y	1.665	Y	1.992	Y	2.376	Y
48 to 96 (5%)	96+ (5%)	42	1.606	1.302	Y	1.682	N	2.018	N	2.419	N

**Key:**

d.o.f. = degrees of freedom for the two categories being compared

t calc = calculated value of t

$\alpha$  = level of significance

t table test values = value for Student's t-distribution for the given value of  $\alpha$

Y = statistically significant difference between groups

N = not a statistically significant difference between groups

**Table 3.5 – Average rate of change for effective diffusion coefficients  $D_{eff}$  obtained from dummy variable regression analysis.**

	Number of Placements	Number of Surveys	Mean Age (months)	Average Rate of Change ( $\text{mm}^2/\text{day}/\text{month}$ )	$R^2$
<b>Monolithic Decks</b>	4	8	94	$-3.613 \times 10^{-4}$	0.64
<b>Conventional Overlay Decks</b>	36	71	87	$-5.182 \times 10^{-4}$	0.94
<b>5% Silica Fume Overlay Decks</b>	42	83	51	$-1.035 \times 10^{-3}$	0.84

**Table 3.6 – Student's t-test for mean adjusted effective diffusion coefficients  $D_{eff}^*$  versus placement age (Figs. 3.30, 3.31)**

				80%	90%	95%	98%				
<b>Bridge Deck Type</b>				<b>Confidence Level <math>\alpha</math></b>							
<b>0 to 48 months old</b>		<b>d.o.f.</b>	<b>t calc</b>	<b>0.20</b>	<b>0.10</b>	<b>0.05</b>	<b>0.02</b>				
7% SFO	5% SFO	49	1.587	1.299	Y	1.677	N	2.010	N	2.405	N
7% SFO	CO	19	0.396	1.328	N	1.729	N	2.093	N	2.540	N
5% SFO	CO	44	0.919	1.301	N	1.680	N	2.015	N	2.414	N
<b>Bridge Deck Type</b>		<b>d.o.f.</b>	<b>t calc</b>	<b>0.20</b>	<b>0.10</b>	<b>0.05</b>	<b>0.02</b>				
<b>48 to 96 months old</b>		<b>d.o.f.</b>	<b>t calc</b>	<b>0.20</b>	<b>0.10</b>	<b>0.05</b>	<b>0.02</b>				
5% SFO	CO	71	1.270	1.294	N	1.667	N	1.994	N	2.380	N
5% SFO	MONO	42	4.466	1.302	Y	1.682	Y	2.018	Y	2.419	Y
CO	MONO	35	3.154	1.306	Y	1.690	Y	2.030	Y	2.438	Y

**Key:**

d.o.f. = degrees of freedom for the two categories being compared

t calc = calculated value of t

$\alpha$  = level of significance

t table test values = value for Student's t-distribution for the given value of  $\alpha$

Y = statistically significant difference between groups

N = not a statistically significant difference between groups

**Table 3.7 – The time (years) to reach corrosion threshold levels at a depth of 76 mm (3 in.) based on adjusted effective diffusion coefficients  $D_{eff}^*$  calculated from data obtained within the first 48 months of deck construction using Fick’s Second Law of Diffusion [Eq. (1.2)]**

<b>Deck Type</b>	<b><math>C_o</math> (kg/m<sup>3</sup>)</b>	<b><math>Adj. D_{eff}</math> (mm<sup>2</sup>/day)</b>	<b>Time (years) to reach 0.60 kg/m<sup>3</sup></b>	<b>Time (years) to reach 1.20 kg/m<sup>3</sup></b>
<b>7% SFO</b>	6.0	0.17	17.6	23.0
<b>5% SFO</b>	6.0	0.13	23.4	30.5
<b>CO</b>	6.0	0.16	18.0	23.5

**Table 3.8 – The time (years) to reach corrosion threshold levels at a depth of 76 mm (3 in.) based on adjusted effective diffusion coefficients  $D_{eff}^*$  calculated from data obtained between 48 and 96 months of deck construction using Fick’s Second Law of Diffusion [Eq. (1.2)]**

<b>Deck Type</b>	<b><math>C_o</math> (kg/m<sup>3</sup>)</b>	<b><math>Adj. D_{eff}</math> (mm<sup>2</sup>/day)</b>	<b>Time (years) to reach 0.60 kg/m<sup>3</sup></b>	<b>Time (years) to reach 1.20 kg/m<sup>3</sup></b>
<b>5% SFO</b>	10.0	0.07	33.4	41.0
<b>CO</b>	10.0	0.09	25.0	30.8
<b>MONO</b>	10.0	0.17	13.6	16.7

**Table 3.9 – Student's t-test for mean adjusted effective diffusion coefficients  $D_{eff}^*$  versus special provision number (Figs. 3.32)**

				80%	90%	95%	98%				
<b>Silica Fume Overlays</b>											
<b>0 to 48 months</b>				<b>Confidence Level <math>\alpha</math></b>							
<b>Special Provision Number</b>	<b>d.o.f.</b>	<b>t calc</b>		<b>0.20</b>	<b>0.10</b>	<b>0.05</b>	<b>0.02</b>				
R1, R2	R3	15	1.346	1.341	Y	1.753	N	2.131	N	2.602	N
R1, R2	R4, R5, R6	27	2.978	1.314	Y	1.703	Y	2.052	Y	2.473	Y
R1, R2	R8, R9	19	2.178	1.328	Y	1.729	Y	2.093	Y	2.539	N
R3	R4, R5, R6	28	1.333	1.313	Y	1.701	N	2.048	N	2.467	N
R3	R8, R9	20	1.261	1.325	N	1.725	N	2.086	N	2.528	N
R4, R5, R6	R8, R9	32	0.606	1.309	N	1.694	N	2.037	N	2.449	N
<b>Silica Fume Overlays</b>											
<b>48 to 96 months</b>											
<b>Special Provision Number</b>	<b>d.o.f.</b>	<b>t calc</b>		<b>0.20</b>	<b>0.10</b>	<b>0.05</b>	<b>0.02</b>				
none	R1, R2	10	0.408	1.372	N	1.812	N	2.228	N	2.764	N
none	R3	15	0.381	1.341	N	1.753	N	2.131	N	2.602	N
none	R4, R5, R6	25	0.401	1.316	N	1.708	N	2.060	N	2.485	N
R1, R2	R3	19	0.952	1.328	N	1.729	N	2.093	N	2.539	N
R1, R2	R4, R5, R6	31	0.848	1.309	N	1.696	N	2.040	N	2.453	N
R3	R4, R5, R6	30	0.255	1.310	N	1.697	N	2.042	N	2.457	N

**Key:**

d.o.f. = degrees of freedom for the two categories being compared

t calc = calculated value of t

$\alpha$  = level of significance

t table test values = value for Student's t-distribution for the given value of  $\alpha$

Y = statistically significant difference between groups

N = not a statistically significant difference between groups

**Table 3.10 – Student's t-test for mean adjusted effective diffusion coefficients  $D_{eff}^*$  versus concrete slump (Figs. 3.33, 3.34, 3.35, 3.36)**

				80%	90%	95%	98%
<b>Silica Fume Overlays</b>							
<b>0 to 48 months</b>				<b>Confidence Level <math>\alpha</math></b>			
<b>slump (mm)</b>	<b>d.o.f.</b>	<b>t calc</b>		<b>0.20</b>	<b>0.10</b>	<b>0.05</b>	<b>0.02</b>
38 (5% SFO)	64 (5% SFO)	22	1.125	1.321 N	1.717 N	2.074 N	2.508 N
38 (5% SFO)	89 (5% SFO)	11	0.180	1.363 N	1.796 N	2.201 N	2.718 N
38 (5% SFO)	>100 (5% SFO)	6	0.930	1.440 N	1.943 N	2.447 N	3.143 N
64 (5% SFO)	89 (5% SFO)	25	0.991	1.316 N	1.708 N	2.060 N	2.485 N
64 (5% SFO)	>100 (5% SFO)	21	0.079	1.323 N	1.721 N	2.080 N	2.518 N
89 (5% SFO)	>100 (5% SFO)	9	0.537	1.383 N	1.833 N	2.262 N	2.821 N
64 (7% SFO)	89 (7% SFO)	8	0.510	1.397 N	1.860 N	2.306 N	2.896 N
64 (7% SFO)	>100 (7% SFO)	3	0.259	1.638 N	2.353 N	3.182 N	4.541 N
89 (7% SFO)	>100 (7% SFO)	7	0.735	1.415 N	1.895 N	2.365 N	2.998 N
<b>Silica Fume Overlays</b>							
<b>48 to 96 months</b>							
<b>slump (mm)</b>	<b>d.o.f.</b>	<b>t calc</b>		<b>0.20</b>	<b>0.10</b>	<b>0.05</b>	<b>0.02</b>
38	64	22	0.893	1.321 N	1.717 N	2.074 N	2.508 N
38	89	11	1.170	1.363 N	1.796 N	2.201 N	2.718 N
38	>100	6	1.369	1.440 N	1.943 N	2.447 N	3.143 N
64	89	25	0.213	1.316 N	1.708 N	2.060 N	2.485 N
64	>100	21	0.064	1.323 N	1.721 N	2.080 N	2.518 N
89	>100	9	0.115	1.383 N	1.833 N	2.262 N	2.821 N

**Key:**

d.o.f. = degrees of freedom for the two categories being compared

t calc = calculated value of t

$\alpha$  = level of significance

t table test values = value for Student's t-distribution for the given value of  $\alpha$

Y = statistically significant difference between groups

N = not a statistically significant difference between groups

**Table 3.10 (con't)– Student's t-test for mean adjusted effective diffusion coefficients  $D_{eff}^*$  versus concrete slump (Figs. 3.33, 3.34, 3.35, 3.36)**

				80%	90%	95%	98%				
<b>Conventional Overlays</b>											
<b>48 to 96 months</b>				<b>Confidence Level <math>\alpha</math></b>							
<b>slump (mm)</b>	<b>d.o.f.</b>	<b>t calc</b>		<b>0.20</b>	<b>0.10</b>	<b>0.05</b>	<b>0.02</b>				
0	6	9	2.994	1.383	Y	1.833	Y	2.262	Y	2.821	Y
0	13	12	1.179	1.356	N	1.782	N	2.179	N	2.681	N
0	19	9	1.633	1.383	Y	1.833	N	2.262	N	2.821	N
6	13	13	0.068	1.350	N	1.771	N	2.160	N	2.650	N
6	>19	10	0.559	1.372	N	1.812	N	2.228	N	2.764	N
13	>19	13	0.278	1.350	N	1.771	N	2.160	N	2.650	N
<b>Conventional Overlays</b>											
<b>96 to 144 months</b>											
<b>slump (mm)</b>	<b>d.o.f.</b>	<b>t calc</b>		<b>0.20</b>	<b>0.10</b>	<b>0.05</b>	<b>0.02</b>				
0	6	9	0.584	1.383	N	1.833	N	2.262	N	2.821	N
0	13	15	0.415	1.341	N	1.753	N	2.131	N	2.602	N
0	19	11	0.913	1.363	N	1.796	N	2.201	N	2.718	N
6	13	12	0.287	1.356	N	1.782	N	2.179	N	2.681	N
6	19	8	0.361	1.397	N	1.860	N	2.306	N	2.896	N
13	19	14	0.604	1.345	N	1.761	N	2.145	N	2.624	N
<b>Monolithic</b>											
<b>over 120 months</b>											
<b>slump (mm)</b>	<b>d.o.f.</b>	<b>t calc</b>		<b>0.20</b>	<b>0.10</b>	<b>0.05</b>	<b>0.02</b>				
44	57	9	1.170	1.383	N	1.833	N	2.262	N	2.821	N
44	89	6	0.306	1.440	N	1.943	N	2.447	N	3.143	N
57	89	7	0.663	1.415	N	1.895	N	2.365	N	2.998	N

**Key:**

d.o.f. = degrees of freedom for the two categories being compared

t calc = calculated value of t

$\alpha$  = level of significance

t table test values = value for Student's t-distribution for the given value of  $\alpha$

Y = statistically significant difference between groups

N = not a statistically significant difference between groups

**Table 3.11 – Student's t-test for mean adjusted effective diffusion coefficients  $D_{eff}^*$  versus air content (Figs. 3.37, 3.38, 3.39, 3.40)**

				80%	90%	95%	98%				
<b>Silica Fume Overlays</b>											
<b>0 to 48 Months</b>											
(%)		d.o.f.	t calc	Confidence Level $\alpha$							
				0.20	0.10	0.05	0.02				
4.5 (5% SFO)	5.5 (5% SFO)	29	1.426	1.311	Y	1.699	N	2.045	N	2.462	N
4.5 (5% SFO)	6.5 (5% SFO)	15	2.107	1.341	Y	1.753	Y	2.131	N	2.602	N
5.5 (5% SFO)	6.5 (5% SFO)	18	1.366	1.330	Y	1.734	N	2.101	N	2.552	N
5.5 (7% SFO)	5.5 (5% SFO)	18	0.045	1.330	N	1.734	N	2.101	N	2.552	N
6.5 (7% SFO)	6.5 (5% SFO)	4	0.161	1.533	N	2.132	N	2.776	N	3.747	N
5.5 (7% SFO)	6.5 (7% SFO)	4	0.698	1.533	N	2.132	N	2.776	N	3.747	N
<b>Silica Fume Overlays</b>											
<b>48 to 96 Months</b>											
(%)		d.o.f.	t calc	0.20	0.10	0.05	0.02				
4.5	5.5	29	0.950	1.311	N	1.699	N	2.045	N	2.462	N
4.5	6.5	15	1.539	1.341	Y	1.753	N	2.131	N	2.602	N
5.5	6.5	18	1.117	1.330	N	1.734	N	2.101	N	2.552	N
<b>Conventional Overlays</b>											
<b>48 to 96 Months</b>											
(%)		d.o.f.	t calc	0.20	0.10	0.05	0.02				
4.375	5.125	9	0.282	1.383	N	1.833	N	2.262	N	2.821	N
4.375	5.875	10	0.322	1.372	N	1.812	N	2.228	N	2.764	N
4.375	6.625	6	1.414	1.440	N	1.943	N	2.447	N	3.143	N
5.125	5.875	13	0.049	1.350	N	1.771	N	2.160	N	2.650	N
5.125	6.625	9	1.486	1.383	Y	1.833	N	2.262	N	2.821	N
5.875	6.625	10	1.478	1.372	Y	1.812	N	2.228	N	2.764	N

**Key:**

d.o.f. = degrees of freedom for the two categories being compared

t calc = calculated value of t

$\alpha$  = level of significance

t table test values = value for Student's t-distribution for the given value of  $\alpha$

Y = statistically significant difference between groups

N = not a statistically significant difference between groups

**Table 3.11 (con't) – Student's t-test for mean adjusted effective diffusion coefficients  $D_{eff}^*$  versus air content (Figs. 3.37, 3.38, 3.39, 3.40)**

				80%	90%	95%	98%				
<b>Conventional Overlays</b>											
<b>96 to 144 Months</b>				<b>Confidence Level <math>\alpha</math></b>							
<b>(%)</b>		<b>d.o.f.</b>	<b>t calc</b>	<b>0.20</b>	<b>0.10</b>	<b>0.05</b>	<b>0.02</b>				
4.375	5.125	7	1.415	1.415	N	1.895	N	2.365	N	2.998	N
4.375	5.875	12	1.356	1.356	N	1.782	N	2.179	N	2.681	N
4.375	6.625	5	1.476	1.476	Y	2.015	N	2.571	N	3.365	N
5.125	5.875	15	1.341	1.341	N	1.753	N	2.131	N	2.602	N
5.125	6.625	8	1.397	1.397	N	1.860	N	2.306	N	2.896	N
5.875	6.625	13	1.350	1.350	Y	1.771	N	2.160	N	2.650	N
<b>Monolithic Decks</b>											
<b>Over 120 Months Old</b>											
<b>(%)</b>		<b>d.o.f.</b>	<b>t calc</b>	<b>0.20</b>	<b>0.10</b>	<b>0.05</b>	<b>0.02</b>				
4.875	5.625	10	1.804	1.372	Y	1.812	N	2.228	N	2.764	N
4.875	6.375	4	0.806	1.533	N	2.132	N	2.776	N	3.747	N
5.625	6.375	8	1.602	1.397	Y	1.860	N	2.306	N	2.896	N

**Key:**

d.o.f. = degrees of freedom for the two categories being compared

t calc = calculated value of t

$\alpha$  = level of significance

t table test values = value for Student's t-distribution for the given value of  $\alpha$

Y = statistically significant difference between groups

N = not a statistically significant difference between groups

**Table 3.12 – Student's t-test for mean adjusted effective diffusion coefficients  $D_{eff}^*$  versus water-cementitious material ratio (Figs. 3.41, 3.42, 3.43)**

				80%	90%	95%	98%				
<b>Silica Fume Overlays</b>				<b>Confidence Level <math>\alpha</math></b>							
<b>0 to 48 Months</b>		<b>d.o.f.</b>	<b>t calc</b>	<b>0.20</b>	<b>0.10</b>	<b>0.05</b>	<b>0.02</b>				
0.37 (7%)	0.38 (5%)	16	0.626	1.337	N	1.746	N	2.120	N	2.583	N
0.37 (7%)	0.40 (5%)	42	1.574	1.302	Y	1.682	N	2.018	N	2.418	N
0.38 (5%)	0.40 (5%)	36	0.400	1.306	N	1.688	N	2.028	N	2.434	N
<b>Silica Fume Overlays</b>											
<b>48 to 96 Months</b>		<b>d.o.f.</b>	<b>t calc</b>	<b>0.20</b>	<b>0.10</b>	<b>0.05</b>	<b>0.02</b>				
0.38 (5%)	0.40 (5%)	36	2.357	1.306	Y	1.688	Y	2.028	Y	2.434	N
<b>Conventional Overlays</b>											
<b>48 to 96 Months</b>		<b>d.o.f.</b>	<b>t calc</b>	<b>0.20</b>	<b>0.10</b>	<b>0.05</b>	<b>0.02</b>				
0.36	0.38	27	1.833	1.314	Y	1.703	Y	2.052	N	2.473	N
0.36	0.40	24	1.328	1.318	Y	1.711	N	2.064	N	2.492	N
0.38	0.40	9	2.283	1.383	Y	1.833	Y	2.262	Y	2.821	N
<b>Conventional Overlays</b>											
<b>96 to 144 Months</b>		<b>d.o.f.</b>	<b>t calc</b>	<b>0.20</b>	<b>0.10</b>	<b>0.05</b>	<b>0.02</b>				
0.36	0.38	27	2.875	1.314	Y	1.703	Y	2.052	Y	2.473	Y
0.36	0.40	24	0.864	1.318	N	1.711	N	2.064	N	2.492	N
0.38	0.40	9	2.851	1.383	Y	1.833	Y	2.262	Y	2.821	Y
<b>Monolithic Decks</b>											
<b>Over 120 Months Old</b>		<b>d.o.f.</b>	<b>t calc</b>	<b>0.20</b>	<b>0.10</b>	<b>0.05</b>	<b>0.02</b>				
0.42	0.44	12	1.627	1.356	Y	1.782	N	2.179	N	2.681	N

**Key:**

d.o.f. = degrees of freedom for the two categories being compared

t calc = calculated value of t

$\alpha$  = level of significance

t table test values = value for Student's t-distribution for the given value of  $\alpha$

Y = statistically significant difference between groups

N = not a statistically significant difference between groups

**Table 3.13 – Student's t-test for mean adjusted effective diffusion coefficients  $D_{eff}^*$  versus percent volume of water and cement (Figs. 3.44)**

				80%	90%	95%	98%				
Monolithic											
Over 120 Months				Confidence Level $\alpha$							
(kg/m <sup>3</sup> )		d.o.f.	t calc	0.20	0.10	0.05	0.02				
27	28	10	0.521	1.372	N	1.812	N	2.228	N	2.764	N
27	29	8	0.703	1.397	N	1.860	N	2.306	N	2.896	N
28	29	4	0.328	1.533	N	2.132	N	2.776	N	3.747	N

**Table 3.14 – Student's t-test for mean adjusted effective diffusion coefficients  $D_{eff}^*$  versus water content (Figs. 3.45)**

				80%	90%	95%	98%				
Monolithic											
Over 120 Months				Confidence Level $\alpha$							
(kg/m <sup>3</sup> )		d.o.f.	t calc	0.20	0.10	0.05	0.02				
147	156	2	2.564	1.886	Y	2.920	N	4.303	N	6.965	N
147	165	11	1.649	1.363	Y	1.796	N	2.201	N	2.718	N
156	165	2	0.360	1.886	N	2.920	N	4.303	N	6.965	N

**Table 3.15 – Student's t-test for mean adjusted effective diffusion coefficients  $D_{eff}^*$  versus cement content (Figs. 3.46)**

				80%	90%	95%	98%				
Monolithic											
Over 120 Months				Confidence Level $\alpha$							
(kg/m <sup>3</sup> )		d.o.f.	t calc	0.20	0.10	0.05	0.02				
357 & 359	379	11	0.749	1.363	N	1.796	N	2.201	N	2.718	N

**Key:**

d.o.f. = degrees of freedom for the two categories being compared

t calc = calculated value of t

$\alpha$  = level of significance

t table test values = value for Student's t-distribution for the given value of  $\alpha$

Y = statistically significant difference between groups

N = not a statistically significant difference between groups

**Table 3.16 – Student's t-test for mean adjusted effective diffusion coefficients  $D_{eff}^*$  versus concrete compressive strength (Figs. 3.47, 3.48, 3.49, 3.50)**

				80%	90%	95%	98%				
<b>Silica Fume Overlays</b>											
<b>0 to 48 Months</b>				<b>Confidence Level <math>\alpha</math></b>							
<b>(MPa)</b>		<b>d.o.f.</b>	<b>t calc</b>	<b>0.20</b>	<b>0.10</b>	<b>0.05</b>	<b>0.02</b>				
38 (5% SFO)	45 (5% SFO)	8	0.513	1.397	N	1.860	N	2.306	N	2.896	N
38 (5% SFO)	52 (5% SFO)	9	0.710	1.383	N	1.833	N	2.262	N	2.821	N
38 (5% SFO)	59 (5% SFO)	6	0.429	1.440	N	1.943	N	2.447	N	3.143	N
45 (5% SFO)	52 (5% SFO)	11	2.009	1.363	Y	1.796	Y	2.201	N	2.718	N
45 (5% SFO)	59 (5% SFO)	8	1.023	1.397	N	1.860	N	2.306	N	2.896	N
52 (5% SFO)	59 (5% SFO)	9	0.071	1.383	N	1.833	N	2.262	N	2.821	N
45 (7% SFO)	52 (7% SFO)	4	0.239	1.533	N	2.132	N	2.776	N	3.747	N
<b>Silica Fume Overlays</b>											
<b>48 to 96 Months</b>											
<b>(MPa)</b>		<b>d.o.f.</b>	<b>t calc</b>	<b>0.20</b>	<b>0.10</b>	<b>0.05</b>	<b>0.02</b>				
38	45	8	1.804	1.397	Y	1.860	N	2.306	N	2.896	N
38	52	9	1.042	1.383	N	1.833	N	2.262	N	2.821	N
38	59	6	1.351	1.440	N	1.943	N	2.447	N	3.143	N
45	52	11	2.436	1.363	Y	1.796	Y	2.201	Y	2.718	N
45	59	8	0.418	1.397	N	1.860	N	2.306	N	2.896	N
52	59	9	1.838	1.383	Y	1.833	Y	2.262	N	2.821	N

**Key:**

d.o.f. = degrees of freedom for the two categories being compared

t calc = calculated value of t

$\alpha$  = level of significance

t table test values = value for Student's t-distribution for the given value of  $\alpha$

Y = statistically significant difference between groups

N = not a statistically significant difference between groups

**Table 3.16 (con't) – Student's t-test for mean adjusted effective diffusion coefficients  $D_{eff}^*$  versus concrete compressive strength (Figs. 3.47, 3.48, 3.49, 3.50)**

				80%	90%	95%	98%
<b>Conventional Overlays</b>							
<b>48 to 96 Months</b>				<b>Confidence Level <math>\alpha</math></b>			
(MPa)	d.o.f.	t calc		0.20	0.10	0.05	0.02
38	45	10	1.238	1.372 N	1.812 N	2.228 N	2.764 N
38	52	9	0.317	1.383 N	1.833 N	2.262 N	2.821 N
45	52	9	0.998	1.383 N	1.833 N	2.262 N	2.821 N
<b>Conventional Overlays</b>							
<b>96 to 144 Months</b>							
(MPa)	d.o.f.	t calc		0.20	0.10	0.05	0.02
38	45	11	0.449	1.363 N	1.796 N	2.201 N	2.718 N
38	52.00	9	0.063	1.383 N	1.833 N	2.262 N	2.821 N
45	52.00	10	0.381	1.372 N	1.812 N	2.228 N	2.764 N
<b>Monolithic Decks</b>							
<b>Over 120 Months Old</b>							
(MPa)	d.o.f.	t calc		0.20	0.10	0.05	0.02
31	38	3	0.579	1.638 N	2.353 N	3.182 N	4.541 N
31	45	4	0.716	1.533 N	2.132 N	2.776 N	3.747 N
38	45	6	0.010	1.440 N	1.943 N	2.447 N	3.143 N

**Key:**

d.o.f. = degrees of freedom for the two categories being compared

t calc = calculated value of t

$\alpha$  = level of significance

t table test values = value for Student's t-distribution for the given value of  $\alpha$

Y = statistically significant difference between groups

N = not a statistically significant difference between groups

**Table 4.1 – Cracking rates obtained from dummy variable regression analysis**

	<b>Number of Bridges</b>	<b>Number of Surveys</b>	<b>Mean Age (months)</b>	<b>Cracking Rate (m/m<sup>2</sup>/month)</b>	<b>R<sup>2</sup></b>
<b>Monolithic Decks</b>	13	29	115	0.0013	0.94
<b>Conventional Overlay Decks</b>	16	36	87	0.0008	0.85
<b>5% Silica Fume Overlay Decks</b>	20	42	53	0.0028	0.86

**Table 4.2 – Student's t-test for mean crack density versus date of construction for individual bridge decks [both age-corrected and non age-corrected (Figs. 4.10, 4.11, 4.12)]**

				<b>80%</b>	<b>90%</b>	<b>95%</b>	<b>98%</b>				
<b>Monolithic Decks</b>		<b>Confidence Level <math>\alpha</math></b>									
<b>(construction years)</b>	<b>d.o.f.</b>	<b>t calc</b>	<b>0.20</b>	<b>0.10</b>	<b>0.05</b>	<b>0.02</b>					
1984-1987	1990-1993	11	1.990	1.363	Y	1.796	Y	2.201	N	2.718	N
1984-1987*	1990-1993*	11	2.803	1.363	Y	1.796	Y	2.201	Y	2.718	Y

**Key:**

d.o.f. = degrees of freedom for the two categories being compared

t calc = calculated value of t

$\alpha$  = level of significance

t table test values = value for Student's t-distribution for the given value of  $\alpha$

Y = statistically significant difference between groups

N = not a statistically significant difference between groups

**Table 4.2 (con't) – Student's t-test for mean crack density versus date of construction for individual bridge decks [both age-corrected and non age-corrected (Figs. 4.10, 4.11, 4.12)]**

				80%	90%	95%	98%				
<b>Conventional Overlays</b>											
<b>(construction years)</b>		<b>d.o.f.</b>	<b>t calc</b>	<b>0.20</b>	<b>0.10</b>	<b>0.05</b>	<b>0.02</b>				
1985-1987	1990-1992	21	2.965	1.323	Y	1.721	Y	2.080	Y	2.518	Y
1985-1987	1993-1995	7	4.257	1.415	Y	1.895	Y	2.365	Y	2.998	Y
1990-1992	1993-1995	18	2.694	1.330	Y	1.734	Y	2.101	Y	2.552	Y
1985-1987*	1990-1992*	21	2.965	1.323	Y	1.721	Y	2.080	Y	2.518	Y
1985-1987*	1993-1995*	7	4.437	1.415	Y	1.895	Y	2.365	Y	2.998	Y
1990-1992*	1993-1995*	18	3.056	1.330	Y	1.734	Y	2.101	Y	2.552	Y
<b>Silica Fume Overlays</b>											
<b>(construction years)</b>		<b>d.o.f.</b>	<b>t calc</b>	<b>0.20</b>	<b>0.10</b>	<b>0.05</b>	<b>0.02</b>				
1990-1991	1995-1996	10	2.616	1.372	Y	1.812	Y	2.228	Y	2.764	N
1990-1991	1997-1998	8	5.598	1.397	Y	1.860	Y	2.306	Y	2.896	Y
1990-1991	2000-2002	10	2.091	1.372	Y	1.812	Y	2.228	N	2.764	N
1995-1996	1997-1998	16	2.048	1.337	Y	1.746	Y	2.120	N	2.583	N
1995-1996	2000-2002	18	1.008	1.330	N	1.734	N	2.101	N	2.552	N
1997-1998	2000-2002	16	0.363	1.337	N	1.746	N	2.120	N	2.583	N
1990-1991*	1995-1996*	10	1.981	1.372	Y	1.812	Y	2.228	N	2.764	N
1990-1991*	1997-1998*	8	4.329	1.397	Y	1.860	Y	2.306	Y	2.896	Y
1990-1991*	2000-2002*	10	1.317	1.372	N	1.812	N	2.228	N	2.764	N
1995-1996*	1997-1998*	16	1.553	1.337	Y	1.746	N	2.120	N	2.583	N
1995-1996*	2000-2002*	18	0.273	1.330	N	1.734	N	2.101	N	2.552	N
1997-1998*	2000-2002*	16	0.738	1.337	N	1.746	N	2.120	N	2.583	N

\*Indicates the age groups that are comprised of age-corrected crack density data.

**Key:**

d.o.f. = degrees of freedom for the two categories being compared

t calc = calculated value of t

$\alpha$  = level of significance

t table test values = value for Student's t-distribution for the given value of  $\alpha$

Y = statistically significant difference between groups

N = not a statistically significant difference between groups

**Table 4.3 – Student's t-test for mean crack density corrected to an age of 78 months versus silica fume special provision number for individual bridge decks (Fig. 4.13)**

			80%	90%	95%	98%					
Silica Fume Overlays (special provision #)			d.o.f.	t calc	Confidence Level $\alpha$						
					0.20	0.10	0.05	0.02			
NONE	R1, R2	4	1.618	1.533	Y	2.132	N	2.776	N	3.747	N
NONE	R3	5	1.583	1.476	Y	2.015	N	2.571	N	3.365	N
NONE	R4, R5, R6	9	5.860	1.383	Y	1.833	Y	2.262	Y	2.821	Y
NONE	R8, R9	10	1.751	1.372	Y	1.812	N	2.228	N	2.764	N
R1, R2	R3	7	0.207	1.415	N	1.895	N	2.365	N	2.998	N
R1, R2	R4, R5, R6	11	1.950	1.363	Y	1.796	Y	2.201	N	2.718	N
R1, R2	R8, R9	12	0.556	1.356	N	1.782	N	2.179	N	2.681	N
R3	R4, R5, R6	12	2.484	1.356	Y	1.782	Y	2.179	Y	2.681	N
R3	R8, R9	13	0.827	1.350	N	1.771	N	2.160	N	2.650	N
R4, R5, R6	R8, R9	17	0.818	1.333	N	1.740	N	2.110	N	2.567	N

**Key:**

d.o.f. = degrees of freedom for the two categories being compared

t calc = calculated value of t

$\alpha$  = level of significance

t table test values = value for Student's t-distribution for the given value of  $\alpha$

Y = statistically significant difference between groups

N = not a statistically significant difference between groups

**Table 5.1 – Student's t-test for mean crack density versus bridge deck type (Fig. 5.1)**

				80%	90%	95%	98%				
				Confidence Level $\alpha$							
Deck Type	d.o.f.	t calc		0.20	0.10	0.05	0.02				
5% SFO	7% SFO	25	0.176	1.316	N	1.708	N	2.060	N	2.485	N
5% SFO	CO	46	0.722	1.300	N	1.679	N	2.013	N	2.410	N
5% SFO	MONO	32	2.042	1.309	Y	1.694	Y	2.037	Y	2.449	N
7% SFO	CO	37	0.665	1.305	N	1.687	N	2.026	N	2.431	N
7% SFO	MONO	23	1.529	1.319	Y	1.714	N	2.069	N	2.500	N
CO	MONO	44	1.418	1.301	Y	1.680	N	2.015	N	2.414	N

**Table 5.2 – Student's t-test for mean crack density versus water content (Figs. 5.2, 5.3, 5.4, 5.5)**

				80%	90%	95%	98%				
				Confidence Level $\alpha$							
Silica Fume Overlays (kg/m <sup>3</sup> )	d.o.f.	t calc		0.20	0.10	0.05	0.02				
138	141	17	0.929	1.333	N	1.740	N	2.110	N	2.567	N
138	148	43	0.024	1.302	N	1.681	N	2.017	N	2.416	N
141	148	36	1.435	1.306	Y	1.688	N	2.028	N	2.434	N
Conventional Overlays (mm)	d.o.f.	t calc		0.20	0.10	0.05	0.02				
133	139	39	1.482	1.304	Y	1.685	N	2.023	N	2.426	N
133	145	37	4.973	1.305	Y	1.687	Y	2.026	Y	2.431	Y
139	145	22	1.963	1.321	Y	1.717	Y	2.074	N	2.508	N

**Key:**

d.o.f. = degrees of freedom for the two categories being compared

t calc = calculated value of t

$\alpha$  = level of significance

t table test values = value for Student's t-distribution for the given value of  $\alpha$

Y = statistically significant difference between groups

N = not a statistically significant difference between groups

**Table 5.2 (con't) – Student's t-test for mean crack density versus water content (Figs. 5.2, 5.3, 5.4, 5.5)**

			80%		90%		95%		98%		
<b>Overlay Subdecks</b>											
<b>(kg/m<sup>3</sup>)</b>	<b>d.o.f.</b>	<b>t calc</b>	<b>0.20</b>	<b>0.10</b>	<b>0.05</b>	<b>0.02</b>					
147	156	44	0.272	1.301	N	1.680	N	2.015	N	2.414	N
147	165	11	1.093	1.363	N	1.796	N	2.201	N	2.718	N
147	174	8	1.141	1.397	N	1.860	N	2.306	N	2.896	N
156	165	41	2.031	1.303	Y	1.683	Y	2.020	Y	2.421	N
156	174	38	1.991	1.304	Y	1.686	Y	2.024	N	2.429	N
165	174	5	0.712	1.476	N	2.015	N	2.571	N	3.365	N
<b>Monolithic</b>											
<b>(kg/m<sup>3</sup>)</b>	<b>d.o.f.</b>	<b>t calc</b>	<b>0.20</b>	<b>0.10</b>	<b>0.05</b>	<b>0.02</b>					
147	156	26	2.974	1.315	Y	1.706	Y	2.056	Y	2.479	Y
147	165	18	∞	1.330	Y	1.734	Y	2.101	Y	2.552	Y
156	165	16	1.697	1.337	Y	1.746	N	2.120	N	2.583	N

**Table 5.3 – Student's t-test for mean crack density versus cement content (Figs. 5.6 and 5.7)**

			80%		90%		95%		98%		
<b>Overlay Subdecks</b>											
<b>(kg/m<sup>3</sup>)</b>	<b>d.o.f.</b>	<b>t calc</b>	<b>Confidence Level <math>\alpha</math></b>								
			<b>0.20</b>	<b>0.10</b>	<b>0.05</b>	<b>0.02</b>					
357	379	49	0.478	1.299	N	1.677	N	2.010	N	2.405	N
357	413	44	2.314	1.301	Y	1.680	Y	2.015	Y	2.414	N
379	413	11	2.286	1.363	Y	1.796	Y	2.201	Y	2.718	N
<b>Monolithic</b>											
<b>(kg/m<sup>3</sup>)</b>	<b>d.o.f.</b>	<b>t calc</b>	<b>0.20</b>	<b>0.10</b>	<b>0.05</b>	<b>0.02</b>					
358	379	28	5.625	1.313	Y	1.701	Y	2.048	Y	2.467	Y

**Key:**

d.o.f. = degrees of freedom for the two categories being compared

t calc = calculated value of t

$\alpha$  = level of significance

t table test values = value for Student's t-distribution for the given value of  $\alpha$

Y = statistically significant difference between groups

N = not a statistically significant difference between groups

**Table 5.4 – Student's t-test for mean crack density versus percent volume of water and cementitious materials (Figs. 5.8 and 5.9)**

				80%	90%	95%	98%				
Overlay Subdecks (%)		d.o.f.	t calc	Confidence Level $\alpha$							
				0.20	0.10	0.05	0.02				
26	27	42	0.606	1.302	N	1.682	N	2.018	N	2.418	N
26	28	9	0.022	1.383	N	1.833	N	2.262	N	2.821	N
26	29	8	0.383	1.397	N	1.860	N	2.306	N	2.896	N
26	30	9	1.434	1.383	Y	1.833	N	2.262	N	2.821	N
27	28	39	0.566	1.304	N	1.685	N	2.023	N	2.426	N
27	29	38	1.138	1.304	N	1.686	N	2.024	N	2.429	N
27	30	39	2.963	1.304	Y	1.685	Y	2.023	Y	2.426	Y
28	29	5	0.445	1.476	N	2.015	N	2.571	N	3.365	N
28	30	6	2.063	1.440	Y	1.943	Y	2.447	N	3.143	N
29	30	5	1.541	1.476	Y	2.015	N	2.571	N	3.365	N
Monolithic (%)		d.o.f.	t calc	0.20	0.10	0.05	0.02				
26	27	20	0.020	1.325	N	1.725	N	2.086	N	2.528	N
26	28	10	3.148	1.372	Y	1.812	Y	2.228	Y	2.764	Y
26	29	11	7.134	1.363	Y	1.796	Y	2.201	Y	2.718	Y
27	28	16	3.279	1.337	Y	1.746	Y	2.120	Y	2.583	Y
27	29	17	5.239	1.333	Y	1.740	Y	2.110	Y	2.567	Y
28	29	7	0.225	1.415	N	1.895	N	2.365	N	2.998	N

**Key:**

d.o.f. = degrees of freedom for the two categories being compared

t calc = calculated value of t

$\alpha$  = level of significance

t table test values = value for Student's t-distribution for the given value of  $\alpha$

Y = statistically significant difference between groups

N = not a statistically significant difference between groups

**Table 5.5 – Student's t-test for mean crack density versus water-cement ratio (Figs. 5.10 and 5.11)**

				80%	90%	95%	98%				
<b>Overlay Subdecks</b>		<b>Confidence Level <math>\alpha</math></b>									
<b>w/cm ratio</b>	<b>d.o.f.</b>	<b>t calc</b>	<b>0.20</b>	<b>0.10</b>	<b>0.05</b>	<b>0.02</b>					
0.40	0.41	10	0.619	1.372	N	1.812	N	2.228	N	2.764	N
0.40	0.42	13	0.440	1.350	N	1.771	N	2.160	N	2.650	N
0.40	0.44	38	1.161	1.304	N	1.686	N	2.024	N	2.429	N
0.40	0.45	11	1.226	1.363	N	1.796	N	2.201	N	2.718	N
0.41	0.42	5	1.082	1.476	N	2.015	N	2.571	N	3.365	N
0.41	0.44	30	1.514	1.310	Y	1.697	N	2.042	N	2.457	N
0.41	0.45	3	3.730	1.638	Y	2.353	Y	3.182	Y	4.541	N
0.42	0.44	33	0.317	1.308	N	1.692	N	2.035	N	2.445	N
0.42	0.45	6	1.045	1.440	N	1.943	N	2.447	N	3.143	N
0.44	0.45	31	0.911	1.309	N	1.696	N	2.040	N	2.453	N
<b>Monolithic</b>											
<b>w/cm ratio</b>	<b>d.o.f.</b>	<b>t calc</b>	<b>0.20</b>	<b>0.10</b>	<b>0.05</b>	<b>0.02</b>					
0.42	0.44	28	0.712	1.313	N	1.701	N	2.048	N	2.467	N

**Key:**

d.o.f. = degrees of freedom for the two categories being compared

t calc = calculated value of t

$\alpha$  = level of significance

t table test values = value for Student's t-distribution for the given value of  $\alpha$

Y = statistically significant difference between groups

N = not a statistically significant difference between groups

**Table 5.6 – Student's t-test for mean crack density versus concrete slump  
(Figs. 5.12, 5.13, 5.14, 5.15)**

				80%	90%	95%	98%				
<b>Silica Fume Overlays</b>				<b>Confidence Level <math>\alpha</math></b>							
<b>(mm)</b>	<b>d.o.f.</b>	<b>t calc</b>		<b>0.20</b>	<b>0.10</b>	<b>0.05</b>	<b>0.02</b>				
26	38	5	0.451	1.476	N	2.015	N	2.571	N	3.365	N
26	51	14	0.521	1.345	N	1.761	N	2.145	N	2.624	N
26	64	10	1.069	1.372	N	1.812	N	2.228	N	2.764	N
26	76	11	0.479	1.363	N	1.796	N	2.201	N	2.718	N
26	≥ 90	12	0.034	1.356	N	1.782	N	2.179	N	2.681	N
38	51	15	0.170	1.341	N	1.753	N	2.131	N	2.602	N
38	64	11	0.859	1.363	N	1.796	N	2.201	N	2.718	N
38	76	12	0.060	1.356	N	1.782	N	2.179	N	2.681	N
38	≥ 90	13	0.612	1.350	N	1.771	N	2.160	N	2.650	N
64	76	17	0.832	1.333	N	1.740	N	2.110	N	2.567	N
64	≥ 90	18	1.525	1.330	Y	1.734	N	2.101	N	2.552	N
76	≥ 90	19	0.718	1.328	N	1.729	N	2.093	N	2.539	N
<b>Conventional Overlays</b>											
<b>(mm)</b>	<b>d.o.f.</b>	<b>t calc</b>		<b>0.20</b>	<b>0.10</b>	<b>0.05</b>	<b>0.02</b>				
0	3	8	5.588	1.397	Y	1.860	Y	2.306	Y	2.896	Y
0	6	18	2.196	1.330	Y	1.734	Y	2.101	Y	2.552	N
0	13	17	1.053	1.333	N	1.740	N	2.110	N	2.567	N
0	19	12	1.151	1.356	N	1.782	N	2.179	N	2.681	N
3	6	12	1.512	1.356	Y	1.782	N	2.179	N	2.681	N
3	13	11	2.139	1.363	Y	1.796	Y	2.201	N	2.718	N
3	19	6	1.175	1.440	N	1.943	N	2.447	N	3.143	N
6	13	16	1.067	1.337	N	1.746	N	2.120	N	2.583	N
6	19	21	0.337	1.323	N	1.721	N	2.080	N	2.518	N
13	19	15	1.070	1.341	N	1.753	N	2.131	N	2.602	N

**Key:**

d.o.f. = degrees of freedom for the two categories being compared

t calc = calculated value of t

$\alpha$  = level of significance

t table test values = value for Student's t-distribution for the given value of  $\alpha$

Y = statistically significant difference between groups

N = not a statistically significant difference between groups

**Table 5.6 (con't) – Student's t-test for mean crack density versus concrete slump (Figs. 5.12, 5.13, 5.14, 5.15)**

				80%	90%	95%	98%				
<b>Overlay Subdecks</b>		<b>d.o.f.</b>	<b>t calc</b>	<b>Confidence Level <math>\alpha</math></b>							
<b>(mm)</b>				<b>0.20</b>	<b>0.10</b>	<b>0.05</b>	<b>0.02</b>				
38	51	19	0.462	1.328	N	1.729	N	2.093	N	2.539	N
38	64	23	0.838	1.319	N	1.714	N	2.069	N	2.500	N
38	$\geq 76$	10	0.625	1.372	N	1.812	N	2.228	N	2.764	N
51	64	36	0.702	1.306	N	1.688	N	2.028	N	2.434	N
51	$\geq 76$	23	0.550	1.319	N	1.714	N	2.069	N	2.500	N
64	$\geq 76$	27	0.073	1.314	N	1.703	N	2.052	N	2.473	N
<b>Monolithic</b>											
<b>(mm)</b>		<b>d.o.f.</b>	<b>t calc</b>	<b>0.20</b>		<b>0.10</b>		<b>0.05</b>		<b>0.02</b>	
38	51	23	0.780	1.319	N	1.714	N	2.069	N	2.500	N
38	64	8	2.053	1.397	Y	1.860	Y	2.306	N	2.896	N
51	64	23	1.320	1.319	Y	1.714	N	2.069	N	2.500	N

**Key:**

d.o.f. = degrees of freedom for the two categories being compared

t calc = calculated value of t

$\alpha$  = level of significance

t table test values = value for Student's t-distribution for the given value of  $\alpha$

Y = statistically significant difference between groups

N = not a statistically significant difference between groups

**Table 5.7 – Influence of slump on crack density corrected for water content for monolithic placements obtained using a dummy variable analysis**

	<b>Number of Bridges</b>	<b>Number of Surveys</b>	<b>Cracking Rate (m/m<sup>2</sup>/mm)</b>	<b>R<sup>2</sup></b>
<b>Monolithic Placements</b>	29	63	0.0029	0.51

**Table 5.8 – Student's t-test for mean crack density versus percent air content (Figs. 5.16, 5.17, 5.18)**

				80%	90%	95%	98%				
<b>Silica Fume Overlays</b>				<b>Confidence Level <math>\alpha</math></b>							
(%)	d.o.f.	t calc		0.20	0.10	0.05	0.02				
4.5	5.5	33	0.416	1.308	N	1.692	N	2.035	N	2.445	N
4.5	6.5	23	0.234	1.319	N	1.714	N	2.069	N	2.500	N
5.5	6.5	28	0.103	1.313	N	1.701	N	2.048	N	2.467	N
<b>Conventional Overlays</b>				0.20	0.10	0.05	0.02				
(%)	d.o.f.	t calc									
4.5	5.5	34	0.159	1.307	N	1.691	N	2.032	N	2.441	N
4.5	6.5	21	0.021	1.323	N	1.721	N	2.080	N	2.518	N
5.5	6.5	25	0.150	1.316	N	1.708	N	2.060	N	2.485	N
<b>Overlay Subdecks</b>				0.20	0.10	0.05	0.02				
(%)	d.o.f.	t calc									
4.5	5.5	40	0.393	1.303	N	1.684	N	2.021	N	2.423	N
4.5	6.5	27	0.592	1.314	N	1.703	N	2.052	N	2.473	N
5.5	6.5	33	0.895	1.308	N	1.692	N	2.035	N	2.445	N
<b>Monolithic</b>				0.20	0.10	0.05	0.02				
(%)	d.o.f.	t calc									
4.5	5.5	26	0.084	1.315	N	1.706	N	2.056	N	2.479	N
4.5	6.5	12	1.069	1.356	N	1.782	N	2.179	N	2.681	N
5.5	6.5	24	1.793	1.318	Y	1.711	Y	2.064	N	2.492	N

**Key:**

d.o.f. = degrees of freedom for the two categories being compared

t calc = calculated value of t

$\alpha$  = level of significance

t table test values = value for Student's t-distribution for the given value of  $\alpha$

Y = statistically significant difference between groups

N = not a statistically significant difference between groups

**Table 5.9 – Student's t-test for mean crack density versus compressive strength (Figs. 5.19, 5.20, 5.21, 5.22)**

			80%	90%	95%	98%					
<b>Silica Fume Overlays</b>			<b>Confidence Level <math>\alpha</math></b>								
<b>(MPa)</b>	<b>d.o.f.</b>	<b>t calc</b>	<b>0.20</b>	<b>0.10</b>	<b>0.05</b>	<b>0.02</b>					
38	45	12	2.969	1.356	Y	1.782	Y	2.179	Y	2.681	Y
38	52	13	2.163	1.350	Y	1.771	Y	2.160	Y	2.650	N
38	59	7	0.554	1.415	N	1.895	N	2.365	N	2.998	N
45	52	19	0.982	1.328	N	1.729	N	2.093	N	2.539	N
45	59	13	1.275	1.350	N	1.771	N	2.160	N	2.650	N
52	59	14	0.747	1.345	N	1.761	N	2.145	N	2.624	N
<b>Conventional Overlays</b>			<b>0.20</b>	<b>0.10</b>	<b>0.05</b>	<b>0.02</b>					
<b>(MPa)</b>	<b>d.o.f.</b>	<b>t calc</b>	<b>0.20</b>	<b>0.10</b>	<b>0.05</b>	<b>0.02</b>					
38	45	24	0.133	1.318	N	1.711	N	2.064	N	2.492	N
38	52	15	1.436	1.341	Y	1.753	N	2.131	N	2.602	N
45	52	19	1.342	1.328	Y	1.729	N	2.093	N	2.539	N
<b>Overlay Subdecks</b>			<b>0.20</b>	<b>0.10</b>	<b>0.05</b>	<b>0.02</b>					
<b>(MPa)</b>	<b>d.o.f.</b>	<b>t calc</b>	<b>0.20</b>	<b>0.10</b>	<b>0.05</b>	<b>0.02</b>					
31	38	22	0.189	1.321	N	1.717	N	2.074	N	2.508	N
31	45	18	1.403	1.330	Y	1.734	N	2.101	N	2.552	N
31	52	9	0.496	1.383	N	1.833	N	2.262	N	2.821	N
38	45	28	1.768	1.313	Y	1.701	Y	2.048	N	2.467	N
38	52	19	0.614	1.328	N	1.729	N	2.093	N	2.539	N
45	52	15	0.600	1.341	N	1.753	N	2.131	N	2.602	N
<b>Monolithic</b>			<b>0.20</b>	<b>0.10</b>	<b>0.05</b>	<b>0.02</b>					
<b>(MPa)</b>	<b>d.o.f.</b>	<b>t calc</b>	<b>0.20</b>	<b>0.10</b>	<b>0.05</b>	<b>0.02</b>					
31	38	17	1.015	1.333	N	1.740	N	2.110	N	2.567	N
31	45	15	2.359	1.341	Y	1.753	Y	2.131	Y	2.602	N
38	45	20	2.012	1.325	Y	1.725	Y	2.086	N	2.528	N

**Key:**

d.o.f. = degrees of freedom for the two categories being compared

t calc = calculated value of t

$\alpha$  = level of significance

t table test values = value for Student's t-distribution for the given value of  $\alpha$

Y = statistically significant difference between groups

N = not a statistically significant difference between groups

**Table 5.10 – Student's t-test for mean crack density versus average air temperature (Figs. 5.23, 5.24, 5.25)**

				80%	90%	95%	98%				
<b>Silica Fume Overlays</b>				<b>Confidence Level <math>\alpha</math></b>							
(°C)	d.o.f.	t calc		0.20	0.10	0.05	0.02				
5	15	33	1.244	1.308	N	1.692	N	2.035	N	2.445	N
5	25	31	0.064	1.309	N	1.696	N	2.040	N	2.453	N
15	25	38	1.267	1.304	N	1.686	N	2.024	N	2.429	N
<b>Conventional Overlays</b>				0.20	0.10	0.05	0.02				
(°C)	d.o.f.	t calc									
5	15	19	0.640	1.328	N	1.729	N	2.093	N	2.539	N
5	25	41	0.847	1.303	N	1.683	N	2.020	N	2.421	N
15	25	52	0.407	1.298	N	1.675	N	2.007	N	2.400	N
<b>Overlay Subdecks</b>				0.20	0.10	0.05	0.02				
(°C)	d.o.f.	t calc									
5	15	19	0.268	1.328	N	1.729	N	2.093	N	2.539	N
5	25	35	0.494	1.306	N	1.690	N	2.030	N	2.438	N
15	25	44	0.202	1.301	N	1.680	N	2.015	N	2.414	N
<b>Monolithic</b>				0.20	0.10	0.05	0.02				
(°C)	d.o.f.	t calc									
5	15	26	0.268	1.315	N	1.706	N	2.056	N	2.479	N
5	25	15	0.347	1.341	N	1.753	N	2.131	N	2.602	N
15	25	17	0.080	1.333	N	1.740	N	2.110	N	2.567	N

**Key:**

d.o.f. = degrees of freedom for the two categories being compared

t calc = calculated value of t

$\alpha$  = level of significance

t table test values = value for Student's t-distribution for the given value of  $\alpha$

Y = statistically significant difference between groups

N = not a statistically significant difference between groups

**Table 5.11 – Student's t-test for mean crack density versus minimum air temperature (Figs. 5.26, 5.27, 5.28)**

				80%	90%	95%	98%				
<b>Silica Fume Overlays</b>				<b>Confidence Level <math>\alpha</math></b>							
(°C)	d.o.f.	t calc		0.20	0.10	0.05	0.02				
0	10	37	1.665	1.305	Y	1.687	N	2.026	N	2.431	N
0	20	23	0.952	1.319	N	1.714	N	2.069	N	2.500	N
10	20	36	2.524	1.306	Y	1.688	Y	2.028	Y	2.434	Y
<b>Conventional Overlays</b>				0.20	0.10	0.05	0.02				
(°C)	d.o.f.	t calc									
0	10	26	0.914	1.315	N	1.706	N	2.056	N	2.479	N
0	20	25	1.430	1.316	Y	1.708	N	2.060	N	2.485	N
10	20	45	1.560	1.301	Y	1.679	N	2.014	N	2.412	N
<b>Overlay Subdecks</b>				0.20	0.10	0.05	0.02				
(°C)	d.o.f.	t calc									
0	10	26	0.399	1.315	N	1.706	N	2.056	N	2.479	N
0	20	25	0.343	1.316	N	1.708	N	2.060	N	2.485	N
10	20	45	0.096	1.301	N	1.679	N	2.014	N	2.412	N
<b>Monolithic</b>				0.20	0.10	0.05	0.02				
(°C)	d.o.f.	t calc									
0	10	25	0.412	1.316	N	1.708	N	2.060	N	2.485	N
0	20	20	0.282	1.325	N	1.725	N	2.086	N	2.528	N
10	20	13	0.450	1.350	N	1.771	N	2.160	N	2.650	N

**Key:**

d.o.f. = degrees of freedom for the two categories being compared

t calc = calculated value of t

$\alpha$  = level of significance

t table test values = value for Student's t-distribution for the given value of  $\alpha$

Y = statistically significant difference between groups

N = not a statistically significant difference between groups

**Table 5.12 – Student's t-test for mean crack density versus maximum air temperature (Figs. 5.29, 5.30, 5.31)**

				80%	90%	95%	98%				
<b>Silica Fume Overlays</b>				<b>Confidence Level <math>\alpha</math></b>							
(°C)		d.o.f.	t calc	0.20	0.10	0.05	0.02				
15	25	39	0.726	1.304	N	1.685	N	2.023	N	2.426	N
15	35	25	0.868	1.316	N	1.708	N	2.060	N	2.485	N
25	35	34	1.610	1.307	Y	1.691	N	2.032	N	2.441	N
<b>Conventional Overlays</b>				0.20	0.10	0.05	0.02				
(°C)		d.o.f.	t calc	0.20	0.10	0.05	0.02				
15	25	31	2.875	1.309	Y	1.696	Y	2.040	Y	2.453	Y
15	35	33	1.752	1.308	Y	1.692	Y	2.035	N	2.445	N
25	35	46	1.121	1.300	N	1.679	N	2.013	N	2.410	N
<b>Overlay Subdecks</b>				0.20	0.10	0.05	0.02				
(°C)		d.o.f.	t calc	0.20	0.10	0.05	0.02				
15	25	32	1.276	1.309	N	1.694	N	2.037	N	2.449	N
15	35	23	1.043	1.319	N	1.714	N	2.069	N	2.500	N
25	35	43	0.441	1.302	N	1.681	N	2.017	N	2.416	N
<b>Monolithic</b>				0.20	0.10	0.05	0.02				
(°C)		d.o.f.	t calc	0.20	0.10	0.05	0.02				
5	15	17	0.912	1.333	N	1.740	N	2.110	N	2.567	N
5	25	11	0.802	1.363	N	1.796	N	2.201	N	2.718	N
5	35	6	1.590	1.440	Y	1.943	N	2.447	N	3.143	N
15	25	22	0.315	1.321	N	1.717	N	2.074	N	2.508	N
15	35	17	0.703	1.333	N	1.740	N	2.110	N	2.567	N
25	35	11	0.281	1.363	N	1.796	N	2.201	N	2.718	N

**Key:**

d.o.f. = degrees of freedom for the two categories being compared

t calc = calculated value of t

$\alpha$  = level of significance

t table test values = value for Student's t-distribution for the given value of  $\alpha$

Y = statistically significant difference between groups

N = not a statistically significant difference between groups

**Table 5.13 – Student's t-test for mean crack density versus daily air temperature range (Figs. 5.32, 5.33, 5.34)**

				80%	90%	95%	98%				
<b>Silica Fume Overlays</b>				<b>Confidence Level <math>\alpha</math></b>							
(°C)	d.o.f.	t calc		0.20	0.10	0.05	0.02				
4	12	39	1.828	1.304	Y	1.685	Y	2.023	N	2.426	N
4	20	21	1.370	1.323	Y	1.721	N	2.080	N	2.518	N
12	20	44	0.546	1.301	N	1.680	N	2.015	N	2.414	N
<b>Conventional Overlays</b>				0.20	0.10	0.05	0.02				
(°C)	d.o.f.	t calc									
4	12	50	0.363	1.299	N	1.676	N	2.009	N	2.403	N
4	20	21	0.525	1.323	N	1.721	N	2.080	N	2.518	N
12	20	49	0.325	1.299	N	1.677	N	2.010	N	2.405	N
<b>Overlay Subdecks</b>				0.20	0.10	0.05	0.02				
(°C)	d.o.f.	t calc									
4	12	42	0.186	1.302	N	1.682	N	2.018	N	2.418	N
4	20	21	0.817	1.323	N	1.721	N	2.080	N	2.518	N
12	20	43	1.135	1.302	N	1.681	N	2.017	N	2.416	N
<b>Monolithic</b>				0.20	0.10	0.05	0.02				
(°C)	d.o.f.	t calc									
4	12	22	0.874	1.321	N	1.717	N	2.074	N	2.508	N
4	20	12	0.937	1.356	N	1.782	N	2.179	N	2.681	N
12	20	30	1.124	1.310	N	1.697	N	2.042	N	2.457	N

**Key:**

d.o.f. = degrees of freedom for the two categories being compared

t calc = calculated value of t

$\alpha$  = level of significance

t table test values = value for Student's t-distribution for the given value of  $\alpha$

Y = statistically significant difference between groups

N = not a statistically significant difference between groups

**Table 5.14 – Student's t-test for mean crack density versus structure type (Figs. 5.35 and 5.36)**

				80%	90%	95%	98%				
<b>Silica Fume Overlays</b>				<b>Confidence Level <math>\alpha</math></b>							
<b>bridge type</b>		<b>d.o.f.</b>	<b>t calc</b>	<b>0.20</b>	<b>0.10</b>	<b>0.05</b>	<b>0.02</b>				
SMCC	SWCC	22	1.029	1.321	N	1.717	N	2.074	N	2.508	N
SMCC	SWCH	9	0.350	1.383	N	1.833	N	2.262	N	2.821	N
SWCC	SWCH	21	1.271	1.323	N	1.721	N	2.080	N	2.518	N
<b>Conventional Overlays</b>				<b>0.20</b>	<b>0.10</b>	<b>0.05</b>	<b>0.02</b>				
<b>bridge type</b>		<b>d.o.f.</b>	<b>t calc</b>	<b>0.20</b>	<b>0.10</b>	<b>0.05</b>	<b>0.02</b>				
SMCC	SWCC	23	1.626	1.319	Y	1.714	N	2.069	N	2.500	N
SMCC	SWCH	13	0.773	1.350	N	1.771	N	2.160	N	2.650	N
SWCC	SWCH	18	3.038	1.330	Y	1.734	Y	2.101	Y	2.552	Y
<b>Monolithic</b>				<b>0.20</b>	<b>0.10</b>	<b>0.05</b>	<b>0.02</b>				
<b>bridge type</b>		<b>d.o.f.</b>	<b>t calc</b>	<b>0.20</b>	<b>0.10</b>	<b>0.05</b>	<b>0.02</b>				
SMCC	SWCC	12	0.414	1.356	N	1.782	N	2.179	N	2.681	N
SMCC	SWCH	7	0.188	1.415	N	1.895	N	2.365	N	2.998	N
SWCC	SWCH	7	0.480	1.415	N	1.895	N	2.365	N	2.998	N
<b>All Bridge Deck Types</b>				<b>0.20</b>	<b>0.10</b>	<b>0.05</b>	<b>0.02</b>				
<b>bridge type</b>		<b>d.o.f.</b>	<b>t calc</b>	<b>0.20</b>	<b>0.10</b>	<b>0.05</b>	<b>0.02</b>				
SMCC	SWCC	59	0.670	1.296	N	1.671	N	2.001	N	2.391	N
SMCC	SWCH	31	0.050	1.309	N	1.696	N	2.040	N	2.453	N
SWCC	SWCH	48	0.482	1.299	N	1.677	N	2.011	N	2.407	N

**Key:**

d.o.f. = degrees of freedom for the two categories being compared

t calc = calculated value of t

$\alpha$  = level of significance

t table test values = value for Student's t-distribution for the given value of  $\alpha$

Y = statistically significant difference between groups

N = not a statistically significant difference between groups

**Table 5.15 – Student's t-test for mean crack density versus top transverse bar size (Figs. 5.37, 5.38, 5.39, 5.40)**

				80%	90%	95%	98%				
<b>Silica Fume Overlays</b>				<b>Confidence Level <math>\alpha</math></b>							
<b>(mm)</b>	<b>d.o.f.</b>	<b>t calc</b>		<b>0.20</b>	<b>0.10</b>	<b>0.05</b>	<b>0.02</b>				
16	19	20	0.403	1.325	N	1.725	N	2.086	N	2.528	N
16	16, 19	18	0.657	1.330	N	1.734	N	2.101	N	2.552	N
19	16, 19	12	1.013	1.356	N	1.782	N	2.179	N	2.681	N
<b>Conventional Overlays</b>				<b>0.20</b>	<b>0.10</b>	<b>0.05</b>	<b>0.02</b>				
<b>(mm)</b>	<b>d.o.f.</b>	<b>t calc</b>									
13, 16	16	22	2.396	1.321	Y	1.717	Y	2.074	Y	2.508	N
13, 16	19	18	0.166	1.330	N	1.734	N	2.101	N	2.552	N
16	19	16	2.773	1.337	Y	1.746	Y	2.120	Y	2.583	Y
<b>Monolithic</b>				<b>0.20</b>	<b>0.10</b>	<b>0.05</b>	<b>0.02</b>				
<b>(mm)</b>	<b>d.o.f.</b>	<b>t calc</b>									
13, 16	16	12	0.910	1.356	N	1.782	N	2.179	N	2.681	N
<b>All Bridge Decks</b>				<b>0.20</b>	<b>0.10</b>	<b>0.05</b>	<b>0.02</b>				
<b>(mm)</b>	<b>d.o.f.</b>	<b>t calc</b>									
13, 16	16	42	0.28048	1.302	N	1.682	N	2.018	N	2.418	N
13, 16	16, 19	16	0.07429	1.337	N	1.746	N	2.120	N	2.583	N
13, 16	19	27	2.56599	1.314	Y	1.703	Y	2.052	Y	2.473	Y
16	16, 19	38	0.17355	1.304	N	1.686	N	2.024	N	2.429	N
16	19	49	2.67844	1.299	Y	1.677	Y	2.010	Y	2.405	Y
16, 19	19	23	2.57128	1.319	Y	1.714	Y	2.069	Y	2.500	Y

**Key:**

d.o.f. = degrees of freedom for the two categories being compared

t calc = calculated value of t

$\alpha$  = level of significance

t table test values = value for Student's t-distribution for the given value of  $\alpha$

Y = statistically significant difference between groups

N = not a statistically significant difference between groups

**Table 5.16 – Student's t-test for mean crack density versus top transverse bar spacing (Figs. 5.41)**

				80%	90%	95%	98%				
Silica Fume Overlays (mm)				Confidence Level $\alpha$							
				d.o.f.	t calc	0.20	0.10	0.05	0.02		
$\leq 153$ ( $\leq 6$ )	$> 153$ ( $> 6$ )	18	2.166	1.330	Y	1.734	Y	2.101	Y	2.552	N
Conventional Overlays (mm)				d.o.f.	t calc	0.20	0.10	0.05	0.02		
$\leq 153$ ( $\leq 6$ )	$> 153$ ( $> 6$ )	28	3.148	1.313	Y	1.701	Y	2.048	Y	2.467	Y

**Table 5.17 – Influence of top transverse bar spacing on crack density corrected for bar size for overlay decks obtained using dummy variable analyses**

	Number of Bridges	Number of Surveys	Cracking Rate (m/m <sup>2</sup> /mm)	R <sup>2</sup>
<b>Silica Fume Overlays</b>	18	32	0.0045	0.17
<b>Conventional Overlays</b>	28	50	0.0025	0.34

**Table 5.18 – Student's t-test for mean crack density versus deck thickness (Figs. 5.43, 5.44, 5.45)**

				80%	90%	95%	98%				
<b>Silica Fume Overlays</b>				<b>Confidence Level <math>\alpha</math></b>							
<b>(mm)</b>	<b>d.o.f.</b>	<b>t calc</b>		<b>0.20</b>	<b>0.10</b>	<b>0.05</b>	<b>0.02</b>				
216	220	19	1.272	1.328	N	1.729	N	2.093	N	2.539	N
216	229	16	0.932	1.337	N	1.746	N	2.120	N	2.583	N
220	229	13	0.169	1.350	N	1.771	N	2.160	N	2.650	N
<b>Conventional Overlays</b>				<b>Confidence Level <math>\alpha</math></b>							
<b>(mm)</b>	<b>d.o.f.</b>	<b>t calc</b>		<b>0.20</b>	<b>0.10</b>	<b>0.05</b>	<b>0.02</b>				
210 & 216	229	26	1.283	1.315	N	1.706	N	2.056	N	2.479	N
<b>Monolithic</b>				<b>Confidence Level <math>\alpha</math></b>							
<b>(mm)</b>	<b>d.o.f.</b>	<b>t calc</b>		<b>0.20</b>	<b>0.10</b>	<b>0.05</b>	<b>0.02</b>				
203	210 & 216	7	1.016	1.415	N	1.895	N	2.365	N	2.998	N
203	222 & 229	5	0.552	1.476	N	2.015	N	2.571	N	3.365	N
210 & 216	222 & 229	8	0.430	1.397	N	1.860	N	2.306	N	2.896	N

**Table 5.19 – Student's t-test for mean crack density versus top cover (Fig. 5.46)**

				80%	90%	95%	98%				
<b>Monolithic</b>				<b>Confidence Level <math>\alpha</math></b>							
<b>(mm)</b>	<b>d.o.f.</b>	<b>t calc</b>		<b>0.20</b>	<b>0.10</b>	<b>0.05</b>	<b>0.02</b>				
64	76	12	1.544	1.356	Y	1.782	N	2.179	N	2.681	N

**Key:**

d.o.f. = degrees of freedom for the two categories being compared

t calc = calculated value of t

$\alpha$  = level of significance

t table test values = value for Student's t-distribution for the given value of  $\alpha$

Y = statistically significant difference between groups

N = not a statistically significant difference between groups

**Table 5.20 – Probability of subsidence (settlement) cracking of fresh concrete based on cover depth, transverse bar size, and concrete slump (Dakhil, Cady, and Carrier 1975)**

		Probability of cracking, percent								
Slump		51 mm (2.0 in.)			76 mm (3.0 in.)			102 mm (4.0 in.)		
Bar Size		No. 13 (No. 4)	No. 16 (No. 5)	No. 19 (No. 6)	No. 13 (No. 4)	No. 16 (No. 5)	No. 19 (No. 6)	No. 13 (No. 4)	No. 16 (No. 5)	No. 19 (No. 6)
Cover	19 mm (0.75 in.)	81	88	93	92	99	100	100	100	100
	38 mm (1.5 in.)	20	35	46	32	48	59	45	62	73
	51 mm (2.0 in.)	0	2	14	0	13	27	6	25	40

**Table 5.21 – Cracking rates for end sections of silica fume and conventional overlays obtained from a dummy variable regression analysis**

	End Condition	Number of End Sections	Mean Age (months)	Cracking Rate (m/m <sup>2</sup> /month)	R <sup>2</sup>
<b>5% Silica Fume Overlays</b>	Fixed	11	59	0.0054	0.89
<b>Conventional Overlays</b>	Fixed	9	93	0.0018	0.93
<b>5% Silica Fume Overlays</b>	Pinned	9	48	0.0032	0.97
<b>Conventional Overlays</b>	Pinned	7	92	0.0019	0.95

**Table 5.22 – Student's t-test for mean crack density versus girder end condition (Figs. 5.47 and 5.48)**

				80%	90%	95%	98%				
<b>Silica Fume Overlays</b>				<b>Confidence Level <math>\alpha</math></b>							
<b>end condition</b>		<b>d.o.f.</b>	<b>t calc</b>	<b>0.20</b>	<b>0.10</b>	<b>0.05</b>	<b>0.02</b>				
fixed	pinned	28	4.183	1.313	Y	1.701	Y	2.048	Y	2.467	Y
<b>Conventional Overlays</b>				<b>0.20</b>	<b>0.10</b>	<b>0.05</b>	<b>0.02</b>				
<b>end condition</b>		<b>d.o.f.</b>	<b>t calc</b>	<b>0.20</b>	<b>0.10</b>	<b>0.05</b>	<b>0.02</b>				
fixed	pinned	28	4.183	1.313	Y	1.701	Y	2.048	Y	2.467	Y
<b>Silica Fume Overlays -- End Section Ratio</b>				<b>0.20</b>	<b>0.10</b>	<b>0.05</b>	<b>0.02</b>				
<b>end condition</b>		<b>d.o.f.</b>	<b>t calc</b>	<b>0.20</b>	<b>0.10</b>	<b>0.05</b>	<b>0.02</b>				
fixed	pinned	28	4.183	1.313	Y	1.701	Y	2.048	Y	2.467	Y
<b>Conventional Overlays -- End Section Ratio</b>				<b>0.20</b>	<b>0.10</b>	<b>0.05</b>	<b>0.02</b>				
<b>end condition</b>		<b>d.o.f.</b>	<b>t calc</b>	<b>0.20</b>	<b>0.10</b>	<b>0.05</b>	<b>0.02</b>				
fixed	pinned	27	3.310	1.314	Y	1.703	Y	2.052	Y	2.473	Y

**Key:**

d.o.f. = degrees of freedom for the two categories being compared

t calc = calculated value of t

$\alpha$  = level of significance

t table test values = value for Student's t-distribution for the given value of  $\alpha$

Y = statistically significant difference between groups

N = not a statistically significant difference between groups

**Table 5.23 – Student's t-test for mean crack density versus span type (Figs. 5.49, 5.50)**

				80%	90%	95%	98%				
<b>Silica Fume Overlays</b>				<b>Confidence Level <math>\alpha</math></b>							
<b>Span Type</b>		<b>d.o.f.</b>	<b>t calc</b>	<b>0.20</b>	<b>0.10</b>	<b>0.05</b>	<b>0.02</b>				
End (F)	End (P)	49	1.092	1.299	N	1.677	N	2.010	N	2.405	N
End (F)	Interior (F)	74	0.372	1.293	N	1.666	N	1.993	N	2.378	N
End (P)	Interior (F)	55	0.809	1.297	N	1.673	N	2.004	N	2.396	N
<b>Conventional Overlays</b>											
<b>Span Type</b>		<b>d.o.f.</b>	<b>t calc</b>	<b>0.20</b>	<b>0.10</b>	<b>0.05</b>	<b>0.02</b>				
End (F)	End (P)	56	0.965	1.297	N	1.673	N	2.003	N	2.395	N
End (F)	Interior (F)	76	0.311	1.293	N	1.665	N	1.992	N	2.376	N
End (P)	Interior (F)	54	0.711	1.297	N	1.674	N	2.005	N	2.397	N
<b>Monolithic</b>											
<b>Span Type</b>		<b>d.o.f.</b>	<b>t calc</b>	<b>0.20</b>	<b>0.10</b>	<b>0.05</b>	<b>0.02</b>				
End (F)	Interior	50	0.490	1.299	N	1.676	N	2.009	N	2.403	N

**Key:**

d.o.f. = degrees of freedom for the two categories being compared

t calc = calculated value of t

$\alpha$  = level of significance

t table test values = value for Student's t-distribution for the given value of  $\alpha$

Y = statistically significant difference between groups

N = not a statistically significant difference between groups

**Table 5.24 – Student's t-test for mean crack density versus bridge skew  
(Figs. 5.51 and 5.52)**

				80%	90%	95%	98%				
<b>Silica Fume Overlays</b>				<b>Confidence Level <math>\alpha</math></b>							
<b>(degrees)</b>	<b>d.o.f.</b>	<b>t calc</b>		<b>0.20</b>	<b>0.10</b>	<b>0.05</b>	<b>0.02</b>				
0	10	13	0.494	1.350	N	1.771	N	2.160	N	2.650	N
0	30	13	2.048	1.350	Y	1.771	Y	2.160	N	2.650	N
0	50	15	0.836	1.341	N	1.753	N	2.131	N	2.602	N
10	30	8	2.305	1.397	Y	1.860	Y	2.306	N	2.896	N
10	50	10	0.332	1.372	N	1.812	N	2.228	N	2.764	N
30	50	10	1.591	1.372	Y	1.812	N	2.228	N	2.764	N
<b>Conventional Overlays</b>				<b>0.20</b>	<b>0.10</b>	<b>0.05</b>	<b>0.02</b>				
<b>(degrees)</b>	<b>d.o.f.</b>	<b>t calc</b>									
0	10	13	0.513	1.350	N	1.771	N	2.160	N	2.650	N
0	30	13	0.348	1.350	N	1.771	N	2.160	N	2.650	N
0	50	12	1.289	1.356	N	1.782	N	2.179	N	2.681	N
10	30	14	0.858	1.345	N	1.761	N	2.145	N	2.624	N
10	50	13	0.530	1.350	N	1.771	N	2.160	N	2.650	N
30	50	13	1.745	1.350	Y	1.771	N	2.160	N	2.650	N
<b>Monolithic</b>				<b>0.20</b>	<b>0.10</b>	<b>0.05</b>	<b>0.02</b>				
<b>(degrees)</b>	<b>d.o.f.</b>	<b>t calc</b>									
0	30	10	0.753	1.372	N	1.812	N	2.228	N	2.764	N
0	50	11	1.108	1.363	N	1.796	N	2.201	N	2.718	N
30	50	5	0.120	1.476	N	2.015	N	2.571	N	3.365	N

**Key:**

d.o.f. = degrees of freedom for the two categories being compared

t calc = calculated value of t

$\alpha$  = level of significance

t table test values = value for Student's t-distribution for the given value of  $\alpha$

Y = statistically significant difference between groups

N = not a statistically significant difference between groups

**Table 5.25 – Student's t-test for mean crack density versus span length  
(Figs. 5.53, 5.54, 5.55)**

				80%	90%	95%	98%				
<b>Silica Fume Overlays</b>				<b>Confidence Level <math>\alpha</math></b>							
<b>(m)</b>	<b>d.o.f.</b>	<b>t calc</b>		<b>0.20</b>	<b>0.10</b>	<b>0.05</b>	<b>0.02</b>				
5	15	20	0.110	1.325	N	1.725	N	2.086	N	2.528	N
5	25	24	0.443	1.318	N	1.711	N	2.064	N	2.492	N
5	35	36	0.076	1.306	N	1.688	N	2.028	N	2.434	N
5	45	10	0.494	1.372	N	1.812	N	2.228	N	2.764	N
5	55	6	0.724	1.440	N	1.943	N	2.447	N	3.143	N
15	25	38	0.526	1.304	N	1.686	N	2.024	N	2.429	N
15	35	50	0.352	1.299	N	1.676	N	2.009	N	2.403	N
15	45	24	0.901	1.318	N	1.711	N	2.064	N	2.492	N
15	55	20	1.287	1.325	N	1.725	N	2.086	N	2.528	N
25	35	54	0.973	1.297	N	1.674	N	2.005	N	2.397	N
25	45	28	1.480	1.313	Y	1.701	N	2.048	N	2.467	N
25	55	24	1.794	1.318	Y	1.711	Y	2.064	N	2.492	N
35	45	40	0.976	1.303	N	1.684	N	2.021	N	2.423	N
35	55	36	1.166	1.306	N	1.688	N	2.028	N	2.434	N
45	55	10	0.578	1.372	N	1.812	N	2.228	N	2.764	N
<b>Conventional Overlays</b>											
<b>(m)</b>	<b>d.o.f.</b>	<b>t calc</b>		<b>0.20</b>	<b>0.10</b>	<b>0.05</b>	<b>0.02</b>				
15	25	75	1.076	1.293	N	1.665	N	1.992	N	2.377	N
15	35	40	0.984	1.303	N	1.684	N	2.021	N	2.423	N
15	45	47	0.980	1.300	N	1.678	N	2.012	N	2.408	N
25	35	47	0.394	1.300	N	1.678	N	2.012	N	2.408	N
25	45	54	0.171	1.297	N	1.674	N	2.005	N	2.397	N
35	45	19	0.363	1.328	N	1.729	N	2.093	N	2.539	N

**Key:**

d.o.f. = degrees of freedom for the two categories being compared

t calc = calculated value of t

$\alpha$  = level of significance

t table test values = value for Student's t-distribution for the given value of  $\alpha$

Y = statistically significant difference between groups

N = not a statistically significant difference between groups

**Table 5.25 (con't) – Student's t-test for mean crack density versus span length (Figs. 5.53, 5.54, 5.55)**

Monolithic		d.o.f.	t calc	0.20		0.10		0.05		0.02	
(m)											
15	25	36	0.415	1.306	N	1.688	N	2.028	N	2.434	N
15	35	20	0.435	1.325	N	1.725	N	2.086	N	2.528	N
25	35	34	0.682	1.307	N	1.691	N	2.032	N	2.441	N

**Table 5.26 – Student's t-test for mean crack density versus bridge length (Fig. 5.56)**

				80%		90%		95%		98%	
Silica Fume Overlays		d.o.f.	t calc	Confidence Level $\alpha$							
(m)				0.20	0.10	0.05	0.02				
50	90	16	2.000	1.337	Y	1.746	Y	2.120	N	2.583	N
50	130	10	1.168	1.372	N	1.812	N	2.228	N	2.764	N
90	130	18	1.565	1.330	Y	1.734	N	2.101	N	2.552	N
Conventional Overlays		d.o.f.	t calc	0.20		0.10		0.05		0.02	
(m)											
50	90	24	1.380	1.318	Y	1.711	N	2.064	N	2.492	N
50	130	15	1.069	1.341	N	1.753	N	2.131	N	2.602	N
90	130	15	0.201	1.341	N	1.753	N	2.131	N	2.602	N
Monolithic		d.o.f.	t calc	0.20		0.10		0.05		0.02	
(m)											
50	90	9	0.248	1.383	N	1.833	N	2.262	N	2.821	N
50	130	4	0.236	1.533	N	2.132	N	2.776	N	3.747	N
90	130	11	0.004	1.363	N	1.796	N	2.201	N	2.718	N

**Key:**

d.o.f. = degrees of freedom for the two categories being compared

t calc = calculated value of t

$\alpha$  = level of significance

t table test values = value for Student's t-distribution for the given value of  $\alpha$

Y = statistically significant difference between groups

N = not a statistically significant difference between groups

**Table 5.27 – Student's t-test for mean crack density versus bridge contractor (Figs. 5.57, 5.58, 5.59)**

				80%	90%	95%	98%				
<b>Silica Fume Overlays</b>				<b>Confidence Level <math>\alpha</math></b>							
<b>(contractor)</b>		<b>d.o.f.</b>	<b>t calc</b>	<b>0.20</b>	<b>0.10</b>	<b>0.05</b>	<b>0.02</b>				
A	B	12	1.087	1.356	N	1.782	N	2.179	N	2.681	N
A	D	11	0.017	1.363	N	1.796	N	2.201	N	2.718	N
A	F	23	1.293	1.319	N	1.714	N	2.069	N	2.500	N
A	H	12	2.771	1.356	Y	1.782	Y	2.179	Y	2.681	Y
B	D	9	1.622	1.383	Y	1.833	N	2.262	N	2.821	N
B	F	21	0.011	1.323	N	1.721	N	2.080	N	2.518	N
B	H	10	4.120	1.372	Y	1.812	Y	2.228	Y	2.764	Y
D	F	20	1.227	1.325	N	1.725	N	2.086	N	2.528	N
D	H	9	3.763	1.383	Y	1.833	Y	2.262	Y	2.821	Y
F	H	21	2.353	1.323	Y	1.721	Y	2.080	Y	2.518	N
<b>Conventional Overlays</b>				<b>0.20</b>	<b>0.10</b>	<b>0.05</b>	<b>0.02</b>				
<b>(contractor)</b>		<b>d.o.f.</b>	<b>t calc</b>	<b>0.20</b>	<b>0.10</b>	<b>0.05</b>	<b>0.02</b>				
B	E	22	3.758	1.321	Y	1.717	Y	2.074	Y	2.508	Y
B	F	48	3.288	1.299	Y	1.677	Y	2.011	Y	2.407	Y
B	G	22	0.902	1.321	N	1.717	N	2.074	N	2.508	N
B	H	22	0.207	1.321	N	1.717	N	2.074	N	2.508	N
E	F	32	1.691	1.309	Y	1.694	N	2.037	N	2.449	N
E	G	6	4.163	1.440	Y	1.943	Y	2.447	Y	3.143	Y
E	H	6	4.831	1.440	Y	1.943	Y	2.447	Y	3.143	Y
F	G	32	1.301	1.309	N	1.694	N	2.037	N	2.449	N
F	H	32	1.931	1.309	Y	1.694	Y	2.037	N	2.449	N
G	H	6	1.716	1.440	Y	1.943	N	2.447	N	3.143	N

**Key:**

d.o.f. = degrees of freedom for the two categories being compared

t calc = calculated value of t

$\alpha$  = level of significance

t table test values = value for Student's t-distribution for the given value of  $\alpha$

Y = statistically significant difference between groups

N = not a statistically significant difference between groups

**Table 5.27 (con't) – Student's t-test for mean crack density versus bridge contractor (Figs. 5.57, 5.58, 5.59)**

Monolithic (contractor)		d.o.f.	t calc	0.20	0.10	0.05	0.02				
A	C	15	0.819	1.341	N	1.753	N	2.131	N	2.602	N
A	I	13	6.407	1.350	Y	1.771	Y	2.160	Y	2.650	Y
C	I	12	6.333	1.356	Y	1.782	Y	2.179	Y	2.681	Y

**Table 5.28 – Student's t-test for mean crack density versus average annual daily traffic (AADT) (Figs. 5.60 and 5.61)**

				80%	90%	95%	98%				
Silica Fume Overlays (AADT)		d.o.f.	t calc	Confidence Level $\alpha$							
				0.20	0.10	0.05	0.02				
2500	7500	16	3.292	1.337	Y	1.746	Y	2.120	Y	2.583	Y
2500	12500	11	0.644	1.363	N	1.796	N	2.201	N	2.718	N
7500	12500	15	1.274	1.341	N	1.753	N	2.131	N	2.602	N
Conventional Overlays (AADT)		d.o.f.	t calc	0.20	0.10	0.05	0.02				
2500	7500	18	0.338	1.330	N	1.734	N	2.101	N	2.552	N
2500	12500	11	1.258	1.363	N	1.796	N	2.201	N	2.718	N
7500	12500	19	1.092	1.328	N	1.729	N	2.093	N	2.539	N
Monolithic (AADT)		d.o.f.	t calc	0.20	0.10	0.05	0.02				
1000	3000	10	3.854	1.372	Y	1.812	Y	2.228	Y	2.764	Y
1000	5000	8	1.765	1.397	Y	1.860	N	2.306	N	2.896	N
3000	5000	6	0.714	1.440	N	1.943	N	2.447	N	3.143	N

**Key:**

d.o.f. = degrees of freedom for the two categories being compared

t calc = calculated value of t

$\alpha$  = level of significance

t table test values = value for Student's t-distribution for the given value of  $\alpha$

Y = statistically significant difference between groups

N = not a statistically significant difference between groups

**Table 5.29 – Average rate of change of crack density as a function of load cycles obtained from dummy variable regression analyses**

	<b>Number of Bridges</b>	<b>Number of Surveys</b>	<b>Weighted Average Intercept (m/m<sup>2</sup>)</b>	<b>Cracking Rate (m/m<sup>2</sup> per 1×10<sup>6</sup> cycles)</b>	<b>R<sup>2</sup></b>
<b>Silica Fume Overlay Decks</b>	27	45	0.25	0.0164	0.80
<b>Conventional Overlay Decks</b>	30	52	0.48	0.0019	0.83
<b>Monolithic Decks</b>	16	32	0.32	0.0078	0.92

**Table 5.30 – Average rate of change of age-corrected crack density as a function of load cycles obtained from dummy variable regression analyses**

	<b>Number of Bridges</b>	<b>Number of Surveys</b>	<b>Weighted Average Intercept (m/m<sup>2</sup>)</b>	<b>Cracking Rate (m/m<sup>2</sup>/ per 1×10<sup>6</sup> cycles)</b>	<b>R<sup>2</sup></b>
<b>Silica Fume Overlay Decks</b>	27	45	0.46	0.0045	0.78
<b>Conventional Overlay Decks</b>	30	52	0.51	0.0003	0.87
<b>Monolithic Decks</b>	16	32	0.33	0.0025	0.92

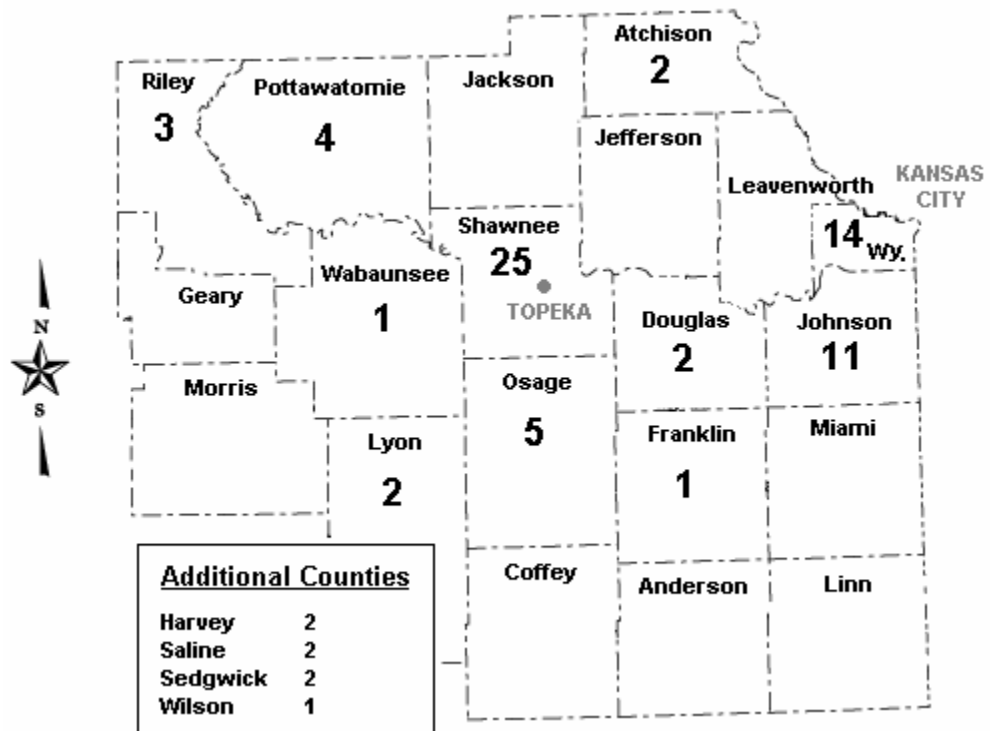


Fig. 2.1 – Breakdown of the number of bridges selected from each county

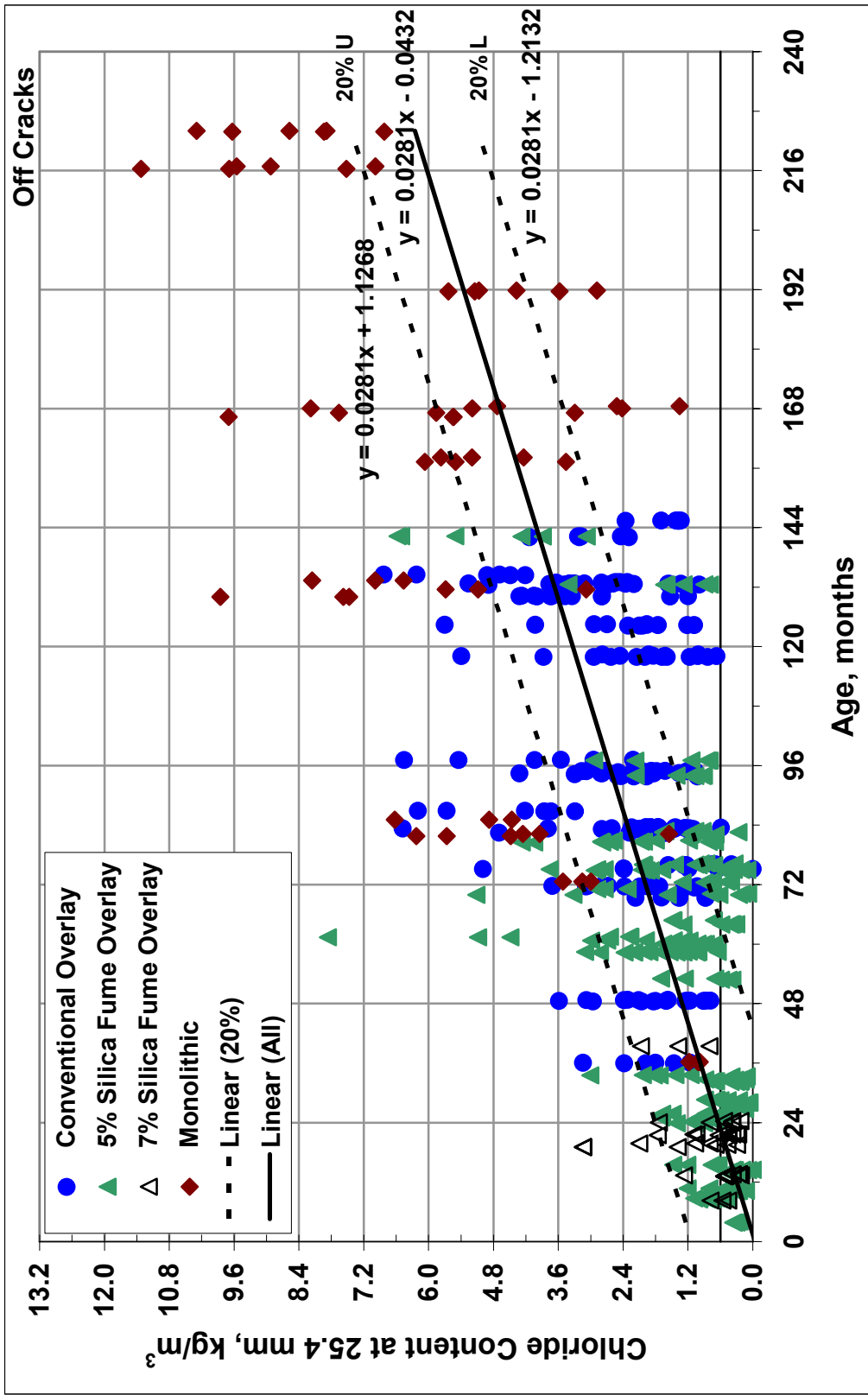


Fig. 3.1 – Chloride content taken away from cracks interpolated at a depth of 25.4 mm (1.0 in.) versus placement age. Twenty percent upper (20% U) and lower (20% L) bound prediction intervals are included.

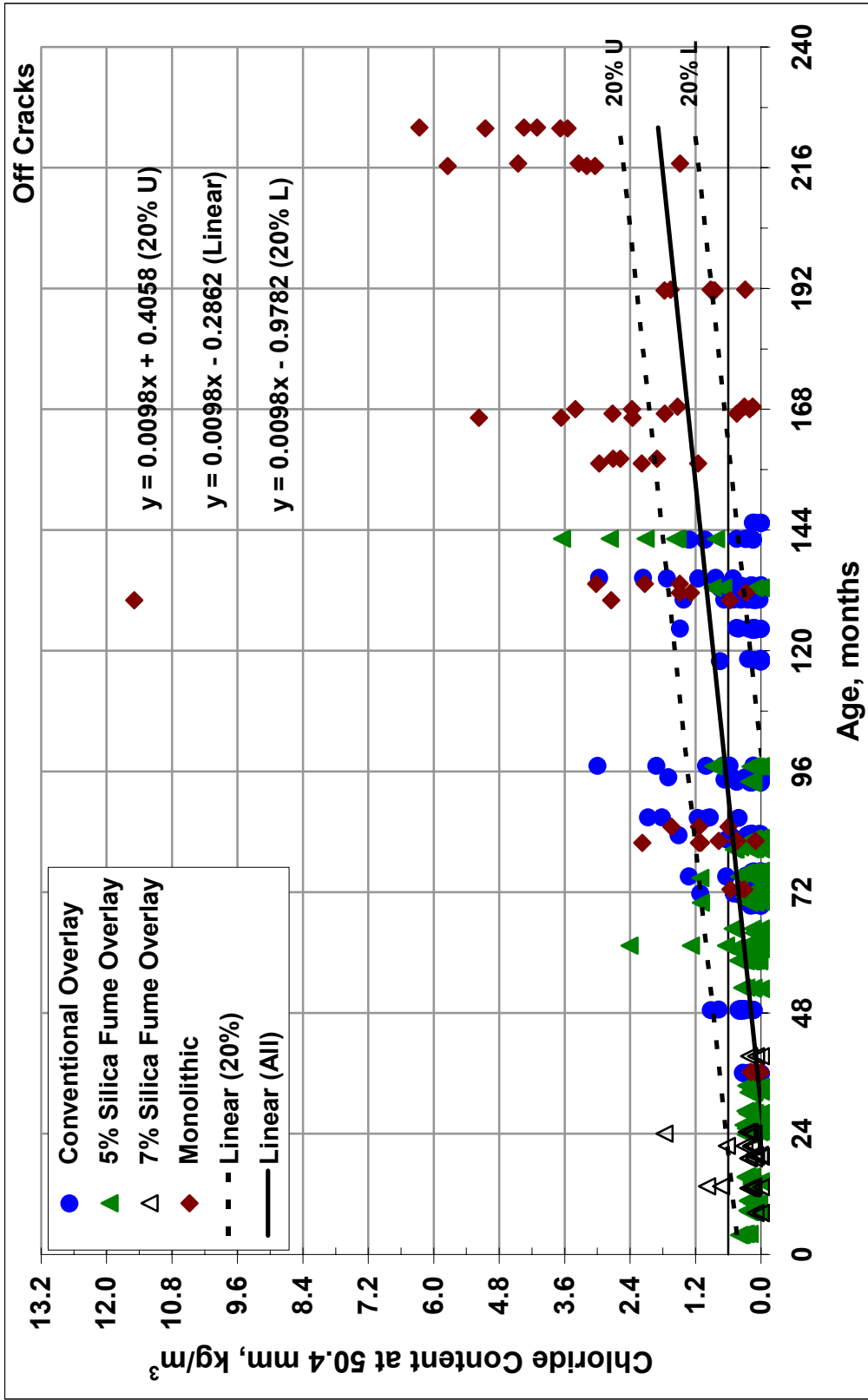


Fig. 3.2 – Chloride content taken away from cracks interpolated at a depth of 50.8 mm (2.0 in.) versus placement age. Twenty percent upper (20% U) and lower (20% L) bound prediction intervals are included.

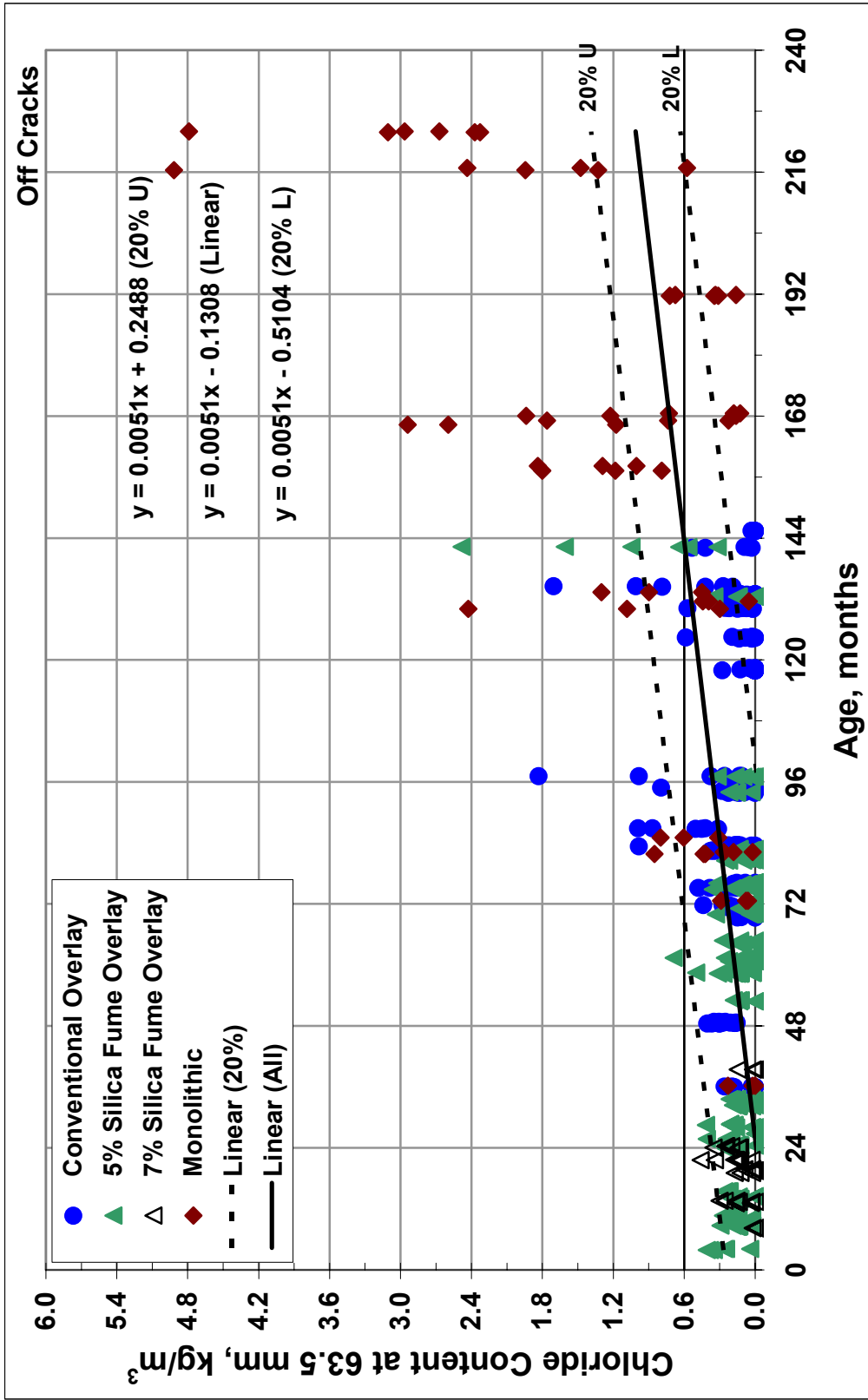


Fig. 3.3 – Chloride content taken away from cracks interpolated at a depth of 63.5 mm (2.5 in.) versus placement age. Twenty percent upper (20% U) and lower (20% L) bound prediction intervals are included.

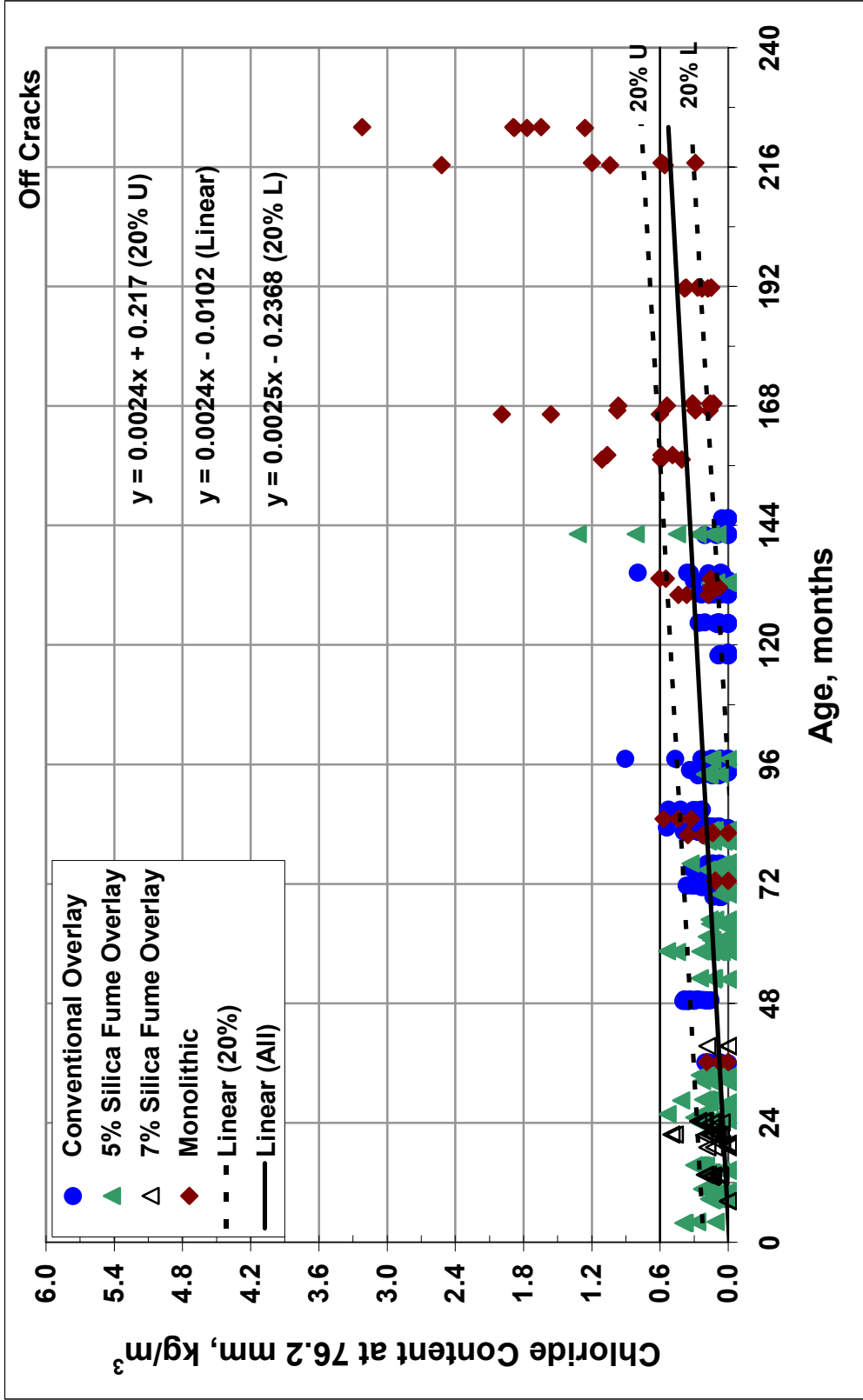


Fig. 3.4 – Chloride content taken away from cracks interpolated at a depth of 76.2 mm (3.0 in.) versus placement age. Twenty percent upper (20% U) and lower (20% L) bound prediction intervals are included.

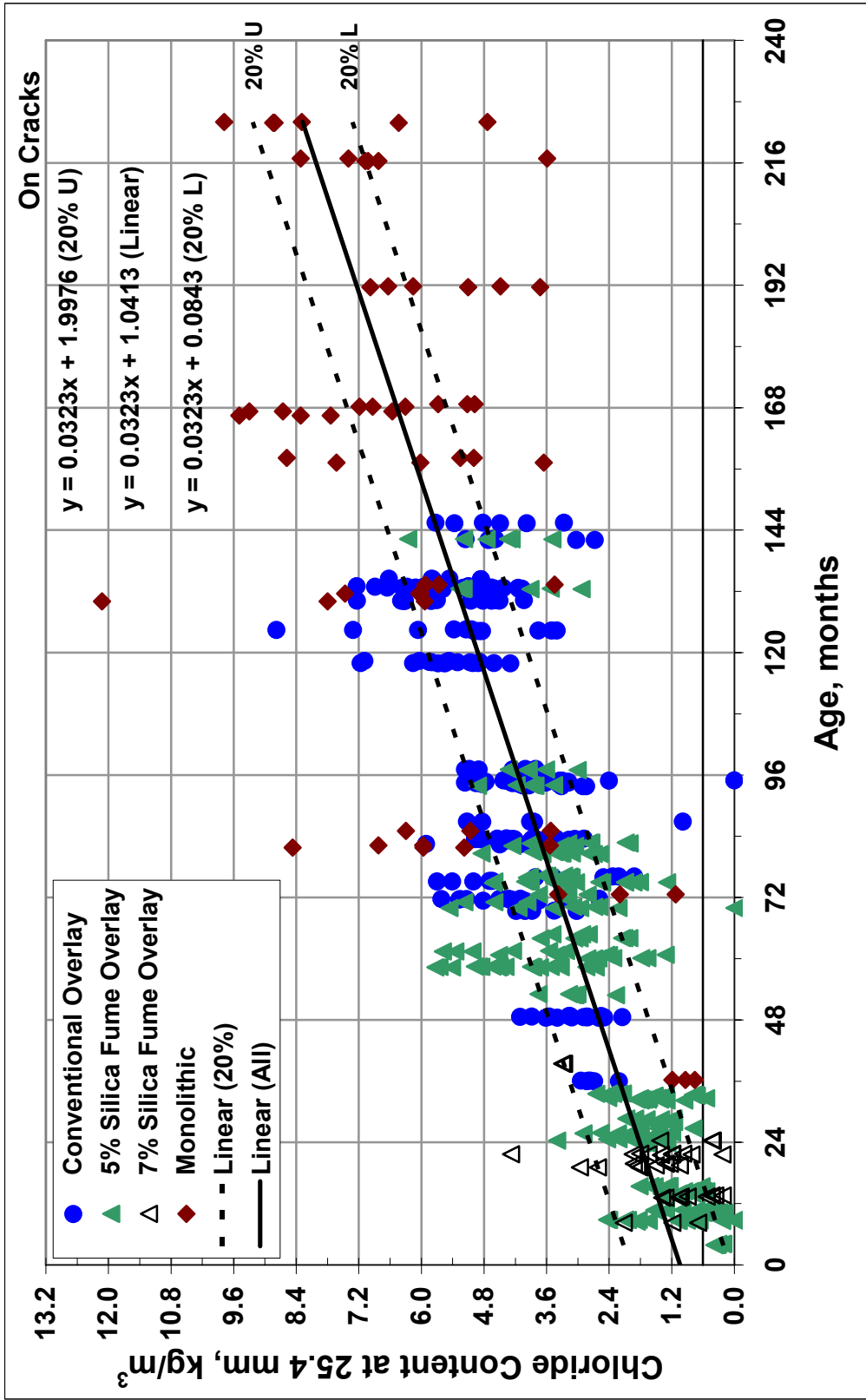


Fig. 3.5 – Chloride content taken on cracks interpolated at a depth of 25.4 mm (1.0 in.) versus placement age. Twenty percent upper (20% U) and lower (20% L) bound prediction intervals are included.

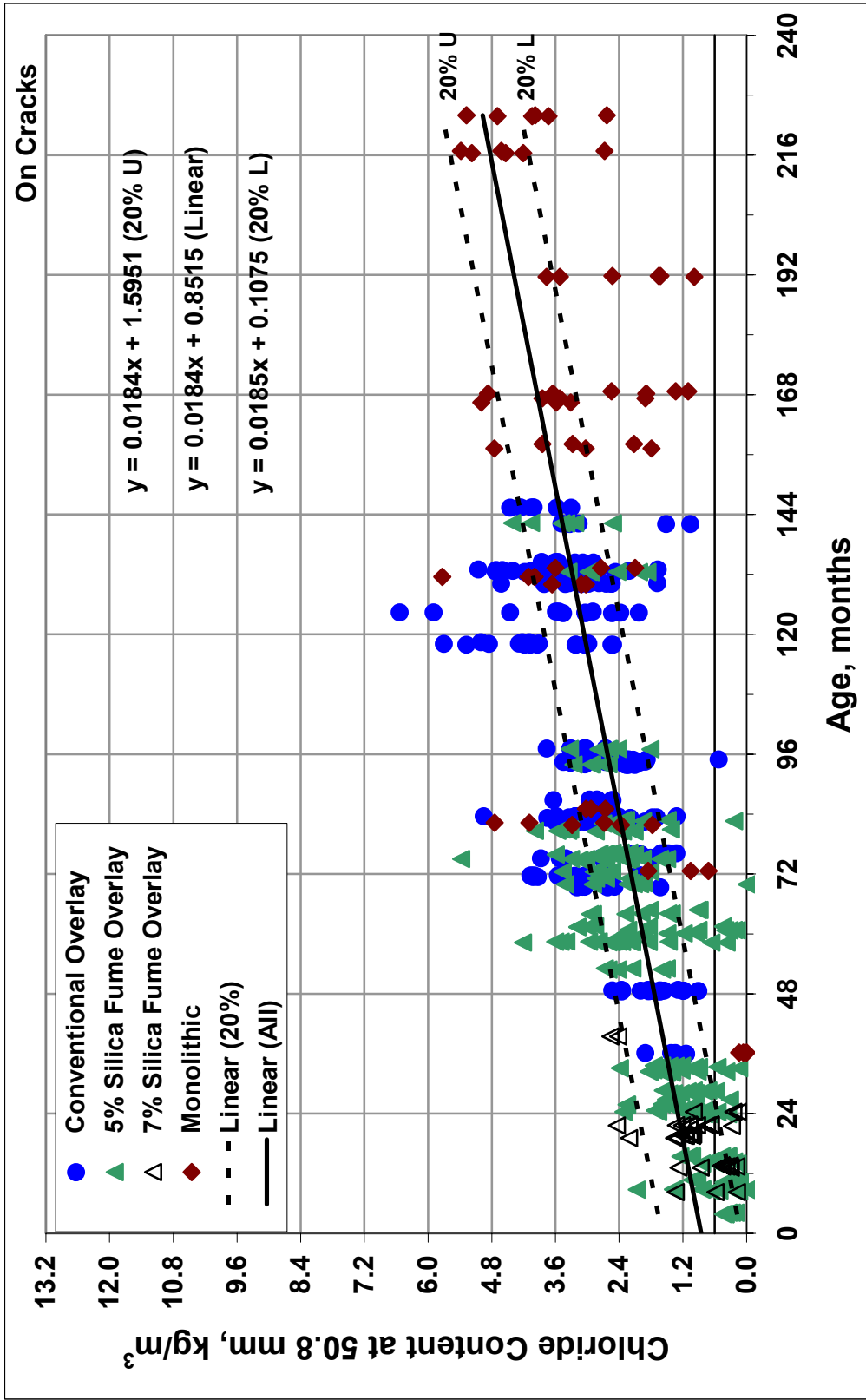


Fig. 3.6 – Chloride content taken on cracks interpolated at a depth of 50.8 mm (2.0 in.) versus placement age. Twenty percent upper (20% U) and lower (20% L) bound prediction intervals are included.

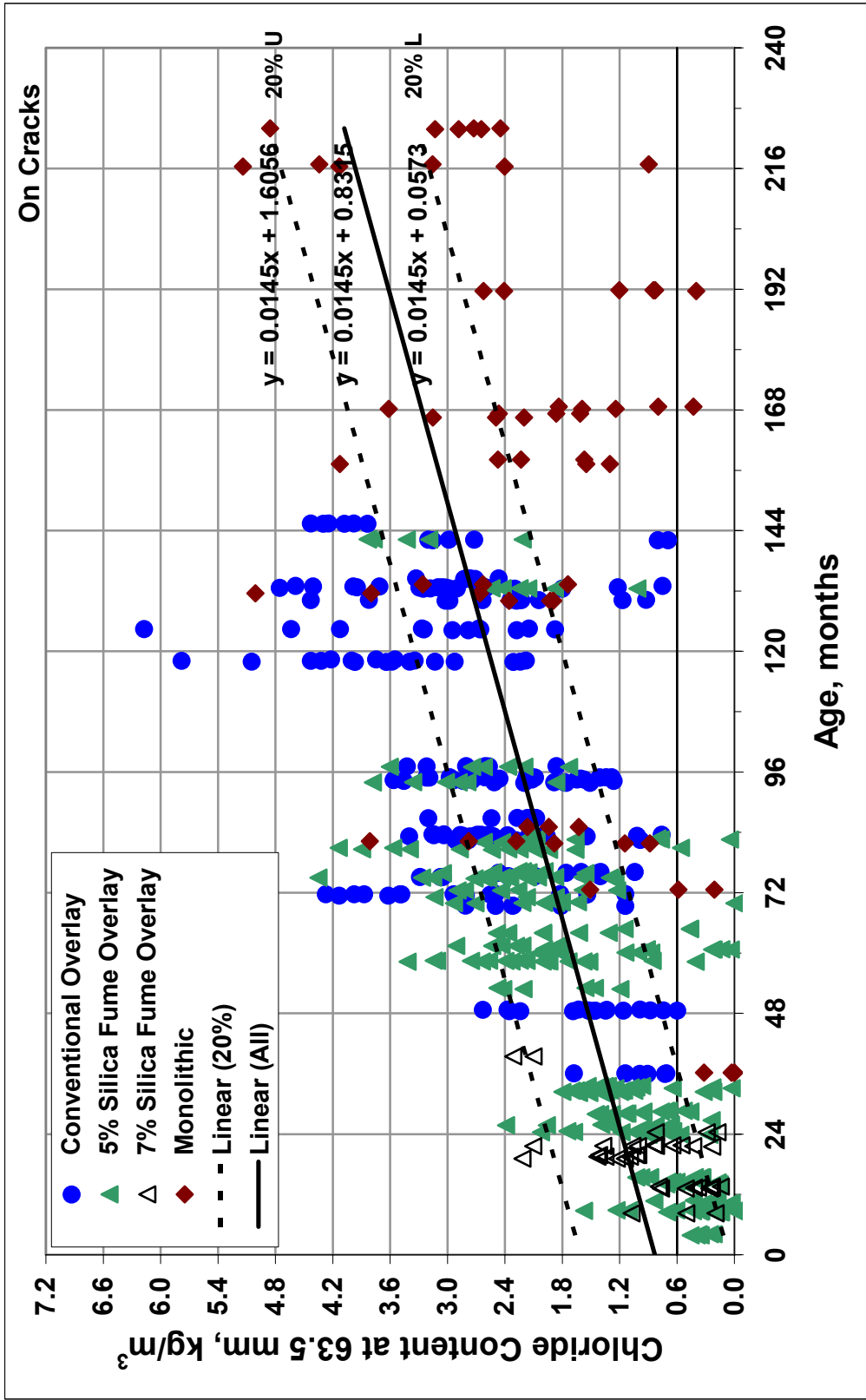


Fig. 3.7 – Chloride content taken on cracks interpolated at a depth of 63.5 mm (2.5 in.) versus placement age. Twenty percent upper (20% U) and lower (20% L) bound prediction intervals are included.

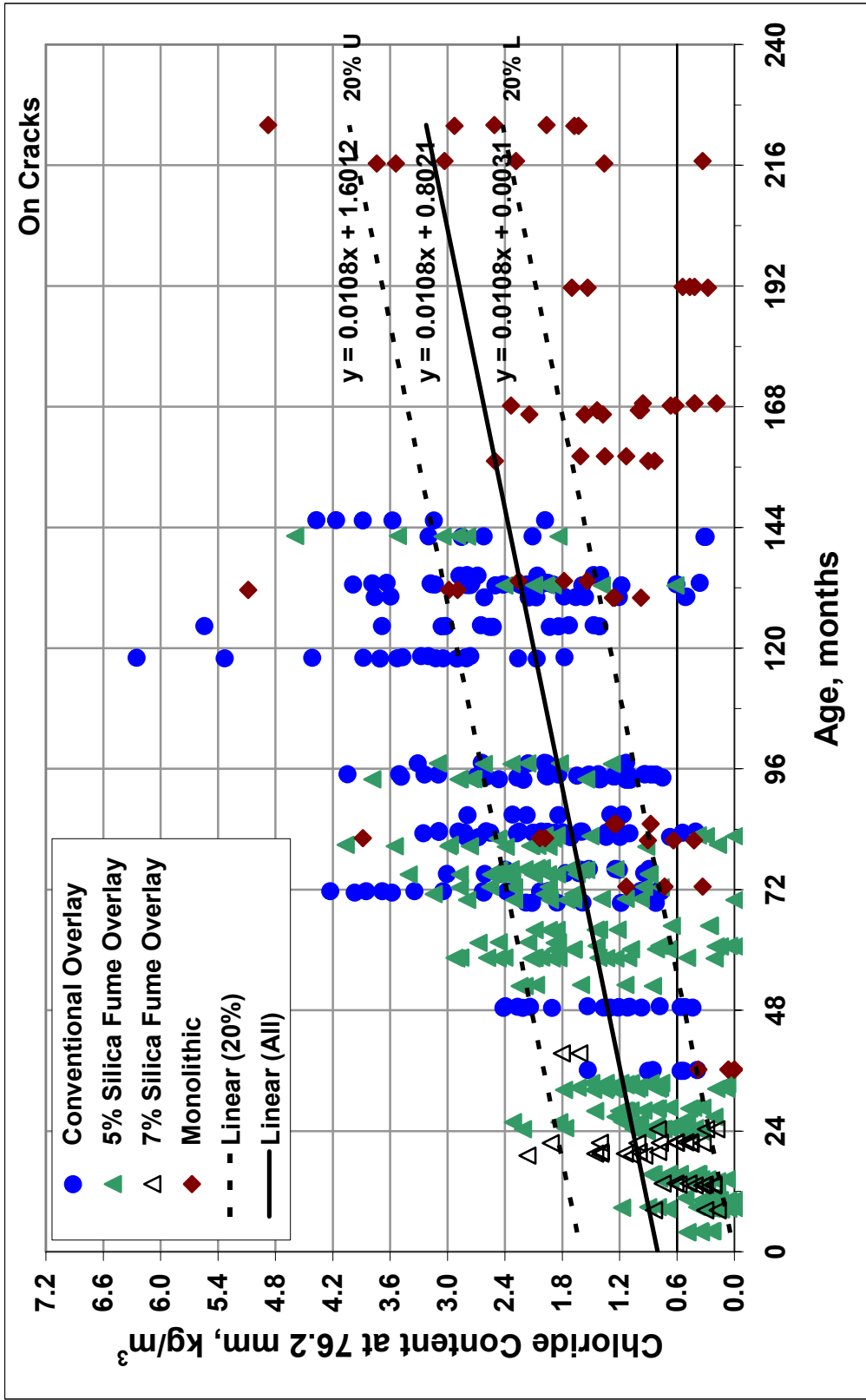


Fig. 3.8 – Chloride content taken on cracks interpolated at a depth of 76.2 mm (3.0 in.) versus placement age. Twenty percent upper (20% U) and lower (20% L) bound prediction intervals are included.

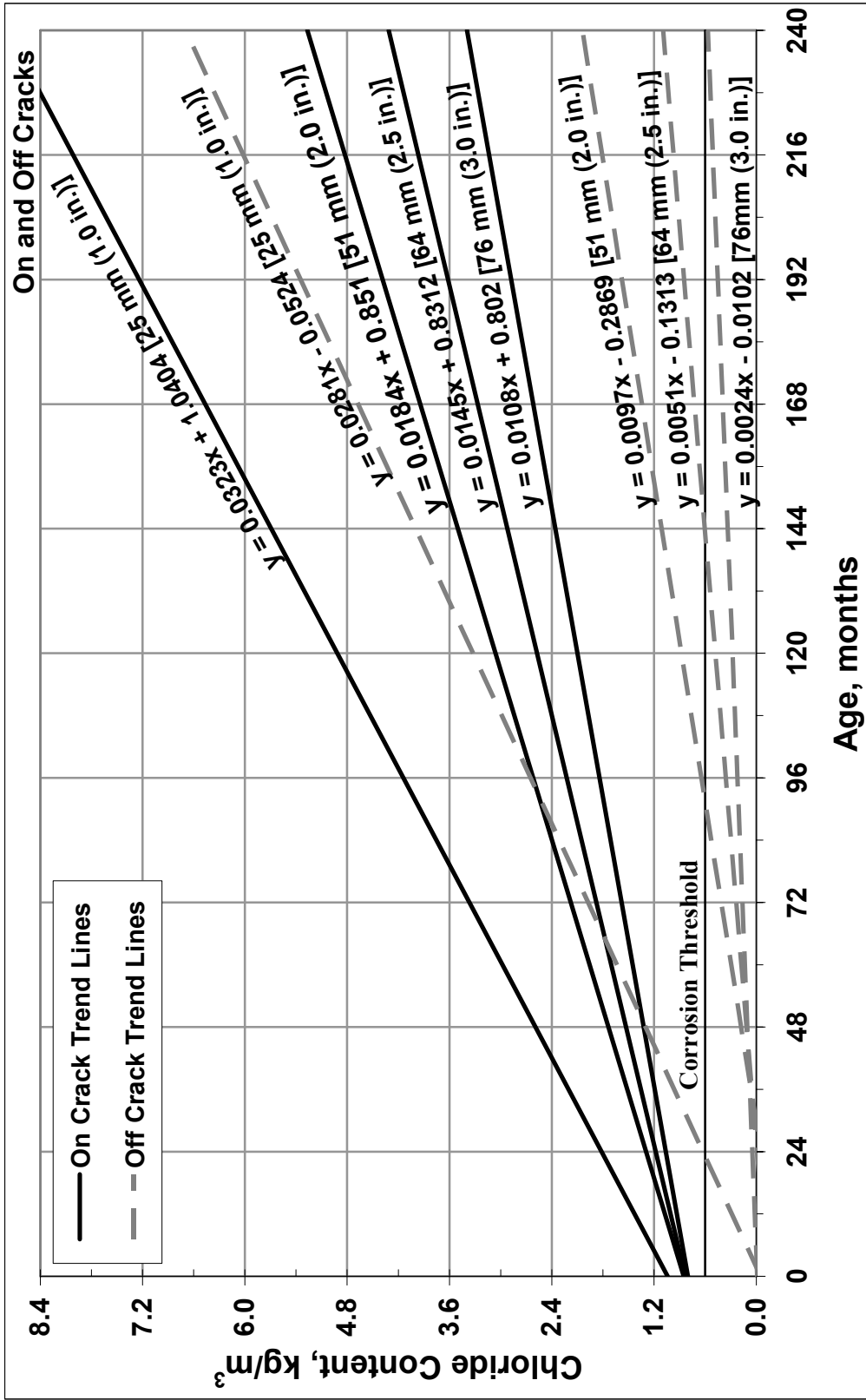


Fig. 3.9 – Linear trend lines for interpolated chloride data taken on and off of cracks at four depths. The depths are 25.4 mm (1.0 in.), 50.8 mm (2.0 in.), 63.5 mm (2.5 in.), and 76.2 mm (3.0 in.) and progress from top to bottom for the two sample types.

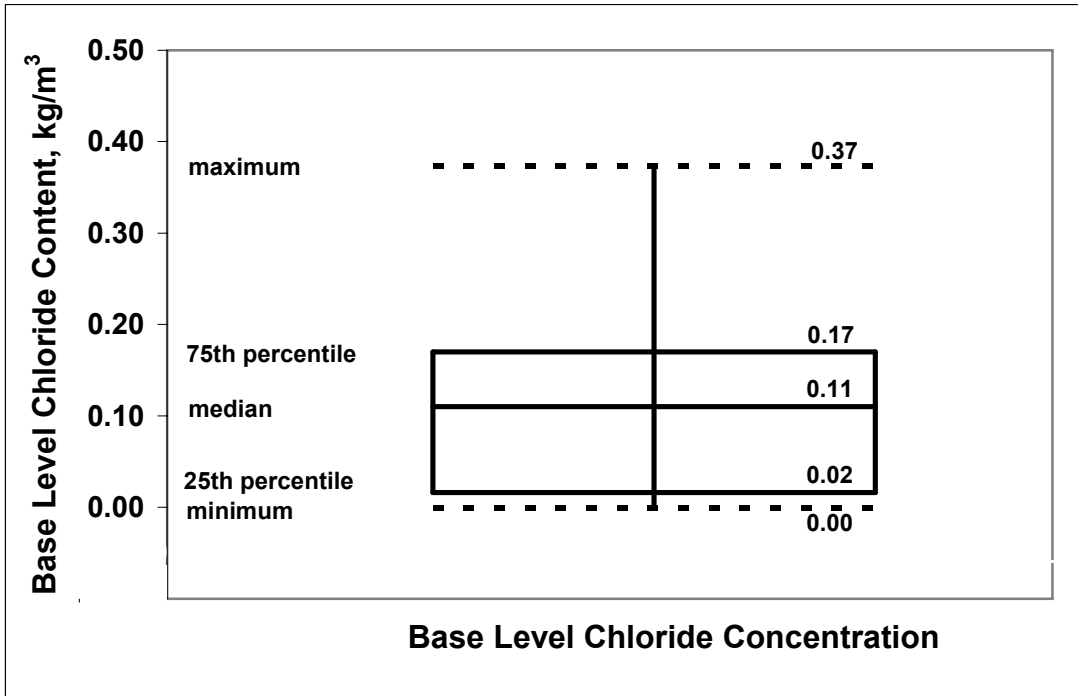


Fig. 3.10 – Box-and-whisker plot of the base level chloride contents for all bridge deck types. (Max, 75th percentile, median, 25th percentile, and min values indicated)

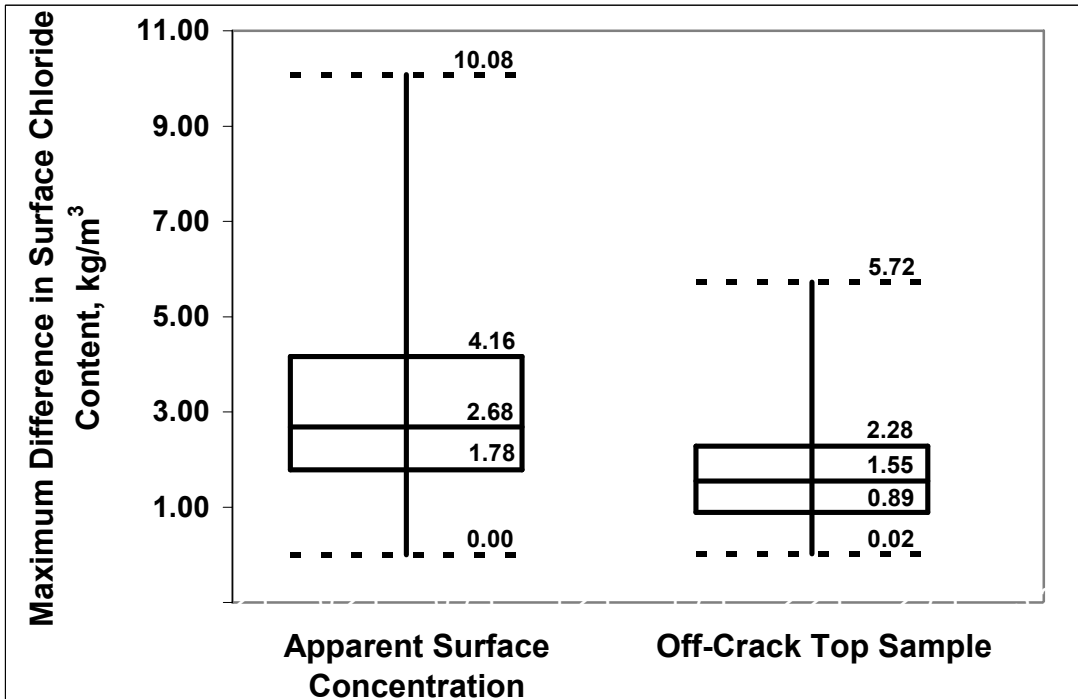


Fig. 3.11 – Box-and-whisker plot of the difference between the maximum and minimum apparent surface concentration and the top sample taken from off-crack locations for each placement. (Max, 75th percentile, median, 25th percentile, and min values indicated)

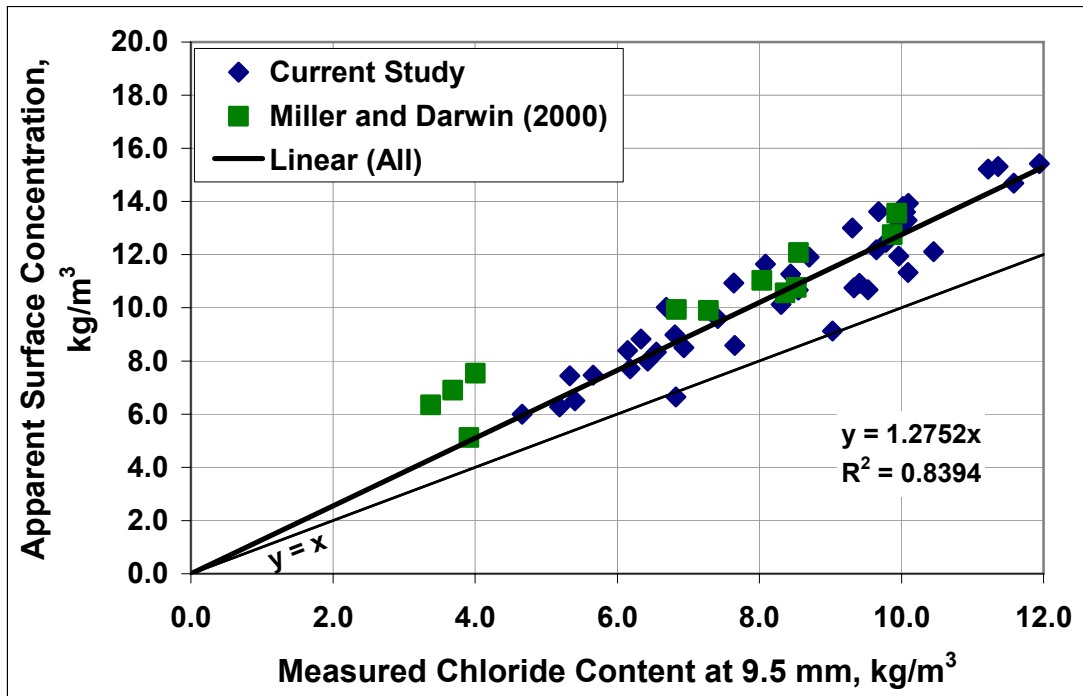


Fig. 3.12 – Apparent surface concentration  $C_o$  calculated from Fick's Second Law versus the measured chloride content away from cracks at 9.5 mm for monolithic bridge decks.

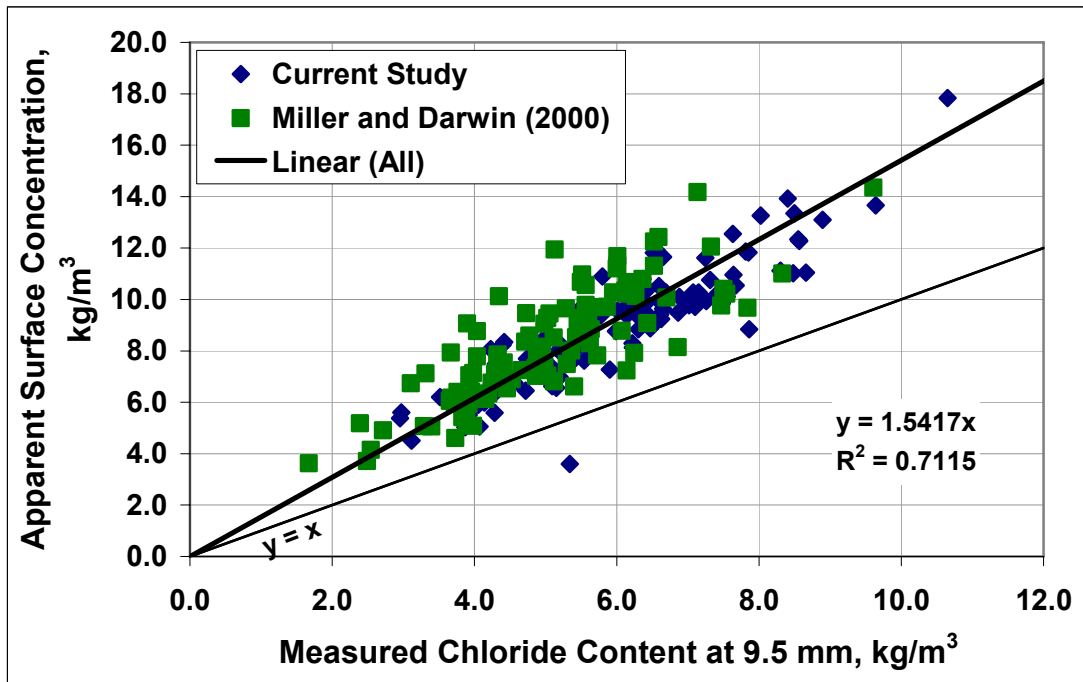


Fig. 3.13 – Apparent surface concentration  $C_o$  calculated from Fick's Second Law versus the measured chloride content away from cracks at 9.5 mm for conventional overlays.

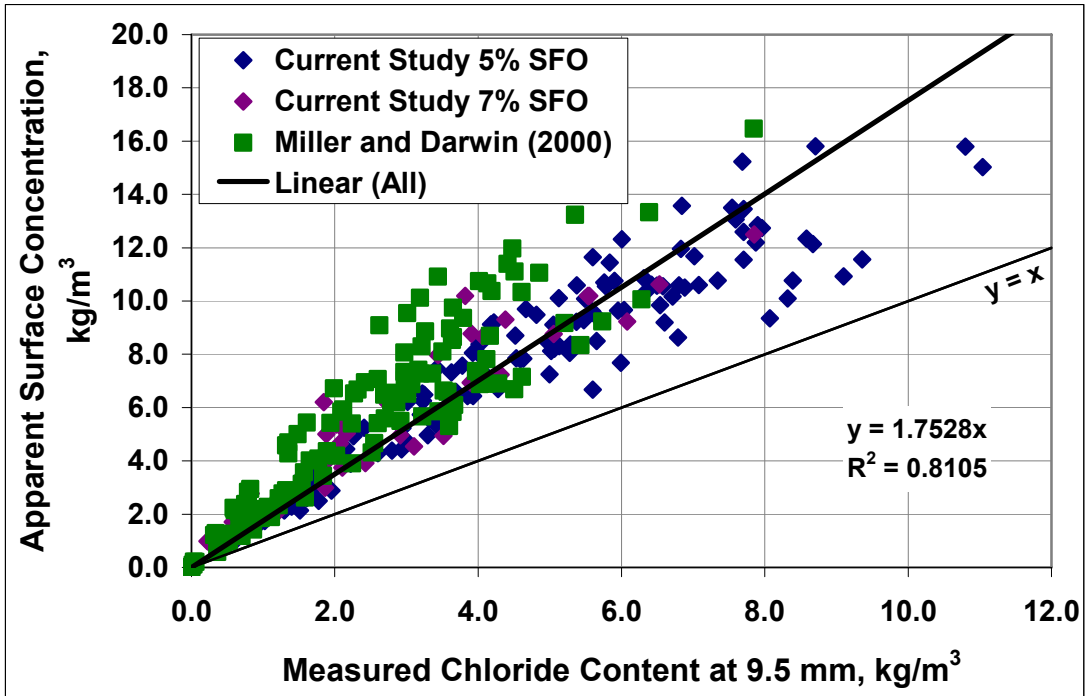


Fig. 3.14 – Apparent surface concentration  $C_o$  calculated from Fick's Second Law versus the measured chloride content away from cracks at 9.5 mm for silica fume overlays.

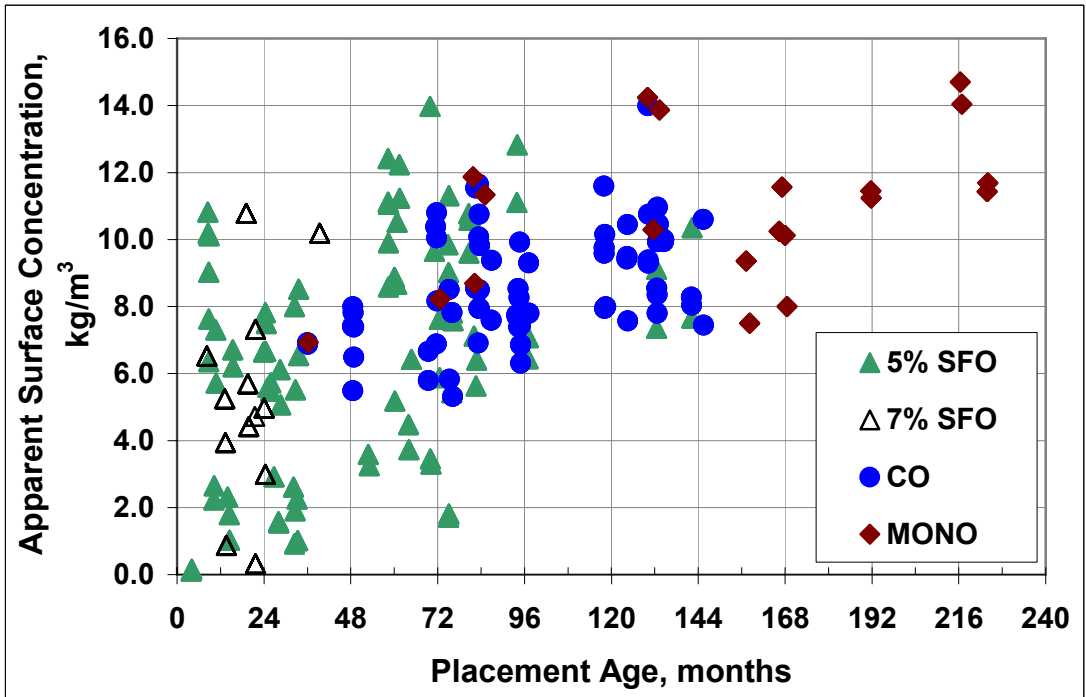


Fig. 3.15 – Average apparent surface concentration  $C_o$  calculated from Fick's Second Law versus bridge deck placement age at the time of sampling.

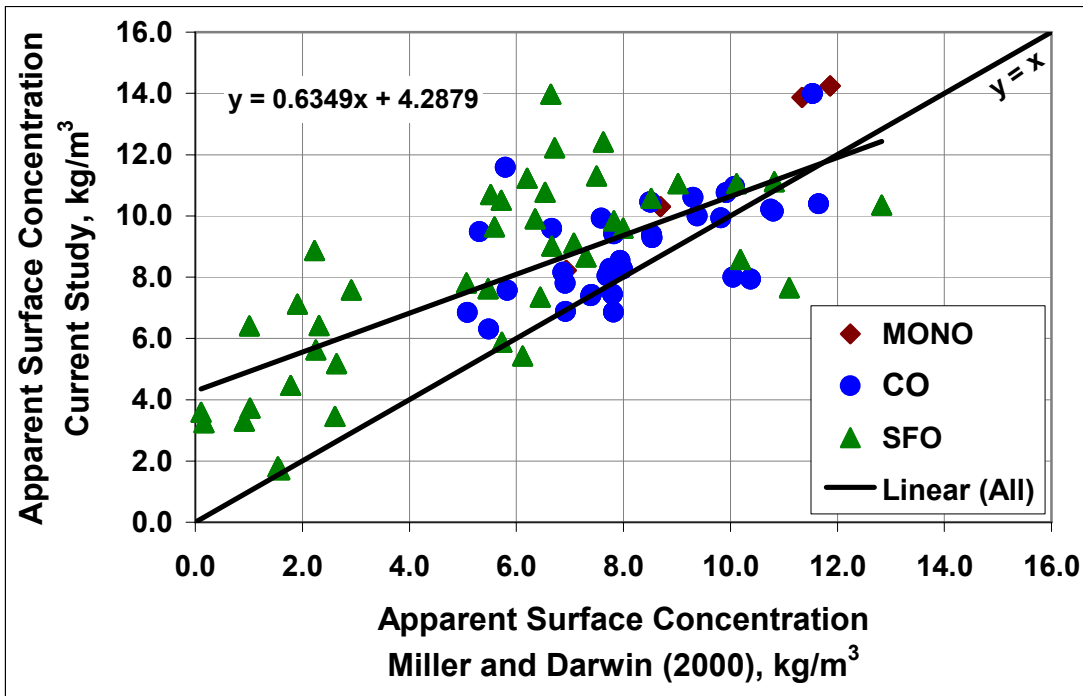


Fig. 3.16 – Average apparent surface concentration  $C_o$  calculated from Fick's Second Law for the current study versus the results based on data obtained by Miller and Darwin (2000).

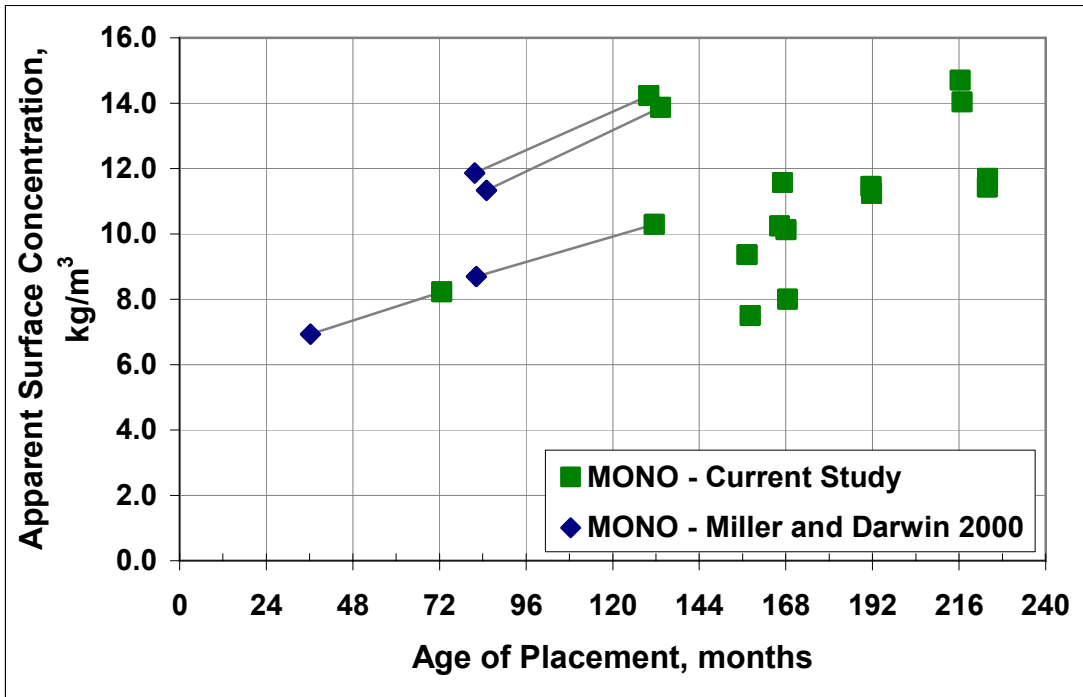


Fig. 3.17 – Average apparent surface concentration  $C_o$  calculated from Fick's Second Law versus age of placement for monolithic deck placements. Observations connected by lines indicate placements surveyed multiple times.

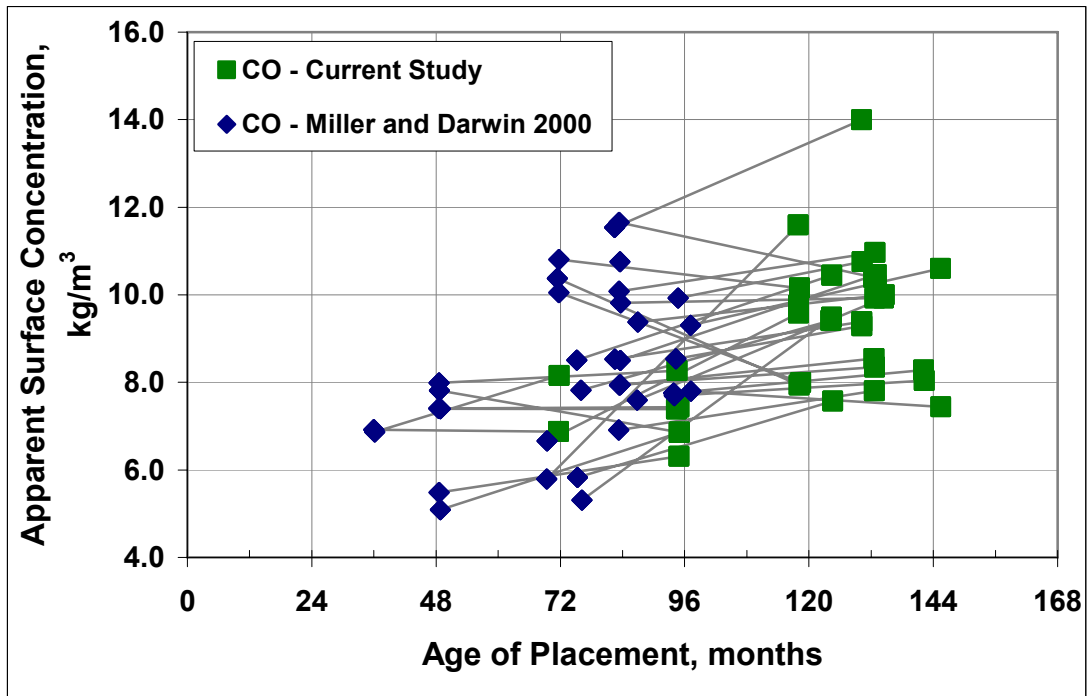


Fig 3.18 – Average apparent surface concentration  $C_o$  calculated from Fick's Second Law versus bridge deck age of placement for conventional overlay deck placements. Observations connected by lines indicate placements surveyed multiple times.

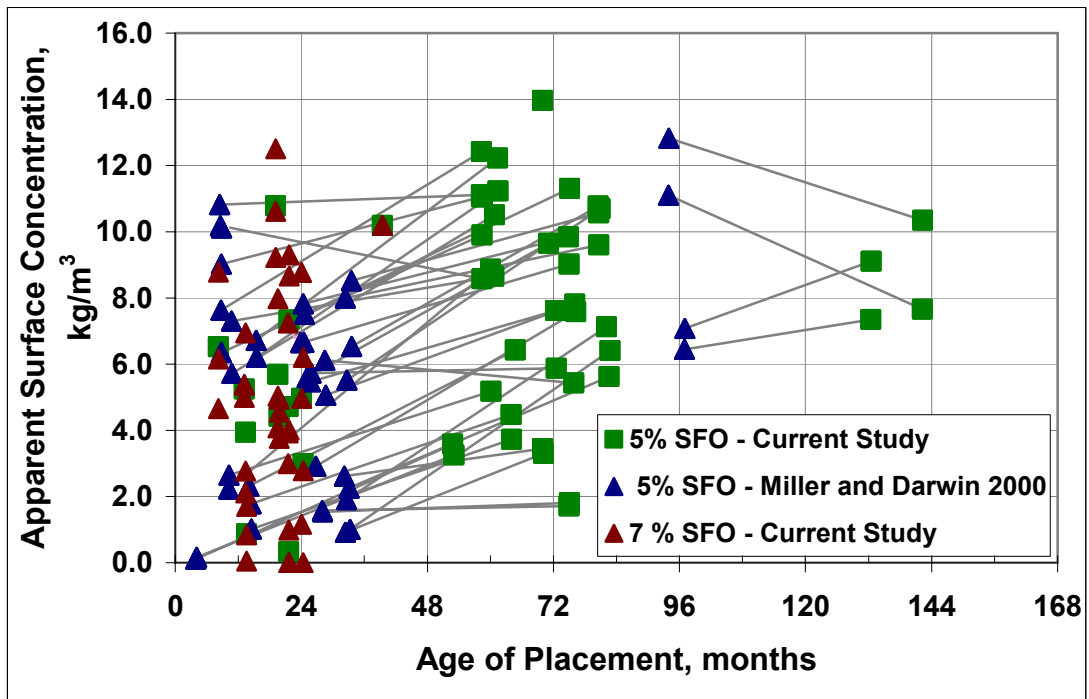


Fig 3.19 – Average apparent surface concentration  $C_o$  calculated from Fick's Second Law versus bridge deck age of placement for silica fume overlay deck placements. Observations connected by lines indicate placements surveyed multiple times.

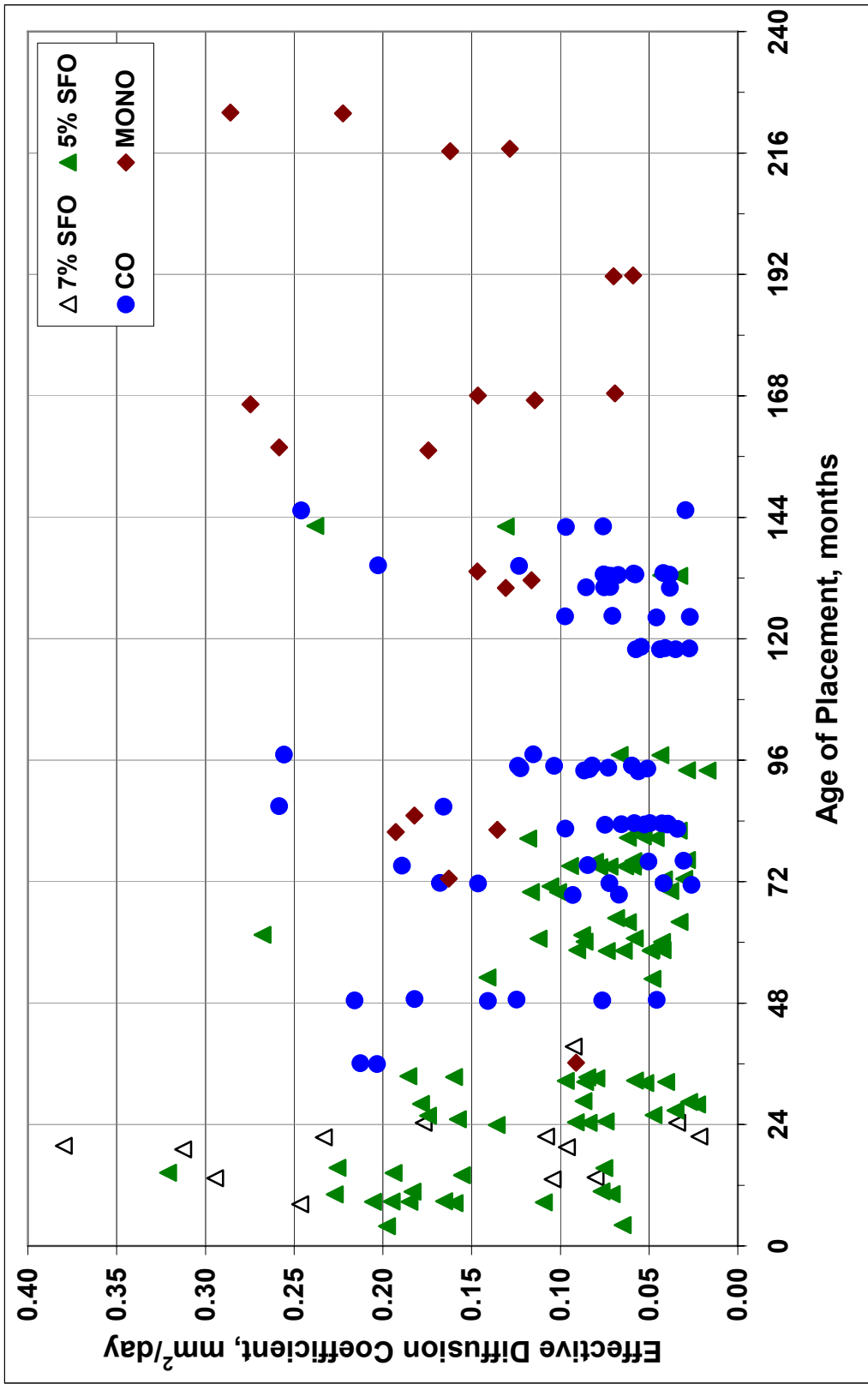


Fig 3.20 – Effective diffusion coefficient  $D_{eff}$  versus age of placement.

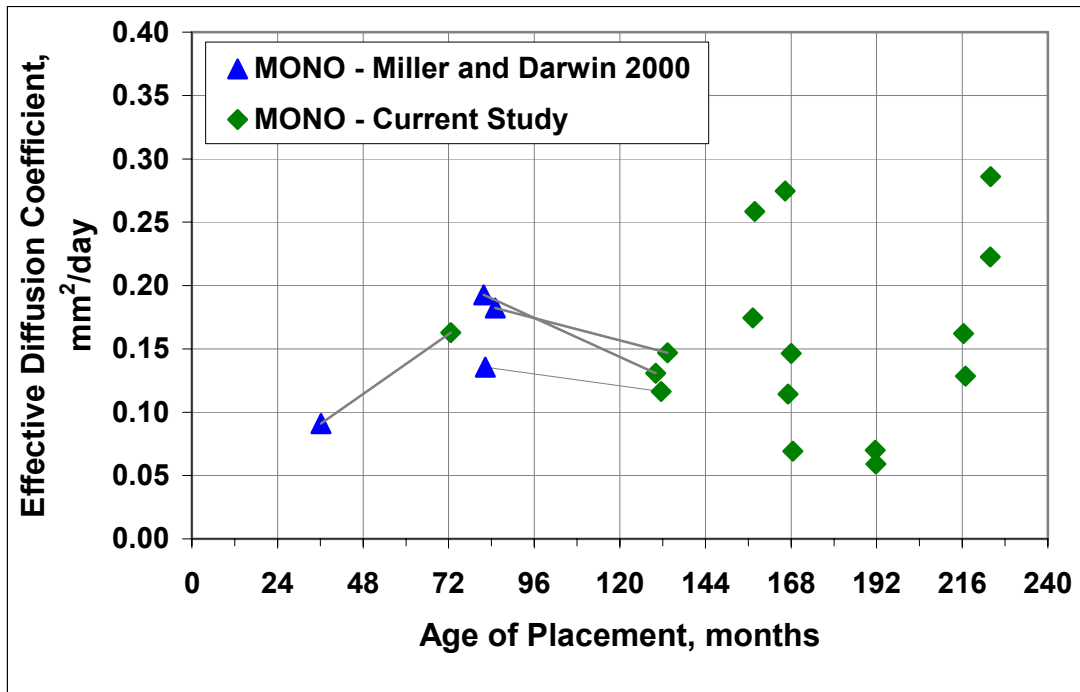


Fig. 3.21 – Effective diffusion coefficient  $D_{eff}$  versus age for monolithic bridge placements. Observations connected by lines indicate the same placement surveyed multiple times.

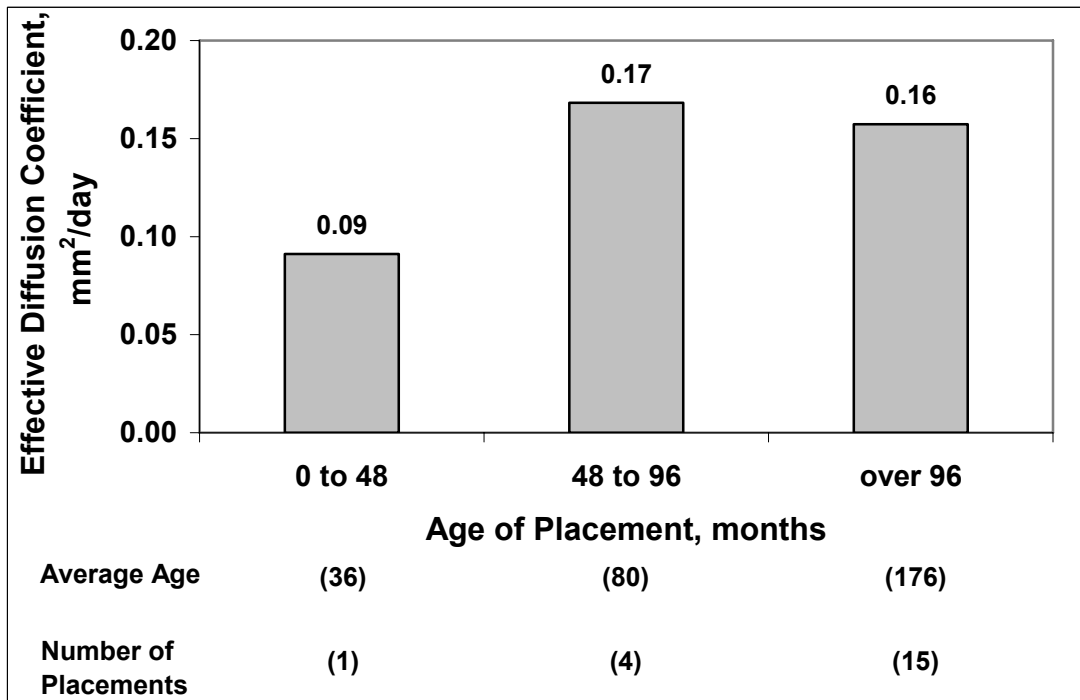


Fig. 3.22 – Mean effective diffusion coefficient  $D_{eff}$  versus placement age for monolithic bridge placements.

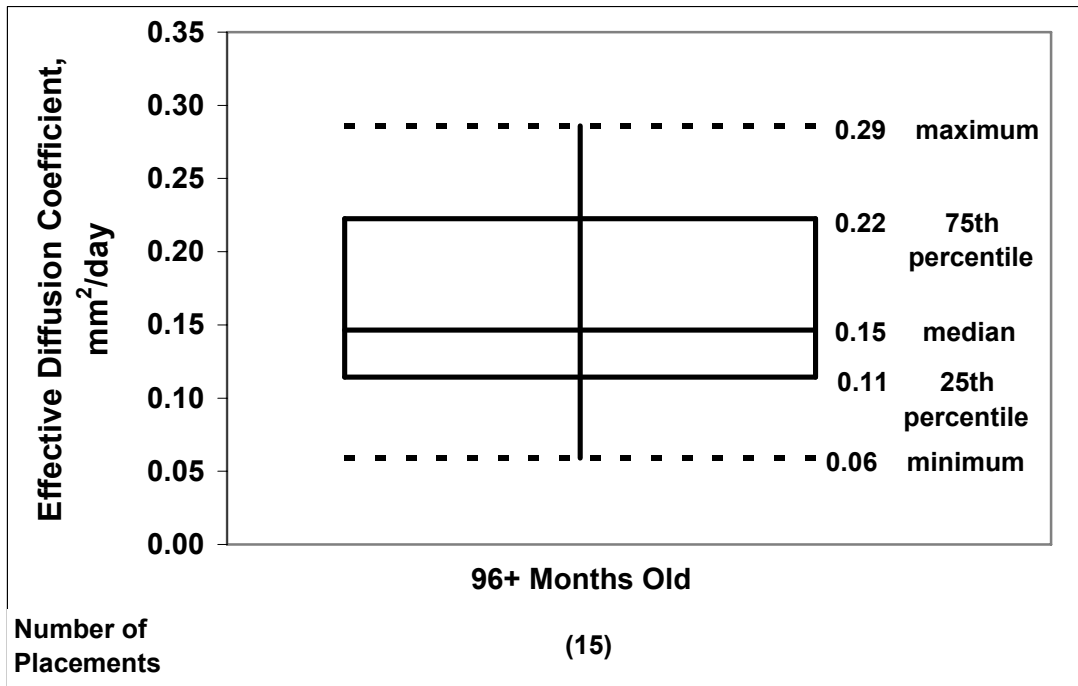


Fig. 3.23 – Box-and-whiskers plot of effective diffusion coefficients  $D_{eff}$  for monolithic placements sampled at an age of 96 months or greater. (max, 75th percentile, median, 25th percentile, and min values indicated)

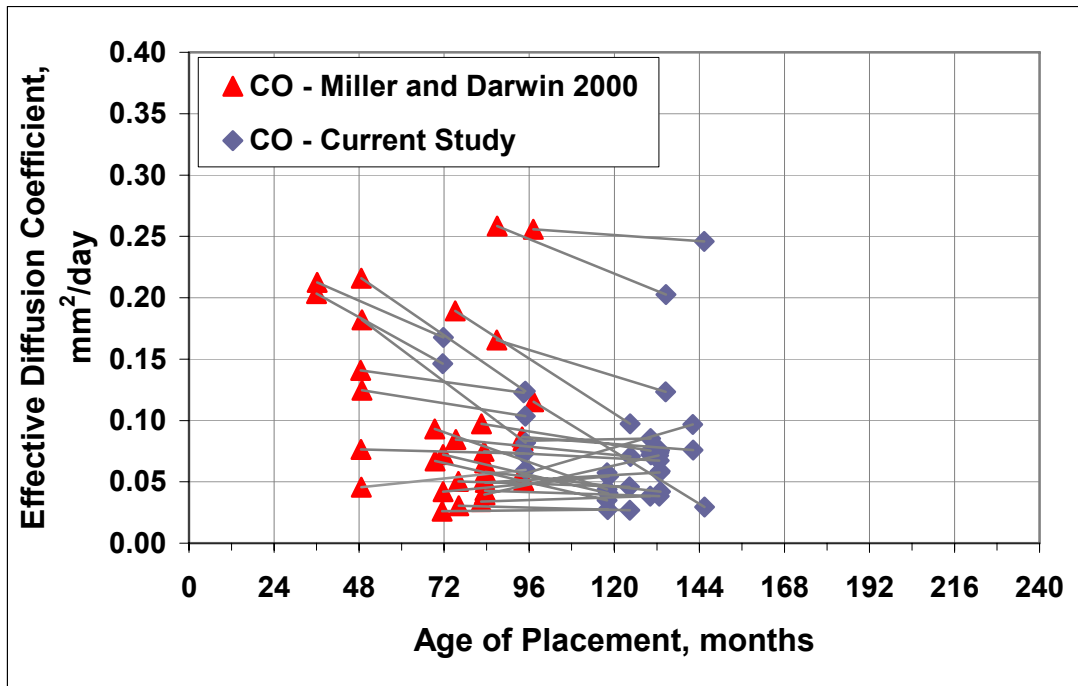


Fig. 3.24 – Effective diffusion coefficient  $D_{eff}$  versus age for conventional overlay bridge placements. Observations connected by lines indicate the same placement surveyed multiple times.

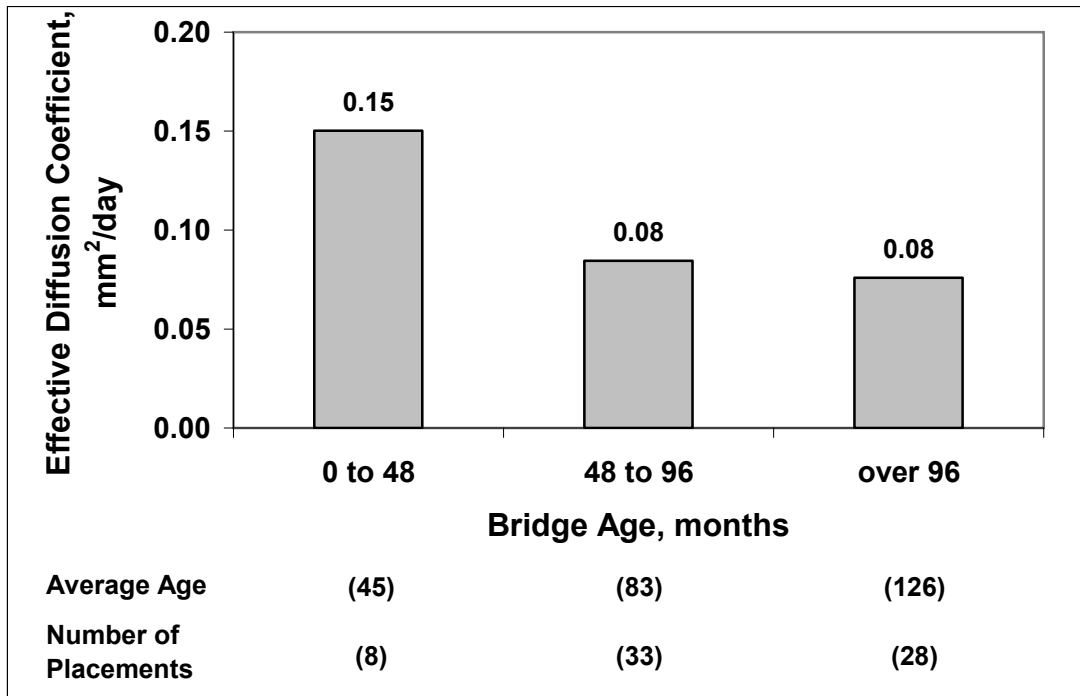


Fig. 3.25 – Mean effective diffusion coefficient  $D_{eff}$  versus placement age range for conventional overlay bridge placements.

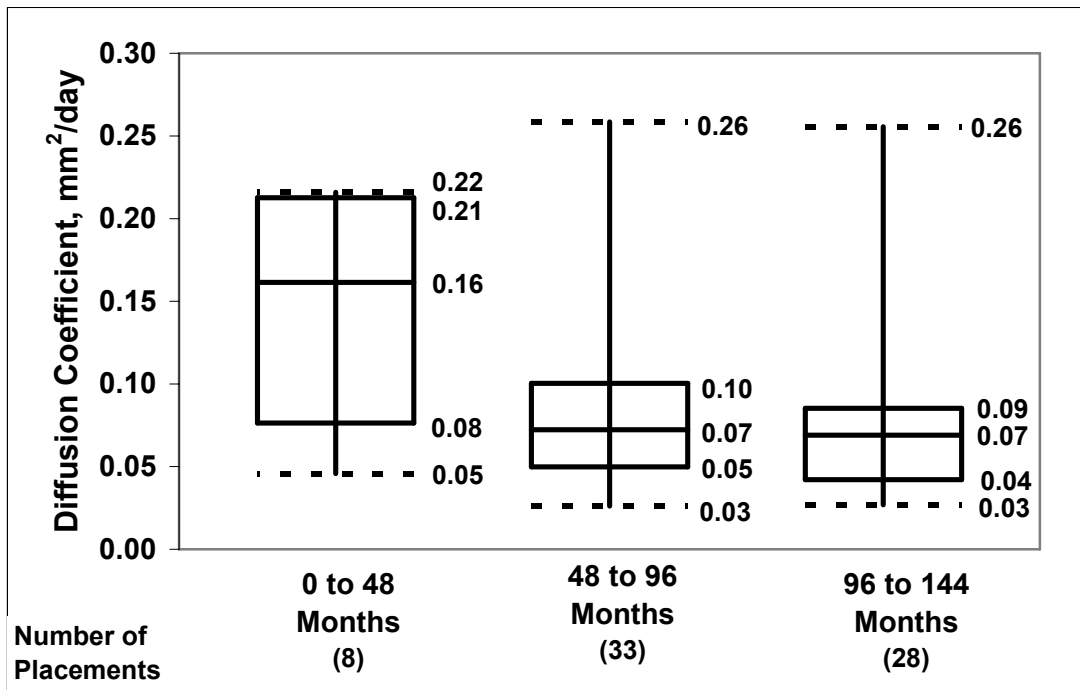


Fig. 3.26 – Box-and-whiskers plot of effective diffusion coefficients  $D_{eff}$  for conventional overlay bridge placements for three age ranges. (max, 75th percentile, median, 25th percentile, and min values indicated)

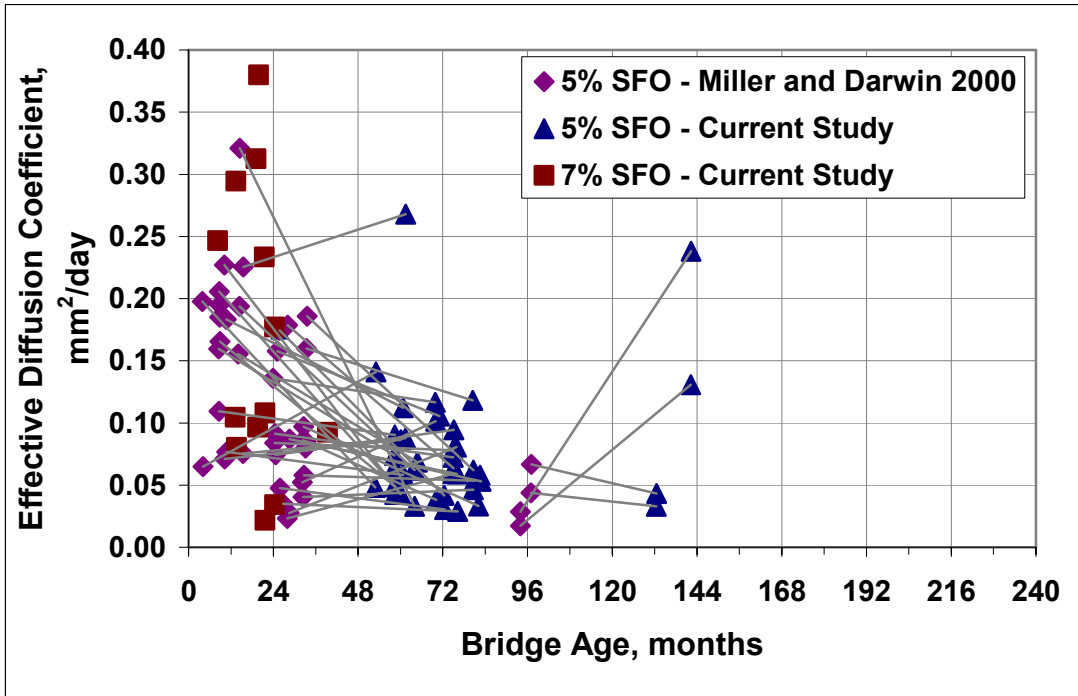


Fig. 3.27 – Effective diffusion coefficient  $D_{eff}$  versus age for silica fume overlay bridge placements. Observations connected by lines indicate the same placement surveyed multiple times.

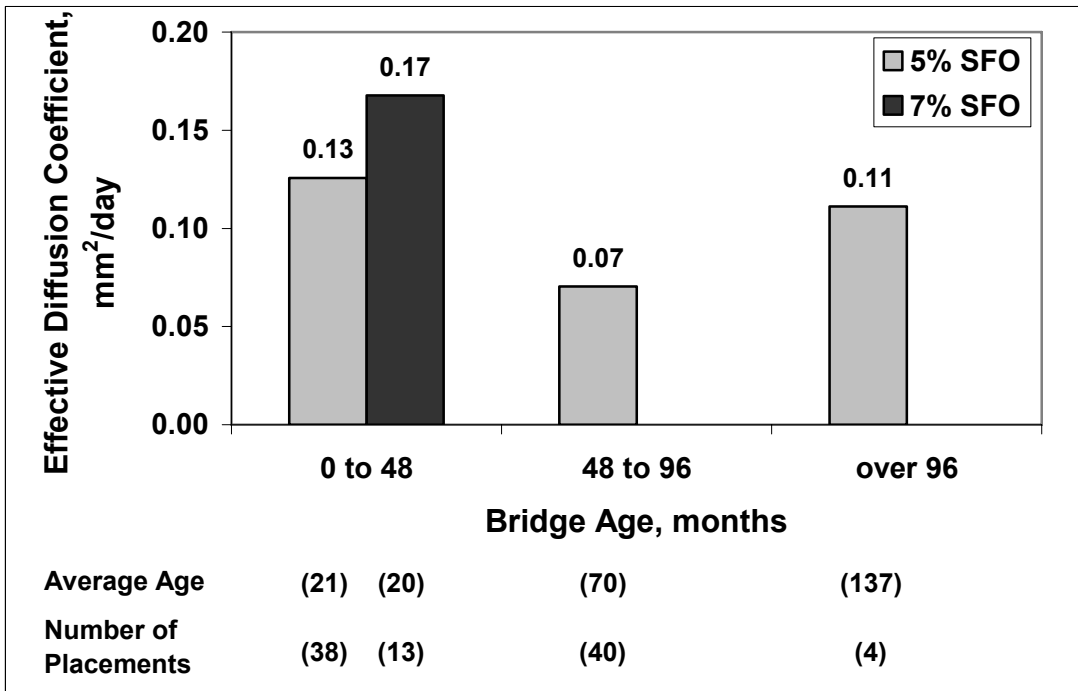


Fig. 3.28 – Mean effective diffusion coefficient  $D_{eff}$  versus placement age range for silica fume overlay bridge placements.

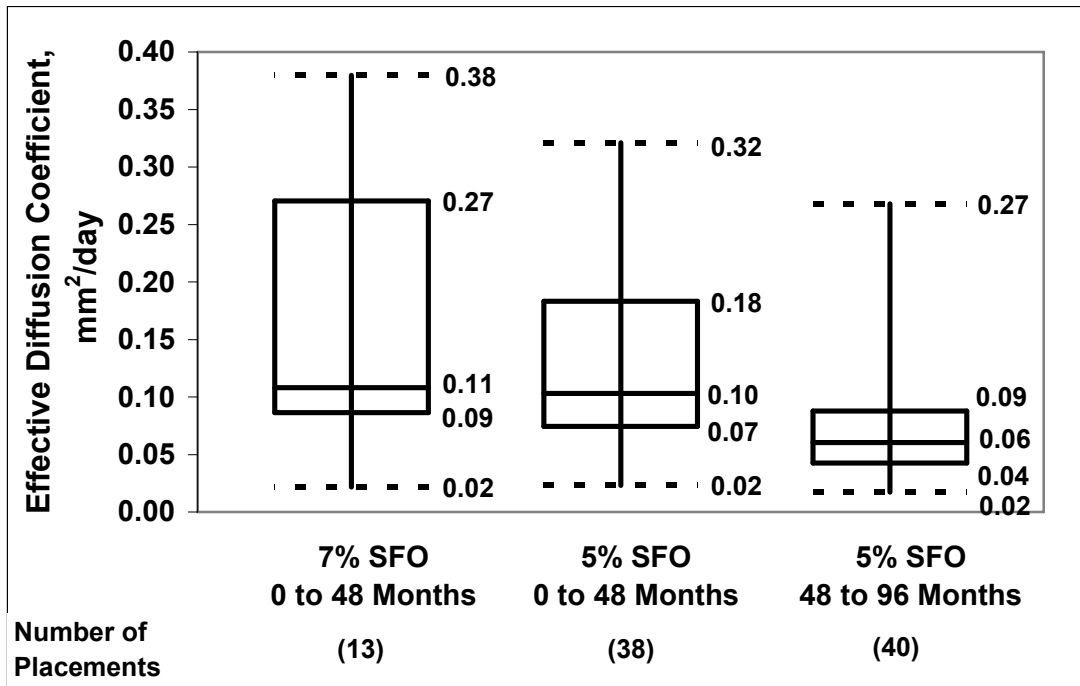


Fig. 3.29 – Box-and-whiskers plot of effective diffusion coefficients  $D_{eff}$  for silica fume overlay bridge placements in two age ranges. (max, 75th percentile, median, 25th percentile, and min values indicated)

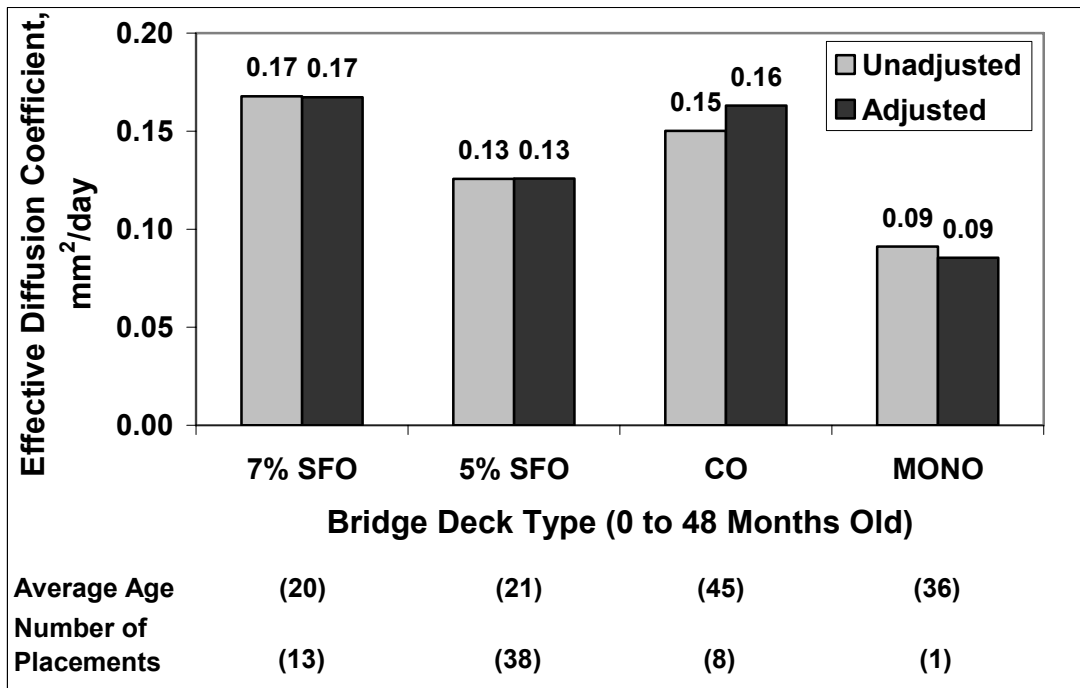


Fig. 3.30 – Mean effective diffusion coefficient  $D_{eff}$  and adjusted mean effective diffusion coefficient  $D_{eff}^*$  versus bridge deck type for individual placements between 0 and 48 months old.

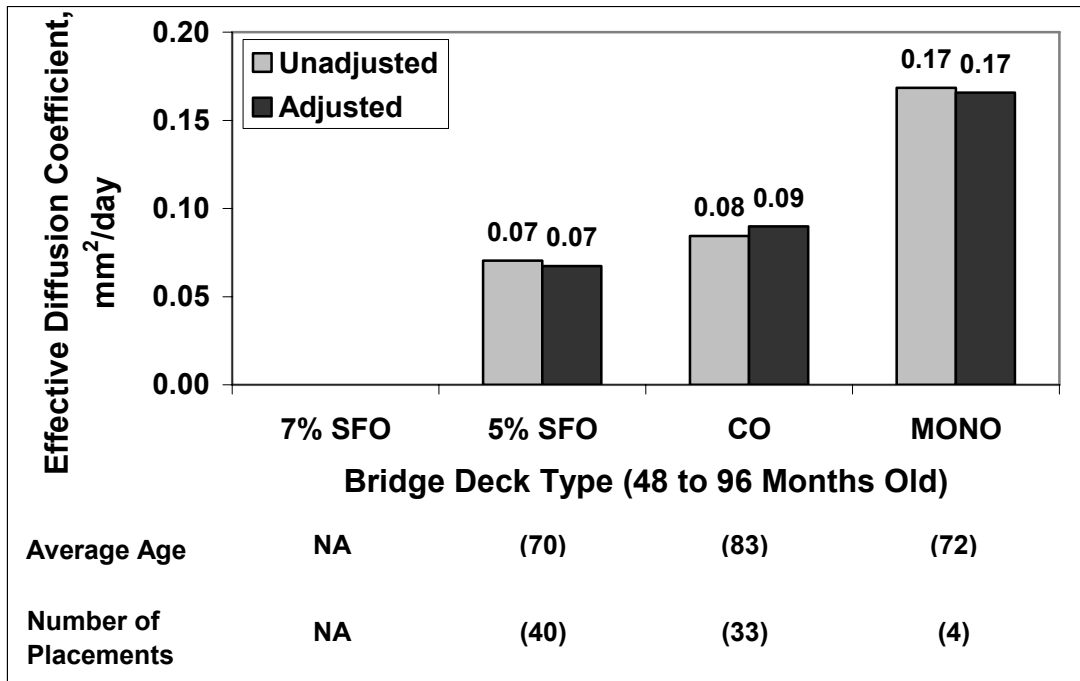


Fig. 3.31 – Mean effective diffusion coefficient  $D_{eff}$  and adjusted mean effective diffusion coefficient  $D_{eff}^*$  versus bridge deck type for individual placements between 48 and 96 months old.

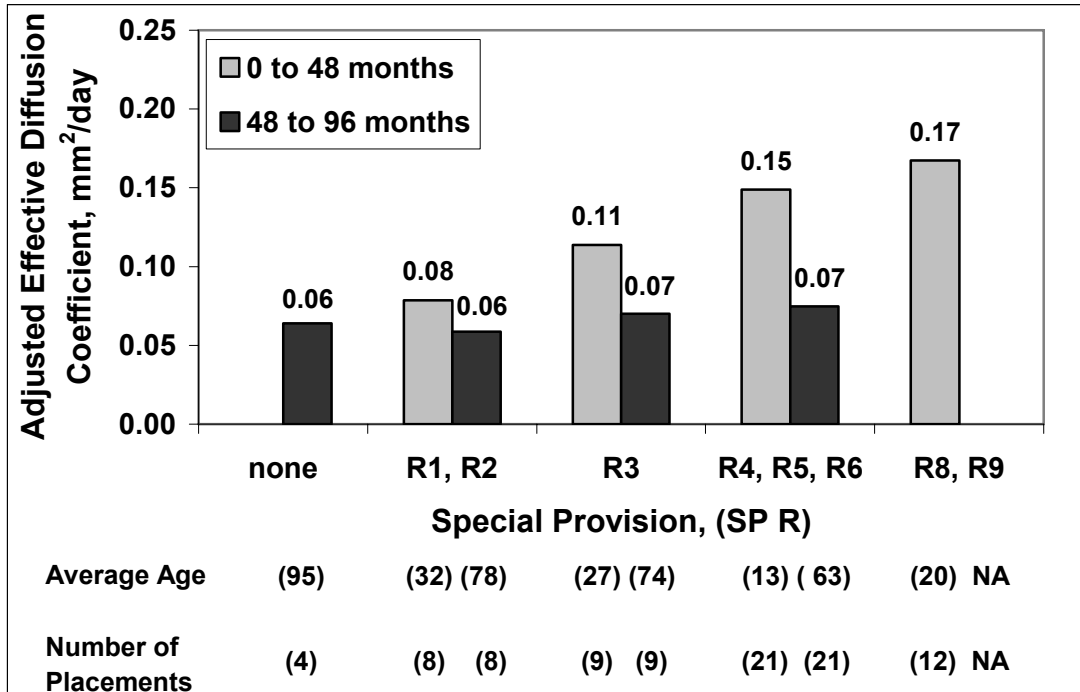


Fig 3.32 – Adjusted mean effective diffusion coefficient  $D_{eff}^*$  of individual placements versus special provision number for silica fume overlay placements between 0 and 48 months and 48 and 96 months old.

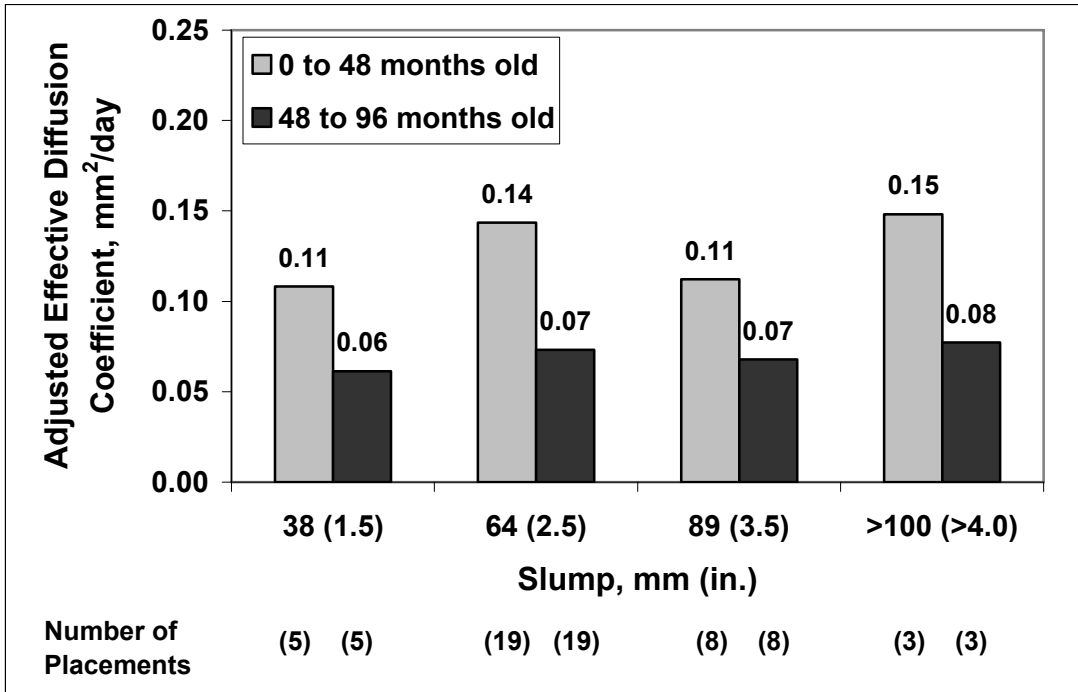


Fig 3.33 – Adjusted mean effective diffusion coefficient  $D_{eff}^*$  of individual placements versus concrete slump for 5% silica fume overlay placements between 0 and 48 months and 48 and 96 months old.

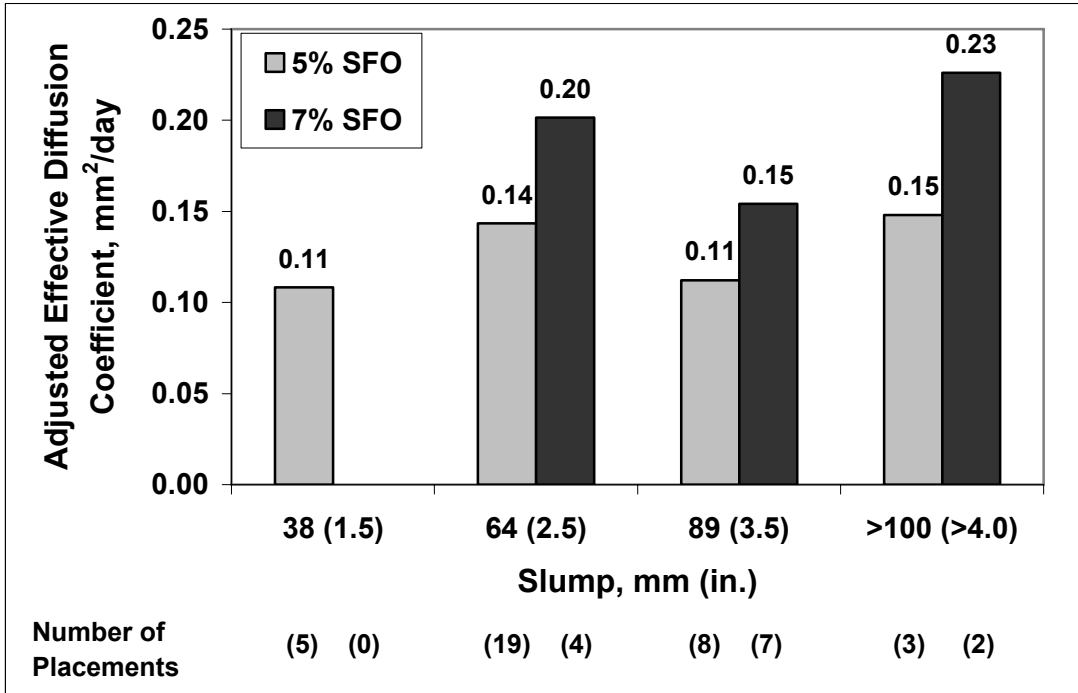


Fig. 3.34 – Adjusted mean effective diffusion coefficient  $D_{eff}^*$  of individual placements versus concrete slump for 5% silica fume and 7% silica fume overlay placements between 0 and 48 months old.

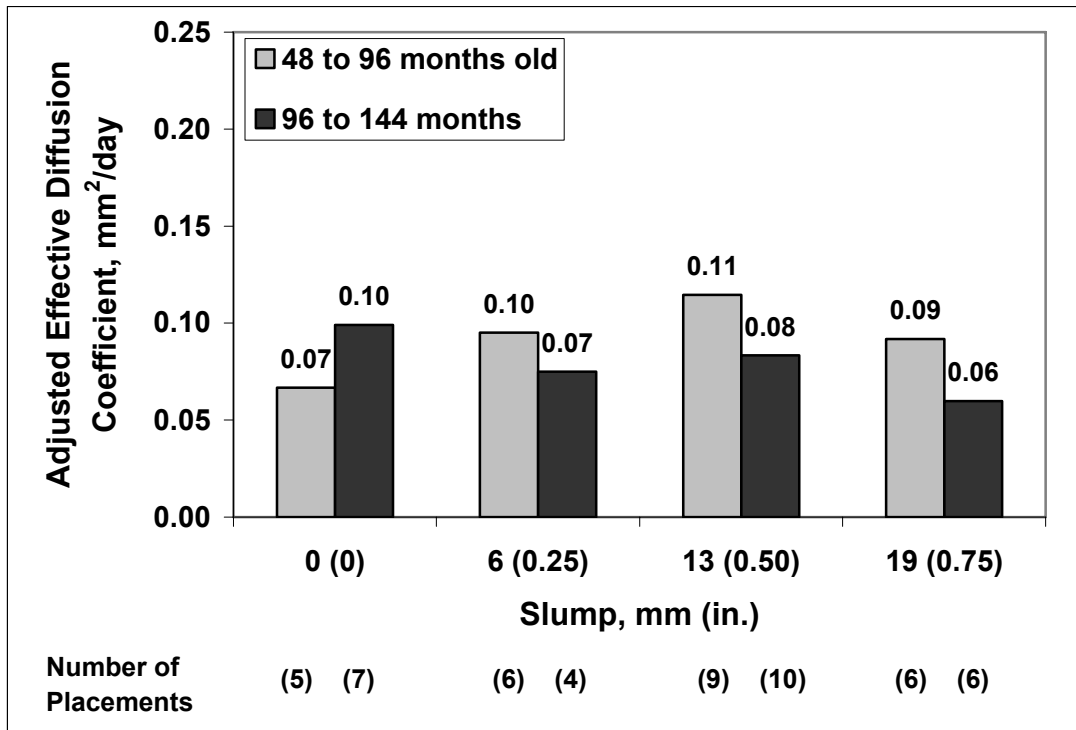


Fig 3.35 – Adjusted mean effective diffusion coefficient  $D_{eff}^*$  of individual placements versus concrete slump for conventional overlay placements between 48 and 96 months and 96 and 144 months old.

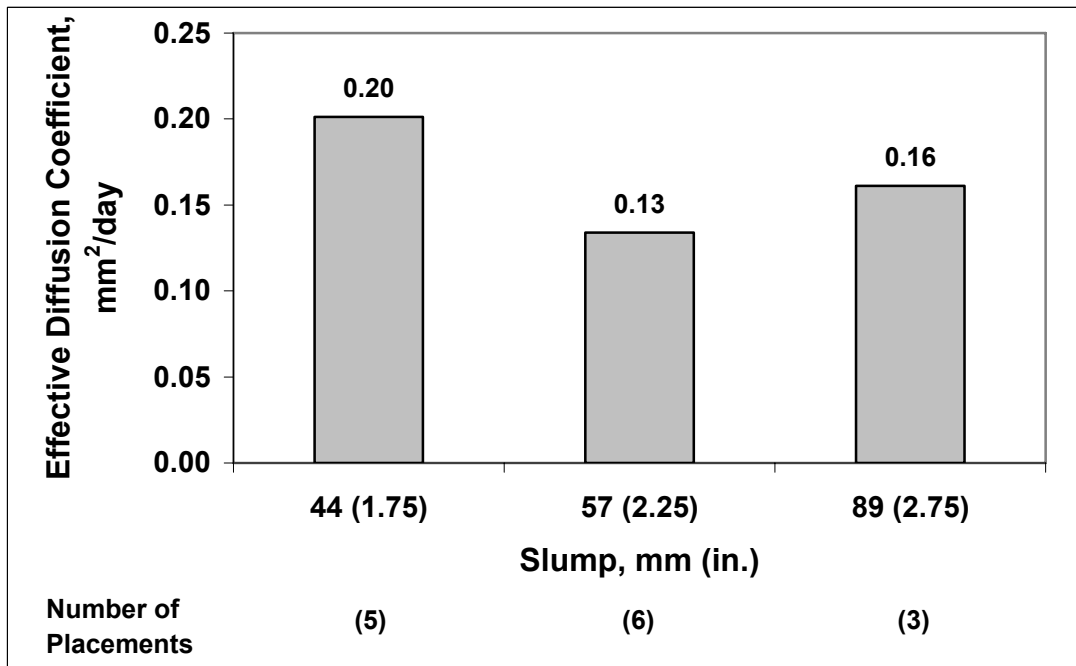


Fig 3.36 – Adjusted mean effective diffusion coefficient  $D_{eff}^*$  of individual placements versus concrete slump for monolithic bridge placements older than 120 months.

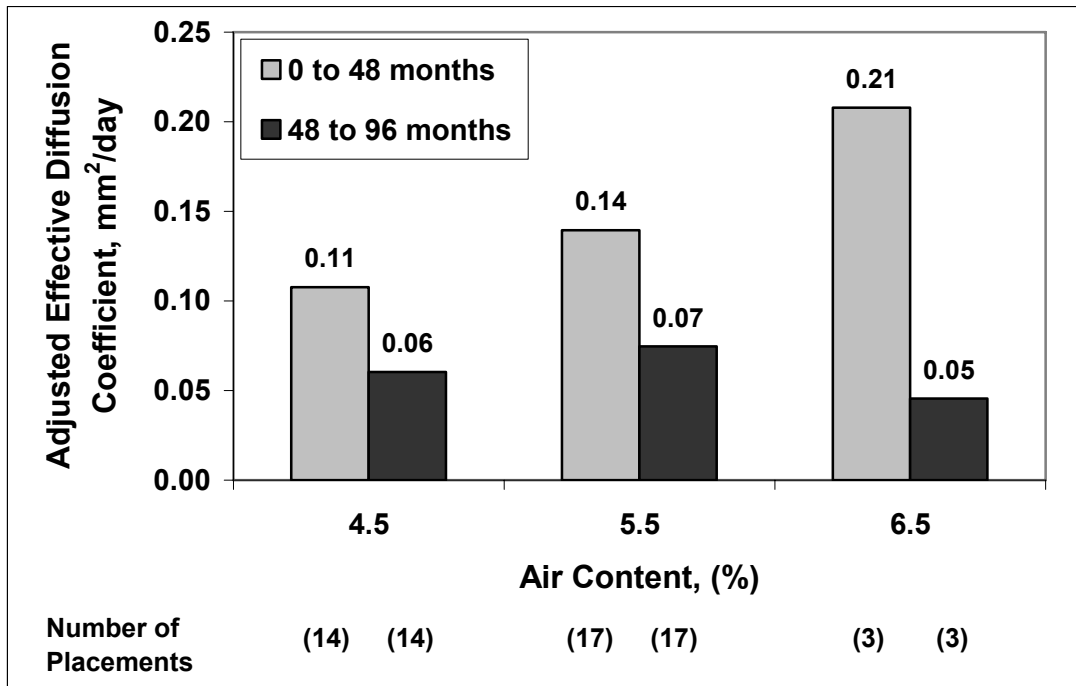


Fig 3.37 – Adjusted mean effective diffusion coefficient  $D_{eff}^*$  of individual placements versus air content for 5% silica fume overlay placements between 0 and 48 months and 48 and 96 months old.

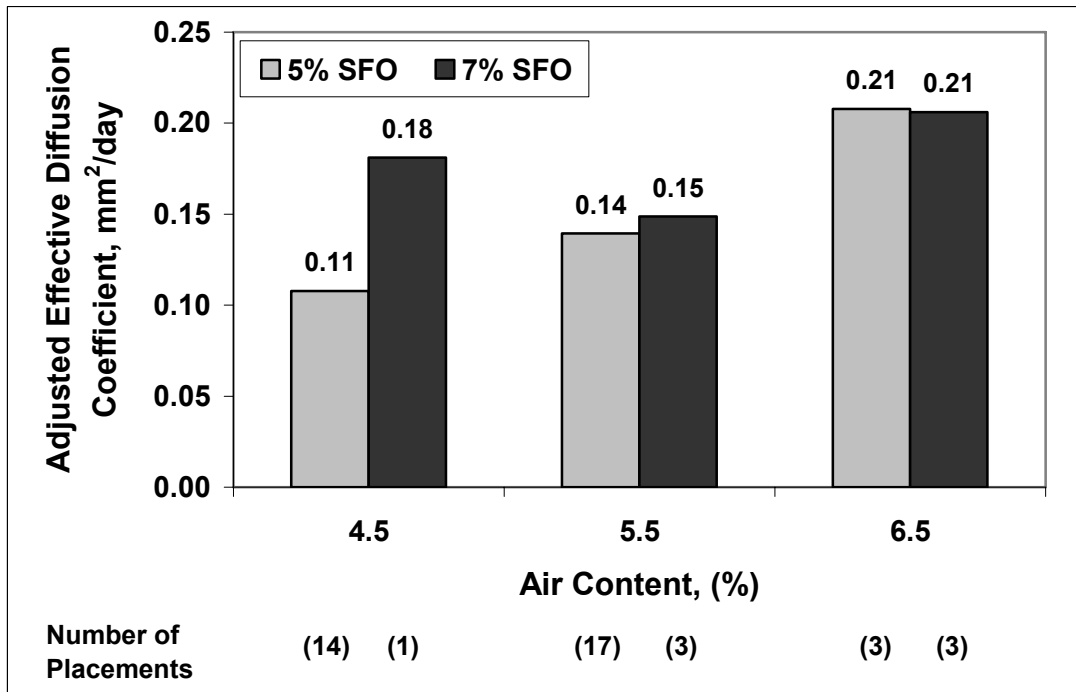


Fig. 3.38 – Adjusted mean effective diffusion coefficient  $D_{eff}^*$  of individual placements versus air content for 5% silica fume and 7% silica fume overlay placements between 0 and 48 months old.

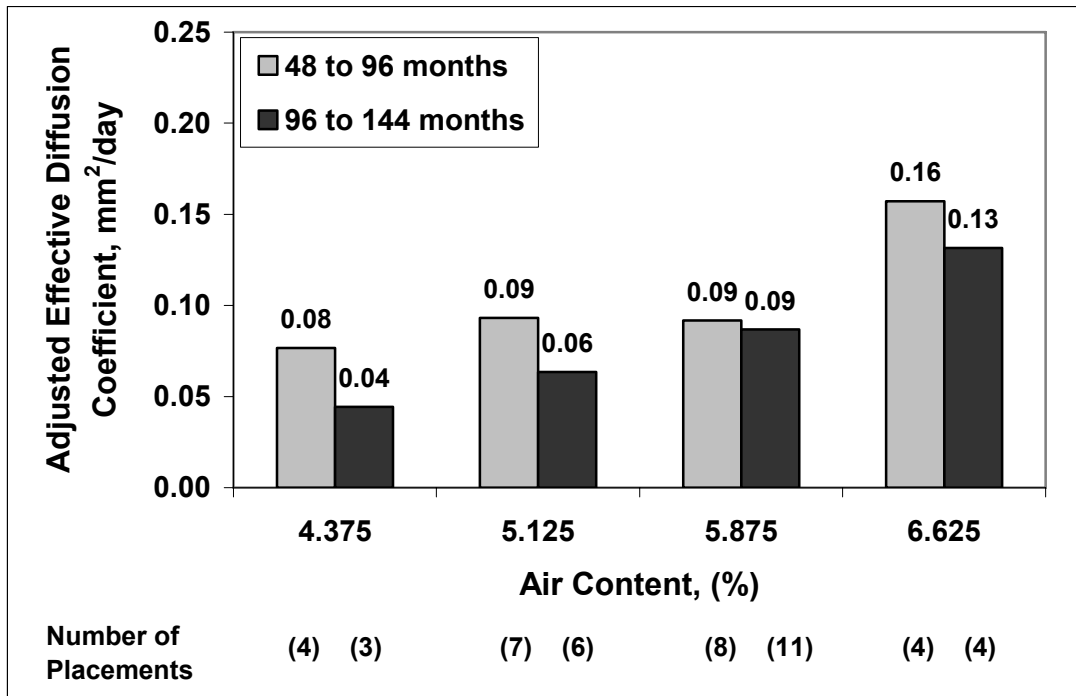


Fig. 3.39 – Adjusted mean effective diffusion coefficient  $D_{eff}^*$  of individual placements versus air content for conventional overlay placements between 48 and 96 months and 96 and 144 months old.

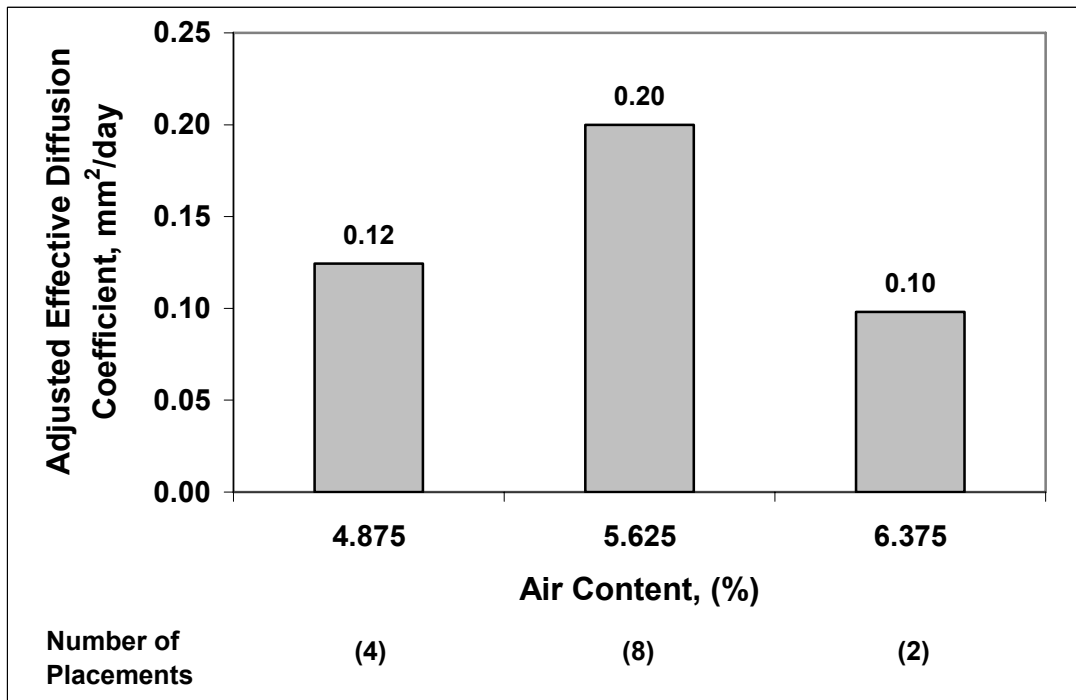


Fig. 3.40 – Adjusted mean effective diffusion coefficient  $D_{eff}^*$  of individual placements versus air content for monolithic bridge placements older than 120 months.

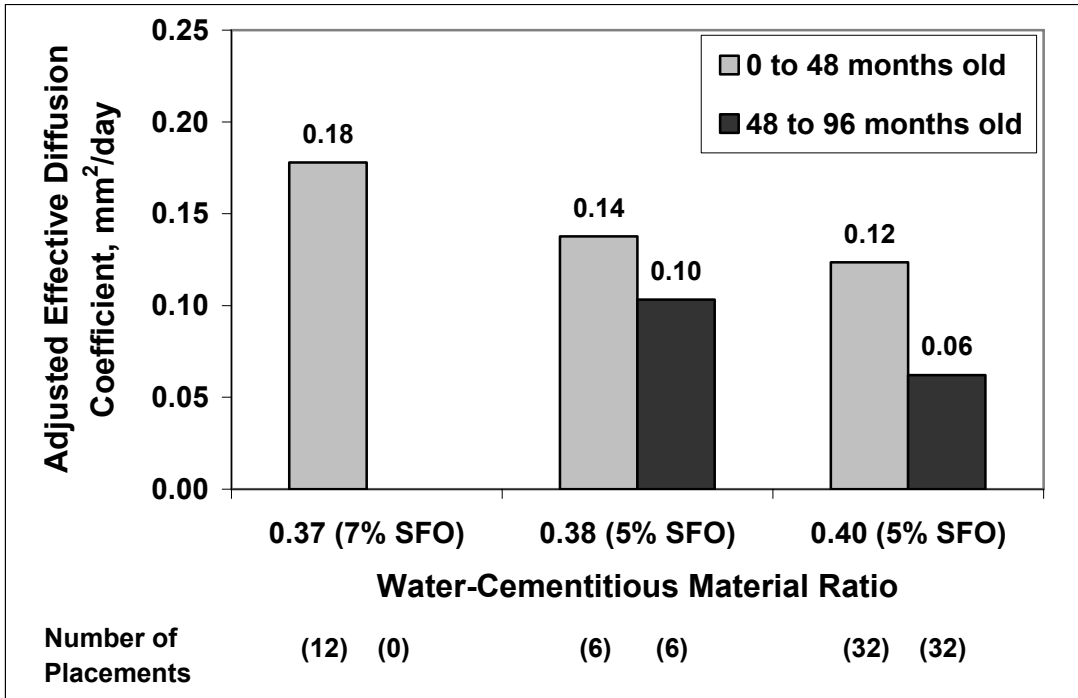


Fig. 3.41 – Adjusted mean effective diffusion coefficient  $D_{eff}^*$  of individual placements versus water-cementitious material ratio for silica fume overlay placements.

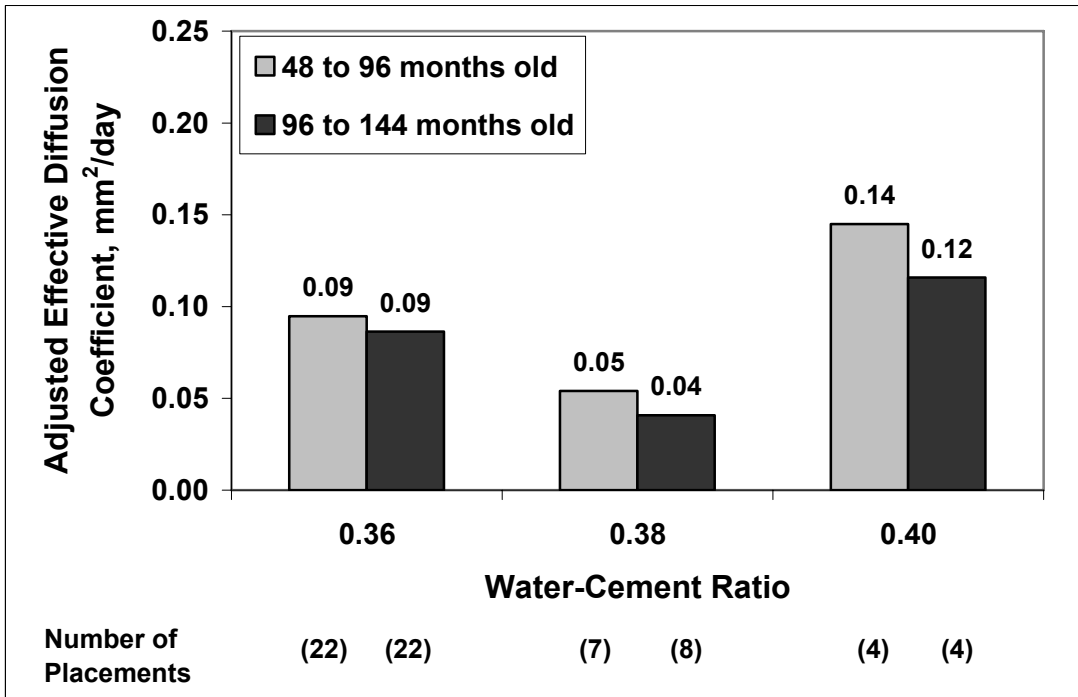


Fig. 3.42 – Adjusted mean effective diffusion coefficient  $D_{eff}^*$  of individual placements versus water-cement ratio for conventional overlay placements.

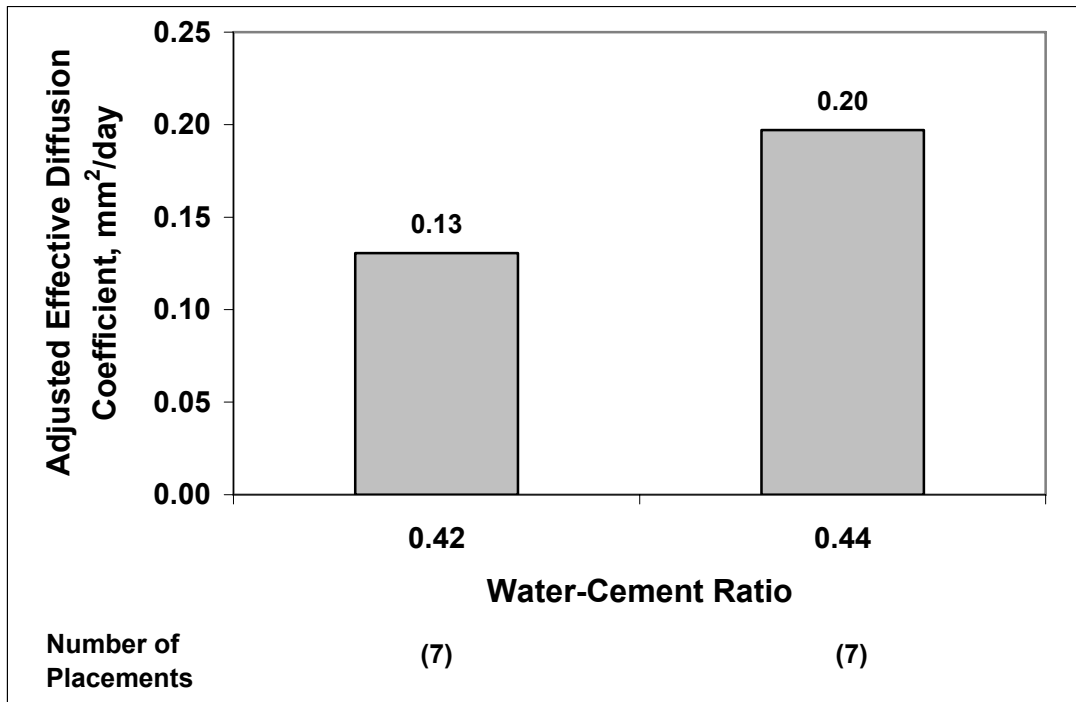


Fig. 3.43 – Adjusted mean effective diffusion coefficient  $D_{eff}^*$  of individual placements versus water-cement ratio for monolithic bridge placements older than 120 months.

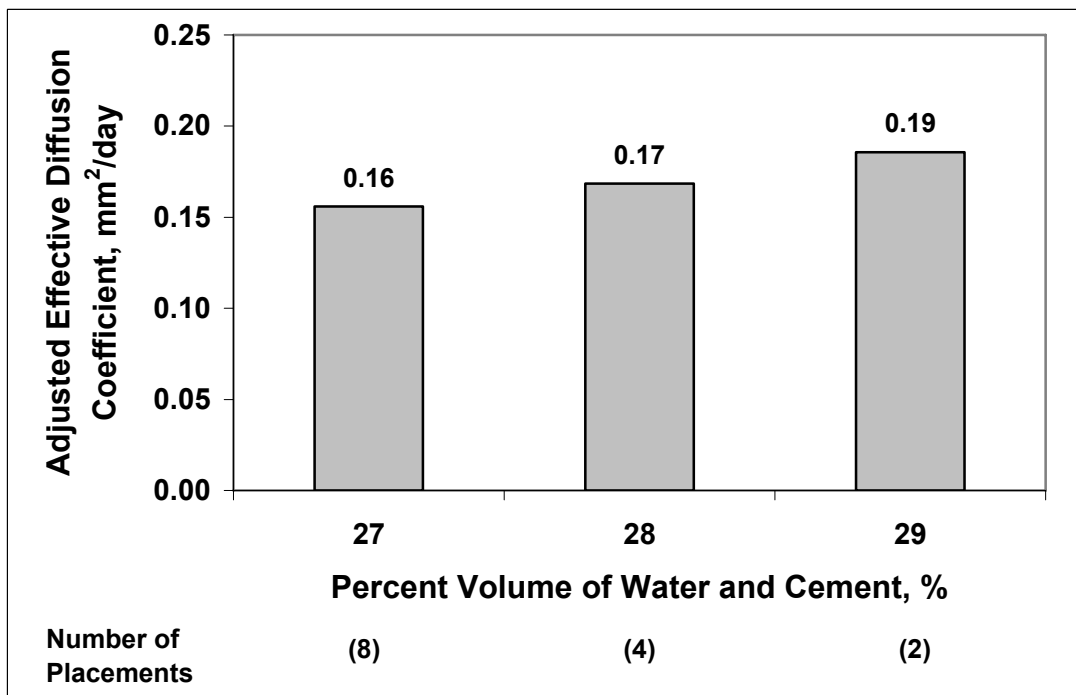


Fig. 3.44 – Adjusted mean effective diffusion coefficient  $D_{eff}^*$  of individual placements versus concrete slump for monolithic bridge placements older than 120 months.

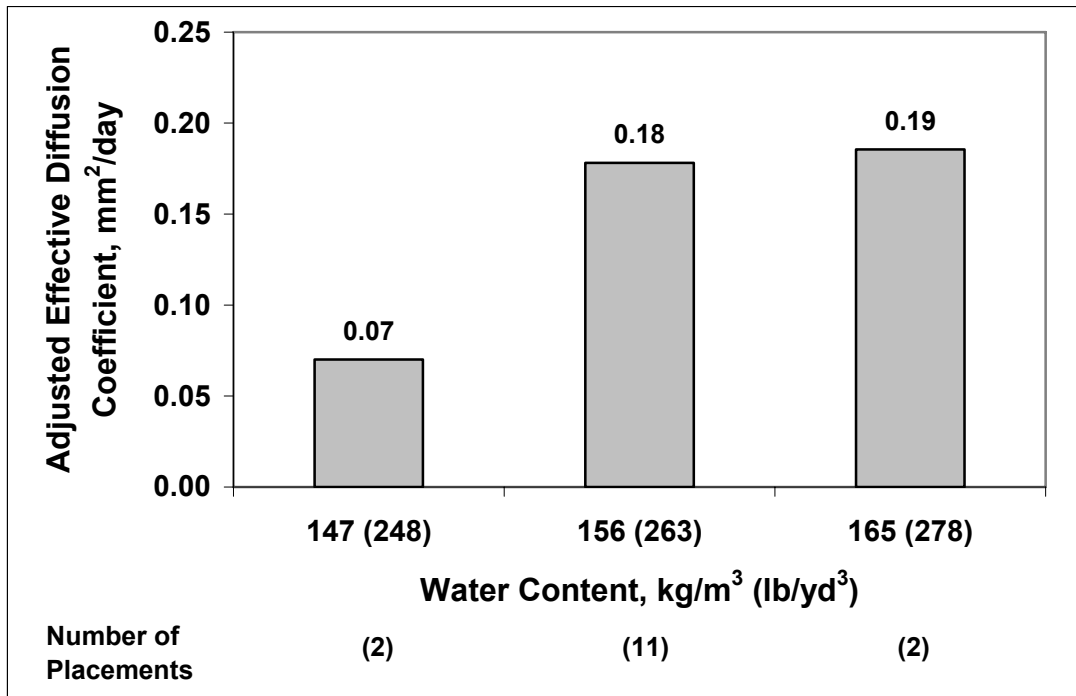


Fig. 3.45 – Adjusted mean effective diffusion coefficient  $D_{eff}^*$  of individual placements versus water content for monolithic bridge placements older than 120 months.

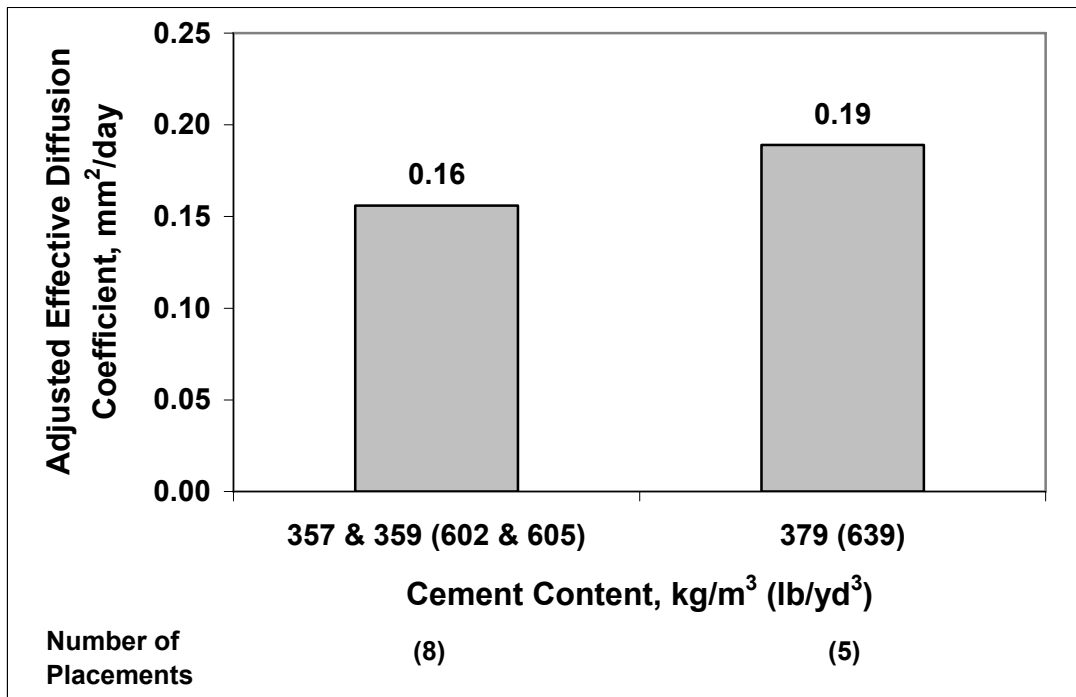


Fig. 3.46 – Adjusted mean effective diffusion coefficient  $D_{eff}^*$  of individual placements versus cement content for monolithic bridge placements older than 120 months.

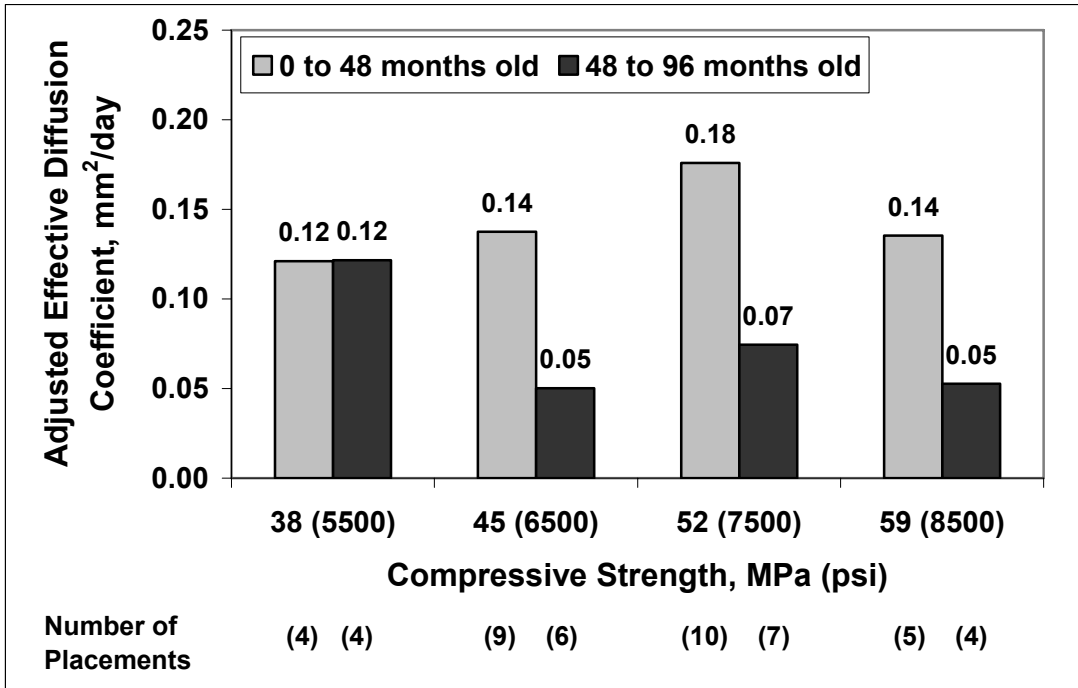


Fig. 3.47 – Adjusted mean effective diffusion coefficient  $D_{eff}^*$  of individual placements versus concrete compressive strength for 5% silica fume overlay placements between 0 and 48 months and 48 and 96 months old.

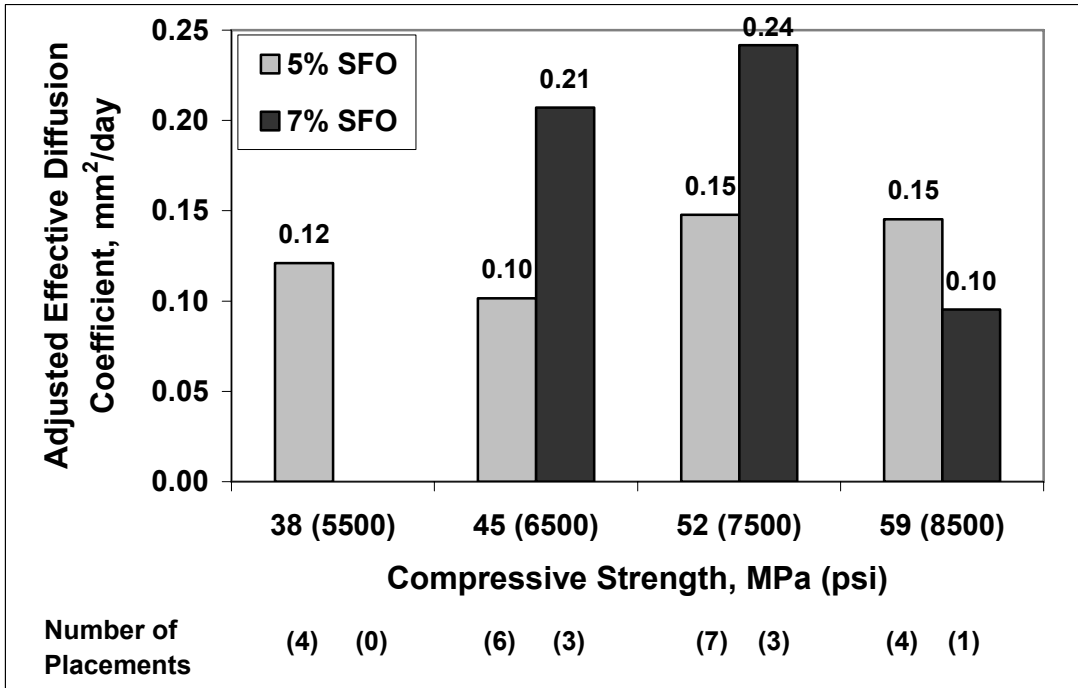


Fig. 3.48 – Adjusted mean effective diffusion coefficient  $D_{eff}^*$  of individual placements versus concrete compressive strength for 5% silica fume and 7% silica fume overlay placements between 0 and 48 months old.

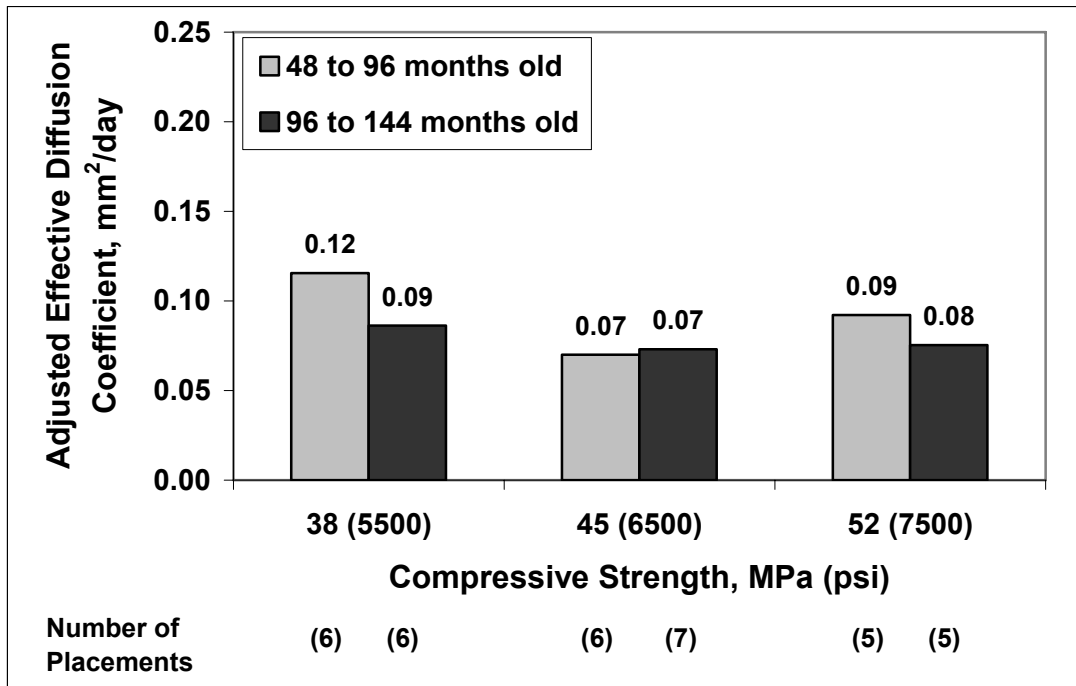


Fig. 3.49 – Adjusted mean effective diffusion coefficient  $D_{eff}^*$  of individual placements versus concrete compressive strength for conventional overlay placements between 48 and 96 months and 96 and 144 months old.

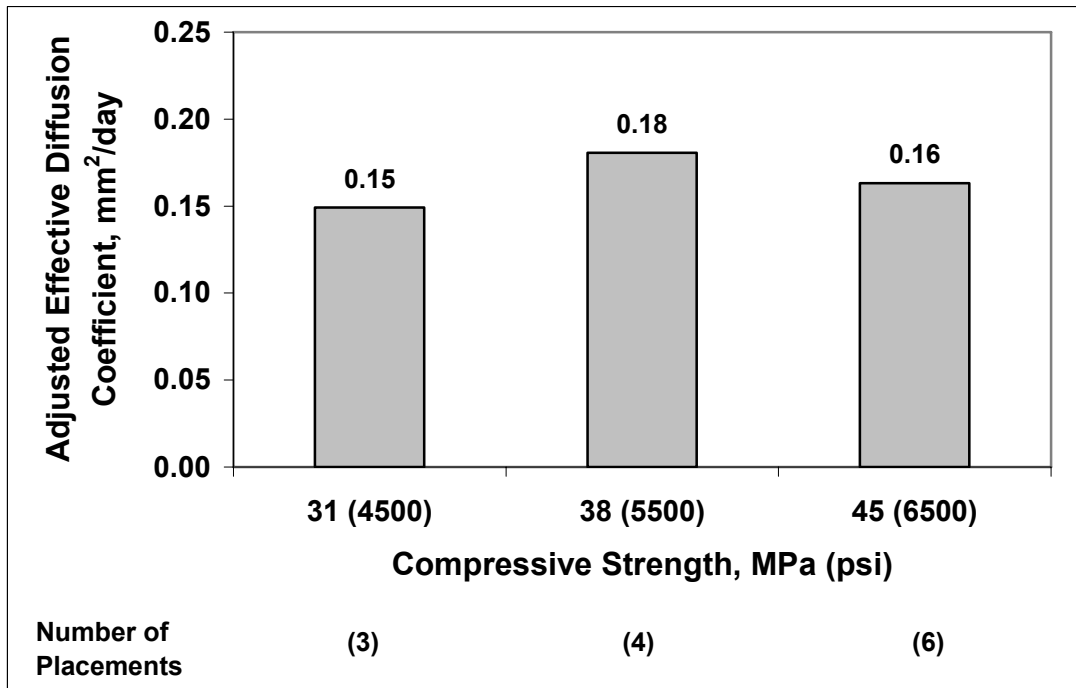


Fig. 3.50 – Adjusted mean effective diffusion coefficient  $D_{eff}^*$  of individual placements versus concrete compressive strength for monolithic bridge placements older than 120 months.

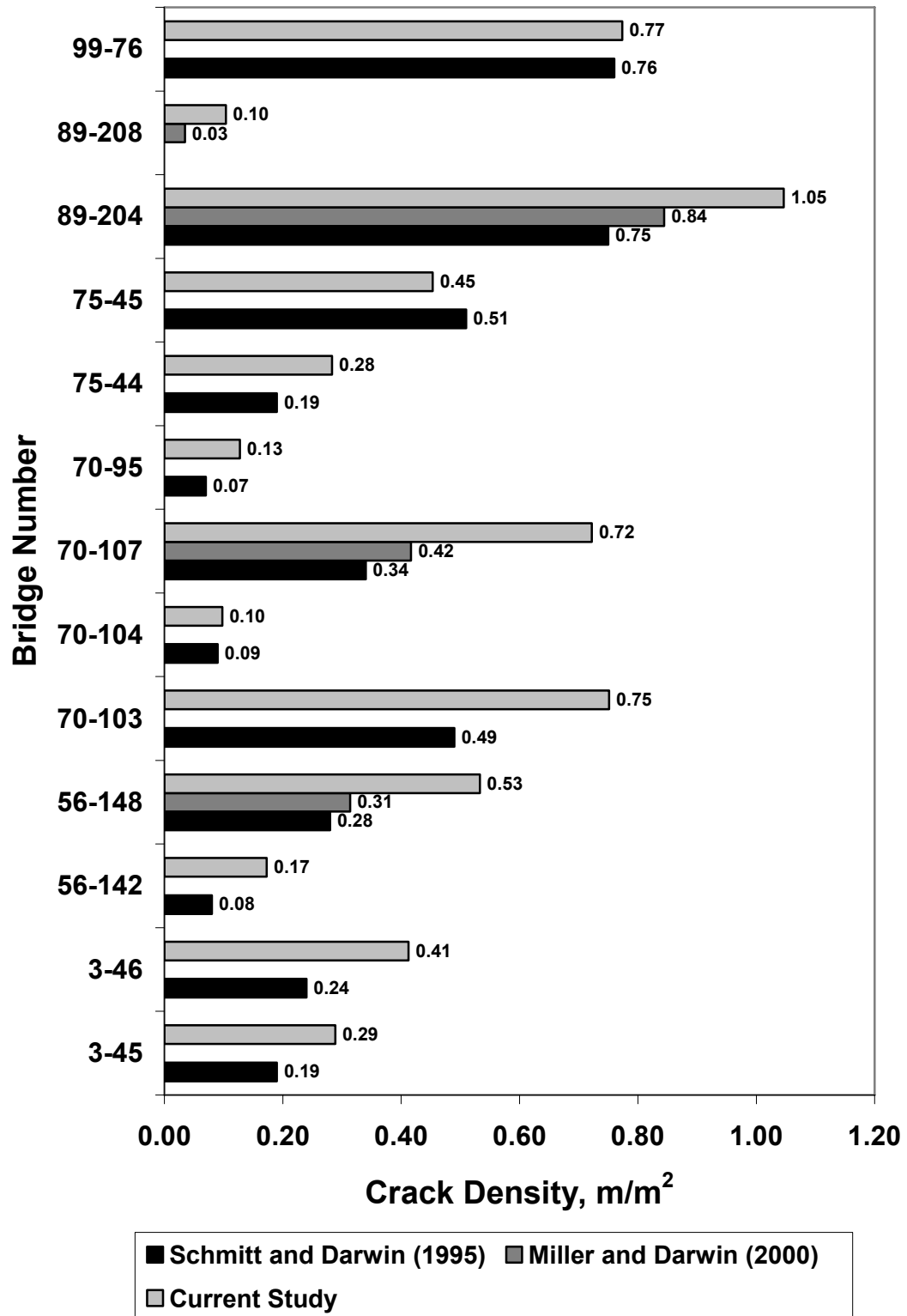


Fig. 4.1 – Crack density of entire **monolithic** bridge decks evaluated in the current study and by Schmitt and Darwin (1995) and/or Miller and Darwin (2000).

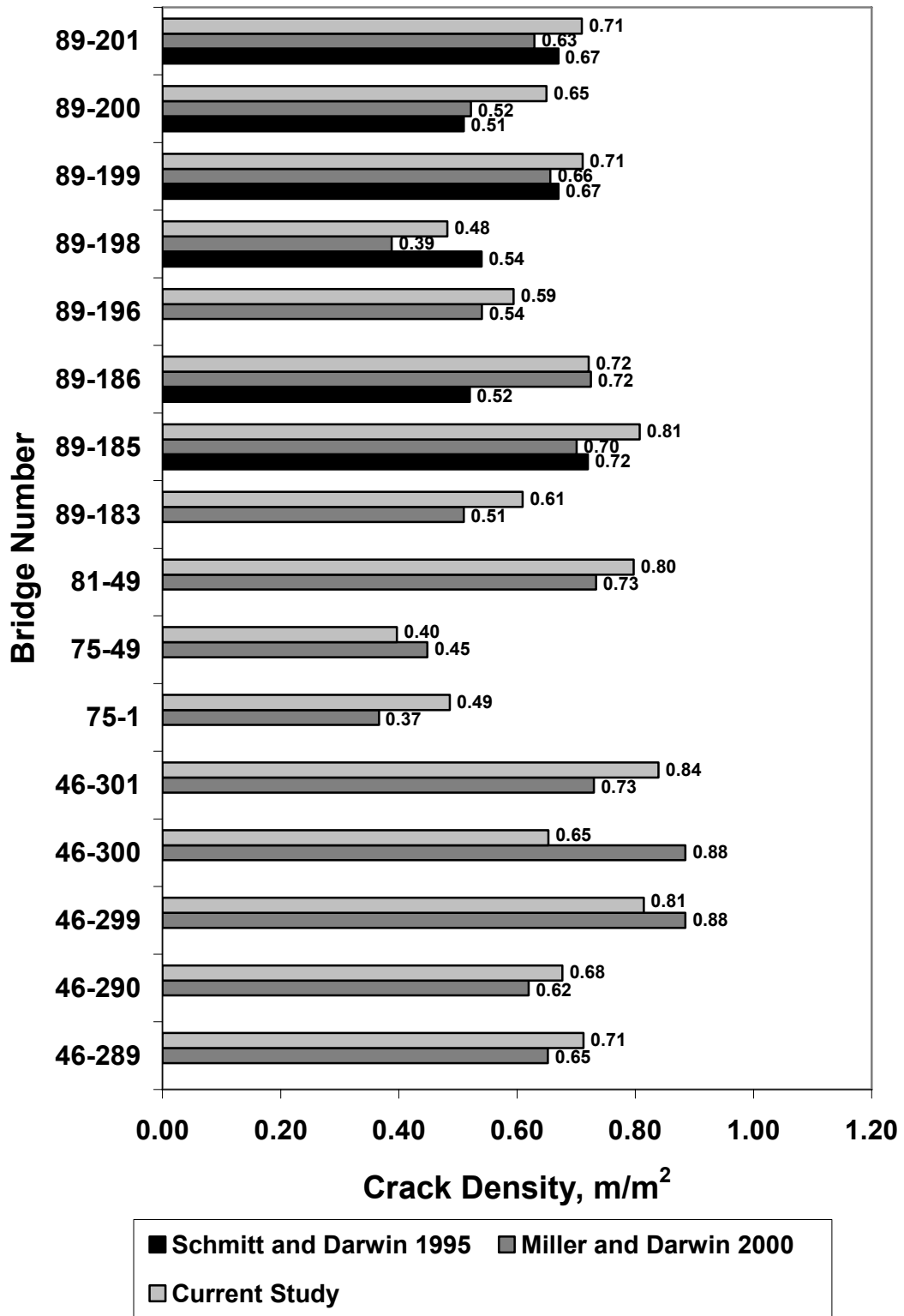


Fig. 4.2 – Crack density of entire **conventional overlay** bridge decks evaluated in the current study and by Schmitt and Darwin (1995) and/or Miller and Darwin (2000).

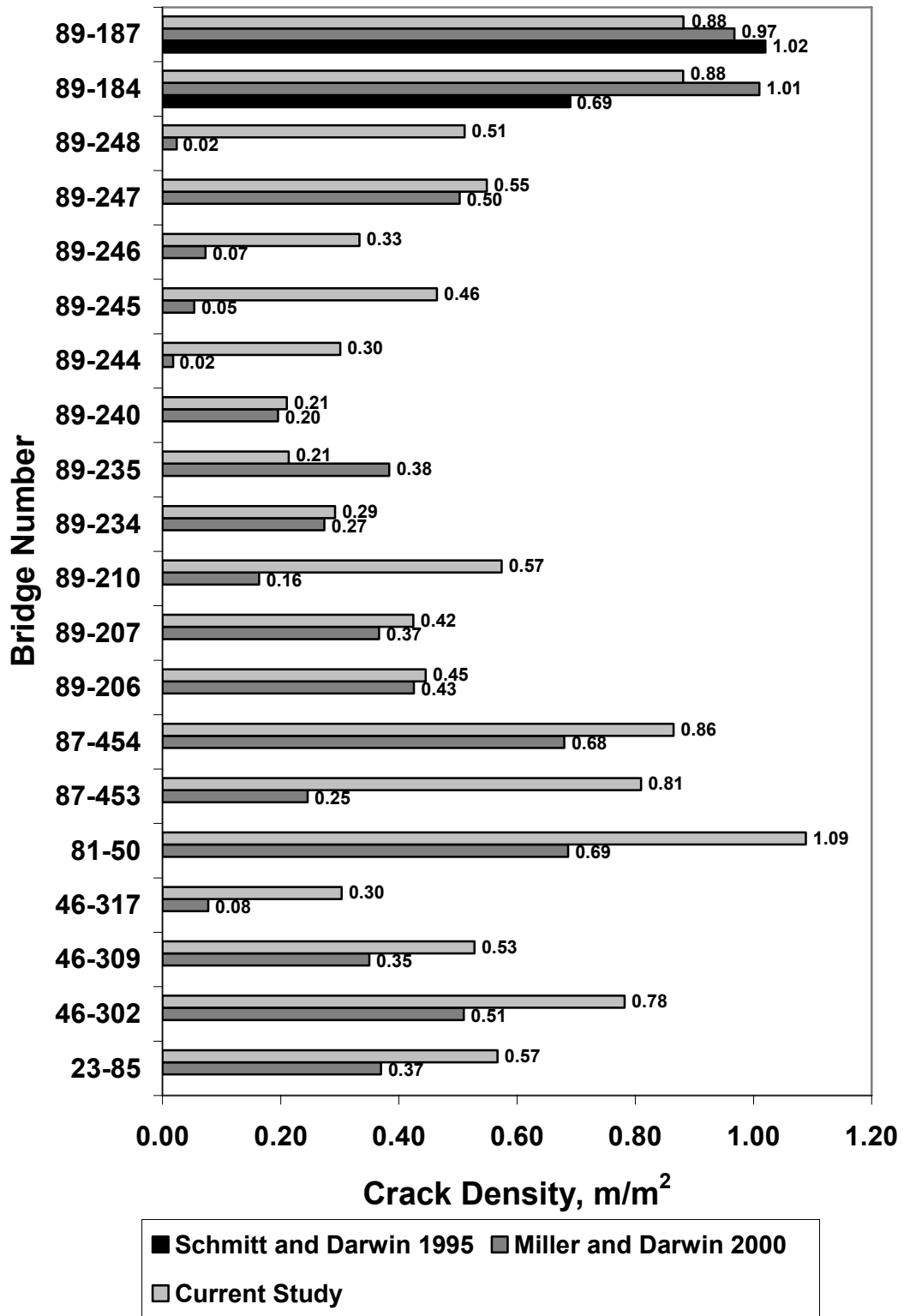


Fig. 4.3 – Crack density of entire **silica fume overlay** bridge decks evaluated in the current study and by Schmitt and Darwin (1995) and/or Miller and Darwin (2000).

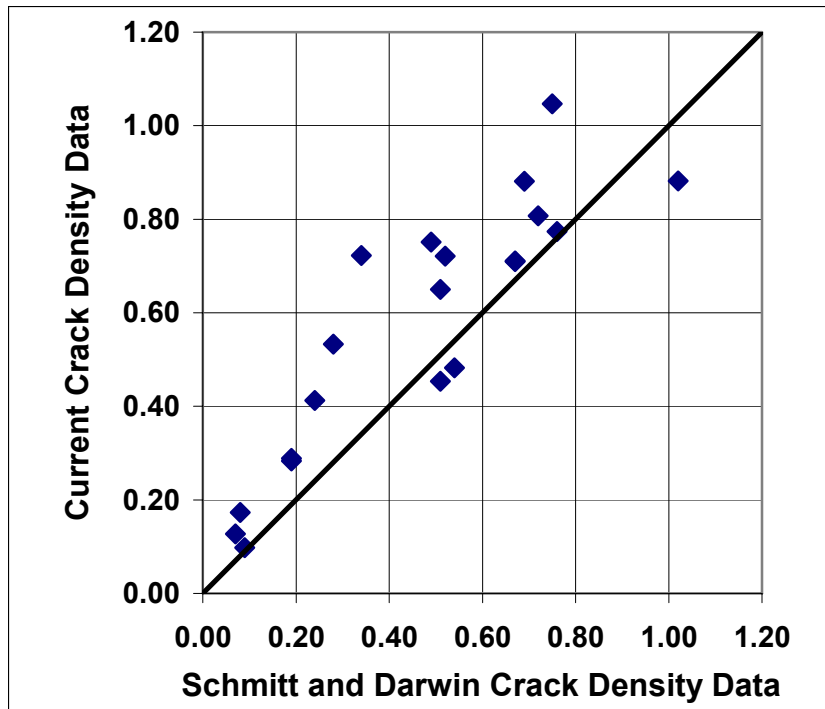


Fig. 4.4 – Correlation of crack density of entire bridge decks for bridges evaluated in the current study and by Schmitt and Darwin (1995).

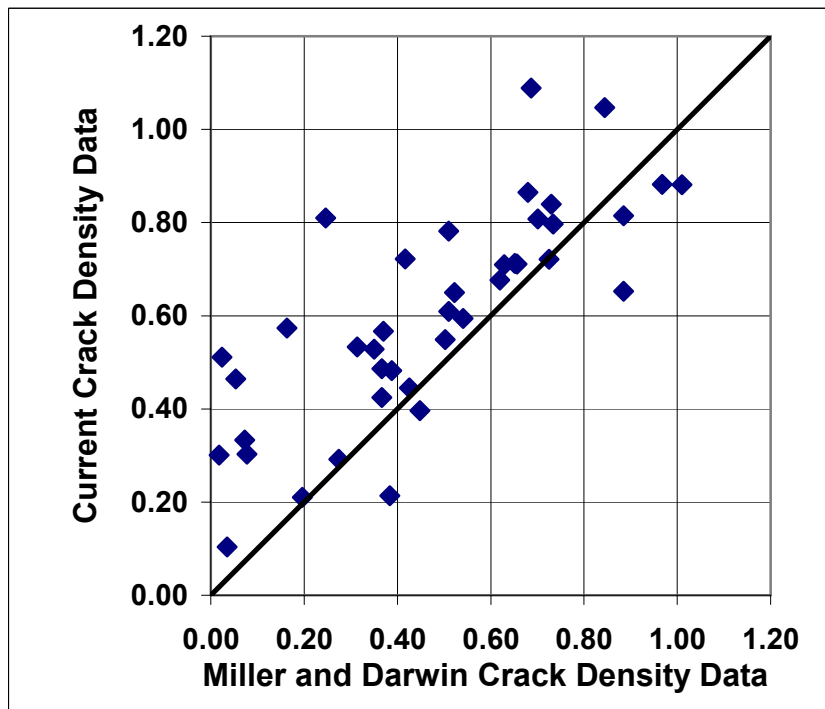


Fig. 4.5 – Correlation of crack density of entire bridge decks for bridges evaluated in the current study and by Miller and Darwin (2000).

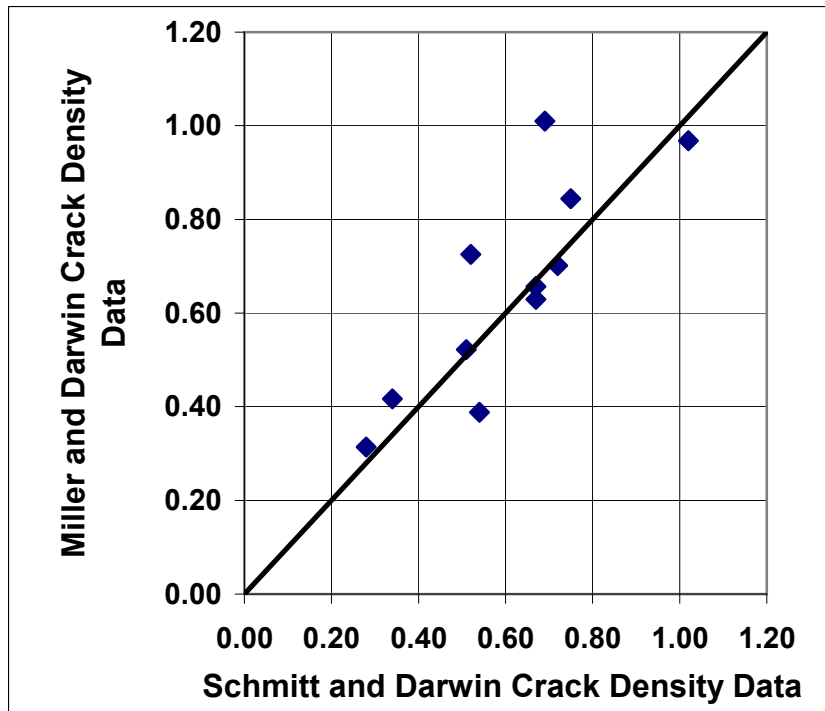


Fig. 4.6 – Correlation of crack density of entire bridge decks for bridges evaluated by Miller and Darwin (2000) and by Schmitt and Darwin (1995).

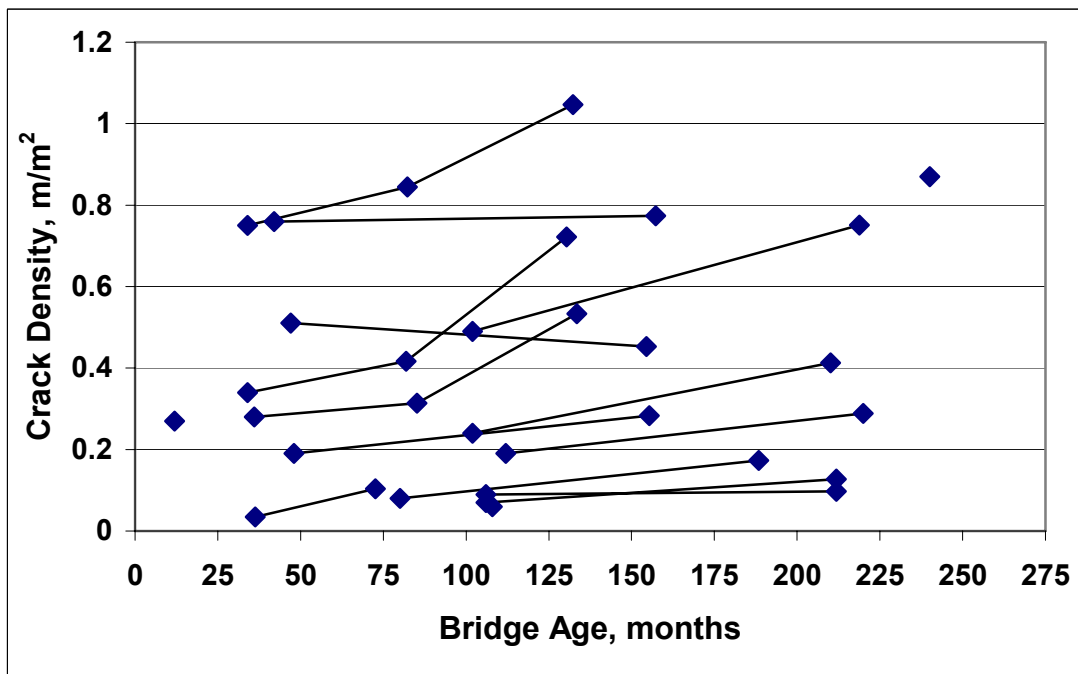


Fig. 4.7 – Crack density of entire bridge decks versus bridge age for all monolithic decks included in the analysis. Observations connected by lines indicate the same bridge surveyed multiple times.

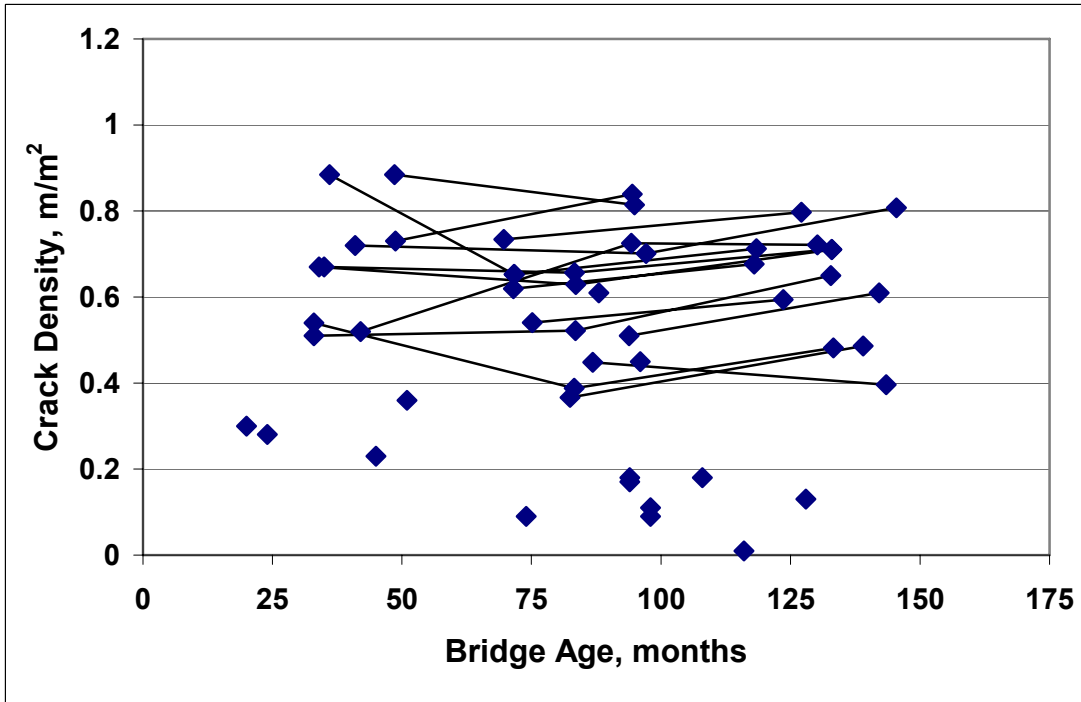


Fig. 4.8 – Crack density of entire bridge decks versus bridge age for all conventional overlays included in the analysis. Observations connected by lines indicate the same bridge surveyed multiple times.

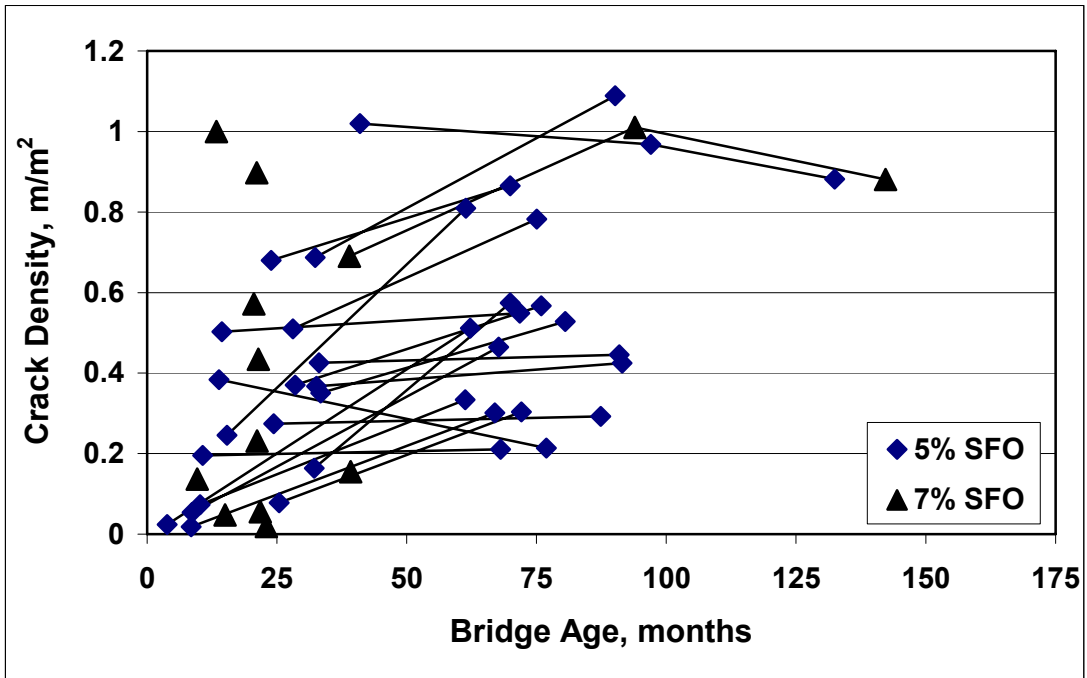


Fig. 4.9 – Crack density of entire bridge decks versus bridge age for all silica fume overlays included in the analysis. Observations connected by lines indicate the same bridge surveyed multiple times.

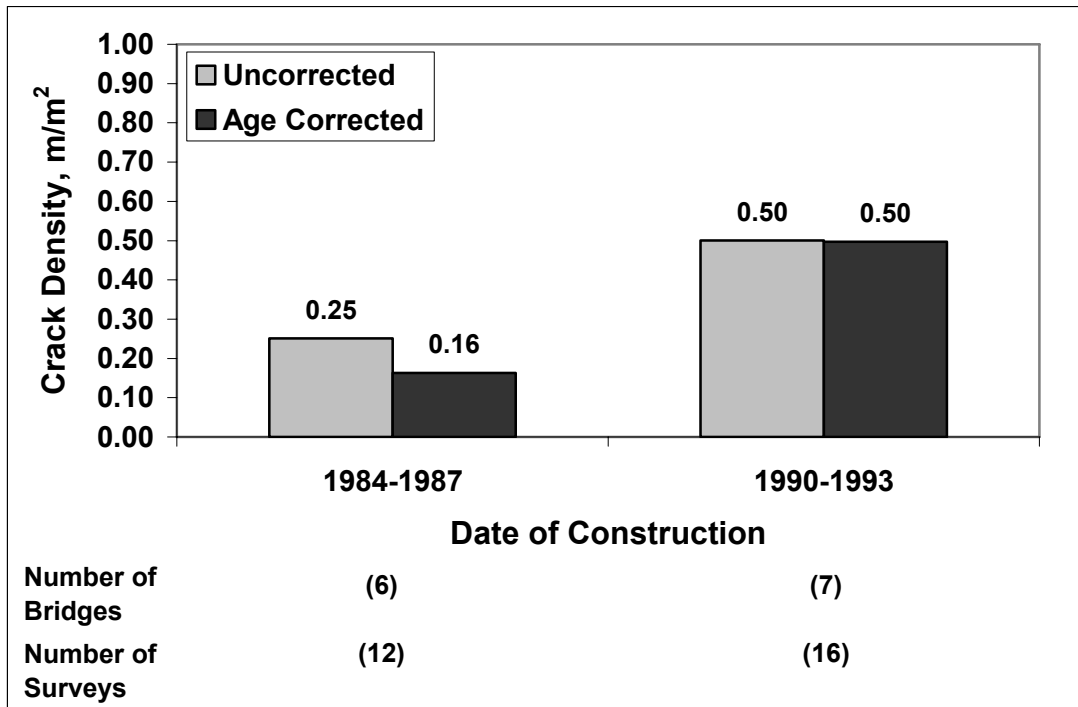


Fig. 4.10 – Mean crack density of entire bridge decks versus date of construction for all monolithic decks included in the analysis.

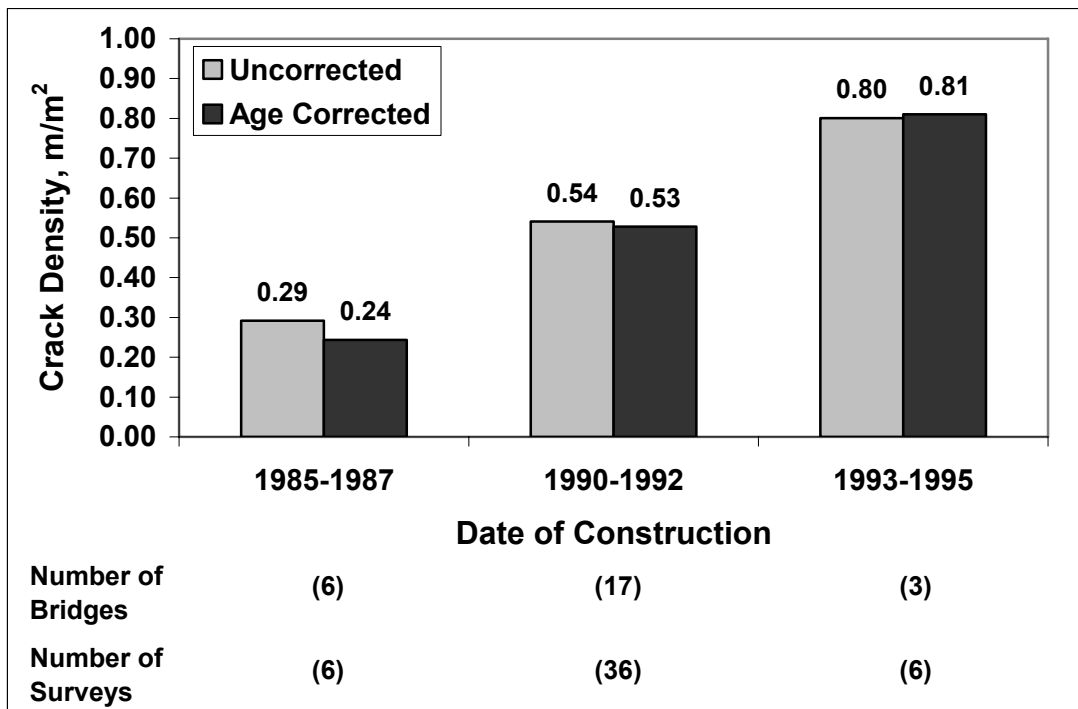


Fig. 4.11 – Mean crack density of entire bridge decks versus date of construction for all conventional overlays included in the analysis.

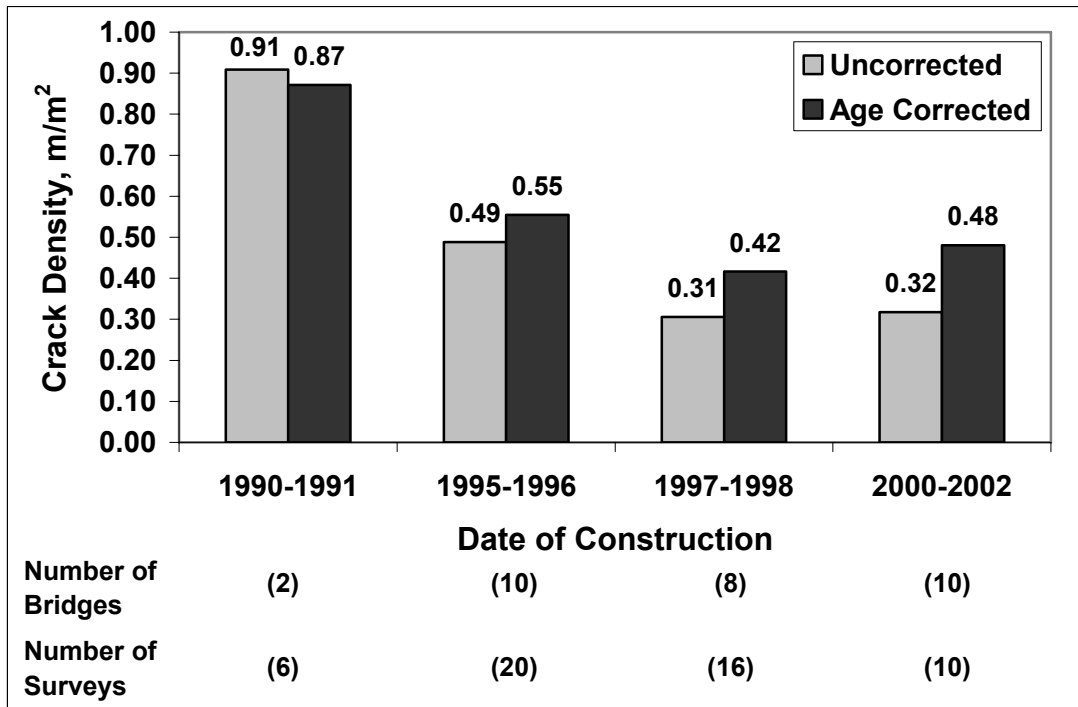


Fig. 4.12 – Mean crack density of entire bridge decks versus date of construction for all silica fume overlays included in the analysis.

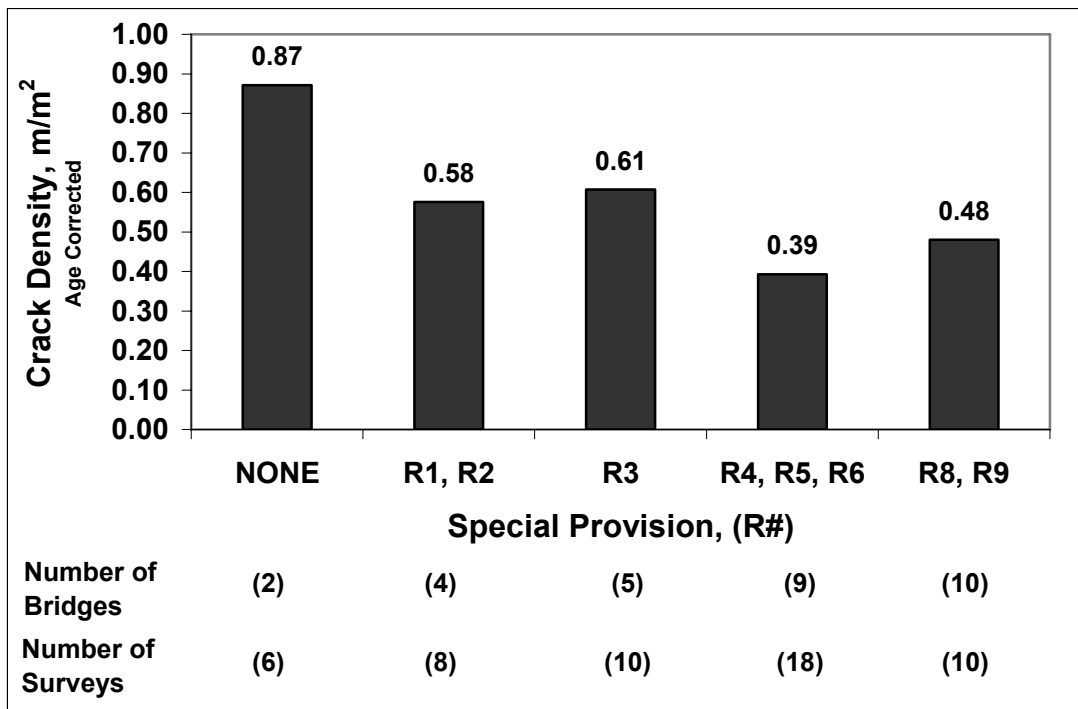


Fig. 4.13 – Mean crack density of entire bridge decks corrected to an age of 78 months versus special provision revision number for silica fume overlay bridge decks.

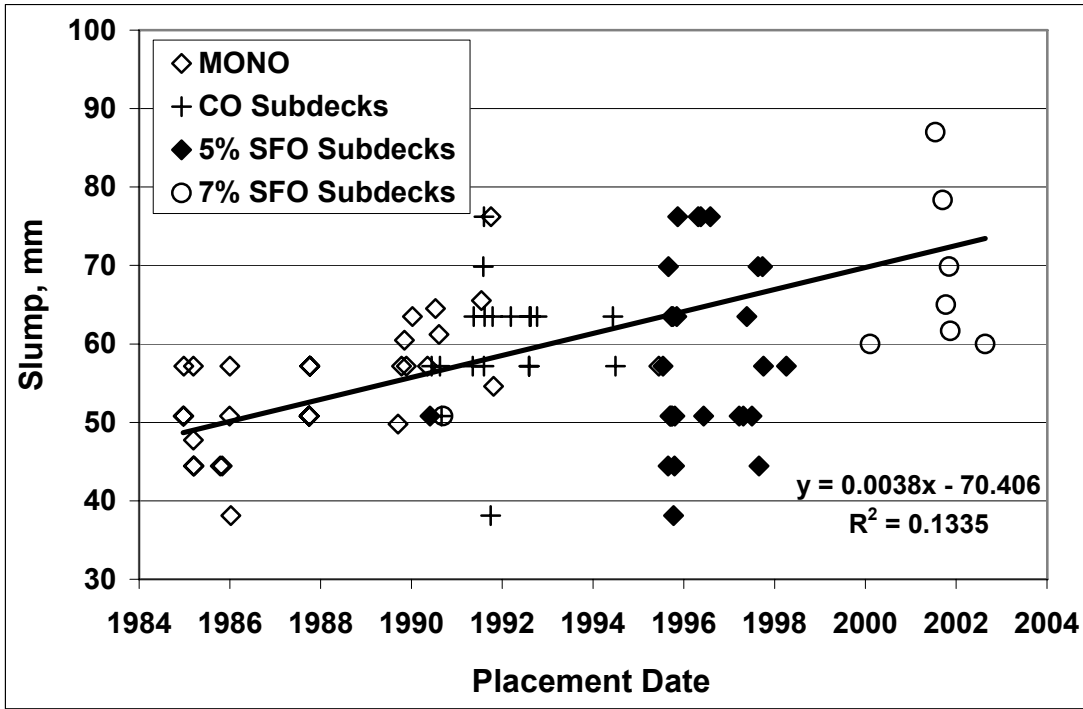


Fig 4.14 – Average concrete slump versus placement date for monolithic decks and overlay subdecks.

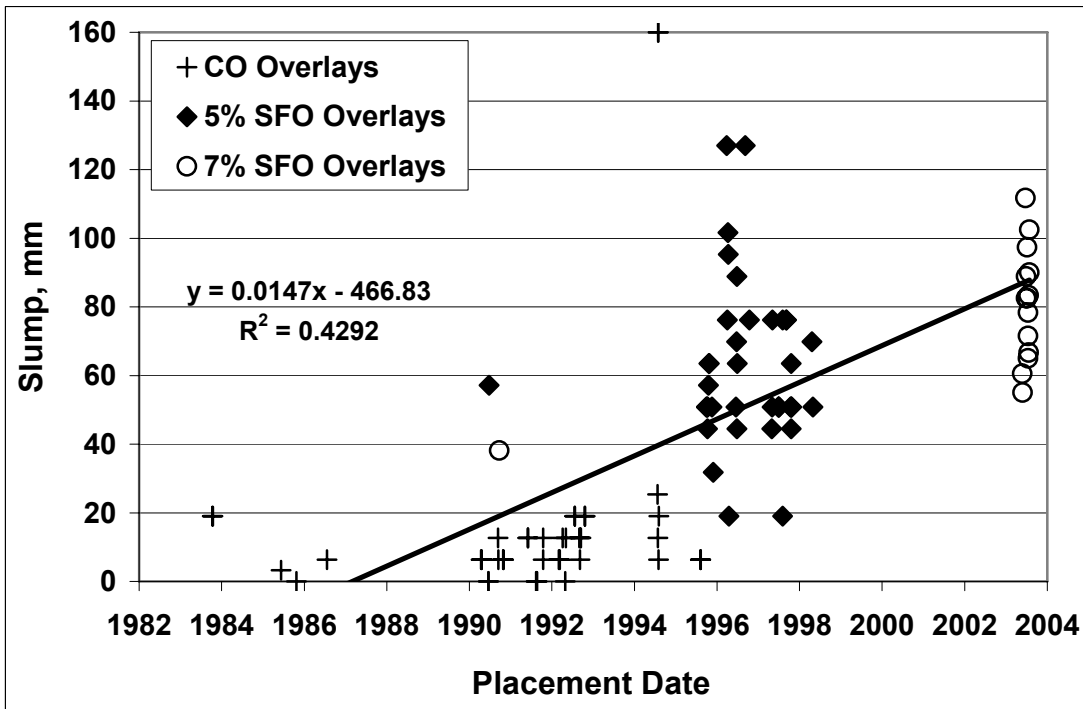


Fig 4.15 – Average concrete slump versus placement date for overlay placements.

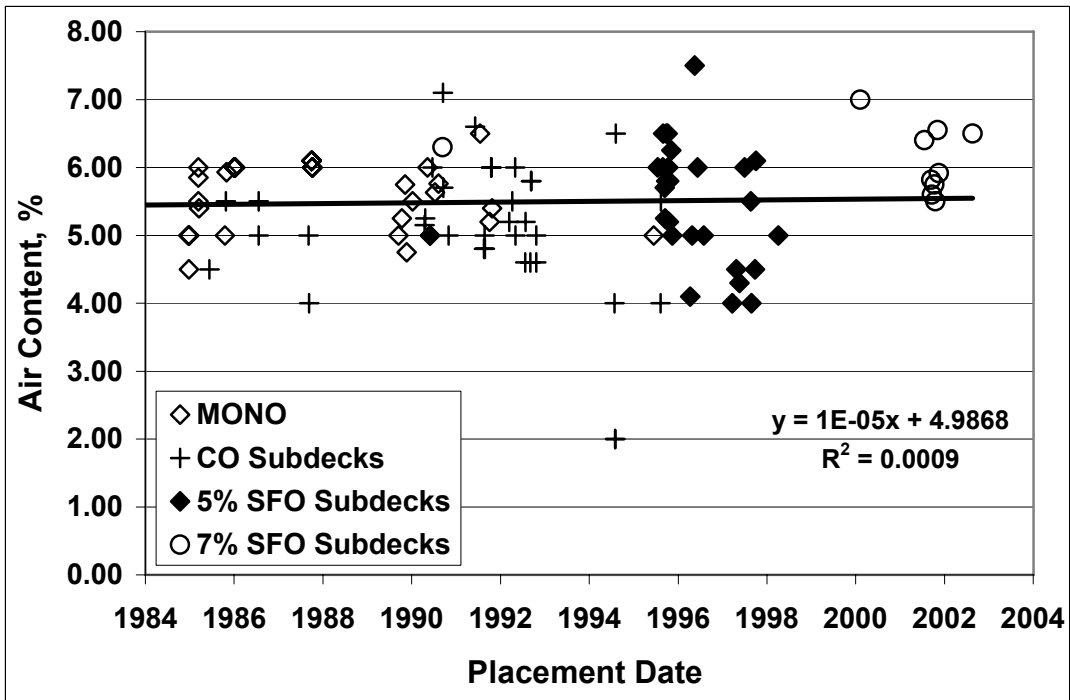


Fig 4.16 – Average air content versus placement date for monolithic decks and overlay subdecks.

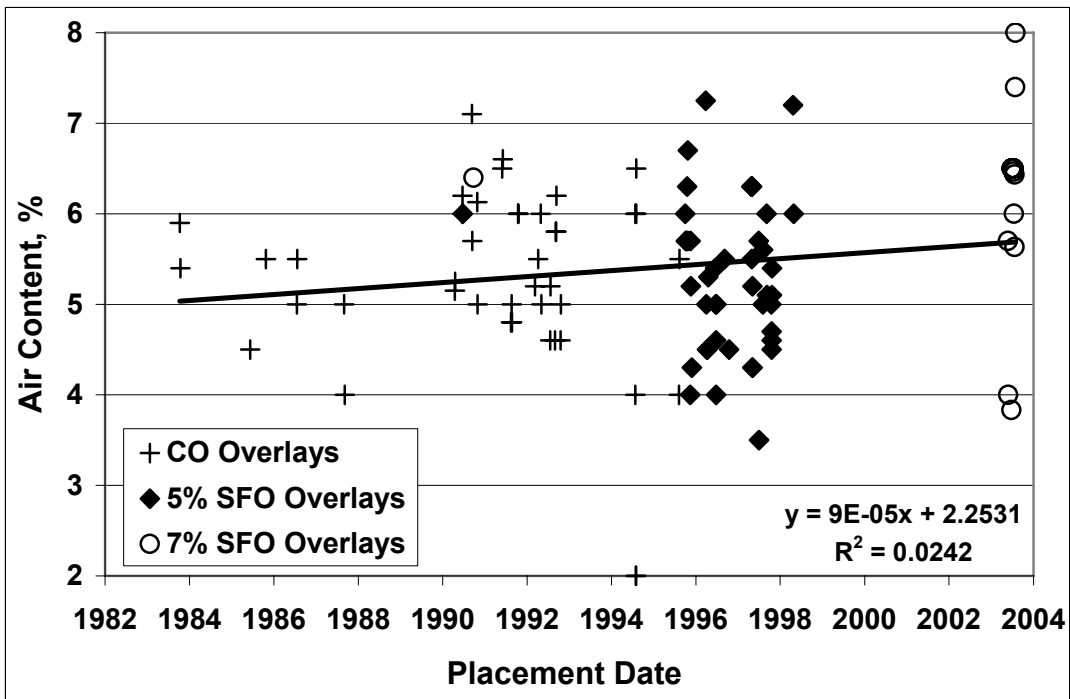


Fig 4.17 – Average concrete air content versus placement date for overlay placements.

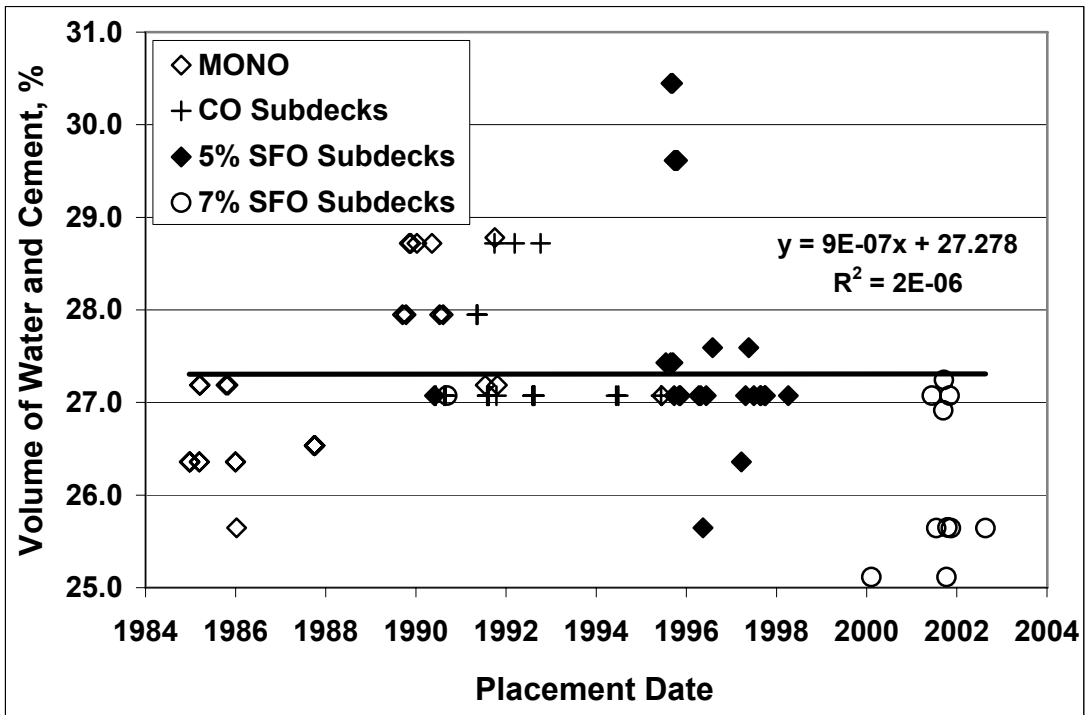


Fig 4.18 – Percent volume of water and cement versus placement date for monolithic decks and overlay subdecks.

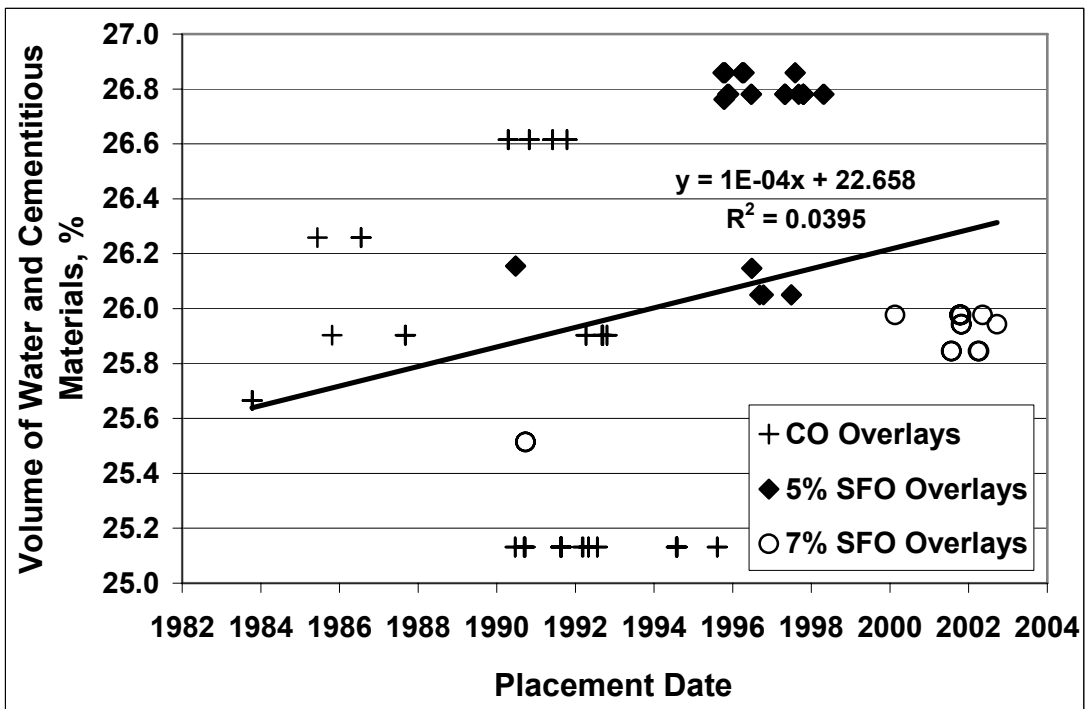


Fig 4.19 – Percent volume of water and cementitious materials versus placement date for overlay placements.

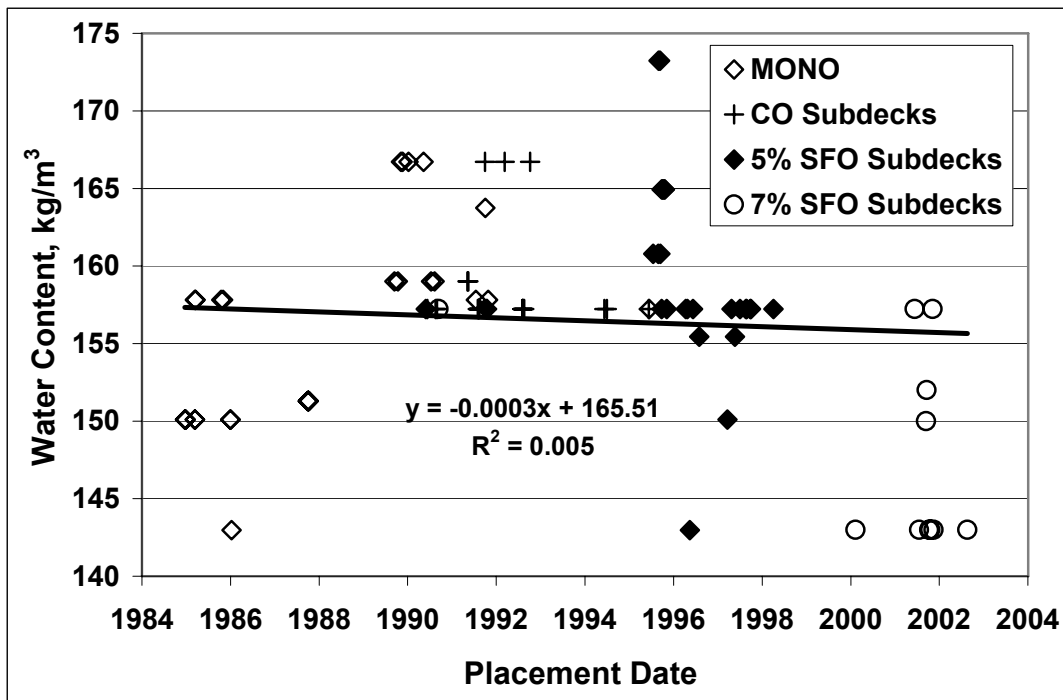


Fig 4.20 – Water content versus placement date for monolithic decks and overlay subdecks.

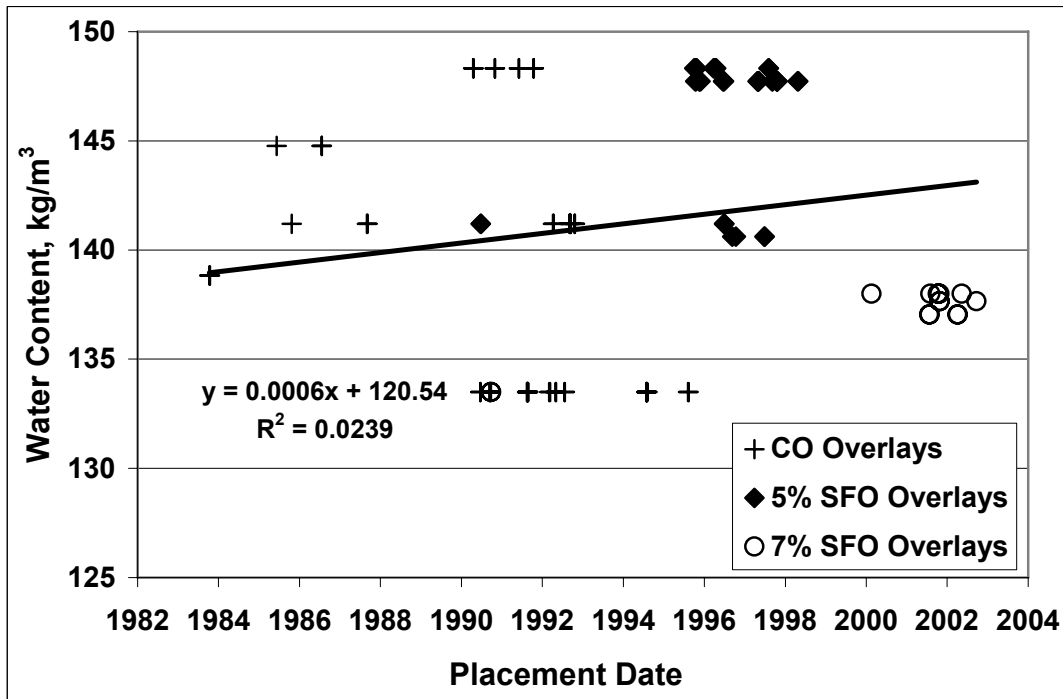


Fig 4.21 – Water content versus placement date for overlay placements.

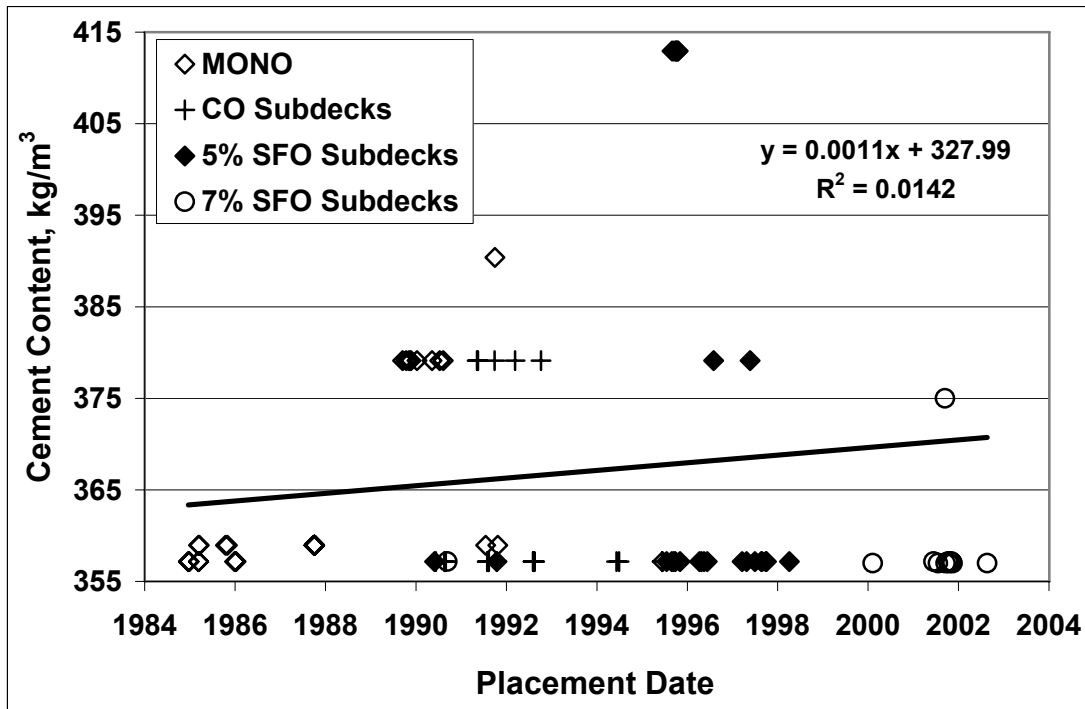


Fig 4.22 – Cement content versus placement date for monolithic decks and overlay subdecks.

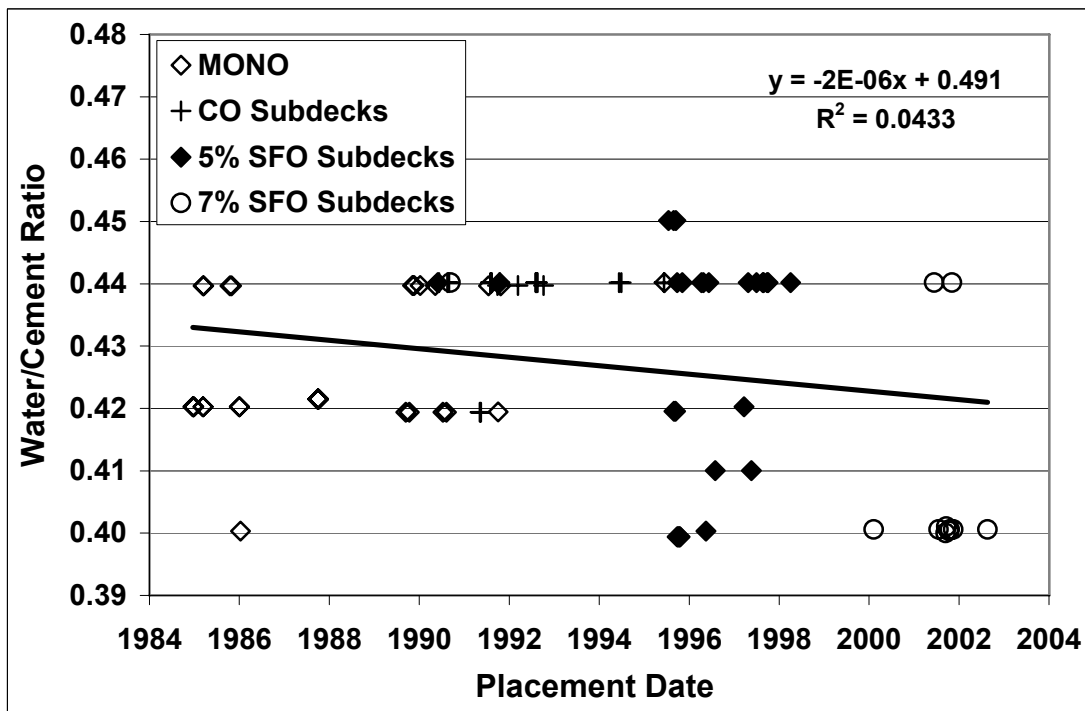


Fig 4.23 – Water/cement ratio versus placement date for monolithic decks and overlay subdecks.

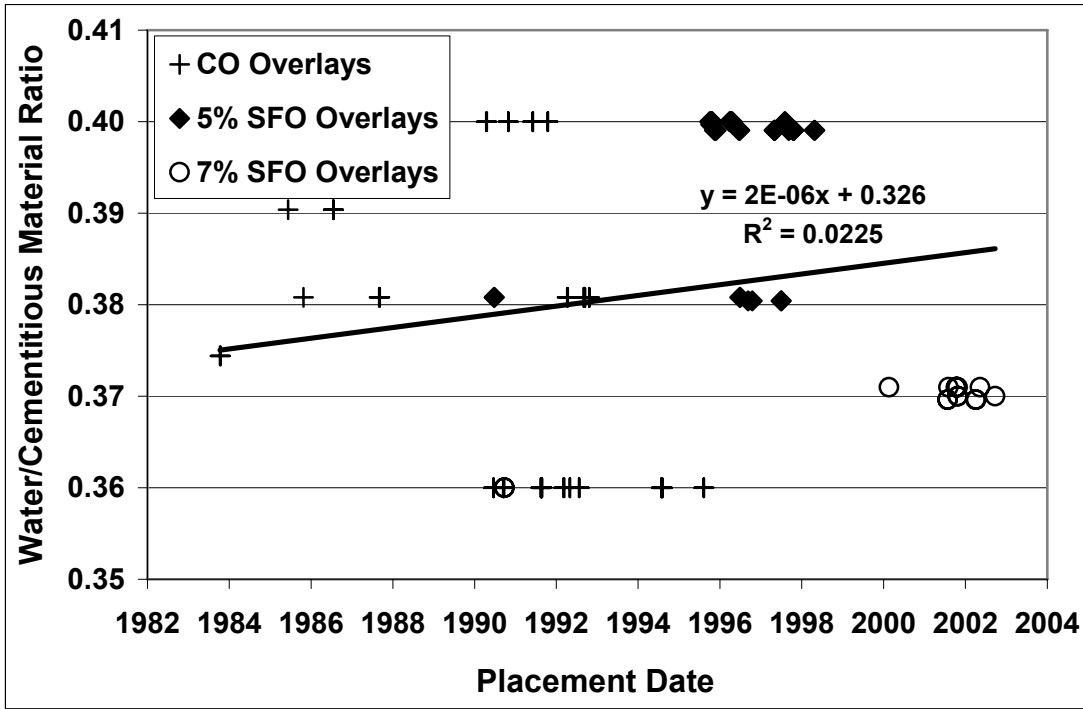


Fig 4.24 – Water/cementitious material ratio versus placement date for overlay placements.

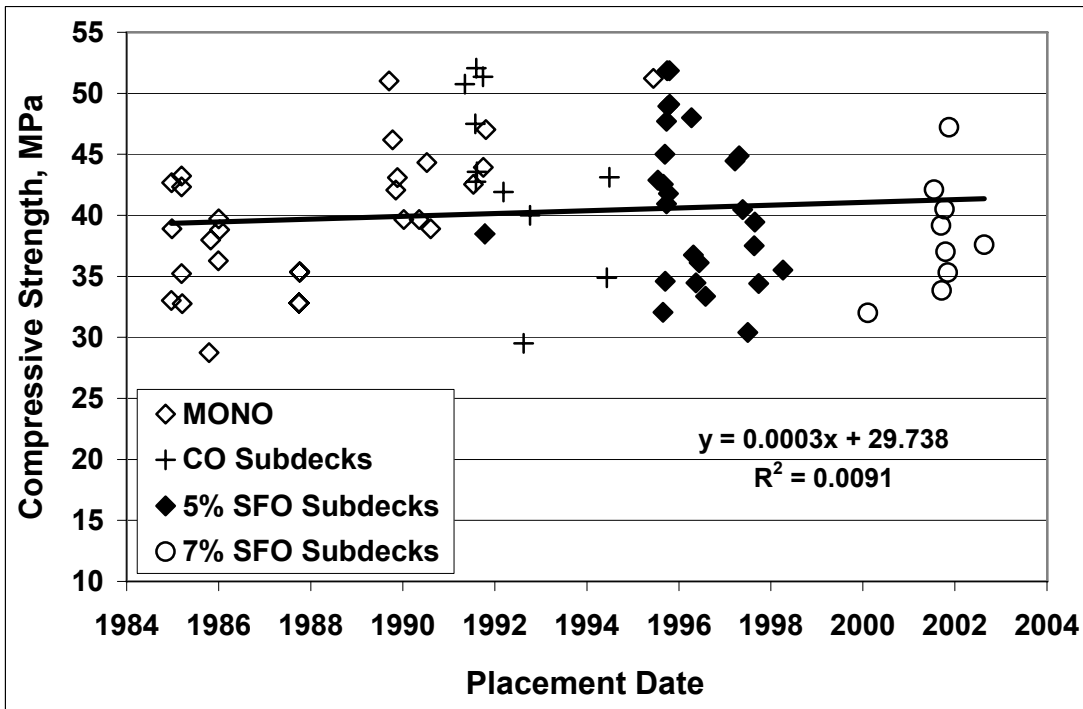


Fig 4.25 – Average concrete compressive strength versus placement date for monolithic decks and overlay subdecks.

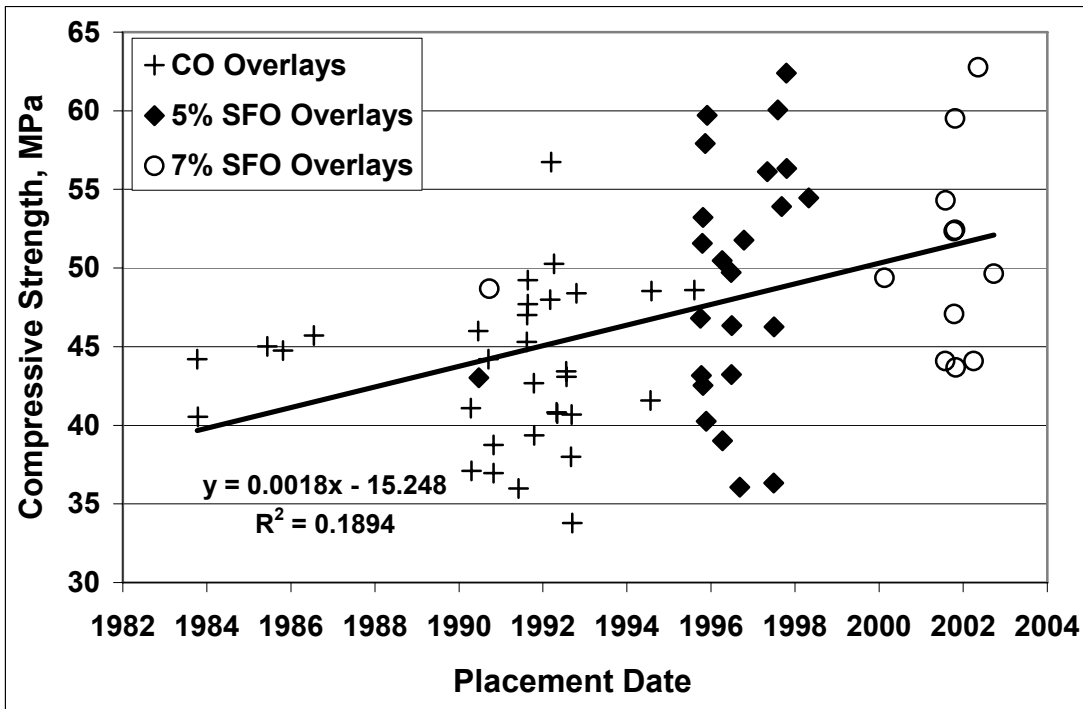


Fig 4.26 – Average concrete compressive strength versus placement date for overlay placements.

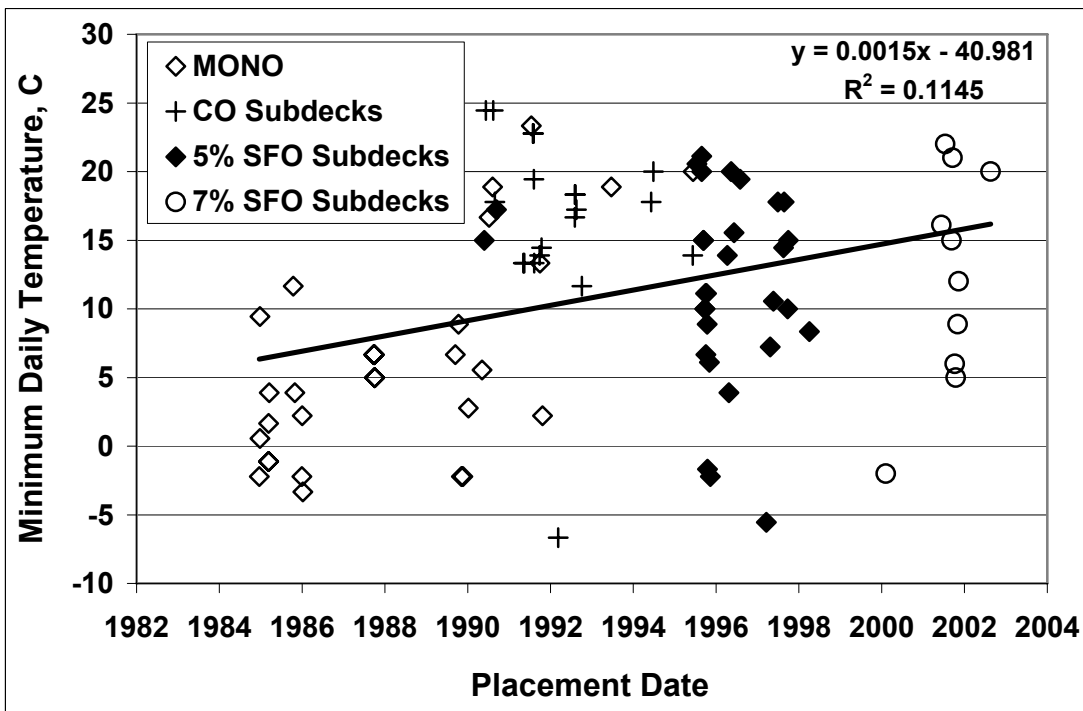


Fig 4.27 – Minimum daily temperature versus placement date for monolithic deck and overlay subdecks.

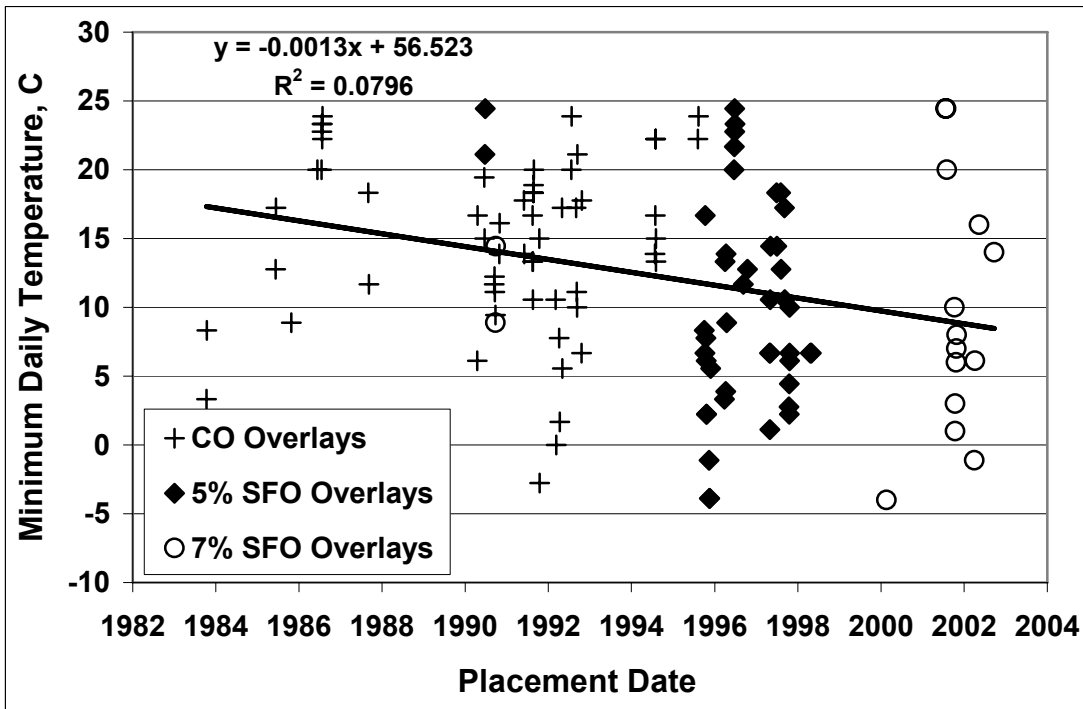


Fig 4.28 – Minimum daily temperature versus placement date for overlay placements.

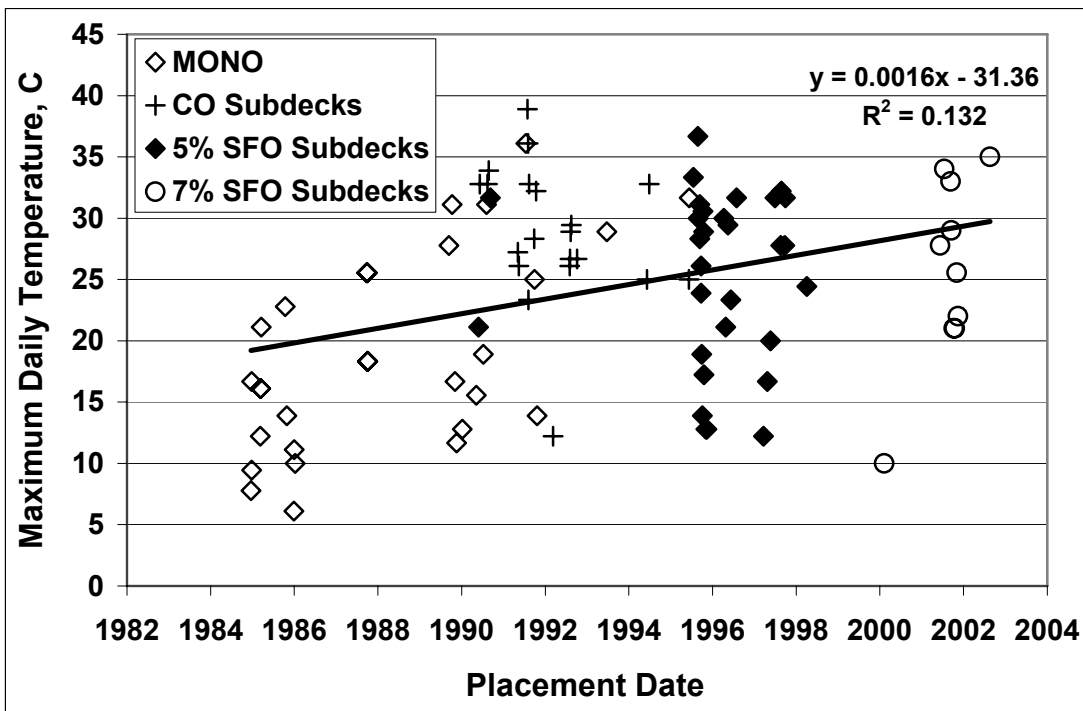


Fig 4.29 – Maximum daily temperature versus placement date for monolithic deck and overlay subdecks.

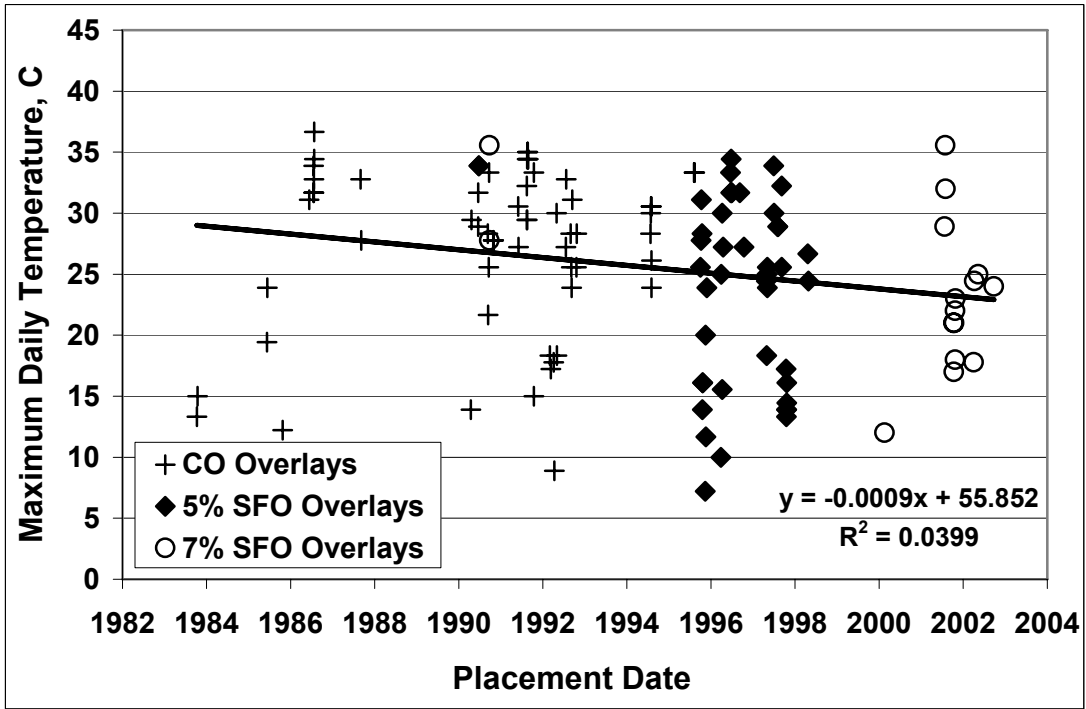


Fig 4.30 – Maximum daily temperature versus placement date for overlay placements.

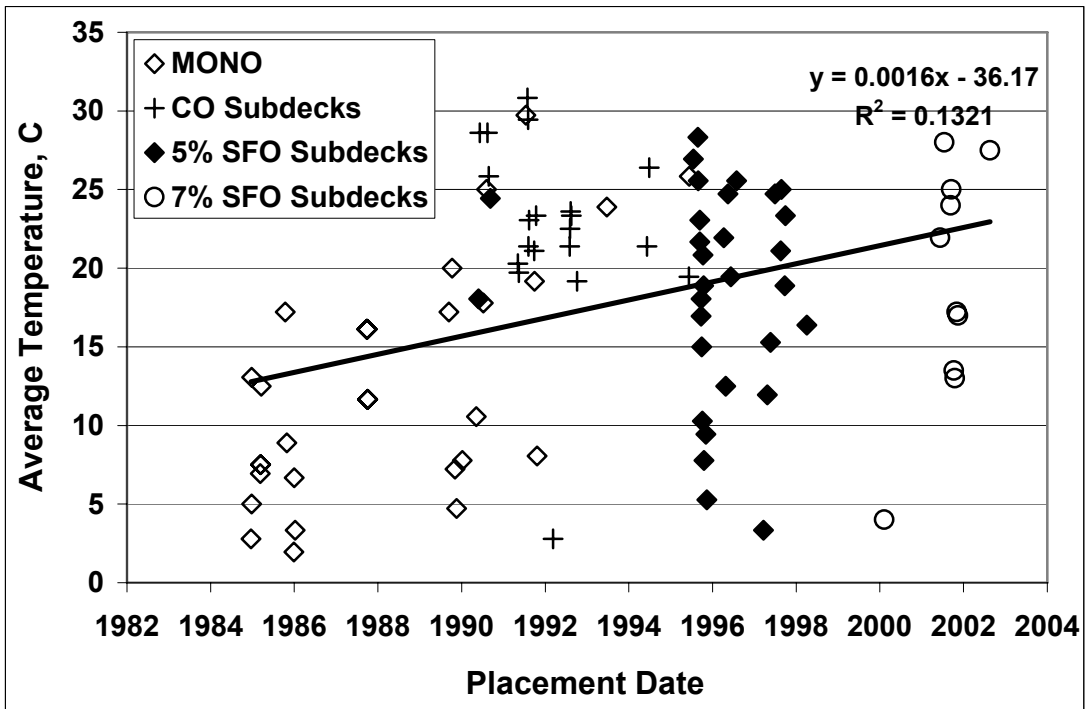


Fig 4.31 – Average temperature versus placement date for monolithic deck and overlay subdecks.

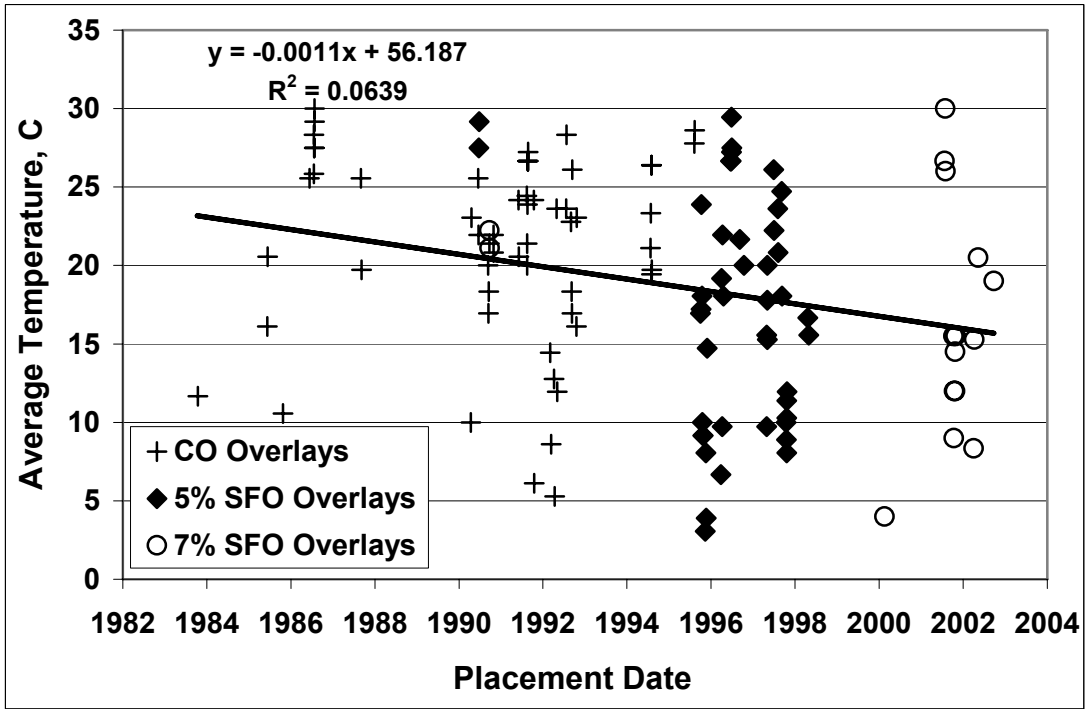


Fig 4.32 – Average temperature versus placement date for overlay placements.

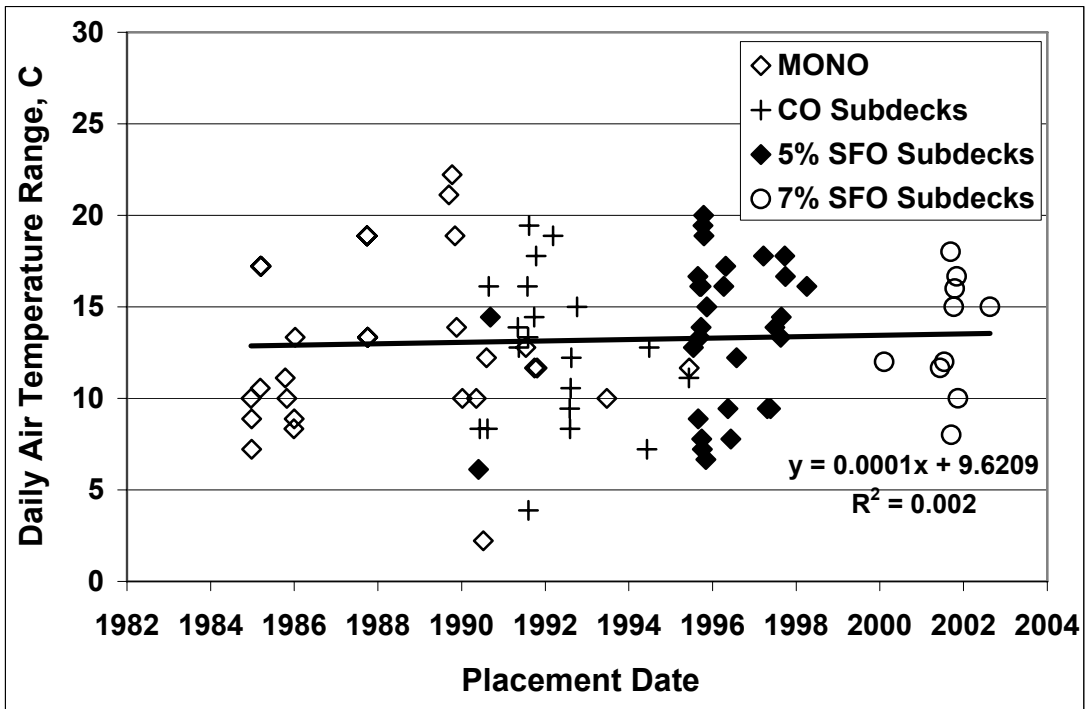


Fig 4.33 – Daily air temperature range versus placement date for monolithic deck and overlay subdecks.

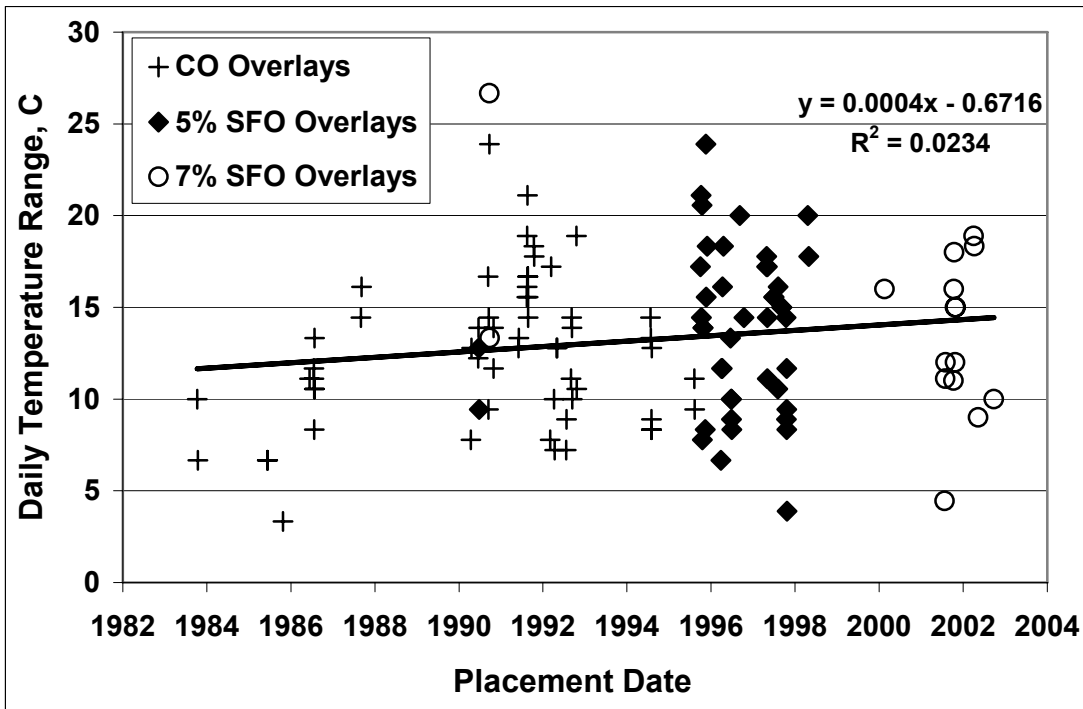


Fig 4.34 – Daily air temperature range versus placement date for overlay placements.

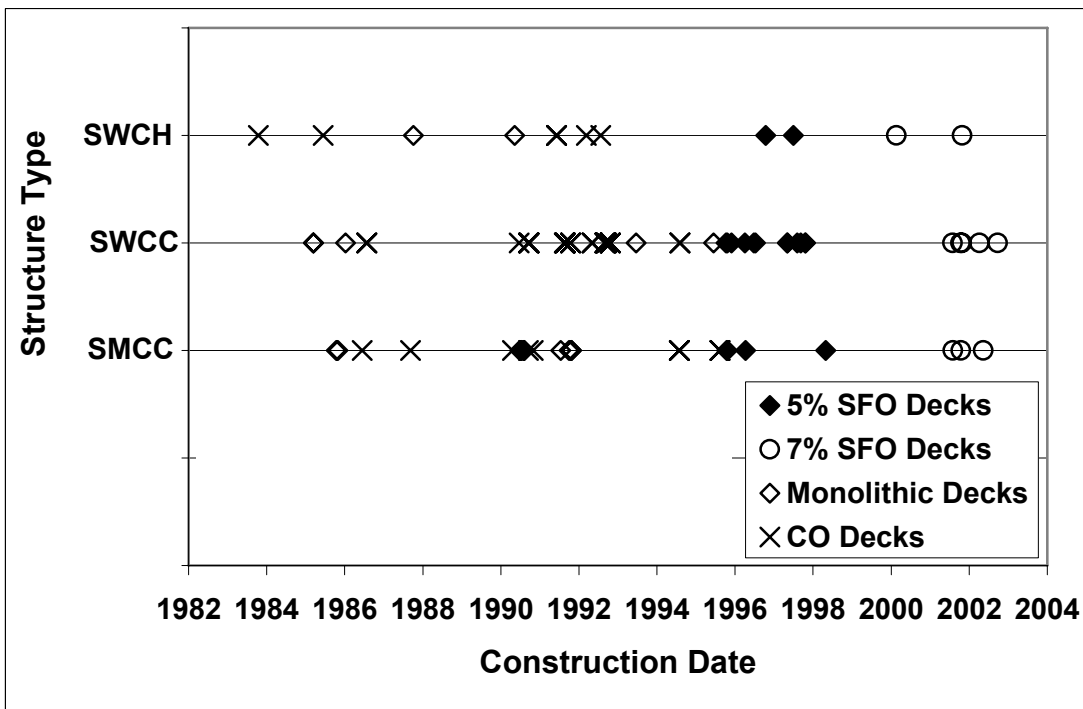


Fig 4.35 – Bridge deck superstructure type versus date of placement for all bridge deck types.



Fig 4.36 – Deck thickness versus the last day of concrete placement.

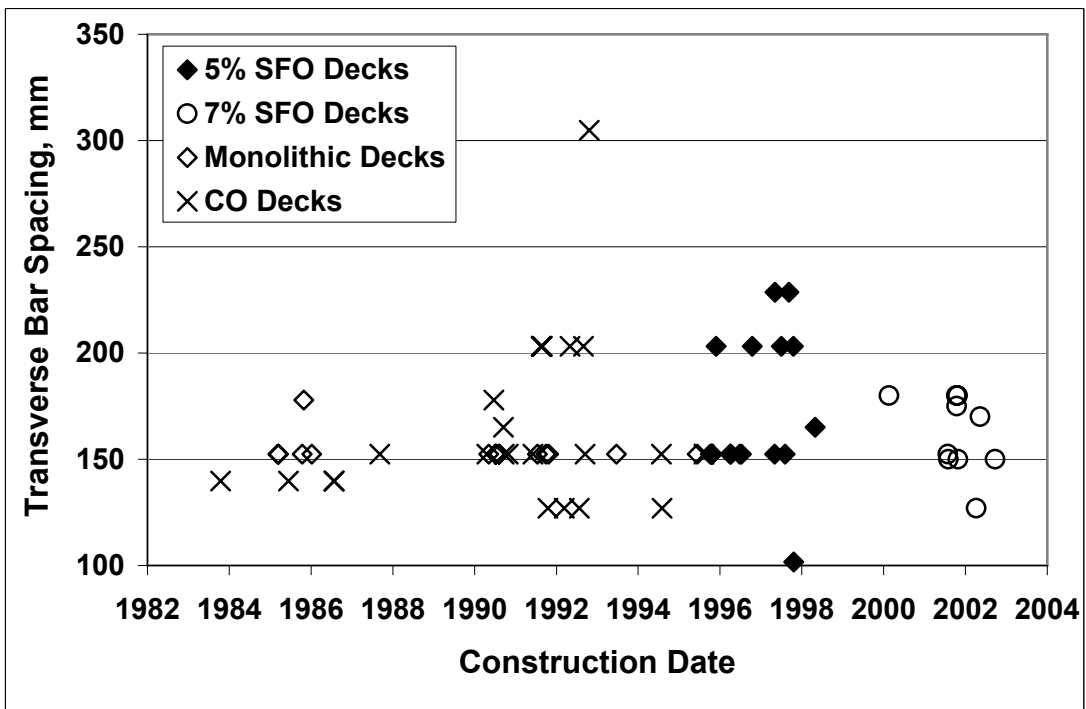


Fig 4.37 – Transverse bar spacing versus the last day of concrete placement.

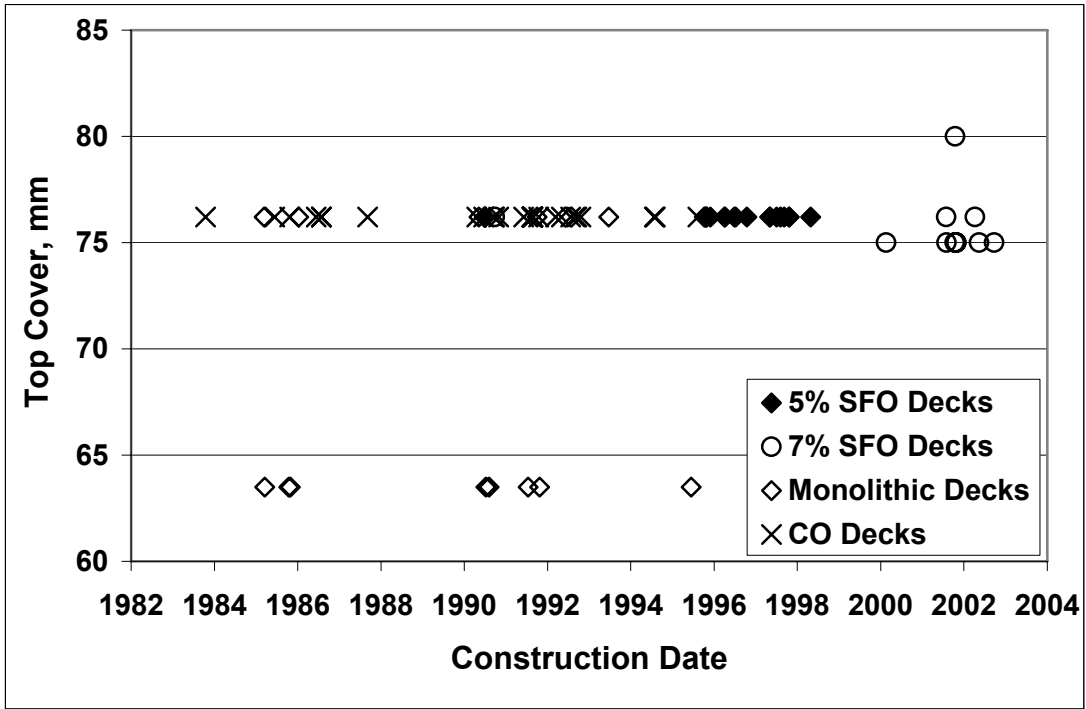


Fig 4.38 – Top cover versus the last day of concrete placement.

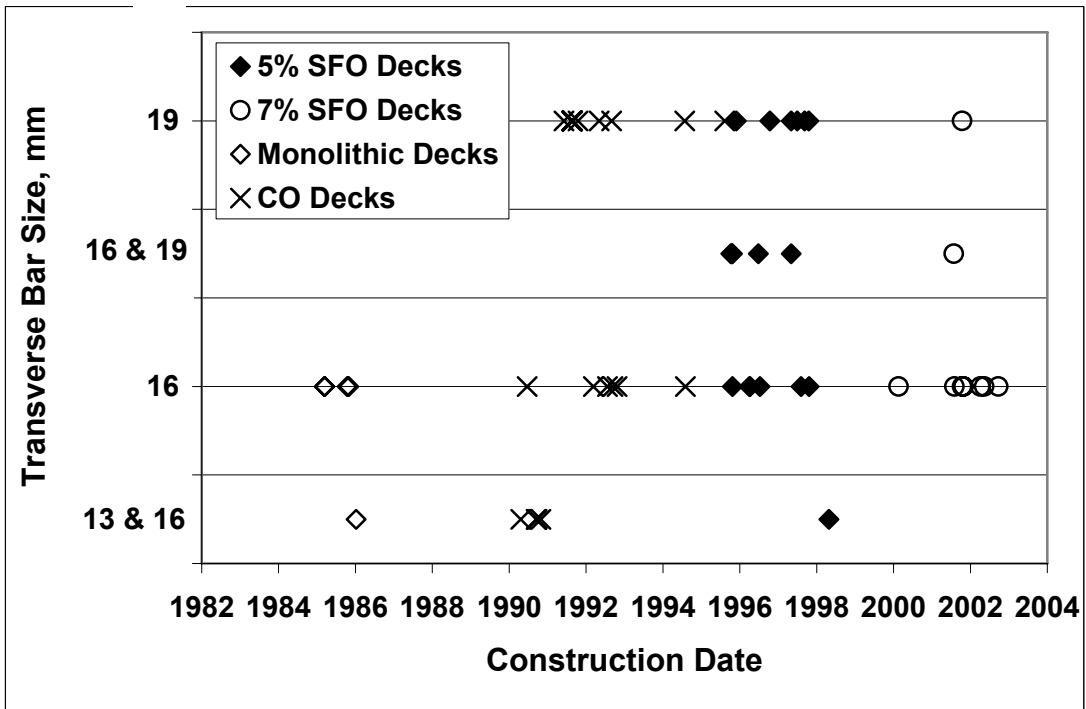


Fig 4.39 – Transverse bar spacing versus the last day of concrete placement.

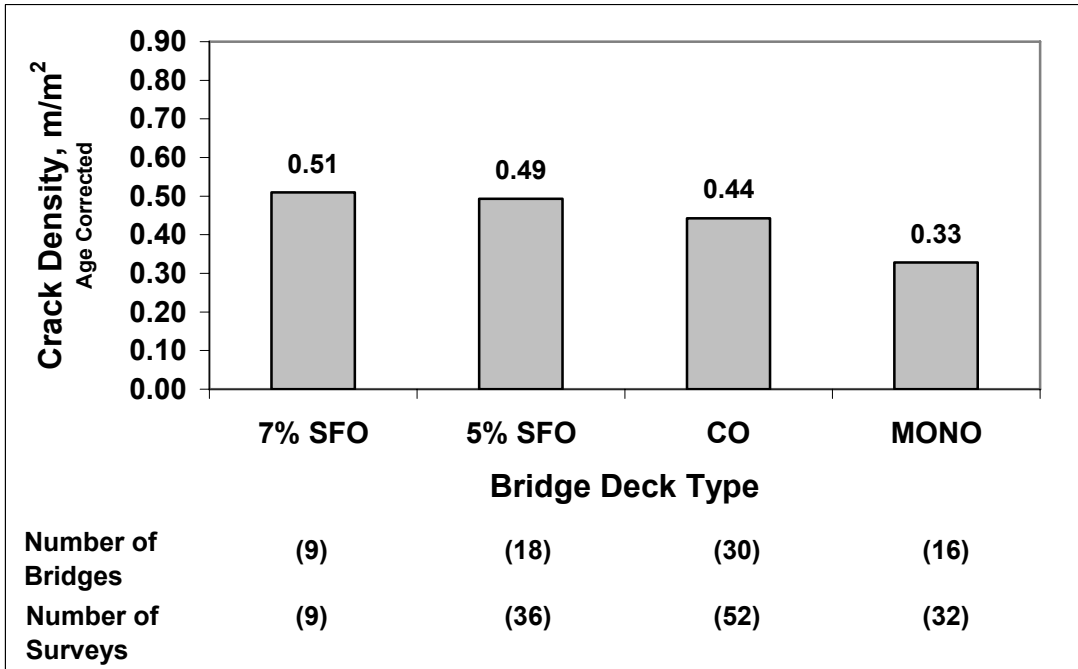


Fig. 5.1 – Mean crack density for individual placements corrected to an age of 78 months versus bridge deck type. Silica Fume Overlay (% SFO); Conventional Overlay (CO); Monolithic Bridge Decks (MONO)

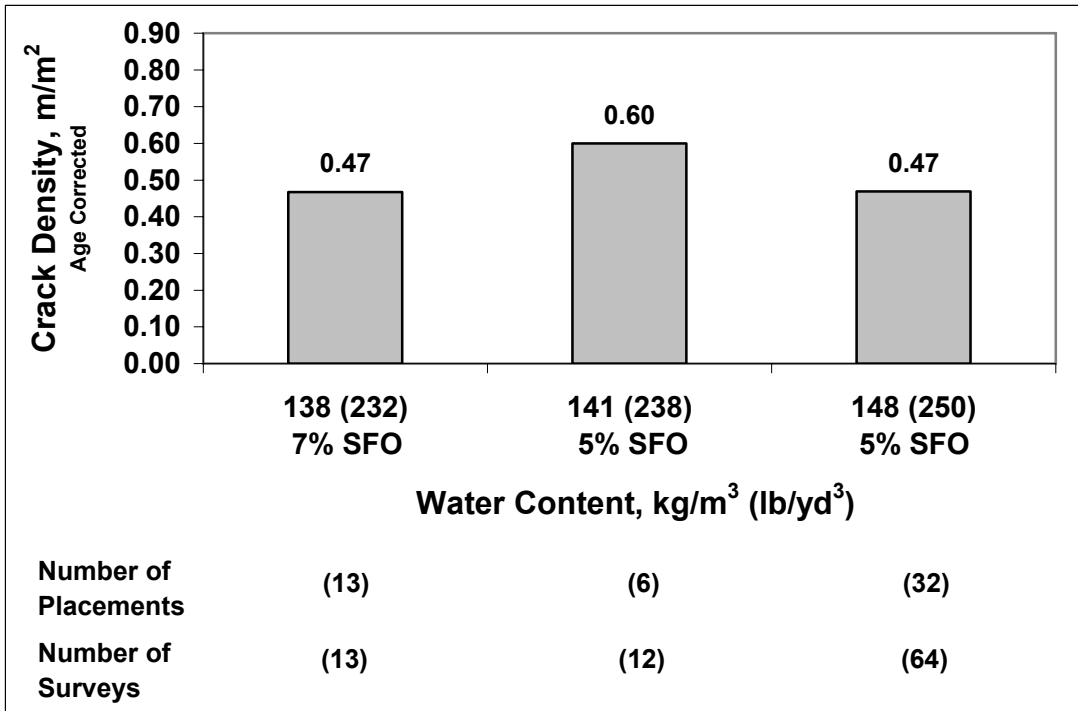


Fig. 5.2 – Mean crack density for individual placements corrected to an age of 78 months versus water content for 5% and 7% silica fume overlay placements.

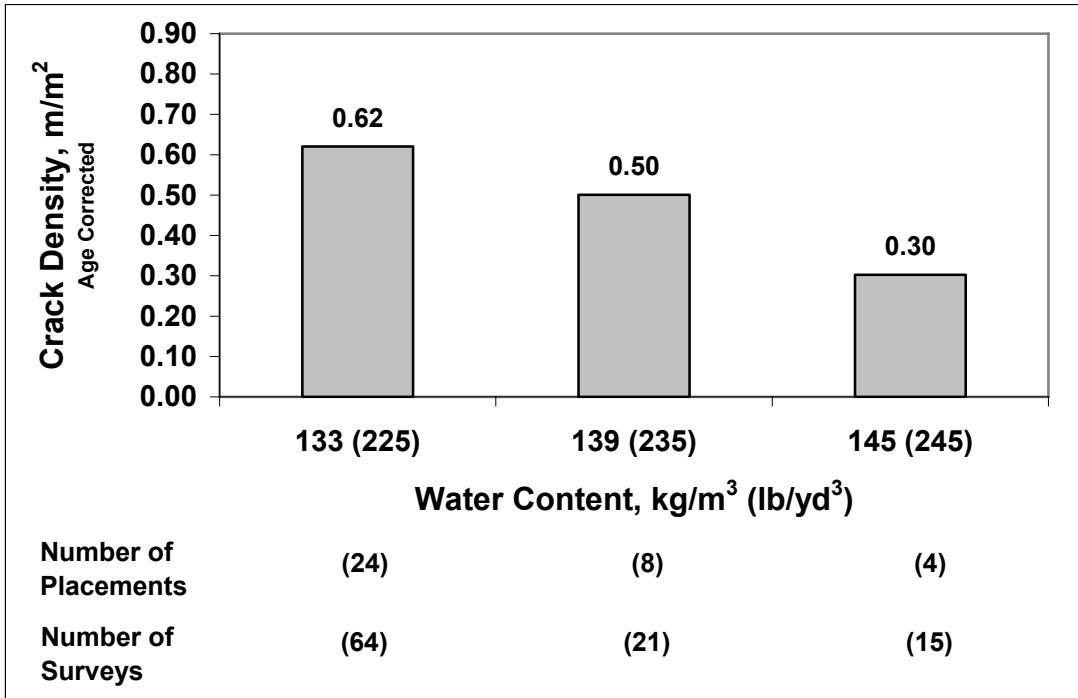


Fig. 5.3 – Mean crack density for individual placements corrected to an age of 78 months versus water content for conventional overlay placements.

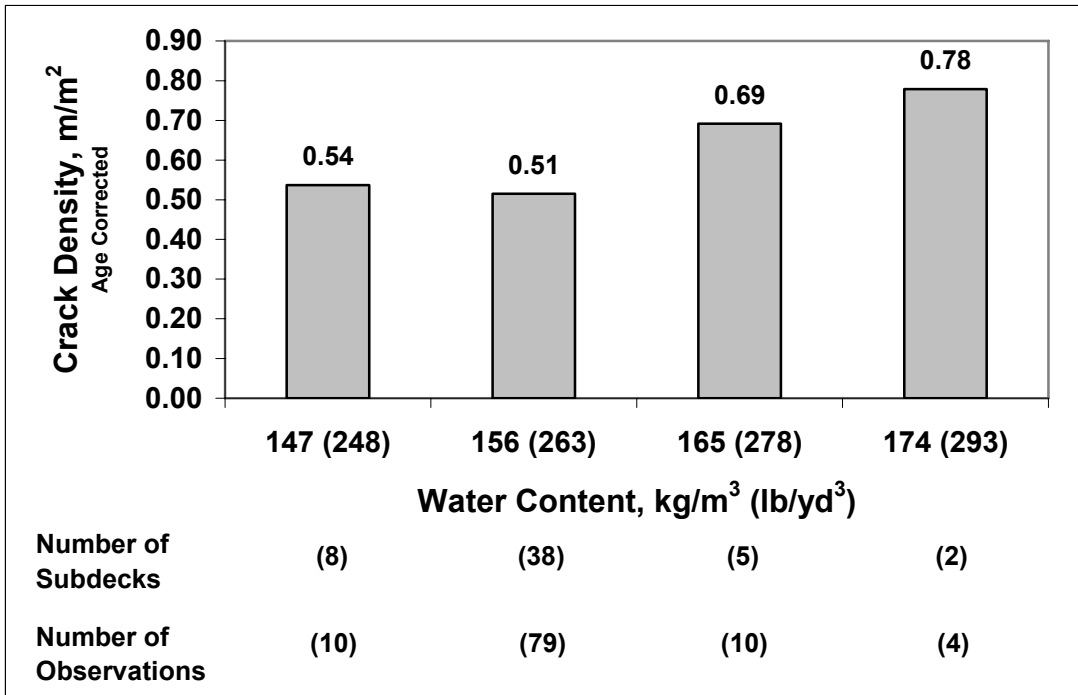


Fig. 5.4 – Mean crack density for individual bridge decks corrected to an age of 78 months versus water content for overlay subdeck placements.

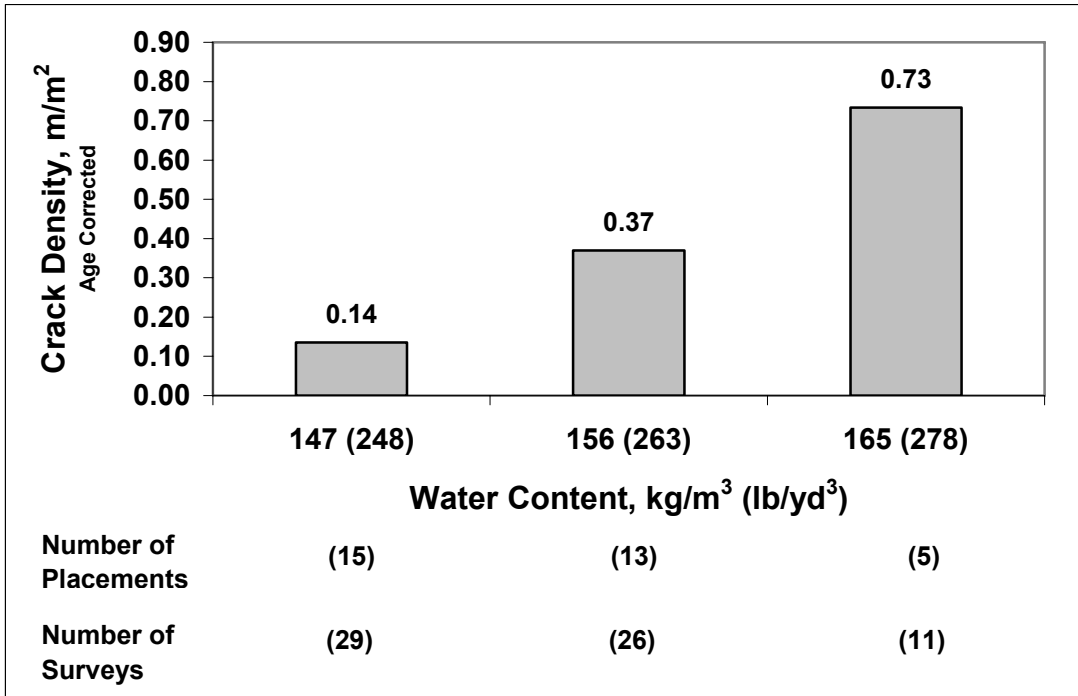


Fig. 5.5 – Mean crack density for individual placements corrected to an age of 78 months versus water content for monolithic placements.

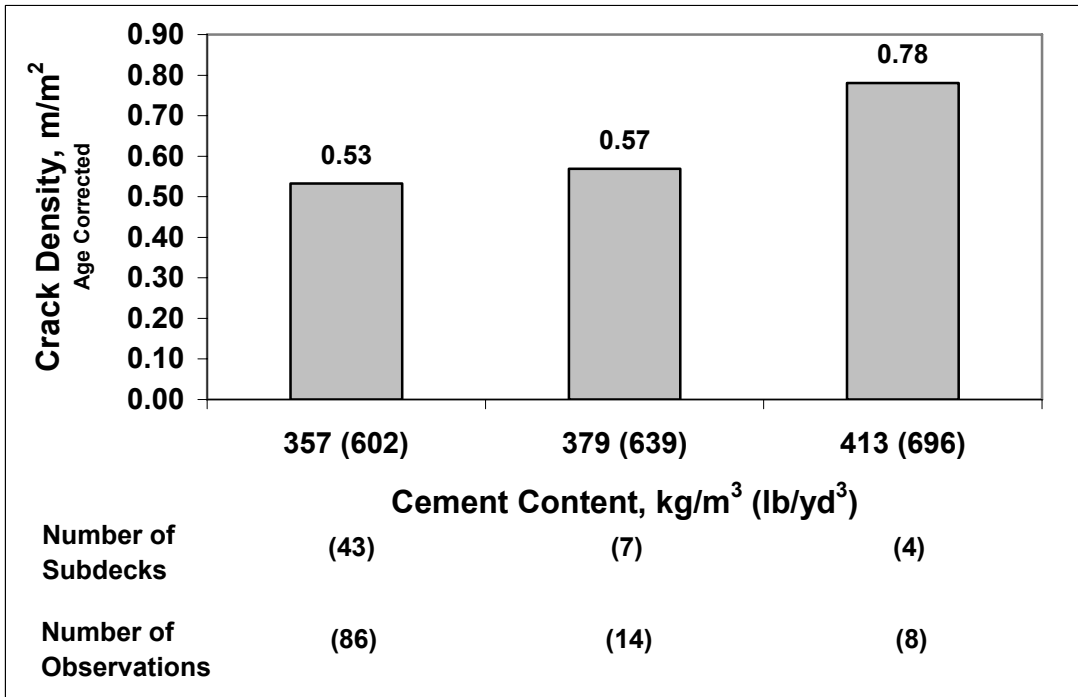


Figure 5.6 – Mean crack density for individual bridge decks corrected to an age of 78 months versus cement content for overlay subdeck placements.

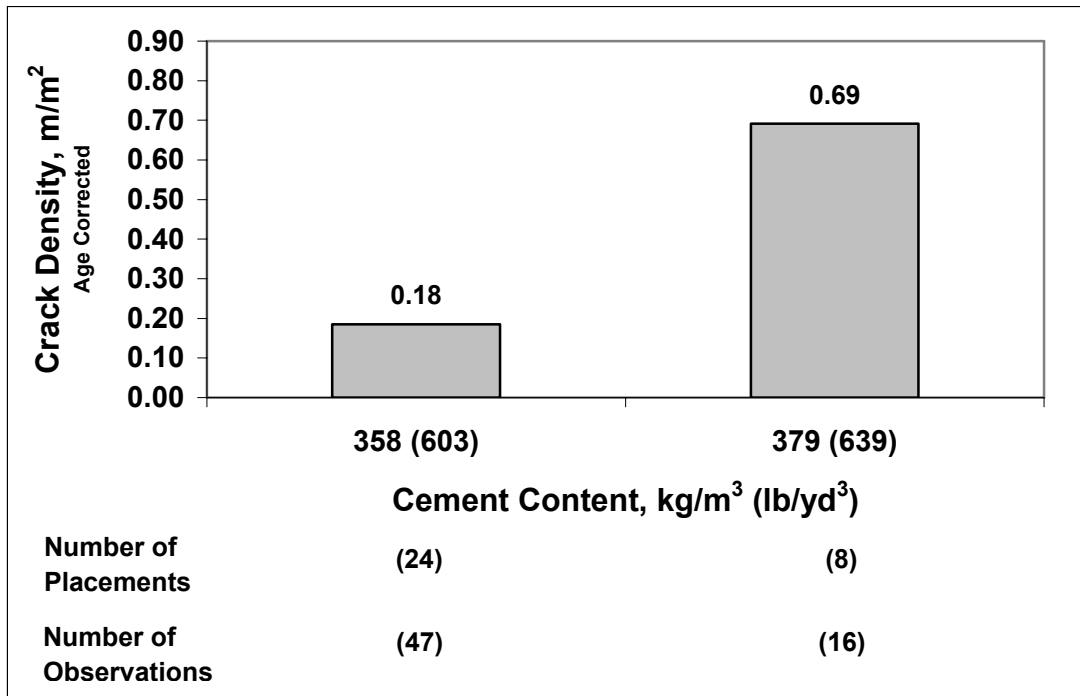


Figure 5.7 – Mean crack density for individual placements corrected to an age of 78 months versus cement content for monolithic placements.

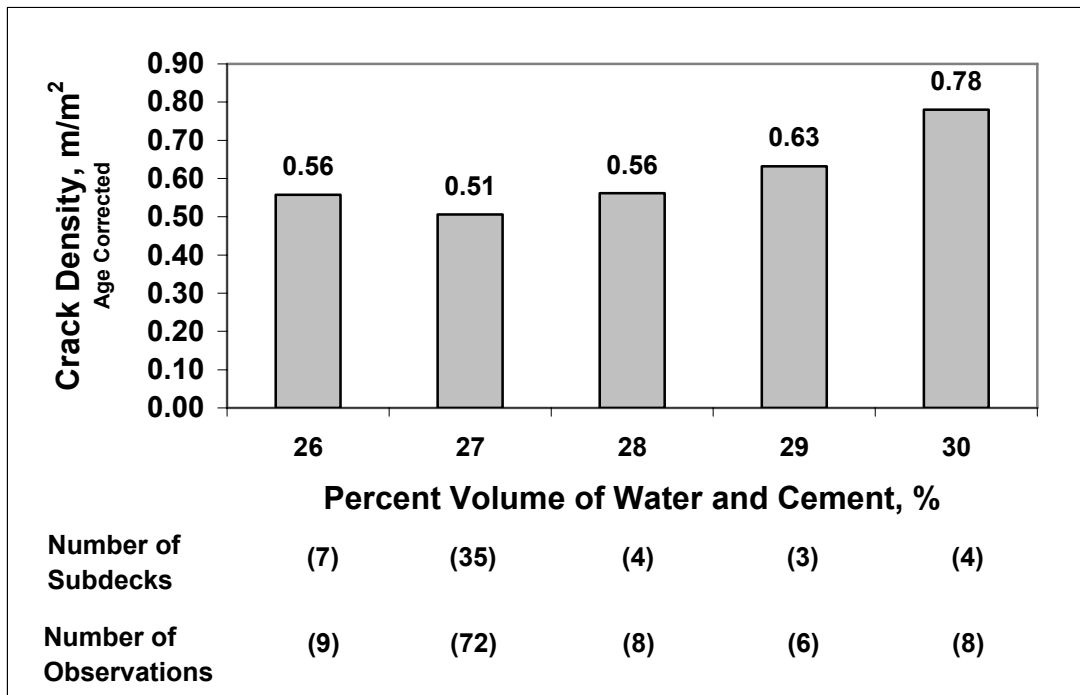


Fig. 5.8 – Mean crack density for individual bridge decks corrected to an age of 78 months versus percent volume of water and cement for overlay subdeck placements.

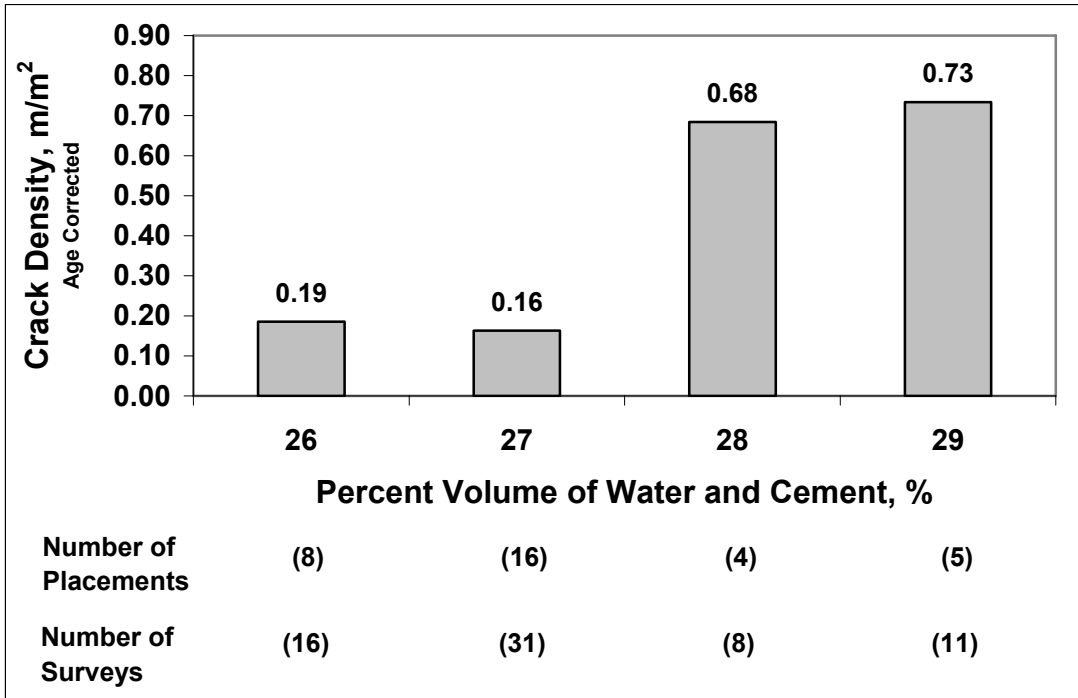


Fig. 5.9 – Mean crack density for individual placements corrected to an age of 78 months versus percent volume of water and cement for monolithic placements.

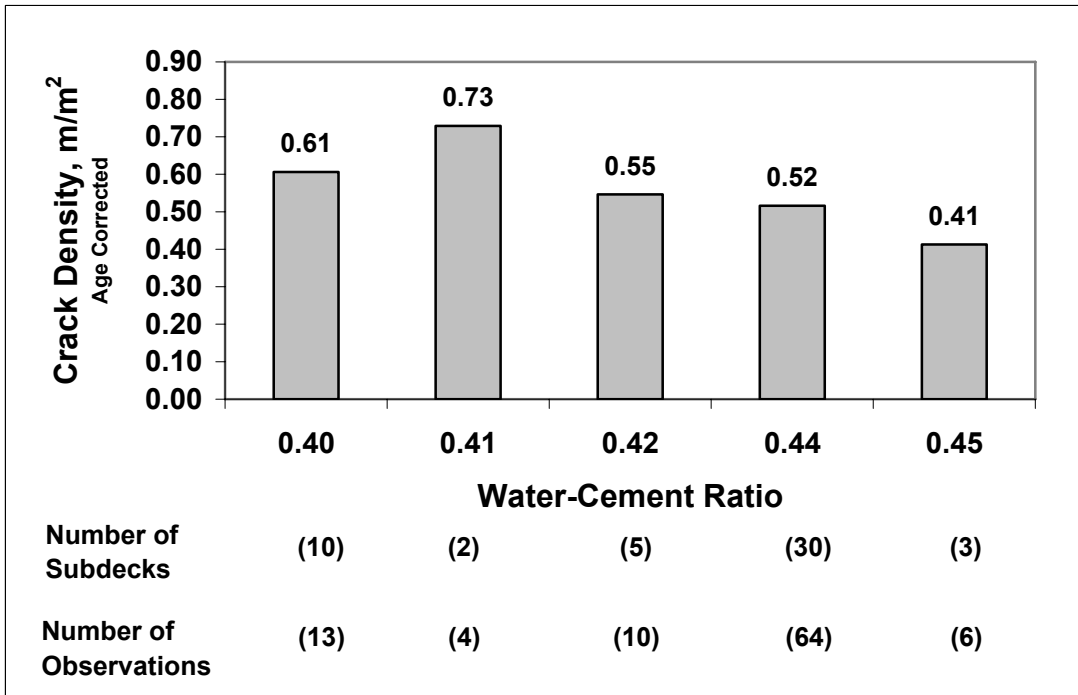


Fig. 5.10 – Mean crack density for individual placements corrected to an age of 78 months versus water-cement ratio for overlay subdeck placements.

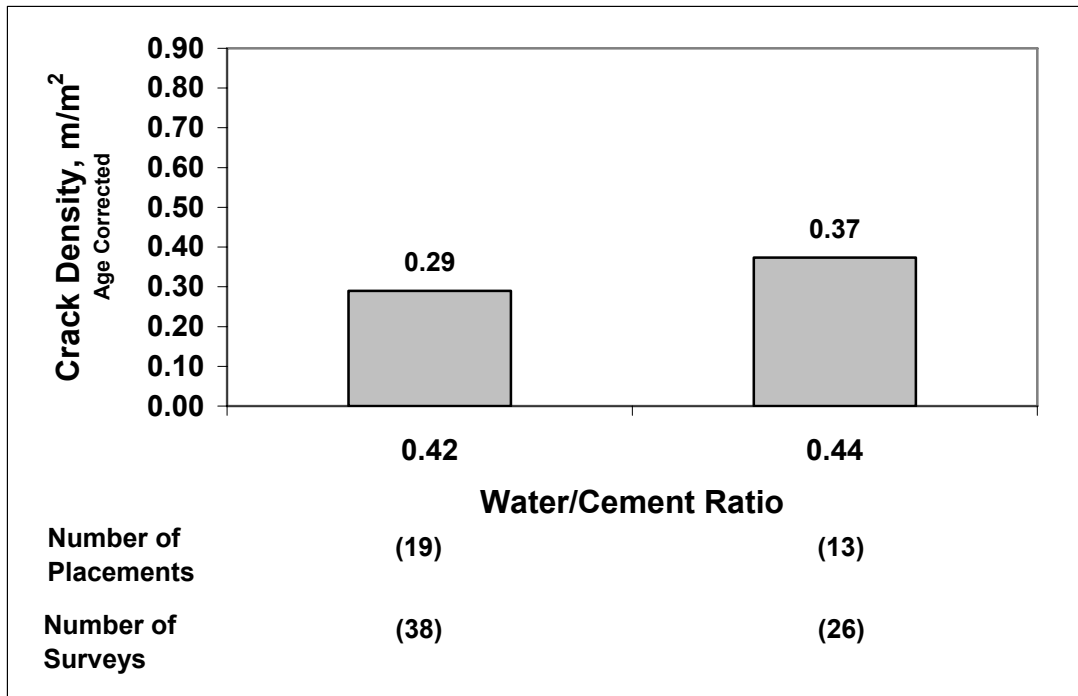


Fig. 5.11 – Mean crack density for individual placements corrected to an age of 78 months versus water-cement ratio for monolithic placements.

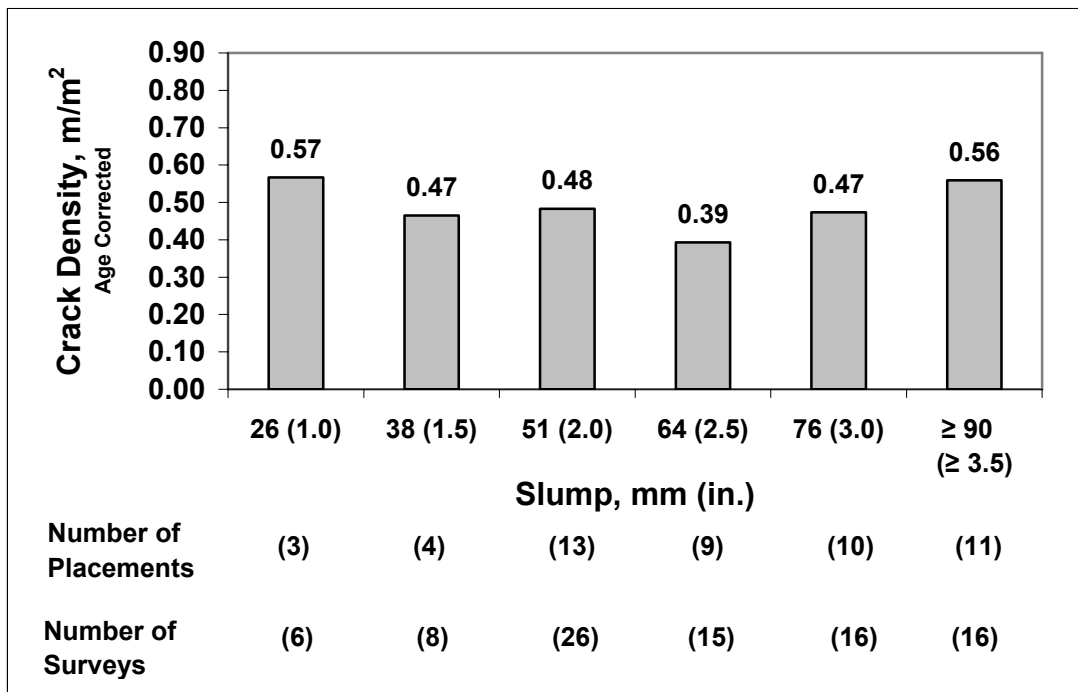


Fig. 5.12 – Mean crack density for individual placements corrected to an age of 78 months versus concrete slump for 5% and 7% silica fume overlay placements.

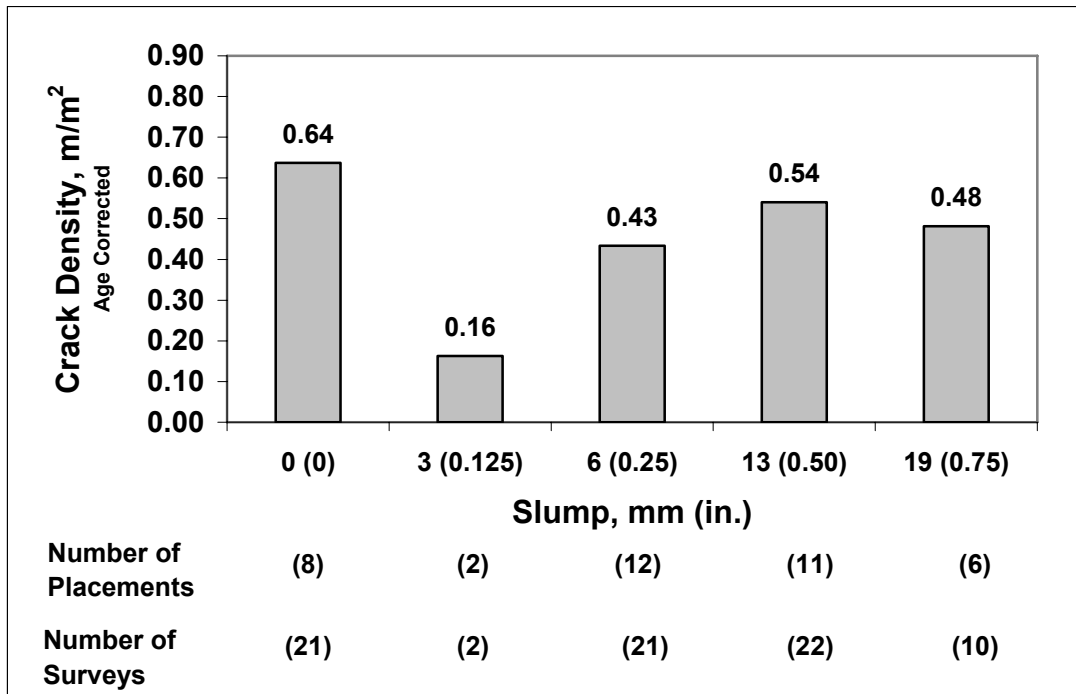


Fig. 5.13 – Mean crack density for individual placements corrected to an age of 78 months versus concrete slump for conventional overlay placements.

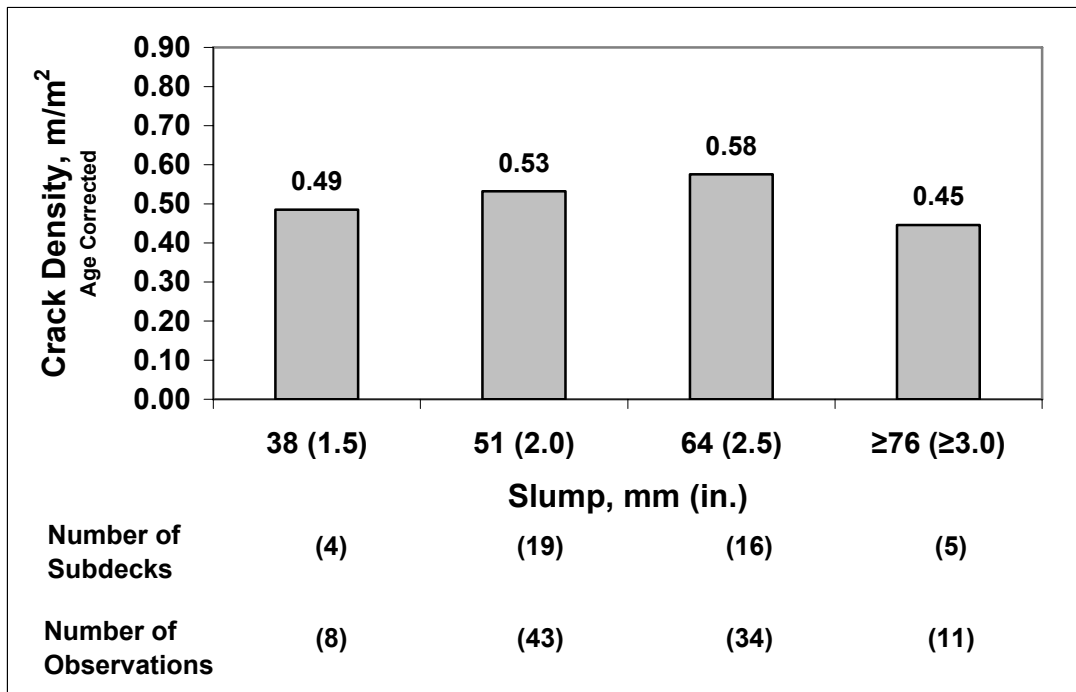


Fig. 5.14 – Mean crack density for individual bridge decks corrected to an age of 78 months versus concrete slump for subdeck placements.

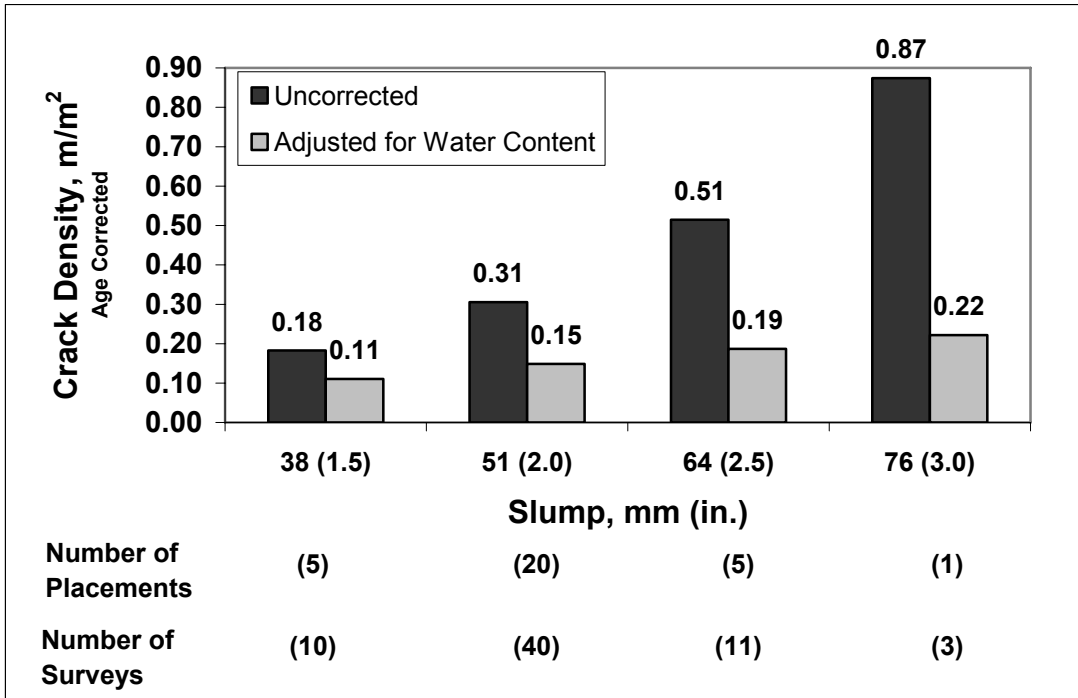


Fig. 5.15 – Mean crack density for individual placements corrected to an age of 78 months versus concrete slump for monolithic placements.

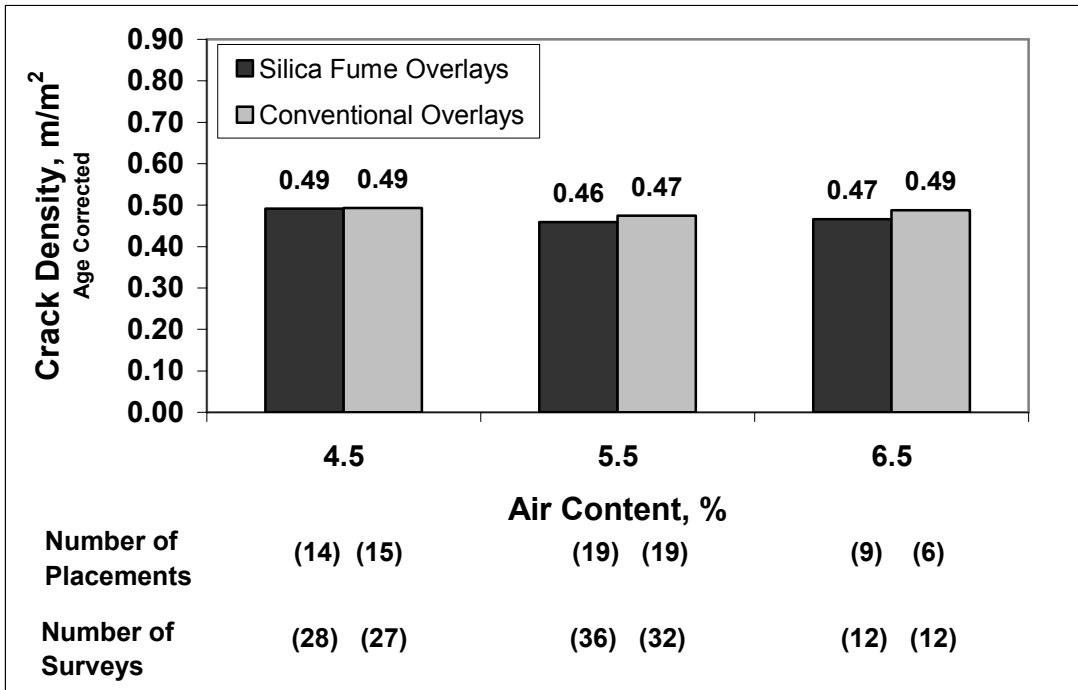


Fig. 5.16 – Mean crack density for individual placements corrected to an age of 78 months versus air content for 5% and 7% silica fume overlay and conventional overlay placements.

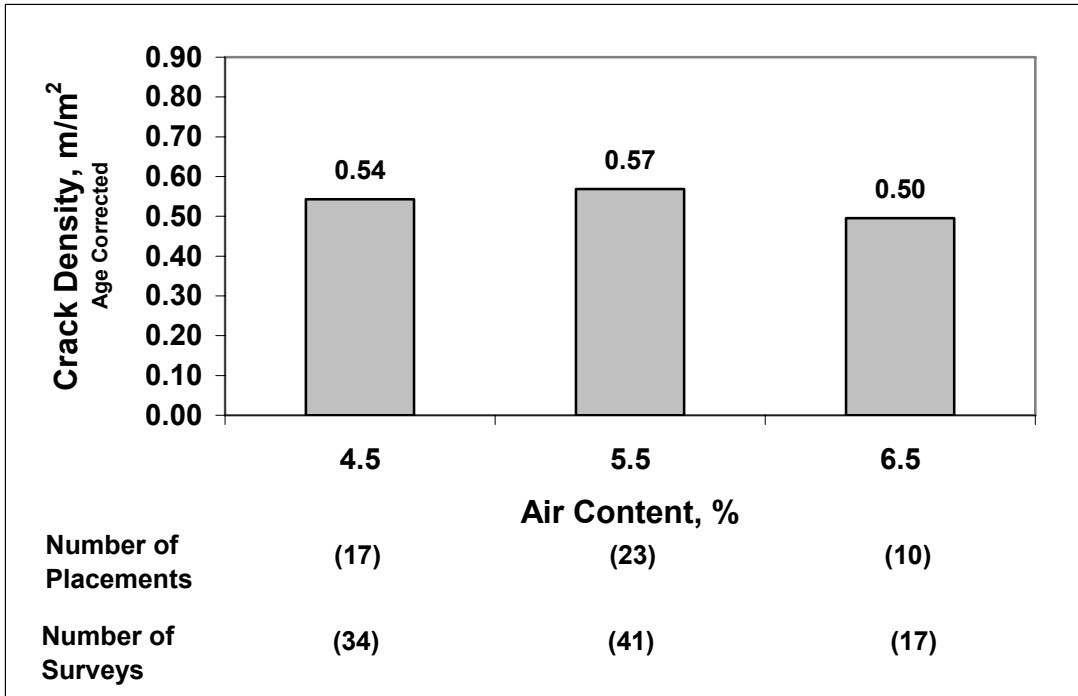


Figure 5.17 – Mean crack density for individual bridge decks corrected to an age of 78 months versus air content for overlay subdeck placements.

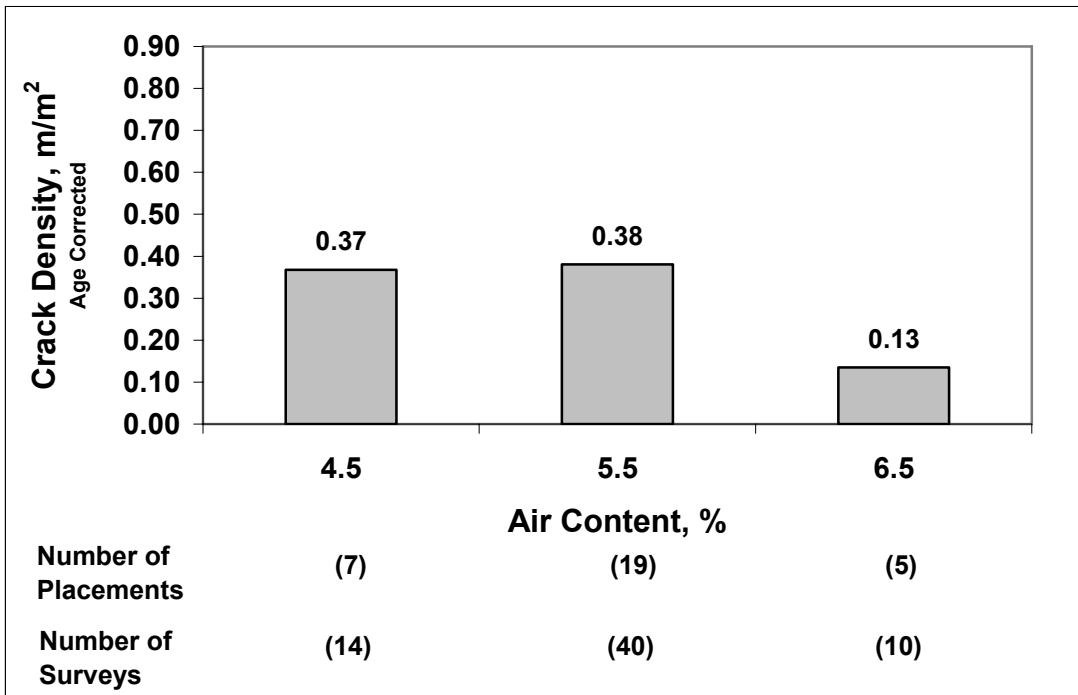


Figure 5.18 – Mean crack density for individual placements corrected to an age of 78 months versus air content for monolithic bridge placements.

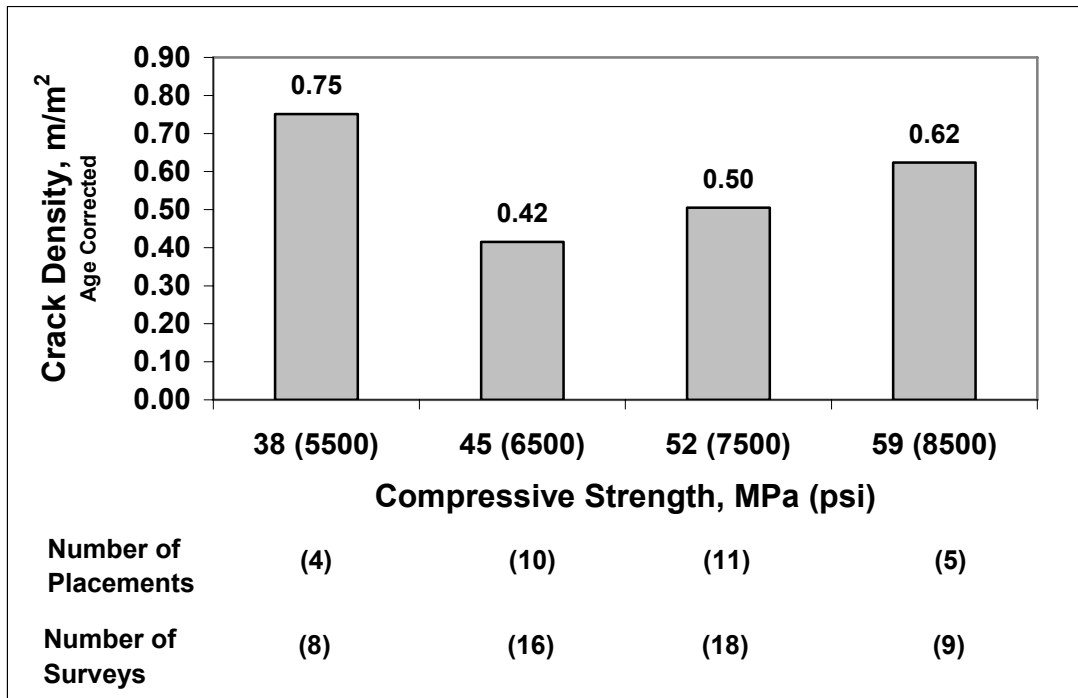


Fig. 5.19 – Mean crack density for individual placements corrected to an age of 78 months versus compressive strength for 5% and 7% silica fume overlay placements.

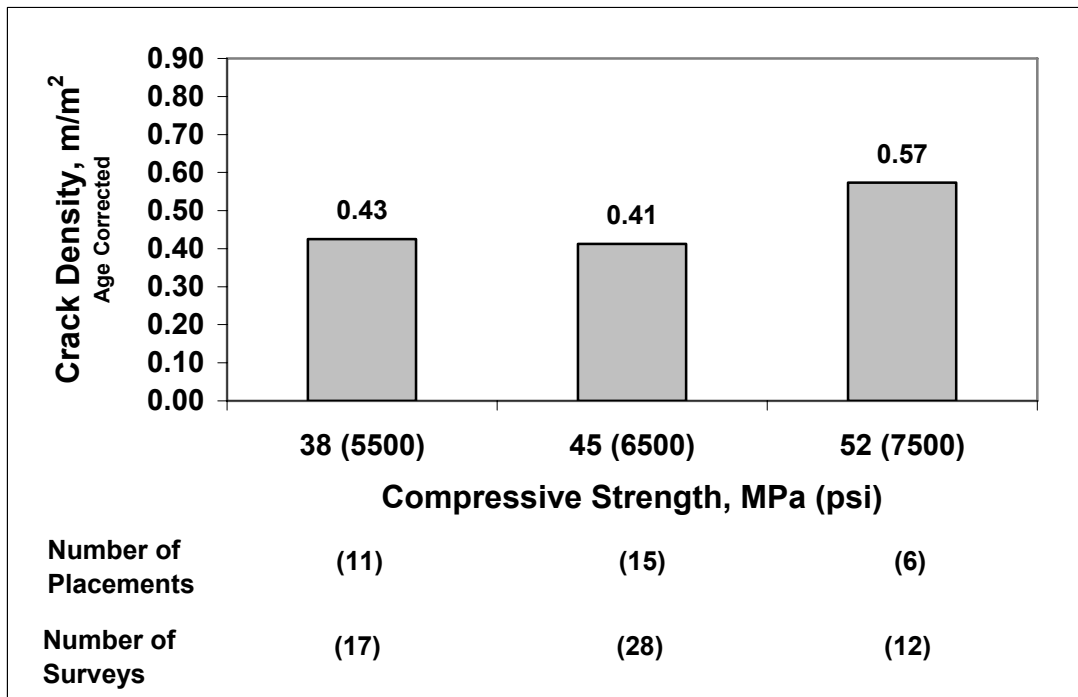


Fig. 5.20 – Mean crack density for individual placements corrected to an age of 78 months versus compressive strength for conventional overlay placements.

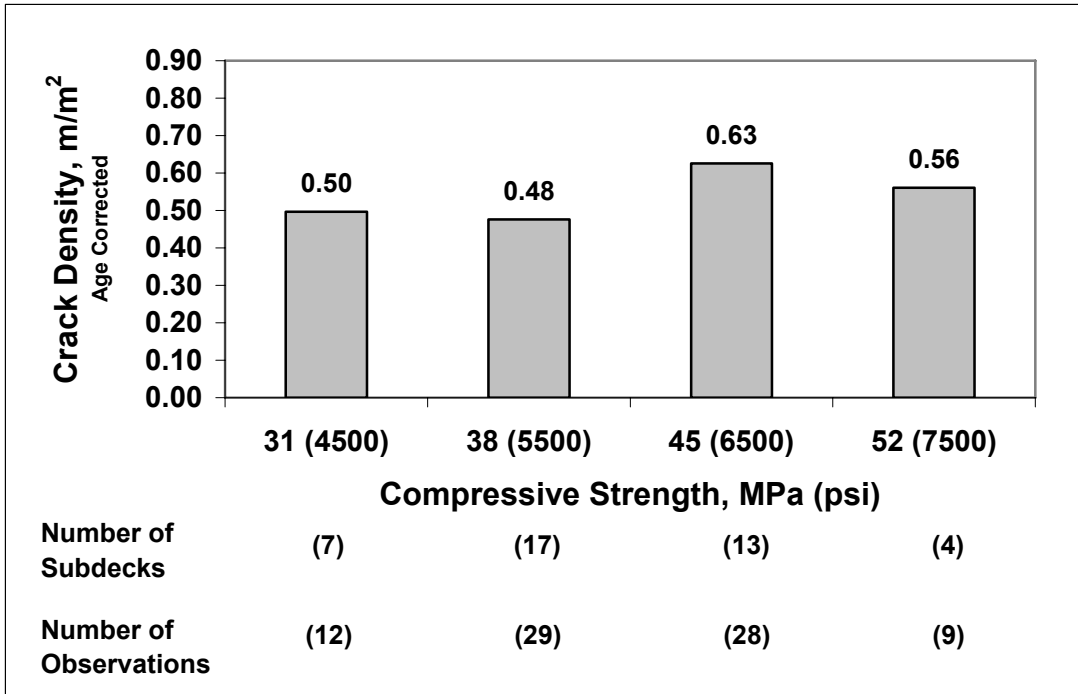


Figure 5.21 – Mean crack density for individual bridge decks corrected to an age of 78 months versus compressive strength for subdeck placements.

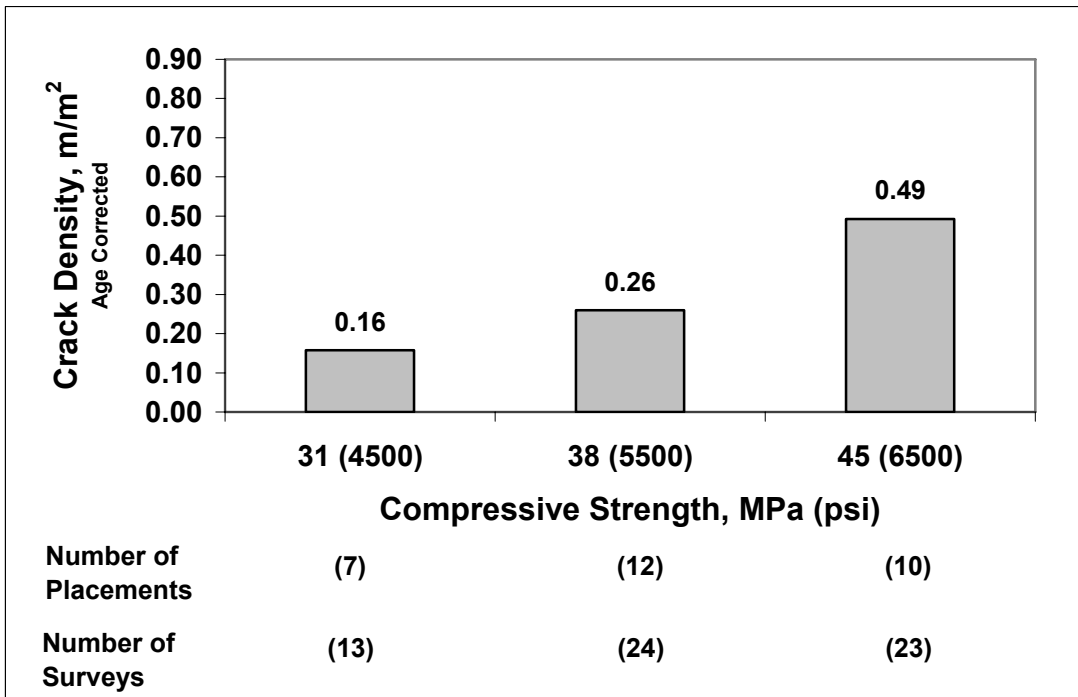


Figure 5.22 – Mean crack density for individual placements corrected to an age of 78 months versus compressive strength for monolithic placements.

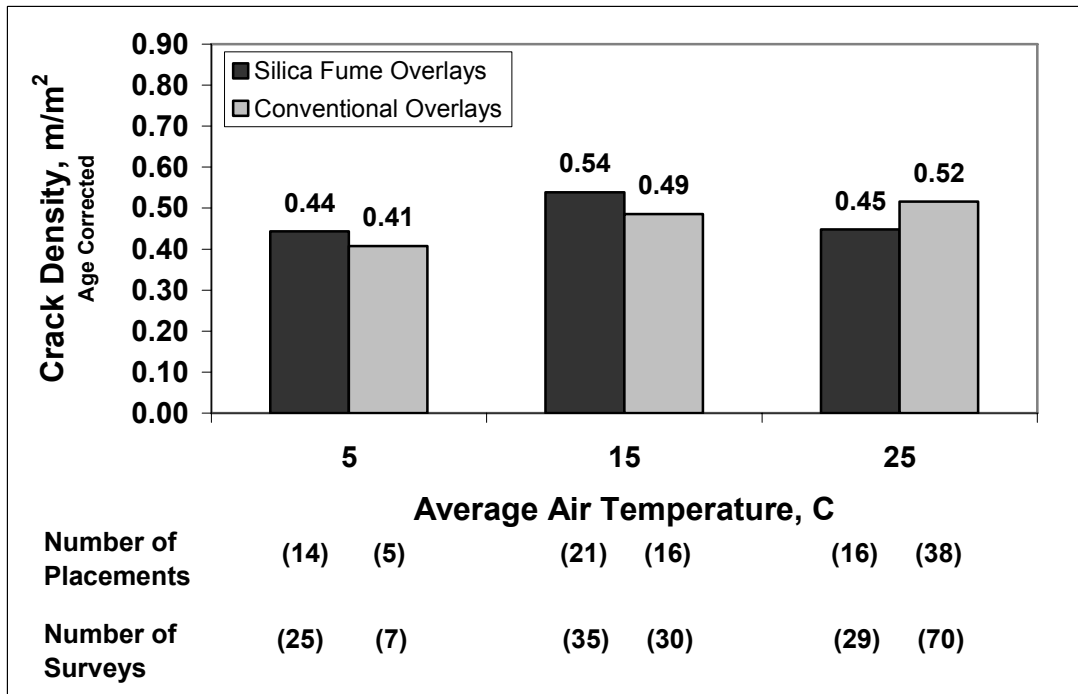


Fig. 5.23 – Mean crack density for individual placements corrected to an age of 78 months versus average air temperature for 5% and 7% silica fume overlay and conventional overlay placements.

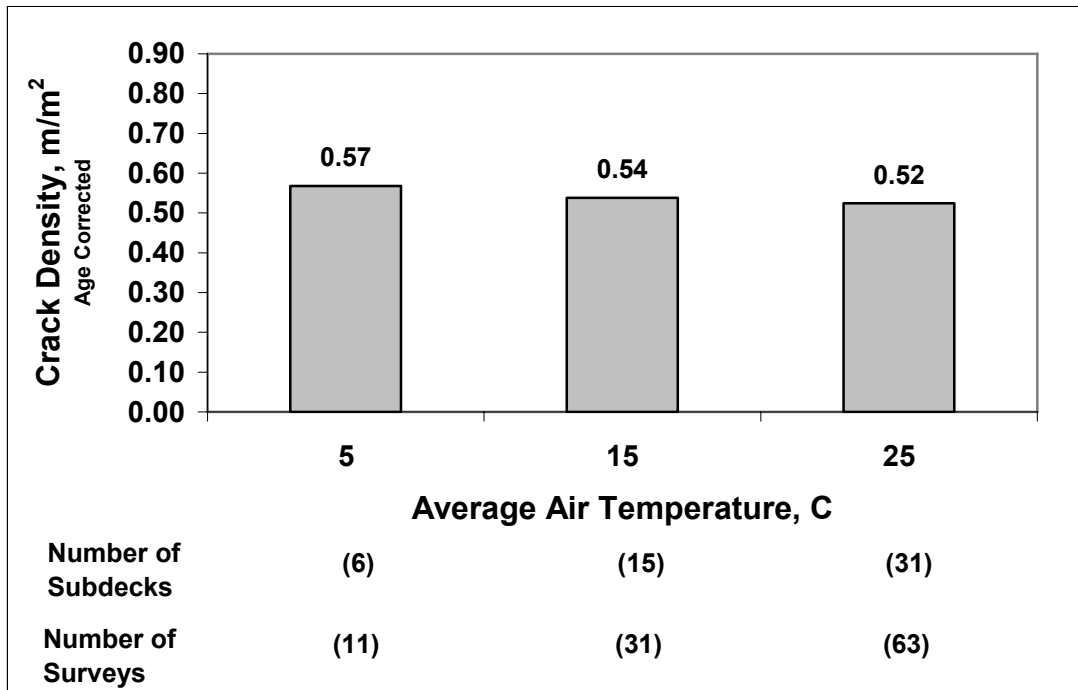


Fig. 5.24 – Mean crack density for individual bridge decks corrected to an age of 78 months versus average air temperature for overlay subdeck placements.

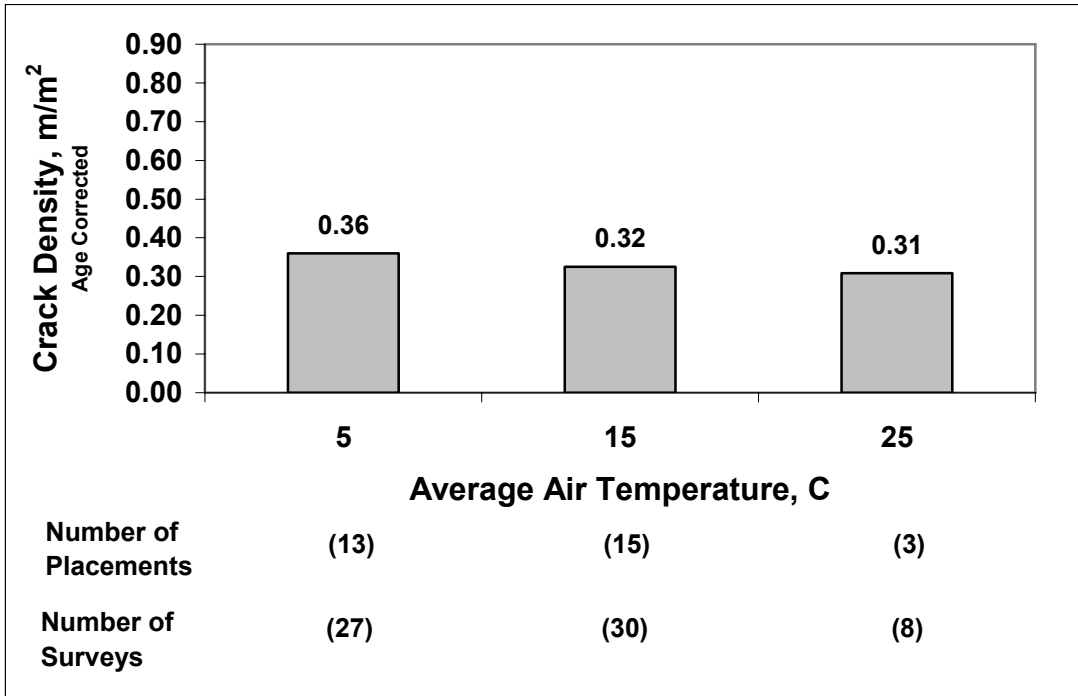


Fig. 5.25 – Mean crack density for individual bridge placements corrected to an age of 78 months versus average air temperature for monolithic placements.

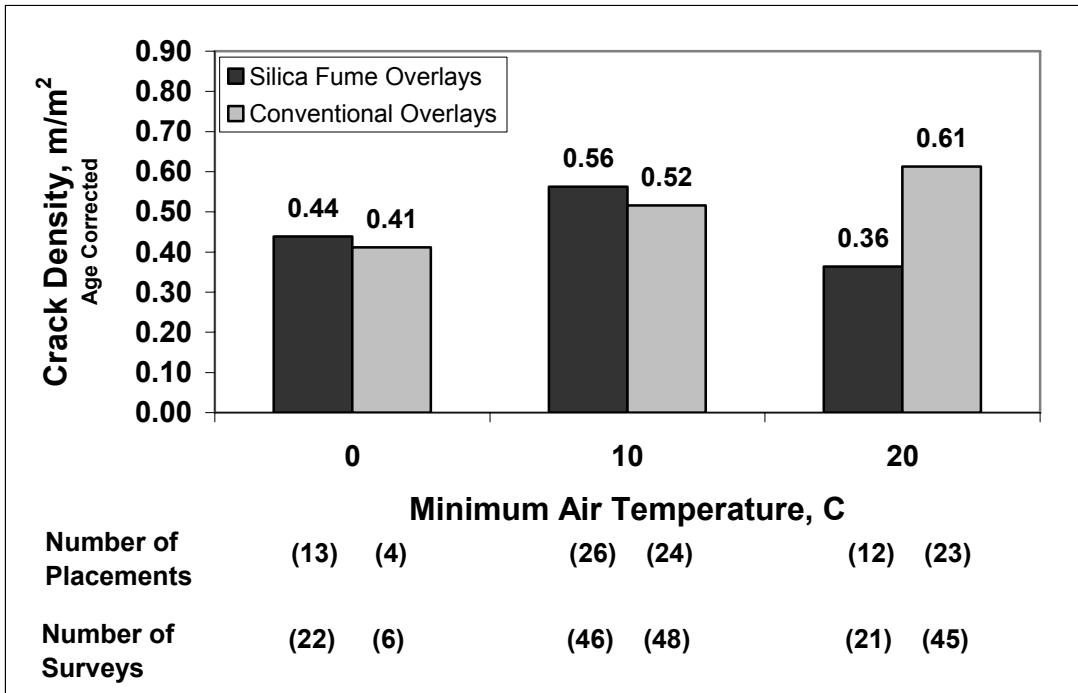


Fig. 5.26 – Mean crack density for individual placements corrected to an age of 78 months versus minimum air temperature for 5% and 7% silica fume overlay and conventional overlay placements.

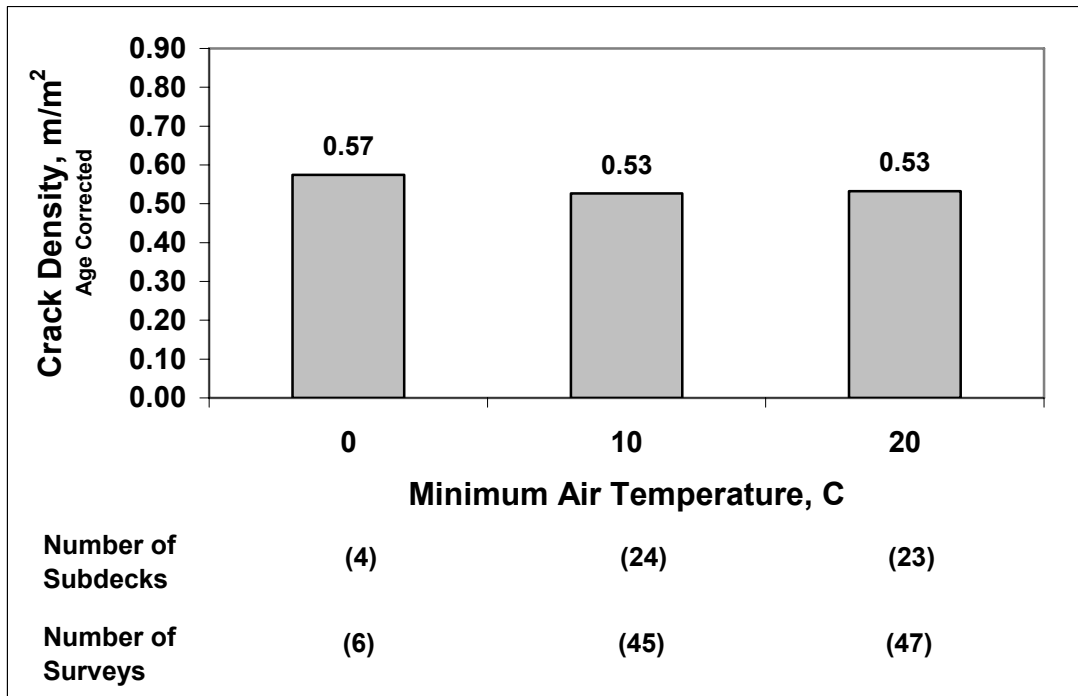


Fig. 5.27 – Mean crack density for individual bridge decks corrected to an age of 78 months versus minimum air temperature for overlay subdeck placements.

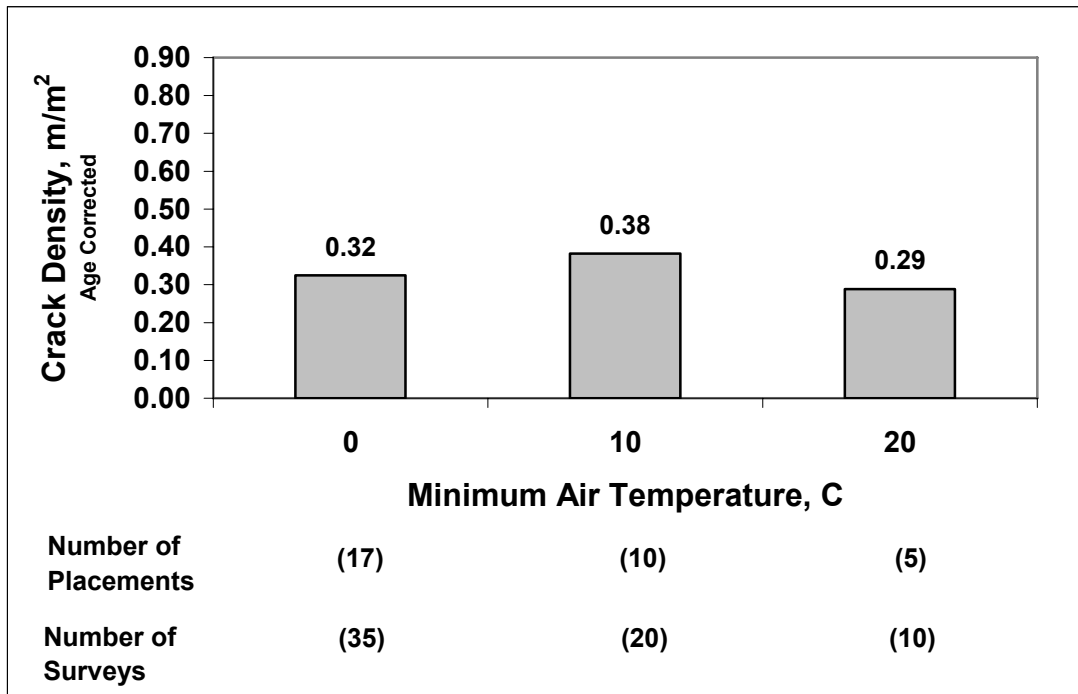


Figure 5.28 – Mean crack density for individual bridge placements corrected to an age of 78 months versus minimum air temperature for monolithic bridge placements.

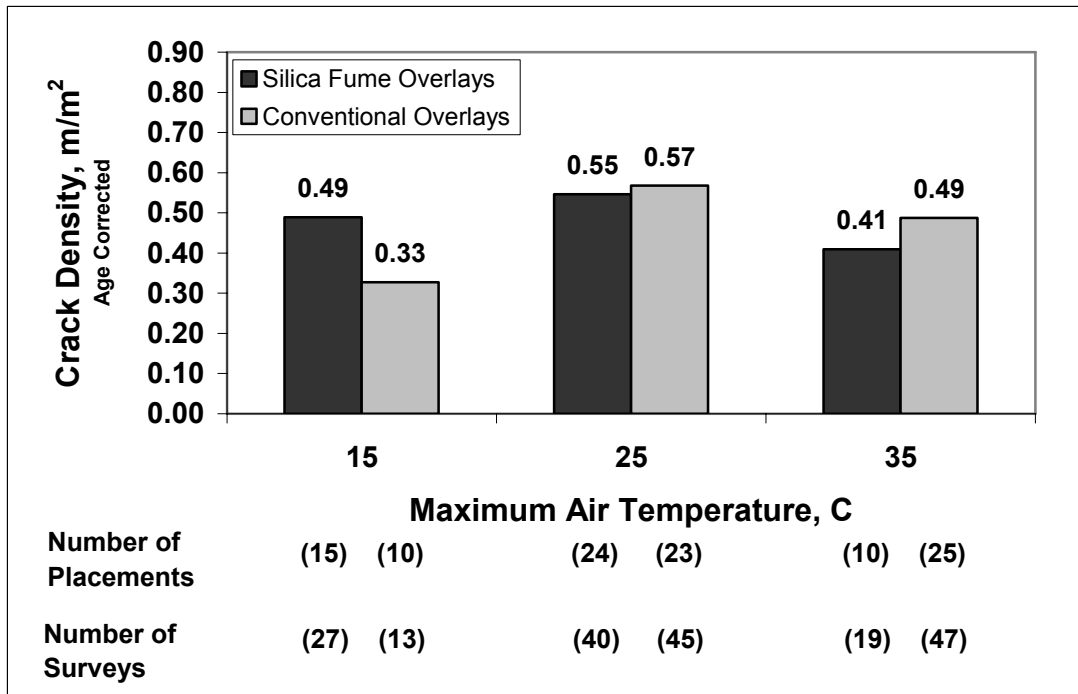


Fig. 5.29 – Mean crack density for individual placements corrected to an age of 78 months versus maximum air temperature for 5% and 7% silica fume overlay and conventional overlay placements.

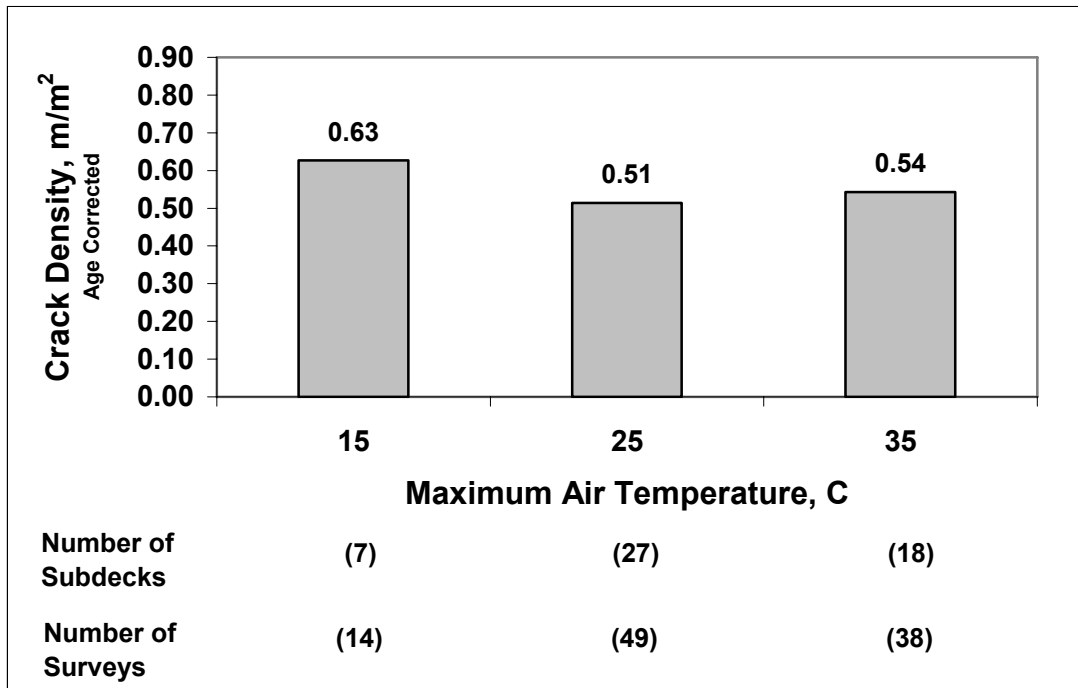


Fig. 5.30 – Mean crack density for individual bridge placements corrected to an age of 78 months versus maximum air temperature for overlay subdeck placements.

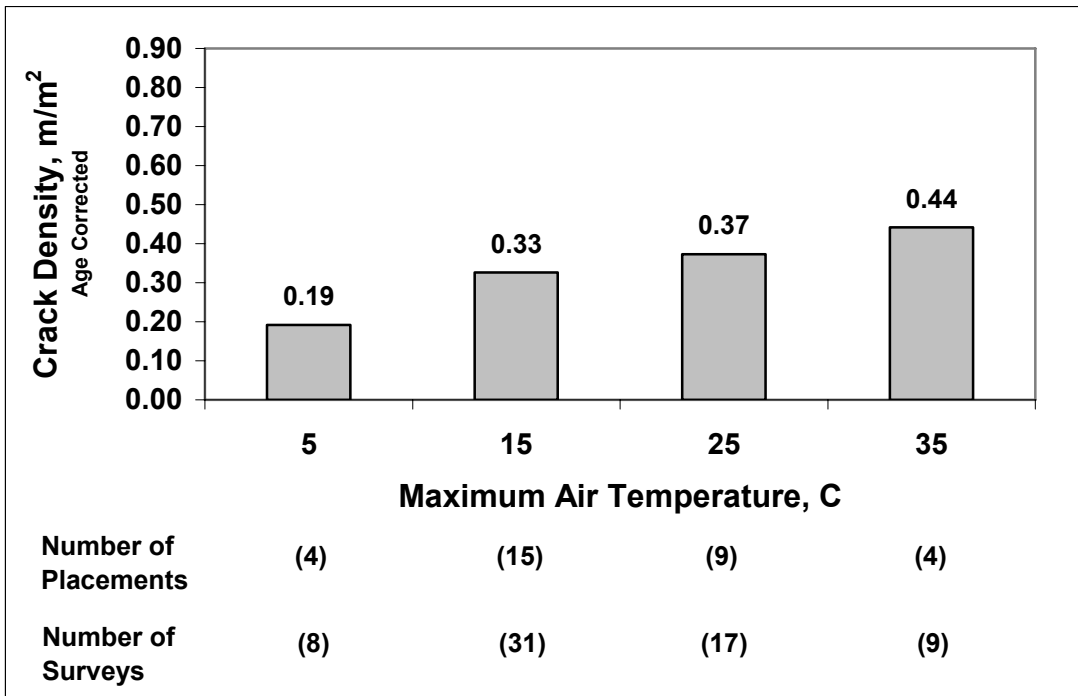


Figure 5.31 – Mean crack density for individual bridge placements corrected to an age of 78 months versus maximum air temperature for monolithic bridge placements.

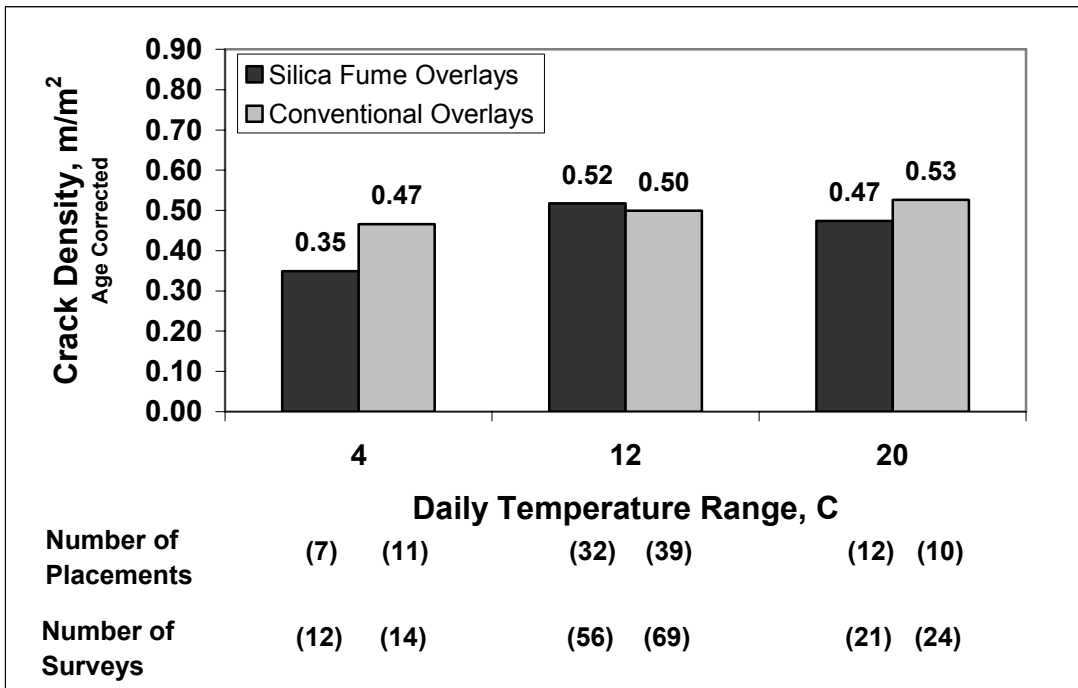


Fig. 5.32 – Mean crack density for individual placements corrected to an age of 78 months versus daily air temperature range for 5% and 7% silica fume overlay and conventional overlay placements.

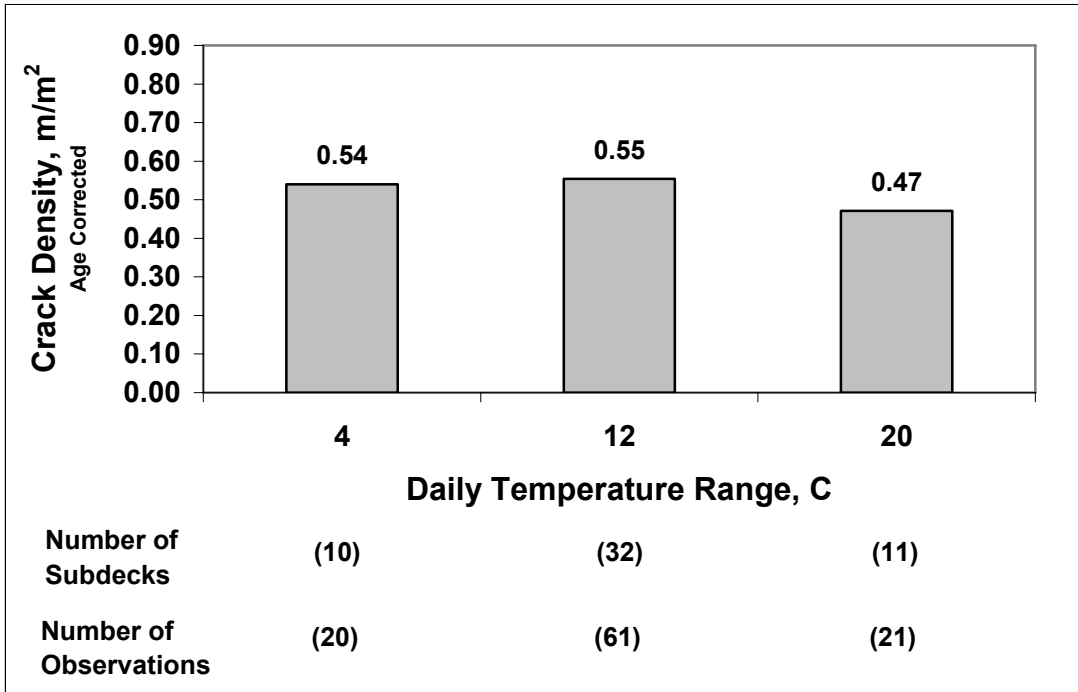


Fig. 5.33 – Mean crack density for individual bridge decks corrected to an age of 78 months versus daily air temperature range for overlay subdeck placements.

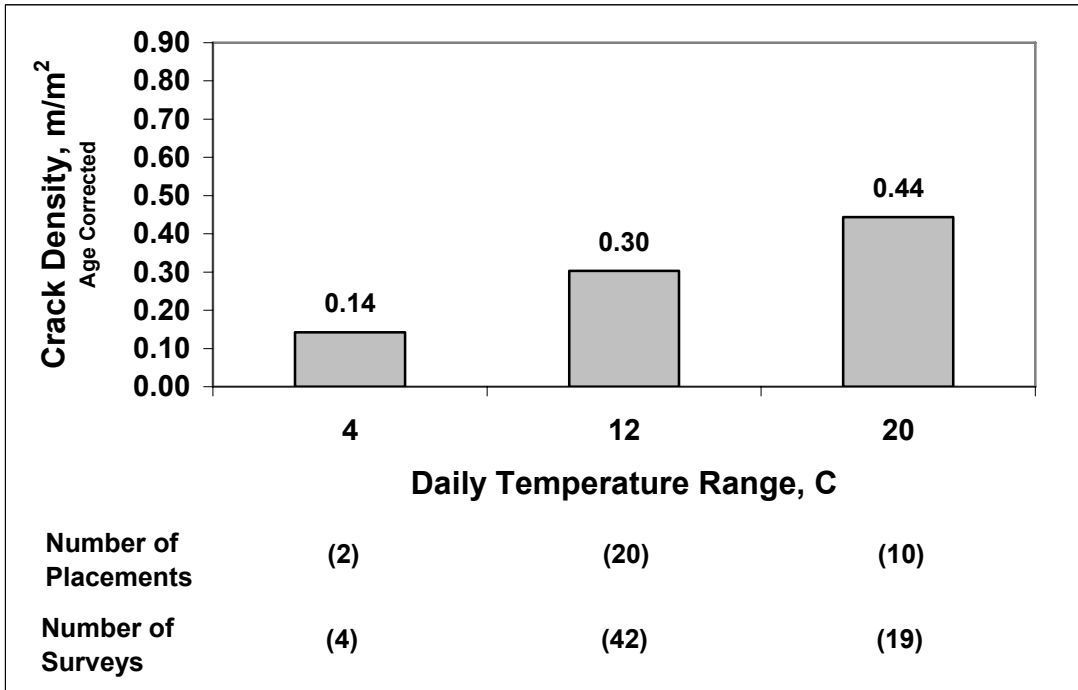


Figure 5.34 – Mean crack density for individual bridge decks corrected to an age of 78 months versus daily air temperature range for monolithic bridge placements.

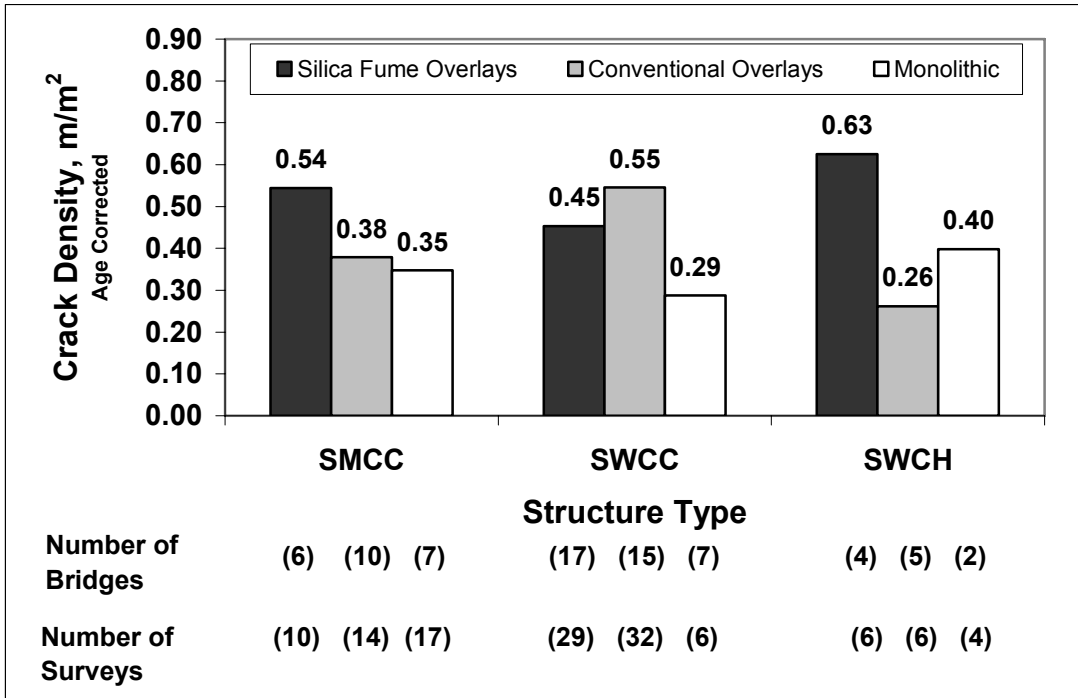


Fig. 5.35 – Mean crack density for bridge decks corrected to an age of 78 months versus structure type, based on deck type, for all bridge deck types.

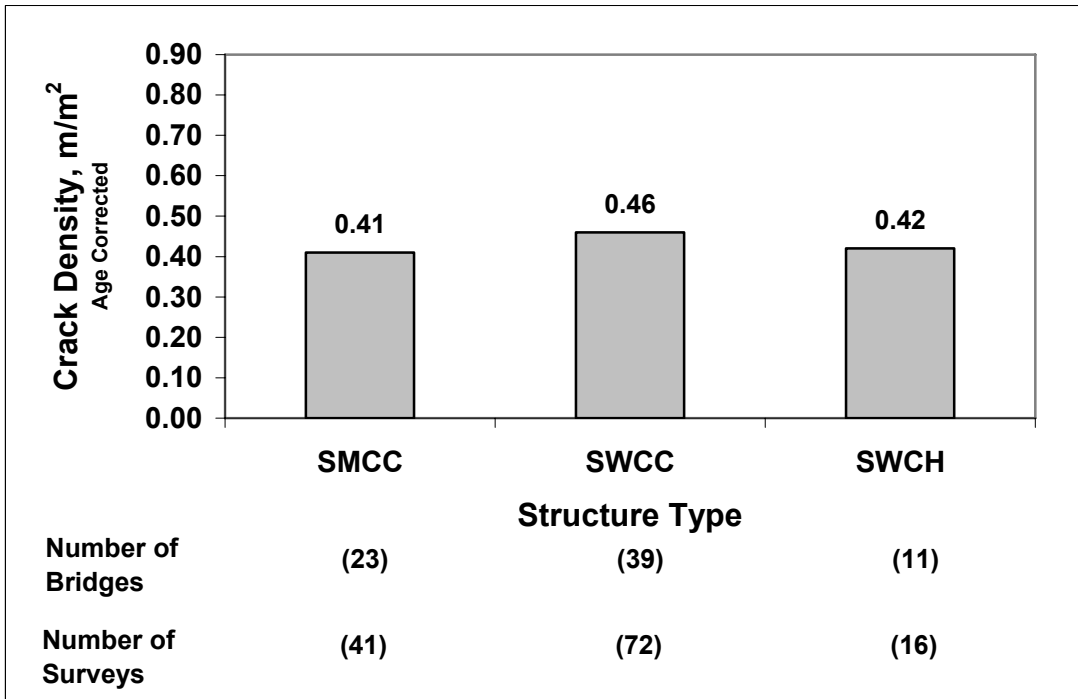


Fig. 5.36 – Mean crack density for bridge decks corrected to an age of 78 months versus structure type for all bridge deck types.

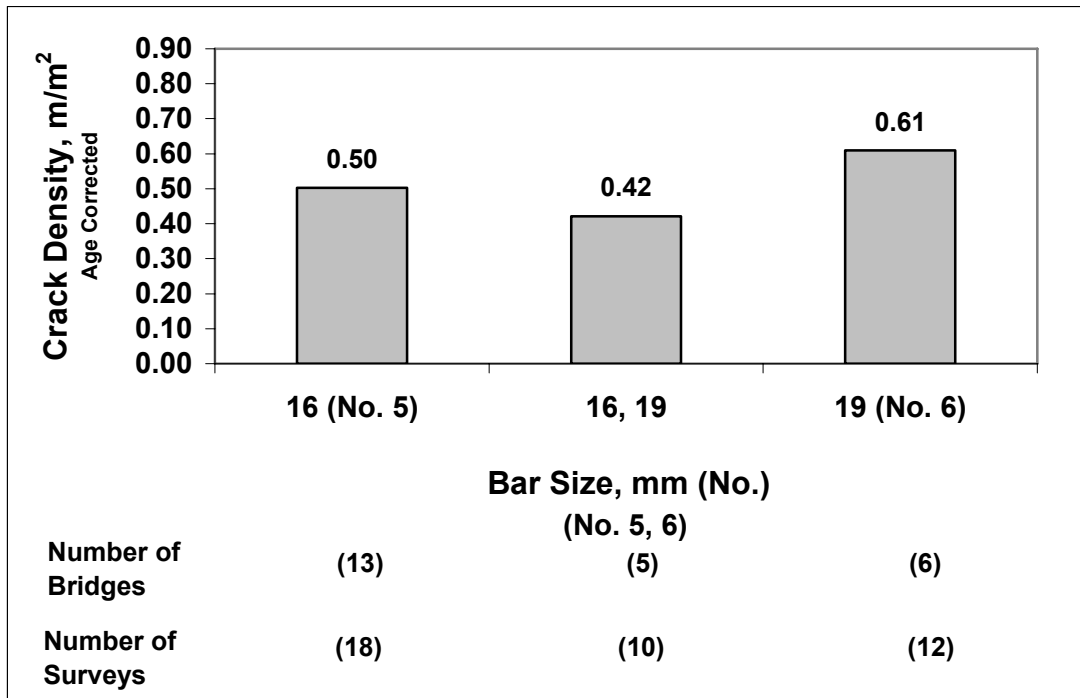


Fig. 5.37 – Mean crack density for bridge decks corrected to an age of 78 months versus top transverse reinforcing bar size for 5% and 7% silica fume overlay bridges.

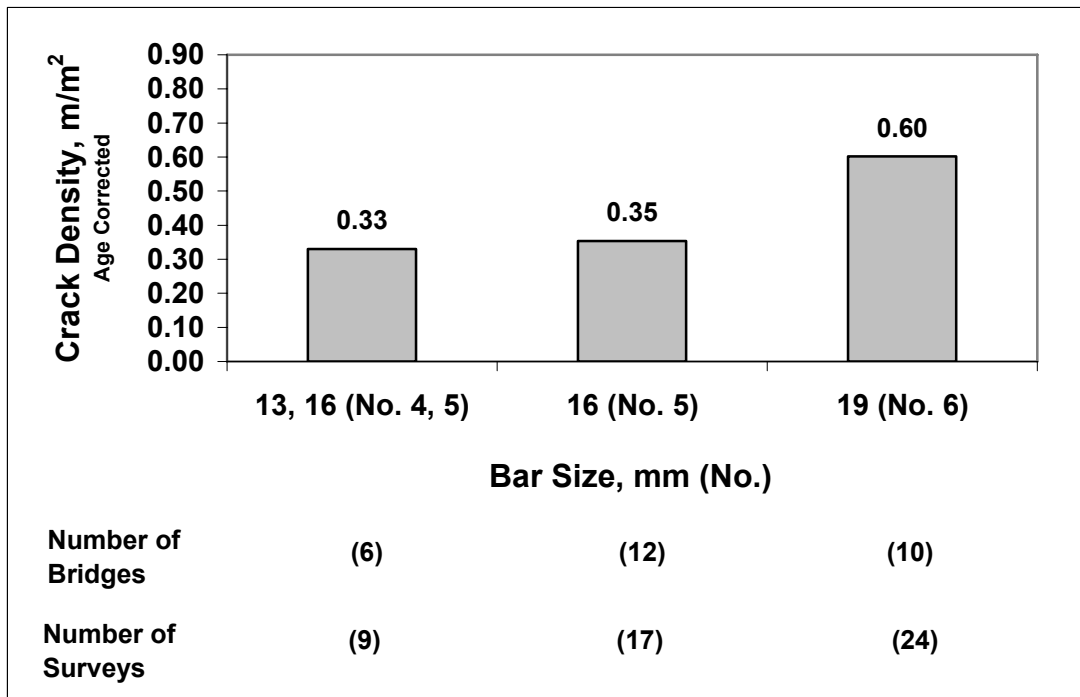


Fig. 5.38 – Mean crack density for bridge decks corrected to an age of 78 months versus top transverse reinforcing bar size for conventional overlay bridges.

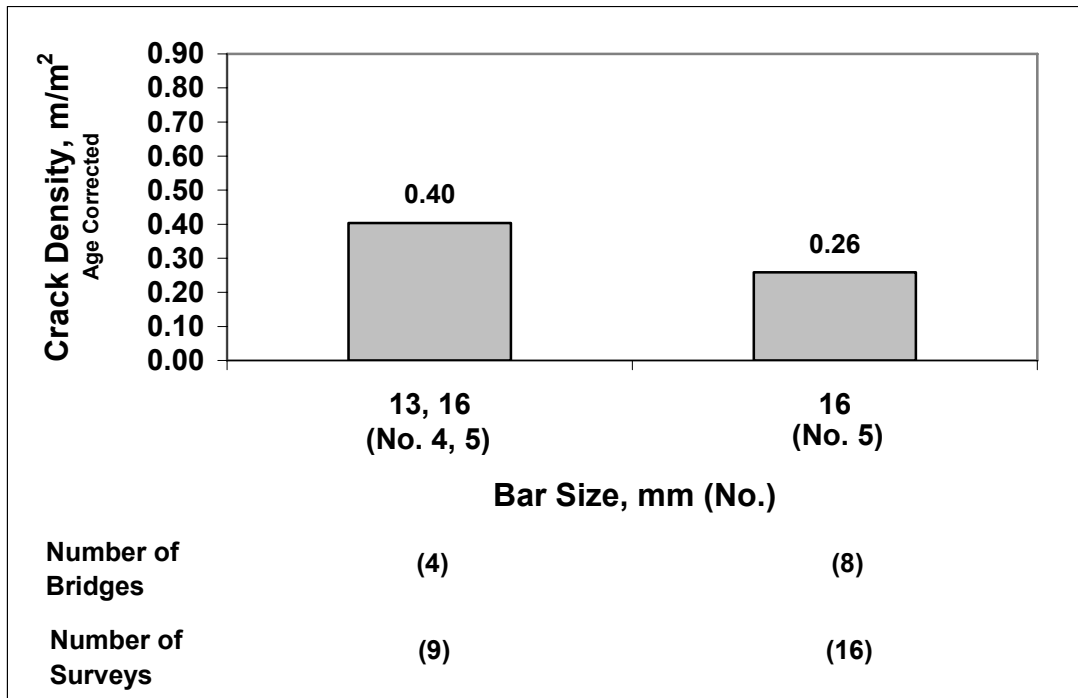


Fig. 5.39 – Mean crack density for bridge decks corrected to an age of 78 months versus top transverse reinforcing bar size for monolithic bridges.

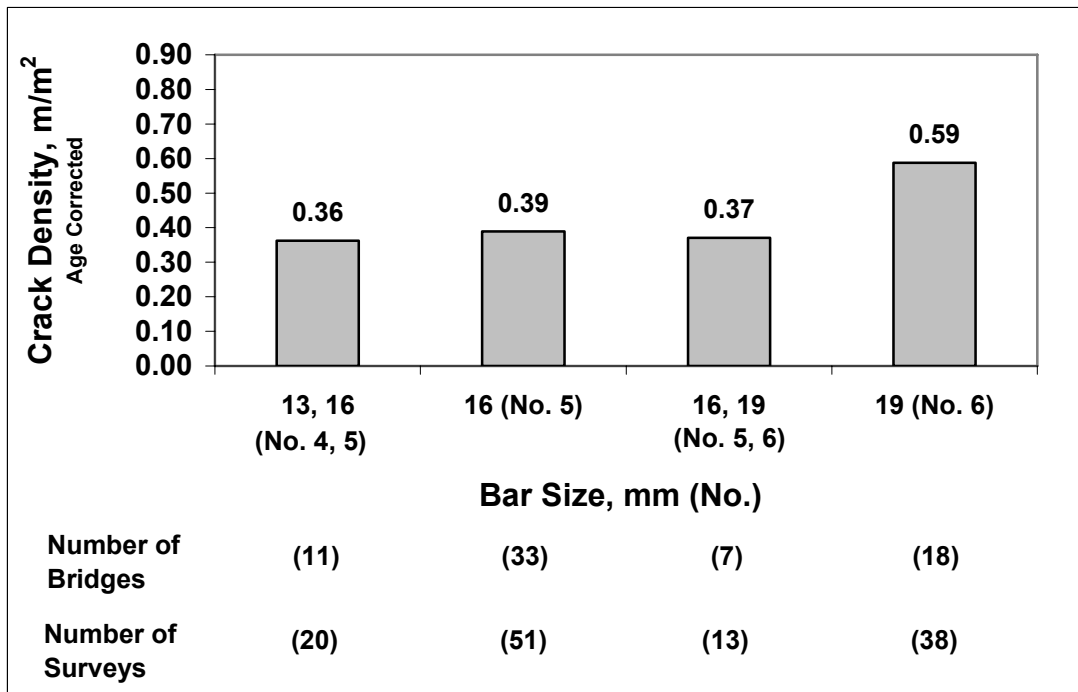


Fig. 5.40 – Mean crack density for bridge decks corrected to an age of 78 months versus top transverse reinforcing bar size for all bridge deck types.

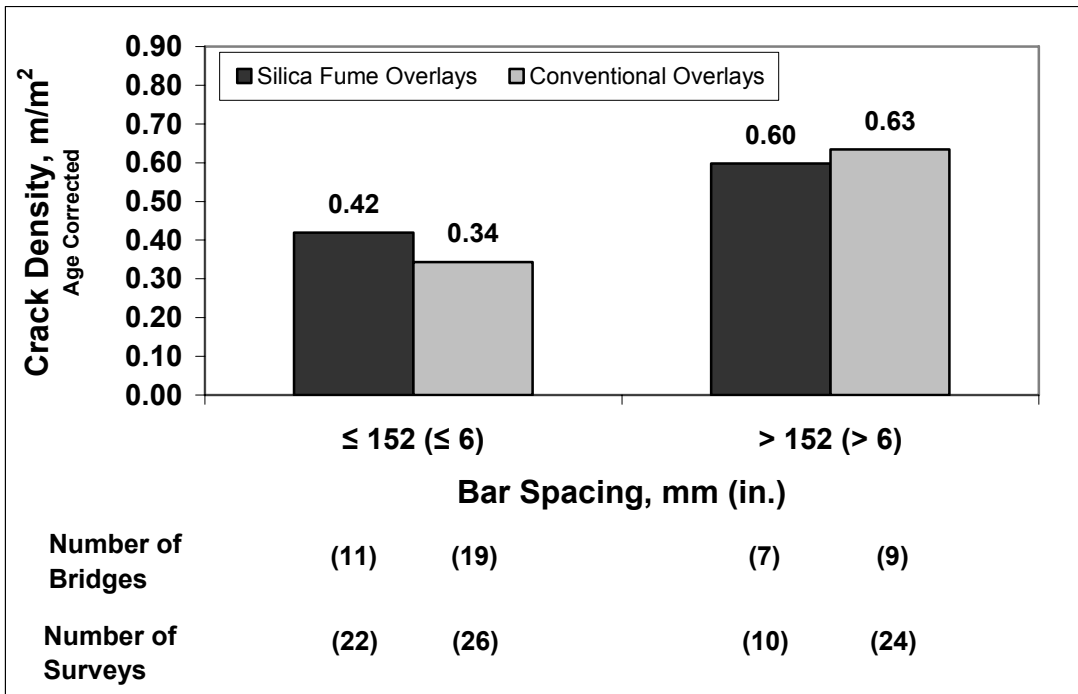


Fig. 5.41 – Mean crack density for bridge decks corrected to an age of 78 months versus top transverse bar spacing for 5% and 7% silica fume and conventional overlay bridges.

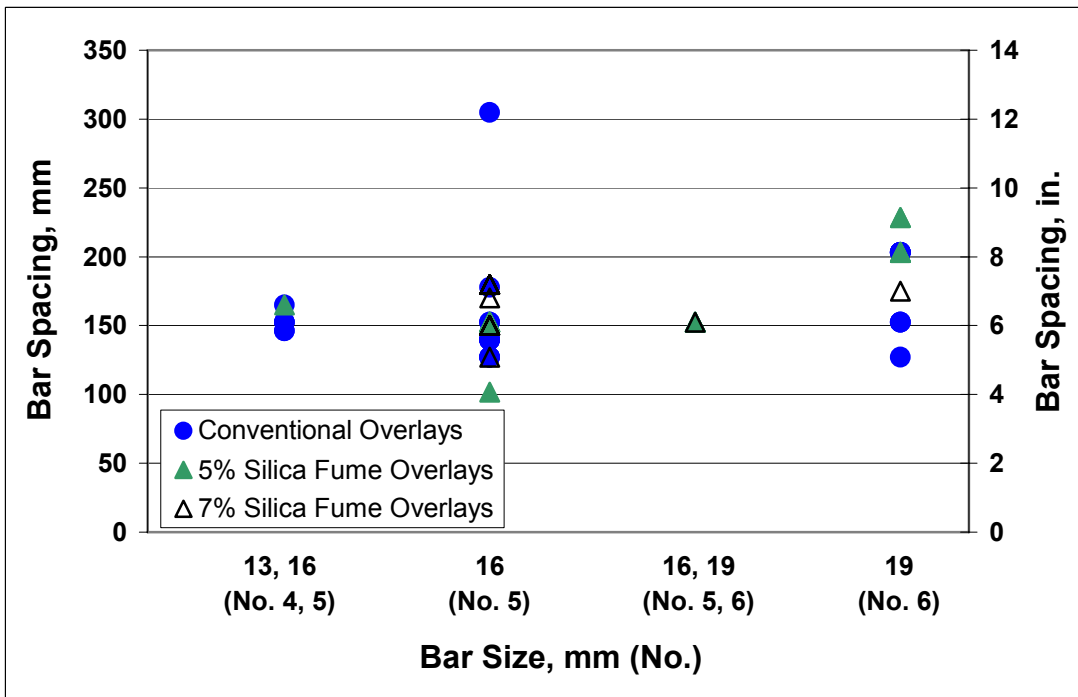


Fig. 5.42 – Top transverse bar spacing versus top transverse bar size for 5% and 7% silica fume and conventional overlay bridges.

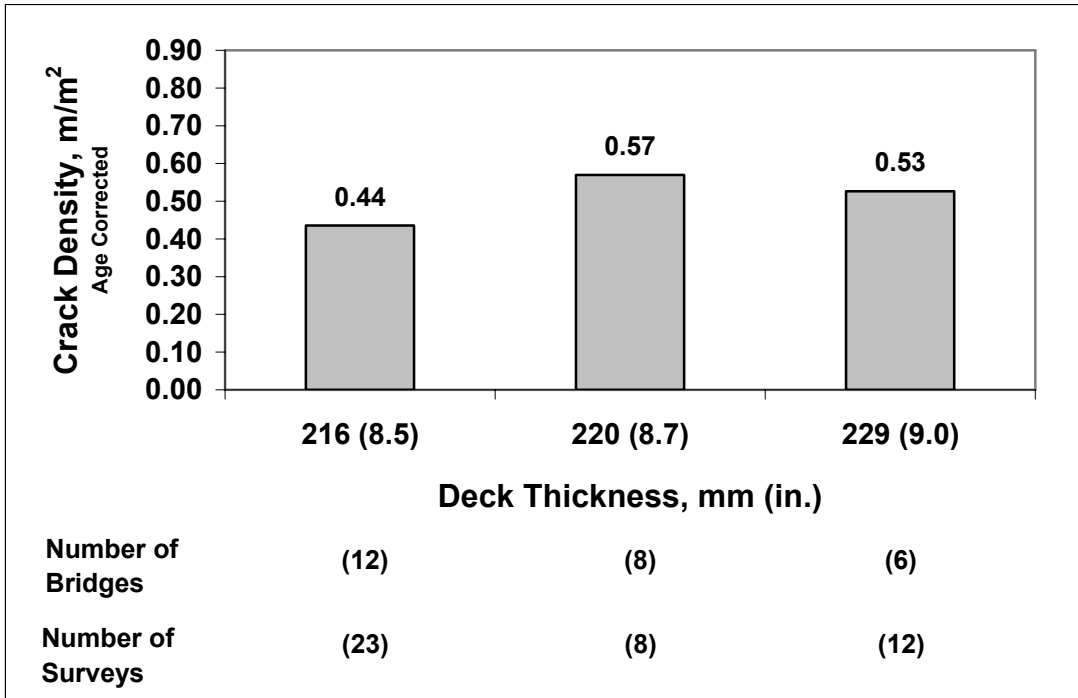


Fig. 5.43 – Mean crack density for bridge decks corrected to an age of 78 months versus deck thickness for 5% and 7% silica fume overlay bridges.

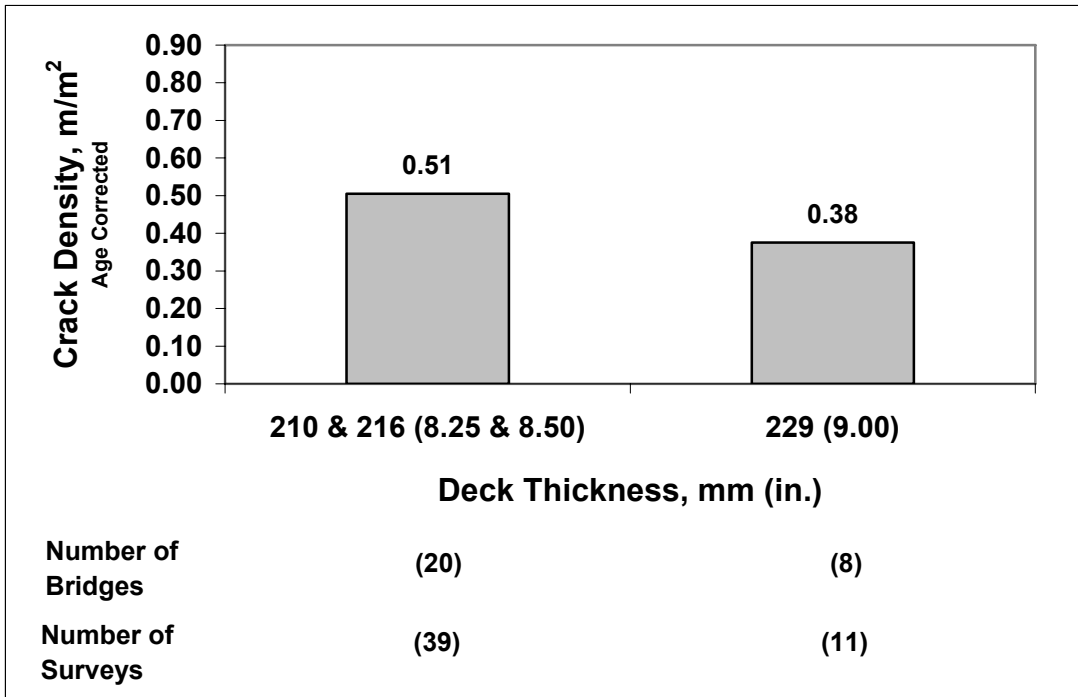


Fig. 5.44 – Mean crack density for bridge decks corrected to an age of 78 months versus deck thickness for conventional overlay bridges.

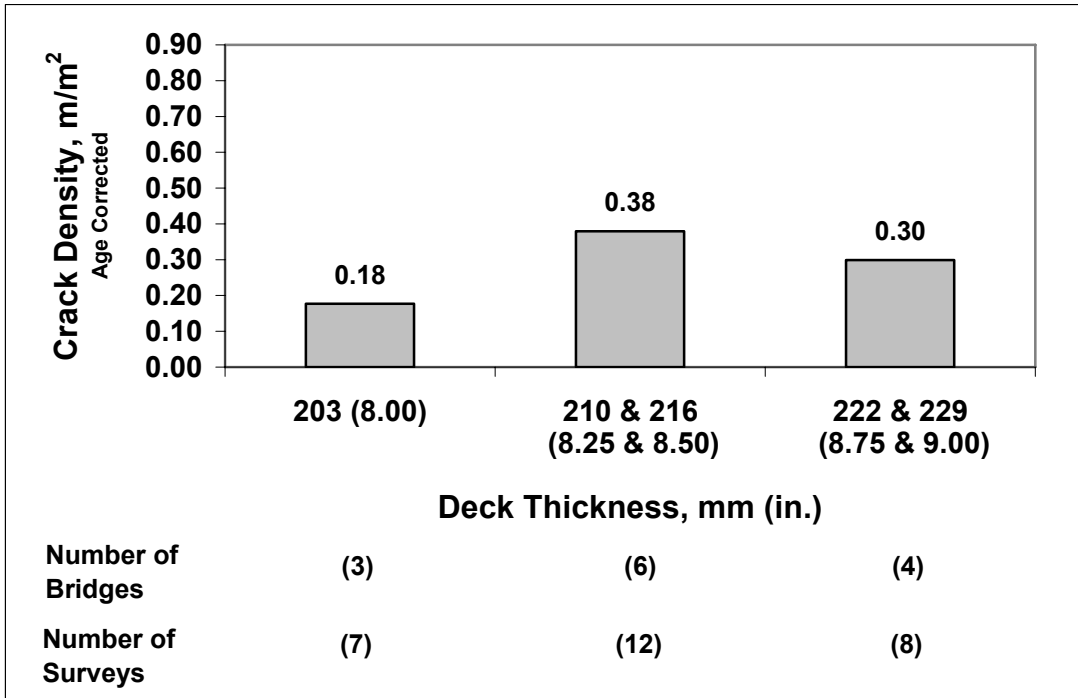


Fig. 5.45 – Mean crack density for bridge decks corrected to an age of 78 months versus deck thickness for monolithic bridges.

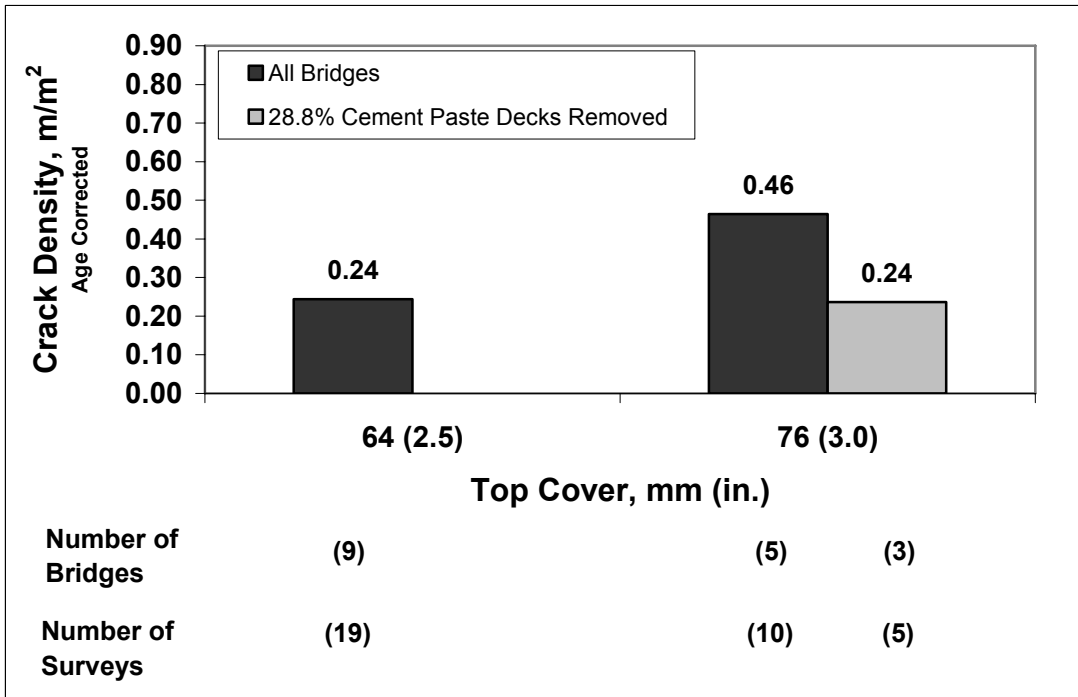


Fig. 5.46 – Mean crack density for bridge decks corrected to an age of 78 months versus top cover for monolithic bridges.

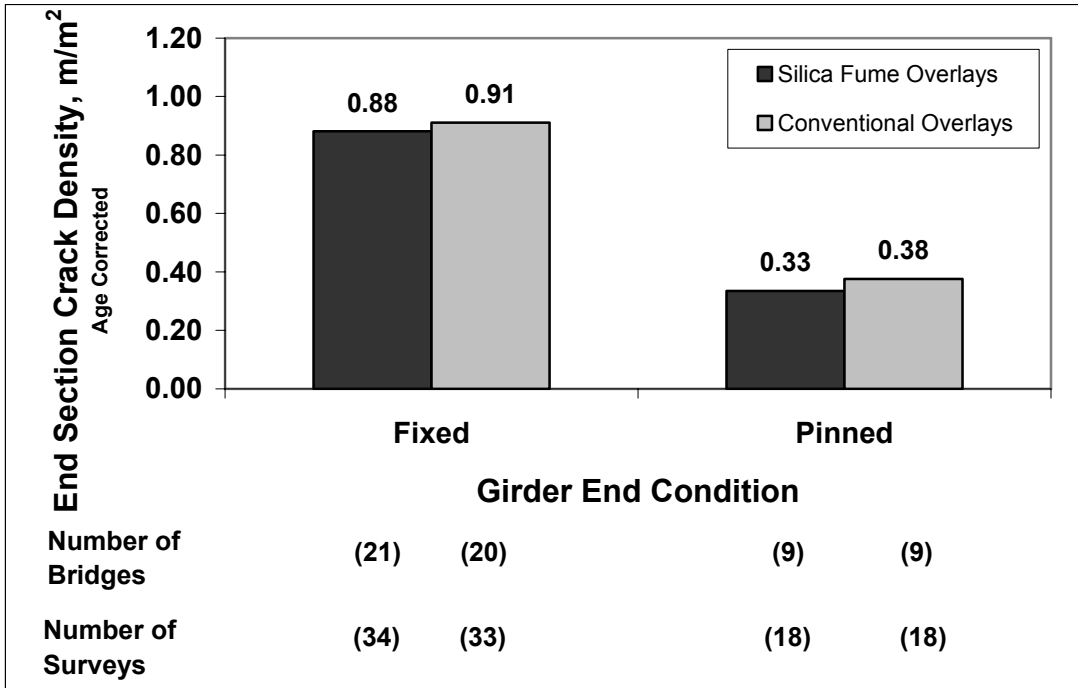


Fig. 5.47 – Mean crack density of end sections corrected to an age of 78 months versus girder end condition for 5% and 7% silica fume overlay and conventional overlay bridges.

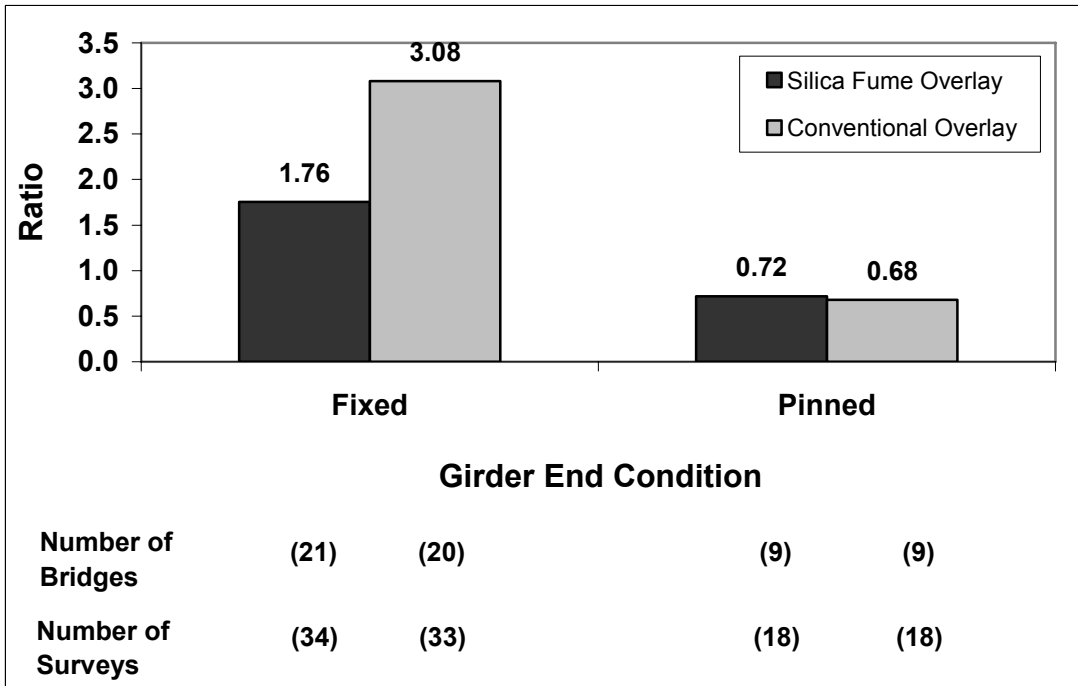


Fig. 5.48 – Ratio of end section crack density to the crack density of the entire deck versus girder end condition for 5% and 7% silica fume overlay and conventional overlay bridges.

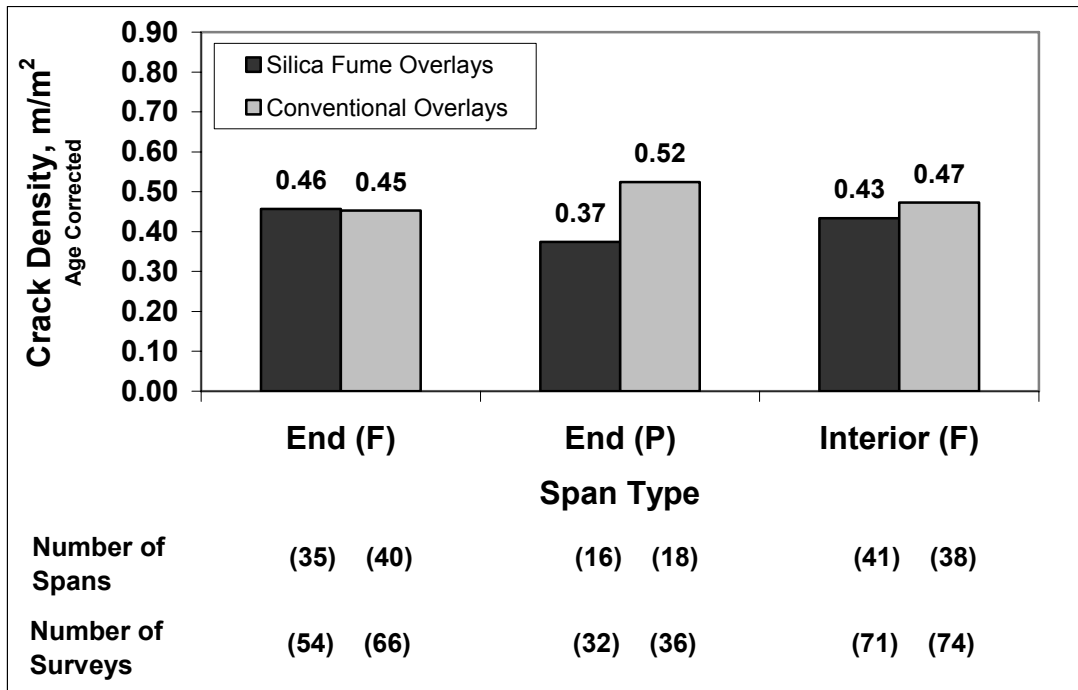


Fig. 5.49 – Mean crack density for individual spans corrected to an age of 78 months versus span type for 5% and 7% silica fume overlay and conventional overlay bridges.

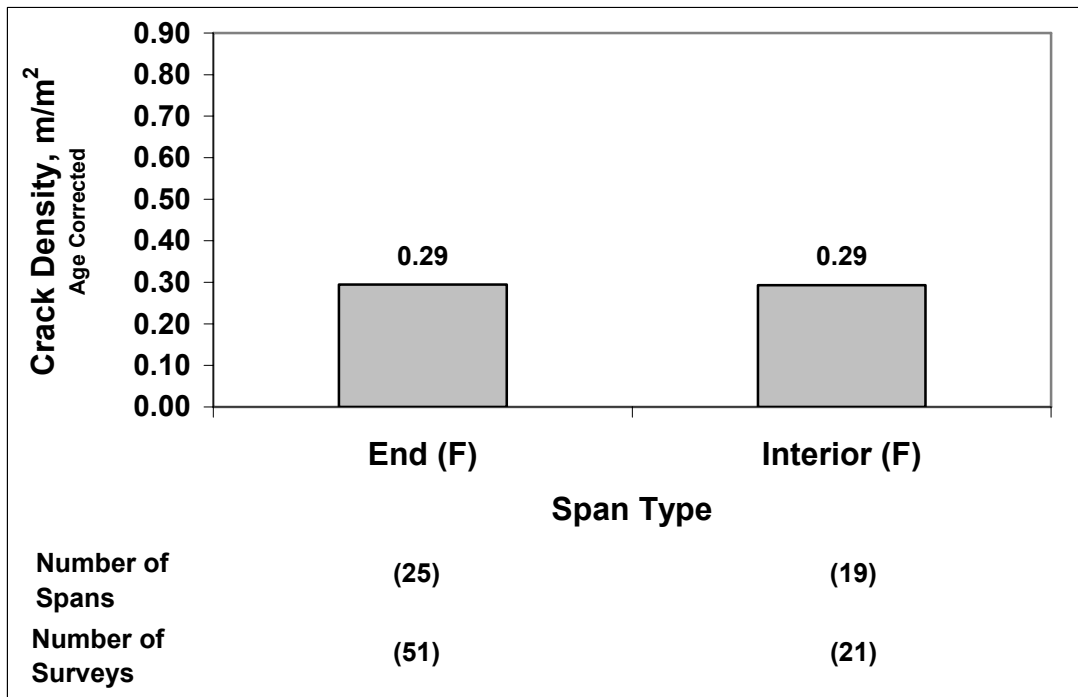


Fig. 5.50 – Mean crack density for individual spans corrected to an age of 78 months versus span type for monolithic bridges.

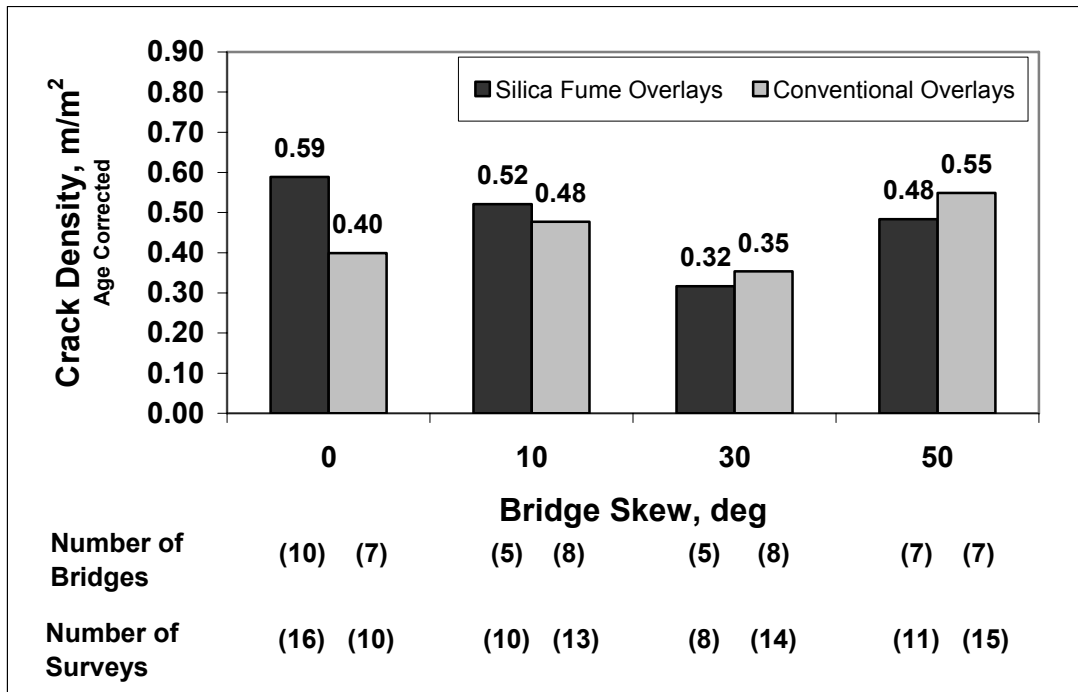


Fig. 5.51 – Mean crack density for bridge decks corrected to an age of 78 months versus bridge skew for 5% and 7% silica fume overlays and conventional overlay bridges.

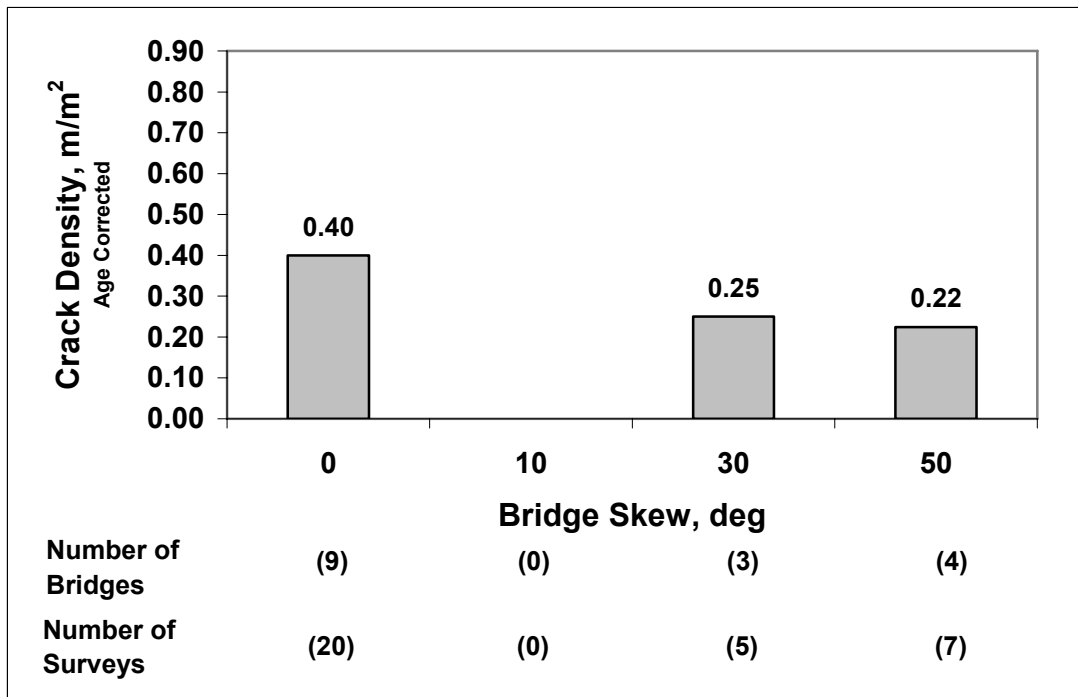


Fig. 5.52 – Mean crack density for bridge decks corrected to an age of 78 months versus bridge skew for monolithic bridges.

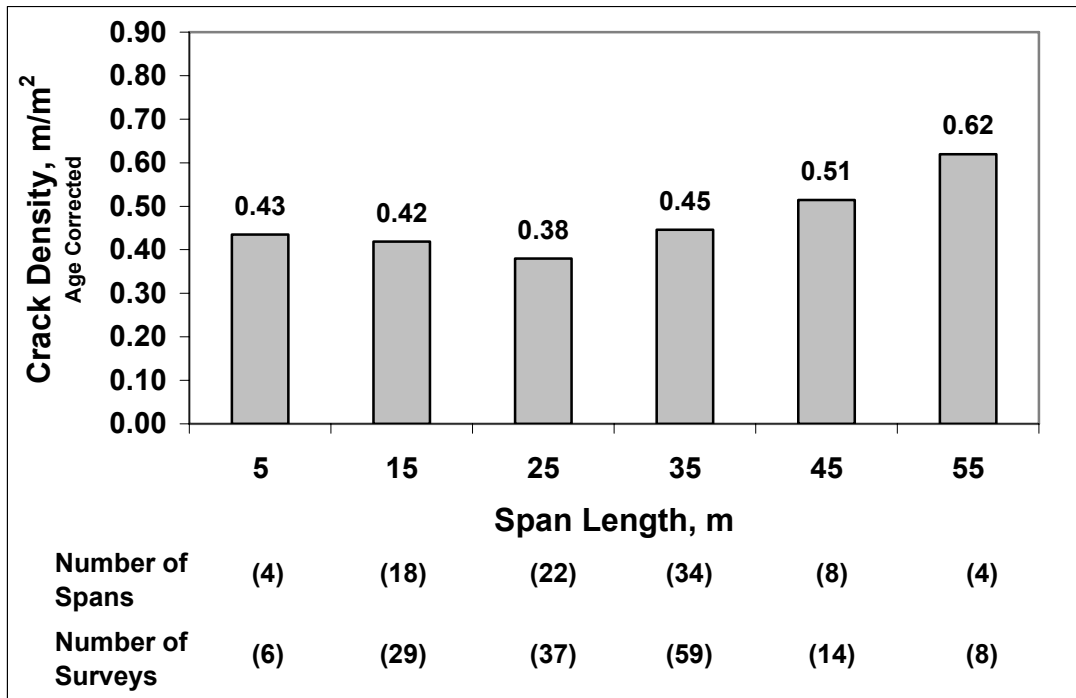


Fig. 5.53 – Mean crack density for individual spans corrected to an age of 78 months versus span length for 5% and 7% silica fume overlay bridges.

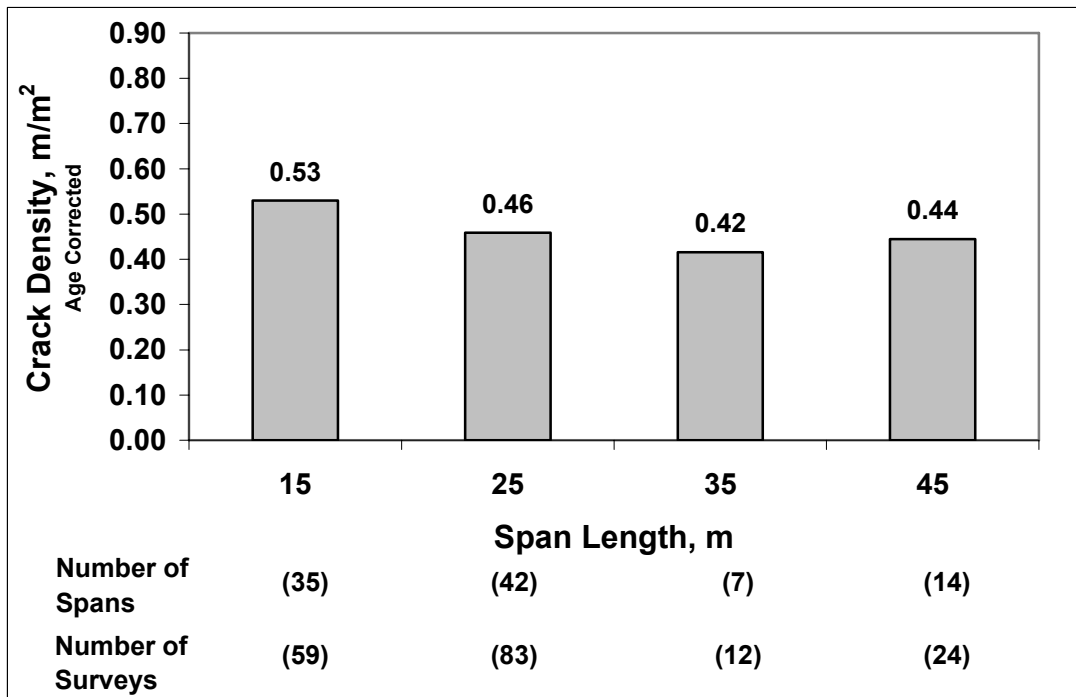


Fig. 5.54 – Mean crack density for individual spans corrected to an age of 78 months versus span length for conventional overlay bridges.

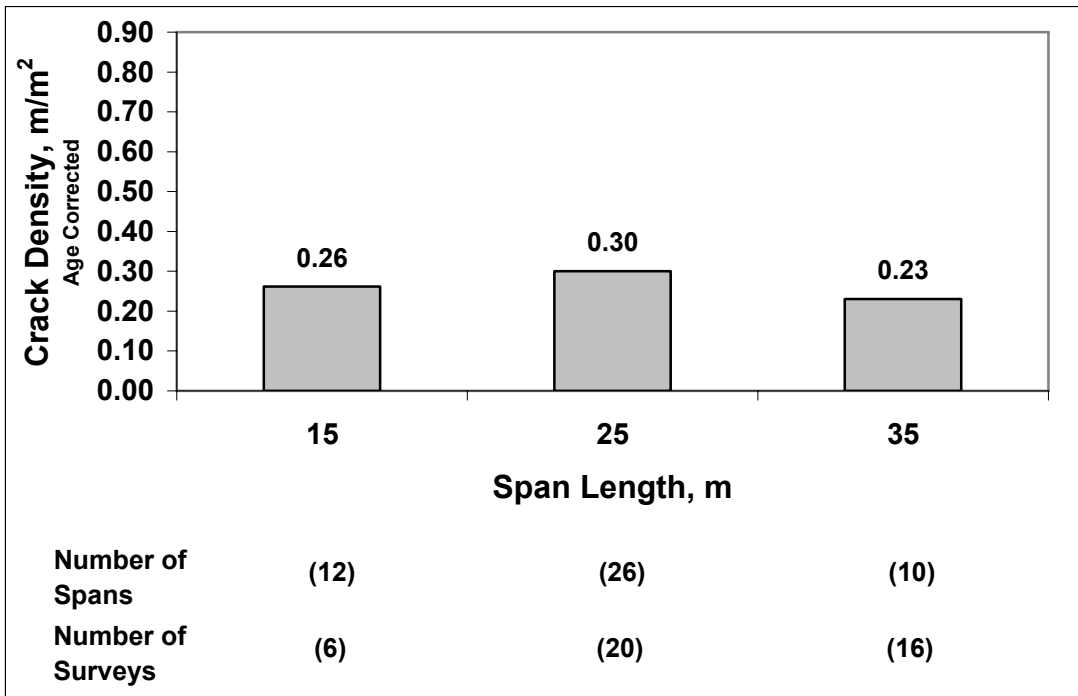


Fig. 5.55 – Mean crack density for individual spans corrected to an age of 78 months versus span length for monolithic bridges.

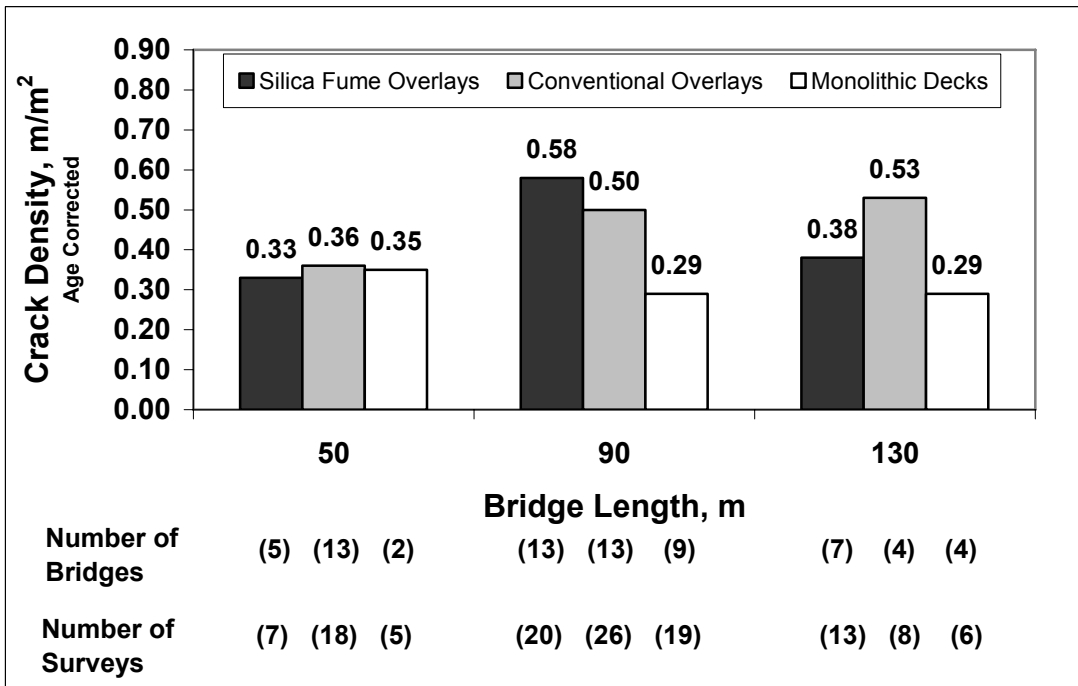


Fig. 5.56 – Mean crack density for bridge decks corrected to an age of 78 months versus bridge length for 5% and 7% silica fume overlay, conventional overlay, and monolithic bridges.

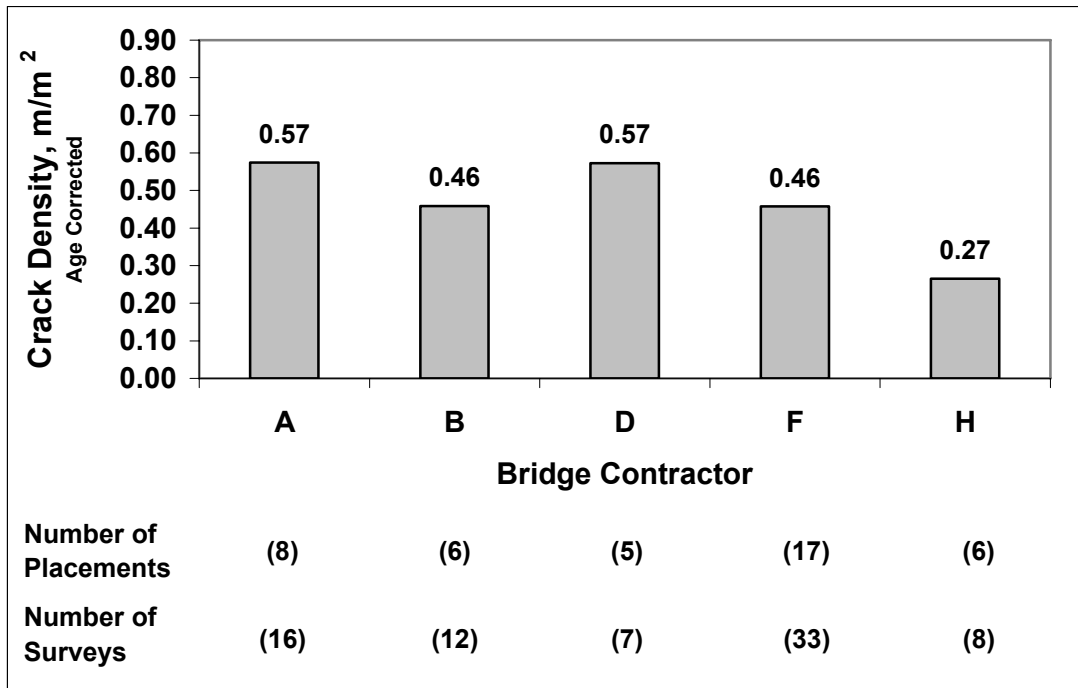


Fig. 5.57 – Mean crack density for individual placements corrected to an age of 78 months versus bridge contractor (names withheld) for 5% and 7% silica fume overlay placements.

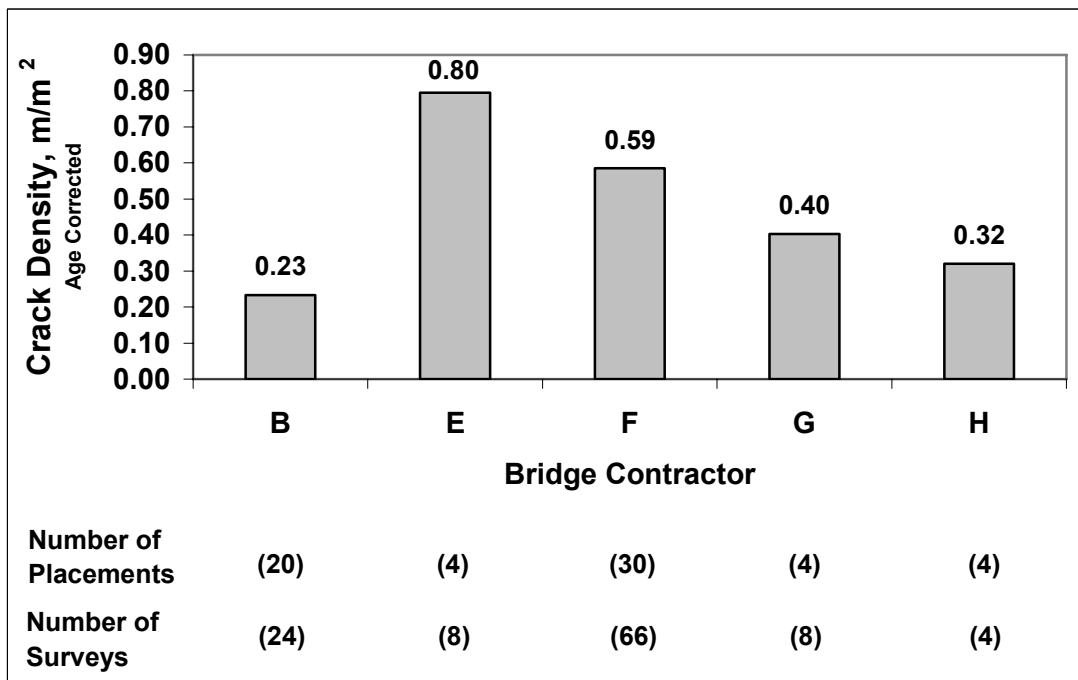


Fig. 5.58 – Mean crack density for individual placements corrected to an age of 78 months versus bridge contractor (names withheld) for conventional overlay placements.

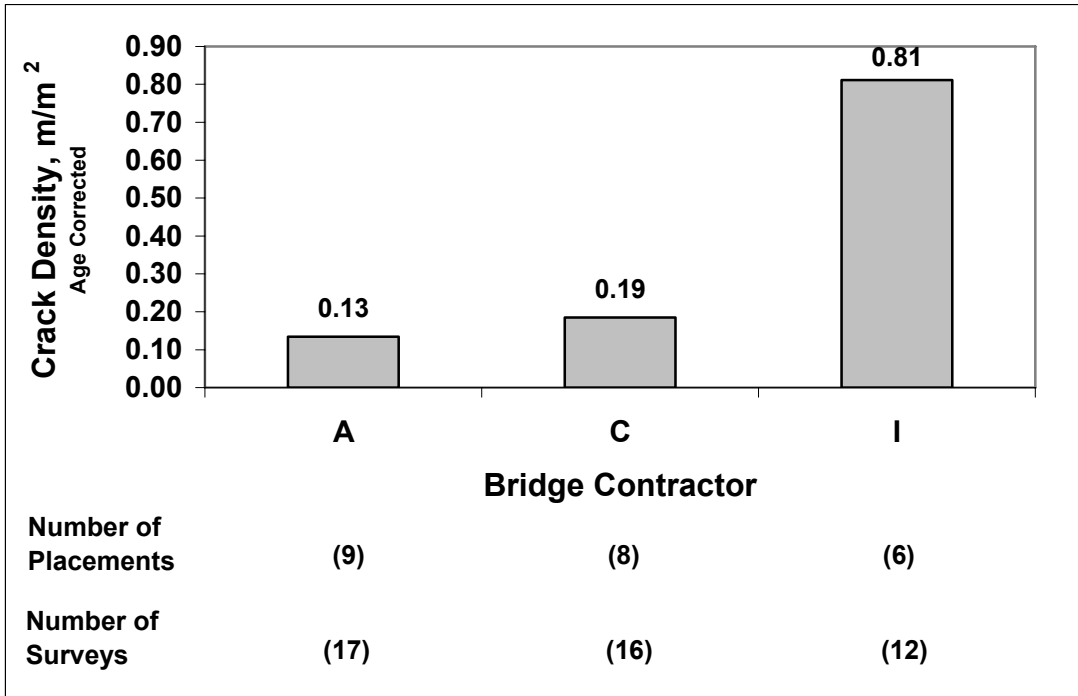


Fig. 5.59 – Mean crack density for individual placements corrected to an age of 78 months versus bridge contractor (names withheld) for monolithic placements.

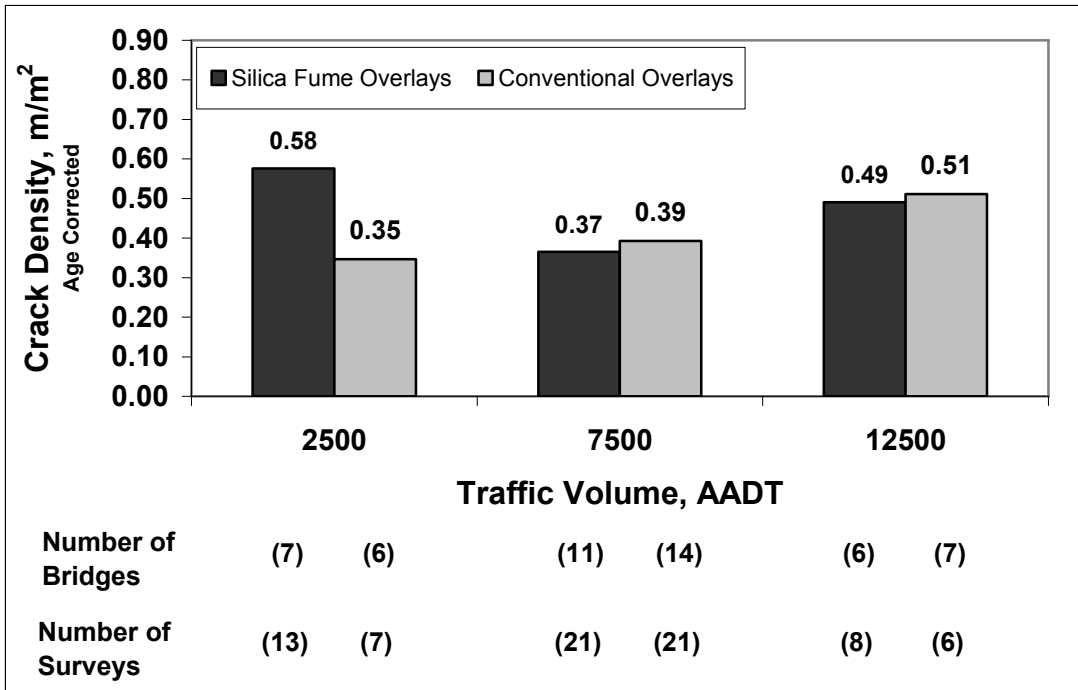


Fig. 5.60 – Mean crack density for entire bridge decks corrected to an age of 78 months versus traffic volume for 5% and 7% silica fume overlays and conventional overlays.

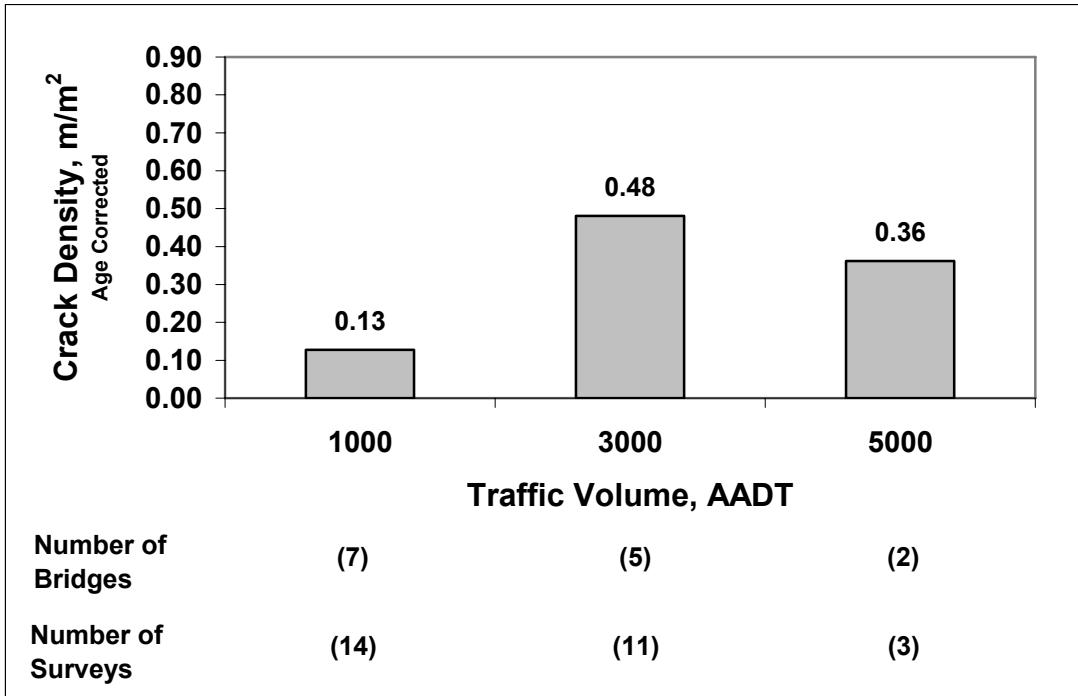


Fig. 5.61 – Mean crack density for entire bridge decks corrected to an age of 78 months versus traffic volume for monolithic bridge decks.

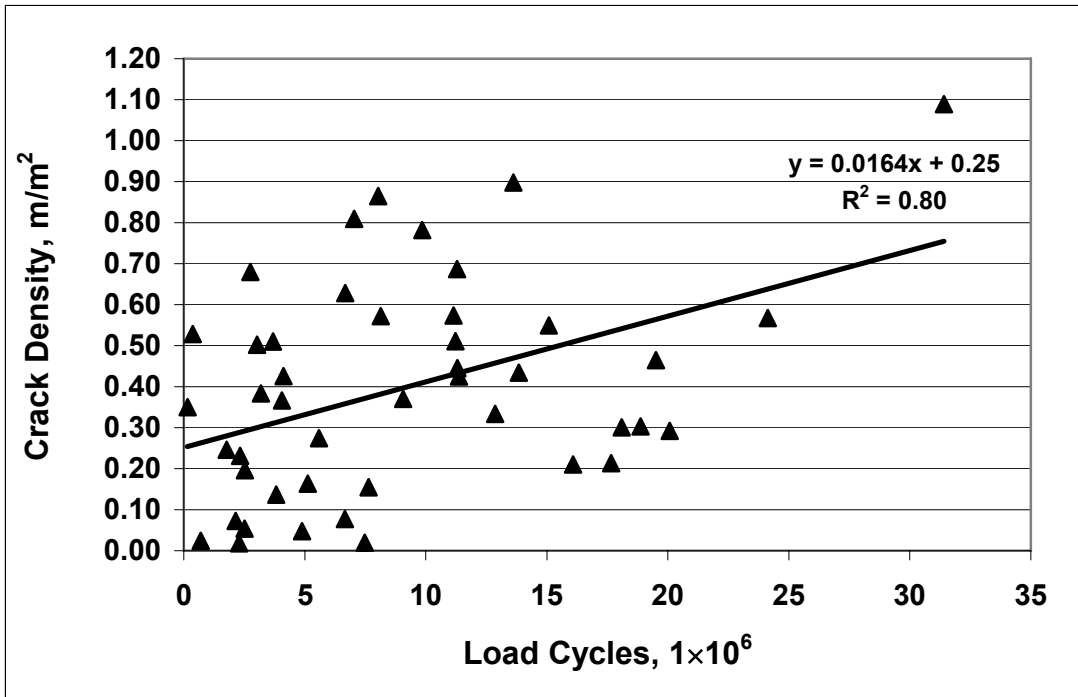


Fig. 5.62 – Crack density and dummy variable analysis results for bridge decks versus total number of load cycles for 5% and 7% silica fume overlay bridges.

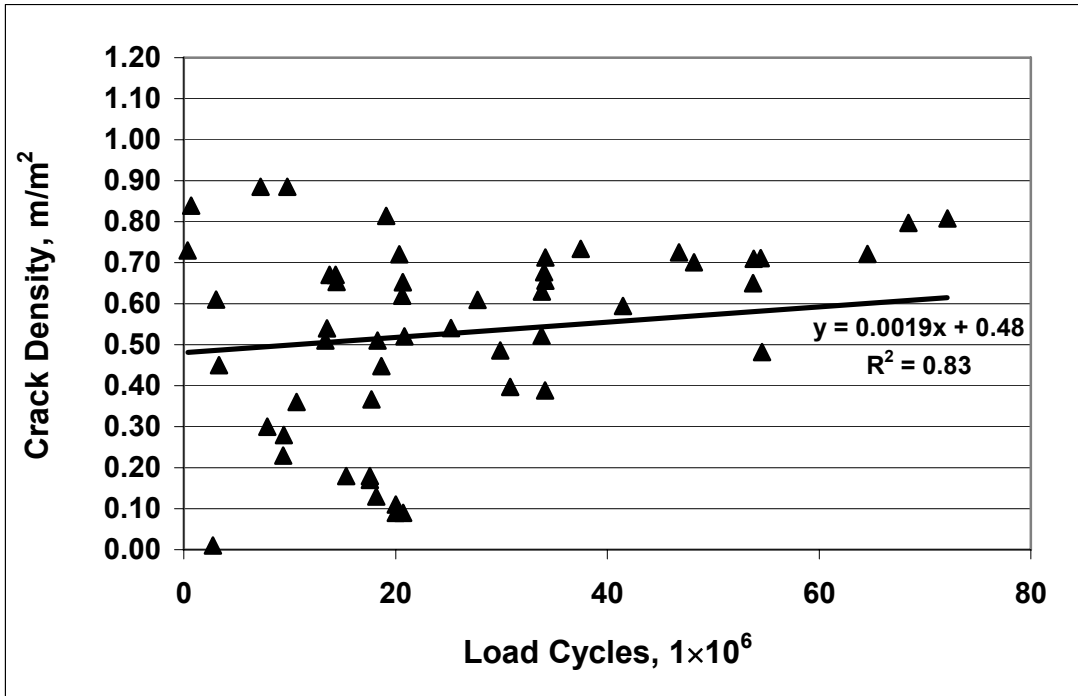
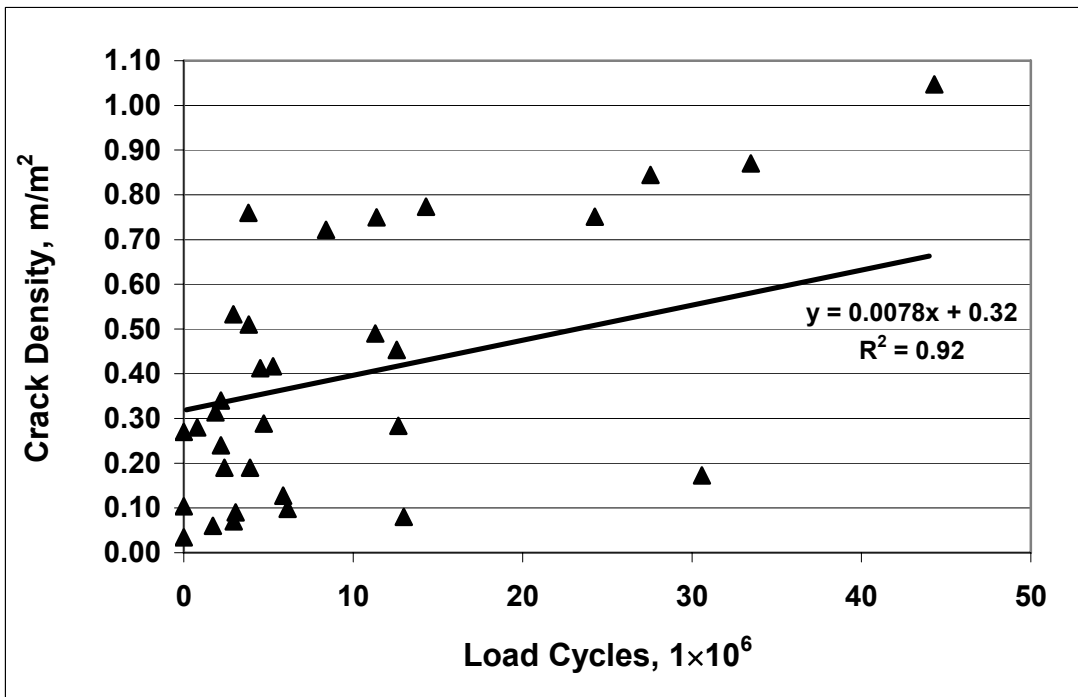


Fig. 5.63 – Crack density and dummy variable analysis results for bridge decks versus total number of load cycles for conventional overlay bridges.



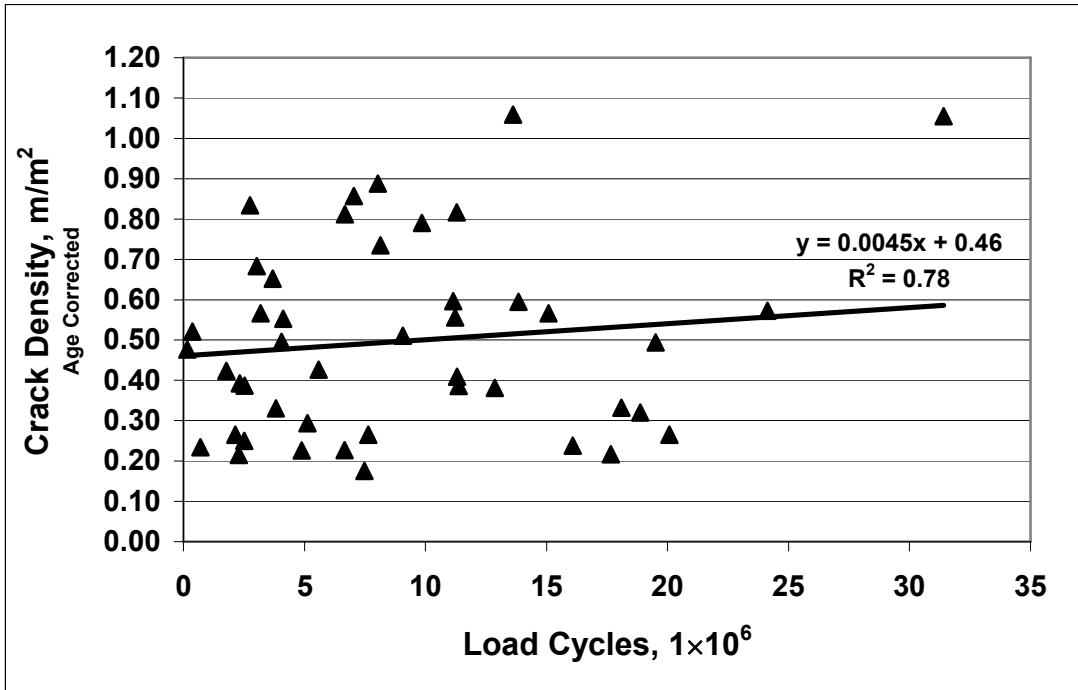


Fig. 5.65 – Crack density and dummy variable analysis results for bridge decks corrected to an age of 78 months versus total number of load cycles for 5% and 7% silica fume overlay bridges.

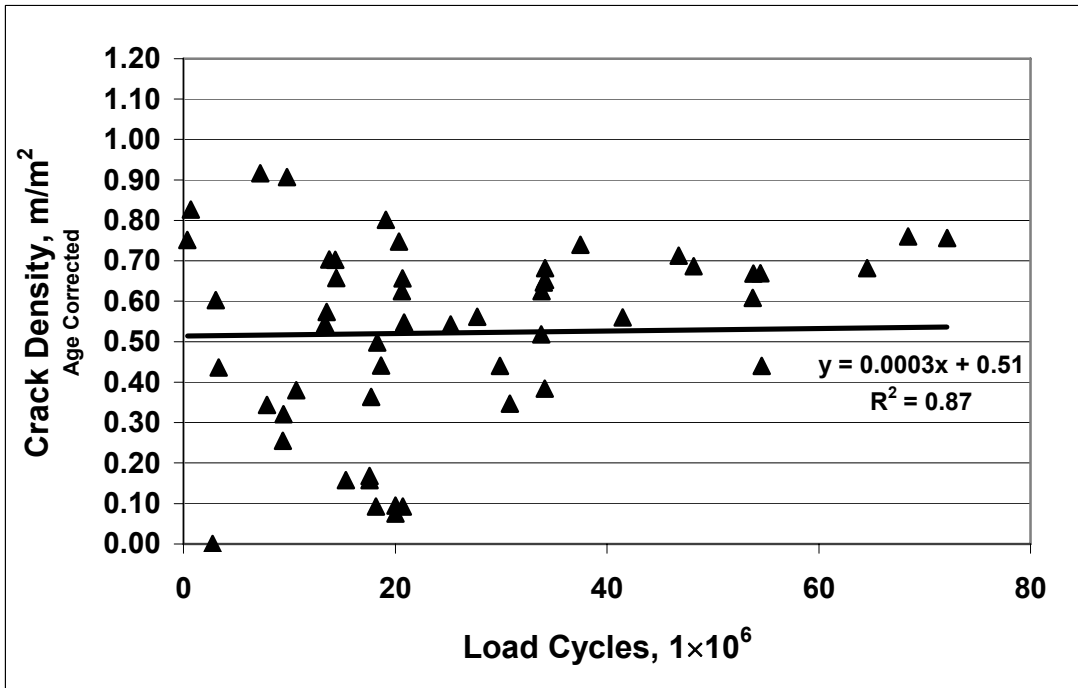


Fig. 5.66 – Crack density and dummy variable analysis results for bridge decks corrected to an age of 78 months versus total number of load cycles for conventional overlay bridges.

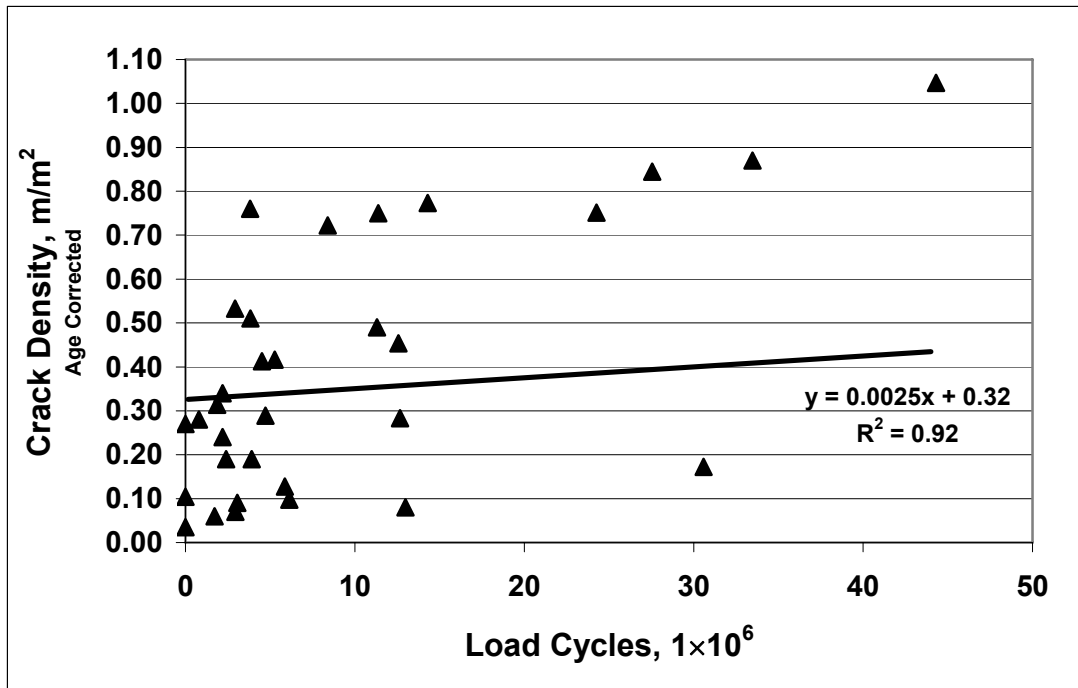


Fig. 5.67 – Crack density and dummy variable analysis results for bridge decks corrected to an age of 78 months versus total number of load cycles for monolithic bridges.

**APPENDIX A**  
**BRIDGE DECK DATA**

Table A.1 – Bridge Data and Deck Properties for 7% Silica Fume Overlays

Bridge Number	Deck Type	Structure Type	Bridge Skew (deg.)	Bridge Length		Total Deck Thickness (mm) (in.)	Overlay Thickness (mm) (in.)		Top Cover (mm) (in.)		Transverse Steel		Angle of Rebar (deg.)			
				(m)	(ft)		(mm)	(in.)	Size (mm)	No.	Spacing (mm) (in.)					
30-93	7% SFO	SMCC	20	70.5	231	220	8.66	40	1.6	75	3.0	16	5	150	5.9	0
40-92	7% SFO	SWCC	0	100.0	328	220	8.66	40	1.6	75	3.0	16	5	180	7.1	0
40-93	7% SFO	SWCC	0	100.0	328	220	8.66	40	1.6	75	3.0	16	5	180	7.1	0
46-332	7% SFO	SMCC	56	76.5	251	220	8.66	40	1.6	75	3.0	16	5	170	6.7	0
81-53	7% SFO	SWCH	0	37.8	124	220	8.66	40	1.6	75	3.0	16	5	180	7.1	0
85-148	7% SFO	WWCH	58	110.0	361	220	8.66	40	1.6	75	3.0	16	5	150	5.9	0
85-149	7% SFO	SWCC	58	111.6	366	220	8.66	40	1.6	75	3.0	16	5	150	5.9	0
89-269	7% SFO	SWCC	39	65.2	214	222	8.75	38	1.5	76	3.0	15, 19	5, 6	152	6.0	0
89-272	7% SFO	SWCC	39	100.6	330	216	8.50	38	1.5	76	3.0	16	5	127	5.0	0
103-56	7% SFO	SMCC	0	70.0	230	220	8.66	40	1.6	80	3.1	19	6	175	6.9	0

Table A.2 – Mix Design Information for 7% Silica Fume Overlay Bridge Placements

Bridge Number	Portion Placed	Date of Placement	Water Content (kg/m <sup>3</sup> ) (lb/yd <sup>3</sup> )	Cement Content (kg/m <sup>3</sup> ) (lb/yd <sup>3</sup> )	Silica Fume Content (kg/m <sup>3</sup> ) (lb/yd <sup>3</sup> )	W/CM Ratio	Volume of W+C+SF	Types of Admixtures
30-93	Subdeck	07/19/01	143	357	0	0.40	25.6	GGBFS <sup>†</sup> , AEA, Type A
30-93	Deck	08/04/01	138	223	26	0.37	26.4	GGBFS <sup>†</sup> , AEA, Type A, Type F
40-92	Subdeck	10/19/01	143	357	0	0.40	25.6	AEA, Type F
40-92	Deck	10/26/01	138	346	26	0.37	26.0	AEA, Type A, Type F
40-93	Subdeck	09/20/01	143	357	0	0.40	25.6	AEA, Type F
40-93	Deck	10/16/01	138	346	26	0.37	26.0	AEA, Type A, Type F
46-332	Subdeck	11/15/01	143	357	0	0.40	25.6	AEA, Type A, Type F
46-332	Deck	05/15/02	138	346	26	0.37	26.0	AEA, Type A, Type F
81-53	Subdeck	02/10/00	143	357	0	0.40	25.6	AEA, type A
81-53	Deck	02/21/00	138	346	26	0.37	26.0	AEA, Type A, Type F
85-148	Subdeck	10/11/01	143	357	0	0.40	25.6	--
85-148	East	10/27/01	138	346	26	0.37	26.0	AEA, Type A, Type F, Type I
85-148	West	10/30/01	138	346	26	0.37	26.0	AEA, Type A, Type F, Type I
85-149	Subdeck	08/22/02	143	357	0	0.40	25.6	--
85-149	Deck	09/26/02	138	346	26	0.37	26.0	AEA, Type A, Type F, Type I
89-269	Subdeck	06/14/01	157	357	0	0.44	27.1	AEA
89-269	Deck -- West	07/26/01	137	345	26	0.37	25.8	AEA
89-269	Deck -- East	07/31/01	137	345	26	0.37	25.8	AEA
89-272	Subdeck	11/06/01	157	357	0	0.44	27.1	AEA
89-272	Deck -- West	04/04/02	137	345	26	0.37	25.8	AEA
89-272	Deck -- East	04/10/02	137	345	26	0.37	25.8	AEA

**Table A.2 (con't) – Mix Design Information for 7% Silica Fume Overlay Bridge Placements**

Bridge Number	Portion Placed	Date of Placement	Water Content (kg/m <sup>3</sup> ) (lb/yd <sup>3</sup> )	Cement Content (kg/m <sup>3</sup> ) (lb/yd <sup>3</sup> )	Silica Fume Content (kg/m <sup>3</sup> ) (lb/yd <sup>3</sup> )	W/CM Ratio	Volume of W+C+SF	Types of Admixtures
103-56	Subdeck	09/14/01	150 253	375 632	0 0	0.40	26.9	AEA
103-56	Deck -- Right	10/12/01	138 233	346 583	26 44	0.37	26.0	AEA, Type II
103-56	Deck -- Left	10/17/01	138 233	346 583	26 44	0.37	26.0	AEA, Type II

\*Contains 33% Ground Granulated Blast Furnace Slag (GGBFS) by weight of cementitious materials.

-- Denotes missing data.

Table A.3 – Field Information and Site Conditions for 7% Silica Fume Overlay Bridge Placements

Bridge Number	Portion Placed	Date of Placement	Average Slump		Compressive Strength (MPa)	Air Content (%)	Air Temperature								
			(mm)	(in.)			Low (C)	Low (F)	High (C)	High (F)	Range (C)	Range (F)	Average (C)	Average (F)	
30-93	Subdeck	07/19/01	87	3.4	42	6110	6.4	--	--	--	--	--	--	--	--
30-93	Deck	08/04/01	55	2.2	54	7880	4.0	--	--	--	--	--	--	--	--
40-92	Subdeck	10/19/01	110	4.3	37	5370	5.5	5	41	21	70	16	61	13	55
40-92	Deck	10/26/01	90	3.5	60	8630	7.4	6	43	18	64	12	54	12	54
40-93	Subdeck	09/20/01	139	5.5	34	4910	5.6	21	70	29	84	8	46	25	77
40-93	Deck	10/16/01	103	4.0	52	7590	8.0	1	34	17	63	16	61	9	48
46-332	Subdeck	11/15/01	62	2.4	47	6850	5.9	12	54	22	72	10	50	17	63
46-332	Deck	05/15/02	112	4.4	63	9100	3.8	16	61	25	77	9	48	21	69
81-53	Subdeck	02/10/00	60	2.4	32	4640	7.0	3	37	7	45	4	39	5	41
81-53	Deck	02/21/00	61	2.4	49	7160	5.7	4	39	9	48	5	41	7	44
85-148	Subdeck	10/11/01	65	2.6	41	5870	5.8	6	43	21	70	15	59	14	56
85-148	West	10/30/01	72	2.8	44	6330	6.0	8	46	23	73	15	59	16	60
85-148	East	10/27/01	65	2.6	52	7600	6.5	7	45	22	72	15	59	15	58
85-149	Subdeck	08/22/02	60	2.4	38	5450	6.5	20	68	35	95	15	59	28	82
85-149	Deck	09/26/02	78	3.1	50	7200	6.5	14	57	24	75	10	50	19	66
89-269	Subdeck	06/14/01	--	--	--	--	--	16	61	28	82	12	53	22	72
89-269	Deck -- West	07/26/01	83	3.3	--	--	6.5	24	76	29	84	4	40	27	80
89-269	Deck -- East	07/31/01	89	3.5	44	6390	6.5	24	76	36	96	11	52	30	86
89-272	Subdeck	11/06/01	70	2.8	35	5120	6.6	9	48	26	78	17	62	17	63
89-272	Deck -- West	04/04/02	97	3.8	44	6390	6.5	-1	30	18	64	19	66	8	47

**Table A.3 (con't) – Field Information and Site Conditions for 7% Silica Fume Overlays**

Bridge Number	Portion Placed	Date of Placement	Average Slump		Compressive Strength (MPa)	Compressive Strength (psi)	Air Content (%)	Air Temperature							
			(mm)	(in.)				Low (C)	Low (F)	High (C)	High (F)	Range (C)	Range (F)	Average (C)	Average (F)
89-272	Deck -- East	04/10/02	83	3.3	--	--	6.5	6	43	24	76	18	65	15	60
103-56	Subdeck	09/14/01	78	3.1	39	5680	5.8	15	59	33	91	18	64	24	75
103-56	Deck -- Right	10/12/01	67	2.6	--	--	6.4	10	50	21	70	11	52	16	60
103-56	Deck -- Left	10/17/01	83	3.3	47	6830	5.6	3	37	21	70	18	64	12	54

**APPENDIX B  
BRIDGE DECK SURVEY SPECIFICATION**

**DRAFT**

**1.0 DESCRIPTION.**

This specification covers the procedures and requirements to perform bridge deck surveys of reinforced concrete bridge decks.

**2.0 SURVEY REQUIREMENTS.**

**a. Pre-Survey Preparation.**

(1) Prior to performing the crack survey, related construction documents need to be gathered to produce a scaled drawing of the bridge deck. The scale must be exactly 1 in. = 10 ft (for use with the scanning software), and the drawing only needs to include the boundaries of the deck surface.

(3) The scaled drawing should also include compass and traffic directions, deck stationing, and a scaled 5 ft by 5 ft grid on the deck.

(4) For curved bridges, the scaled drawing need not be curved, i.e., the curve may be approximated using straight lines.

(5) Coordinate with traffic control so that at least one side (or one lane) of the bridge can be closed during the time that the crack survey is being performed.

**b. Preparation of Surface.**

(1) After traffic has been closed, station the bridge in the longitudinal direction at ten feet intervals. The stationing shall be done as close to the centerline as possible. For curved bridges, the stationing shall follow the curve.

(2) Prior to beginning the “crack survey,” mark a 5 ft by 5 ft grid using lumber crayons on the portion of the bridge closed to traffic corresponding to the grid on the scaled drawing. Measure and document any drains, repaired areas, unusual cracking, or any other items of interest.

(3) Starting with one end of the closed portion of the deck, begin tracing cracks that can be seen while bending at the waist. After beginning to trace cracks, continue to the end of the crack, even if this includes portions of the crack that were not initially seen while bending at the waist. Areas covered by sand or other debris need not be surveyed. Trace the cracks using a different color crayon than was used to mark the grid and stationing.

(4) At least one person shall check over the marked portion of the deck for any additional cracks. The goal is not to mark every crack on the deck, only those cracks that can initially be seen while bending at the waist.

**c. Weather Limitations.**

(1) Surveys are limited to days when the expected temperature during the survey will not be below 60° F.

(2) Surveys are further limited to days that are forecasted to be at least mostly sunny for a majority of the day.

(3) Regardless of the weather conditions, the bridge deck must be completely dry before the survey can begin.

**3.0 BRIDGE SURVEY.****a. Crack Surveys.**

Using the grid as a guide, transfer the cracks from the deck to the scaled drawing. Areas that are not surveyed should be marked on the scaled drawing. Spalls, regions of scaling, and other areas of special interest need not be included on the scale drawings but should be noted.

**b. Delamination Survey.**

At any time during or after the crack survey, bridge decks shall be checked for delamination. Any areas of delamination shall be noted and drawn on a separate drawing of the bridge. This second drawing need not be to scale.

**c. Under Deck Survey.**

Following the crack and delamination survey, the underside of the deck shall be examined and any unusual or excessive cracking noted.

**APPENDIX C**  
**CRACK DENSITY CALCULATION PROGRAM LISTING**

```

*****
*
* PROGRAM NAME:  AngLen
*
* VERSION:      3.1  originally written in Fortran 77
*
* LAST MODIFIED: September 2, 2003
*
* CREATED BY:   Tony R. Schmitt , 1993
*               University of Kansas
*               Department of Civil Engineering
*
* LAST
* UPDATED BY:  Will D. Lindquist, 2005
*               University of Kansas
*               Department of Civil, Environmental and
*               Engineering
*
* FUNCTION:     Takes an ascii file created from a .tif file,
*               locates pixels that are within a user specified
*               gray-level range, groups pixels that are
*               adjacent to one another (these groups represent
*               cracks), and then calculates the length and
*               then calculates the length and angle of each
*               crack.
*****
*
* INSTRUCTIONS:
*
*   Step 1:     The scale drawing is made of the cracks on the
*               This program is designed to work with a scale of
*               1 inch = 10 feet.
*
*   Step 2:     Photocopy the scale drawing to get a clean copy.
*
*   Step 3:     Scan the drawing into a computer in black and
*               white at 100 dpi and saved as a TIFF image file
*               (uncompressed). Record the image size in pixels
*               for use in the program. The width of the bridge
*               is the X coordinate and the length of the bridge
*               is the Y coordinate.
*
*   Step 4:     Remove all lines from the scanned image file that
*               do not represent cracks. Draw a single black line
*               from the top of the page to the top left corner of
*               the bridge. This represents the starting point.
*
*   Step 5:     Use the programs created by Prof. John Gauch at
*               the University of Kansas. The programs are
*               available at:
*               http://www.ittc.ku.edu/~jgauch/research/kuim/source.html
*
*               The following 2 programs are used as follows:
*

```

```

*          covert_raw -x Xsize -y Ysize TIFFfilename
*          IMfilename Note: the Y dimension needs to be
*          slightly larger than the actual image to get all
*          of the pixel information.
*
*          make_raw -A IMfilename TXTfilename
*
* Step 6:   The ascii file created by this method includes
*          various tags and a number representing the color
*          of each pixel 0 = black and 255 = white. The
*          Anglen program only needs the color of the pixels,
*          so the ascii file must be opened and the tags that
*          do not represent pixel colors must be removed.
*          This can be performed in Microsoft Notepad or
*          Excel. Save the ascii file as a text file or
*          as a space delimited file (*.prn).
*
* Step 7:   The *.txt or *.prn file containing only the pixel
*          colors can then be used as the input file.
*
*****
*
* VARIABLE DEFINITIONS
*
* REAL VARIABLES:
*
* ANGLE      Angle of crack. Horizontal = 0 degrees.
*            Cracks increasing from left to right are positive.
* AREA       Bridge deck area in square meters.
* AREAL      Bridge deck in square feet.
* AREAPLAC   Area of an individual concrete placement.
* D          Distance between two pixels. This is used to
*            establish the length of a given crack.
* DENS       Crack density of a given deck area.
* DIVTOTD    Total crack density of a bridge division.
* DIVTOTL    Total length of all cracks in a division.
* DIVTRD     Transverse crack density of a bridge division.
* DIVTRL     Total length of all transverse cracks in a
*            division.
* LENBERG    Length of bridge in feet.
* LENDIV     Length of each bridge division.
* LENGTH     Length of an individual crack. This is calculated
*            as the greatest distance between any two pixels
*            in a given crack.
* LENPLACE   Length of an individual concrete placement.
* RDIVS      Number of bridge divisions. (real number format)
* RDWY       Width of roadway in feet.
* RHIGH      Real number variation of integer variable HIGH.
* RLOW       Real number variation of integer variable LOW.
* RTEMP      Real number variation of integer variable ITEMP.
* SCALE      Drawing scale in ft./in. Note that many conversion
*            factors are built into the program and must be
*            modified if the scale of the input image is
*            altered.

```

```

*      SKEW          Skew of the end of the bridge in degrees.
*      SPANAREA     Area of an individual span.
*      SPANG        Special angle, in degrees, defined by user to
*                  investigate angles other than the default angles.
*      SPANLEN      Length of a span.
*      SPDENS       Density of cracks at defined special angle.
*      SPTL         Total length of cracks at defined special angle.
*      TLPG         Total length of cracks in a given angle group.
*      TOL          Tolerance, in degrees, for the special angle.
*      TOTDENS      Total crack density.
*      TOTLEN       Total length of all cracks.
*      WIDPLACE     Width of concrete placement.
*      X1           X coordinate of a pixel.
*      X2           X coordinate of a pixel.
*      Y1           Y coordinate of a pixel.
*      Y2           Y coordinate of a pixel.
*
*      INTEGER VARIABLES:
*
*      BOTBND       Bottom bound of bridge section being considered.
*      CHECK        Used in subroutine GROUP to determine when the
*                  last of the pixels have been collected into crack
*                  groups.
*      CHOICE       Represents "main menu" option.
*      CX           X coordinate of a pixel within graylevel range.
*      CY           Y coordinate of a pixel within graylevel range.
*      DIVTOTC      Total number of cracks in a division
*      DIVTRC       Total number of transverse cracks in a division.
*      HIGH         Used to define angle groups.
*      ITEMP        Used to increment YLOCATOR in division analysis.
*      JUMP         The number of rows in the ascii file that
*                  represent
*                  one row of pixels in the .tif file.
*      LDPIX        Length of division in units of pixels.
*      LENPIX       Length of an individual placement in units of
*                  pixels.
*      LEVEL        Graylevel of a pixel. Takes on a value of 0
*                  (black) to 255 (white)
*      LOW          Used to define angle groups
*      LOWER        Lower graylevel bound.
*      LTBND        Left bound. Used to define the section of bridge
*                  being analyzed.
*      N            Total number of pixels in input file.
*      NCL          Limit on number of cracks program will handle.
*      NCPG         Number of cracks per angle group.
*      NUM          Number of additional specified angles
*      NUMCRCKS     Number of cracks.
*      NUMDIVS      Number of divisions.
*      NUMPIX       Number of pixels.
*      NUMPLACE     Number of placements.
*      NUMSPANS     Number of spans.
*      PCL          Limit on maximum number of pixels allowed in a
*                  crack.
*      RDWYPIX      Width of roadway in units of pixels.

```

```

*      RES           Resolution in DPI (dots per inch).
*      RTBND        Right bound. Used to define the section of bridge
*                  being analyzed.
*      SLPIX        Span Length in units of pixels.
*      SPNC         Number of cracks at the specified angle.
*      TCHECK       Total number of cracks in all angle groups.
*      TOPBND       Top bound. Used in defining a span.
*      TPL          Total pixel limit.
*      UPPER        Upper graylevel bound.
*      WIDPIX       Width of a placement in units of pixels.
*      X            X coordinate of a pixel.
*      XCOUNT       Counter used to assign proper X coordinate to a
*                  selected pixel.
*      XEDGE        X coordinate of line used to locate starting
*                  pixel.
*      XLOCATOR     Used to define section of bridge being analyzed.
*      XPERM        Permanent list of X coordinates of pixels within
*                  defined graylevel range.
*      XPT2         Used to define section of bridge being analyzed.
*      XSIZE        Number of pixels along X axis in input image.
*      XSTART       X coordinate of starting point pixel.
*      Y            Y coordinate of a pixel.
*      YBOTPT       Used to define section of bridge being analyzed.
*      YCOUNT      Counter used to assign proper Y coordinate to a
*                  selected pixel.
*      YLOCATOR     Used to define section of bridge being analyzed.
*      YPERM        Permanent list of Y coordinates of pixels within
*                  defined graylevel range.
*      YPT2         Used to define section of bridge being analyzed.
*      YSIZE        Number of pixels along Y axis in input image.
*      YSTART       Y coordinate of starting point pixel.
*      YTOPPT       Used to define section of bridge being analyzed.
*
* CHARACTER VARIABLES:
*
*      INFILE*14    Name of input ascii file.
*      OUTFILE*18   Name of output file.
*      YESNO        See subroutine SPECANG.
*
*****
* BEGIN
*****
PROGRAM MAIN
REAL LENGTH, ANGLE, AREA, DENS, TLPG, SCALE, TOTLEN,
+      TOTDENS, SPANG, SPTL, SPDENS, AREAL, SPANLEN, SKEW, RDWY,
+      SPANAREA, LENBRG, WIDPLACE, AREAPLAC, LENPLACE,
+      RTEMP, RDIVS, LENDIV, DIVTRL, DIVTRD, DIVTOTL, DIVTOTD
INTEGER X, Y, NUMCRCKS, NUMPIX, CX, CY, NCPG, RES, SPNC,
+      TCHECK, LOWER, UPPER, N, TPL, PCL, NCL, XPERM, YPERM,
+      CHOICE, NUMSPANS, XLOCATOR, YLOCATOR, LTBND, RTBND,
+      RTBND, BOTBND, TOPBND, XPT2, YPT2, RDWYPIX, SLPIX,
+      YTOPPT, YBOTPT, NUMPLACE, WIDPIX, LENPIX, ITEMP, LDPIX,
+      NUMDIVS, XSTART, YSTART, DIVTRC, DIVTOTC, JOUT
CHARACTER INFILE*14, OUTFILE*18

```

```

        DIMENSION      X(900000),Y(900000),NUMPIX(8000),CX(4000,4000),
+
+       CY(4000,4000),LENGTH(3000),ANGLE(3000),
+       NCPG(20),TLPG(20),DENS(20),SPANG(10),SPNC(10),
+       SPTL(10),SPDENS(10),XPERM(800000),YPERM(800000),
+       SPANLEN(12),SLPIX(12),SPANAREA(12),WIDPLACE(8),
+       WIDPIX(8),AREAPLAC(8),LENPLACE(8),LENPIX(8),
+       DIVTRC(100),DIVTRL(100),DIVTRD(100),DIVTOTC(100),
+       DIVTOTL(100),DIVTOTD(100)
*****
*   INPUT INFORMATION SECTION
*
        RES = 100
        SCALE = 10.0
        TPL = 800000
        PCL = 6000
        NCL = 3000
        WRITE(6, 1009)
1009  FORMAT (//, 'CURRENT SETTINGS:')
        WRITE(6,*) ' '
        WRITE(6,*) ' Resolution (DPI).....',RES
        WRITE(6,*) ' Drawing Scale (ft./in.).....',SCALE
        WRITE(6,*) ' Total Pixel Limit.....',TPL
        WRITE(6,*) ' Pixels per Crack Limit.....',PCL
        WRITE(6,*) ' Number of Cracks Limit.....',NCL
        WRITE(6,*) ' Lower Graylevel Bound (suggested)... 0'
        WRITE(6,*) ' Upper Graylevel Bound (suggested)... 200'
        WRITE(6,*) ' '
        WRITE (6,*) 'ENTER INPUT FILE NAME.'
        READ (5,1010) INFILE
1010  FORMAT(A)
        WRITE (6,*) 'ENTER LOWER GRAYLEVEL BOUND.'
        READ (5,*) LOWER
        WRITE (6,*) 'ENTER UPPER GRAYLEVEL BOUND.'
        READ (5,*) UPPER
        WRITE (6,*) ' '
*
*****
*   MAIN SECTION
*
CCC=> The following subroutine scans the ascii file, records the
C     coordinates of each pixel within the specified gray-level
C     range, and identifies the starting point pixel from which all
C     distances are measured (span length, placement width, etc.).
C     and identifies the starting point pixel from which all
*
        CALL COORDS (INFILE,XPERM,YPERM,LOWER,UPPER,N,XSTART,YSTART)
*
CCC=> The following lines represent the program's "main menu". The
C     IF statement in line 699 divides the main program into
C     sections containing the commands for each menu option.
*
701  WRITE(6,*) ' '
        WRITE (6, *) 'CRACK DENSITY CALCULATION OPTIONS.'
        WRITE(6,*) ' (1) ENTIRE BRIDGE'

```

```

WRITE(6,*)' (2) SPANS'
WRITE(6,*)' (3) PLACEMENTS'
WRITE(6,*)' (4) DIVISIONS'
WRITE(6,*)' (5) FIRST AND LAST DIVISON'
WRITE(6,*)' (6) QUIT'
WRITE(6,*)' '
WRITE(6,*)'ENTER CHOICE.'
700 READ(5,*) CHOICE
   IF ((CHOICE.LT.1) .OR. (CHOICE.GT.6)) THEN
       WRITE(6,*)'ENTER 1, 2, 3, 4, 5, OR 6.'
       GO TO 700
   END IF
*
*****
CCC=>Option 1 -- Entire Bridge.
C   This section taken alone is essentially the same as version
C   1.0 of this program.
*
699 IF (CHOICE .EQ. 1) THEN
      DO 702 I = 1,N
          X(I) = XPERM(I)
          Y(I) = YPERM(I)
702  CONTINUE
      WRITE (6, '(//,A)') 'ENTER OUTPUT FILE NAME.'
      READ (5,1010) OUTFILE
      OPEN (13, FILE = OUTFILE, STATUS = 'UNKNOWN')
      WRITE (6, '(//,A)') 'ENTER BRIDGE DECK AREA (ft.^2).'
      READ (5,*) AREA
      AREA1 = AREA
      AREA = AREA*(0.09290304)
*
      WRITE(13, *) OUTFILE
      WRITE(13,*) ''
      WRITE (13,*) 'OPTION 1: ENTIRE BRIDGE'
      WRITE(13,*) ''
      WRITE(13,*)'AREA = ',AREA1,' (ft^2)'
      WRITE(13,*)'AREA = ',AREA,' (m^2)'
      WRITE(13,*)''
*
      CALL GROUP (N, X, Y, NUMCRCKS, NUMPIX, CX, CY)
      CALL CALCS (NUMCRCKS, NUMPIX, ANGLE, LENGTH, CX, CY)
      CALL OUTINFO (NUMCRCKS, ANGLE, LENGTH, AREA, NCPG,
+                 TLPG,TOTLEN,TOTDENS, TCHECK, DENS)
      CALL OUTPUT (NCPG, TLPG,DENS,TCHECK,AREA,AREA1,NUMCRCKS,
+                 TOTLEN, TOTDENS, OUTFILE)
      CALL SPECANG (AREA, NUMCRCKS, ANGLE, LENGTH, SPANG, SPNC,
+                 SPTL, SPDENS)
*
      CLOSE(13)
      GO TO 701
*
*****
CCC=>Option 2 -- Spans.
*

```

```

ELSEIF (CHOICE .EQ. 2) THEN
  WRITE(6,*)'ENTER OUTPUT FILE NAME.'
  READ(5, 1010) OUTFILE
  OPEN(13, FILE = OUTFILE, STATUS = 'UNKNOWN')
  WRITE(6,'(//,A)')'ENTER WIDTH OF ROADWAY. (ft.)'
  READ(5,*) RDWY
  RDWYPIX = NINT(RDWY*10)
  WRITE(6,'(//,A)')'ENTER NUMBER OF SPANS.'
  READ(5, *)NUMSPANS
  DO 710 I = 1,NUMSPANS
    WRITE(6,*)'ENTER LENGTH OF SPAN',I,'. (ft.)'
    WRITE(6,*)'(NOTE: Span 1 is at the top of the TIFF
+ image.)'
    READ(5,*)SPANLEN(I)
    SLPIX(I) = NINT(SPANLEN(I)*10)
    SPANAREA(I) = SPANLEN(I) *RDWY
    SPANAREA(I) = SPANAREA(I)*(0.09290304)
710  CONTINUE
    WRITE(6,'(//,A)')'ENTER SKEW. [(+) OP. (-) DEGREES]'
    READ(5,*) SKEW
    XLOCATOR = XSTART
    YLOCATOR = YSTART
    LTBND = XSTART
    RTBND = LTBND + RDWYPIX
    DO 712 I = 1, NUMSPANS
      AREA = SPANAREA(I)
      AREA1 = AREA/0.09290304
      IF (SKEW .EQ. 0) THEN
        BOTBND = YLOCATOR + SLPIX(I)
        TOPBND = YLOCATOR
        DO 714 J = 1,N
          IF ((XPERM(J).LT.LTBND).OR.(XPERM(J).GT.RTBND)) THEN
            X(J) = 0
            Y(J) = 0
          ELSEIF
+ ((YPERM(J).LT.TOPBND).OR.(YPERM(J).GT.BOTBND))THEN
            X(J) = 0
            Y(J) = 0
          ELSE
            X(J) = XPERM(J)
            Y(J) = YPERM(J)
          END IF
714  CONTINUE
        ELSE
          YPT2 = YLOCATOR - NINT(TAND(SKEW)*RDWY*10)
          XPT2 = RTBND
          DO 716 J = 1,N
            IF ((XPERM(J).LT.LTBND).OR.(XPERM(J).GT.RTBND)) THEN
              X(J) = 0
              Y(J) = 0
            ELSE
              YTOPPT = YLOCATOR + ( (-XPERM (J) +XLOCATOR) *
+ (YLOCATOR-YPT2) ) /RDWYPIX
              YBOTPT = YTOPPT + SLPIX(I)

```

```

                IF((YPERM(J).LT.YTOPPT).OR.(YPERM(J).GT.YBOTPT))THEN
                    X(J) = 0
                    Y(J) = 0
                ELSE
                    X(J) = XPERM(J)
                    Y(J) = YPERM(J)
                ENDIF
            ENDIF
716          CONTINUE
        ENDIF
*
        WRITE(13, *) OUTFILE
        WRITE(13,*) ''
        WRITE (13,*) 'OPTION 2: SPANS'
        WRITE(13,*) ''
        WRITE(13,*)'AREA = ',AREA1,' (ft^2)'
        WRITE(13,*)'AREA = ',AREA,' (m^2)'
        WRITE(13,*)''
        WRITE(13,*)'SPAN #:',I
        WRITE(13,*)'SPAN LENGTH (ft):',SPANLEN(I)
        WRITE(13,*)''
*
        CALL GROUP (N, X, Y, NUMCRCKS, NUMPIX, CX, CY)
        CALL CALCS (NUMCRCKS, NUMPIX, ANGLE, LENGTH, CX, CY)
        CALL OUTINFO (NUMCRCKS,ANGLE,LENGTH,AREA,NCPG,TLPG,TOTLEN,
+          TOTDENS, TCHECK, DENS)
+       CALL OUTPUT (NCPG,TLPG,DENS,TCHECK,AREA,AREA1,NUMCRCKS,
+          TOTLEN,TOTDENS,OUTFILE)
+       CALL SPECANG (AREA, NUMCRCKS, ANGLE, LENGTH, SPANG, SPNC,
+          SPTL, SPDENS)
        YLOCATOR = YLOCATOR + SLPIX(I)
*
712          CONTINUE
          CLOSE (13)
          GO TO 701
*
*****
CCC=>Option 3 -- Placements.
*
        ELSEIF (CHOICE .EQ. 3) THEN
            WRITE(6,*)'ENTER OUTPUT FILE NAME.'
            READ(5, 1010) OUTFILE
            OPEN(13, FILE = OUTFILE, STATUS = 'UNKNOWN')
            WRITE(6,'(//,A)')'ENTER SKEW. [(+) OR (-) DEGREES]'
            READ(5,*) SKEW
            WRITE(6,'(//,A)')'PLACEMENTS ARE . . .'
            WRITE(6,*)' (1) FULL LENGTH/PARTIAL WIDTH'
            WRITE(6,*)' (2) PARTIAL LENGTH/FULL WIDTH'
            WRITE(6,*)' '
            WRITE(6,*) 'ENTER CHOICE.'
720          READ(5,*) CHOICE
            IF ((CHOICE.NE.1) .AND. (CHOICE.NE.2)) THEN
                WRITE(6,*)'ENTER 1 OR 2.'
                GO TO 720
            
```

```

ENDIF
IF (CHOICE .EQ. 1) THEN
  WRITE(6, '(//,A)') 'ENTER LENGTH OF BRIDGE. (ft.)'
  READ(5, *) LENBRG
  WRITE(6, '(//,A)') 'ENTER NUMBER OF PLACEMENTS.'
  READ(5, *) NUMPLACE
  DO 722 I = 1, NUMPLACE
    WRITE(6, *) 'ENTER WIDTH OF PLACEMENT' , I, '. (ft.)'
    READ(5, *) WIDPLACE(I)
    WIDPIX(I) = NINT(WIDPLACE(I)*10)
    AREAPLAC(I) = LENBRG * WIDPLACE(I)*0.09290304
722  CONTINUE
    XLOCATOR = XSTART
    DO 724 I = 1, NUMPLACE
      LTBND = XLOCATOR
      RTBND = LTBND + WIDPIX(I)
      AREA = AREAPLAC (I)
      AREA1 = AREA/0.09290304
      DO 726 J = 1, N
        IF ((XPERM(J) .LT. LTBND) .OR. (XPERM(J) .GT.
          + RTBND)) THEN
          X(J) = 0
          Y(J) = 0
        ELSE
          X(J) = XPERM(J)
          Y(J) = YPERM(J)
        ENDIF
726  CONTINUE
      *
      WRITE(13, *) 'OUTFILE'
      WRITE(13, *) ''
      WRITE (13, *) 'OPTION 3: PLACEMENTS'
      WRITE(13, *) ''
      WRITE(13, *) 'AREA = ', AREA1, ' (ft^2)'
      WRITE(13, *) 'AREA = ', AREA, ' (m^2)'
      WRITE(13, *) ''
      WRITE(13, *) 'FULL LENGTH / PARTIAL WIDTH'
      WRITE(13, *) 'PLACEMENT #:', I
      WRITE(13, *) 'WIDTH OF PLACEMENT (ft):', WIDPLACE(I)
      WRITE(13, *) ''
      *
      CALL GROUP (N, X, Y, NUMCRCKS, NUMPIX, CX, CY)
      CALL CALCS (NUMCRCKS, NUMPIX, ANGLE, LENGTH, CX, CY)
      CALL OUTINFO (NUMCRCKS, ANGLE, LENGTH, AREA, NCPG, TLPG, TOTLEN,
+         TOTDENS, TCHECK, DENS)
      CALL OUTPUT (NCPG, TLPG, DENS, TCHECK, AREA, AREA1,
+         NUMCRCKS, TOTLEN, TOTDENS, OUTFILE)
      CALL SPECANG (AREA, NUMCRCKS, ANGLE, LENGTH, SPANG, SPNC,
+         SPTL, SPDENS)
      *
      XLOCATOR = RTBND
724  CONTINUE
    ELSE
      WRITE(6, *) 'ENTER NUMBER OF PLACEMENTS.'

```

```

READ(5, *) NUMPLACE
WRITE(6,*)'ENTER WIDTH OF ROADWAY. (ft.^2).'
```

730

```

READ(5,*) RDWY
RDWYPIX = NINT(RDWY*10)
DO 730 I = 1,NUMPLACE
  WRITE(6,*)'ENTER LENGTH OF PLACEMENT',I,'. (ft.).'
  READ(5,*) LENPLACE(I)
  LENPIX(I) = NINT(LENPLACE(I)*10)
  AREAPLAC(I) = RDWY * LENPLACE(I) *0.09290304
CONTINUE
XLOCATOR = XSTART
YLOCATOR = YSTART
LTBND = XSTART
RTBND = LTBND + RDWYPIX
DO 732 I = 1,NUMPLACE
  AREA = AREAPLAC(I)
  AREA1 = AREA/0.09290304
  IF (SKEW .EQ. 0) THEN
    BOTBND = YLOCATOR + LENPIX(I)
    TOPBND = YLOCATOR
    DO 734 J = 1,N
      IF ((XPERM(J).LT.LTBND).OR.(XPERM(J).GT.RTBND))THEN
        X(J) = 0
        Y(J) = 0
      ELSEIF((YPERM(J).LT.TOPBND).OR.(YPERM(J).GT.BOTBND))
        THEN
        X(J) = 0
        Y(J) = 0
      ELSE
        X(J) = XPERM(J)
        Y(J) = YPERM(J)
      END IF
    CONTINUE
  ELSE
    YPT2 = YLOCATOR - NINT(TAND(SKEW)*RDWY*10)
    XPT2 = RTBND
    DO 736 J = 1,N
      IF ((XPERM(J) .LT. LTBND) .OR. (XPERM(J) .GT. RTBND))
        THEN
        X(J) = 0
        Y(J) = 0
      ELSE
        YTOPPT = YLOCATOR + ( (-XPERM(J) + XLOCATOR)*
          (YLOCATOR-YPT2) ) /RDWYPIX
        YBOTPT = YTOPPT + LENPIX(I)
        IF((YPERM(J).LT.YTOPPT).OR.(YPERM(J).GT.YBOTPT))
          THEN
          X(J) = 0
          Y(J) = 0
        ELSE
          X(J) = XPERM(J)
          Y(J) = YPERM(J)
        END IF
      ENDIF
    ENDIF
  ENDIF

```

```

736      CONTINUE
          ENDIF
*
          WRITE(13, *) OUTFILE
          WRITE(13,*) ''
          WRITE (13,*) 'OPTION 3: PLACEMENTS'
          WRITE(13,*) ''
          WRITE(13,*)'AREA = ',AREA1,' (ft^2)'
          WRITE(13,*)'AREA = ',AREA,' (m^2)'
          WRITE(13,*)''
          WRITE(13,*)'PARTIAL LENGTH / FULL WIDTH'
          WRITE(13,*)'PLACEMENT #:',I
          WRITE(13,*)'LENGHT OF PLACEMENT (ft):',LENPLACE(I)
          WRITE(13,*)''
*
          CALL GROUP (N, X, Y, NUMCRCKS, NUMPIX, CX, CY)
          CALL CALCS (NUMCRCKS, NUMPIX, ANGLE, LENGTH, CX, CY)
          CALL OUTINFO (NUMCRCKS,ANGLE,LENGTH,AREA,NCPG,TLPG,
+                     TOTLEN,TOTDENS, TCHECK, DENS)
          CALL OUTPUT (NCPG,TLPG,DENS,TCHECK,AREA,AREA1,NUMCRCKS,
+                     TOTLEN,TOTDENS,OUTFILE)
          CALL SPECANG (AREA, NUMCRCKS, ANGLE, LENGTH, SPANG,
+                     SPNC,SPTL, SPDENS)
*
          YLOCATOR = YLOCATOR + LENPIX(I)
732      CONTINUE
          ENDIF
          CLOSE(13)
          GO TO 701
*
*****
CCC=>Option 4 -- Divisions.
*
      ELSEIF (CHOICE .EQ. 4) THEN
          WRITE(6,*) 'ENTER OUTPUT FILE NAME.'
          READ(5, 1010)OUTFILE
          OPEN(13, FILE=OUTFILE,STATUS='UNKNOWN')
          WRITE(6,*) 'ENTER WIDTH OF ROADWAY. (ft.)'
          READ(5,*) RDWY
          RDWYPIX = NINT(RDWY*10)
          WRITE(6,*) 'ENTER LENGTH OF BRIDGE. (ft.)'
          READ(5,*) LENBRG
*
*      THE FOLLOWING LINES WERE CHANGED SO THAT THE LENGTH OF
*      DIVISION COULD BE CHOSEN INSTEAD OF THE NUMBER OF DIVISIONS
*      WRITE(6,*) 'ENTER NUMBER OF DIVISIONS.'
*      READ(5,*) NUMDIVS
*      RDIVS = REAL(NUMDIVS)
*      LENDIV = LENBRG/RDIVS
*      LDPIX = NINT(LENDIV*10)
*
*      THE CHANGES START HERE
          WRITE(6,*) 'NOTE!'
          WRITE(6,*) 'THE LAST DIVISION WILL NOT NECESSARILY BE THE

```

```

+           CHOSEN LENGTH'
WRITE(6,*) 'IF THE BRIDGE LENGTH IS NOT EVENLY DIVISIBLE BY
+           THE DIVISION LENGTH'
WRITE(6,*)
WRITE(6,*) 'ENTER LENGTH OF DIVISIONS (ft)'
READ(5,*) LENDIV
LDPIX = NINT(LENDIV*10)
RDIIVS = LENBRG/LENDIV
NUMDIIVS = (INT(RDIIVS)+1)
*
*           END OF CHANGES
*
AREA = LENDIV*RDWY* 0.09290304
AREA1 = AREA/0.09290304
WRITE(6,*) 'ENTER SKEW. [(+) OR (-) DEGREES]'
READ(5,*) SKEW
XLOCATOR = XSTART
YLOCATOR = YSTART
LTBND = XLOCATOR
RTBND = LTBND + RDWYPIX
DO 742 I = 1,NUMDIIVS
  IF (SKEW .EQ. 0) THEN
    BOTBND = YLOCATOR + LDPIX
    TOPBND = YLOCATOR
    DO 744 J = 1,N
      IF ((XPERM(J).LT. LTBND) .OR. (XPERM(J).GT. RTBND))
THEN
        X(J) = 0
        Y(J) = 0
      ELSEIF((YPERM(J).LT.TOPBND) .OR. (YPERM(J).GT.BOTBND))
THEN
        X(J) = 0
        Y(J) = 0
      ELSE
        X(J) = XPERM(J)
        Y(J) = YPERM(J)
      ENDIF
    CONTINUE
  ELSE
    YPT2 = YLOCATOR - NINT(TAND(SKEW)*RDWY*10)
    XPT2 = RTBND
    DO 746 J = 1,N
      IF ((XPERM(J).LT.LTBND) .OR. (XPERM(J).GT.RTBND)) THEN
        X(J) = 0
        Y(J) = 0
      ELSE
        YTOPPT = YLOCATOR + ((-XPERM(J) + XLOCATOR) *
+           (YLOCATOR-YPT2)) / RDWYPIX
        YBOTPT = YTOPPT + LDPIX
        IF((YPERM(J).LT.YTOPPT) .OR. (YPERM(J).GT.YBOTPT)) THEN
          X(J) = 0
          Y(J) = 0
        ELSE
          X(J) = XPERM(J)
          Y(J) = YPERM(J)
        ENDIF
      ENDIF
    ENDIF
  ENDIF
ENDIF

```

```

                ENDIF
                ENDIF
746          CONTINUE
                END IF
*
                CALL GROUP (N, X, Y, NUMCRCKS, NUMPIX, CX, CY)
                CALL CALCS (NUMCRCKS, NUMPIX, ANGLE, LENGTH, CX, CY)
                CALL OUTINFO (NUMCRCKS, ANGLE, LENGTH, AREA, NCPG, TLPG, TOTLEN,
+                 TOTDENS, TCHECK, DENS)
*
                DIVTRC(I) = NCPG(1)
                DIVTRL(I) = TLPG(1)
                DIVTRD(I) = DENS(1)
                DIVTOTC(I) = TCHECK
                DIVTOTL(I) = TOTLEN
                DIVTOTD(I) = TOTDENS
                RTEMP = I*LENDIV*10
                ITEMP = NINT(RTEMP)
                YLOCATOR = YSTART + ITEMP
742          CONTINUE
                DO 747 J = 1,2
                IF (J .EQ. 1) THEN
                    JOUT = 6
                ELSE
                    JOUT = 13
                ENDIF
                WRITE (JOUT, *) OUTFILE
                WRITE(JOUT,*) ''
                WRITE (JOUT,*) 'OPTION 4: DIVISIONS'
                WRITE(JOUT,*)
                WRITE(JOUT,*) 'DIVISION LENGTH =',LENDIV,' (ft.)'
                WRITE(JOUT,*) '                        =',LENDIV*0.3048,' (m)'
                WRITE(JOUT,*) ' '
                WRITE(JOUT,*) 'NUMBER OF DIVISIONS',NUMDIVS
                WRITE(JOUT,*) ' '
                WRITE(JOUT,*) 'DIVISION AREA =',AREA1,' (ft.^2)'
                WRITE(JOUT,*) '                        =',AREA,' (m^2)'
                WRITE(JOUT,*) ' '
                WRITE (JOUT,1730)
                WRITE (JOUT,1732)
                WRITE (JOUT,1734)
                WRITE (JOUT,1736)
                DO 745 I = 1,NUMDIVS
                    WRITE(JOUT,1745)I, DIVTRC(I), DIVTRL(I), DIVTRD(I),
+                 DIVTOTC(I), DIVTOTL(I), DIVTOTD(I)
745          CONTINUE
747          CONTINUE
                WRITE(JOUT,*) ''
1730          FORMAT (7X, '-----TRANSVERSE-----', 2X,
+                 '-----TOTAL-----')
1732          FORMAT ('DIV.', 3X, '#CRACKS', 2X, 'LENGTH', 2X, 'DENSITY', 2X,
+                 '#CRACKS', 2X, 'LENGTH', 2X, 'DENSITY')
1734          FORMAT (18X, '(m)', 3X, '(m/m^2)', 13X, '(m)', 3X, '(m/m^2)')
1736          FORMAT ('----', 3X, '-----', 1X, '-----', 1X, '-----', 2X,

```

```

+          '-----',1X,'-----',1X,'-----')
1745  FORMAT(2X,I2,5X,I3,4X,F6.2,3X,F5.3,5X,I3,4X,F6.2,3X,F5.3)
      CLOSE(13)
      GO TO 701
*
*****
CCC=>Option 5 - First and Last 10 ft (or other length) of bridge
deck
*
      ELSEIF (CHOICE .EQ. 5) THEN
        WRITE(6,*) 'ENTER OUTPUT FILE NAME.'
        READ(5, 1010)OUTFILE
        OPEN(13, FILE=OUTFILE,STATUS='UNKNOWN')
        WRITE(6,*) 'ENTER WIDTH OF ROADWAY. (ft.)'
        READ(5,*) RDWY
        RDWYPIX = NINT(RDWY*10)
        WRITE(6,*) 'ENTER LENGTH OF BRIDGE. (ft.)'
        READ(5,*) LENBRG
        WRITE(6,*) 'ENTER LENGTH OF FIRST AND LAST DIVISIONS. (ft.)'
(10)'
        READ(5,*) LENDIV
*
        LENDIV is now the length in feet of the first and last
*
        division
        RDIVS = LENBRG/LENDIV
        LDPIX = NINT(LENDIV*10)
*
        10 pixels per foot for a 100 dpi image
*
        LDPIX is the number of pixels for the length of the division
        AREA = LENDIV*RDWY* 0.09290304
*
        1 square ft = 0.09290304 square meters
*
        AREA is area of the div in square meters
        AREA1 = AREA/0.09290304
*
        AREA1 is the area of the div in square ft.
        WRITE(6,*) 'ENTER SKEW. [(+) OR (-) DEGREES]'
        READ(5,*) SKEW
        XLOCATOR = XSTART
        YLOCATOR = YSTART
        LTBND = XLOCATOR
        RTBND = LTBND + RDWYPIX
*
        DO 2742 I = 1,2
          IF (SKEW .EQ. 0) THEN
            BOTBND = YLOCATOR + LDPIX
            TOPBND = YLOCATOR
            DO 2744 J = 1,N
              IF ((XPERM(J).LT. LTBND) .OR. (XPERM(J).GT. RTBND))
THEN
                X(J) = 0
                Y(J) = 0
              ELSEIF((YPERM(J).LT.TOPBND).OR.(YPERM(J).GT.BOTBND))
THEN
                X(J) = 0
                Y(J) = 0
              ELSE
                X(J) = XPERM(J)

```

```

          Y(J) = YPERM(J)
        ENDIF
2744      CONTINUE
      ELSE
        YPT2 = YLOCATOR - NINT(TAND(SKEW)*RDWY*10)
        XPT2 = RTBND
        DO 2746 J = 1,N
          IF ((XPERM(J).LT.LTBND).OR.(XPERM(J).GT.RTBND)) THEN
            X(J) = 0
            Y(J) = 0
          ELSE
            YTOPPT = YLOCATOR + ((-XPERM(J) + XLOCATOR) *
+              (YLOCATOR-YPT2)) / RDWYPIX
            YBOTPT = YTOPPT + LDPIX
            IF((YPERM(J).LT.YTOPPT).OR.(YPERM(J).GT.YBOTPT))THEN
              X(J) = 0
              Y(J) = 0
            ELSE
              X(J) = XPERM(J)
              Y(J) = YPERM(J)
            ENDIF
          ENDIF
        ENDIF
2746      CONTINUE
      END IF
*
      CALL GROUP (N, X, Y, NUMCRCKS, NUMPIX, CX, CY)
      CALL CALCS (NUMCRCKS, NUMPIX, ANGLE, LENGTH, CX, CY)
      CALL OUTINFO (NUMCRCKS, ANGLE, LENGTH, AREA, NCPG, TLPG, TOTLEN,
+        TOTDENS, TCHECK, DENS)
*
      WRITE (13, *) OUTFILE
      WRITE(13,*) ' '
      WRITE (13,*) 'OPTION 5: FIRST AND LAST DIVISION'
      WRITE (13,*)
      WRITE (13,*) 'DIVISION NUMBER ',I
      WRITE(13,*)
      WRITE(13,*)'DIVISION LENGTH =',LENDIV,' (ft.)'
      WRITE(13,*)'                    =',LENDIV*0.3048,' (m)'
      WRITE(13,*)'DIVISION AREA =',AREAL,' (ft.^2)'
      WRITE(13,*)'                    =',AREA,' (m^2)'
      WRITE(13,*)' '
      WRITE (13,*)'DIVISON 1 IS THE FIRST ',LENDIV,' (ft.)OF
+        THE BRIDGE DECK'
      WRITE (13,*)'DIVISON 2 IS THE LAST ',LENDIV,' (ft.)OF THE
+        BRIDGE DECK'
      WRITE(13,*)' '
*
      CALL OUTPUT (NCPG, TLPG, DENS, TCHECK, AREA, AREAL, NUMCRCKS,
+        TOTLEN, TOTDENS, OUTFILE)
*
*
      Cracks between -5 and 5 degrees are considered transverse
      DIVTRC(I) = NCPG(1)
      DIVTRL(I) = TLPG(1)

```

```

DIVTRD(I) = DENS(1)
DIVTOTC(I) = TCHECK
DIVTOTL(I) = TOTLEN
DIVTOTD(I) = TOTDENS
*
*   Set YLOCATOR to a distance LENDIV or LDPIX from the far
*   end of the bridge
RTEMP = (LENBRG - LENDIV)*10
ITEMP = NINT(RTEMP)
YLOCATOR = YSTART + ITEMP
2742 CONTINUE
*
DO 2747 J = 1,2
  IF (J .EQ. 1) THEN
    JOUT = 6
  ELSE
    JOUT = 13
  ENDIF
  WRITE (JOUT, *) OUTFILE
  WRITE(JOUT,*) ' '
  WRITE (JOUT,*) 'OPTION 5: FIRST AND LAST DIVISION'
  WRITE(JOUT,*)
  WRITE(JOUT,*) 'DIVISION LENGTH = ',LENDIV,' (ft.)'
  WRITE(JOUT,*) '                        = ',LENDIV*0.3048,' (m)'
  WRITE(JOUT,*) 'DIVISION AREA = ',AREAL,' (ft.^2)'
  WRITE(JOUT,*) '                        = ',AREA,' (m^2)'
  WRITE(JOUT,*) ' '
  WRITE (JOUT,*) 'DIVISON 1 IS THE FIRST ',LENDIV,' (ft.)OF
+           THE BRIDGE DECK'
  WRITE (JOUT,*) 'DIVISON 2 IS THE LAST ',LENDIV,' (ft.)OF
+           THE BRIDGE DECK'
  WRITE(JOUT,*) ' '
  WRITE (JOUT,3730)
  WRITE (JOUT,3732)
  WRITE (JOUT,3734)
  WRITE (JOUT,3736)
  DO 2745 I = 1,2
    WRITE(JOUT,3745) I, DIVTRC(I), DIVTRL(I), DIVTRD(I),
+           DIVTOTC(I), DIVTOTL(I), DIVTOTD(I)
2745 CONTINUE
2747 CONTINUE
  WRITE(JOUT,*) ' '
3730 FORMAT (7X, '-----TRANSVERSE-----', 2X,
+          '-----TOTAL-----')
3732 FORMAT ('DIV.', 3X, '#CRACKS', 2X, 'LENGTH', 2X, 'DENSITY', 2X,
+          '#CRACKS', 2X, 'LENGTH', 2X, 'DENSITY')
3734 FORMAT (18X, '(m)', 3X, '(m/m^2)', 13X, '(m)', 3X, '(m/m^2)')
3736 FORMAT ('----', 3X, '-----', 1X, '-----', 1X, '-----', 2X,
+          '-----', 1X, '-----', 1X, '-----')
3745 FORMAT(2X, I2, 5X, I3, 4X, F6.2, 3X, F5.3, 5X, I3, 4X, F6.2, 3X, F5.3)
  CLOSE(13)
  GO TO 701
*
*****

```

```

CCC=>Option 6 -- Quit.
*
      ELSE
        WRITE(6,*) 'END!'
      ENDIF
    END
*
*****
*   SUBROUTINE GROUP
*****
*   DIVIDES PIXELS INTO CRACK GROUPS
*   NUMCRCKS = TOTAL NUMBER OF CRACKS IN SECTION CONSIDERED
*   NUMPIX(K) = TOTAL NUMBER OF PIXELS IN A GIVEN CRACK K
*   N = TOTAL NUMBER OF PIXELS IN THE INPUT FILE
*
      SUBROUTINE GROUP (N,X,Y,NUMCRCKS,NUMPIX,CX,CY)
      INTEGER N,X,Y,NUMCRCKS,NUMPIX,CX,CY,CHECK,H
      DIMENSION X(900000),Y(900000),NUMPIX(8000),CX(4000,4000),
+           CY(4000,4000)
*
*
      DO 24 I = 1,1000
        DO 23 J = 1,1000
          CX(J,I) = 0
          CY(J,I) = 0
23      CONTINUE
24      CONTINUE
      NUMCRCKS = 0
      H = 0
      DO 50 K = 1,3000
        H=H + 1
        WRITE(6,*) 'K = ',K
        WRITE(6,*) 'H = ',H
        CHECK = 0
        DO 25 M = 1,N
          CHECK = CHECK + X(M)
25      CONTINUE
        WRITE(6,*) 'check = ',CHECK
        IF (CHECK .EQ. 0) THEN
          GO TO 60
        ELSE
          NUMPIX(H) = 1
          DO 5 L = 1,N
            IF (X(L) .NE. 0) THEN
              CX(1,H) = X(L)
              CY(1,H) = Y(L)
              X(L) = 0
              Y(L) = 0
              GO TO 8
            ENDIF
          CONTINUE
5          CONTINUE
8          DO 40 J = 1,3000
            IF (CX(J,H) .NE. 0) THEN
              DO 30 I = 1,N

```

```

      IF (X(I).NE.0) THEN
      IF ((X(I).EQ.CX(J,H)).OR.(X(I).EQ.(CX(J,H)+1)).OR.
+      (X(I).EQ.(CX(J,H)-1)))
+      .AND.
+
((Y(I).EQ.CY(J,H)).OR.(Y(I).EQ.(CY(J,H)+1)).OR.
+      (Y(I).EQ.(CY(J,H)-1)))) THEN
      NUMPIX(H) = NUMPIX(H) + 1
      CX(NUMPIX(H),H) = X(I)
      CY(NUMPIX(H),H) = Y(I)
      X(I) = 0
      Y(I) = 0
      ENDIF
      ENDIF
30      CONTINUE
*
      IF (NUMPIX(H).EQ.1) THEN
      NUMCRCKS = NUMCRCKS-1
      H=H-1
      ENDIF
      ELSE
      GO TO 45
      ENDIF
40      CONTINUE
45      CONTINUE
      NUMCRCKS = NUMCRCKS + 1
      END IF
50      CONTINUE
60      CONTINUE
      WRITE(6,*)'numcrcks = ',NUMCRCKS
      RETURN
      END
*
*****
* SUBROUTINE CALCS
*****
* CALCULATES LENGTH AND ANGLE OF EVERY CRACK
* K = CRACK NUMBER
* J = FIXED (BASE) PIXEL FROM WHICH DISTANCES ARE MEASURED
* I = VARIABLE (ENDPOINT) PIXEL
*
      SUBROUTINE CALCS (NUMCRCKS, NUMPIX, ANGLE, LENGTH, CX, CY)
      REAL ANGLE,LENGTH,D,X1,Y1,X2,Y2
      INTEGER NUMCRCKS, NUMPIX, CX, CY
      DIMENSION ANGLE(3000),LENGTH(3000),NUMPIX(8000),CX(4000,4000),
+      CY(4000,4000),D(6000)
*
*
      DO 78 I = 1,3000
      ANGLE(I) = 0
78      CONTINUE
      DO 90 K = 1,NUMCRCKS
      LENGTH(K) = 0
      DO 80 J = 1,NUMPIX(K)

```

```

X1 = REAL(CX(J,K))
Y1 = REAL(CY(J,K))
DO 70 I = 1,NUMPIX(K)
  X2 = REAL(CX(I,K))
  Y2 = REAL(CY(I,K))
*   D calculates the distance between two pixels
  D(K)=SQRT(((X1-X2)**2)+((Y1-Y2)**2))
  IF (D(K) .GT. LENGTH(K)) THEN
    LENGTH(K) = D(K)
    IF (X1 .EQ. X2) THEN
      ANGLE(K) = 90
    ELSEIF (Y1 .EQ. Y2) THEN
      ANGLE(K) = 0
    ELSE
*   Angle is the angle in degrees between the first pixel in the
*   crack and the last pixel in the crack.
      ANGLE(K)=(ATAN((Y1-Y2)/(X1-X2)))*(-180/3.14159265)
    ENDIF
  END IF
70   CONTINUE
80   CONTINUE
90   CONTINUE
*
CCC=> THE FOLLOWING LINES CONVERT THE LENGTHS FROM PIXELS TO METERS.
CCC=> IF THE RESOLUTION OR DRAWING SCALE CHANGES, THE CONVERSION
CCC=> FACTOR MUST CHANGE ACCORDINGLY.
CCC=> (1 in./100 pix)*(10 feet/1 in.)*(0.3048m/foot) = 0.03048m/pix
*
DO 95 K = 1,NUMCRCKS
  LENGTH(K) = LENGTH(K) * (0.03048)
95  CONTINUE
RETURN
END
*
*****
* SUBROUTINE OUTINFO
*****
* CREATES INFORMATION FOR OUTPUT
*   NCPG = NUMBER OF CRACKS PER GROUP
*   TLPG = TOTAL LENGTH PER GROUP
*   DENS = CRACK DENSITY PER GROUP (LIN. m/m^2)
*
*
SUBROUTINE OUTINFO
(NUMCRCKS,ANGLE,LENGTH,AREA,NCPG,TLPG,TOTLEN,
+  TOTDENS, TCHECK, DENS)
REAL ANGLE, LENGTH, AREA, TLPG, TOTLEN, TOTDENS, DENS
INTEGER NUMCRCKS , NCPG, TCHECK, LOW, HIGH
DIMENSION ANGLE(3000),LENGTH(3000),NCPG(20),TLPG(20),DENS(20)
*
*
DO 110 L = 1,19
  NCPG(L) = 0
  TLPG(L) = 0

```

```

      DENS(L) = 0
110  CONTINUE
      DO 130 K = 1,NUMCRCKS
          LOW = -5
          HIGH = 5
          DO 120 L = 1,9
              IF ((ANGLE(K).GE. LOW) .AND. (ANGLE(K).LT. HIGH)) THEN
                  NCPG(L) = NCPG(L) + 1
                  TLPG(L) = TLPG(L) + LENGTH(K)
                  GO TO 130
              ENDIF
              LOW = LOW + 10
              HIGH = HIGH + 10
120  CONTINUE
          IF ((ANGLE(K).GE.85).AND.(ANGLE(K).LE.90)) .OR.
+         ((ANGLE(K).LT.-85).AND.(ANGLE(K).GT.-90))) THEN
              NCPG(10) = NCPG(10) + 1
              TLPG(10) = TLPG(10) + LENGTH(K)
          END IF
          LOW = -15
          HIGH = -5
          DO 125 L = 11,18
              IF ((ANGLE(K) .GE. LOW) .AND. (ANGLE(K) .LT. HIGH)) THEN
                  NCPG(L) = NCPG(L) + 1
                  TLPG(L) = TLPG(L) + LENGTH(K)
                  GO TO 130
              ENDIF
              LOW = LOW - 10
              HIGH = HIGH - 10
125  CONTINUE
130  CONTINUE
          DO 140 L = 1,18
              DENS(L) = TLPG(L)/AREA
140  CONTINUE
          TOTLEN = 0
          DO 145 K = 1,NUMCRCKS
              TOTLEN = TOTLEN + LENGTH(K)
145  CONTINUE
          TOTDENS = TOTLEN/AREA
          TCHECK = 0
          DO 147 I = 1,18
              TCHECK      = TCHECK + NCPG(I)
147  CONTINUE
          RETURN
          END
*
*****
*   SUBROUTINE OUTPUT
*****
*   WRITES RESULTS TO THE SCREEN AND TO AN OUTPUT FILE
*
      SUBROUTINE OUTPUT (NCPG,TLPG,DENS,TCHECK,AREA,AREA1,NUMCRCKS,
+      TOTLEN,TOTDENS,OUTFILE)
      REAL TLPG, DENS, AREA, AREA1 , TOTLEN, TOTDENS

```

```

INTEGER NCPG, TCHECK, NUMCRCKS, LOW, HIGH
CHARACTER OUTFILE*18
DIMENSION NCPG(20), TLPG(20), DENS(20)
*
WRITE(6,*) ''
WRITE(6,1012)
WRITE(6,1014)
WRITE(6,1016)
WRITE(6,1018)
LOW = -5
HIGH = 5
1012 FORMAT(15X, '# OF', 6X, 'TOTAL', 8X, 'CRACK')
1014 FORMAT(4X, 'ANGLE', 5X, 'CRACKS', 4X, 'LENGTH', 7X, 'DENSITY')
1016 FORMAT(4X, '(deg)', 17X, '(m)', 6X, '(Lin. m/m^2)')
1018 FORMAT('-----', 4X, '----', 5X, '-----', 5X, '-----')
1020 FORMAT(1x, '(', I3, ') - (', I3, ')', 4x, I3, 3x, F8.2, 8X, F9.7)
DO 150 I = 1, 10
    WRITE(6,1020) LOW, HIGH, NCPG(I), TLPG(I), DENS(I)
    LOW = LOW + 10
    HIGH = HIGH + 10
150 CONTINUE
LOW = -5
HIGH = -15
DO 160 I = 11, 18
    WRITE(6,1020) LOW, HIGH, NCPG(I), TLPG(I), DENS(I)
    LOW = LOW - 10
    HIGH = HIGH - 10
160 CONTINUE
WRITE(6,1030) 'TOTAL', NUMCRCKS, TOTLEN, TOTDENS
WRITE(6, 1037) 'CHECK', TCHECK
WRITE(6,*) ''
1030 FORMAT (4X,A5,7X,I3,3X,F8.2,8X,F9.7)
*
WRITE(13,1012)
WRITE(13,1014)
WRITE(13,1016)
WRITE(13,1018)
LOW = -5
HIGH = 5
DO 170 I = 1, 10
    WRITE(13,1020) LOW, HIGH, NCPG(I), TLPG(I), DENS(I)
    LOW = LOW + 10
    HIGH = HIGH + 10
170 CONTINUE
LOW = -5
HIGH = -15
DO 180 I = 11, 18
    WRITE(13,1020) LOW, HIGH, NCPG(I), TLPG(I), DENS(I)
    LOW = LOW - 10
    HIGH = HIGH - 10
180 CONTINUE
WRITE(13,1030) 'TOTAL', NUMCRCKS, TOTLEN, TOTDENS
WRITE(13,1037) 'CHECK', TCHECK
WRITE(13,*) ''

```

```

        WRITE(13,*)''
1037  FORMAT (4X,A5,7X,I3)
        RETURN
        END
*
*****
*   SUBROUTINE SPECANG
*****
*   SPECIFIED ANGLE SECTION
*
        SUBROUTINE SPECANG (AREA, NUMCRCKS, ANGLE, LENGTH, SPANG,
+           SPNC,SPTL, SPDENS)
        REAL AREA, ANGLE, LENGTH, SPANG, SPTL, SPDENS, RLOW, RHIGH,
+           TOL
        INTEGER NUMCRCKS, SPNC, NUM
        CHARACTER YESNO
        DIMENSION ANGLE(20),LENGTH(20),SPANG(10),SPNC(10),SPTL(10),
+           SPDENS (10)
*
        WRITE(6, 1050)
1050  FORMAT(//,//,' DO YOU WISH TO SEE INFORMATION FOR ANGLES
+           OTHER')
        WRITE(6,*)'THAN THOSE LISTED?'
1051  FORMAT (A1)
        READ(5,1051) YESNO
        IF (YESNO .EQ. 'Y' .OR. YESNO .EQ. 'y') THEN
            WRITE(6,*)'ENTER THE NO. OF ADDITIONAL ANGLES DESIRED.'
            READ(5, *)NUM
            WRITE(6,*)'ENTER TOLERANCE FOR EACH ANGLE (+/- ___deg.).'
            READ(5,*) TOL
            DO 190 I = 1,NUM
                WRITE(6,*)'ENTER ANGLE',I,'(deg.).'
                READ(5,*) SPANG(I)
190          CONTINUE
                DO 195 I = 1,10
                    SPNC(I) = 0
                    SPTL(I) = 0
                    SPDENS(I) = 0
195          CONTINUE
                DO 200 K = 1,NUMCRCKS
                    DO 198 I = 1,NUM
                        IF((ANGLE(K).GT.(SPANG(I)-TOL)) .AND.
+                          (ANGLE(K).LT.(SPANG(I)+TOL))) THEN
                            SPNC(I) = SPNC(I) + 1
                            SPTL(I) = SPTL(I) + LENGTH(K)
                        ENDIF
198          CONTINUE
200          CONTINUE
                DO 210 I = 1,NUM
                    SPDENS(I) = SPTL(I)/AREA
210          CONTINUE
        WRITE(6, 1052)
1052  FORMAT(//, 'SPECIFIED ANGLES:')
*
        See the end of the Subroutine for the format statements

```

```

WRITE(6,*)' '
WRITE(6,1062)
WRITE(6,1064)
WRITE(6,1066)
WRITE(6,1068)
WRITE(13, 1052)
WRITE(13,*)' '
WRITE(13,1062)
WRITE(13,1064)
WRITE(13,1066)
WRITE(13,1068)
DO 220 I = 1,NUM
    RLOW = SPANG(I) - TOL
    RHIGH = SPANG(I) + TOL
    WRITE(6,1060)RLOW, RHIGH, SPNC(I),SPTL(I),SPDENS(I)
    WRITE(13,1060)RLOW, RHIGH, SPNC(I),SPTL(I),SPDENS(I)
220 CONTINUE
END IF
1060 FORMAT(1X,'( ',F5.1')-( ',F5.1,')',4X,I3,3X,F6.2,8X,F9.7)
1062 FORMAT(19X,'# OF',4X,'TOTAL',8X,'CRACK')
1064 FORMAT(6X,'ANGLE',7X,'CRACKS',2X,'LENGTH',7X,'DENSITY')
1066 FORMAT(6X,'(deg)',17X,'(m)',6X,'(Lin. m/m^2)')
1068 FORMAT('-----',4X,'---',3X,'-----',5X,'-----'
+         -')
WRITE(13,*)''
WRITE(13,*)''
RETURN
END
*
*****
* SUBROUTINE COORDS
*****
* SELECTS ALL "DARK" PIXELS FROM ASCII FILE AND WRITES THEIR
* COORDINATES TO FILE coords.dat
*
SUBROUTINE COORDS (INFILE,XPERM,YPERM,LOWER,UPPER,N,XSTART,
+ YSTART)
INTEGER LEVEL, XCOUNT, YCOUNT, XPERM, YPERM, LOWER, UPPER, N,
+ XSIZE, YSIZE, CHOICE, JUMP, XEDGE, XSTART, YSTART
INTEGER SHIFT,CHECK
CHARACTER INFILE*14
DIMENSION LEVEL(20),XPERM(900000),YPERM(900000)
*
XSIZE = 600
YSIZE = 4200
WRITE(6,*)'DEFAULT IMAGE SIZE:      ',XSIZE,' x ',YSIZE
WRITE(6,*)' (1) USE DEFAULT'
WRITE(6,*)' (2) SPECIFY NEW SIZE'
WRITE(6,*)' '
WRITE(6,*) 'ENTER CHOICE'
600 READ(5,*)CHOICE
IF ((CHOICE .NE. 1) .AND. (CHOICE .NE. 2)) THEN
    WRITE(6,*)'ENTER 1 OR 2.'
    GO TO 600

```

```

ENDIF
IF (CHOICE .EQ. 2) THEN
  WRITE(6,*)
  WRITE(6,*)
  WRITE(6,*)'BOTH X AND Y DIMENSIONS MUST BE MULTIPLES OF 20'
  WRITE(6,*)'FOR THE PROGRAM TO FUNCTION CORRECTLY!!!'
  WRITE(6,*)
  WRITE(6,*)
  601  WRITE(6,*)'ENTER X-DIMENSION.'
      READ(5,*)XSIZE
      WRITE(6,*) 'ENTER Y-DIMENSION.'
      READ(5,*)YSIZE
      WRITE(6,*)'NEW IMAGE SIZE:  ',XSIZE,' x',YSIZE
      WRITE(6,*)' (1) ACCEPT'
      WRITE(6,*)' (2) MODIFY'
      WRITE(6,*)' '
      WRITE(6,*) 'ENTER CHOICE'
  602  READ(5,*)CHOICE
      IF ((CHOICE .NE. 1) .AND. (CHOICE .NE. 2)) THEN
        WRITE(6,*)'ENTER 1 OR 2.'
        GO TO 602
      END IF
      IF (CHOICE .EQ. 2) THEN
        GO TO 601
      ENDIF
ENDIF
ENDIF
*
* 20 is the number of columns of data in the ASCII file.
* JUMP is the number of rows of the ASCII file that make up one
* row of the TIFF image.
* JUMP = XSIZE/20
* WRITE(6,*)'SCANNING ASCII FILE . . .'
1002  FORMAT (20(I3,1X))
*****
* This group of lines opens the data file and reads in the first
* lines so that the program can determine in which column the
* data starts. SHIFT represents the number of empty columns
* before the first data point.
* REWIND should tell the program to go back to the beginning of
* the data file.
*
SHIFT = 0
CHECK = 0
OPEN (11,FILE=INFILE,STATUS='OLD')
READ (11,1002) (LEVEL(I), I=1,20)
DO 300 I = 1,20
  IF (LEVEL(I).NE.0) THEN
    CHECK = 1
  ENDIF
  IF ((LEVEL(I).EQ.0).AND.(CHECK.EQ.0)) THEN
    SHIFT = SHIFT + 1
  ENDIF
300  CONTINUE
REWIND (11)

```

```

*
* The first row requires an additional if then so that XCOUNT
* starts at 1 in the correct column.
*
N = 0
YCOUNT = 1
XCOUNT=0
IF (SHIFT.EQ.0) THEN
  GO TO 320
ENDIF
READ (11,1002) (LEVEL(I), I=1,SHIFT)
DO 310 I = 1,20
  IF (I.GT.SHIFT) THEN
    XCOUNT = XCOUNT + 1
    IF ((LEVEL(I).GE.LOWER).AND.(LEVEL(I).LE.UPPER)) THEN
      N = N + 1
      XPERM(N) = XCOUNT
      YPERM(N) = YCOUNT
    END IF
  ENDIF
310 CONTINUE
*
* The following lines examine the remaining rows
* This is where the program begins if SHIFT = 0
320 DO 3 K = 1,YSIZE
  DO 2 J = 1,JUMP
    READ (11,1002) (LEVEL(I), I=1,20)
    DO 1 I = 1,20
* If XCOUNT = XSIZE then the end of a row has been reached and
* the next row needs to be started.
      IF ((XCOUNT.EQ.XSIZE).AND.(YCOUNT.EQ.YSIZE)) THEN
        GO TO 330
      ENDIF
      IF (XCOUNT.EQ.XSIZE) THEN
        XCOUNT = 0
        YCOUNT = YCOUNT + 1
      ENDIF
      XCOUNT = XCOUNT + 1
      IF ((LEVEL(I).GE.LOWER).AND.(LEVEL(I).LE.UPPER)) THEN
        N = N + 1
        XPERM(N) = XCOUNT
        YPERM(N) = YCOUNT
      END IF
1      CONTINUE
2      CONTINUE
3      CONTINUE
*
330 CLOSE (11)
*
*****
CCC=>The following lines locate the starting point pixel.
      IF (YPERM(1).NE.1) THEN
        WRITE(6,*)'ERROR!! CHECK TIFF FILE.'
        STOP

```

```
ENDIF
XEDGE = XPERM(1)
J= 1
DO 610 I = 1,N
  IF ((XPERM(I).EQ. XEDGE) .AND. (YPERM(I).EQ. J)) THEN
    XSTART = XPERM(I)
    YSTART = YPERM(I)
    J=J+1
    XPERM(I) = 0
    YPERM(I) = 0
  END IF
610 CONTINUE
CCC=>
OPEN (12,FILE='coords.dat',STATUS='UNKNOWN')
*
WRITE (12,*) 'SHIFT:',SHIFT,' CHECK:',CHECK
WRITE (12,*) 'XSIZE:',XSIZE,' YSIZE:',YSIZE
*
1003 FORMAT (3X,I3,4X,I4)
DO 4 I = 1,N
  IF (XPERM(I).NE.0) THEN
    WRITE (12,1003) XPERM(I),YPERM(I)
  ENDIF
4 CONTINUE
CLOSE (12)
*
WRITE(6,*)'TOTAL NUMBER OF "DARK" PIXELS =',N,','
RETURN
END
```

**APPENDIX D**  
**BRIDGE DECK CHLORIDE CONTENTS AND DIFFUSION DATA**

**Table D.1 – Chloride Concentration Data**

<b>Bridge:</b>		<b>30-93</b>		<b>Bridge:</b>		<b>40-92</b>		
<b>Placement:</b>		Deck		<b>Placement:</b>		Deck		
<b>Placement Date:</b>		08/04/01		<b>Placement Date:</b>		10/26/01		
<b>Survey Date:</b>		08/15/03		<b>Survey Date:</b>		06/12/03		
<b>Off Crack</b>		<b>On Crack</b>		<b>Off Crack</b>		<b>On Crack</b>		<b>Mean Depth</b>
<b>Sample</b>	<b>kg/m<sup>3</sup></b>	<b>Sample</b>	<b>kg/m<sup>3</sup></b>	<b>Sample</b>	<b>kg/m<sup>3</sup></b>	<b>Sample</b>	<b>kg/m<sup>3</sup></b>	<b>(mm)</b>
2A	1.06	1A	1.97	2A	1.76	1A	3.73	9.5
2B	0.24	1B	1.31	2B	0.00	1B	1.06	28.6
2C	0.21	1C	1.04	2C	0.00	1C	1.01	47.6
2D	0.20	1D	0.78	2D	0.00	1D	1.11	66.7
2E	0.21	1E	0.82	2E	0.00	1E	1.18	85.7
4A	2.08	3A	1.40	4A	3.44	3A	4.24	9.5
4B	0.22	3B	0.22	4B	0.14	3B	1.39	28.6
4C	0.23	3C	0.24	4C	0.00	3C	1.10	47.6
4D	0.26	3D	0.30	4D	0.00	3D	1.50	66.7
4E	0.27	3E	0.29	4E	0.00	3E	1.41	85.7
6A	0.12	5A	1.66	6A	2.17	5A	2.35	9.5
6B	0.25	5B	0.19	6B	0.13	5B	0.78	28.6
6C	0.27	5C	0.16	6C	0.11	5C	1.09	47.6
6D	0.24	5D	0.18	6D	0.00	5D	1.40	66.7
6E	0.21	5E	0.20	6E	0.00	5E	1.40	85.7
<b>Bridge:</b>		<b>40-93</b>		<b>Bridge:</b>		<b>46-332</b>		
<b>Placement:</b>		Deck		<b>Placement:</b>		Deck		
<b>Placement Date:</b>		10/16/01		<b>Placement Date:</b>		05/15/02		
<b>Survey Date:</b>		06/11/03		<b>Survey Date:</b>		07/02/03		
<b>Off Crack</b>		<b>On Crack</b>		<b>Off Crack</b>		<b>On Crack</b>		<b>Mean Depth</b>
<b>Sample</b>	<b>kg/m<sup>3</sup></b>	<b>Sample</b>	<b>kg/m<sup>3</sup></b>	<b>Sample</b>	<b>kg/m<sup>3</sup></b>	<b>Sample</b>	<b>kg/m<sup>3</sup></b>	<b>(mm)</b>
2A	3.53	1A	5.72	2A	0.81	1A	0.16	9.5
2B	0.25	1B	1.17	2B	0.15	1B	0.49	28.6
2C	0.00	1C	1.19	2C	0.14	1C	0.53	47.6
2D	0.11	1D	1.46	2D	0.16	1D	0.18	66.7
2E	0.00	1E	1.34	2E	0.00	1E	1.05	85.7
4A	3.12	3A	2.56	4A	0.25	3A	0.43	9.5
4B	0.66	3B	0.97	4B	0.40	3B	0.18	28.6
4C	0.14	3C	1.00	4C	1.16	3C	0.36	47.6
4D	0.00	3D	1.03	4D	0.13	3D	0.10	66.7
4E	0.00	3E	0.97	4E	0.23	3E	0.86	85.7
6A	2.12	5A	2.16	6A	0.52	5A	0.19	9.5
6B	2.10	5B	1.15	6B	0.21	5B	0.40	28.6
6C	0.15	5C	1.09	6C	0.85	5C	0.40	47.6
6D	0.00	5D	0.99	6D	0.14	5D	0.87	66.7
6E	0.00	5E	0.60	6E	0.27	5E	0.63	85.7

Table D.1 (con't) – Chloride Concentration Data

<b>Off Crack</b>		<b>On Crack</b>		<b>Off Crack</b>		<b>On Crack</b>		<b>Mean Depth</b>
<b>Sample</b>	<b>kg/m<sup>3</sup></b>	<b>Sample</b>	<b>kg/m<sup>3</sup></b>	<b>Sample</b>	<b>kg/m<sup>3</sup></b>	<b>Sample</b>	<b>kg/m<sup>3</sup></b>	<b>(mm)</b>
2A	5.62	1A	5.77	2A	6.64	1A	7.43	9.5
2B	1.36	1B	2.81	2B	2.45	1B	1.65	28.6
2C	0.24	1C	2.63	2C	0.25	1C	1.42	47.6
2D	0.13	1D	2.25	2D	0.16	1D	1.09	66.7
2E	0.24	1E	1.36	2E	0.21	1E	0.79	85.7
3A	3.91	4A	7.18	4A	7.96	3A	7.78	9.5
3B	0.18	4B	2.48	4B	2.18	3B	2.00	28.6
3C	0.00	4C	2.50	4C	0.26	3C	2.21	47.6
3D	0.00	4D	2.02	4D	0.10	3D	2.22	66.7
3E	0.00	4E	1.22	4E	0.15	3E	2.11	85.7
5A	5.64			6A	6.19	5A	4.98	9.5
5B	0.53			6B	0.43	5B	1.19	28.6
5C	0.11			6C	0.15	5C	1.32	47.6
5D	0.00			6D	0.00	5D	1.21	66.7
5E	0.00			6E	0.00	5E	0.93	85.7

<b>Bridge:</b>		<b>81-53</b>		<b>Bridge:</b>		<b>85-148</b>		
<b>Placement:</b>		Deck		<b>Placement:</b>		West 32 ft		
<b>Placement Date:</b>		02/21/00		<b>Placement Date:</b>		10/30/01		
<b>Survey Date:</b>		06/05/03		<b>Survey Date:</b>		06/03/03		
<b>Bridge:</b>		<b>85-149</b>		<b>Bridge:</b>		<b>85-149</b>		
<b>Placement:</b>		Deck		<b>Placement:</b>		West 32 ft		
<b>Placement Date:</b>		09/26/02		<b>Placement Date:</b>		10/30/01		
<b>Survey Date:</b>		06/04/03		<b>Survey Date:</b>		06/03/03		

<b>Off Crack</b>		<b>On Crack</b>		<b>Off Crack</b>		<b>On Crack</b>		<b>Mean Depth</b>
<b>Sample</b>	<b>kg/m<sup>3</sup></b>	<b>Sample</b>	<b>kg/m<sup>3</sup></b>	<b>Sample</b>	<b>kg/m<sup>3</sup></b>	<b>Sample</b>	<b>kg/m<sup>3</sup></b>	<b>(mm)</b>
2A	2.07	1A	3.01					9.5
2B	0.13	1B	0.23					28.6
2C	0.00	1C	0.18					47.6
2D	0.00	1D	0.20					66.7
2E	0.00	1E	0.15					85.7
4A	3.91	3A	5.27					9.5
4B	0.16	3B	1.49					28.6
4C	0.00	3C	1.40					47.6
4D	0.00	3D	1.01					66.7
4E	0.00	3E	0.67					85.7
6A	2.74	5A	3.03					9.5
6B	0.13	5B	0.82					28.6
6C	0.12	5C	0.61					47.6
6D	0.00	5D	0.48					66.7
6E	0.00	5E	0.13					85.7

Table D.1 (con't) – Chloride Concentration Data

<b>Bridge:</b>		<b>89-269</b>		<b>Bridge:</b>		<b>89-269</b>		
<b>Placement:</b>		West 1/2 SFO		<b>Placement:</b>		East 1/2 SFO		
<b>Placement Date:</b>		08/04/01		<b>Placement Date:</b>		10/26/01		
<b>Survey Date:</b>		08/15/03		<b>Survey Date:</b>		06/12/03		
<b>Off Crack</b>		<b>On Crack</b>		<b>Off Crack</b>		<b>On Crack</b>		<b>Mean Depth</b>
<b>Sample</b>	<b>kg/m<sup>3</sup></b>	<b>Sample</b>	<b>kg/m<sup>3</sup></b>	<b>Sample</b>	<b>kg/m<sup>3</sup></b>	<b>Sample</b>	<b>kg/m<sup>3</sup></b>	<b>(mm)</b>
1A	4.51	4A	2.44	7A	4.41	8A	2.58	9.5
1B	0.35	4B	1.49	7B	1.23	8B	1.17	28.6
1C	0.17	4C	1.31	7C	0.19	8C	0.29	47.6
1D	0.18	4D	0.72	7D	0.14	8D	0.22	66.7
1E	0.00	4E	0.50	7E	0.14	8E	0.69	85.7
2A	4.20	5A	2.90	9A	1.96			9.5
2B	0.48	5B	1.76	9B	0.15			28.6
2C	0.14	5C	1.32	9C	0.17			47.6
2D	0.17	5D	1.38	9D	0.15			66.7
2E	0.17	5E	1.43	9E	0.27			85.7
3A	2.02	6A	5.29	10A	2.52			9.5
3B	0.15	6B	4.08	10B	0.26			28.6
3C	0.19	6C	0.90	10C	0.14			47.6
3D	0.00	6D	1.10	10D	0.14			66.7
3E	0.13	6E	0.46	10E	0.12			85.7
<b>Bridge:</b>		<b>89-272</b>		<b>Bridge:</b>		<b>89-272</b>		
<b>Placement:</b>		West 1/2 SFO		<b>Placement:</b>		East 1/2 SFO		
<b>Placement Date:</b>		04/04/02		<b>Placement Date:</b>		04/10/02		
<b>Survey Date:</b>		05/16/03		<b>Survey Date:</b>		05/16/03		
<b>Off Crack</b>		<b>On Crack</b>		<b>Off Crack</b>		<b>On Crack</b>		<b>Mean Depth</b>
<b>Sample</b>	<b>kg/m<sup>3</sup></b>	<b>Sample</b>	<b>kg/m<sup>3</sup></b>	<b>Sample</b>	<b>kg/m<sup>3</sup></b>	<b>Sample</b>	<b>kg/m<sup>3</sup></b>	<b>(mm)</b>
1A	1.31	7A	2.91	4A	2.05	10A	1.88	9.5
1B	0.00	7B	0.65	4B	0.23	10B	0.91	28.6
1C	0.18	7C	0.38	4C	0.22	10C	0.95	47.6
1D	0.13	7D	0.38	4D	0.00	10D	0.42	66.7
1E	0.14	7E	0.24	4E	0.15	10E	0.25	85.7
2A	1.66	8A	3.01	5A	2.20	11A	5.08	9.5
2B	0.26	8B	0.47	5B	0.18	11B	0.57	28.6
2C	0.00	8C	0.18	5C	0.17	11C	0.31	47.6
2D	0.00	8D	0.25	5D	0.16	11D	0.25	66.7
2E	0.14	8E	0.19	5E	0.16	11E	0.20	85.7
3A	3.99	9A	0.60	6A	2.19	12A	0.41	9.5
3B	0.73	9B	0.52	6B	0.20	12B	1.58	28.6
3C	0.19	9C	0.47	6C	0.25	12C	1.41	47.6
3D	0.00	9D	0.41	6D	0.15	12D	0.64	66.7
3E	0.17	9E	0.76	6E	0.15	12E	0.19	85.7

Table D.1 (con't) – Chloride Concentration Data

<b>Bridge:</b>		<b>103-56</b>		<b>Bridge:</b>		<b>103-56</b>		
<b>Placement:</b>		South 1/2 SFO		<b>Placement:</b>		North 1/2 SFO		
<b>Placement Date:</b>		10/12/01		<b>Placement Date:</b>		10/17/01		
<b>Survey Date:</b>		08/15/03		<b>Survey Date:</b>		08/06/03		
<b>Off Crack</b>		<b>On Crack</b>		<b>Off Crack</b>		<b>On Crack</b>		<b>Mean Depth</b>
<b>Sample</b>	<b>kg/m<sup>3</sup></b>	<b>Sample</b>	<b>kg/m<sup>3</sup></b>	<b>Sample</b>	<b>kg/m<sup>3</sup></b>	<b>Sample</b>	<b>kg/m<sup>3</sup></b>	<b>(mm)</b>
8A	5.18	7A	3.69	2A	0.57	1A	0.45	9.5
8B	1.05	7B	1.43	2B	0.25	1B	1.35	28.6
8C	0.14	7C	1.19	2C	0.16	1C	1.10	47.6
8D	0.14	7D	0.54	2D	0.12	1D	0.99	66.7
8E	0.16	7E	0.39	2E	0.19	1E	1.04	85.7
10A	3.04	9A	2.08	4A	0.33	3A	0.27	9.5
10B	0.35	9B	1.01	4B	0.26	3B	0.22	28.6
10C	0.17	9C	0.71	4C	0.27	3C	0.83	47.6
10D	0.12	9D	0.52	4D	0.50	3D	0.35	66.7
10E	0.16	9E	0.71	4E	0.50	3E	0.31	85.7
12A	0.77	11A	2.54	5A	0.26	6A	3.51	9.5
12B	0.31	11B	0.67	5B	0.40	6B	0.28	28.6
12C	2.12	11C	0.64	5C	0.70	6C	2.53	47.6
12D	0.00	11D	0.88	5D	0.27	6D	2.02	66.7
12E	0.12	11E	0.14	5E	0.67	6E	1.82	85.7
<b>Bridge:</b>		<b>23-85</b>		<b>Bridge:</b>		<b>23-85</b>		
<b>Placement:</b>		East 1/2 SFO		<b>Placement:</b>		West 1/2 SFO		
<b>Placement Date:</b>		03/29/96		<b>Placement Date:</b>		04/03/96		
<b>Survey Date:</b>		07/31/02		<b>Survey Date:</b>		07/31/02		
<b>Off Crack</b>		<b>On Crack</b>		<b>Off Crack</b>		<b>On Crack</b>		<b>Mean Depth</b>
<b>Sample</b>	<b>kg/m<sup>3</sup></b>	<b>Sample</b>	<b>kg/m<sup>3</sup></b>	<b>Sample</b>	<b>kg/m<sup>3</sup></b>	<b>Sample</b>	<b>kg/m<sup>3</sup></b>	<b>(mm)</b>
8A	5.71	7A	6.93	2A	2.96	1A	6.14	9.5
8B	1.30	7B	3.32	2B	0.27	1B	3.55	28.6
8C	0.17	7C	2.92	2C	0.00	1C	3.73	47.6
8D	0.35	7D	2.00	2D	0.13	1D	2.91	66.7
8E	0.31	7E	0.49	2E	0.00	1E	2.01	85.7
10A	4.71	9A	4.92	4A	3.57	3A	4.43	9.5
10B	0.79	9B	2.80	4B	0.49	3B	2.86	28.6
10C	0.18	9C	2.58	4C	0.00	3C	2.75	47.6
10D	0.00	9D	2.51	4D	0.00	3D	2.08	66.7
10E	0.00	9E	1.88	4E	0.11	3E	1.12	85.7
12A	3.66	11A	5.01	6A	3.96	5A	7.14	9.5
12B	0.54	11B	2.81	6B	1.62	5B	2.83	28.6
12C	0.09	11C	2.69	6C	0.36	5C	2.24	47.6
12D	0.00	11D	2.50	6D	0.00	5D	1.42	66.7
12E	0.00	11E	2.18	6E	0.00	5E	1.68	85.7

Table D.1 (con't) – Chloride Concentration Data

Off Crack		On Crack		Off Crack		On Crack		Mean Depth
Sample	kg/m <sup>3</sup>	Sample	kg/m <sup>3</sup>	Sample	kg/m <sup>3</sup>	Sample	kg/m <sup>3</sup>	(mm)
8A	0.93	7A	4.64	2A	1.08	1A	2.44	9.5
8B	0.24	7B	2.18	2B	0.47	1B	1.83	28.6
8C	0.08	7C	2.29	2C	0.13	1C	5.90	47.6
8D	0.00	7D	2.15	2D	0.00	1D	2.74	66.7
8E	0.00	7E	1.56	2E	0.00	1E	3.00	85.7
10A	1.31	9A	2.02	4A	0.62	3A	2.12	9.5
10B	0.16	9B	1.77	4B	0.00	3B	2.09	28.6
10C	0.00	9C	1.93	4C	0.00	3C	2.99	47.6
10D	0.00	9D	2.08	4D	0.00	3D	3.18	66.7
10E	0.00	9E	1.82	4E	0.00	3E	1.03	85.7
12A	1.04	11A	2.56	5A	1.30	5A	2.94	9.5
12B	0.28	11B	2.00	5B	0.00	5B	0.96	28.6
12C	0.00	11C	2.17	5C	0.00	5C	3.05	47.6
12D	0.00	11D	2.48	5D	0.00	5D	4.61	66.7
12E	0.00	11E	2.31	5E	0.00	5E	2.20	85.7

<b>Bridge:</b> 46-302		<b>Bridge:</b> 46-302						
<b>Placement:</b> Lt. 1/2 SFO	<b>Placement:</b> Rt. 1/2 SFO	<b>Placement:</b> Lt. 1/2 SFO	<b>Placement:</b> Rt. 1/2 SFO					
<b>Placement Date:</b> 04/09/96	<b>Placement Date:</b> 04/11/96	<b>Placement Date:</b> 10/20/95	<b>Placement Date:</b> 10/24/95					
<b>Survey Date:</b> 07/11/02	<b>Survey Date:</b> 07/11/02	<b>Survey Date:</b> 07/10/02	<b>Survey Date:</b> 07/10/02					
Off Crack		On Crack		Off Crack		On Crack		Mean Depth
Sample	kg/m <sup>3</sup>	Sample	kg/m <sup>3</sup>	Sample	kg/m <sup>3</sup>	Sample	kg/m <sup>3</sup>	(mm)
2A	7.90	1A	5.56	8A	6.73	7A	7.18	9.5
2B	1.79	1B	2.63	8B	2.00	7B	2.98	28.6
2C	0.17	1C	2.16	8C	0.21	7C	2.92	47.6
2D	0.00	1D	2.08	8D	0.08	7D	2.46	66.7
2E	0.00	1E	2.19	8E	0.00	7E	2.32	85.7
4A	6.58	3A	6.09	10A	7.47	9A	5.37	9.5
4B	1.17	3B	2.74	10B	3.36	9B	2.16	28.6
4C	0.00	3C	2.39	10C	0.57	9C	2.22	47.6
4D	0.00	3D	2.36	10D	0.15	9D	1.55	66.7
4E	0.00	3E	1.89	10E	0.12	9E	0.29	85.7
6A	5.13	5A	5.57	12A	8.71	11A	4.22	9.5
6B	1.39	5B	2.86	12B	3.39	11B	2.25	28.6
6C	0.15	5C	2.43	12C	0.52	11C	2.43	47.6
6D	0.00	5D	2.21	12D	0.20	11D	1.84	66.7
6E	0.00	5E	1.91	12E	0.16	11E	2.05	85.7

Table D.1 (con't) – Chloride Concentration Data

Off Crack		On Crack		Off Crack		On Crack		Mean Depth
Sample	kg/m <sup>3</sup>	Sample	kg/m <sup>3</sup>	Sample	kg/m <sup>3</sup>	Sample	kg/m <sup>3</sup>	(mm)
8A	2.26	7A	3.98	2A	4.52	1A	4.86	9.5
8B	0.13	7B	2.58	2B	0.17	1B	3.04	28.6
8C	0.13	7C	2.61	2C	0.00	1C	1.96	47.6
8D	0.00	7D	2.19	2D	0.00	1D	1.08	66.7
8E	0.00	7E	1.69	2E	0.00	1E	0.46	85.7
10A	3.42	9A	5.44	4A	4.05	3A	4.75	9.5
10B	0.27	9B	3.41	4B	0.75	3B	2.87	28.6
10C	0.11	9C	2.81	4C	0.11	3C	2.99	47.6
10D	0.00	9D	2.82	4D	0.00	3D	2.33	66.7
10E	0.00	9E	2.29	4E	0.00	3E	2.28	85.7
12A	2.41	11A	4.40	5A	3.23	5A	4.94	9.5
12B	0.00	11B	2.96	5B	0.24	5B	2.98	28.6
12C	0.00	11C	2.77	5C	0.00	5C	3.61	47.6
12D	0.00	11D	1.35	5D	0.00	5D	2.75	66.7
12E	0.00	11E	0.54	5E	0.00	5E	2.99	85.7

<b>Bridge:</b> 46-317		<b>Bridge:</b> 46-317						
<b>Placement:</b> North 12 ft	<b>Placement:</b> South 16 ft	<b>Placement Date:</b> 06/28/96	<b>Placement Date:</b> 07/01/96					
<b>Survey Date:</b> 07/15/02	<b>Survey Date:</b> 07/15/02	<b>Survey Date:</b> 07/15/02	<b>Survey Date:</b> 07/15/02					
Off Crack		On Crack		Off Crack		On Crack		Mean Depth
Sample	kg/m <sup>3</sup>	Sample	kg/m <sup>3</sup>	Sample	kg/m <sup>3</sup>	Sample	kg/m <sup>3</sup>	(mm)
8A	2.26	7A	3.98	2A	4.52	1A	4.86	9.5
8B	0.13	7B	2.58	2B	0.17	1B	3.04	28.6
8C	0.13	7C	2.61	2C	0.00	1C	1.96	47.6
8D	0.00	7D	2.19	2D	0.00	1D	1.08	66.7
8E	0.00	7E	1.69	2E	0.00	1E	0.46	85.7
10A	3.42	9A	5.44	4A	4.05	3A	4.75	9.5
10B	0.27	9B	3.41	4B	0.75	3B	2.87	28.6
10C	0.11	9C	2.81	4C	0.11	3C	2.99	47.6
10D	0.00	9D	2.82	4D	0.00	3D	2.33	66.7
10E	0.00	9E	2.29	4E	0.00	3E	2.28	85.7
12A	2.41	11A	4.40	5A	3.23	5A	4.94	9.5
12B	0.00	11B	2.96	5B	0.24	5B	2.98	28.6
12C	0.00	11C	2.77	5C	0.00	5C	3.61	47.6
12D	0.00	11D	1.35	5D	0.00	5D	2.75	66.7
12E	0.00	11E	0.54	5E	0.00	5E	2.99	85.7

<b>Bridge:</b> 81-50		<b>Bridge:</b> 81-50						
<b>Placement:</b> SFO Rt. Unit 2	<b>Placement:</b> SFO Lt. Unit 2	<b>Placement Date:</b> 11/21/95	<b>Placement Date:</b> 11/30/95					
<b>Survey Date:</b> 08/19/02	<b>Survey Date:</b> 08/19/02	<b>Survey Date:</b> 08/19/02	<b>Survey Date:</b> 08/19/02					
Off Crack		On Crack		Off Crack		On Crack		Mean Depth
Sample	kg/m <sup>3</sup>	Sample	kg/m <sup>3</sup>	Sample	kg/m <sup>3</sup>	Sample	kg/m <sup>3</sup>	(mm)
2A	5.49	1A	7.39	8A	3.20	7A	4.76	9.5
2B	0.32	1B	2.67	8B	0.20	7B	2.40	28.6
2C	0.00	1C	1.64	8C	0.00	7C	3.61	47.6
2D	0.11	1D	0.34	8D	0.00	7D	3.35	66.7
2E	0.00	1E	0.00	8E	0.00	7E	2.18	85.7
4A	6.85	3A	6.54	9A	4.07	10A	5.77	9.5
4B	1.72	3B	2.83	9B	0.16	10B	2.86	28.6
4C	0.46	3C	3.46	9C	0.00	10C	4.01	47.6
4D	0.00	3D	3.59	9D	0.00	10D	3.87	66.7
4E	0.00	3E	2.36	9E	0.00	10E	3.23	85.7
6A	6.33	5A	7.06	11A	8.71	12A	8.85	9.5
6B	0.89	5B	3.22	11B	1.43	12B	4.05	28.6
6C	0.00	5C	3.12	11C	0.13	12C	3.48	47.6
6D	0.00	5D	4.34	11D	0.00	12D	2.75	66.7
6E	0.00	5E	3.79	11E	0.00	12E	3.23	85.7

Table D.1 (con't) – Chloride Concentration Data

Off Crack		On Crack		Off Crack		On Crack		Mean Depth
Sample	kg/m <sup>3</sup>	Sample	kg/m <sup>3</sup>	Sample	kg/m <sup>3</sup>	Sample	kg/m <sup>3</sup>	(mm)
2A	6.42	1A	5.37	8A	8.32	7A	10.43	9.5
2B	1.89	1B	2.80	8B	3.72	7B	4.33	28.6
2C	0.35	1C	1.84	8C	0.77	7C	3.25	47.6
2D	0.00	1D	1.85	8D	0.00	7D	2.84	66.7
2E	0.00	1E	1.84	8E	0.00	7E	2.51	85.7
4A	7.96	3A	6.47	10A	11.04	9A	9.52	9.5
4B	1.13	3B	2.97	10B	7.23	9B	4.80	28.6
4C	0.22	3C	2.96	10C	2.84	9C	3.11	47.6
4D	0.00	3D	2.33	10D	0.26	9D	242.00	66.7
4E	0.00	3E	1.98	10E	0.12	9E	1.34	85.7
6A	6.34	5A	6.48	12A	9.36	11A	8.40	9.5
6B	1.48	5B	3.80	12B	4.23	11B	4.35	28.6
6C	0.00	5C	LIP	12C	1.54	11C	3.41	47.6
6D	0.00	5D	2.66	12D	0.00	11D	2.06	66.7
6E	0.00	5E	2.27	12E	0.00	11E	1.66	85.7

<b>Bridge:</b> 87-453		<b>Bridge:</b> 87-453						
<b>Placement:</b> North 22 ft	<b>Placement:</b> South 18 ft	<b>Placement Date:</b> 06/30/97	<b>Placement Date:</b> 07/03/97					
<b>Survey Date:</b> 08/15/02	<b>Survey Date:</b> 08/15/02	<b>Survey Date:</b> 08/15/02	<b>Survey Date:</b> 08/15/02					
Off Crack		On Crack		Off Crack		On Crack		Mean Depth
Sample	kg/m <sup>3</sup>	Sample	kg/m <sup>3</sup>	Sample	kg/m <sup>3</sup>	Sample	kg/m <sup>3</sup>	(mm)
2A	7.08	1A	9.33	8A	LIP	7A	LIP	9.5
2B	2.04	1B	4.35	8B	LIP	7B	LIP	28.6
2C	0.21	1C	2.76	8C	LIP	7C	LIP	47.6
2D	0.00	1D	3.21	8D	0.00	7D	LIP	66.7
2E	0.00	1E	3.08	8E	0.00	7E	LIP	85.7
4A	6.54	3A	7.48	10A	8.67	9A	6.79	9.5
4B	1.98	3B	4.03	10B	2.25	9B	3.61	28.6
4C	0.36	3C	2.31	10C	0.26	9C	2.94	47.6
4D	0.00	3D	1.78	10D	0.00	9D	2.66	66.7
4E	0.00	3E	2.19	10E	0.00	9E	2.93	85.7
6A	5.66	5A	5.02	12A	10.80	11A	9.25	9.5
6B	1.65	5B	3.76	12B	3.98	11B	4.70	28.6
6C	0.32	5C	2.77	12C	1.29	11C	3.54	47.6
6D	0.10	5D	2.05	12D	0.14	11D	2.81	66.7
6E	0.00	5E	1.32	12E	0.00	11E	1.80	85.7

Table D.1 (con't) – Chloride Concentration Data

Off Crack		On Crack		Off Crack		On Crack		Mean Depth
Sample	kg/m <sup>3</sup>	Sample	kg/m <sup>3</sup>	Sample	kg/m <sup>3</sup>	Sample	kg/m <sup>3</sup>	(mm)
8A	9.10	7A	8.56	2A	6.79	1A	6.19	9.5
8B	6.07	7B	5.79	2B	3.78	1B	3.89	28.6
8C	3.06	7C	4.58	2C	1.83	1C	3.45	47.6
8D	1.32	7D	3.61	2D	0.31	1D	3.14	66.7
8E	0.31	7E	2.19	2E	0.00	1E	2.45	85.7
10A	8.39	9A	4.76	4A	5.99	3A	5.38	9.5
10B	6.13	9B	4.26	4B	3.47	3B	3.11	28.6
10C	3.94	9C	3.08	4C	1.75	3C	2.59	47.6
10D	2.19	9D	3.98	4D	0.42	3D	2.14	66.7
10E	0.46	9E	5.21	4E	0.12	3E	1.54	85.7
12A	8.07	11A	8.01	6A	5.60	5A	6.95	9.5
12B	4.99	11B	4.62	6B	2.57	5B	4.31	28.6
12C	2.38	11C	4.12	6C	0.95	5C	3.50	47.6
12D	0.78	11D	3.78	6D	0.19	5D	3.41	66.7
12E	0.12	11E	3.26	6E	0.00	5E	2.69	85.7

<b>Bridge:</b>		<b>89-184</b>	<b>Bridge:</b>		<b>89-184</b>
<b>Placement:</b>	Inside		<b>Placement:</b>	Outside	
<b>Placement Date:</b>	09/26/90		<b>Placement Date:</b>	09/28/90	
<b>Survey Date:</b>	08/05/02		<b>Survey Date:</b>	08/05/02	

Off Crack		On Crack		Off Crack		On Crack		Mean Depth
Sample	kg/m <sup>3</sup>	Sample	kg/m <sup>3</sup>	Sample	kg/m <sup>3</sup>	Sample	kg/m <sup>3</sup>	(mm)
8A	7.81	7A	9.07	2A	5.42	1A	8.94	9.5
8B	2.53	7B	4.42	2B	0.83	1B	4.47	28.6
8C	1.02	7C	3.09	2C	0.11	1C	3.13	47.6
8D	0.21	7D	2.43	2D	0.16	1D	1.96	66.7
8E	0.00	7E	1.51	2E	0.16	1E	2.85	85.7
10A	5.38	9A	5.88	4A	3.37	3A	5.89	9.5
10B	0.00	9B	3.05	4B	0.28	3B	2.34	28.6
10C	0.83	9C	2.48	4C	0.00	3C	2.06	47.6
10D	0.00	9D	2.20	4D	0.00	3D	1.84	66.7
10E	0.00	9E	1.99	4E	0.00	3E	0.93	85.7
12A	4.38	11A	8.53	6A	4.16	5A	6.17	9.5
12B	0.66	11B	4.62	6B	1.14	5B	3.46	28.6
12C	0.00	11C	3.59	6C	0.00	5C	2.08	47.6
12D	0.00	11D	2.19	6D	0.00	5D	0.80	66.7
12E	0.00	11E	1.61	6E	0.00	5E	0.43	85.7

Table D.1 (con't) – Chloride Concentration Data

<b>Bridge:</b>		<b>89-206</b>		<b>Bridge:</b>		<b>89-206</b>		
<b>Placement:</b>		Right of CL		<b>Placement:</b>		Left of CL		
<b>Placement Date:</b>		10/04/95		<b>Placement Date:</b>		10/10/95		
<b>Survey Date:</b>		08/28/02		<b>Survey Date:</b>		08/28/02		
<b>Off Crack</b>		<b>On Crack</b>		<b>Off Crack</b>		<b>On Crack</b>		<b>Mean Depth</b>
<b>Sample</b>	<b>kg/m<sup>3</sup></b>	<b>Sample</b>	<b>kg/m<sup>3</sup></b>	<b>Sample</b>	<b>kg/m<sup>3</sup></b>	<b>Sample</b>	<b>kg/m<sup>3</sup></b>	<b>(mm)</b>
8A	3.38	7A	5.08	1A	1.61	2A	5.45	9.5
8B	0.44	7B	2.32	1B	0.00	2B	2.73	28.6
8C	0.14	7C	1.66	1C	0.00	2C	2.25	47.6
8D	0.13	7D	0.63	1D	0.00	2D	0.47	66.7
8E	0.11	7E	0.13	1E	0.00	2E	0.13	85.7
10A	4.61	9A	4.10	3A	4.63	4A	4.95	9.5
10B	1.02	9B	2.47	3B	1.07	4B	1.42	28.6
10C	0.00	9C	2.36	3C	0.00	4C	0.28	47.6
10D	0.16	9D	2.13	3D	0.00	4D	0.00	66.7
10E	0.15	9E	1.84	3E	0.00	4E	0.00	85.7
12A	3.43	11A	3.39	5A	3.85	6A	5.92	9.5
12B	0.59	11B	1.82	5B	0.57	6B	3.50	28.6
12C	0.00	11C	2.32	5C	0.20	6C	2.52	47.6
12D	0.00	11D	2.02	5D	0.00	6D	1.49	66.7
12E	0.00	11E	1.70	5E	0.00	6E	1.52	85.7
<b>Bridge:</b>		<b>89-207</b>		<b>Bridge:</b>		<b>89-207</b>		
<b>Placement:</b>		Left of CL		<b>Placement:</b>		Right of CL		
<b>Placement Date:</b>		10/24/95		<b>Placement Date:</b>		04/19/96		
<b>Survey Date:</b>		08/27/02		<b>Survey Date:</b>		08/27/02		
<b>Off Crack</b>		<b>On Crack</b>		<b>Off Crack</b>		<b>On Crack</b>		<b>Mean Depth</b>
<b>Sample</b>	<b>kg/m<sup>3</sup></b>	<b>Sample</b>	<b>kg/m<sup>3</sup></b>	<b>Sample</b>	<b>kg/m<sup>3</sup></b>	<b>Sample</b>	<b>kg/m<sup>3</sup></b>	<b>(mm)</b>
7A	3.34	8A	6.85	1A	4.22	2A	5.04	9.5
7B	0.16	8B	3.74	1B	0.19	2B	3.30	28.6
7C	0.15	8C	2.77	1C	0.00	2C	2.66	47.6
7D	0.13	8D	2.36	1D	0.00	2D	1.85	66.7
7E	0.11	8E	2.59	1E	0.00	2E	1.56	85.7
9A	3.72	10A	5.71	3A	4.18	4A	5.20	9.5
9B	0.64	10B	2.52	3B	0.32	4B	3.34	28.6
9C	0.14	10C	2.53	3C	0.00	4C	2.40	47.6
9D	0.13	10D	2.64	3D	0.00	4D	2.23	66.7
9E	0.00	10E	2.30	3E	0.00	4E	1.80	85.7
11A	3.87	12A	4.29	5A	2.03	6A	5.40	9.5
11B	0.33	12B	3.14	5B	0.00	6B	2.84	28.6
11C	0.15	12C	2.53	5C	0.00	6C	2.21	47.6
11D	0.11	12D	2.07	5D	0.00	6D	2.21	66.7
11E	0.00	12E	1.72	5E	0.00	6E	1.93	85.7

Table D.1 (con't) – Chloride Concentration Data

<b>Off Crack</b>		<b>On Crack</b>		<b>Off Crack</b>		<b>On Crack</b>		<b>Mean Depth</b>
<b>Sample</b>	<b>kg/m<sup>3</sup></b>	<b>Sample</b>	<b>kg/m<sup>3</sup></b>	<b>Sample</b>	<b>kg/m<sup>3</sup></b>	<b>Sample</b>	<b>kg/m<sup>3</sup></b>	<b>(mm)</b>
8A	0.52	7A	3.83	2A	3.45	1A	6.44	9.5
8B	0.00	7B	2.34	2B	1.20	1B	2.87	28.6
8C	0.00	7C	2.11	2C	0.26	1C	2.10	47.6
8D	0.00	7D	1.76	2D	0.00	1D	2.24	66.7
8E	0.00	7E	0.20	2E	0.00	1E	1.62	85.7
10A	3.22	9A	4.15	4A	1.53	3A	3.83	9.5
10B	0.29	9B	2.39	4B	0.00	3B	2.78	28.6
10C	0.12	9C	2.01	4C	0.13	3C	2.30	47.6
10D	0.00	9D	1.56	4D	0.00	3D	1.93	66.7
10E	0.00	9E	0.71	4E	0.00	3E	1.44	85.7
12A	1.16	11A	4.99	6A	1.97	5A	3.08	9.5
12B	0.00	11B	2.71	6B	0.35	5B	2.05	28.6
12C	0.00	11C	2.28	6C	0.13	5C	2.04	47.6
12D	0.00	11D	1.71	6D	0.00	5D	1.83	66.7
12E	0.00	11E	1.06	6E	0.00	5E	1.68	85.7

<b>Bridge:</b>		<b>89-210</b>	<b>Bridge:</b>		<b>89-210</b>
<b>Placement:</b>	Right of CL		<b>Placement:</b>	Left of CL	
<b>Placement Date:</b>	10/12/95		<b>Placement Date:</b>	10/18/95	
<b>Survey Date:</b>	08/16/01		<b>Survey Date:</b>	08/16/01	

<b>Off Crack</b>		<b>On Crack</b>		<b>Off Crack</b>		<b>On Crack</b>		<b>Mean Depth</b>
<b>Sample</b>	<b>kg/m<sup>3</sup></b>	<b>Sample</b>	<b>kg/m<sup>3</sup></b>	<b>Sample</b>	<b>kg/m<sup>3</sup></b>	<b>Sample</b>	<b>kg/m<sup>3</sup></b>	<b>(mm)</b>
1A	8.00	2A	7.73	13A	5.70	14A	6.03	9.5
1B	2.91	2B	3.98	13B	1.32	14B	2.94	28.6
1C	0.45	2C	2.90	13C	0.14	14C	2.75	47.6
1D	0.14	2D	2.01	13D	0.12	14D	2.60	66.7
1E	0.13	2E	2.18	13E	0.00	14E	2.49	85.7
3A	7.83	4A	6.66	15A	5.95	16A	5.05	9.5
3B	1.89	4B	3.42	15B	1.22	16B	2.03	28.6
3C	0.21	4C	2.45	15C	0.12	16C	1.56	47.6
3D	0.13	4D	1.76	15D	0.00	16D	1.18	66.7
3E	0.10	4E	1.54	15E	0.00	16E	0.59	85.7
5A	6.84	6A	7.38	17A	5.02	18A	4.78	9.5
5B	1.92	6B	3.34	17B	1.01	18B	2.69	28.6
5C	0.22	6C	2.34	17C	0.13	18C	1.71	47.6
5D	0.00	6D	1.44	17D	0.13	18D	1.22	66.7
5E	1.52	6E	0.35	17E	0.00	18E	0.56	85.7

Table D.1 (con't) – Chloride Concentration Data

<b>Bridge:</b>		<b>89-234</b>		<b>Bridge:</b>		<b>89-235</b>		
<b>Placement:</b>		SFO Center 12 ft		<b>Placement:</b>		SFO Right 18 ft		
<b>Placement Date:</b>		06/28/96		<b>Placement Date:</b>		05/01/97		
<b>Survey Date:</b>		09/23/02		<b>Survey Date:</b>		09/24/02		
<b>Off Crack</b>		<b>On Crack</b>		<b>Off Crack</b>		<b>On Crack</b>		<b>Mean Depth</b>
<b>Sample</b>	<b>kg/m<sup>3</sup></b>	<b>Sample</b>	<b>kg/m<sup>3</sup></b>	<b>Sample</b>	<b>kg/m<sup>3</sup></b>	<b>Sample</b>	<b>kg/m<sup>3</sup></b>	<b>(mm)</b>
8A	6.60	7A	8.09	1A	5.03	2A	5.10	9.5
8B	2.19	7B	3.07	1B	0.78	2B	2.48	28.6
8C	1.30	7C	2.22	1C	0.16	2C	0.99	47.6
8D	0.17	7D	2.37	1D	0.12	2D	0.36	66.7
8E	0.20	7E	2.58	1E	0.11	2E	0.17	85.7
10A	5.39	9A	7.49	3A	3.01	4A	5.66	9.5
10B	1.19	9B	4.06	3B	1.16	4B	2.22	28.6
10C	0.11	9C	3.25	3C	0.58	4C	1.03	47.6
10D	0.00	9D	2.61	3D	0.21	4D	0.35	66.7
10E	0.00	9E	2.04	3E	0.12	4E	0.16	85.7
12A	6.91	11A	5.68	5A	3.39	6A	6.53	9.5
12B	0.98	11B	2.76	5B	0.19	6B	2.88	28.6
12C	0.12	11C	2.67	5C	0.00	6C	1.99	47.6
12D	0.13	11D	2.55	5D	0.00	6D	0.98	66.7
12E	0.12	11E	2.26	5E	0.00	6E	0.33	85.7
<b>Bridge:</b>		<b>89-240</b>		<b>Bridge:</b>		<b>89-240</b>		
<b>Placement:</b>		Rt. 22 ft SFO		<b>Placement:</b>		Lt. 22 ft SFO		
<b>Placement Date:</b>		08/05/97		<b>Placement Date:</b>		08/07/97		
<b>Survey Date:</b>		08/29/02		<b>Survey Date:</b>		08/29/02		
<b>Off Crack</b>		<b>On Crack</b>		<b>Off Crack</b>		<b>On Crack</b>		<b>Mean Depth</b>
<b>Sample</b>	<b>kg/m<sup>3</sup></b>	<b>Sample</b>	<b>kg/m<sup>3</sup></b>	<b>Sample</b>	<b>kg/m<sup>3</sup></b>	<b>Sample</b>	<b>kg/m<sup>3</sup></b>	<b>(mm)</b>
1A	5.52	2A	5.25	7A	5.09	8A	5.32	9.5
1B	0.65	2B	3.05	7B	0.39	8B	1.82	28.6
1C	0.00	2C	2.29	7C	0.00	8C	0.22	47.6
1D	0.00	2D	1.93	7D	0.00	8D	0.00	66.7
1E	0.10	2E	0.95	7E	0.00	8E	0.00	85.7
3A	5.93	4A	6.37	9A	6.98	10A	8.12	9.5
3B	0.35	4B	1.67	9B	1.84	10B	2.40	28.6
3C	0.00	4C	0.27	9C	0.18	10C	0.35	47.6
3D	0.00	4D	0.11	9D	0.13	10D	0.21	66.7
3E	0.11	4E	0.00	9E	0.15	10E	0.18	85.7
6A	5.79	6A	4.74	11A	5.16	12A	7.86	9.5
6B	1.22	6B	0.63	11B	2.56	12B	3.84	28.6
6C	0.19	6C	0.90	11C	0.58	12C	0.45	47.6
6D	0.12	6D	0.92	11D	0.15	12D	0.17	66.7
6E	0.00	6E	0.65	11E	0.15	12E	0.13	85.7

Table D.1 (con't) – Chloride Concentration Data

Off Crack		On Crack		Off Crack		On Crack		Mean Depth
Sample	kg/m <sup>3</sup>	Sample	kg/m <sup>3</sup>	Sample	kg/m <sup>3</sup>	Sample	kg/m <sup>3</sup>	(mm)
7A	6.19	8A	6.35	1A	7.83	2A	8.85	9.5
7B	0.82	8B	4.00	1B	1.83	2B	5.11	28.6
7C	0.20	8C	3.11	1C	0.23	2C	4.41	47.6
7D	0.17	8D	2.25	1D	0.11	2D	3.22	66.7
7E	0.00	8E	1.93	1E	0.10	2E	2.59	85.7
10A	7.17	9A	8.62	4A	7.72	3A	7.61	9.5
10B	2.29	9B	5.06	4B	1.09	3B	1.67	28.6
10C	0.46	9C	3.82	4C	0.16	3C	0.37	47.6
10D	0.24	9D	2.54	4D	0.29	3D	0.41	66.7
10E	0.20	9E	2.63	4E	0.10	3E	LIP	85.7
12A	2.95	11A	7.47	5A	4.13	6A	7.19	9.5
12B	0.19	11B	3.90	5B	0.42	6B	4.00	28.6
12C	0.00	11C	2.99	5C	0.31	6C	0.45	47.6
12D	0.17	11D	2.01	5D	0.12	6D	1.73	66.7
12E	0.32	11E	2.20	5E	0.00	6E	0.76	85.7

Off Crack		On Crack		Off Crack		On Crack		Mean Depth
Sample	kg/m <sup>3</sup>	Sample	kg/m <sup>3</sup>	Sample	kg/m <sup>3</sup>	Sample	kg/m <sup>3</sup>	(mm)
19A	7.04	20A	7.29	14A	4.71	13A	8.48	9.5
19B	1.02	20B	4.42	14B	0.27	13B	4.13	28.6
19C	0.12	20C	3.46	14C	0.19	13C	3.60	47.6
19D	0.00	20D	3.08	14D	0.11	13D	3.01	66.7
19E	0.00	20E	2.65	14E	0.10	13E	2.84	85.7
21A	5.32	22A	7.54	16A	5.64	15A	6.03	9.5
21B	0.55	22B	4.06	16B	0.42	15B	3.47	28.6
21C	0.17	22C	2.84	16C	0.13	15C	2.53	47.6
21D	0.00	22D	2.51	16D	0.00	15D	1.85	66.7
21E	0.00	22E	2.30	16E	0.00	15E	0.99	85.7
24A	5.01	23A	7.75	18A	4.06	17A	6.37	9.5
24B	0.42	23B	4.42	18B	0.43	17B	2.95	28.6
24C	0.29	23C	2.56	18C	0.18	17C	1.62	47.6
24D	0.54	23D	2.18	18D	0.14	17D	0.70	66.7
24E	0.54	23E	1.86	18E	0.00	17E	0.29	85.7

Table D.1 (con't) – Chloride Concentration Data

Off Crack		On Crack		Off Crack		On Crack		Mean Depth
Sample	kg/m <sup>3</sup>	Sample	kg/m <sup>3</sup>	Sample	kg/m <sup>3</sup>	Sample	kg/m <sup>3</sup>	(mm)
7A	7.68	8A	7.72	1A	6.04	2A	6.47	9.5
7B	0.76	8B	3.11	1B	0.33	2B	3.18	28.6
7C	0.14	8C	2.31	1C	0.00	2C	2.21	47.6
7D	0.12	8D	1.62	1D	0.21	2D	1.88	66.7
7E	0.27	8E	0.60	1E	0.11	2E	1.94	85.7
9A	5.19	10A	5.75	4A	5.58	3A	5.94	9.5
9B	0.81	10B	2.26	4B	0.58	3B	3.44	28.6
9C	0.21	10C	1.91	4C	0.17	3C	2.59	47.6
9D	0.12	10D	1.51	4D	0.18	3D	2.28	66.7
9E	0.18	10E	1.17	4E	0.13	3E	1.96	85.7
11A	5.92	12A	6.14	5A	7.89	6A	9.96	9.5
11B	1.46	12B	2.77	5B	1.27	6B	4.50	28.6
11C	0.18	12C	2.43	5C	0.14	6C	2.59	47.6
11D	0.17	12D	1.92	5D	0.35	6D	2.65	66.7
11E	0.00	12E	1.76	5E	0.55	6E	2.30	85.7

<b>Bridge:</b> 89-245		<b>Bridge:</b> 89-245						
<b>Placement:</b> Rt. of CL Unit #2	<b>Placement:</b> Rt. of CL Unit #1	<b>Placement Date:</b> 10/23/97	<b>Placement Date:</b> 10/24/97					
<b>Survey Date:</b> 09/03/02	<b>Survey Date:</b> 09/03/02	<b>Survey Date:</b> 09/03/02	<b>Survey Date:</b> 09/03/02					
Off Crack		On Crack		Off Crack		On Crack		Mean Depth
Sample	kg/m <sup>3</sup>	Sample	kg/m <sup>3</sup>	Sample	kg/m <sup>3</sup>	Sample	kg/m <sup>3</sup>	(mm)
7A	3.09	8A	3.00	1A	6.06	2A	4.57	9.5
7B	0.23	8B	1.54	1B	0.44	2B	2.47	28.6
7C	0.11	8C	1.23	1C	0.15	2C	2.38	47.6
7D	0.13	8D	0.96	1D	0.13	2D	1.86	66.7
7E	0.10	8E	0.68	1E	0.10	2E	1.89	85.7
9A	3.99	10A	3.79	4A	3.98	3A	4.44	9.5
9B	1.19	10B	1.24	4B	0.30	3B	2.34	28.6
9C	0.26	10C	0.97	4C	0.22	3C	2.29	47.6
9D	0.14	10D	0.85	4D	0.00	3D	1.99	66.7
9E	0.11	10E	0.54	4E	0.00	3E	1.37	85.7
12A	2.70	11A	4.35	6A	3.07	5A	4.52	9.5
12B	0.69	11B	1.92	6B	0.43	5B	2.23	28.6
12C	0.16	11C	1.58	6C	0.13	5C	1.96	47.6
12D	0.12	11D	1.05	6D	0.00	5D	1.79	66.7
12E	0.00	11E	1.11	6E	0.00	5E	1.59	85.7

Table D.1 (con't) – Chloride Concentration Data

<b>Off Crack</b>		<b>On Crack</b>		<b>Off Crack</b>		<b>On Crack</b>		<b>Mean Depth</b>
<b>Sample</b>	<b>kg/m<sup>3</sup></b>	<b>Sample</b>	<b>kg/m<sup>3</sup></b>	<b>Sample</b>	<b>kg/m<sup>3</sup></b>	<b>Sample</b>	<b>kg/m<sup>3</sup></b>	<b>(mm)</b>
8A	1.85	7A	4.42	3A	3.77	1A	6.69	9.5
8B	0.00	7B	1.70	3B	0.79	1B	3.12	28.6
8C	0.00	7C	1.43	3C	0.13	1C	3.09	47.6
8D	0.00	7D	1.29	3D	0.13	1D	2.22	66.7
8E	0.00	7E	1.15	3E	0.00	1E	1.66	85.7
10A	1.65	9A	3.01	4A	1.75	2A	4.62	9.5
10B	0.12	9B	1.93	4B	0.15	2B	2.76	28.6
10C	0.00	9C	1.97	4C	0.00	2C	3.00	47.6
10D	0.12	9D	2.01	4D	0.00	2D	2.38	66.7
10E	0.00	9E	0.82	4E	0.00	2E	1.80	85.7
12A	1.58	11A	3.52	5A	2.30	6A	4.59	9.5
12B	0.17	11B	1.71	5B	0.24	6B	2.64	28.6
12C	0.00	11C	1.44	5C	0.13	6C	2.35	47.6
12D	0.00	11D	1.66	5D	0.12	6D	1.93	66.7
12E	0.00	11E	1.24	5E	0.20	6E	1.79	85.7

<b>Bridge:</b>		<b>89-247</b>	<b>Bridge:</b>		<b>89-247</b>
<b>Placement:</b>	SFO West 13 ft		<b>Placement:</b>	SFO East 26 ft	
<b>Placement Date:</b>	05/05/97		<b>Placement Date:</b>	05/07/97	
<b>Survey Date:</b>	09/05/02		<b>Survey Date:</b>	09/05/02	

<b>Off Crack</b>		<b>On Crack</b>		<b>Off Crack</b>		<b>On Crack</b>		<b>Mean Depth</b>
<b>Sample</b>	<b>kg/m<sup>3</sup></b>	<b>Sample</b>	<b>kg/m<sup>3</sup></b>	<b>Sample</b>	<b>kg/m<sup>3</sup></b>	<b>Sample</b>	<b>kg/m<sup>3</sup></b>	<b>(mm)</b>
2A	2.07	1A	5.92	7A	1.74	8A	3.56	9.5
2B	0.42	1B	3.32	7B	0.19	8B	3.00	28.6
2C	0.14	1C	2.72	7C	0.16	8C	2.65	47.6
2D	0.12	1D	2.43	7D	0.13	8D	2.37	66.7
2E	0.16	1E	1.72	7E	0.14	8E	2.12	85.7
3A	3.59	4A	4.08	10A	1.48	10A	3.42	9.5
3B	1.32	4B	2.99	10B	0.16	10B	2.97	28.6
3C	0.30	4C	1.51	10C	0.00	10C	2.48	47.6
3D	0.11	4D	1.45	10D	0.00	10D	2.15	66.7
3E	0.39	4E	0.83	10E	0.12	10E	2.24	85.7
6A	1.69	5A	4.45	11A	2.24	12A	2.72	9.5
6B	1.17	5B	2.72	11B	0.26	12B	2.18	28.6
6C	0.39	5C	2.30	11C	0.00	12C	1.69	47.6
6D	0.14	5D	1.41	11D	0.00	12D	1.09	66.7
6E	0.11	5E	1.80	11E	0.00	12E	0.61	85.7

Table D.1 (con't) – Chloride Concentration Data

Off Crack		On Crack		Off Crack		On Crack		Mean Depth
Sample	kg/m <sup>3</sup>	Sample	kg/m <sup>3</sup>	Sample	kg/m <sup>3</sup>	Sample	kg/m <sup>3</sup>	(mm)
8A	4.30	7A	7.13	2A	2.97	1A	7.61	9.5
8B	0.35	7B	5.14	2B	0.21	1B	4.56	28.6
8C	0.00	7C	4.18	2C	0.00	1C	3.83	47.6
8D	0.00	7D	3.66	2D	0.00	1D	4.42	66.7
8E	0.00	7E	2.74	2E	0.00	1E	3.34	85.7
10A	5.18	9A	7.91	4A	4.42	3A	6.37	9.5
10B	1.27	9B	5.66	4B	0.34	3B	5.09	28.6
10C	0.00	9C	4.39	4C	0.00	3C	5.68	47.6
10D	0.00	9D	3.38	4D	0.00	3D	5.80	66.7
10E	0.00	9E	2.14	4E	0.00	3E	6.70	85.7
12A	6.01	11A	9.09	6A	5.19	5A	6.42	9.5
12B	2.14	11B	6.69	6B	0.75	5B	5.68	28.6
12C	0.28	11C	5.20	6C	0.00	5C	4.96	47.6
12D	0.00	11D	4.02	6D	0.00	5D	4.32	66.7
12E	0.00	11E	2.53	6E	0.00	5E	4.51	85.7

<b>Bridge:</b> 46-289		<b>Bridge:</b> 46-289						
<b>Placement:</b> Inside 24 ft		<b>Placement:</b> Outside 20 ft						
<b>Placement Date:</b> 09/02/92		<b>Placement Date:</b> 09/11/92						
<b>Survey Date:</b> 07/17/02		<b>Survey Date:</b> 07/17/02						
Off Crack		On Crack		Off Crack		On Crack		Mean Depth
Sample	kg/m <sup>3</sup>	Sample	kg/m <sup>3</sup>	Sample	kg/m <sup>3</sup>	Sample	kg/m <sup>3</sup>	(mm)
2A	6.38	1A	8.08	8A	4.14	7A	7.37	9.5
2B	1.67	1B	4.24	8B	0.17	7B	5.21	28.6
2C	0.15	1C	3.18	8C	0.00	7C	3.29	47.6
2D	0.00	1D	1.98	8D	0.00	7D	2.85	66.7
2E	0.00	1E	1.57	8E	0.00	7E	2.75	85.7
4A	5.67	3A	8.05	10A	8.50	9A	7.89	9.5
4B	0.81	3B	5.40	10B	2.95	9B	5.81	28.6
4C	0.00	3C	4.36	10C	0.87	9C	4.33	47.6
4D	0.00	3D	3.93	10D	0.16	9D	3.43	66.7
4E	0.14	3E	3.01	10E	0.00	9E	2.81	85.7
6A	6.19	5A	8.66	12A	6.60	11A	9.00	9.5
6B	0.97	5B	4.87	12B	1.26	11B	6.80	28.6
6C	0.00	5C	4.05	12C	0.00	11C	5.33	47.6
6D	0.00	5D	3.20	12D	0.00	11D	4.99	66.7
6E	0.00	5E	2.41	12E	0.00	11E	5.67	85.7

Table D.1 (con't) – Chloride Concentration Data

Off Crack		On Crack		Off Crack		On Crack		Mean Depth
Sample	kg/m <sup>3</sup>	Sample	kg/m <sup>3</sup>	Sample	kg/m <sup>3</sup>	Sample	kg/m <sup>3</sup>	(mm)
2A	5.18	1A	7.36	8A	5.09	7A	4.76	9.5
2B	1.22	1B	3.60	8B	1.44	7B	3.06	28.6
2C	0.00	1C	2.03	8C	0.00	7C	2.25	47.6
2D	0.00	1D	1.13	8D	0.00	7D	2.05	66.7
2E	0.00	1E	0.75	8E	0.00	7E	0.99	85.7
4A	4.00	3A	6.07	10A	4.88	9A	3.95	9.5
4B	0.54	3B	3.26	10B	2.72	9B	2.09	28.6
4C	0.00	3C	2.44	10C	1.92	9C	2.00	47.6
4D	0.00	3D	1.12	10D	0.57	9D	1.29	66.7
4E	0.00	3E	0.74	10E	0.10	9E	0.45	85.7
6A	3.63	5A	5.60	12A	4.07	11A	5.82	9.5
6B	1.22	5B	4.19	12B	0.64	11B	3.33	28.6
6C	0.00	5C	3.32	12C	0.00	11C	2.32	47.6
6D	0.00	5D	1.87	12D	0.00	11D	1.22	66.7
6E	0.00	5E	0.97	12E	0.00	11E	0.42	85.7

<b>Bridge:</b> 46-299		<b>Bridge:</b> 46-299	
<b>Placement:</b> Rt. of CL 22 ft	<b>Placement:</b> Lt. of CL 18 ft	<b>Placement Date:</b> 07/28/94	<b>Placement Date:</b> 07/30/94
<b>Survey Date:</b> 06/27/02	<b>Survey Date:</b> 06/27/02		

Off Crack		On Crack		Off Crack		On Crack		Mean Depth
Sample	kg/m <sup>3</sup>	Sample	kg/m <sup>3</sup>	Sample	kg/m <sup>3</sup>	Sample	kg/m <sup>3</sup>	(mm)
2A	4.10	1A	7.64	8A	6.29	7A	3.83	9.5
2B	2.03	1B	4.80	8B	1.96	7B	2.34	28.6
2C	0.46	1C	3.22	8C	0.26	7C	2.11	47.6
2D	0.15	1D	1.20	8D	0.00	7D	1.76	66.7
2E	0.17	1E	0.33	8E	0.00	7E	0.20	85.7
4A	5.24	3A	6.11	10A	5.36	9A	6.25	9.5
4B	1.46	3B	3.90	10B	2.60	9B	3.67	28.6
4C	0.00	3C	3.40	10C	1.28	9C	2.23	47.6
4D	0.00	3D	2.38	10D	0.27	9D	0.92	66.7
4E	0.00	3E	1.68	10E	0.00	9E	0.67	85.7
6A	5.40	5A	5.97	12A	6.37	11A	7.44	9.5
6B	2.62	5B	3.98	12B	3.18	11B	3.70	28.6
6C	0.40	5C	3.12	12C	0.57	11C	2.72	47.6
6D	0.00	5D	2.78	12D	0.16	11D	2.45	66.7
6E	0.00	5E	1.98	12E	0.17	11E	1.43	85.7

Table D.1 (con't) – Chloride Concentration Data

Off Crack		On Crack		Off Crack		On Crack		Mean Depth
Sample	kg/m <sup>3</sup>	Sample	kg/m <sup>3</sup>	Sample	kg/m <sup>3</sup>	Sample	kg/m <sup>3</sup>	(mm)
2A	6.24	1A	11.11	8A	3.13	7A	LIP	9.5
2B	2.13	1B	3.97	8B	0.66	7B	LIP	28.6
2C	0.11	1C	2.39	8C	0.00	7C	LIP	47.6
2D	0.00	1D	2.06	8D	0.00	7D	3.13	66.7
2E	0.00	1E	1.85	8E	0.00	7E	3.88	85.7
4A	5.42	3A	5.66	10A	6.39	9A	6.50	9.5
4B	1.60	3B	3.20	10B	1.30	9B	3.52	28.6
4C	0.00	3C	2.17	10C	0.00	9C	2.29	47.6
4D	0.00	3D	1.54	10D	0.13	9D	2.15	66.7
4E	0.00	3E	0.96	10E	0.00	9E	1.78	85.7
6A	4.56	5A	6.11	12A	4.29	11A	5.15	9.5
6B	0.72	5B	2.59	12B	2.42	11B	4.06	28.6
6C	0.00	5C	1.99	12C	0.65	11C	2.90	47.6
6D	0.00	5D	1.49	12D	0.00	11D	2.99	66.7
6E	0.00	5E	1.04	12E	0.00	11E	5.10	85.7

<b>Bridge:</b> 46-301		<b>Bridge:</b> 46-301						
<b>Placement:</b> Rt. of CL 24 ft	<b>Placement:</b> Lt. of CL 24 to 36 ft	<b>Placement:</b> Lt. of CL 24 ft	<b>Placement:</b> Lt. of CL 24 to 36 ft					
<b>Placement Date:</b> 08/03/94	<b>Placement Date:</b> 08/06/94	<b>Placement Date:</b> 08/06/94	<b>Placement Date:</b> 08/06/94					
<b>Survey Date:</b> 06/20/02	<b>Survey Date:</b> 07/03/02	<b>Survey Date:</b> 06/20/02	<b>Survey Date:</b> 06/20/02					
Off Crack		On Crack		Off Crack		On Crack		Mean Depth
Sample	kg/m <sup>3</sup>	Sample	kg/m <sup>3</sup>	Sample	kg/m <sup>3</sup>	Sample	kg/m <sup>3</sup>	(mm)
2A	5.08	1A	7.64	8A	7.15	7A	8.24	9.5
2B	2.28	1B	3.71	8B	3.75	7B	4.29	28.6
2C	0.17	1C	2.93	8C	0.80	7C	3.42	47.6
2D	0.00	1D	3.24	8D	0.00	7D	3.59	66.7
2E	0.00	1E	2.95	8E	0.00	7E	3.38	85.7
4A	6.61	3A	6.74	10A	5.34	9A	6.63	9.5
4B	2.48	3B	3.63	10B	1.13	9B	3.64	28.6
4C	0.32	3C	2.64	10C	0.00	9C	2.64	47.6
4D	0.11	3D	2.07	10D	0.00	9D	2.76	66.7
4E	0.00	3E	1.61	10E	0.00	9E	2.43	85.7
6A	3.92	5A	5.42	12A	6.22	11A	6.34	9.5
6B	1.35	5B	2.88	12B	2.10	11B	3.83	28.6
6C	0.00	5C	2.87	12C	0.00	11C	3.12	47.6
6D	0.00	5D	3.29	12D	0.00	11D	2.89	66.7
6E	0.00	5E	3.19	12E	0.00	11E	2.51	85.7

Table D.1 (con't) – Chloride Concentration Data

Off Crack		On Crack		Off Crack		On Crack		Mean Depth
Sample	kg/m <sup>3</sup>	Sample	kg/m <sup>3</sup>	Sample	kg/m <sup>3</sup>	Sample	kg/m <sup>3</sup>	(mm)
2A	4.34	1A	6.13	8A	6.37	7A	10.41	9.5
2B	0.57	1B	4.56	8B	0.56	7B	5.49	28.6
2C	0.00	1C	2.62	8C	0.11	7C	3.51	47.6
2D	0.14	1D	2.18	8D	0.00	7D	2.92	66.7
2E	0.10	1E	0.94	8E	0.00	7E	2.31	85.7
4A	7.13	3A	6.74	10A	10.72	9A	8.68	9.5
4B	3.07	3B	4.24	10B	2.65	9B	5.24	28.6
4C	0.81	3C	3.16	10C	0.14	9C	4.02	47.6
4D	0.00	3D	2.04	10D	0.15	9D	2.77	66.7
4E	0.15	3E	1.27	10E	0.18	9E	1.53	85.7
6A	8.62	5A	8.78	12A	8.47	11A	10.03	9.5
6B	3.46	5B	5.91	12B	1.66	11B	5.61	28.6
6C	0.44	5C	3.01	12C	0.13	11C	3.32	47.6
6D	0.00	5D	0.80	12D	0.00	11D	2.07	66.7
6E	0.00	5E	0.22	12E	0.00	11E	2.07	85.7

<b>Bridge:</b> 75-49		<b>Bridge:</b> 75-49						
<b>Placement:</b> Eastbound		<b>Placement:</b> Westbound						
<b>Placement Date:</b> 06/04/91		<b>Placement Date:</b> 06/07/91						
<b>Survey Date:</b> 08/20/02		<b>Survey Date:</b> 08/20/02						
Off Crack		On Crack		Off Crack		On Crack		Mean Depth
Sample	kg/m <sup>3</sup>	Sample	kg/m <sup>3</sup>	Sample	kg/m <sup>3</sup>	Sample	kg/m <sup>3</sup>	(mm)
2A	7.39	1A	9.17	8A	7.48	7A	7.24	9.5
2B	5.99	1B	6.11	8B	3.89	7B	4.38	28.6
2C	3.28	1C	3.88	8C	1.33	7C	3.36	47.6
2D	1.39	1D	2.18	8D	0.24	7D	2.58	66.7
2E	0.20	1E	0.62	8E	0.11	7E	1.54	85.7
4A	7.86	3A	7.32	10A	8.66	9A	6.66	9.5
4B	4.05	3B	5.09	10B	4.17	9B	4.50	28.6
4C	0.97	3C	4.13	10C	0.59	9C	3.15	47.6
4D	0.13	3D	2.49	10D	0.11	9D	2.74	66.7
4E	0.00	3E	0.45	10E	0.00	9E	3.01	85.7
6A	8.48	5A	6.16	12A	6.47	11A	7.97	9.5
6B	6.50	5B	5.73	12B	3.76	11B	5.34	28.6
6C	2.45	5C	3.61	12C	1.96	11C	2.90	47.6
6D	0.72	5D	3.27	12D	0.55	11D	2.81	66.7
6E	0.00	5E	2.32	12E	0.12	11E	2.56	85.7

Table D.1 (con't) – Chloride Concentration Data

Off Crack		On Crack		Off Crack		On Crack		Mean Depth (mm)
Sample	kg/m <sup>3</sup>	Sample	kg/m <sup>3</sup>	Sample	kg/m <sup>3</sup>	Sample	kg/m <sup>3</sup>	
2A	5.82	1A	5.48	7A	4.90	8A	6.87	9.5
2B	0.94	1B	2.99	7B	1.47	8B	4.43	28.6
2C	0.00	1C	2.50	7C	0.19	8C	3.09	47.6
2D	0.10	1D	1.75	7D	0.00	8D	2.72	66.7
2E	0.12	1E	1.07	7E	0.19	8E	2.33	85.7
4A	5.06	3A	6.08	9A	6.20	10A	7.77	9.5
4B	0.29	3B	2.99	9B	1.28	10B	4.43	28.6
4C	0.00	3C	1.72	9C	0.15	10C	3.58	47.6
4D	0.00	3D	3.55	9D	0.13	10D	2.82	66.7
4E	0.00	3E	2.57	9E	0.00	10E	2.30	85.7
6A	4.42	5A	6.44	11A	6.63	12A	8.37	9.5
6B	0.57	5B	3.22	11B	1.44	12B	4.20	28.6
6C	0.00	5C	3.13	11C	0.12	12C	2.60	47.6
6D	0.00	5D	2.56	11D	0.00	12D	2.21	66.7
6E	0.00	5E	1.11	11E	0.00	12E	1.65	85.7

<b>Bridge:</b>		<b>81-49</b>	<b>Bridge:</b>		<b>81-49</b>			
<b>Placement:</b>	Rt. 22 ft		<b>Placement:</b>	Rt. of CL 12 ft				
<b>Placement Date:</b>	04/08/92		<b>Placement Date:</b>	04/13/92				
<b>Survey Date:</b>	08/20/02		<b>Survey Date:</b>	08/21/02				
Off Crack		On Crack		Off Crack		On Crack		Mean Depth (mm)
Sample	kg/m <sup>3</sup>	Sample	kg/m <sup>3</sup>	Sample	kg/m <sup>3</sup>	Sample	kg/m <sup>3</sup>	
14A	4.30	13A	8.68	20A	5.54	19A	9.22	9.5
14B	0.54	13B	4.28	20B	0.80	19B	4.97	28.6
14C	0.00	13C	3.17	20C	0.00	19C	4.02	47.6
14D	0.00	13D	3.44	20D	0.00	19D	3.56	66.7
14E	0.00	13E	3.61	20E	0.00	19E	2.24	85.7
16A	5.47	15A	8.11	22A	7.65	21A	7.73	9.5
16B	0.92	15B	4.27	22B	1.62	21B	5.11	28.6
16C	0.00	15C	3.03	22C	0.00	21C	4.10	47.6
16D	0.00	15D	3.15	22D	0.00	21D	3.94	66.7
16E	0.00	15E	2.94	22E	0.00	21E	3.47	85.7
18A	6.65	17A	6.84	24A	8.04	23A	6.35	9.5
18B	1.07	17B	4.16	24B	1.92	23B	3.88	28.6
18C	0.00	17C	2.62	24C	0.00	23C	2.56	47.6
18D	0.00	17D	2.16	24D	0.00	23D	2.26	66.7
18E	0.00	17E	2.36	24E	0.00	23E	1.87	85.7

Table D.1 (con't) – Chloride Concentration Data

Off Crack		On Crack		Off Crack		On Crack		Mean Depth
Sample	kg/m <sup>3</sup>	Sample	kg/m <sup>3</sup>	Sample	kg/m <sup>3</sup>	Sample	kg/m <sup>3</sup>	(mm)
8A	4.94	7A	6.72	2A	5.54	1A	5.06	9.5
8B	2.89	7B	4.84	2B	2.74	1B	2.20	28.6
8C	0.53	7C	3.61	2C	1.15	1C	1.15	47.6
8D	0.00	7D	2.86	2D	0.41	1D	0.60	66.7
8E	0.00	7E	2.38	2E	0.00	1E	0.00	85.7
10A	5.08	9A	6.95	4A	7.26	3A	4.82	9.5
10B	1.91	9B	4.11	4B	3.51	3B	2.67	28.6
10C	0.32	9C	3.27	4C	1.53	3C	1.69	47.6
10D	0.00	9D	2.61	4D	0.20	3D	0.62	66.7
10E	0.00	9E	1.61	4E	0.00	3E	0.00	85.7
12A	7.10	11A	6.32	6A	5.90	5A	6.69	9.5
12B	2.39	11B	4.28	6B	1.57	5B	4.32	28.6
12C	0.34	11C	3.39	6C	0.17	5C	3.37	47.6
12D	0.00	11D	3.16	6D	0.00	5D	3.11	66.7
12E	0.00	11E	3.23	6E	0.00	5E	2.59	85.7

<b>Bridge:</b>		<b>89-183</b>	<b>Bridge:</b>		<b>89-183</b>
<b>Placement:</b>	Rt. Side		<b>Placement:</b>	Lt. Side	
<b>Placement Date:</b>	09/21/90		<b>Placement Date:</b>	09/25/90	
<b>Survey Date:</b>	07/30/02		<b>Survey Date:</b>	07/30/02	

Off Crack		On Crack		Off Crack		On Crack		Mean Depth
Sample	kg/m <sup>3</sup>	Sample	kg/m <sup>3</sup>	Sample	kg/m <sup>3</sup>	Sample	kg/m <sup>3</sup>	(mm)
8A	6.52	7A	8.52	2A	3.53	1A	6.28	9.5
8B	0.33	7B	4.73	2B	1.00	1B	2.66	28.6
8C	0.00	7C	4.49	2C	0.14	1C	4.06	47.6
8D	0.00	7D	4.26	2D	0.00	1D	3.96	66.7
8E	0.00	7E	2.89	2E	0.00	1E	LIP	85.7
10A	6.56	9A	6.92	4A	2.97	3A	6.49	9.5
10B	0.36	9B	3.39	4B	1.44	3B	4.49	28.6
10C	0.00	9C	3.11	4C	0.18	3C	4.21	47.6
10D	0.00	9D	4.27	4D	0.00	3D	4.47	66.7
10E	0.00	9E	3.50	4E	0.11	3E	3.86	85.7
12A	4.23	11A	5.63	6A	6.34	5A	8.10	9.5
12B	1.98	11B	4.26	6B	0.33	5B	5.25	28.6
12C	0.00	11C	3.51	6C	0.00	5C	3.95	47.6
12D	0.00	11D	3.90	6D	0.00	5D	4.30	66.7
12E	0.00	11E	2.38	6E	0.00	5E	4.44	85.7

Table D.1 (con't) – Chloride Concentration Data

Off Crack		On Crack		Off Crack		On Crack		Mean Depth
Sample	kg/m <sup>3</sup>	Sample	kg/m <sup>3</sup>	Sample	kg/m <sup>3</sup>	Sample	kg/m <sup>3</sup>	(mm)
7A	6.73	8A	6.45	2A	7.69	1A	15.49	9.5
7B	2.00	8B	4.20	2B	2.48	1B	5.58	28.6
7C	0.21	8C	2.89	2C	0.26	1C	4.67	47.6
7D	0.08	8D	2.23	2D	0.13	1D	4.38	66.7
7E	0.00	8E	1.33	2E	0.13	1E	3.14	85.7
9A	7.47	10A	6.83	4A	5.54	3A	6.66	9.5
9B	3.36	10B	3.47	4B	3.06	3B	4.73	28.6
9C	0.57	10C	1.87	4C	1.63	3C	3.60	47.6
9D	0.15	10D	0.73	4D	0.36	3D	2.44	66.7
9E	0.12	10E	0.27	4E	0.11	3E	1.86	85.7
11A	8.71	12A	8.21	6A	7.16	5A	6.95	9.5
11B	3.39	12B	5.20	6B	3.04	5B	4.01	28.6
11C	0.52	12C	3.22	6C	0.61	5C	2.66	47.6
11D	0.20	12D	3.94	6D	0.14	5D	1.92	66.7
11E	0.16	12E	3.25	6E	0.17	5E	0.49	85.7

<b>Bridge:</b>		<b>89-186</b>	<b>Bridge:</b>		<b>89-186</b>
<b>Placement:</b>	Inside		<b>Placement:</b>	Outside	
<b>Placement Date:</b>	09/14/90		<b>Placement Date:</b>	09/17/90	
<b>Survey Date:</b>	07/24/01		<b>Survey Date:</b>	07/24/01	

Off Crack		On Crack		Off Crack		On Crack		Mean Depth
Sample	kg/m <sup>3</sup>	Sample	kg/m <sup>3</sup>	Sample	kg/m <sup>3</sup>	Sample	kg/m <sup>3</sup>	(mm)
2A	6.12	1A	7.90	8A	8.37	7A	10.81	9.5
2B	2.30	1B	4.59	8B	3.16	7B	8.37	28.6
2C	0.51	1C	3.08	8C	0.49	7C	6.62	47.6
2D	0.13	1D	1.96	8D	0.00	7D	6.08	66.7
2E	0.28	1E	0.98	8E	0.00	7E	5.00	85.7
4A	4.12	3A	5.99	10A	9.71	9A	8.17	9.5
4B	1.53	3B	5.25	10B	4.90	9B	5.64	28.6
4C	0.17	3C	3.82	10C	1.71	9C	4.54	47.6
4D	0.00	3D	2.44	10D	0.36	9D	4.04	66.7
4E	0.18	3E	1.02	10E	0.16	9E	2.00	85.7
6A	5.74	5A	6.82	12A	5.22	11A	10.61	9.5
6B	2.09	5B	4.68	12B	1.31	11B	6.65	28.6
6C	0.14	5C	3.60	12C	0.27	11C	6.21	47.6
6D	0.00	5D	3.20	12D	0.00	11D	4.32	66.7
6E	0.15	5E	3.10	12E	0.18	11E	3.05	85.7

Table D.1 (con't) – Chloride Concentration Data

Off Crack		On Crack		Off Crack		On Crack		Mean Depth
Sample	kg/m <sup>3</sup>	Sample	kg/m <sup>3</sup>	Sample	kg/m <sup>3</sup>	Sample	kg/m <sup>3</sup>	(mm)
8A	7.79	7A	10.06	2A	4.81	1A	10.00	9.5
8B	2.40	7B	5.97	2B	0.88	1B	4.72	28.6
8C	0.16	7C	4.69	2C	0.00	1C	4.72	47.6
8D	0.00	7D	2.97	2D	0.12	1D	4.76	66.7
8E	0.14	7E	1.52	2E	0.19	1E	3.21	85.7
10A	6.74	9A	9.57	4A	5.46	3A	7.05	9.5
10B	2.39	9B	5.42	4B	1.55	3B	4.75	28.6
10C	0.19	9C	2.46	4C	0.00	3C	3.58	47.6
10D	0.11	9D	0.97	4D	0.00	3D	2.40	66.7
10E	0.13	9E	0.24	4E	0.15	3E	1.39	85.7
12A	9.01	11A	9.61	6A	6.23	5A	6.88	9.5
12B	4.51	11B	5.71	6B	3.27	5B	4.41	28.6
12C	0.90	11C	4.18	6C	0.57	5C	2.84	47.6
12D	0.12	11D	2.88	6D	0.12	5D	2.59	66.7
12E	0.16	11E	1.95	6E	0.15	5E	1.46	85.7

<b>Bridge:</b>		<b>89-198</b>	<b>Bridge:</b>		<b>89-198</b>
<b>Placement:</b>	Lt. Side		<b>Placement:</b>	Rt. Side	
<b>Placement Date:</b>	08/24/91		<b>Placement Date:</b>	08/27/91	
<b>Survey Date:</b>	09/16/02		<b>Survey Date:</b>	09/16/02	

Off Crack		On Crack		Off Crack		On Crack		Mean Depth
Sample	kg/m <sup>3</sup>	Sample	kg/m <sup>3</sup>	Sample	kg/m <sup>3</sup>	Sample	kg/m <sup>3</sup>	(mm)
2A	3.87	1A	6.92	8A	7.18	7A	8.64	9.5
2B	0.42	1B	3.50	8B	1.85	7B	5.53	28.6
2C	0.00	1C	2.88	8C	0.00	7C	3.83	47.6
2D	0.00	1D	3.24	8D	0.00	7D	1.99	66.7
2E	0.00	1E	2.35	8E	0.19	7E	1.19	85.7
4A	7.64	3A	6.55	10A	7.86	9A	8.27	9.5
4B	2.92	3B	4.20	10B	4.30	9B	5.05	28.6
4C	0.83	3C	3.14	10C	0.89	9C	4.41	47.6
4D	0.00	3D	2.85	10D	0.00	9D	3.02	66.7
4E	0.00	3E	2.67	10E	0.19	9E	1.98	85.7
6A	6.65	5A	7.94	12A	6.91	11A	6.24	9.5
6B	2.85	5B	5.24	12B	1.85	11B	3.70	28.6
6C	0.29	5C	3.85	12C	0.00	11C	2.64	47.6
6D	0.00	5D	2.81	12D	0.00	11D	1.63	66.7
6E	0.00	5E	1.64	12E	0.00	11E	0.73	85.7

Table D.1 (con't) – Chloride Concentration Data

Off Crack		On Crack		Off Crack		On Crack		Mean Depth
Sample	kg/m <sup>3</sup>	Sample	kg/m <sup>3</sup>	Sample	kg/m <sup>3</sup>	Sample	kg/m <sup>3</sup>	(mm)
8A	5.90	7A	8.60	2A	6.35	1A	11.47	9.5
8B	1.61	7B	4.40	2B	2.09	1B	5.97	28.6
8C	0.19	7C	3.40	2C	0.13	1C	3.83	47.6
8D	0.11	7D	2.49	2D	0.11	1D	4.52	66.7
8E	0.14	7E	1.41	2E	0.15	1E	3.05	85.7
10A	6.56	9A	6.40	4A	6.49	3A	7.75	9.5
10B	1.64	9B	4.64	4B	1.78	3B	5.59	28.6
10C	0.00	9C	1.90	4C	0.00	3C	4.90	47.6
10D	0.00	9D	0.52	4D	0.00	3D	3.80	66.7
10E	0.00	9E	0.50	4E	0.14	3E	2.55	85.7
12A	7.37	11A	8.00	6A	7.92	5A	7.56	9.5
12B	1.57	11B	7.09	6B	2.78	5B	6.02	28.6
12C	0.00	11C	5.17	6C	0.42	5C	4.82	47.6
12D	0.00	11D	4.47	6D	0.00	5D	3.49	66.7
12E	0.61	11E	2.80	6E	0.00	5E	2.01	85.7

<b>Bridge:</b>		<b>89-200</b>	<b>Bridge:</b>		<b>89-200</b>
<b>Placement:</b>	Rt. Side		<b>Placement:</b>	Lt. Side	
<b>Placement Date:</b>	08/17/91		<b>Placement Date:</b>	08/20/91	
<b>Survey Date:</b>	09/17/02		<b>Survey Date:</b>	09/17/02	

Off Crack		On Crack		Off Crack		On Crack		Mean Depth
Sample	kg/m <sup>3</sup>	Sample	kg/m <sup>3</sup>	Sample	kg/m <sup>3</sup>	Sample	kg/m <sup>3</sup>	(mm)
8A	6.76	7A	16.37	2A	4.79	1A	7.26	9.5
8B	2.72	7B	10.97	2B	0.64	1B	3.86	28.6
8C	0.62	7C	11.96	2C	0.00	1C	3.75	47.6
8D	0.12	7D	15.87	2D	0.00	1D	3.20	66.7
8E	0.13	7E	2.80	2E	0.17	1E	3.06	85.7
10A	6.95	9A	7.32	4A	5.53	3A	6.37	9.5
10B	1.72	9B	4.12	4B	0.77	3B	3.70	28.6
10C	0.13	9C	3.92	4C	0.00	3C	3.27	47.6
10D	0.00	9D	2.88	4D	0.00	3D	2.97	66.7
10E	0.17	9E	1.26	4E	0.17	3E	1.86	85.7
12A	6.42	11A	7.56	6A	5.02	5A	6.75	9.5
12B	1.82	11B	4.59	6B	1.82	5B	4.89	28.6
12C	0.15	11C	4.08	6C	0.14	5C	3.71	47.6
12D	0.00	11D	3.92	6D	0.00	5D	2.37	66.7
12E	0.00	11E	2.41	6E	0.00	5E	1.97	85.7

Table D.1 (con't) – Chloride Concentration Data

<b>Bridge:</b>		<b>56-142</b>		<b>Bridge:</b>		<b>56-142</b>		
<b>Placement:</b>		South End		<b>Placement:</b>		South Pier		
<b>Placement Date:</b>		10/01/87		<b>Placement Date:</b>		10/06/87		
<b>Survey Date:</b>		09/25/03		<b>Survey Date:</b>		09/25/03		
<b>Off Crack</b>		<b>On Crack</b>		<b>Off Crack</b>		<b>On Crack</b>		<b>Mean Depth</b>
<b>Sample</b>	<b>kg/m<sup>3</sup></b>	<b>Sample</b>	<b>kg/m<sup>3</sup></b>	<b>Sample</b>	<b>kg/m<sup>3</sup></b>	<b>Sample</b>	<b>kg/m<sup>3</sup></b>	<b>(mm)</b>
2A	7.79	1A	8.35	6A	8.29	5A	7.01	9.5
2B	3.69	1B	5.72	6B	5.10	5B	3.98	28.6
2C	1.90	1C	2.86	6C	2.03	5C	1.86	47.6
2D	0.43	1D	0.87	6D	0.46	5D	0.62	66.7
2E	0.11	1E	0.21	6E	0.31	5E	0.31	85.7
4A	10.17	3A	10.56	8A	7.62	7A	8.18	9.5
4B	4.05	3B	5.85	8B	2.77	7B	4.49	28.6
4C	1.07	3C	1.82	8C	0.98	7C	3.74	47.6
4D	0.19	3D	0.65	8D	0.22	7D	2.40	66.7
4E	0.55	3E	0.18	8E	0.24	7E	1.00	85.7
12A	6.96	11A	6.69	10A	10.19	9A	10.08	9.5
12B	2.07	11B	3.13	10B	4.14	9B	6.36	28.6
12C	0.32	11C	1.13	10C	1.03	9C	4.11	47.6
12D	0.13	11D	0.25	10D	0.17	9D	2.07	66.7
12E	0.17	11E	0.30	10E	0.19	9E	1.00	85.7
<b>Bridge:</b>		<b>56-148</b>		<b>Bridge:</b>		<b>70-95</b>		
<b>Placement:</b>		Deck		<b>Placement:</b>		Deck		
<b>Placement Date:</b>		07/18/91		<b>Placement Date:</b>		10/31/95		
<b>Survey Date:</b>		08/27/02		<b>Survey Date:</b>		11/12/03		
<b>Off Crack</b>		<b>On Crack</b>		<b>Off Crack</b>		<b>On Crack</b>		<b>Mean Depth</b>
<b>Sample</b>	<b>kg/m<sup>3</sup></b>	<b>Sample</b>	<b>kg/m<sup>3</sup></b>	<b>Sample</b>	<b>kg/m<sup>3</sup></b>	<b>Sample</b>	<b>kg/m<sup>3</sup></b>	<b>(mm)</b>
2A	13.19	1A	10.27	2A	13.39	1A	12.06	9.5
2B	5.75	1B	4.75	2B	8.95	1B	6.01	28.6
2C	1.75	1C	2.77	2C	3.47	1C	4.66	47.6
2D	0.19	1D	2.60	2D	0.90	1D	1.95	66.7
2E	0.12	1E	0.96	2E	0.22	1E	0.77	85.7
4A	9.68	3A	9.39	4A	12.73	3A	0.64	9.5
4B	7.85	3B	5.23	4B	11.04	3B	8.06	28.6
4C	3.45	3C	3.69	4C	5.95	3C	4.39	47.6
4D	0.87	3D	3.17	4D	4.71	3D	5.29	66.7
4E	0.23	3E	1.34	4E	0.33	3E	2.19	85.7
6A	9.78	5A	6.22	6A	10.12	5A	8.75	9.5
6B	5.80	5B	2.89	6B	7.00	5B	6.74	28.6
6C	2.44	5C	2.19	6C	3.51	5C	5.44	47.6
6D	0.59	5D	1.65	6D	1.63	5D	3.87	66.7
6E	0.62	5E	1.43	6E	0.45	5E	3.21	85.7

Table D.1 (con't) – Chloride Concentration Data

<b>Off Crack</b>		<b>On Crack</b>		<b>Off Crack</b>		<b>On Crack</b>		<b>Mean Depth</b>
<b>Sample</b>	<b>kg/m<sup>3</sup></b>	<b>Sample</b>	<b>kg/m<sup>3</sup></b>	<b>Sample</b>	<b>kg/m<sup>3</sup></b>	<b>Sample</b>	<b>kg/m<sup>3</sup></b>	<b>(mm)</b>
2A	10.09	1A	10.02	8A	9.53	7A	11.51	9.5
2B	8.27	1B	9.73	8B	6.28	7B	8.28	28.6
2C	4.47	1C	4.30	8C	3.84	7C	4.39	47.6
2D	2.31	1D	2.41	8D	2.08	7D	2.30	66.7
2E	0.98	1E	2.61	8E	1.68	7E	1.05	85.7
4A	9.33	3A	7.72	10A	9.91	9A	11.11	9.5
4B	7.60	3B	4.14	10B	9.58	9B	8.39	28.6
4C	4.69	3C	2.68	10C	5.54	9C	5.15	47.6
4D	2.62	3D	2.40	10D	2.62	9D	2.43	66.7
4E	1.16	3E	1.53	10E	0.92	9E	0.83	85.7
6A	9.31	5A	11.91	12A	8.55	11A	8.16	9.5
6B	10.49	5B	7.57	12B	7.81	11B	6.09	28.6
6C	6.63	5C	5.38	12C	4.02	11C	3.88	47.6
6D	4.42	5D	4.75	12D	1.99	11D	2.98	66.7
6E	2.02	5E	5.00	12E	0.53	11E	2.87	85.7

<b>Bridge:</b>		<b>70-103</b>	<b>Bridge:</b>		<b>70-103</b>			
<b>Placement:</b>	Right		<b>Placement:</b>	Left				
<b>Placement Date:</b>	03/14/85		<b>Placement Date:</b>	03/19/85				
<b>Survey Date:</b>	11/13/03		<b>Survey Date:</b>	11/13/03				
<b>Off Crack</b>		<b>On Crack</b>		<b>Off Crack</b>		<b>On Crack</b>		<b>Mean Depth</b>
<b>Sample</b>	<b>kg/m<sup>3</sup></b>	<b>Sample</b>	<b>kg/m<sup>3</sup></b>	<b>Sample</b>	<b>kg/m<sup>3</sup></b>	<b>Sample</b>	<b>kg/m<sup>3</sup></b>	<b>(mm)</b>
2A	10.61	1A	0.35	2A	12.10	1A	13.75	9.5
2B	6.26	1B	4.24	2B	6.67	1B	6.61	28.6
2C	1.71	1C	3.12	2C	0.64	1C	3.31	47.6
2D	0.35	1D	0.45	2D	0.23	1D	1.61	66.7
2E	0.23	1E	0.21	2E	0.12	1E	0.34	85.7
4A	11.52	3A	10.14	4A	11.38	3A	8.43	9.5
4B	9.16	3B	7.95	4B	6.69	3B	12.86	28.6
4C	4.96	3C	5.64	4C	3.16	3C	3.99	47.6
4D	1.93	3D	4.08	4D	0.67	3D	2.03	66.7
4E	0.47	3E	1.98	4E	0.21	3E	0.51	85.7
6A	11.74	5A	12.59	6A	12.56	5A	9.76	9.5
6B	8.36	5B	6.36	6B	9.31	5B	5.17	28.6
6C	3.81	5C	4.99	6C	13.76	5C	3.41	47.6
6D	1.01	5D	2.79	6D	0.16	5D	1.63	66.7
6E	0.16	5E	1.78	6E	0.57	5E	0.87	85.7

Table D.1 (con't) – Chloride Concentration Data

<b>Bridge:</b>		<b>75-44</b>		<b>Bridge:</b>		<b>75-45</b>		
<b>Placement:</b>		Deck		<b>Placement:</b>		Deck		
<b>Placement Date:</b>		07/12/90		<b>Placement Date:</b>		08/10/90		
<b>Survey Date:</b>		09/16/03		<b>Survey Date:</b>		09/17/03		
<b>Off Crack</b>		<b>On Crack</b>		<b>Off Crack</b>		<b>On Crack</b>		<b>Mean Depth</b>
<b>Sample</b>	<b>kg/m<sup>3</sup></b>	<b>Sample</b>	<b>kg/m<sup>3</sup></b>	<b>Sample</b>	<b>kg/m<sup>3</sup></b>	<b>Sample</b>	<b>kg/m<sup>3</sup></b>	<b>(mm)</b>
2A	4.66	1A	7.69	2A	9.41	1A	8.32	9.5
2B	4.16	1B	4.46	2B	4.72	1B	5.56	28.6
2C	2.13	1C	2.26	2C	2.44	1C	3.40	47.6
2D	0.78	1D	1.43	2D	0.93	1D	1.18	66.7
2E	0.20	1E	0.83	2E	0.25	1E	0.49	85.7
4A	6.94	3A	9.83	4A	8.52	3A	10.13	9.5
4B	5.54	3B	8.33	4B	5.58	3B	7.13	28.6
4C	2.90	3C	4.19	4C	3.26	3C	4.91	47.6
4D	0.97	3D	2.13	4D	1.51	3D	3.97	66.7
4E	0.20	3E	0.58	4E	0.71	3E	1.04	85.7
6A	6.43	5A	6.55	6A	5.19	5A	5.68	9.5
6B	4.95	5B	4.99	6B	3.11	5B	3.25	28.6
6C	2.93	5C	3.54	6C	1.24	5C	1.91	47.6
6D	1.62	5D	1.97	6D	0.70	5D	1.18	66.7
6E	0.51	5E	1.25	6E	0.12	5E	0.62	85.7
<b>Bridge:</b>		<b>89-204</b>		<b>Bridge:</b>		<b>89-208</b>		
<b>Placement:</b>		Deck		<b>Placement:</b>		Deck		
<b>Placement Date:</b>		10/03/91		<b>Placement Date:</b>		06/15/95		
<b>Survey Date:</b>		09/19/02		<b>Survey Date:</b>		07/03/01		
<b>Off Crack</b>		<b>On Crack</b>		<b>Off Crack</b>		<b>On Crack</b>		<b>Mean Depth</b>
<b>Sample</b>	<b>kg/m<sup>3</sup></b>	<b>Sample</b>	<b>kg/m<sup>3</sup></b>	<b>Sample</b>	<b>kg/m<sup>3</sup></b>	<b>Sample</b>	<b>kg/m<sup>3</sup></b>	<b>(mm)</b>
2A	6.30	1A	8.53	2A	5.38	1A	1.19	9.5
2B	2.44	1B	5.51	2B	2.52	1B	1.11	28.6
2C	0.33	1C	4.47	2C	0.47	1C	0.75	47.6
2D	0.00	1D	2.30	2D	0.00	1D	0.55	66.7
2E	0.16	1E	3.49	2E	0.00	1E	0.91	85.7
4A	8.56	3A	9.78	4A	6.19	3A	3.78	9.5
4B	4.39	3B	7.00	4B	2.55	3B	1.88	28.6
4C	1.51	3C	5.91	4C	0.37	3C	1.26	47.6
4D	0.17	3D	4.83	4D	0.00	3D	LIP	66.7
4E	0.11	3E	5.34	4E	0.23	3E	0.66	85.7
6A	8.82	5A	8.79	6A	6.38	5A	6.32	9.5
6B	5.06	5B	5.49	6B	2.94	5B	2.79	28.6
6C	1.75	5C	4.04	6C	0.63	5C	1.94	47.6
6D	0.18	5D	3.75	6D	0.22	5D	1.42	66.7
6E	0.13	5E	2.22	6E	0.00	5E	0.84	85.7

Table D.1 (con't) – Chloride Concentration Data

Off Crack		On Crack		Off Crack		On Crack		Mean Depth (mm)
Sample	kg/m <sup>3</sup>	Sample	kg/m <sup>3</sup>	Sample	kg/m <sup>3</sup>	Sample	kg/m <sup>3</sup>	
2A	6.84	1A	8.01	6A	8.45	5A	8.97	9.5
2B	4.31	1B	5.21	6B	4.54	5B	6.83	28.6
2C	1.73	1C	2.72	6C	2.65	5C	4.16	47.6
2D	0.53	1D	1.66	6D	0.94	5D	1.08	66.7
2E	0.10	1E	0.25	6E	0.14	5E	0.25	85.7
4A	5.55	3A	8.58	20A	10.20	19A	9.52	9.5
4B	0.52	3B	4.43	20B	7.78	19B	6.42	28.6
4C	0.16	3C	1.47	20C	3.77	19C	5.19	47.6
4D	0.12	3D	0.66	20D	1.57	19D	3.30	66.7
4E	0.20	3E	0.17	20E	0.36	19E	1.37	85.7
24A	5.81	23A	9.12	22A	6.97	21A	9.14	9.5
24B	1.86	23B	4.15	22B	1.51	21B	5.74	28.6
24C	0.34	23C	1.27	22C	0.22	21C	2.05	47.6
24D	0.15	23D	0.26	22D	0.15	21D	1.08	66.7
24E	0.11	23E	0.11	22E	0.14	21E	0.15	85.7

<b>Bridge:</b> 99-76		<b>Bridge:</b> 99-76						
<b>Placement:</b> South End	<b>Placement:</b> Placement 2	<b>Placement:</b> Placement 3	<b>Placement:</b> Placement 4					
<b>Placement Date:</b> 09/01/89	<b>Placement Date:</b> 09/15/89	<b>Placement Date:</b> 10/13/89	<b>Placement Date:</b> 11/07/89					
<b>Survey Date:</b> 09/17/03	<b>Survey Date:</b> 09/17/03	<b>Survey Date:</b> 09/17/03	<b>Survey Date:</b> 09/17/03					
Off Crack		On Crack		Off Crack		On Crack		Mean Depth (mm)
Sample	kg/m <sup>3</sup>	Sample	kg/m <sup>3</sup>	Sample	kg/m <sup>3</sup>	Sample	kg/m <sup>3</sup>	
8A	9.81	7A	10.63	10A	10.20	9A	8.54	9.5
8B	5.07	7B	5.74	10B	9.60	9B	9.68	28.6
8C	2.02	7C	1.98	10C	5.73	9C	5.46	47.6
8D	0.48	7D	1.54	10D	2.38	9D	2.69	66.7
8E	0.10	7E	0.41	10E	1.60	9E	1.60	85.7
18A	7.82	17A	8.47	12A	9.15	11A	9.49	9.5
18B	2.39	17B	9.47	12B	4.81	11B	8.08	28.6
18C	0.50	17C	4.19	12C	2.65	11C	3.86	47.6
18D	0.17	17D	2.12	12D	0.88	11D	2.22	66.7
18E	0.16	17E	0.75	12E	0.32	11E	0.91	85.7
16A	10.26	15A	7.29	14A	6.67	13A	10.10	9.5
16B	7.14	15B	8.93	14B	5.32	13B	7.27	28.6
16C	2.96	15C	3.93	14C	3.93	13C	3.59	47.6
16D	1.52	15D	1.45	14D	2.33	13D	1.92	66.7
16E	0.43	15E	0.55	14E	0.79	13E	0.83	85.7

Table D.2 – Calculated Surface Concentrations and Diffusion Coefficients

Bridge Number	Portion Placed	Date of Placement	Calculated using current study data				Calculated using Miller and Darwin (2000) data							
			Apparent Surface Concentrations (kg/m <sup>3</sup> )		Base Cl <sup>-</sup> (kg/m <sup>3</sup> )	$D_{eff}$ (mm <sup>2</sup> /day)	$D_{eff}^*$ (mm <sup>2</sup> /day)	Apparent Surface Concentrations (kg/m <sup>3</sup> )		Base Cl <sup>-</sup> (kg/m <sup>3</sup> )	$D_{eff}$ (mm <sup>2</sup> /day)	$D_{eff}^*$ (mm <sup>2</sup> /day)		
			1	2				3	1				2	3
<b>7% Silica Fume Overlay Bridges</b>														
30-93	Deck	08/04/01	2.78	6.20	0.00	0.23	0.03	0.04	--	--	--	--	--	--
40-92	Deck	10/26/01	4.07	7.97	5.03	0.00	0.10	0.10	--	--	--	--	--	--
40-93	Deck	10/16/01	4.94	4.55	3.75	0.02	0.38	0.38	--	--	--	--	--	--
46-332	Deck	05/15/02	1.74	0.05	0.87	0.23	0.08	0.07	--	--	--	--	--	--
81-53	Deck	02/21/00	10.19	10.03	6.86	0.09	0.09	0.11	--	--	--	--	--	--
85-148	West 32 ft	10/30/01	10.62	12.50	9.23	0.11	0.31	0.31	--	--	--	--	--	--
85-148	East 18 ft SFO	10/27/01	--	--	--	--	--	--	--	--	--	--	--	--
85-149	Deck	09/26/02	4.65	8.78	6.15	0.00	0.25	0.23	--	--	--	--	--	--
89-269	West 1/2 SFO	07/26/01	9.30	8.66	4.00	0.13	0.11	0.11	--	--	--	--	--	--
89-269	East 1/2 SFO	07/31/01	7.24	2.99	3.92	0.10	0.23	0.23	--	--	--	--	--	--
89-272	West 1/2 SFO	04/04/02	2.11	2.76	6.94	0.10	0.29	0.29	--	--	--	--	--	--
89-272	East 1/2 SFO	04/10/02	4.99	5.39	5.36	0.17	0.10	0.10	--	--	--	--	--	--
103-56	North 1/2 SFO	10/17/01	0.99	0.00	0.00	0.35	0.02	0.02	--	--	--	--	--	--
103-56	South 1/2 SFO	10/12/01	8.77	4.97	1.17	0.13	0.18	0.18	--	--	--	--	--	--
<b>5% Silica Fume Overlay Bridges</b>														
23-85	East 1/2 SFO	03/29/96	9.62	7.82	6.00	0.12	0.06	0.06	5.58	5.41	4.19	0.20	0.09	0.10
23-85	West 1/2 SFO	04/03/96	4.44	5.42	6.43	0.03	0.08	0.08	9.09	4.68	4.58	0.23	0.03	0.04

Table D.2 (con't) – Calculated Surface Concentrations and Diffusion Coefficients

Bridge Number	Portion Placed	Date of Placement	Calculated using current study data				Calculated using Miller and Darwin (2000) data							
			Apparent Surface Concentrations (kg/m <sup>3</sup> )		Base Cl <sup>-</sup> (kg/m <sup>3</sup> )	D <sub>eff</sub> (mm <sup>2</sup> /day)	Apparent Surface Concentrations (kg/m <sup>3</sup> )		Base Cl <sup>-</sup> (kg/m <sup>3</sup> )	D <sub>eff</sub> (mm <sup>2</sup> /day)				
			1	2	3	1	2	3	1	2	3			
46-302	Lt. 1/2 SFO	04/09/96	1.55	2.14	1.74	0.02	0.06	0.07	1.42	2.63	0.58	0.02	0.18	0.19
46-302	Rt. 1/2 SFO	04/11/96	1.94	1.03	2.17	0.00	0.06	0.06	1.28	1.21	2.24	0.07	0.02	0.03
46-309	Rt. 1/2 SFO	10/20/95	12.85	10.55	8.30	0.00	0.06	0.07	10.06	8.35	7.15	0.17	0.19	0.20
46-309	Lt. 1/2 SFO	10/24/95	9.19	10.77	12.35	0.13	0.12	0.13	6.88	5.83	6.90	0.17	0.16	0.17
46-317	North 12 ft	06/28/96	4.93	7.46	5.24	0.00	0.03	0.03	5.42	5.92	5.84	0.20	0.05	0.05
46-317	South 16 ft	07/01/96	8.71	7.91	6.24	0.00	0.04	0.04	3.44	6.88	6.09	0.23	0.17	0.18
81-50	SFO Rt. Unit 1	11/15/95	--	--	--	--	--	--	--	--	--	--	--	--
81-50	SFO Lt. Unit 1	11/18/95	--	--	--	--	--	--	--	--	--	--	--	--
81-50	SFO Rt. Unit 2	11/21/95	9.28	11.96	10.85	0.02	0.05	0.06	8.10	4.37	4.09	0.14	0.06	0.07
81-50	SFO Lt. Unit 2	11/30/95	5.73	7.26	15.80	0.00	0.05	0.05	8.07	7.07	8.85	0.20	0.04	0.05
87-453	North 22 ft	06/30/97	10.61	12.74	10.34	0.00	0.09	0.26	4.66	7.37	6.59	0.27	0.23	0.22
87-453	South 18 ft	07/03/97	10.10	15.02	11.56	0.00	0.27	0.08	6.95	6.52	6.67	0.25	0.08	0.07
87-454	Left of CL	09/10/96	10.60	9.84	8.49	0.00	0.11	0.10	3.90	5.66	7.22	0.25	0.16	0.16
87-454	Right of CL	10/16/96	--	12.14	15.80	0.00	0.12	0.11	7.81	6.63	5.49	0.23	0.14	0.14
89-184	Inside	09/26/90	10.92	10.78	9.35	0.00	0.24	0.31	13.33	16.46	8.69	0.17	0.03	0.10
89-184	Outside	09/28/90	8.63	7.68	6.67	0.00	0.13	0.20	8.96	13.24	11.11	0.17	0.02	0.09
89-187	Inside	06/26/90	12.59	8.05	6.70	0.10	0.04	0.10	6.69	5.30	9.23	0.10	0.07	0.15
89-187	Outside	06/28/90	9.22	5.63	7.20	0.05	0.03	0.09	9.17	4.31	5.85	0.23	0.04	0.12
89-206	Right of CL	10/04/95	5.63	7.85	5.75	0.08	0.05	0.06	0.96	1.05	1.02	0.20	0.08	0.10
89-206	Left of CL	10/10/95	2.61	7.84	6.42	0.00	0.06	0.07	3.14	1.72	1.90	0.00	0.08	0.09

Table D.2 (con't) – Calculated Surface Concentrations and Diffusion Coefficients

Bridge Number	Portion Placed	Date of Placement	Calculated using current study data				Calculated using Miller and Darwin (2000) data							
			Apparent Surface Concentrations (kg/m <sup>3</sup> )	Base Cl <sup>-</sup> (kg/m <sup>3</sup> )	D <sub>eff</sub> (mm <sup>2</sup> /day)	D <sub>eff</sub> <sup>*</sup> (mm <sup>2</sup> /day)	Apparent Surface Concentrations (kg/m <sup>3</sup> )	Base Cl <sup>-</sup> (kg/m <sup>3</sup> )	D <sub>eff</sub> (mm <sup>2</sup> /day)	D <sub>eff</sub> <sup>*</sup> (mm <sup>2</sup> /day)				
			1	2	3			1	2	3				
89-207	Left of CL	10/24/95	6.48	7.32	7.57	0.09	0.03	0.04	1.85	1.53	2.33	0.00	0.10	0.11
89-207	Right of CL	04/19/96	9.19	9.12	4.41	0.00	0.03	0.03	4.28	2.09	2.38	0.19	0.04	0.04
89-210	Right of CL	10/12/95	1.05	6.52	2.33	0.00	0.04	0.04	0.87	1.00	0.87	0.16	0.09	0.10
89-210	Left of CL	10/18/95	5.32	2.14	2.89	0.02	0.10	0.10	1.63	2.19	4.01	0.11	0.05	0.06
89-234	SFO South 20 ft	06/20/96	12.20	11.55	10.16	0.13	0.09	0.10	7.41	8.54	6.55	0.16	0.07	0.08
89-234	SFO North 18 ft	06/25/96	9.29	9.64	8.13	0.00	0.07	0.07	7.27	6.19	6.52	0.00	0.09	0.10
89-234	SFO Center 12 ft	06/28/96	10.58	8.36	10.58	0.11	0.08	0.08	10.34	6.88	6.24	0.11	0.08	0.09
89-235	SFO Left 20 ft	04/26/97	--	--	--	--	--	--	--	--	--	--	--	--
89-235	SFO Right 18 ft	05/01/97	8.47	5.22	5.57	0.07	0.07	0.06	2.77	1.26	2.89	0.15	0.16	0.15
89-235	SFO Center 12 ft	05/06/97	--	--	--	--	--	--	--	--	--	--	--	--
89-240	Rt. 22 ft SFO	08/05/97	10.08	10.75	10.70	0.03	0.06	0.05	5.44	5.00	6.72	0.17	0.08	0.07
89-240	Lt. 22 ft SFO	08/07/97	7.25	10.51	8.21	0.10	0.11	0.10	3.57	7.27	11.05	0.19	0.18	0.17
89-244	Right of CL	10/17/97	9.66	11.69	4.39	0.16	0.09	0.08	10.11	10.91	9.54	0.17	0.11	0.10
89-244	Left of CL	10/21/97	13.45	13.06	6.83	0.13	0.07	0.06	11.98	10.74	9.75	0.14	0.16	0.15
89-245	Lt. of CL Unit #2	10/20/97	13.57	10.11	9.48	0.20	0.05	0.03	11.39	8.29	10.66	0.12	0.17	0.15
89-245	Lt. of CL Unit #1	10/22/97	9.69	11.64	8.37	0.04	0.04	0.03	7.19	5.39	6.48	0.11	0.20	0.18
89-245	Rt. of CL Unit #2	10/23/97	13.50	9.11	10.56	0.14	0.06	0.05	7.34	9.36	10.37	0.17	0.19	0.17
89-245	Rt. of CL Unit #1	10/24/97	11.44	10.58	15.23	0.20	0.05	0.03	7.19	8.64	7.04	0.11	0.21	0.19
89-246	East 1/2 SFO	09/08/97	4.75	6.49	4.29	0.10	0.09	0.07	2.84	2.94	2.15	0.17	0.07	0.06
89-246	West 1/2 SFO	09/10/97	12.32	8.06	6.22	0.05	0.04	0.03	1.81	2.28	2.59	0.09	0.23	0.22

Table D.2 (con't) – Calculated Surface Concentrations and Diffusion Coefficients

Bridge Number	Portion Placed	Date of Placement	Calculated using current study data				Calculated using Miller and Darwin (2000) data							
			Apparent Surface Concentrations (kg/m <sup>3</sup> )		Base Cl <sup>-</sup> (kg/m <sup>3</sup> )	D <sub>eff</sub> (mm <sup>2</sup> /day)	Apparent Surface Concentrations (kg/m <sup>3</sup> )		Base Cl <sup>-</sup> (kg/m <sup>3</sup> )	D <sub>eff</sub> (mm <sup>2</sup> /day)				
			1	2	3	1	2	3	1	2	3			
89-247	SFO West 13 ft	05/05/97	4.06	3.63	3.48	0.01	0.03	0.02	0.00	1.88	1.18	0.00	0.32	0.31
89-247	SFO East 26 ft	05/07/97	6.59	2.92	3.90	0.08	0.06	0.05	1.03	2.81	1.52	0.00	0.19	0.19
89-248	Westbound Lane	04/24/98	2.50	4.97	2.29	0.29	0.14	0.12	0.00	0.22	0.10	0.29	0.06	0.05
89-248	Eastbound Lane	05/01/98	3.42	2.88	4.45	0.08	0.05	0.03	0.00	0.21	0.11	0.36	0.20	0.18
<b>Conventional Overlay Bridges</b>														
46-289	Inside 24 ft	09/02/92	6.40	8.02	9.57	0.00	0.05	0.05	10.69	7.78	11.68	0.27	0.04	0.04
46-289	Outside 20 ft	09/11/92	5.60	8.34	9.87	0.00	0.03	0.03	10.12	11.94	9.07	0.23	0.03	0.03
46-290	Inside 24 ft	09/08/92	10.80	9.38	10.27	0.02	0.04	0.04	10.14	12.06	10.22	0.26	0.07	0.07
46-290	Outside 10 ft	09/15/92	5.99	13.34	9.93	0.00	0.06	0.06	--	--	--	--	--	--
46-299	Rt. of CL 22 ft	07/28/94	8.32	6.29	5.96	0.00	0.06	0.05	7.93	6.74	8.77	0.17	0.05	0.03
46-299	Lt. of CL 18 ft	07/30/94	6.62	7.25	5.05	0.00	0.12	0.11	5.08	6.77	4.61	0.17	0.22	0.20
46-300	Lt. of CL 22 ft	08/14/95	5.90	6.98	7.75	0.05	0.15	0.15	7.25	6.12	7.38	0.06	0.20	0.18
46-300	Rt. of CL 18 ft	08/10/95	8.13	7.50	8.85	0.07	0.17	0.17	6.54	5.42	8.65	0.16	0.21	0.19
46-301	Rt. of CL 24 ft	08/03/94	9.71	8.33	6.76	0.00	0.07	0.06	9.06	7.85	7.05	0.32	0.08	0.06
46-301	Lt. of CL 24 to 38 ft	08/06/94	4.50	9.20	6.85	0.02	0.08	0.07	4.14	2.28	8.84	0.34	0.12	0.17
46-301	Rt. of CL 24 to 38 ft	08/05/94	7.39	9.41	5.51	0.00	0.10	0.09	6.34	8.53	7.34	0.37	0.14	0.11
46-301	Lt. of CL 24 ft	08/06/94	10.27	3.60	8.30	0.00	0.12	0.11	7.04	7.13	8.01	0.27	0.18	0.13
75-1	Lt. of CL	10/17/91	5.59	10.28	12.28	0.06	0.08	0.08	5.31	5.94	14.34	0.33	0.10	0.10
75-1	Rt. of CL	10/19/91	10.23	17.83	13.93	0.07	0.04	0.04	10.97	14.17	9.46	0.33	0.03	0.04

Table D.2 (con't) – Calculated Surface Concentrations and Diffusion Coefficients

Bridge Number	Portion Placed	Date of Placement	Calculated using current study data				Calculated using Miller and Darwin (2000) data							
			Apparent Surface Concentrations (kg/m <sup>3</sup> )		Base Cl <sup>-</sup> (kg/m <sup>3</sup> )	$D_{eff}$ (mm <sup>2</sup> /day)	Apparent Surface Concentrations (kg/m <sup>3</sup> )		Base Cl <sup>-</sup> (kg/m <sup>3</sup> )	$D_{eff}$ (mm <sup>2</sup> /day)	$D_{eff}^*$ (mm <sup>2</sup> /day)			
			1	2	3			1	2	3				
75-49	Eastbound	06/04/91	10.14	8.84	11.02	0.00	0.20	0.21	9.77	8.15	10.22	0.20	0.26	0.27
75-49	Westbound	06/07/91	9.85	11.05	8.88	0.00	0.12	0.13	7.83	7.93	7.02	0.29	0.17	0.17
81-49	Rt. 22 ft	04/08/92	10.89	9.35	8.23	0.02	0.03	0.03	7.12	3.63	5.18	0.10	0.03	0.03
81-49	Rt. of CL 12 ft	04/13/92	7.91	9.82	10.53	0.04	0.05	0.05	8.59	7.73	7.14	0.13	0.05	0.05
81-49	Lt. 22 ft	10/21/92	7.50	9.60	11.66	0.00	0.03	0.03	6.40	7.54	6.05	0.08	0.07	0.07
81-49	Lt. of CL 12 ft	10/23/92	8.96	12.55	13.26	0.02	0.04	0.04	6.41	5.92	5.05	0.07	0.09	0.09
89-183	Rt. Side	09/21/90	7.36	7.05	9.71	0.00	0.08	0.09	8.78	6.90	7.41	0.15	0.09	0.10
89-183	Lt. Side	09/25/90	7.62	9.94	7.28	0.00	0.10	0.11	9.15	5.95	8.15	0.15	0.06	0.07
89-185	Outside	06/23/90	11.82	11.90	8.08	0.00	0.02	0.26	9.67	11.01	7.23	0.23	0.26	0.24
89-185	Inside	06/21/90	6.20	5.38	10.75	0.02	0.03	0.04	9.08	6.82	7.49	0.08	0.12	0.10
89-186	Inside	09/14/90	9.18	10.76	12.34	0.16	0.07	0.08	9.71	10.35	9.71	0.23	0.05	0.06
89-186	Outside	09/17/90	10.11	7.98	9.78	0.14	0.09	0.09	7.23	8.30	10.08	0.21	0.08	0.09
89-196	Rt. Side	05/01/92	8.76	5.80	8.15	0.13	0.07	0.07	8.71	5.07	3.72	0.08	0.08	0.09
89-196	Lt. Side	05/05/92	11.12	13.66	6.57	0.07	0.10	0.10	0.09	10.41	6.61	0.25	0.19	0.19
89-198	Lt. Side	08/24/91	10.55	9.25	13.10	0.12	0.08	0.08	9.28	10.68	10.27	0.23	0.05	0.06
89-198	Rt. Side	08/27/91	6.45	7.58	9.37	0.09	0.07	0.07	5.80	9.05	5.88	0.11	0.07	0.08
89-199	Lt. Side	08/26/91	5.03	10.96	9.64	0.00	0.07	0.08	7.88	6.90	9.03	0.20	0.07	0.07
89-199	Rt. Side	08/28/91	9.83	11.86	9.49	0.05	0.07	0.08	12.43	11.21	11.32	0.17	0.04	0.04
89-200	Rt. Side	08/17/91	9.37	10.39	11.61	0.12	0.04	0.05	6.17	10.80	8.52	0.15	0.06	0.06
89-200	Lt. Side	08/20/91	9.39	9.45	11.83	0.07	0.06	0.06	9.46	12.25	10.56	0.17	0.04	0.04

Table D.2 (con't) – Calculated Surface Concentrations and Diffusion Coefficients

Bridge Number	Portion Placed	Date of Placement	Calculated using current study data			Calculated using Miller and Darwin (2000) data								
			Apparent Surface Concentrations (kg/m <sup>3</sup> )	Base Cl <sup>-</sup> (kg/m <sup>3</sup> )	$D_{eff}$ (mm <sup>2</sup> /day)	Apparent Surface Concentrations (kg/m <sup>3</sup> )	Base Cl <sup>-</sup> (kg/m <sup>3</sup> )	$D_{eff}$ (mm <sup>2</sup> /day)						
			1	2	3	1	2	3						
89-201	Rt. Side	08/19/91	10.28	10.10	9.41	0.07	0.06	0.06	8.36	11.31	9.79	0.17	0.05	0.05
89-201	Lt. Side	08/21/91	7.70	8.91	8.44	0.05	0.04	0.04	4.90	9.65	9.28	0.11	0.04	0.05
<b>Monolithic Bridges</b>														
56-142	North End	10/01/87	--	--	--	--	--	--	--	--	--	--	--	--
56-142	N. + Moment	10/01/87	--	--	--	--	--	--	--	--	--	--	--	--
56-142	S. + Moment	10/01/87	--	--	--	--	--	--	--	--	--	--	--	--
56-142	South End	10/01/87	10.93	13.81	8.98	0.15	0.06	0.06	--	--	--	--	--	--
56-142	N. Pier	10/06/87	--	--	--	--	--	--	--	--	--	--	--	--
56-142	Ctr. Pier	10/06/87	--	--	--	--	--	--	--	--	--	--	--	--
56-142	South Pier	10/06/87	11.64	9.59	13.12	0.21	0.07	0.08	--	--	--	--	--	--
56-148	Deck	07/18/91	15.52	13.62	12.46	0.00	0.15	0.13	10.56	13.56	9.90	0.22	0.18	0.15
70-95	Deck	10/31/85	15.22	16.95	11.94	0.16	0.16	0.18	--	--	--	--	--	--
70-103	Right	03/14/85	11.33	10.75	13.00	0.00	0.29	0.30	--	--	--	--	--	--
70-103	Left	03/19/85	10.68	12.94	10.67	0.00	0.22	0.24	--	--	--	--	--	--
70-104	Deck	10/17/85	12.11	15.31	14.69	0.16	0.13	0.14	--	--	--	--	--	--
70-107	Deck	10/25/91	15.50	15.32	12.07	0.00	0.14	0.11	10.77	12.76	12.07	0.22	0.19	0.16
75-44	Deck	07/12/90	6.00	8.50	8.00	0.00	0.26	0.25	--	--	--	--	--	--
75-45	Deck	08/10/90	10.92	10.89	6.27	0.00	0.17	0.17	--	--	--	--	--	--
89-204	Deck	10/03/91	7.71	11.27	11.91	0.12	0.12	0.10	5.12	9.93	11.03	0.10	0.14	0.10

Table D.2 (con't) – Calculated Surface Concentrations and Diffusion Coefficients

Bridge Number	Portion Placed	Date of Placement	Calculated using current study data				Calculated using Miller and Darwin (2000) data												
			Apparent Surface Concentrations (kg/m <sup>3</sup> )	Base Cl <sup>-</sup> (kg/m <sup>3</sup> )	$D_{eff}$ (mm <sup>2</sup> /day)	$D_{eff}^*$ (mm <sup>2</sup> /day)	Apparent Surface Concentrations (kg/m <sup>3</sup> )	Base Cl <sup>-</sup> (kg/m <sup>3</sup> )	$D_{eff}$ (mm <sup>2</sup> /day)	$D_{eff}^*$ (mm <sup>2</sup> /day)									
			1	2	3														
89-208	Deck	06/15/95	7.44	8.39	8.83	0.05	0.16	0.13	0.13	6.35	7.53	6.90	0.10	0.09	0.04				
99-76	South End	09/01/89	10.02	6.50	7.47	0.15	0.07	0.07	0.07	--	--	--	--	--	--				
99-76	Placement 2	09/15/89	6.65	13.61	10.12	0.15	0.15	0.14	0.14	--	--	--	--	--	--				
99-76	Placement 3	10/13/89	12.19	8.58	13.93	0.17	0.11	0.11	0.11	--	--	--	--	--	--				
99-76	Placement 4	11/07/89	13.29	9.12	8.34	0.12	0.27	0.27	0.27	--	--	--	--	--	--				
99-76	Placement 5	11/21/89	--	--	--	--	--	--	--	--	--	--	--	--	--				
99-76	North (West Ln.)	01/09/90	--	--	--	--	--	--	--	--	--	--	--	--	--				
99-76	North (East Ln.)	05/11/90	--	--	--	--	--	--	--	--	--	--	--	--	--				

**APPENDIX E**  
**FIELD SURVEY RESULTS AND AGE-CORRECTED CRACK DENSITIES**

Table E.1 – Field Survey Results for All Bridges Decks

Bridge Number	Deck Type	Current Study			Miller and Darwin (2000)		Schmitt and Darwin (1995)		All Studies Mean Age-Corrected Crack Density (m/m <sup>2</sup> )
		Delaminated Area [m <sup>2</sup> (%)]	Crack Density (m/m <sup>2</sup> )	Age-Corrected Crack Density (m/m <sup>2</sup> )	Crack Density (m/m <sup>2</sup> )	Age-Corrected Crack Density (m/m <sup>2</sup> )	Crack Density (m/m <sup>2</sup> )	Age-Corrected Crack Density (m/m <sup>2</sup> )	
<b>7% Silica Fume Overlay Bridges</b>									
30-93	7% SFO	0.0	0.06	0.21	--	--	--	--	0.21
40-92	7% SFO	0.0	0.90	1.06	--	--	--	--	1.06
40-93	7% SFO	0.1 (0.0)	0.43	0.60	--	--	--	--	0.60
46-332	7% SFO	0.0	0.63	0.81	--	--	--	--	0.81
81-53	7% SFO	2.4 (0.5)	0.15	0.26	--	--	--	--	0.26
85-148	7% SFO	0.0	0.57	0.73	--	--	--	--	0.73
85-149	7% SFO	0.1 (0.0)	0.14	0.33	--	--	--	--	0.33
89-269	7% SFO	0.0	0.02	0.18	--	--	--	--	0.18
89-272	7% SFO	0.1 (0.0)	0.05	0.23	--	--	--	--	0.23
103-56	7% SFO	1.5 (0.2)	0.23	0.39	--	--	--	--	0.39
<b>5% Silica Fume Overlay Bridges</b>									
23-85	5% SFO	0.0	0.57	0.57	0.37	0.51	--	--	0.54
46-302	5% SFO	0.0	0.78	0.79	0.51	0.65	--	--	0.72
46-309	5% SFO	0.0	0.53	0.52	0.35	0.48	--	--	0.50
46-317	5% SFO	0.0	0.30	0.32	0.08	0.23	--	--	0.27
81-50	5% SFO	0.6 (0.0)	1.09	1.05	0.69	0.82	--	--	0.94
87-453	5% SFO	0.0	0.81	0.86	0.25	0.42	--	--	0.64
87-454	5% SFO	0.0	0.86	0.89	0.68	0.83	--	--	0.86

Table E.1 (con't) – Field Survey Results for All Bridges Decks

Bridge Number	Deck Type	Current Study			Miller and Darwin (2000)		Schmitt and Darwin (1995)		All Studies Mean Age-Corrected Crack Density (m/m <sup>2</sup> )
		Delaminated Area (%)	Crack Density (m/m <sup>2</sup> )	Age-Corrected Crack Density (m/m <sup>2</sup> )	Crack Density (m/m <sup>2</sup> )	Age-Corrected Crack Density (m/m <sup>2</sup> )	Crack Density (m/m <sup>2</sup> )	Age-Corrected Crack Density (m/m <sup>2</sup> )	
89-184	5% SFO	0.0	0.88	0.70	1.01	0.96	0.69	0.80	0.82
89-187	5% SFO	--	0.88	0.73	0.97	0.91	1.02	1.13	0.92
89-206	5% SFO	0.0	0.45	0.41	0.43	0.55	--	--	0.48
89-207	5% SFO	0.0	0.42	0.39	0.37	0.50	--	--	0.44
89-210	5% SFO	--	0.57	0.60	0.16	0.29	--	--	0.45
89-234	5% SFO	0.0	0.29	0.27	0.27	0.43	--	--	0.35
89-235	5% SFO	0.0	0.21	0.22	0.38	0.57	--	--	0.39
89-240	5% SFO	0.0	0.21	0.24	0.20	0.39	--	--	0.31
89-244	5% SFO	0.0	0.30	0.33	0.02	0.22	--	--	0.27
89-245	5% SFO	0.0	0.46	0.49	0.05	0.25	--	--	0.37
89-246	5% SFO	0.0	0.33	0.38	0.07	0.27	--	--	0.32
89-247	5% SFO	0.0	0.55	0.57	0.50	0.68	--	--	0.62
89-248	5% SFO	2.7 (0.3)	0.51	0.56	0.02	0.23	--	--	0.40
<b>Conventional Overlay Bridges</b>									
46-289	CO	1.1 (0.1)	0.71	0.68	0.65	0.66	--	--	0.67
46-290	CO	0	0.68	0.65	0.62	0.62	--	--	0.64
46-294	CO	--	--	--	--	--	0.30	0.34	0.34
46-295	CO	--	--	--	--	--	0.28	0.32	0.32
46-299	CO	0	0.81	0.80	0.88	0.91	--	--	0.85

Table E.1 (con't) – Field Survey Results for All Bridges Decks

Bridge Number	Deck Type	Current Study			Miller and Darwin (2000)		Schmitt and Darwin (1995)		All Studies Mean Age-Corrected Crack Density (m/m <sup>2</sup> )
		Delaminated Area (%)	Crack Density (m/m <sup>2</sup> )	Age-Corrected Crack Density (m/m <sup>2</sup> )	Crack Density (m/m <sup>2</sup> )	Age-Corrected Crack Density (m/m <sup>2</sup> )	Crack Density (m/m <sup>2</sup> )	Age-Corrected Crack Density (m/m <sup>2</sup> )	
46-300	CO	--	0.65	0.66	0.88	0.92	--	--	0.79
46-301	CO	0.0	0.84	0.83	0.73	0.75	--	--	0.79
75-1	CO	0.1 (0.0)	0.49	0.44	0.37	0.36	--	--	0.40
75-49	CO	0.1 (0.0)	0.40	0.35	0.45	0.44	--	--	0.39
81-49	CO	0.0	0.80	0.76	0.73	0.74	--	--	0.75
89-179	CO	--	--	--	--	--	0.23	0.25	0.25
89-180	CO	--	--	--	--	--	0.36	0.38	0.38
89-183	CO	0.0	0.61	0.56	0.51	0.50	--	--	0.53
89-185	CO	0.0	0.81	0.76	0.70	0.69	0.72	0.75	0.73
89-186	CO	--	0.72	0.68	0.72	0.71	0.52	0.55	0.65
89-196	CO	0.0	0.59	0.56	0.54	0.54	--	--	0.55
89-198	CO	0.0	0.48	0.44	0.39	0.38	0.54	0.57	0.47
89-199	CO	0.0	0.71	0.67	0.66	0.65	0.67	0.70	0.67
89-200	CO	--	0.65	0.61	0.52	0.52	0.51	0.54	0.56
89-201	CO	--	0.71	0.67	0.63	0.63	0.67	0.70	0.67
105-021	CO	--	--	--	--	--	0.09	0.09	0.09
105-225	CO	--	--	--	--	--	0.18	0.17	0.17
105-226	CO	--	--	--	--	--	0.17	0.16	0.16
105-230	CO	--	--	--	--	--	0.09	0.07	0.07
105-231	CO	--	--	--	--	--	0.11	0.09	0.09

Table E.1 (con't) – Field Survey Results for All Bridges Decks

Bridge Number	Deck Type	Current Study			Miller and Darwin (2000)		Schmitt and Darwin (1995)		All Studies Mean Age-Corrected Crack Density (m/m <sup>2</sup> )
		Delaminated Area (%)	Crack Density (m/m <sup>2</sup> )	Age-Corrected Crack Density (m/m <sup>2</sup> )	Crack Density (m/m <sup>2</sup> )	Age-Corrected Crack Density (m/m <sup>2</sup> )	Crack Density (m/m <sup>2</sup> )	Age-Corrected Crack Density (m/m <sup>2</sup> )	
105-262	CO	--	--	--	--	--	0.18	0.16	0.16
105-263	CO	--	--	--	--	--	0.13	0.09	0.09
105-265	CO	--	--	--	--	--	0.01	0.00	0.00
105-268	CO	--	--	--	--	--	0.61	0.60	0.60
105-269	CO	--	--	--	--	--	0.45	0.44	0.44
<b>Monolithic Bridges</b>									
3-45	MONO	--	0.29	0.11	--	--	0.19	0.15	0.13
3-46	MONO	--	0.41	0.25	--	--	0.24	0.21	0.23
56-142	MONO	--	0.17	0.03	--	--	0.08	0.08	0.06
56-148	MONO	--	0.53	0.46	0.31	0.30	0.28	0.33	0.37
70-95	MONO	--	0.13	0.00	--	--	0.07	0.03	0.02
70-101	MONO	--	--	--	--	--	0.06	0.02	0.02
70-103	MONO	--	0.75	0.57	--	--	0.49	0.46	0.52
70-104	MONO	--	0.10	0.00	--	--	0.09	0.05	0.03
70-107	MONO	--	0.72	0.66	0.42	0.41	0.34	0.40	0.49
75-44	MONO	--	0.28	0.19	--	--	0.19	0.23	0.21
75-45	MONO	--	0.45	0.36	--	--	0.51	0.55	0.45
89-204	MONO	--	1.05	0.98	0.84	0.84	0.75	0.81	0.87
89-208	MONO	--	0.10	0.11	0.03	0.09	--	--	0.10

**Table E.1 (con't) – Field Survey Results for All Bridges Decks**

Bridge Number	Deck Type	Current Study			Miller and Darwin (2000)		Schmitt and Darwin (1995)		All Studies Mean Age-Corrected Crack Density (m/m <sup>2</sup> )
		Delaminated Area (%)	Crack Density (m/m <sup>2</sup> )	Age-Corrected Crack Density (m/m <sup>2</sup> )	Crack Density (m/m <sup>2</sup> )	Age-Corrected Crack Density (m/m <sup>2</sup> )	Crack Density (m/m <sup>2</sup> )	Age-Corrected Crack Density (m/m <sup>2</sup> )	
99-76	MONO	--	0.77	0.67	--	--	0.76	0.81	0.74
105-000 <sup>†</sup>	MONO	--	--	--	--	--	0.27	0.35	0.35
105-46	MONO	--	--	--	--	--	0.87	0.67	0.67

<sup>†</sup>Bridge has no assigned serial number. Project No. is 105-U-1262-01.

-- Denotes bridges that were not surveyed during a particular study or missing data.

Table E.2 – Crack Densities for Individual Bridge Placements

Bridge Number	Portion Placed	Date of Placement	Current Study		Miller and Darwin (2000)		Schmitt and Darwin (1995)		All Studies Mean Age-Corrected Crack Density (m/m <sup>2</sup> )
			Crack Density (m/m <sup>2</sup> )	Age-Corrected Crack Density (m/m <sup>2</sup> )	Crack Density (m/m <sup>2</sup> )	Age-Corrected Crack Density (m/m <sup>2</sup> )	Crack Density (m/m <sup>2</sup> )	Age-Corrected Crack Density (m/m <sup>2</sup> )	
<b>7% Silica Fume Overlay Bridges</b>									
30-93	Deck	08/04/01	0.06	0.21	--	--	--	--	0.21
40-92	Deck	10/26/01	0.90	1.06	--	--	--	--	1.06
40-93	Deck	10/16/01	0.43	0.60	--	--	--	--	0.60
46-332	Deck	05/15/02	0.63	0.81	--	--	--	--	0.81
81-53	Deck	02/21/00	0.15	0.26	--	--	--	--	0.26
85-148	West 32 ft	10/30/01	0.59	0.75	--	--	--	--	0.75
85-148	East 18 ft SFO	10/27/01	0.54	0.70	--	--	--	--	0.70
85-149	Deck	09/26/02	0.14	0.33	--	--	--	--	0.33
89-269	West 1/2 SFO	07/26/01	0.02	0.18	--	--	--	--	0.18
89-269	East 1/2 SFO	07/31/01	0.02	0.17	--	--	--	--	0.17
89-272	West 1/2 SFO	04/04/02	0.05	0.23	--	--	--	--	0.23
89-272	East 1/2 SFO	04/10/02	0.04	0.22	--	--	--	--	0.22
103-56	North 1/2 SFO	10/17/01	0.16	0.32	--	--	--	--	0.32
103-56	South 1/2 SFO	10/12/01	0.28	0.44	--	--	--	--	0.44
<b>5% Silica Fume Overlay Bridges</b>									
23-85	East 1/2 SFO	03/29/96	0.54	0.55	0.37	0.51	--	--	0.53
23-85	West 1/2 SFO	04/03/96	0.59	0.60	0.37	0.51	--	--	0.56

Table E.2 (con't) – Crack Densities for Individual Bridge Placements

Bridge Number	Portion Placed	Date of Placement	Current Study		Miller and Darwin (2000)		Schmitt and Darwin (1995)		All Studies Mean Age-Corrected Crack Density (m/m <sup>2</sup> )
			Crack Density (m/m <sup>2</sup> )	Age-Corrected Crack Density (m/m <sup>2</sup> )	Crack Density (m/m <sup>2</sup> )	Age-Corrected Crack Density (m/m <sup>2</sup> )	Crack Density (m/m <sup>2</sup> )	Age-Corrected Crack Density (m/m <sup>2</sup> )	
46-302	Lt. 1/2 SFO	04/09/96	0.71	0.72	0.43	0.57	--	--	0.65
46-302	Rt. 1/2 SFO	04/11/96	0.85	0.86	0.56	0.70	--	--	0.78
46-309	Rt. 1/2 SFO	10/20/95	0.50	0.49	0.32	0.44	--	--	0.47
46-309	Lt 1/2 SFO	10/24/95	0.56	0.55	0.38	0.51	--	--	0.53
46-317	North 12 ft	06/28/96	0.19	0.20	0.07	0.22	--	--	0.21
46-317	South 16 ft	07/01/96	0.39	0.41	0.08	0.23	--	--	0.32
81-50	SFO Rt. Unit 1	11/15/95	--	--	--	--	--	--	--
81-50	SFO Lt. Unit 1	11/18/95	--	--	--	--	--	--	--
81-50	SFO Rt. Unit 2	11/21/95	0.90	0.90	0.67	0.80	--	--	0.85
81-50	SFO Lt. Unit 2	11/30/95	1.28	1.28	0.70	0.83	--	--	1.05
87-453	North 22 ft	06/30/97	0.71	0.76	0.19	0.36	--	--	0.56
87-453	South 18 ft	07/03/97	0.92	0.97	0.32	0.50	--	--	0.73
87-454	Left of CL	09/10/96	0.80	0.82	0.66	0.81	--	--	0.81
87-454	Right of CL	10/16/96	0.93	0.95	0.82	0.97	--	--	0.96
89-184	Inside	09/26/90	0.90	0.72	0.94	0.89	0.68	0.79	0.80
89-184	Outside	09/28/90	0.88	0.69	1.06	1.01	0.70	0.81	0.84
89-187	Inside	06/26/90	0.99	0.83	1.21	1.15	1.46	1.57	1.18
89-187	Outside	06/28/90	0.83	0.67	0.79	0.73	0.65	0.76	0.72
89-206	Right of CL	10/04/95	0.58	0.70	0.41	0.38	--	--	0.54
89-206	Left of CL	10/10/95	0.27	0.40	0.48	0.44	--	--	0.42

Table E.2 (con't) – Crack Densities for Individual Bridge Placements

Bridge Number	Portion Placed	Date of Placement	Current Study		Miller and Darwin (2000)		Schmitt and Darwin (1995)		All Studies Mean Age-Corrected Crack Density (m/m <sup>2</sup> )
			Crack Density (m/m <sup>2</sup> )	Age-Corrected Crack Density (m/m <sup>2</sup> )	Crack Density (m/m <sup>2</sup> )	Age-Corrected Crack Density (m/m <sup>2</sup> )	Crack Density (m/m <sup>2</sup> )	Age-Corrected Crack Density (m/m <sup>2</sup> )	
89-207	Left of CL	10/24/95	0.40	0.36	0.33	0.46	--	--	0.41
89-207	Right of CL	04/19/96	0.45	0.43	0.39	0.53	--	--	0.48
89-210	Right of CL	10/12/95	0.62	0.64	0.17	0.30	--	--	0.47
89-210	Left of CL	10/18/95	0.55	0.57	0.15	0.29	--	--	0.43
89-234	SFO South 20 ft	06/20/96	0.18	0.15	0.17	0.33	--	--	0.24
89-234	SFO North 18 ft	06/25/96	0.24	0.21	0.23	0.38	--	--	0.30
89-234	SFO Center 12 ft	06/28/96	0.57	0.54	0.51	0.66	--	--	0.60
89-235	SFO Left 20 ft	04/26/97	--	--	--	--	--	--	--
89-235	SFO Right 18 ft	05/01/97	0.21	0.22	0.38	0.56	--	--	0.39
89-235	SFO Center 12 ft	05/06/97	--	--	--	--	--	--	--
89-240	Rt. 22 ft SFO	08/05/97	0.10	0.13	0.01	0.20	--	--	0.17
89-240	Lt. 22 ft SFO	08/07/97	0.32	0.35	0.41	0.60	--	--	0.47
89-244	Right of CL	10/17/97	0.45	0.48	0.03	0.23	--	--	0.35
89-244	Left of CL	10/21/97	0.15	0.19	0.00	0.20	--	--	0.19
89-245	Lt. of CL Unit #2	10/20/97	0.54	0.57	0.03	0.23	--	--	0.40
89-245	Lt. of CL Unit #1	10/22/97	0.47	0.49	0.03	0.23	--	--	0.36
89-245	Rt. of CL Unit #2	10/23/97	0.45	0.48	0.05	0.25	--	--	0.37
89-245	Rt. of CL Unit #1	10/24/97	0.35	0.38	0.09	0.28	--	--	0.33
89-246	East 1/2 SFO	09/08/97	0.37	0.42	0.08	0.27	--	--	0.35
89-246	West 1/2 SFO	09/10/97	0.29	0.34	0.06	0.26	--	--	0.30

Table E.2 (con't) – Crack Densities for Individual Bridge Placements

Bridge Number	Portion Placed	Date of Placement	Current Study		Miller and Darwin (2000)		Schmitt and Darwin (1995)		All Studies Mean Age-Corrected Crack Density (m/m <sup>2</sup> )
			Crack Density (m/m <sup>2</sup> )	Age-Corrected Crack Density (m/m <sup>2</sup> )	Crack Density (m/m <sup>2</sup> )	Age-Corrected Crack Density (m/m <sup>2</sup> )	Crack Density (m/m <sup>2</sup> )	Age-Corrected Crack Density (m/m <sup>2</sup> )	
89-247	SFO West 13 ft	05/05/97	0.62	0.64	0.47	0.65	--	--	0.64
89-247	SFO East 26 ft	05/07/97	0.51	0.53	0.52	0.70	--	--	0.62
89-248	Westbound Lane	04/24/98	0.48	0.52	0.02	0.23	--	--	0.38
89-248	Eastbound Lane	05/01/98	0.55	0.59	0.03	0.24	--	--	0.41
<b>Conventional Overlay Bridges</b>									
46-289	Inside 24 ft	09/02/92	0.75	0.72	0.66	0.66	--	--	0.69
46-289	Outside 20 ft	09/11/92	0.65	0.62	0.64	0.64	--	--	0.63
46-290	Inside 24 ft	09/08/92	0.75	0.72	0.66	0.66	--	--	0.69
46-290	Outside 10 ft	09/15/92	0.51	0.48	0.53	0.54	--	--	0.51
46-294	Left	07/23/92	--	--	--	--	0.40	0.44	0.44
46-294	Right	07/25/92	--	--	--	--	0.20	0.24	0.24
46-295	Left	03/06/92	--	--	--	--	0.43	0.47	0.47
46-295	Right	03/14/92	--	--	--	--	0.15	0.19	0.19
46-299	Rt. of CL 22 ft	07/28/94	0.67	0.65	0.69	0.71	--	--	0.68
46-299	Lt. of CL 18 ft	07/30/94	1.00	0.99	1.12	1.14	--	--	1.06
46-300	Lt. of CL 22 ft	08/14/95	0.68	0.69	0.98	1.01	--	--	0.85
46-300	Rt. of CL 18 ft	08/10/95	0.63	0.63	0.49	0.52	--	--	0.58
46-301	Rt. of CL 24 ft	08/03/94	0.72	0.71	0.98	1.00	--	--	0.85
46-301	Lt. of CL 24 to 38 ft	08/06/94	1.12	1.10	0.92	0.94	--	--	1.02

Table E.2 (con't) – Crack Densities for Individual Bridge Placements

Bridge Number	Portion Placed	Date of Placement	Current Study		Miller and Darwin (2000)		Schmitt and Darwin (1995)		All Studies Mean Age-Corrected Crack Density (m/m <sup>2</sup> )
			Crack Density (m/m <sup>2</sup> )	Age-Corrected Crack Density (m/m <sup>2</sup> )	Crack Density (m/m <sup>2</sup> )	Age-Corrected Crack Density (m/m <sup>2</sup> )	Crack Density (m/m <sup>2</sup> )	Age-Corrected Crack Density (m/m <sup>2</sup> )	
46-301	Rt. of CL 24 to 38 ft	08/05/94	0.78	0.77	0.43	0.45	--	--	0.61
46-301	Lt. of CL 24 ft	08/06/94	0.83	0.82	0.57	0.59	--	--	0.70
75-1	Lt. of CL	10/17/91	0.41	0.36	0.35	0.34	--	--	0.35
75-1	Rt. of CL	10/19/91	0.58	0.54	0.39	0.39	--	--	0.46
75-49	Eastbound	06/04/91	0.36	0.31	0.41	0.40	--	--	0.36
75-49	Westbound	06/07/91	0.44	0.39	0.49	0.49	--	--	0.44
81-49	Rt. 22 ft	04/08/92	0.69	0.64	0.58	0.58	--	--	0.61
81-49	Rt. of CL 12 ft	04/13/92	1.06	1.02	0.80	0.80	--	--	0.91
81-49	Lt. 22 ft	10/21/92	0.67	0.63	0.71	0.72	--	--	0.67
81-49	Lt. of CL 12 ft	10/23/92	0.99	0.95	1.01	1.02	--	--	0.98
89-179	Right	10/30/90	--	--	--	--	0.19	0.21	0.21
89-179	Left	11/01/90	--	--	--	--	0.28	0.30	0.30
89-180	Right	04/18/90	--	--	--	--	0.37	0.39	0.39
89-180	Left	04/23/90	--	--	--	--	0.35	0.37	0.37
89-183	Rt. Side	09/21/90	0.56	0.52	0.44	0.43	--	--	0.47
89-183	Lt. Side	09/25/90	0.64	0.59	0.58	0.56	--	--	0.58
89-185	Outside	06/21/90	0.95	0.90	0.81	0.79	0.60	0.63	0.77
89-185	Inside	06/23/90	0.63	0.58	0.57	0.55	0.95	0.98	0.70
89-186	Inside	09/14/90	0.79	0.75	0.69	0.68	0.56	0.59	0.67
89-186	Outside	09/17/90	0.70	0.66	0.75	0.74	0.45	0.48	0.63

Table E.2 (con't) – Crack Densities for Individual Bridge Placements

Bridge Number	Portion Placed	Date of Placement	Current Study		Miller and Darwin (2000)		Schmitt and Darwin (1995)		All Studies Mean Age-Corrected Crack Density (m/m <sup>2</sup> )
			Crack Density (m/m <sup>2</sup> )	Age-Corrected Crack Density (m/m <sup>2</sup> )	Crack Density (m/m <sup>2</sup> )	Age-Corrected Crack Density (m/m <sup>2</sup> )	Crack Density (m/m <sup>2</sup> )	Age-Corrected Crack Density (m/m <sup>2</sup> )	
89-196	Rt. Side	05/01/92	0.76	0.72	0.66	0.67	--	--	0.69
89-196	Lt. Side	05/05/92	0.43	0.40	0.40	0.41	--	--	0.40
89-198	Lt. Side	08/24/91	0.45	0.40	0.36	0.35	0.70	0.73	0.50
89-198	Rt. Side	08/27/91	0.51	0.47	0.41	0.41	0.40	0.43	0.44
89-199	Lt. Side	08/26/91	0.67	0.63	0.75	0.75	0.64	0.67	0.68
89-199	Rt. Side	08/28/91	0.73	0.69	0.54	0.54	0.71	0.74	0.66
89-200	Rt. Side	08/17/91	0.77	0.73	0.67	0.67	0.57	0.60	0.67
89-200	Lt. Side	08/20/91	0.51	0.47	0.44	0.43	0.45	0.48	0.46
89-201	Rt. Side	08/19/91	0.69	0.65	0.66	0.66	0.59	0.62	0.64
89-201	Lt. Side	08/21/91	0.73	0.69	0.59	0.59	0.77	0.80	0.69
105-021	East	09/04/87	--	--	--	--	0.11	0.11	0.11
105-021	West	09/09/87	--	--	--	--	0.08	0.08	0.08
105-225	East	07/22/86	--	--	--	--	0.21	0.20	0.20
105-225	West	07/26/86	--	--	--	--	0.11	0.10	0.10
105-225	Center	07/29/86	--	--	--	--	0.29	0.28	0.28
105-226	East	07/23/86	--	--	--	--	0.12	0.11	0.11
105-226	West	07/25/86	--	--	--	--	0.17	0.16	0.16
105-226	Center	07/28/86	--	--	--	--	0.27	0.26	0.26

Table E.2 (con't) – Crack Densities for Individual Bridge Placements

Bridge Number	Portion Placed	Date of Placement	Current Study		Miller and Darwin (2000)		Schmitt and Darwin (1995)		All Studies Mean Age-Corrected Crack Density (m/m <sup>2</sup> )
			Crack Density (m/m <sup>2</sup> )	Age-Corrected Crack Density (m/m <sup>2</sup> )	Crack Density (m/m <sup>2</sup> )	Age-Corrected Crack Density (m/m <sup>2</sup> )	Crack Density (m/m <sup>2</sup> )	Age-Corrected Crack Density (m/m <sup>2</sup> )	
105-230	Center	--	--	--	--	--	0.09	0.07	0.07
105-230	East	--	--	--	--	--	0.10	0.08	0.08
105-230	West	--	--	--	--	--	0.08	0.06	0.06
105-231	Center	--	--	--	--	--	0.12	0.10	0.10
105-231	East	--	--	--	--	--	0.13	0.11	0.11
105-231	West	--	--	--	--	--	0.09	0.07	0.07
105-262	Center	06/12/85	--	--	--	--	0.15	0.13	0.13
105-262	Right	06/14/85	--	--	--	--	0.23	0.21	0.21
105-262	Left	--	--	--	--	--	--	--	--
105-263	Center	10/13/83	--	--	--	--	0.12	0.08	0.08
105-263	East	10/18/83	--	--	--	--	0.14	0.10	0.10
105-263	West	--	--	--	--	--	--	--	--
105-268	Left	06/14/86	--	--	--	--	0.67	0.66	0.66
105-268	Right	06/14/86	--	--	--	--	0.56	0.55	0.55
105-269	Deck	10/26/85	--	--	--	--	0.45	0.44	0.44
<b>Monolithic Bridges</b>									
3-045	West Deck	12/21/84	0.43	0.25	--	--	0.12	0.08	0.16
3-045	East Deck	12/26/84	0.39	0.20	--	--	0.21	0.17	0.19
3-045	W. Ctr. Deck	12/27/84	0.20	0.02	--	--	0.18	0.14	0.08

Table E.2 (con't) – Crack Densities for Individual Bridge Placements

Bridge Number	Portion Placed	Date of Placement	Current Study		Miller and Darwin (2000)		Schmitt and Darwin (1995)		All Studies Mean Age-Corrected Crack Density (m/m <sup>2</sup> )
			Crack Density (m/m <sup>2</sup> )	Age-Corrected Crack Density (m/m <sup>2</sup> )	Crack Density (m/m <sup>2</sup> )	Age-Corrected Crack Density (m/m <sup>2</sup> )	Crack Density (m/m <sup>2</sup> )	Age-Corrected Crack Density (m/m <sup>2</sup> )	
3-045	Ctr. Deck	03/13/85	0.28	0.10	--	--	0.23	0.19	0.14
3-045	E. Ctr. Deck	03/14/85	0.31	0.13	--	--	0.15	0.11	0.12
3-046	West Deck	12/31/85	0.40	0.24	--	--	0.33	0.30	0.27
3-046	East Deck	01/02/86	0.53	0.36	--	--	0.42	0.39	0.38
3-046	Ctr. Deck	01/10/86	0.34	0.18	--	--	0.15	0.12	0.15
56-142	North End	10/01/87	0.35	0.21	--	--	0.22	0.22	0.22
56-142	N. + Moment	10/01/87	0.04	0.00	--	--	0.00	0.00	0.00
56-142	S. + Moment	10/01/87	0.19	0.05	--	--	0.08	0.08	0.06
56-142	South End	10/01/87	--	--	--	--	0.03	0.03	0.03
56-142	N. Pier	10/06/87	0.36	0.22	--	--	0.20	0.20	0.21
56-142	Ctr. Pier	10/06/87	0.07	0.00	--	--	0.02	0.02	0.01
56-142	South Pier	10/06/87	0.07	0.00	--	--	0.05	0.05	0.02
56-148	Deck	07/18/91	0.53	0.46	0.31	0.31	0.28	0.33	0.37
70-95	Deck	10/31/85	0.13	0.00	--	--	0.07	0.03	0.02
70-101	North	--	--	--	--	--	0.07	0.03	0.03
70-101	South	--	--	--	--	--	0.04	0.00	0.00
70-103	Right	03/14/85	0.66	0.48	--	--	0.40	0.37	0.43
70-103	Left	03/19/85	0.84	0.66	--	--	0.57	0.54	0.60
70-104	Deck	10/17/85	0.10	0.00	--	--	0.09	0.05	0.03
70-107	Deck	10/25/91	0.72	0.66	0.42	0.42	0.34	0.40	0.49

Table E.2 (con't) – Crack Densities for Individual Bridge Placements

Bridge Number	Portion Placed	Date of Placement	Current Study		Miller and Darwin (2000)		Schmitt and Darwin (1995)		All Studies Mean Age-Corrected Crack Density (m/m <sup>2</sup> )
			Crack Density (m/m <sup>2</sup> )	Age-Corrected Crack Density (m/m <sup>2</sup> )	Crack Density (m/m <sup>2</sup> )	Age-Corrected Crack Density (m/m <sup>2</sup> )	Crack Density (m/m <sup>2</sup> )	Age-Corrected Crack Density (m/m <sup>2</sup> )	
75-44	Deck	07/12/90	0.28	0.19	--	--	0.19	0.23	0.21
75-45	Deck	08/10/90	0.45	0.36	--	--	0.51	0.55	0.45
89-204	Deck	10/03/91	1.05	0.98	0.84	0.84	0.75	0.81	0.87
89-208	Deck	06/15/95	0.11	0.11	0.03	0.09	--	--	0.10
99-76	South End	09/01/89	1.04	0.93	--	--	1.48	1.53	1.23
99-76	Placement 2	09/15/89	0.81	0.70	--	--	0.95	1.00	0.85
99-76	Placement 3	10/13/89	0.93	0.83	--	--	0.94	0.99	0.91
99-76	Placement 4	11/07/89	0.74	0.63	--	--	0.90	0.95	0.79
99-76	Placement 5	11/21/89	0.57	0.47	--	--	0.77	0.82	0.64
99-76	North (West Ln.)	01/09/90	0.55	0.45	--	--	0.42	0.47	0.46
99-76	North (East Ln.)	05/11/90	0.48	0.37	--	--	0.46	0.51	0.44
105-000 <sup>†</sup>	Deck	06/23/93	--	--	--	--	0.27	0.32	0.32

<sup>†</sup>Bridge has no assigned serial number. Project No. is 105-U-1262-01.

-- Denotes bridges that were not surveyed during a particular study or missing data.

Table E.3 – Crack Densities for End Sections

Bridge Number	End Condition	End Section Crack Densities											
		Current Study			Miller and Darwin (2000)			Schmitt and Darwin (1995)			All Studies		
		End 1 (m/m <sup>2</sup> )	End 2 (m/m <sup>2</sup> )	Mean Age-Corrected (m/m <sup>2</sup> )	End 1 (m/m <sup>2</sup> )	End 2 (m/m <sup>2</sup> )	Mean Age-Corrected (m/m <sup>2</sup> )	End 1 (m/m <sup>2</sup> )	End 2 (m/m <sup>2</sup> )	Mean Age-Corrected (m/m <sup>2</sup> )	End 1 (m/m <sup>2</sup> )	End 2 (m/m <sup>2</sup> )	Mean Age-Corrected (m/m <sup>2</sup> )
<b>7% Silica Fume Overlay Bridges</b>													
30-93	F	0.04	0.00	0.38	--	--	--	--	--	--	--	--	0.38
40-92	F	0.37	0.94	1.00	--	--	--	--	--	--	--	--	1.00
40-93	F	0.02	0.04	0.32	--	--	--	--	--	--	--	--	0.32
46-332	F	0.97	0.72	1.15	--	--	--	--	--	--	--	--	1.15
81-53	F	0.61	0.22	0.72	--	--	--	--	--	--	--	--	0.72
85-148	F	0.90	0.60	0.95	--	--	--	--	--	--	--	--	0.95
85-149	F	0.54	0.22	0.69	--	--	--	--	--	--	--	--	0.69
89-269	F	0.10	0.07	0.38	--	--	--	--	--	--	--	--	0.38
89-272	F	0.25	0.11	0.52	--	--	--	--	--	--	--	--	0.52
103-56	F	0.30	0.16	0.53	--	--	--	--	--	--	--	--	0.53
<b>5% Silica Fume Overlay Bridges</b>													
23-85	F	1.11	0.77	0.94	0.34	0.27	0.30	--	--	--	--	--	0.62
46-302	F	0.73	0.79	0.76	0.32	0.58	0.45	--	--	--	--	--	0.61
46-309	F	0.68	1.25	0.97	0.26	0.61	0.44	--	--	--	--	--	0.70
46-317	P	0.10	0.55	0.32	0.00	0.00	0.00	--	--	--	--	--	0.16
81-50	P	--	1.15	1.15	--	0.76	0.76	--	--	--	--	--	0.96
87-453	F	1.74	1.87	1.80	0.30	1.61	0.96	--	--	--	--	--	1.38

Table E.3 (con't) – Crack Densities for End Sections

Bridge Number	End Condition	End Section Crack Densities											
		Current Study			Miller and Darwin (2000)			Schmitt and Darwin (1995)			All Studies		
		End 1 (m/m <sup>2</sup> )	End 2 (m/m <sup>2</sup> )	Mean Age-Corrected (m/m <sup>2</sup> )	End 1 (m/m <sup>2</sup> )	End 2 (m/m <sup>2</sup> )	Mean Age-Corrected (m/m <sup>2</sup> )	End 1 (m/m <sup>2</sup> )	End 2 (m/m <sup>2</sup> )	Mean Age-Corrected (m/m <sup>2</sup> )	End 1 (m/m <sup>2</sup> )	End 2 (m/m <sup>2</sup> )	Mean Age-Corrected (m/m <sup>2</sup> )
87-454	F	1.46	1.91	1.68	0.89	2.32	1.61	--	--	--	--	--	1.64
89-206	P	0.36	0.28	0.32	0.32	0.00	0.16	--	--	--	--	--	0.24
89-207	P	0.12	0.22	0.17	0.12	0.03	0.08	--	--	--	--	--	0.12
89-210	F	1.07	1.18	1.13	0.01	0.19	0.10	--	--	--	--	--	0.61
89-234	F	0.52	0.52	0.52	0.63	0.52	0.58	--	--	--	--	--	0.55
89-235	F	0.86	--	0.86	2.43	0.00	1.21	--	--	--	--	--	1.04
89-240	P	0.07	0.10	0.09	0.13	0.17	0.15	--	--	--	--	--	0.12
89-244	P	0.21	0.13	0.17	0.00	0.00	0.00	--	--	--	--	--	0.08
89-245	P	0.26	0.27	0.26	0.00	0.00	0.00	--	--	--	--	--	0.13
89-246	P	0.19	0.00	0.10	0.00	0.00	0.00	--	--	--	--	--	0.05
89-247	P	0.28	0.49	0.38	0.31	0.02	0.17	--	--	--	--	--	0.27
89-248	F	0.60	1.08	0.84	0.00	0.00	0.00	--	--	--	--	--	0.42
89-184	F	1.35	1.99	1.67	1.46	1.92	1.69	1.16	1.16	1.16	1.16	1.16	1.51
89-187	F	1.47	1.17	1.32	1.85	1.57	1.71	1.05	1.66	1.66	1.66	1.36	1.46
<b>Conventional Overlay Bridges</b>													
46-294	P	--	--	--	--	--	--	0.33	0.16	0.35	0.35	0.35	0.35
46-295	P	--	--	--	--	--	--	0.20	0.14	0.27	0.27	0.27	0.27
46-289	P	0.52	0.19	0.28	0.50	0.13	0.33	--	--	--	--	--	0.30

Table E.3 (con't) – Crack Densities for End Sections

Bridge Number	End Condition	End Section Crack Densities												
		Current Study			Miller and Darwin (2000)			Schmitt and Darwin (1995)			All Studies			
		End 1 (m/m <sup>2</sup> )	End 2 (m/m <sup>2</sup> )	Mean Age-Corrected (m/m <sup>2</sup> )	End 1 (m/m <sup>2</sup> )	End 2 (m/m <sup>2</sup> )	Mean Age-Corrected (m/m <sup>2</sup> )	End 1 (m/m <sup>2</sup> )	End 2 (m/m <sup>2</sup> )	Mean Age-Corrected (m/m <sup>2</sup> )	End 1 (m/m <sup>2</sup> )	End 2 (m/m <sup>2</sup> )	Mean Age-Corrected (m/m <sup>2</sup> )	
46-290	P	0.49	0.20	0.27	0.46	0.17	0.32	--	--	--	--	--	--	0.30
46-299	P	0.80	1.08	0.91	0.33	0.93	0.68	--	--	--	--	--	--	0.79
46-300	P	0.32	0.36	0.35	0.33	0.40	0.44	--	--	--	--	--	--	0.40
46-301	F	1.52	0.92	1.19	1.75	1.27	1.56	--	--	--	--	--	--	1.37
75-1	P	0.35	0.39	0.26	0.30	0.12	0.20	--	--	--	--	--	--	0.23
75-49	F	--	0.57	0.46	0.76	0.92	0.83	--	--	--	--	--	--	0.64
81-49	F	1.25	1.24	1.16	0.98	0.88	0.94	--	--	--	--	--	--	1.05
89-179	F	--	--	--	--	--	--	1.01	1.19	1.16	1.16	1.16	1.16	1.16
89-180	F	--	--	--	--	--	--	0.64	0.99	0.86	0.86	0.86	0.86	0.86
89-183	F	1.45	1.24	1.23	1.30	1.10	1.17	--	--	--	--	--	--	1.20
89-185	F	1.01	2.09	1.43	1.43	1.99	1.68	--	--	--	--	--	--	1.55
89-186	F	1.09	1.23	1.07	1.09	1.23	1.13	--	--	--	--	--	--	1.10
89-196	F	1.13	1.30	1.13	1.06	1.47	1.27	--	--	--	--	--	--	1.20
89-198	P	0.33	0.34	0.23	0.40	0.19	0.29	--	--	--	--	--	--	0.26
89-199	P	0.33	0.53	0.33	0.24	0.56	0.39	--	--	--	--	--	--	0.36
89-200	F	1.79	1.48	1.54	1.64	1.48	1.55	--	--	--	--	--	--	1.54
89-201	F	1.66	1.61	1.53	1.8	1.59	1.69	--	--	--	--	--	--	1.61
105-021	--	--	--	--	--	--	--	--	--	--	--	--	--	--
105-225	F	--	--	--	--	--	--	0.88	0.74	0.78	0.78	0.78	0.78	0.78

Table E.3 (con't) – Crack Densities for End Sections

Bridge Number	End Condition	End Section Crack Densities											
		Current Study			Miller and Darwin (2000)			Schmitt and Darwin (1995)			All Studies		
		End 1 (m/m <sup>2</sup> )	End 2 (m/m <sup>2</sup> )	Mean Age-Corrected (m/m <sup>2</sup> )	End 1 (m/m <sup>2</sup> )	End 2 (m/m <sup>2</sup> )	Mean Age-Corrected (m/m <sup>2</sup> )	End 1 (m/m <sup>2</sup> )	End 2 (m/m <sup>2</sup> )	Mean Age-Corrected (m/m <sup>2</sup> )	End 1 (m/m <sup>2</sup> )	End 2 (m/m <sup>2</sup> )	Mean Age-Corrected (m/m <sup>2</sup> )
105-226	F	--	--	--	--	--	1.02	1.07	1.02	1.02	1.02	1.02	1.02
105-230	F	--	--	--	--	--	0.71	0.88	0.71	0.71	0.71	0.76	0.76
105-231	F	--	--	--	--	--	0.53	0.63	0.53	0.53	0.53	0.54	0.54
105-262	F	--	--	--	--	--	0.37	0.20	0.37	0.37	0.37	0.23	0.23
105-263	F	--	--	--	--	--	0.08	0.00	0.08	0.08	0.08	0.00	0.00
105-265	F	--	--	--	--	--	0.00	0.12	0.00	0.00	0.00	0.00	0.00
105-268	F	--	--	--	--	--	1.03	0.98	1.03	1.03	1.03	0.99	0.99
105-269	F	--	--	--	--	--	0.51	0.92	0.51	0.51	0.51	0.68	0.68
<b>Monolithic Bridges</b>													
3-45	F	--	0.39	--	--	--	0.24	0.35	0.24	0.24	0.24	--	--
3-46	F	0.77	0.39	--	--	--	0.54	0.17	0.54	0.54	0.54	--	--
56-142	P	--	0.00	--	--	--	0.00	0.00	0.00	0.00	0.00	--	--
56-148	F	0.89	0.89	--	0.63	0.30	0.41	0.09	0.41	0.41	0.41	--	--
70-101	F	--	--	--	--	--	0.00	0.18	0.00	0.00	0.00	--	--
70-103	F	0.94	0.55	--	--	--	0.11	0.29	0.11	0.11	0.11	--	--
70-104	F	0.16	0.30	--	--	--	0.95	0.50	0.95	0.95	0.95	--	--
70-107	F	--	--	--	0.53	0.56	0.00	0.03	0.00	0.00	0.00	--	--
70-95	F	0.30	0.30	--	--	--	0.55	0.20	0.55	0.55	0.55	--	--

Table E.3 (con't) – Crack Densities for End Sections

Bridge Number	End Condition	End Section Crack Densities									
		Current Study			Miller and Darwin (2000)			Schmitt and Darwin (1995)			All Studies
		End 1 (m/m <sup>2</sup> )	End 2 (m/m <sup>2</sup> )	Mean Age-Corrected (m/m <sup>2</sup> )	End 1 (m/m <sup>2</sup> )	End 2 (m/m <sup>2</sup> )	Mean Age-Corrected (m/m <sup>2</sup> )	End 1 (m/m <sup>2</sup> )	End 2 (m/m <sup>2</sup> )	Mean Age-Corrected (m/m <sup>2</sup> )	Mean Age-Corrected (m/m <sup>2</sup> )
75-44	F	0.61	0.46	--	--	--	0.36	0.13	--	--	
75-45	F	0.43	1.35	--	--	--	0.06	0.76	--	--	
89-204	F	1.01	1.03	--	0.72	0.64	0.43	0.41	--	--	
89-208	F	0.03	0.08	--	0.02	0.04	--	--	--	--	
99-76	P	0.45	0.21	--	--	--	0.45	--	--	--	
105-000 <sup>†</sup>	F	--	--	--	--	--	0.61	--	--	--	
105-46	F	--	--	--	--	--	--	--	--	--	

<sup>†</sup>Bridge has no assigned serial number. Project No. is 105-U-1262-01.

-- Denotes bridges that were not surveyed during a particular study or missing data.

Table E.4 – Crack Densities and Data for Individual Spans

Bridge Number	Span Type	Span Location	Span Length		Current Study		Miller and Darwin (2000)		Schmitt and Darwin (1995)		All Studies Mean Age-Corrected Crack Density (m/m <sup>2</sup> )
			(ft)	(m)	Crack Density (m/m <sup>2</sup> )	Age-Corrected Crack Density (m/m <sup>2</sup> )	Crack Density (m/m <sup>2</sup> )	Age-Corrected Crack Density (m/m <sup>2</sup> )	Crack Density (m/m <sup>2</sup> )	Age-Corrected Crack Density (m/m <sup>2</sup> )	
<b>7% Silica Fume Overlay Bridges</b>											
30-93	End	West	126	38.5	0.02	0.06	--	--	--	--	0.06
30-93	End	East	105	32.0	0.09	0.13	--	--	--	--	0.13
40-92	End	South	62	19.0	0.84	0.88	--	--	--	--	0.88
40-92	Int.	S. Center	102	31.0	0.93	0.97	--	--	--	--	0.97
40-92	Int.	N. Center	102	31.0	0.90	0.94	--	--	--	--	0.94
40-92	End	North	62	19.0	0.89	0.93	--	--	--	--	0.93
40-93	End	South	62	19.0	0.36	0.40	--	--	--	--	0.40
40-93	Int.	S. Center	102	31.0	0.36	0.40	--	--	--	--	0.40
40-93	Int.	N. Center	102	31.0	0.47	0.51	--	--	--	--	0.51
40-93	End	North	62	19.0	0.55	0.59	--	--	--	--	0.59
46-332	End	West	72	22.0	0.70	0.75	--	--	--	--	0.75
46-332	Int.	Center	107	32.5	0.68	0.73	--	--	--	--	0.73
46-332	End	East	72	22.0	0.38	0.43	--	--	--	--	0.43
85-148	End	South	125	38.0	0.44	0.48	--	--	--	--	0.48
85-148	Int.	Center	141	43.0	0.68	0.72	--	--	--	--	0.72
85-148	End	North	95	29.0	0.56	0.60	--	--	--	--	0.60
85-149	End	South	125	38.0	0.09	0.14	--	--	--	--	0.14
85-149	Int.	Center	141	43.0	0.20	0.25	--	--	--	--	0.25
85-149	End	North	95	29.0	0.10	0.15	--	--	--	--	0.15

Table E.4 (con't) – Crack Densities and Data for Individual Spans

Bridge Number	Span Type	Span Location	Span Length		Current Study		Miller and Darwin (2000)		Schmitt and Darwin (1995)		All Studies Mean Age-Corrected Crack Density (m/m <sup>2</sup> )
			(ft)	(m)	Crack Density (m/m <sup>2</sup> )	Age-Corrected Crack Density (m/m <sup>2</sup> )	Crack Density (m/m <sup>2</sup> )	Age-Corrected Crack Density (m/m <sup>2</sup> )	Crack Density (m/m <sup>2</sup> )	Age-Corrected Crack Density (m/m <sup>2</sup> )	
89-269	End	South	65	19.8	0.00	0.04	--	--	--	--	0.04
89-269	Int.	Center	84	25.6	0.02	0.06	--	--	--	--	0.06
89-269	End	North	65	19.8	0.02	0.06	--	--	--	--	0.06
89-272	End	South	70	21.3	0.02	0.07	--	--	--	--	0.07
89-272	Int.	S. Center	100	30.5	0.00	0.05	--	--	--	--	0.05
89-272	Int.	N. Center	100	30.5	0.01	0.06	--	--	--	--	0.06
89-272	End	North	60	18.3	0.14	0.19	--	--	--	--	0.19
103-56	End	West	66	20.0	0.23	0.27	--	--	--	--	0.27
103-56	Int.	Center	98	30.0	0.23	0.27	--	--	--	--	0.27
103-56	End	East	66	20.0	0.21	0.25	--	--	--	--	0.25
<b>5% Silica Fume Overlay Bridges</b>											
23-85	End	South	124	37.8	0.67	0.67	0.46	0.50	--	--	0.58
23-85	End	North	124	37.8	0.46	0.46	0.27	0.31	--	--	0.39
46-302	End	South	61	18.6	0.75	0.75	0.41	0.44	--	--	0.60
46-302	Int.	S. Center	85	25.9	0.75	0.75	0.57	0.61	--	--	0.68
46-302	Int.	N. Center	85	25.9	0.84	0.84	0.50	0.54	--	--	0.69
46-302	End	North	61	18.6	0.79	0.79	0.48	0.52	--	--	0.65
46-309	End	South	51	15.5	0.54	0.54	0.40	0.43	--	--	0.48
46-309	Int.	S. Center	85	25.9	0.46	0.46	0.32	0.36	--	--	0.41

Table E.4 (con't) – Crack Densities and Data for Individual Spans

Bridge Number	Span Type	Span Location	Span Length		Current Study		Miller and Darwin (2000)		Schmitt and Darwin (1995)		All Studies Mean Age-Corrected Crack Density (m/m <sup>2</sup> )
			(ft)	(m)	Crack Density (m/m <sup>2</sup> )	Age-Corrected Crack Density (m/m <sup>2</sup> )	Crack Density (m/m <sup>2</sup> )	Age-Corrected Crack Density (m/m <sup>2</sup> )	Crack Density (m/m <sup>2</sup> )	Age-Corrected Crack Density (m/m <sup>2</sup> )	
46-309	Int.	N. Center	85	25.9	0.46	0.46	0.32	0.35	--	--	0.41
46-309	End	North	51	15.5	0.72	0.72	0.39	0.42	--	--	0.57
46-317	End	West	90	27.4	0.27	0.27	0.03	0.07	--	--	0.17
46-317	Int.	W. Center	127	38.7	0.43	0.43	0.07	0.11	--	--	0.27
46-317	Int.	Center	192	58.5	0.37	0.37	0.07	0.11	--	--	0.24
46-317	Int.	E. Center	127	38.7	0.27	0.27	0.11	0.15	--	--	0.21
81-50	End	North	140	42.7	0.95	0.94	0.67	0.71	--	--	0.82
81-50	Int.	N. Center	175	53.3	1.11	1.10	0.74	0.78	--	--	0.94
81-50	Int.	N. Center	175	53.3	1.16	1.15	0.80	0.83	--	--	0.99
81-50	Int.	N. Center	150	45.7	1.12	1.11	0.72	0.76	--	--	0.93
81-50	Int.	Center	20	6.1	1.15	1.14	0.64	0.67	--	--	0.91
87-453	End	West	110	33.5	0.84	0.85	0.19	0.23	--	--	0.54
87-453	Int.	Center	158	48.2	0.65	0.66	0.10	0.14	--	--	0.40
87-453	End	East	110	33.5	1.00	1.01	0.51	0.56	--	--	0.79
87-454	End	West	102	31.1	0.93	0.94	0.57	0.61	--	--	0.77
87-454	Int.	Center	147	44.8	0.69	0.70	0.54	0.59	--	--	0.65
87-454	End	East	102	31.1	1.05	1.06	1.21	1.25	--	--	1.16
89-184	End	West	48	14.6	0.96	0.91	0.99	0.98	0.77	0.80	0.90
89-184	Int.	W. Center	93	28.3	0.77	0.73	0.83	0.82	0.58	0.61	0.72
89-184	Int.	E. Center	70	21.3	0.87	0.82	1.06	1.05	0.73	0.76	0.88

Table E.4 (con't) – Crack Densities and Data for Individual Spans

Bridge Number	Span Type	Span Location	Span Length (ft)	Span Length (m)	Current Study		Miller and Darwin (2000)		Schmitt and Darwin (1995)			All Studies Mean Age- Corrected Crack Density (m/m <sup>2</sup> )
					Crack Density (m/m <sup>2</sup> )	Age-Corrected Crack Density (m/m <sup>2</sup> )	Crack Density (m/m <sup>2</sup> )	Age-Corrected Crack Density (m/m <sup>2</sup> )	Crack Density (m/m <sup>2</sup> )	Age-Corrected Crack Density (m/m <sup>2</sup> )		
89-184	End	East	50	15.2	1.03	0.98	1.17	1.16	0.78	0.81	0.98	
89-187	End	West	45	13.7	0.73	0.69	0.80	0.79	0.94	0.97	0.81	
89-187	Int.	W. Center	60	18.3	0.95	0.91	1.00	0.99	1.12	1.15	1.01	
89-187	Int.	E. Center	60	18.3	0.88	0.84	0.98	0.96	0.97	1.00	0.93	
89-187	End	East	45	13.7	0.96	0.91	1.08	1.06	1.00	1.03	1.00	
89-206	End	West	84	25.6	0.54	0.53	0.45	0.48	--	--	0.51	
89-206	Int.	W. Center	116	35.4	0.44	0.43	0.43	0.47	--	--	0.45	
89-206	Int.	E. Center	116	35.4	0.45	0.44	0.42	0.46	--	--	0.45	
89-206	End	East	84	25.6	0.34	0.33	0.40	0.43	--	--	0.38	
89-207	End	West	84	25.6	0.34	0.33	0.31	0.34	--	--	0.33	
89-207	Int.	W. Center	116	35.4	0.47	0.46	0.42	0.45	--	--	0.46	
89-207	Int.	E. Center	116	35.4	0.45	0.44	0.45	0.49	--	--	0.46	
89-207	End	East	84	25.6	0.42	0.41	0.21	0.25	--	--	0.33	
89-210	End	South	65	19.8	0.51	0.52	0.07	0.11	--	--	0.31	
89-210	Int.	Center	82	25.0	0.53	0.54	0.11	0.15	--	--	0.34	
89-210	End	North	65	19.8	0.69	0.70	0.17	0.21	--	--	0.45	
89-234	End	West	73	22.3	0.26	0.25	0.28	0.32	--	--	0.28	
89-234	Int.	W. Center	131	39.9	0.27	0.26	0.26	0.30	--	--	0.28	
89-234	Int.	E. Center	110	33.5	0.31	0.30	0.28	0.32	--	--	0.31	
89-234	End	East	60	18.3	0.35	0.34	0.29	0.33	--	--	0.34	

Table E.4 (con't) – Crack Densities and Data for Individual Spans

Bridge Number	Span Type	Span Location	Span Length		Current Study		Miller and Darwin (2000)		Schmitt and Darwin (1995)		All Studies Mean Age-Corrected Crack Density (m/m <sup>2</sup> )
			(ft)	(m)	Crack Density (m/m <sup>2</sup> )	Age-Corrected Crack Density (m/m <sup>2</sup> )	Crack Density (m/m <sup>2</sup> )	Age-Corrected Crack Density (m/m <sup>2</sup> )	Crack Density (m/m <sup>2</sup> )	Age-Corrected Crack Density (m/m <sup>2</sup> )	
89-235	End	West	71	21.6	0.46	0.46	0.98	1.03	--	--	0.75
89-235	Int.	W. Center	131	39.9	0.16	0.16	0.27	0.32	--	--	0.24
89-235	Int.	E. Center	110	33.5	0.28	0.28	0.15	0.20	--	--	0.24
89-235	End	East	51	15.5	0.38	0.38	0.32	0.36	--	--	0.37
89-240	End	South	70	21.3	0.26	0.27	0.31	0.36	--	--	0.32
89-240	Int.	S. Center	100	30.5	0.27	0.28	0.34	0.39	--	--	0.33
89-240	Int.	N. Center	100	30.5	0.18	0.19	0.29	0.34	--	--	0.26
89-240	End	North	60	18.3	0.10	0.11	0.14	0.19	--	--	0.15
89-244	End	South	96	29.3	0.20	0.21	0.01	0.06	--	--	0.14
89-244	Int.	S. Center	120	36.6	0.33	0.34	0.01	0.06	--	--	0.20
89-244	Int.	N. Center	124	37.8	0.37	0.38	0.03	0.08	--	--	0.23
89-244	End	North	110	33.5	0.27	0.28	0.02	0.07	--	--	0.18
89-245	End	West	110	33.5	0.48	0.49	0.06	0.11	--	--	0.30
89-245	Int.	W. Center	170	51.8	0.37	0.38	0.07	0.12	--	--	0.25
89-245	Int.	W. Center	25	7.6	0.47	0.48	0.09	0.14	--	--	0.31
89-245	Int.	Center	155	47.2	0.66	0.67	0.03	0.09	--	--	0.38
89-245	Int.	E. Center	202	61.6	0.30	0.31	0.03	0.08	--	--	0.20
89-245	End	East	150	45.7	0.52	0.53	0.08	0.13	--	--	0.33
89-246	End	South	123	37.5	0.40	0.41	0.09	0.14	--	--	0.27
89-246	End	North	130	39.6	0.27	0.28	0.06	0.11	--	--	0.20

Table E.4 (con't) – Crack Densities and Data for Individual Spans

Bridge Number	Span Type	Span Location	Span Length		Current Study		Miller and Darwin (2000)		Schmitt and Darwin (1995)		All Studies Mean Age-Corrected Crack Density (m/m <sup>2</sup> )
			(ft)	(m)	Crack Density (m/m <sup>2</sup> )	Age-Corrected Crack Density (m/m <sup>2</sup> )	Crack Density (m/m <sup>2</sup> )	Age-Corrected Crack Density (m/m <sup>2</sup> )	Crack Density (m/m <sup>2</sup> )	Age-Corrected Crack Density (m/m <sup>2</sup> )	
89-247	End	South	123	37.5	0.60	0.60	0.66	0.71	--	--	0.66
89-247	End	North	130	39.6	0.50	0.50	0.35	0.40	--	--	0.45
89-248	End	West	60	18.3	0.45	0.46	0.02	0.07	--	--	0.27
89-248	Int.	Center	75	22.9	0.47	0.48	0.04	0.10	--	--	0.29
89-248	End	East	60	18.3	0.52	0.53	0.01	0.07	--	--	0.30
<b>Conventional Overlay Bridges</b>											
46-289	End	West	79	24.1	0.77	0.74	0.68	0.69	--	--	0.71
46-289	Int.	W. Center	137	41.8	0.79	0.76	0.70	0.70	--	--	0.73
46-289	Int.	E. Center	137	41.8	0.74	0.71	0.70	0.71	--	--	0.71
46-289	End	East	79	24.1	0.43	0.40	0.47	0.48	--	--	0.44
46-290	End	West	79	24.1	0.71	0.68	0.66	0.67	--	--	0.67
46-290	Int.	W. Center	137	41.8	0.69	0.66	0.63	0.64	--	--	0.65
46-290	Int.	E. Center	137	41.8	0.73	0.70	0.65	0.66	--	--	0.68
46-290	End	East	79	24.1	0.54	0.51	0.49	0.50	--	--	0.50
46-294	End	South	150	45.7	--	--	--	--	0.27	0.31	0.31
46-294	End	North	150	45.7	--	--	--	--	0.32	0.36	0.36
46-295	End	South	150	45.7	--	--	--	--	0.25	0.29	0.29
46-295	End	North	150	45.7	--	--	--	--	0.31	0.35	0.35
46-299	End	South	40	12.2	1.01	1.00	0.81	0.83	--	--	0.91

Table E.4 (con't) – Crack Densities and Data for Individual Spans

Bridge Number	Span Type	Span Location	Span Length		Current Study		Miller and Darwin (2000)		Schmitt and Darwin (1995)		All Studies Mean Age-Corrected Crack Density (m/m <sup>2</sup> )
			(ft)	(m)	Crack Density (m/m <sup>2</sup> )	Age-Corrected Crack Density (m/m <sup>2</sup> )	Crack Density (m/m <sup>2</sup> )	Age-Corrected Crack Density (m/m <sup>2</sup> )	Crack Density (m/m <sup>2</sup> )	Age-Corrected Crack Density (m/m <sup>2</sup> )	
46-299	Int.	S. Center	64	19.5	0.92	0.91	0.92	0.94	--	--	0.92
46-299	Int.	N. Center	64	19.5	0.64	0.63	0.79	0.82	--	--	0.72
46-299	End	North	40	12.2	0.73	0.72	1.03	1.05	--	--	0.88
46-300	End	South	40	12.2	0.62	0.62	0.75	0.78	--	--	0.70
46-300	Int.	S. Center	64	19.5	0.66	0.66	0.80	0.83	--	--	0.75
46-300	Int.	N. Center	64	19.5	0.66	0.66	0.69	0.73	--	--	0.70
46-300	End	North	40	12.2	0.68	0.68	0.57	0.61	--	--	0.64
46-301	End	West	55	16.8	1.06	1.05	0.96	0.98	--	--	1.01
46-301	Int.	W. Center	90	27.4	0.86	0.85	0.69	0.71	--	--	0.78
46-301	Int.	E. Center	90	27.4	0.70	0.69	0.55	0.57	--	--	0.63
46-301	End	East	55	16.8	0.76	0.75	0.90	0.93	--	--	0.84
75-1	End	West	128	39.0	0.44	0.39	0.34	0.33	--	--	0.36
75-1	Int.	Center	160	48.8	0.57	0.52	0.51	0.51	--	--	0.52
75-1	End	East	128	39.0	0.43	0.38	0.22	0.22	--	--	0.30
75-49	End	West	128	39.0	0.46	0.41	0.40	0.40	--	--	0.40
75-49	Int.	Center	160	48.8	0.44	0.39	0.47	0.47	--	--	0.43
75-49	End	East	128	39.0	0.30	0.25	0.45	0.44	--	--	0.34
81-49	End	South	77	23.5	0.88	0.84	0.73	0.73	--	--	0.79
81-49	Int.	Center	110	33.5	0.68	0.64	0.60	0.61	--	--	0.63
81-49	End	North	77	23.5	0.87	0.83	0.79	0.80	--	--	0.82

Table E.4 (con't) – Crack Densities and Data for Individual Spans

Bridge Number	Span Type	Span Location	Span Length		Current Study		Miller and Darwin (2000)		Schmitt and Darwin (1995)		All Studies Mean Age-Corrected Crack Density (m/m <sup>2</sup> )
			(ft)	(m)	Crack Density (m/m <sup>2</sup> )	Age-Corrected Crack Density (m/m <sup>2</sup> )	Crack Density (m/m <sup>2</sup> )	Age-Corrected Crack Density (m/m <sup>2</sup> )	Crack Density (m/m <sup>2</sup> )	Age-Corrected Crack Density (m/m <sup>2</sup> )	
89-179	End	West	55	16.8	--	--	--	--	0.32	0.34	0.34
89-179	Int.	Center	70	21.3	--	--	--	--	0.14	0.16	0.16
89-179	End	East	55	16.8	--	--	--	--	0.25	0.27	0.27
89-180	End	West	55	16.8	--	--	--	--	0.28	0.30	0.30
89-180	Int.	Center	70	21.3	--	--	--	--	0.33	0.35	0.35
89-180	End	East	55	16.8	--	--	--	--	0.50	0.52	0.52
89-183	End	South	67	20.4	0.66	0.61	0.51	0.50	--	--	0.56
89-183	Int.	S. Center	88	26.8	0.57	0.52	0.56	0.55	--	--	0.53
89-183	Int.	N. Center	88	26.8	0.55	0.50	0.48	0.46	--	--	0.48
89-183	End	North	67	20.4	0.58	0.53	0.45	0.44	--	--	0.48
89-185	End	West	49	14.9	0.62	0.57	0.63	0.62	0.90	0.93	0.71
89-185	Int.	W. Center	84	25.6	0.59	0.54	0.50	0.49	0.53	0.56	0.53
89-185	Int.	E. Center	71	21.6	0.88	0.83	0.77	0.76	0.93	0.96	0.85
89-185	End	East	51	15.5	1.24	1.19	0.94	0.93	0.47	0.50	0.87
89-186	End	West	45	13.7	0.86	0.82	0.84	0.83	0.56	0.59	0.74
89-186	Int.	W. Center	60	18.3	0.74	0.70	0.67	0.66	0.59	0.62	0.66
89-186	Int.	E. Center	60	18.3	0.62	0.58	0.64	0.63	0.39	0.42	0.54
89-186	End	East	45	13.7	0.70	0.66	0.76	0.75	0.54	0.57	0.66
89-196	End	South	46	14.0	0.66	0.63	0.54	0.54	--	--	0.58
89-196	Int.	Center	68	20.7	0.47	0.44	0.41	0.41	--	--	0.42

**Table E.4 (con't) – Crack Densities and Data for Individual Spans**

Bridge Number	Span Type	Span Location	Span Length (ft) (m)	Current Study		Miller and Darwin (2000)		Schmitt and Darwin (1995)		All Studies Mean Age-Corrected Crack Density (m/m <sup>2</sup> )
				Crack Density (m/m <sup>2</sup> )	Age-Corrected Crack Density (m/m <sup>2</sup> )	Crack Density (m/m <sup>2</sup> )	Age-Corrected Crack Density (m/m <sup>2</sup> )	Crack Density (m/m <sup>2</sup> )	Age-Corrected Crack Density (m/m <sup>2</sup> )	
89-196	End	North	46 14.0	0.71	0.68	0.71	0.71	--	--	0.69
89-198	End	South	66 20.1	0.46	0.46	0.42	0.38	0.40	0.43	0.42
89-198	Int.	S. Center	97 29.6	0.51	0.48	0.41	0.42	0.68	0.71	0.54
89-198	Int.	N. Center	97 29.6	0.59	0.55	0.38	0.38	0.52	0.55	0.49
89-198	End	North	80 24.4	0.33	0.33	0.30	0.26	0.51	0.54	0.38
89-199	End	South	66 20.1	0.60	0.56	0.54	0.54	0.63	0.66	0.59
89-199	Int.	S. Center	97 29.6	0.69	0.65	0.66	0.65	0.83	0.86	0.72
89-199	Int.	N. Center	97 29.6	0.81	0.77	0.73	0.73	0.67	0.70	0.73
89-199	End	North	80 24.4	0.64	0.60	0.65	0.64	0.52	0.55	0.60
89-200	End	South	84 25.6	0.85	0.81	0.70	0.69	0.60	0.63	0.71
89-200	Int.	Center	150 45.7	0.49	0.45	0.40	0.40	0.45	0.48	0.44
89-200	End	North	84 25.6	0.73	0.69	0.68	0.68	0.55	0.58	0.65
89-201	End	South	84 25.6	0.78	0.74	0.77	0.76	0.99	1.02	0.84
89-201	Int.	Center	150 45.7	0.54	0.50	0.41	0.41	0.44	0.47	0.46
89-201	End	North	84 25.6	0.95	0.91	0.83	0.83	0.76	0.79	0.84
105-021	End	South	74 22.6	--	--	--	--	0.14	0.20	0.20
105-021	End	North	67 20.4	--	--	--	--	0.06	0.12	0.12
105-225	End	South	51 15.5	--	--	--	--	0.25	0.24	0.24
105-225	Int.	Center	76 23.2	--	--	--	--	0.10	0.09	0.09
105-225	End	North	60 18.3	--	--	--	--	0.23	0.22	0.22

Table E.4 (con't) – Crack Densities and Data for Individual Spans

Bridge Number	Span Type	Span Location	Span Length		Current Study		Miller and Darwin (2000)		Schmitt and Darwin (1995)		All Studies Mean Age-Corrected Crack Density (m/m <sup>2</sup> )
			(ft)	(m)	Crack Density (m/m <sup>2</sup> )	Age-Corrected Crack Density (m/m <sup>2</sup> )	Crack Density (m/m <sup>2</sup> )	Age-Corrected Crack Density (m/m <sup>2</sup> )	Crack Density (m/m <sup>2</sup> )	Age-Corrected Crack Density (m/m <sup>2</sup> )	
105-226	End	South	60	18.3	--	--	--	--	0.26	0.25	0.25
105-226	Int.	Center	76	23.2	--	--	--	--	0.05	0.04	0.04
105-226	End	North	45	13.7	--	--	--	--	0.27	0.26	0.26
105-230	End	South	47	14.3	--	--	--	--	0.22	0.20	0.20
105-230	Int.	S. Center	66	20.1	--	--	--	--	0.04	0.02	0.02
105-230	Int.	N. Center	66	20.1	--	--	--	--	0.00	0.00	0.00
105-230	End	North	47	14.3	--	--	--	--	0.16	0.14	0.14
105-231	End	South	47	14.3	--	--	--	--	0.25	0.23	0.23
105-231	Int.	S. Center	66	20.1	--	--	--	--	0.04	0.02	0.02
105-231	Int.	N. Center	66	20.1	--	--	--	--	0.05	0.03	0.03
105-231	End	North	47	14.3	--	--	--	--	0.17	0.15	0.15
105-262	End	South	67	20.4	--	--	--	--	0.14	0.12	0.12
105-262	Int.	Center	135	41.1	--	--	--	--	0.18	0.16	0.16
105-262	End	North	67	20.4	--	--	--	--	0.20	0.18	0.18
105-263	End	South	67	20.4	--	--	--	--	0.17	0.13	0.13
105-263	Int.	Center	135	41.1	--	--	--	--	0.17	0.13	0.13
105-263	End	North	67	20.4	--	--	--	--	0.00	0.00	0.00
105-265	End	South	43	13.1	--	--	--	--	0.04	0.01	0.01
105-265	Int.	Center	57	17.4	--	--	--	--	0.00	0.00	0.00
105-265	End	North	43	13.1	--	--	--	--	0.01	0.00	0.00

Table E.4 (con't) – Crack Densities and Data for Individual Spans

Bridge Number	Span Type	Span Location	Span Length (ft)	Span Length (m)	Current Study		Miller and Darwin (2000)		Schmitt and Darwin (1995)		All Studies Mean Age-Corrected Crack Density (m/m <sup>2</sup> )
					Crack Density (m/m <sup>2</sup> )	Age-Corrected Crack Density (m/m <sup>2</sup> )	Crack Density (m/m <sup>2</sup> )	Age-Corrected Crack Density (m/m <sup>2</sup> )	Crack Density (m/m <sup>2</sup> )	Age-Corrected Crack Density (m/m <sup>2</sup> )	
105-268	End	West	57	17.4	--	--	--	--	0.60	0.59	0.59
105-268	Int.	Center	57	17.4	--	--	--	--	0.72	0.71	0.71
105-268	End	East	75	22.9	--	--	--	--	0.54	0.53	0.53
105-269	End	West	122	37.2	--	--	--	--	0.45	0.44	0.44
105-269	End	East	122	37.2	--	--	--	--	0.45	0.44	0.44
<b>Monolithic Bridges</b>											
3-045	End	West	64	19.5	0.43	0.32	--	--	--	--	0.32
3-045	Int.	W. Center	80	24.4	0.20	0.09	--	--	--	--	0.09
3-045	Int.	E. Center	80	24.4	0.31	0.20	--	--	--	--	0.20
3-045	End	East	64	19.5	0.39	0.28	--	--	--	--	0.28
3-046	End	West	100	30.5	0.40	0.30	--	--	--	--	0.30
3-046	Int.	Center	120	36.6	0.34	0.24	--	--	--	--	0.24
3-046	End	East	100	30.5	0.53	0.43	--	--	--	--	0.43
56-142	End	South	88	26.8	0.08	0.00	--	--	--	--	0.00
56-142	Int.	S. Center	112	34.1	0.21	0.13	--	--	--	--	0.13
56-142	Int.	N. Center	112	34.1	0.27	0.19	--	--	--	--	0.19
56-142	End	North	88	26.8	0.06	0.00	--	--	--	--	0.00
56-148	End	West	72	21.9	0.64	0.60	0.37	0.36	--	--	0.48

Table E.4 (con't) – Crack Densities and Data for Individual Spans

Bridge Number	Span Type	Span Location	Span Length (ft)	Span Length (m)	Current Study		Miller and Darwin (2000)		Schmitt and Darwin (1995)		All Studies Mean Age-Corrected Crack Density (m/m <sup>2</sup> )
					Crack Density (m/m <sup>2</sup> )	Age-Corrected Crack Density (m/m <sup>2</sup> )	Crack Density (m/m <sup>2</sup> )	Age-Corrected Crack Density (m/m <sup>2</sup> )	Crack Density (m/m <sup>2</sup> )	Age-Corrected Crack Density (m/m <sup>2</sup> )	
56-148	Int.	Center	100	30.5	0.49	0.45	0.32	0.32	--	--	0.38
56-148	End	East	72	21.9	0.50	0.46	0.25	0.24	--	--	0.35
70-095	End	South	74	22.6	0.10	0.00	--	--	--	--	0.00
70-095	Int.	Center	90	27.4	0.15	0.05	--	--	--	--	0.05
70-095	End	North	74	22.6	0.13	0.03	--	--	--	--	0.03
70-101	End	West	80	24.4	--	--	--	--	0.02	0.00	0.00
70-101	Int.	Center	100	30.5	--	--	--	--	0.06	0.04	0.04
70-101	End	East	80	24.4	--	--	--	--	0.08	0.06	0.06
70-103	End	South	80	24.4	0.88	0.77	--	--	0.54	0.52	0.65
70-103	Int.	Center	100	30.5	0.77	0.66	--	--	0.54	0.52	0.59
70-103	End	North	80	24.4	0.58	0.47	--	--	0.36	0.34	0.41
70-104	End	South	56	17.1	0.16	0.06	--	--	0.17	0.15	0.10
70-104	Int.	S. Center	70	21.3	0.08	0.00	--	--	0.08	0.06	0.03
70-104	Int.	N. Center	70	21.3	0.05	0.00	--	--	0.06	0.04	0.02
70-104	End	North	56	17.1	0.11	0.01	--	--	0.04	0.02	0.01
70-107	End	South	60	18.3	0.92	0.88	0.46	0.46	0.45	0.48	0.61
70-107	Int.	Center	80	24.4	0.60	0.56	0.39	0.39	0.36	0.39	0.45
70-107	End	North	60	18.3	0.70	0.66	0.40	0.39	0.19	0.22	0.43
75-044	End	South	37	11.3	0.25	0.19	--	--	0.12	0.14	0.17

Table E.4 (con't) – Crack Densities and Data for Individual Spans

Bridge Number	Span Type	Span Location	Span Length (ft) (m)	Current Study		Miller and Darwin (2000)		Schmitt and Darwin (1995)		All Studies Mean Age-Corrected Crack Density (m/m <sup>2</sup> )
				Crack Density (m/m <sup>2</sup> )	Age-Corrected Crack Density (m/m <sup>2</sup> )	Crack Density (m/m <sup>2</sup> )	Age-Corrected Crack Density (m/m <sup>2</sup> )	Crack Density (m/m <sup>2</sup> )	Age-Corrected Crack Density (m/m <sup>2</sup> )	
75-044	Int.	Center	46 14.0	0.22	0.16	--	--	0.16	0.18	0.17
75-044	End	North	37 11.3	0.39	0.33	--	--	0.27	0.29	0.31
75-045	End	South	62 18.9	0.36	0.30	--	--	0.26	0.28	0.29
75-045	Int.	S. Center	77 23.5	0.42	0.36	--	--	0.77	0.79	0.58
75-045	Int.	N. Center	77 23.5	0.51	0.45	--	--	0.58	0.60	0.53
75-045	End	North	62 18.9	0.51	0.45	--	--	0.34	0.36	0.41
89-204	End	West	70 21.3	1.06	1.02	0.86	0.89	--	--	0.96
89-204	End	Center	88 26.8	1.16	1.12	0.99	0.98	--	--	1.05
89-204	End	East	70 21.3	0.90	0.86	0.63	0.66	--	--	0.76
89-208	End	West	68 20.7	0.10	0.10	0.01	0.05	--	--	0.08
89-208	Int.	W. Center	106 32.3	0.11	0.11	0.03	0.07	--	--	0.09
89-208	Int.	E. Center	106 32.3	0.12	0.12	0.04	0.07	--	--	0.10
89-208	End	East	83 25.3	0.08	0.08	0.02	0.05	--	--	0.07
99-76	End	South	75 22.9	--	--	--	--	--	--	--
99-76	Int.	--	100 30.5	--	--	--	--	--	--	--
99-76	Int.	--	128 39.0	--	--	--	--	--	--	--
99-76	Int.	--	128 39.0	--	--	--	--	--	--	--
99-76	Int.	--	128 39.0	--	--	--	--	--	--	--
99-76	Int.	--	128 39.0	--	--	--	--	--	--	--

**Table E.4 (con't) – Crack Densities and Data for Individual Spans**

Bridge Number	Span Type	Span Location	Span Length (ft) (m)	Current Study		Miller and Darwin (2000)		Schmitt and Darwin (1995)		All Studies Mean Age-Corrected Crack Density (m/m <sup>2</sup> )
				Crack Density (m/m <sup>2</sup> )	Age-Corrected Crack Density (m/m <sup>2</sup> )	Crack Density (m/m <sup>2</sup> )	Age-Corrected Crack Density (m/m <sup>2</sup> )	Crack Density (m/m <sup>2</sup> )	Age-Corrected Crack Density (m/m <sup>2</sup> )	
99-76	Int.	--	128 39.0	--	--	--	--	--	--	--
99-76	Int.	--	100 30.5	--	--	--	--	--	--	--
99-76	Int.	--	75 22.9	--	--	--	--	--	--	--
105-000 <sup>†</sup>	Int.	--	74 22.6	--	--	--	--	0.17	0.22	0.22
105-000 <sup>†</sup>	Int.	--	74 22.6	--	--	--	--	0.42	0.47	0.47
105-000 <sup>†</sup>	Int.	--	48 14.5	--	--	--	--	0.12	0.17	0.17
105-000 <sup>†</sup>	End	North	87 26.4	--	--	--	--	0.33	0.38	0.38

<sup>†</sup>Bridge has no assigned serial number. Project No. is 105-U-1262-01.

-- Denotes bridges that were not surveyed or missing data.

Table E.5 – Bridge Traffic Data

Bridge Number	Average Traffic Volume <sup>†</sup> (AADT)	Current Study		Miller and Darwin (2000)		Schmitt and Darwin (1995)	
		Bridge Age at the Time of Survey (months)	Load Cycles ( $\times 10^6$ cycles)	Bridge Age at the Time of Survey (months)	Load Cycles ( $\times 10^6$ cycles)	Bridge Age at the Time of Survey (months)	Load Cycles ( $\times 10^6$ cycles)
<b>7% Silica Fume Overlay Bridges</b>							
30-93	16000	22	10.6	--	--	--	--
40-92	21200	21	13.6	--	--	--	--
40-93	21200	21	13.8	--	--	--	--
46-332	16400	13	6.7	--	--	--	--
81-53	6400	39	7.6	--	--	--	--
85-148	13000	21	8.1	--	--	--	--
85-149	13000	10	3.8	--	--	--	--
89-269	10700	23	7.5	--	--	--	--
89-272	10700	15	4.9	--	--	--	--
103-56	3600	21	2.3	--	--	--	--
<b>5% Silica Fume Overlay Bridges</b>							
23-85	10445	76	24.1	29	9.1	--	--
46-302	4311	75	9.8	28	3.7	--	--
46-309	150	81	0.4	33	0.2	--	--
46-317	8600	72	18.9	25	6.7	--	--
81-50	11448	90	31.4	32	11.3	--	--
87-453	3770	61	7.0	15	1.8	--	--
87-454	3770	70	8.0	24	2.7	--	--

Table E.5 (con't) – Bridge Traffic Data

Bridge Number	Average Traffic Volume <sup>†</sup> (AADT)	Current Study		Miller and Darwin (2000)		Schmitt and Darwin (1995)	
		Bridge Age at the Time of Survey (months)	Load Cycles ( $\times 10^6$ cycles)	Bridge Age at the Time of Survey (months)	Load Cycles ( $\times 10^6$ cycles)	Bridge Age at the Time of Survey (months)	Load Cycles ( $\times 10^6$ cycles)
89-184	12877	142	55.8	94	36.81	39.00	15.29
89-187	14273	132	57.6	4	42.1	41	17.8
89-206	4085	91	11.3	97	4.1	--	--
89-207	4085	91	11.4	33	4.1	--	--
89-210	5235	70	11.1	33	5.1	--	--
89-234	7545	87	20.1	32	5.6	--	--
89-235	7545	77	17.7	24	3.2	--	--
89-240	7758	68	16.1	14	2.5	--	--
89-244	8870	67	18.1	11	2.3	--	--
89-245	9465	68	19.5	8	2.5	--	--
89-246	6898	61	12.9	9	2.1	--	--
89-247	6898	72	15.1	10	3.0	--	--
89-248	5930	62	11.2	14	0.7	--	--
<b>Conventional Overlay Bridges</b>							
46-289	9473	118	34.1	72	20.7	--	--
46-290	9473	118	34.0	71	20.6	--	--
46-294	12955	--	--	--	--	20	7.9
46-295	12955	--	--	--	--	24	9.5
46-299	6613	95	19.1	49	9.8	--	--

Table E.5 (con't) – Bridge Traffic Data

Bridge Number	Average Traffic Volume <sup>†</sup> (AADT)	Current Study		Miller and Darwin (2000)		Schmitt and Darwin (1995)	
		Bridge Age at the Time of Survey (months)	Load Cycles ( $\times 10^6$ cycles)	Bridge Age at the Time of Survey (months)	Load Cycles ( $\times 10^6$ cycles)	Bridge Age at the Time of Survey (months)	Load Cycles ( $\times 10^6$ cycles)
46-300	6613	72	14.4	36	7.2	--	--
46-301	245	94	0.7	49	0.4	--	--
75-1	7063	139	29.9	82	17.7	--	--
75-49	7063	143	30.8	87	18.7	--	--
81-49	17690	127	68.4	70	37.5	--	--
89-179	6865	--	--	--	--	45	9.4
89-180	6865	--	--	--	--	51	10.7
89-183	6410	142	27.7	94	18.3	--	--
89-185	16293	145	72.1	97	48.2	41	20.3
89-186	16293	130	64.6	94	46.8	42	20.8
89-196	11028	124	41.5	75	25.2	--	--
89-198	13462	133	54.6	83	34.1	33	13.5
89-199	13462	133	54.5	83	34.1	35	14.3
89-200	13300	133	53.8	83	33.8	33	13.4
89-201	13300	133	53.8	84	33.8	34	13.8
105-021	9189	--	--	--	--	74	20.7
105-225	6140	--	--	--	--	94	17.6
105-226	6140	--	--	--	--	94	17.6
105-230	6710	--	--	--	--	98	20.0
105-231	6710	--	--	--	--	98	20.0

Table E.5 (con't) – Bridge Traffic Data

Bridge Number	Average Traffic Volume <sup>†</sup> (AADT)	Current Study		Miller and Darwin (2000)		Schmitt and Darwin (1995)	
		Bridge Age at the Time of Survey (months)	Load Cycles ( $\times 10^6$ cycles)	Bridge Age at the Time of Survey (months)	Load Cycles ( $\times 10^6$ cycles)	Bridge Age at the Time of Survey (months)	Load Cycles ( $\times 10^6$ cycles)
105-262	4665	--	--	--	--	108	15.3
105-263	4665	--	--	--	--	128	18.2
105-265	780	--	--	--	--	116	2.8
105-268	1135	--	--	--	--	88	3.0
105-269	1135	--	--	--	--	96	3.3
<b>Monolithic Bridges</b>							
3-45	705	220	4.7	--	--	112	2.4
3-46	705	210	4.5	--	--	102	2.2
56-142	5333	188	30.6	--	--	80	13.0
56-148	718	133	2.9	85	1.9	36	0.8
70-101	520	--	--	--	--	108	1.7
70-103	3643	219	24.3	--	--	102	11.3
70-104	950	212	6.1	--	--	106	3.1
70-107	2117	130	8.4	82	5.3	34	2.2
70-95	910	212	5.9	--	--	106	2.9
75-44	2675	155	12.7	--	--	48	3.9
75-45	2675	154	12.6	--	--	47	3.8
89-204	11003	132	44.3	82	27.5	34	11.4
89-208	0	73	0.0	36	0.0	--	--

**Table E.5 (con't) – Bridge Traffic Data**

Bridge Number	Average Traffic Volume <sup>†</sup> (AADT)	Current Study		Miller and Darwin (2000)		Schmitt and Darwin (1995)	
		Bridge Age at the Time of Survey (months)	Load Cycles ( $\times 10^6$ cycles)	Bridge Age at the Time of Survey (months)	Load Cycles ( $\times 10^6$ cycles)	Bridge Age at the Time of Survey (months)	Load Cycles ( $\times 10^6$ cycles)
99-76	2988	157	14.3	--	--	42	3.8
105-000 <sup>‡</sup>	4582	--	--	--	--	12	1.7
105-46	4582	--	--	--	--	240	33.5

<sup>†</sup>Calculated using data from the Kansas Department of Transportation Bridge Log at the time of each survey.

<sup>‡</sup>Bridge has no assigned serial number. Project No. is 105-U-1262-01.

-- Denotes bridges that were not surveyed during a particular study or missing data.

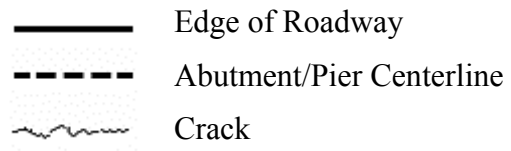


Fig. E.1 – Legend for Bridge Deck Cracking Patterns.

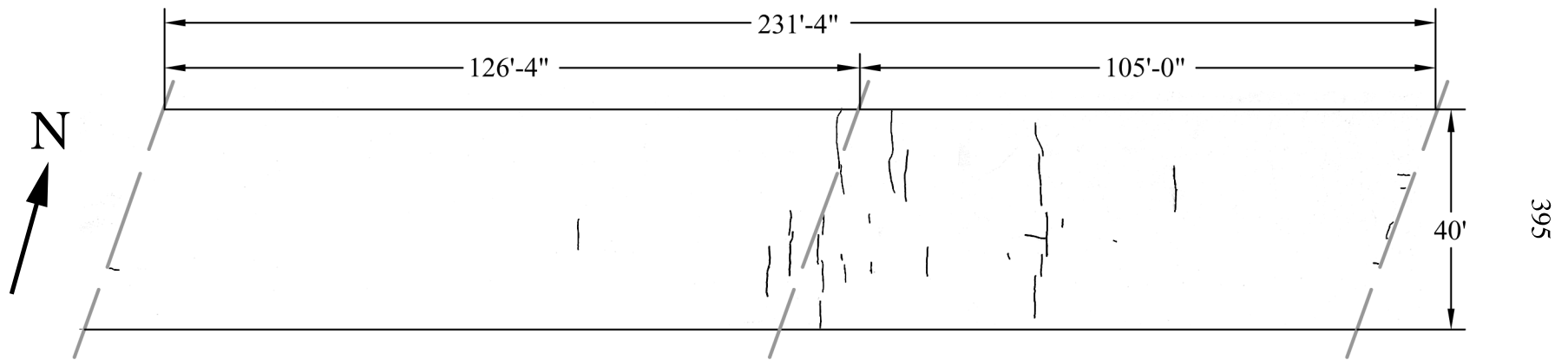


Fig. E.2 – Bridge Number 30-93 (7% Silica Fume Overlay). Scale 1" = 30'-0"

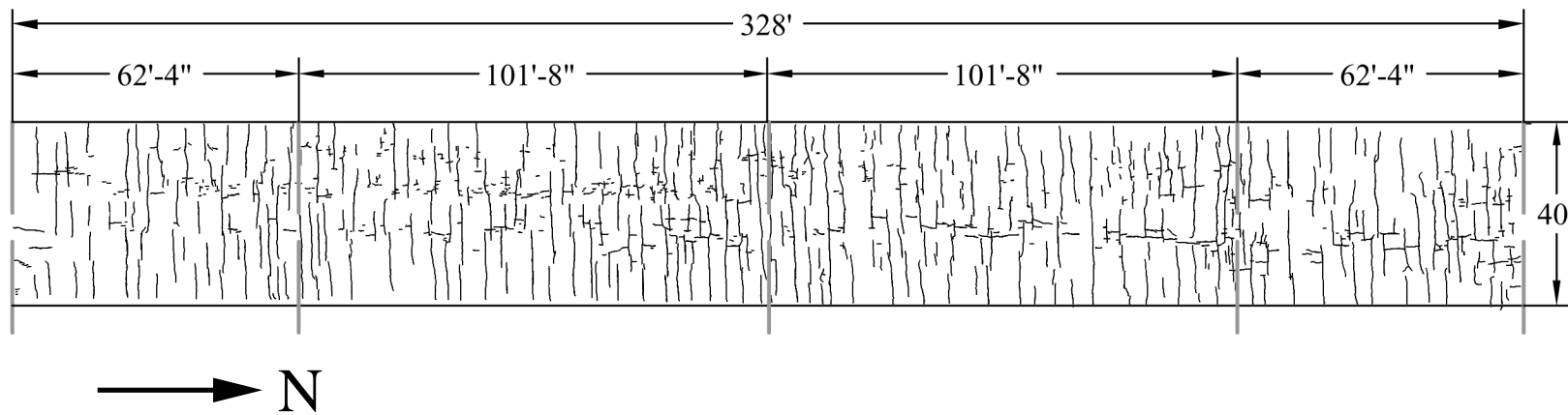


Fig. E.3 – Bridge Number 40-92 (7% Silica Fume Overlay). Scale 1" = 40'-0"

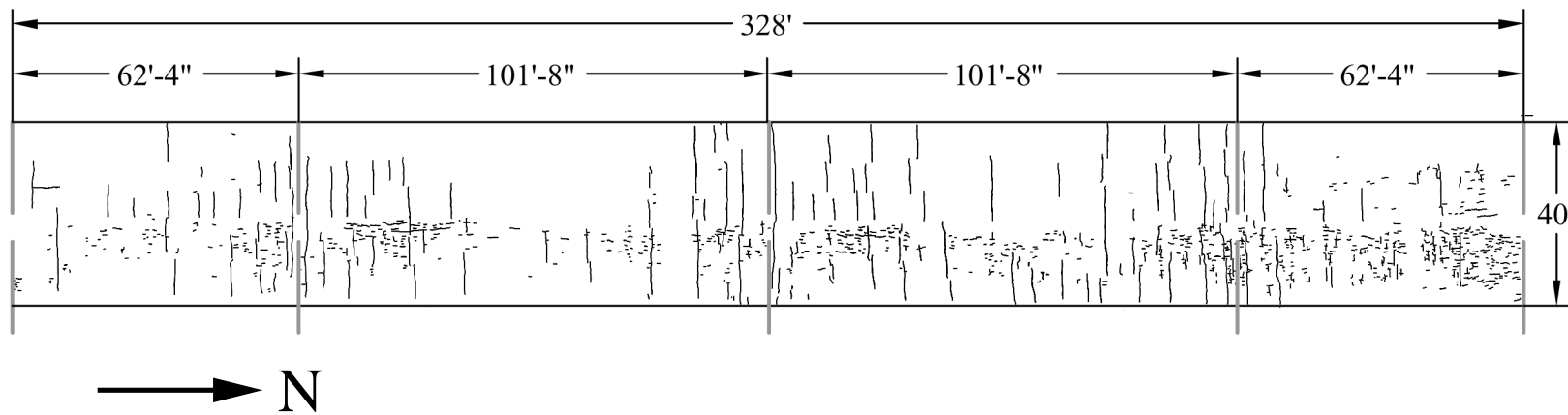


Fig. E.4 – Bridge Number 40-93 (7% Silica Fume Overlay). Scale 1" = 40'-0"

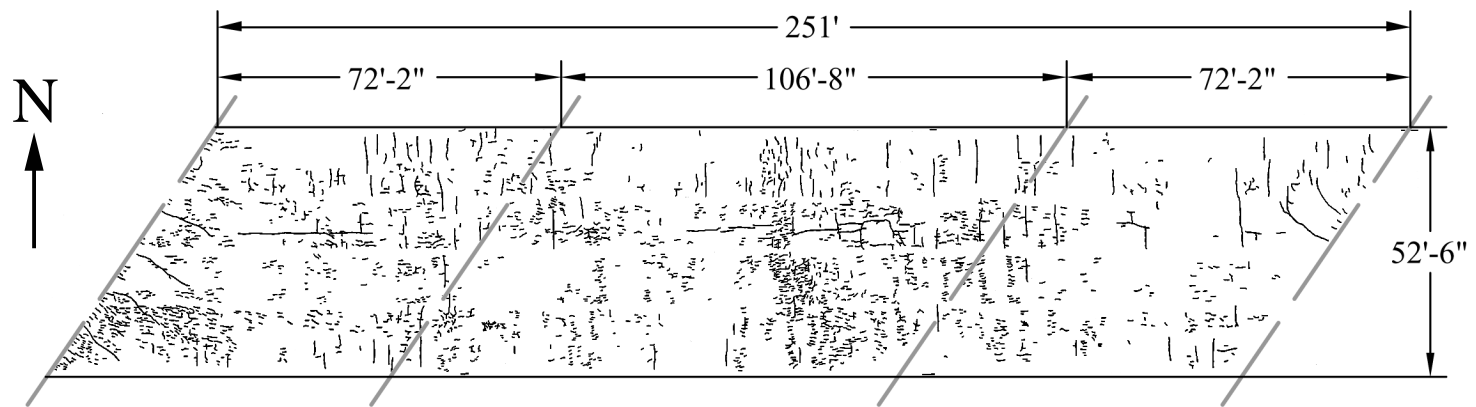


Fig. E.5 – Bridge Number 46-332 (7% Silica Fume Overlay). Scale 1" = 40'-0"

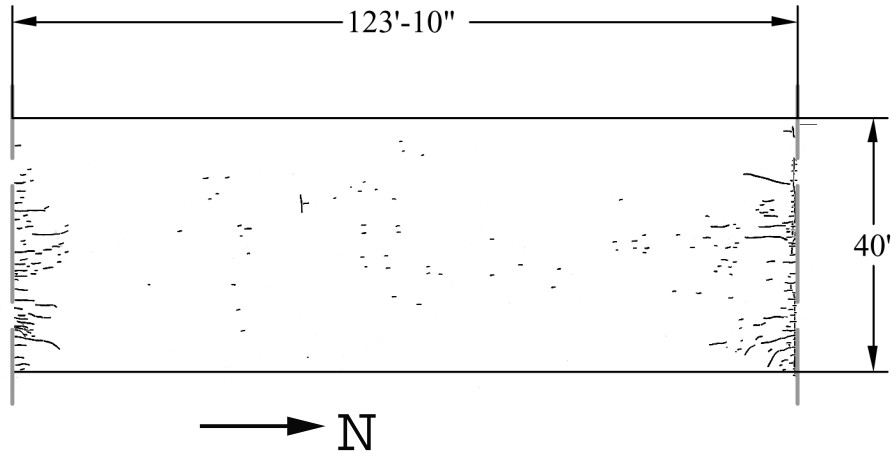
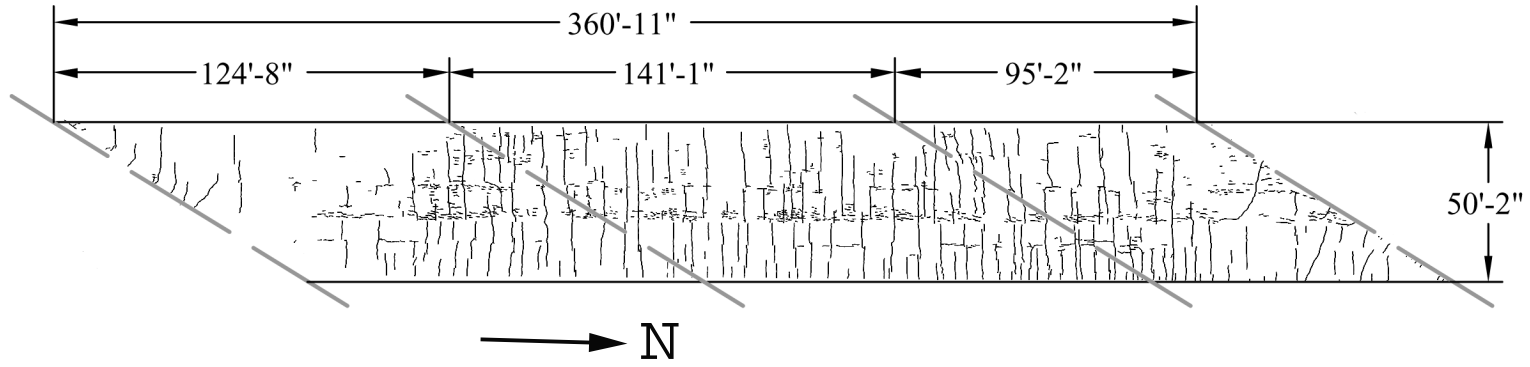


Fig. E.6 – Bridge Number 81-53 (7% Silica Fume Overlay). Scale 1" = 40'-0"



400

Fig. E.7 – Bridge Number 85-148 (7% Silica Fume Overlay). Scale 1" = 60'-0"

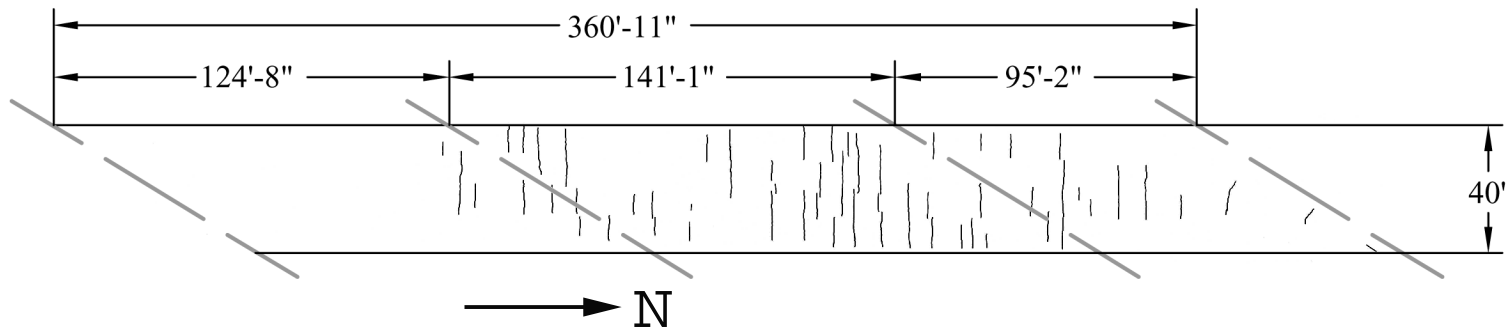


Fig. E.8 – Bridge Number 85-149 (7% Silica Fume Overlay). Scale 1" = 40'-0"

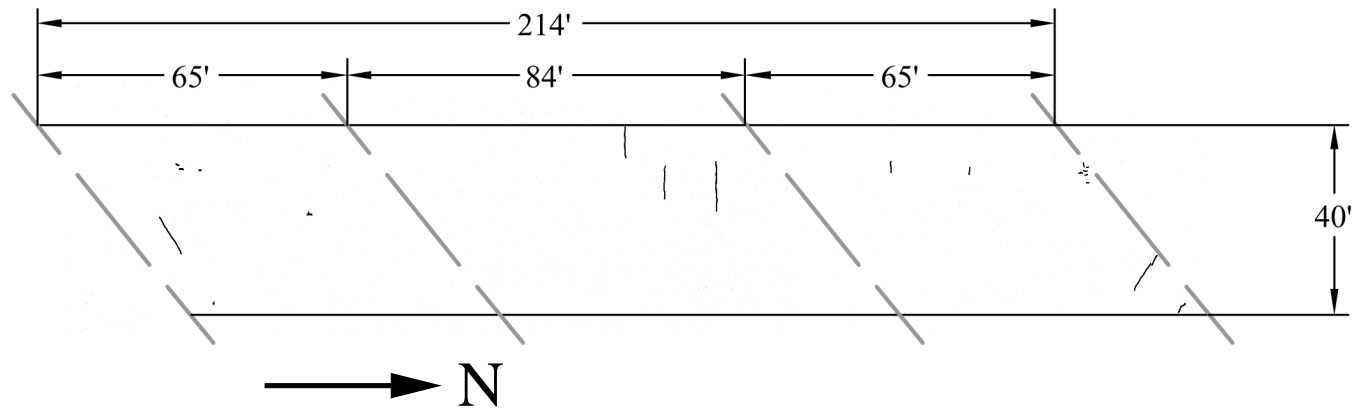


Fig. E.9 – Bridge Number 89-269 (7% Silica Fume Overlay). Scale 1" = 40'-0"

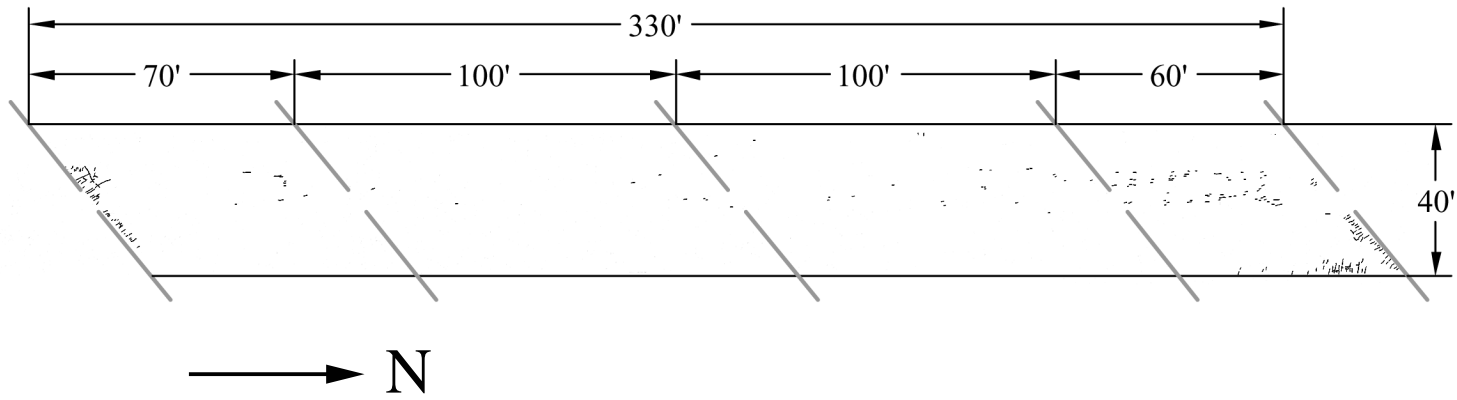


Fig. E.10 – Bridge Number 89-272 (5% Silica Fume Overlay). Scale 1" = 40'-0"

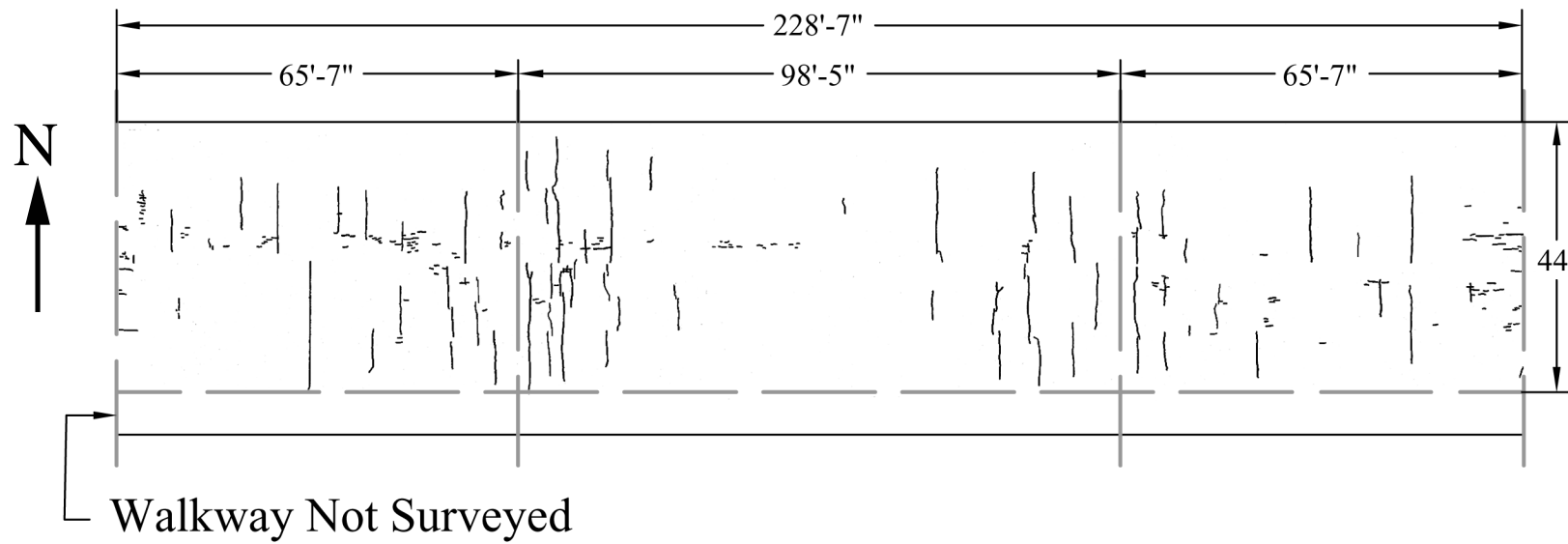


Fig. E.11 – Bridge Number 103-56 (7% Silica Fume Overlay). Scale 1" = 30'-0"

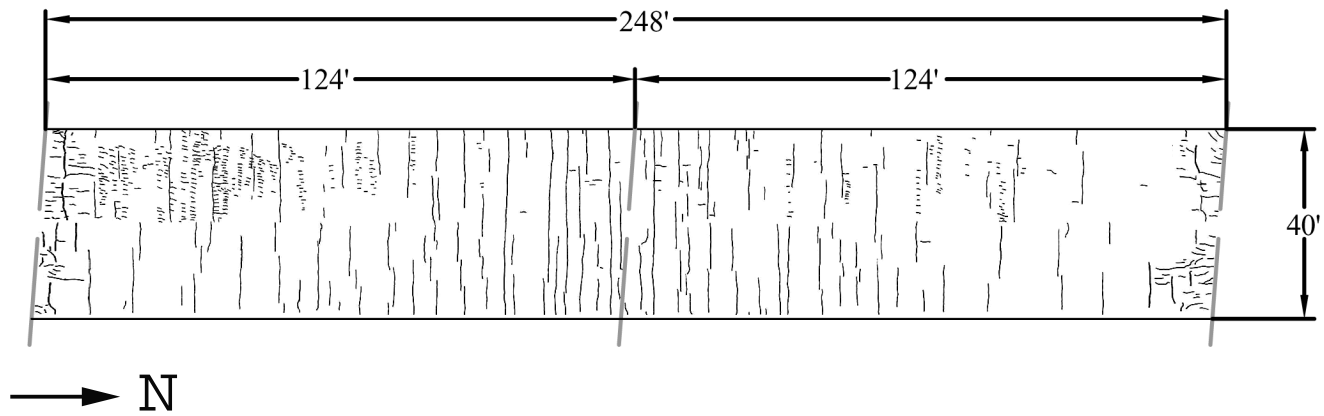
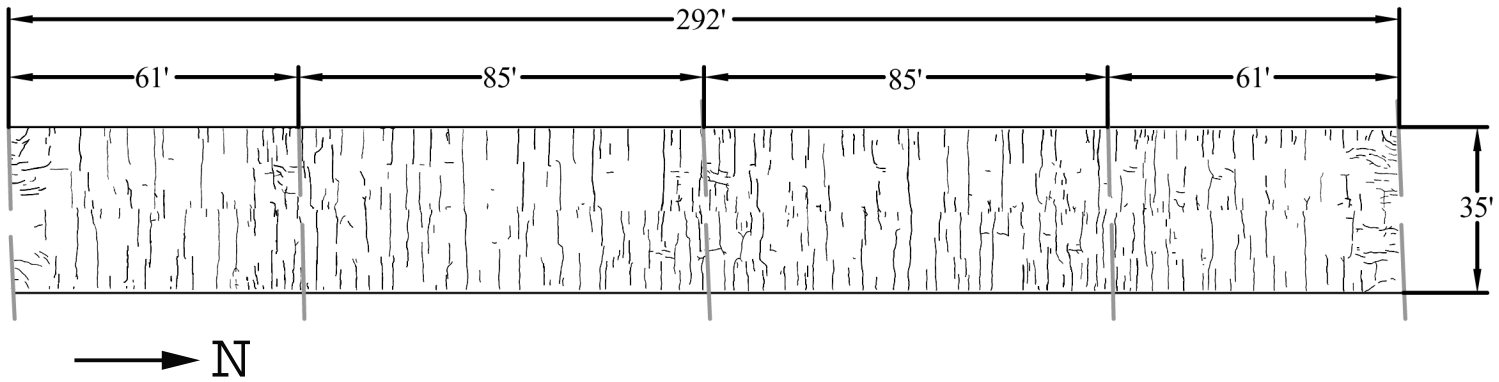


Fig. E.12 – Bridge Number 23-85 (5% Silica Fume Overlay). Scale 1" = 40'-0"



406

Fig. E.13 – Bridge Number 46-302 (5% Silica Fume Overlay). Scale 1" = 40'-0"

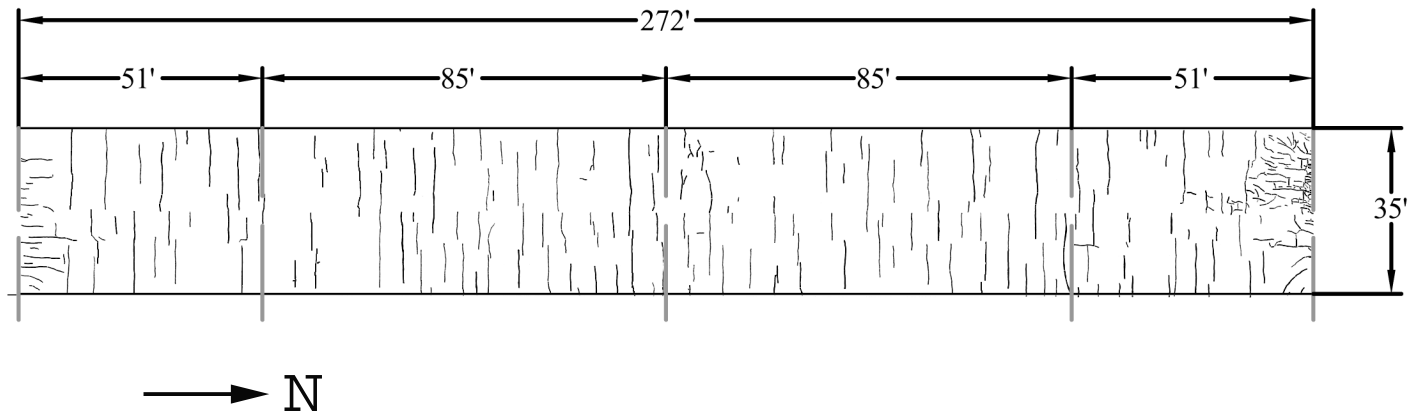
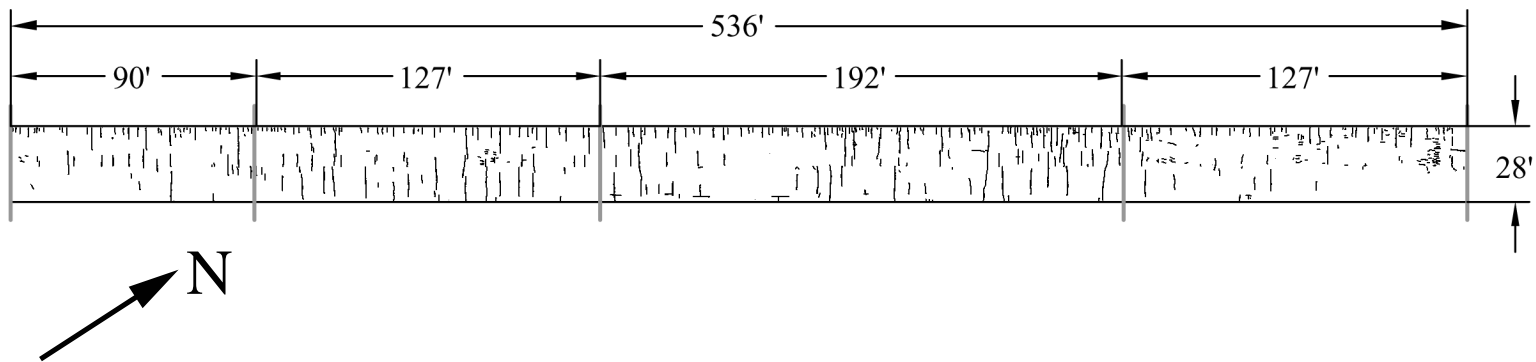


Fig. E.14 – Bridge Number 46-309 (5% Silica Fume Overlay). Scale 1" = 40'-0"



408

Fig. E.15 – Bridge Number 46-317, Unit 1 (5% Silica Fume Overlay). Scale 1" = 70'-0"

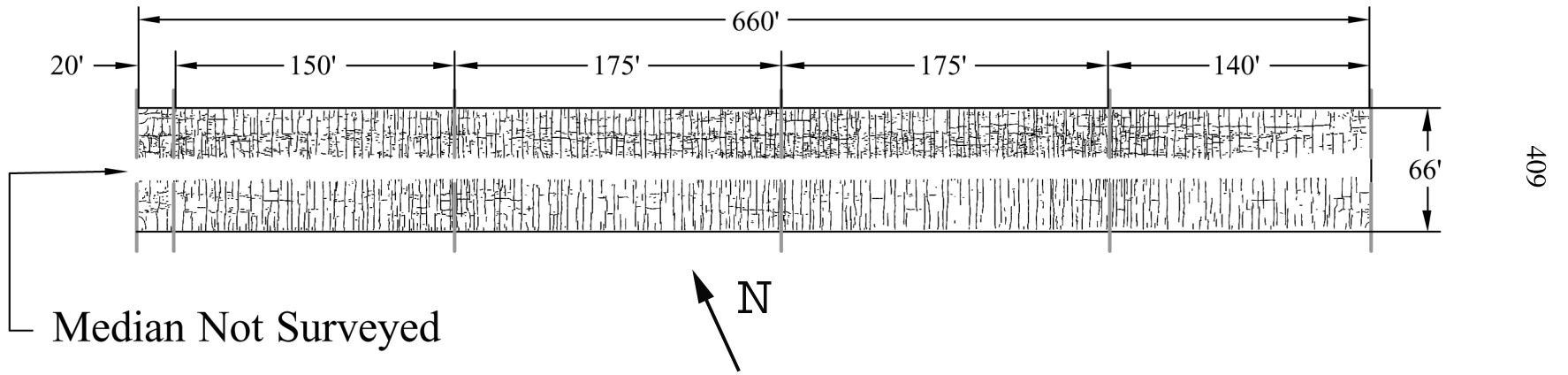
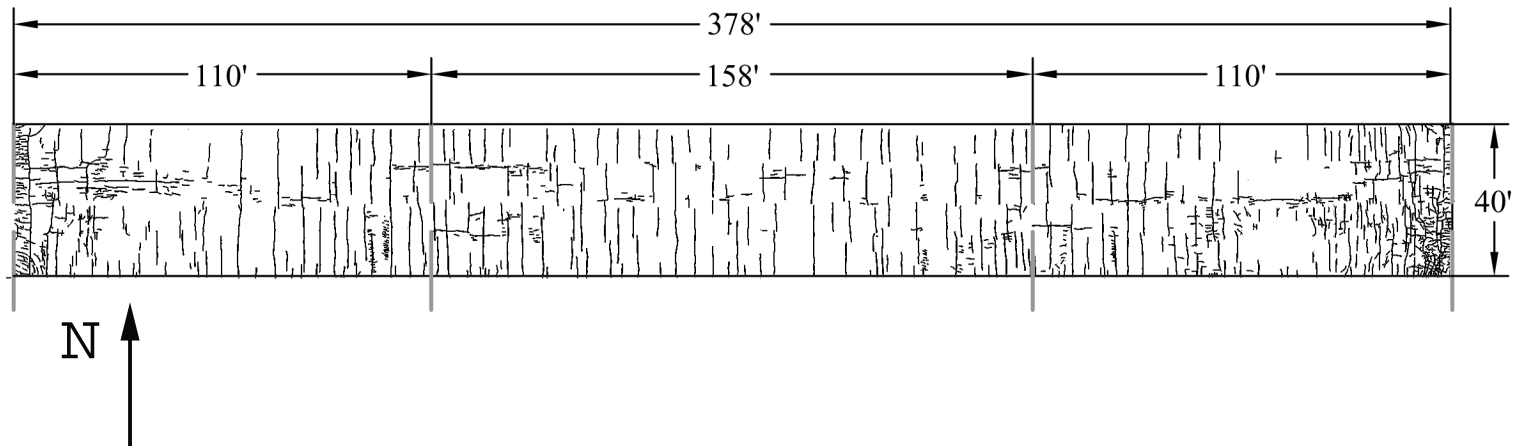


Fig. E.16 – Bridge Number 81-50, Unit 2 (5% Silica Fume Overlay). Scale 1" = 90'-0"



410

Fig. E.17 – Bridge Number 87-453 (5% Silica Fume Overlay). Scale 1" = 50'-0"

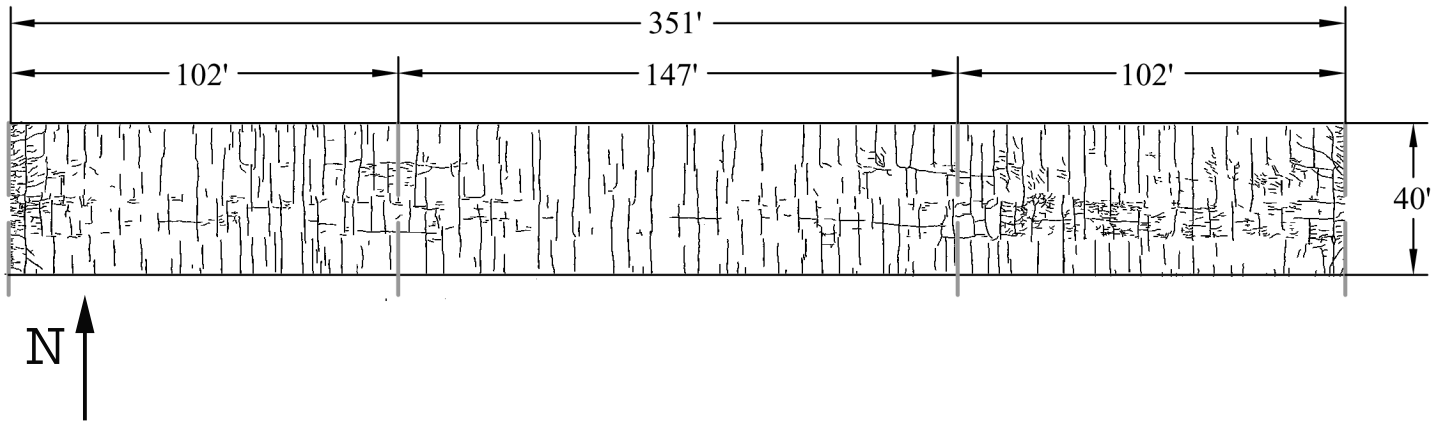


Fig. E.18 – Bridge Number 87-454 (5% Silica Fume Overlay). Scale 1" = 50'-0"

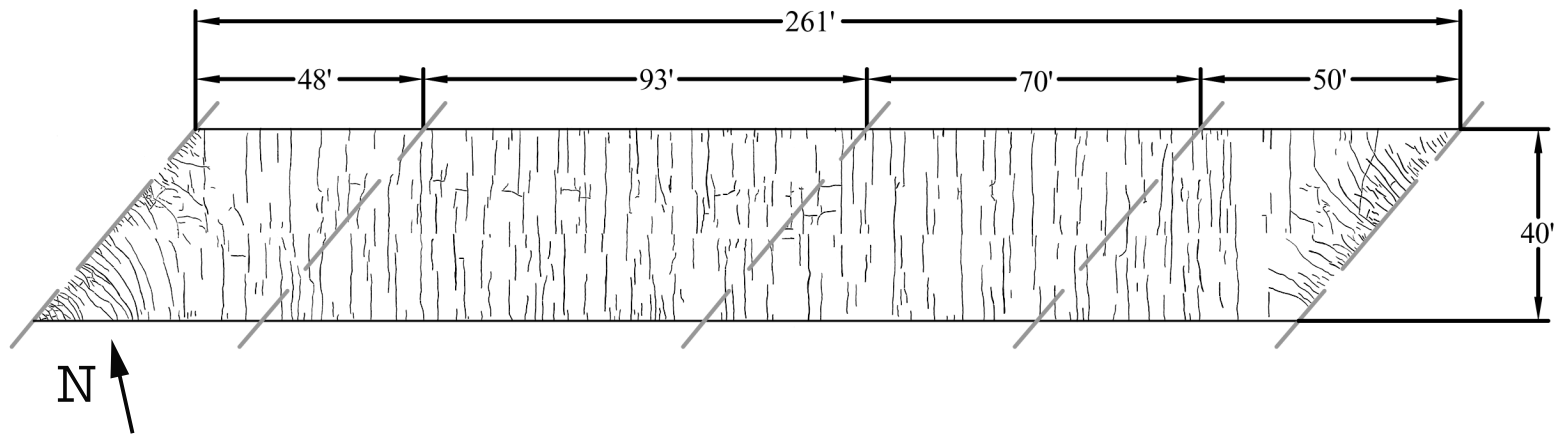


Fig. E.19 – Bridge Number 89-184 (7% Silica Fume Overlay). Scale 1" = 40'-0"

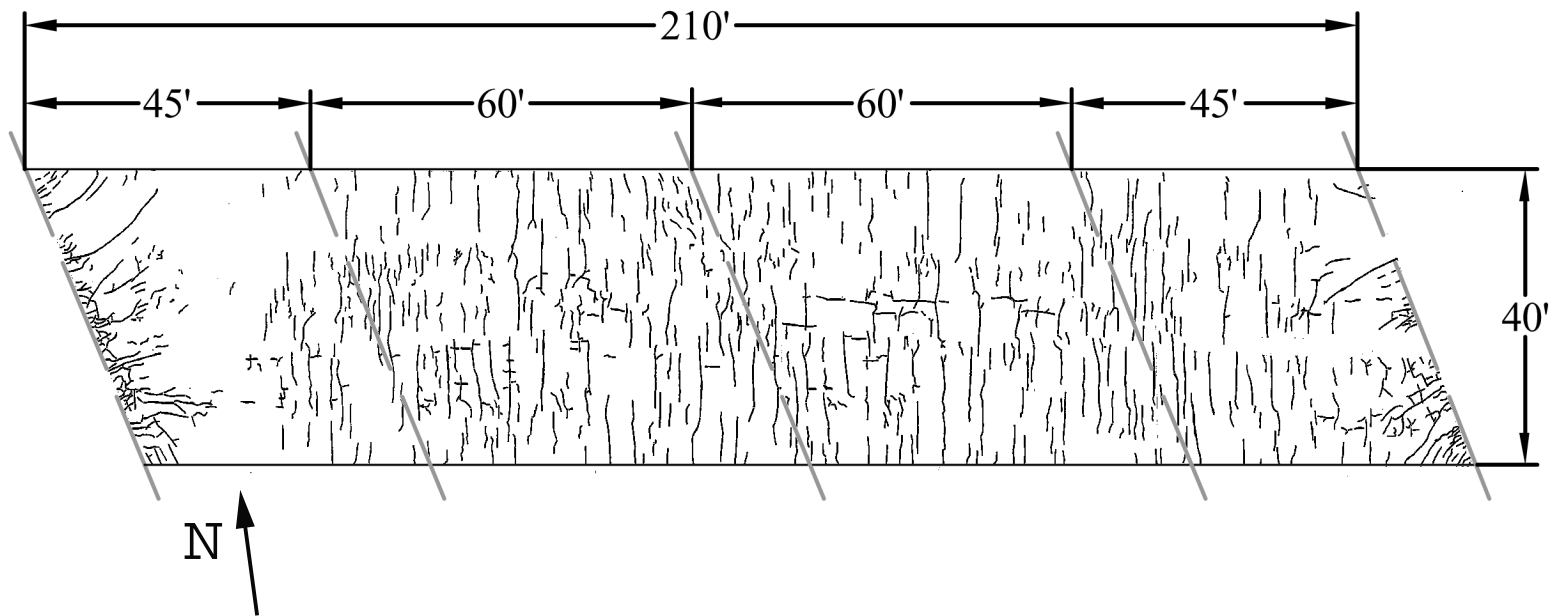


Fig. E.20 – Bridge Number 89-187 (5% Silica Fume Overlay). Scale 1" = 40'

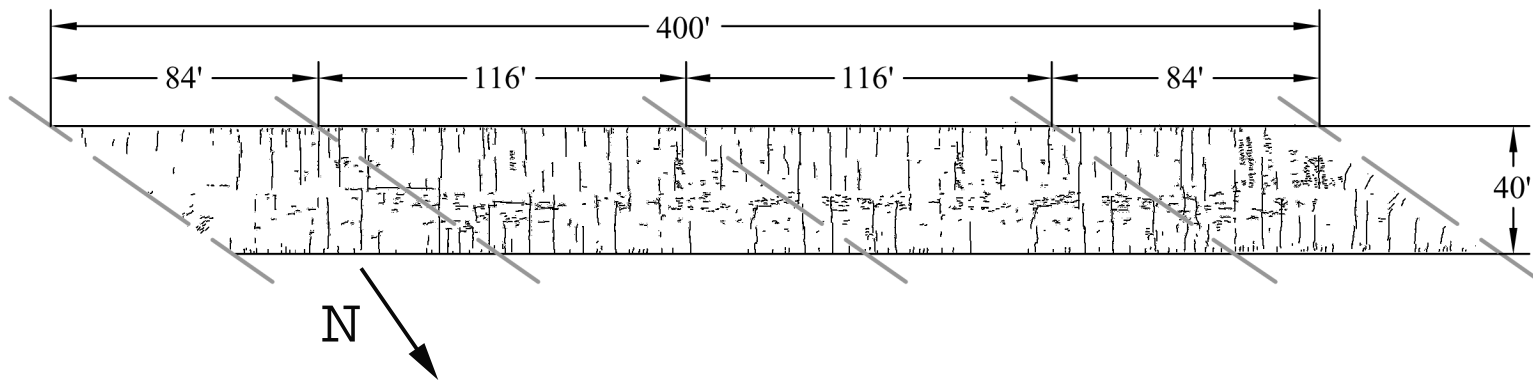


Fig. E.21 – Bridge Number 89-206 (5% Silica Fume Overlay). Scale 1" = 60'-0"

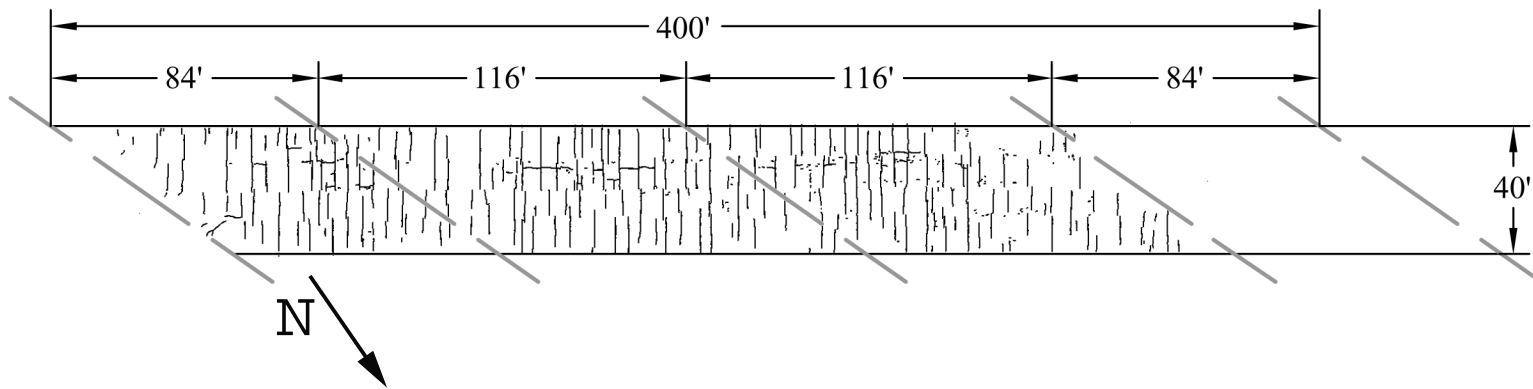


Fig. E.22 – Bridge Number 89-207 (5% Silica Fume Overlay). Scale 1" = 60'-0"

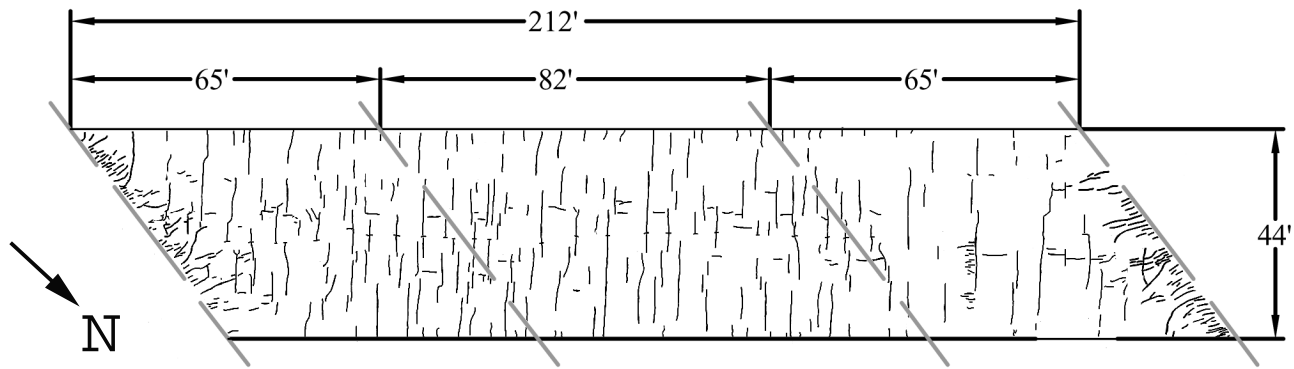


Fig. E.23 – Bridge Number 89-210 (5% Silica Fume Overlay). Scale 1" = 40'-0"

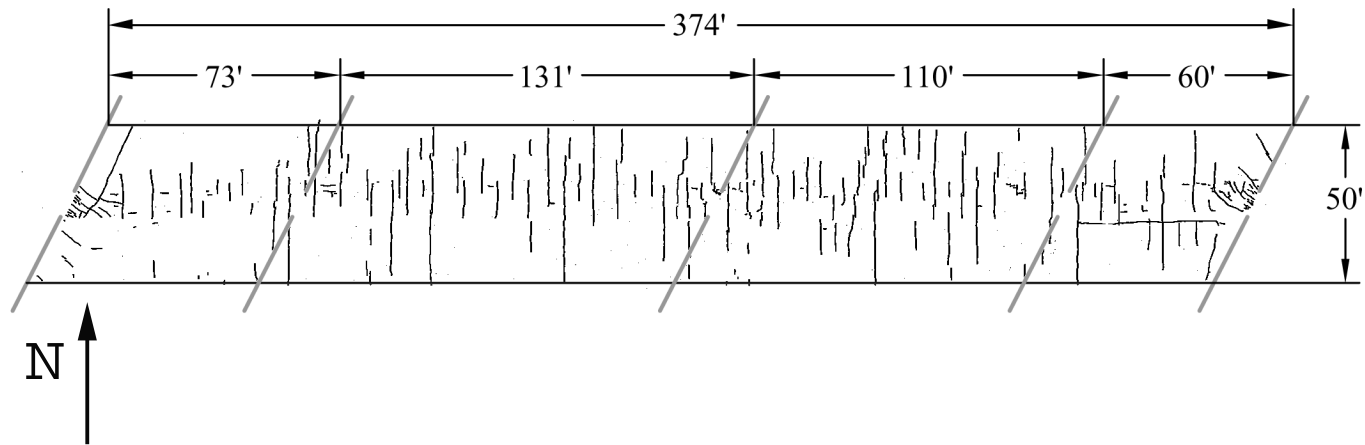


Fig. E.24 – Bridge Number 89-234 (5% Silica Fume Overlay). Scale 1" = 60'-0"

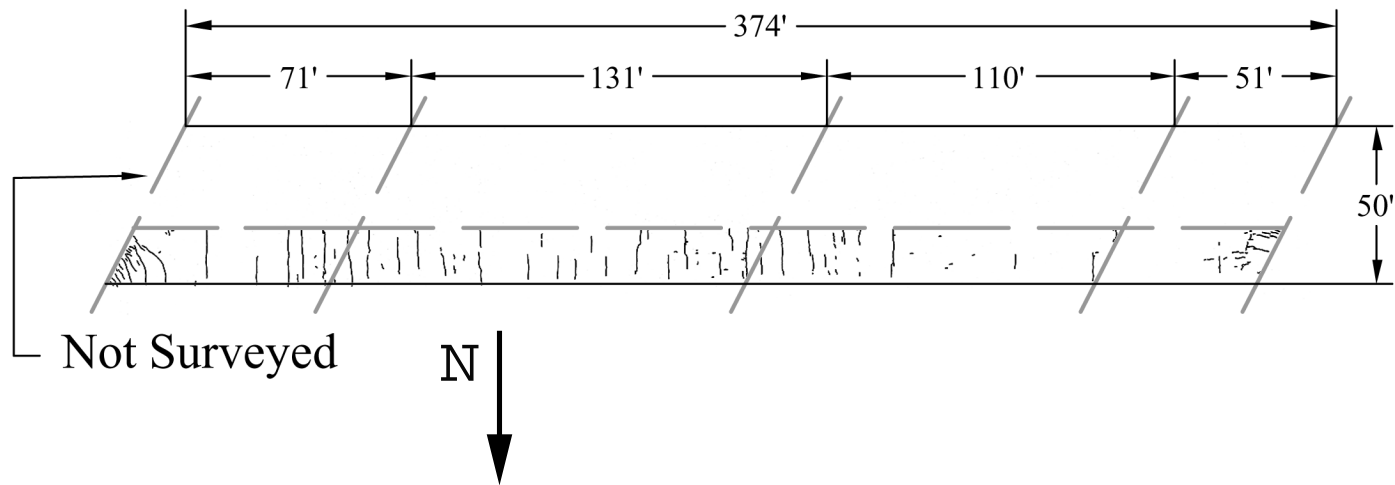


Fig. E.25 – Bridge Number 89-235 (5% Silica Fume Overlay). Scale 1" = 60'-0"

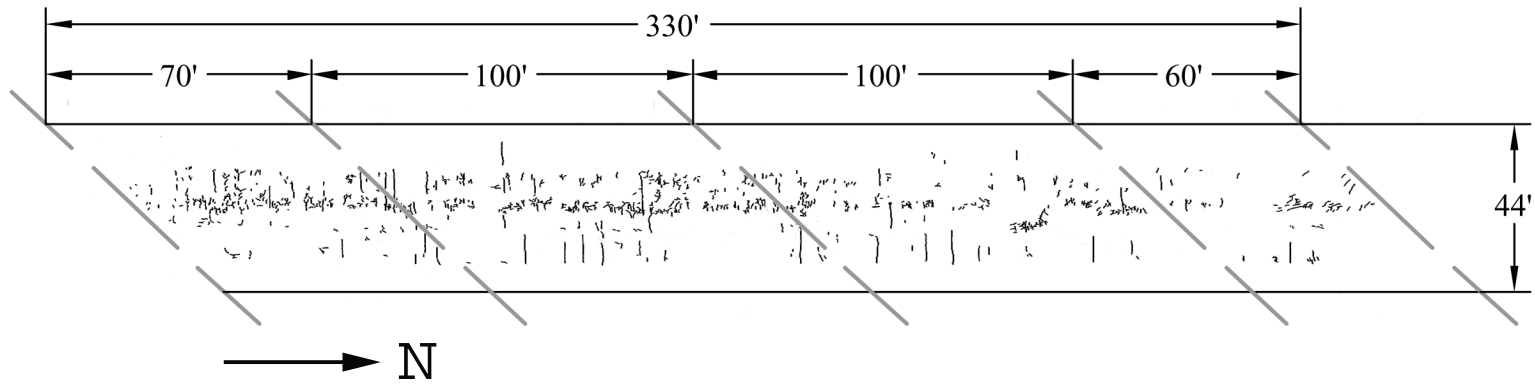


Fig. E.26 – Bridge Number 89-240 (5% Silica Fume Overlay). Scale 1" = 50'-0"

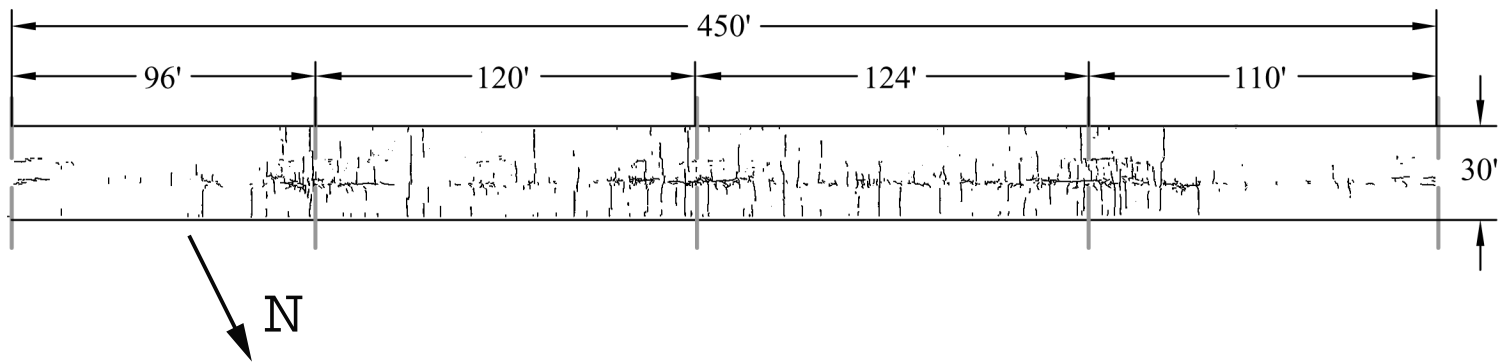


Fig. E.27 – Bridge Number 89-244 (5% Silica Fume Overlay). Scale 1" = 60'-0"

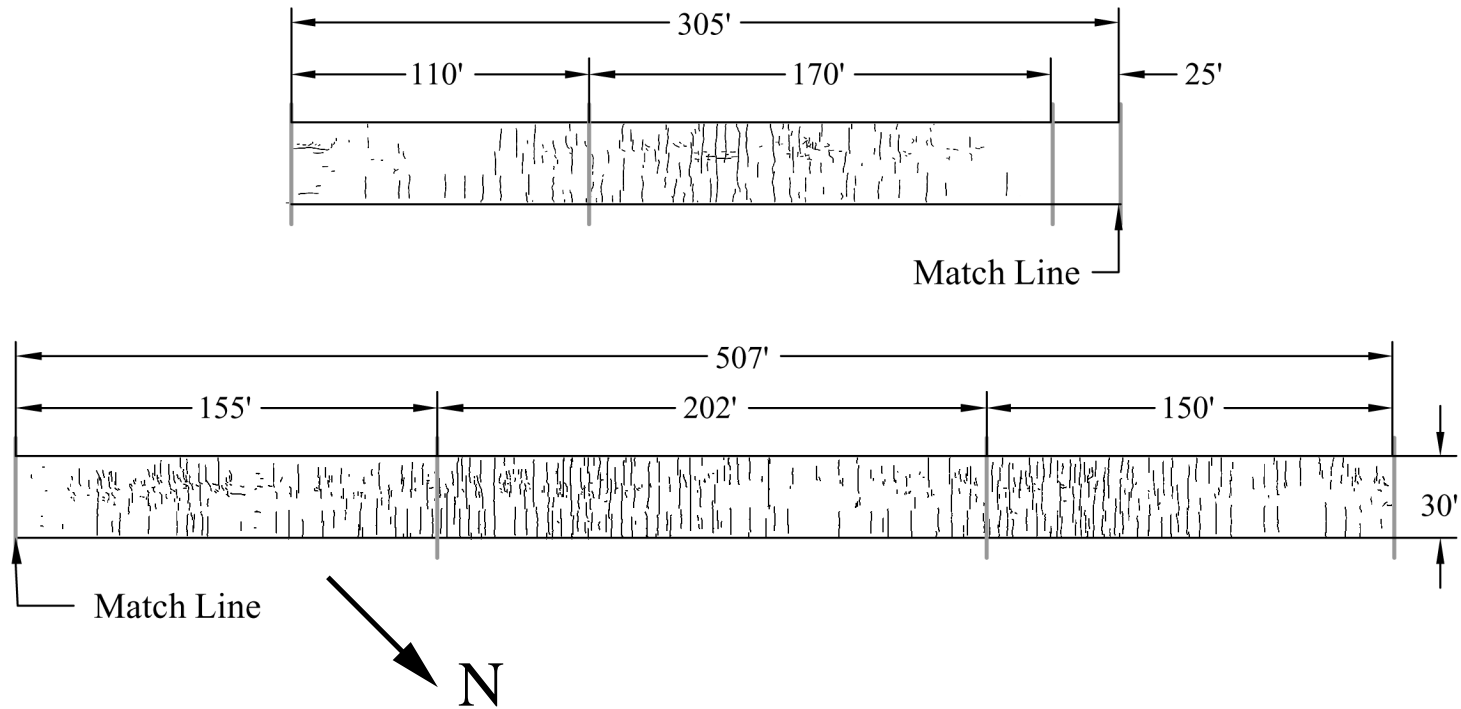


Fig. E.28 – Bridge Number 89-245 (5% Silica Fume Overlay). Scale 1" = 70'-0"

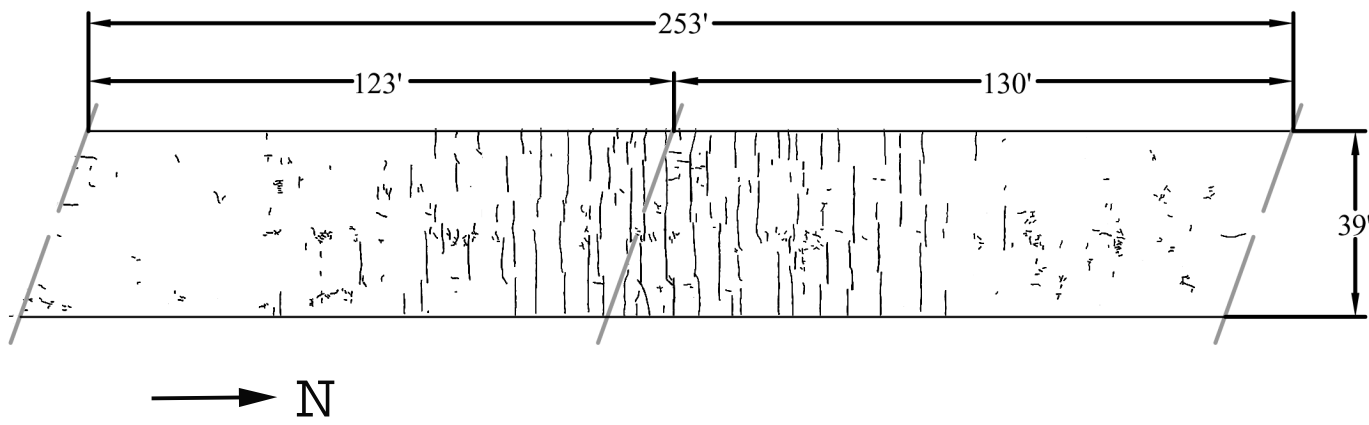


Fig. E.29 – Bridge Number 89-246 (5% Silica Fume Overlay). Scale 1" = 40'-0"

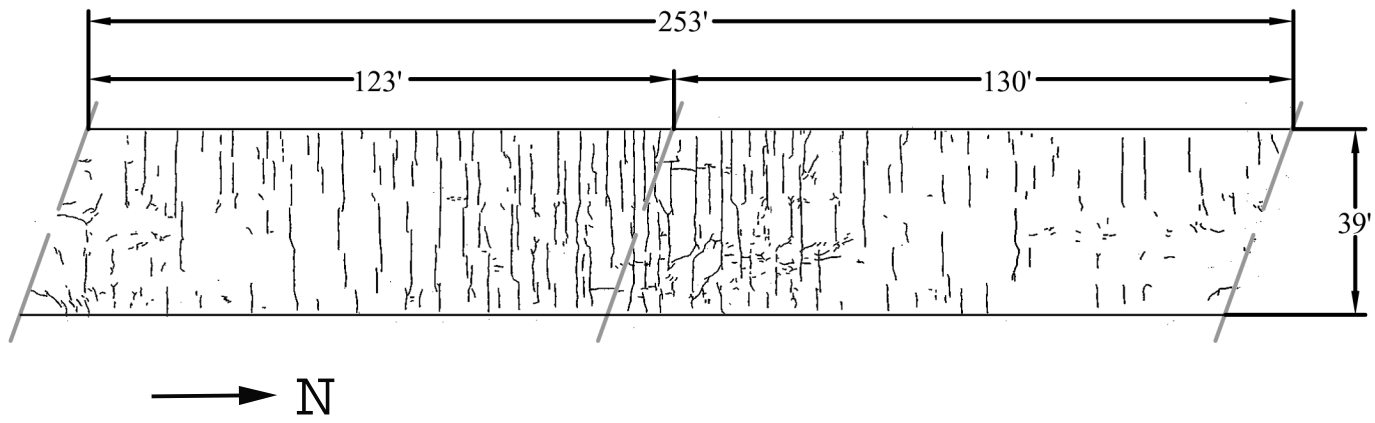


Fig. E.30 – Bridge Number 89-247 (5% Silica Fume Overlay). Scale 1" = 40'-0"

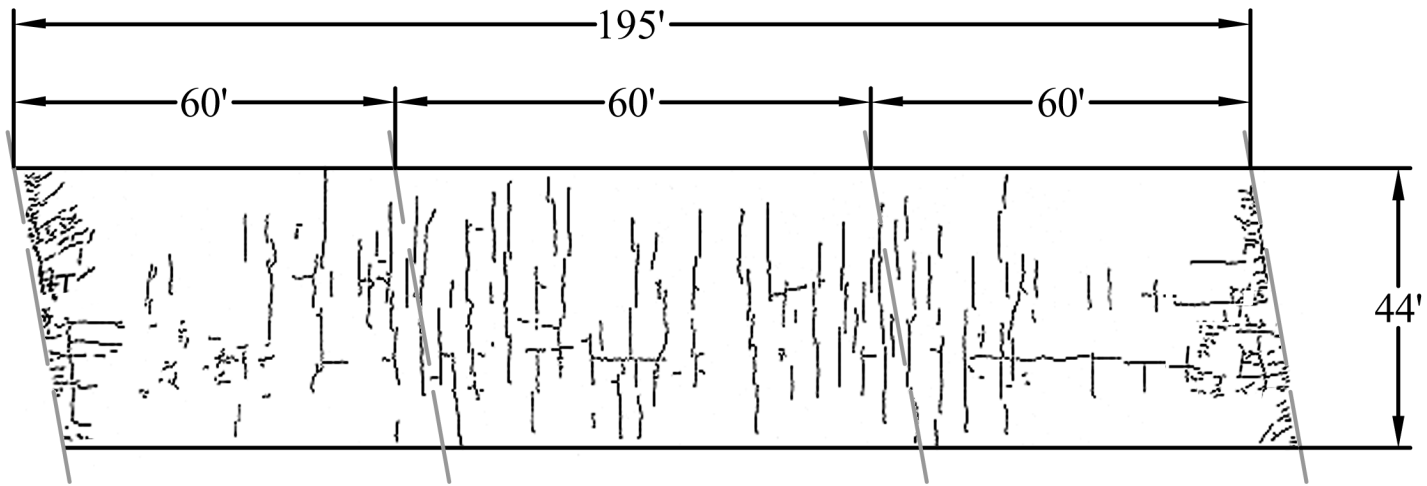


Fig. E.31 – Bridge Number 89-248 (5% Silica Fume Overlay). Scale 1" = 30'-0"

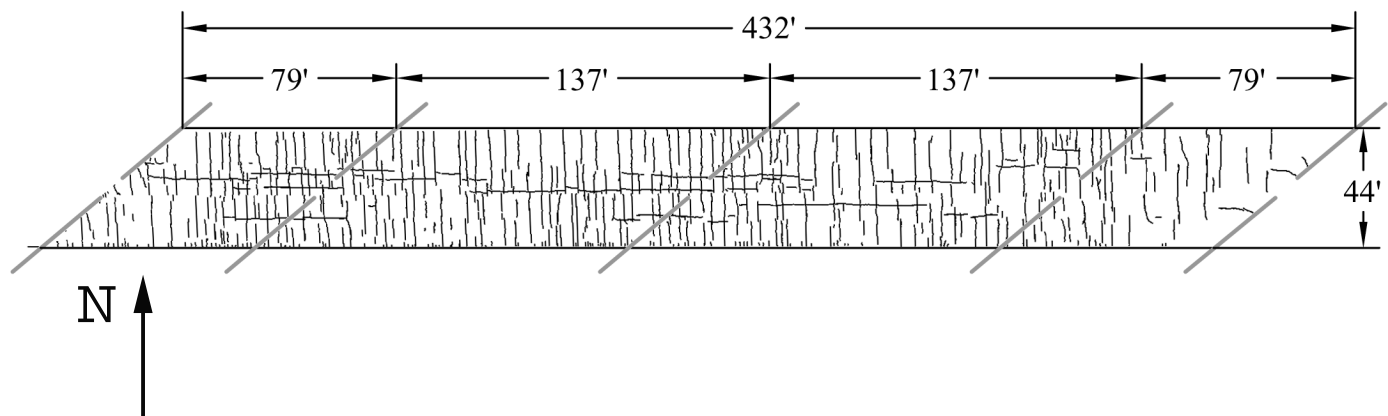


Fig. E.32 – Bridge Number 46-289 (Conventional Overlay). Scale 1" = 70'-0"

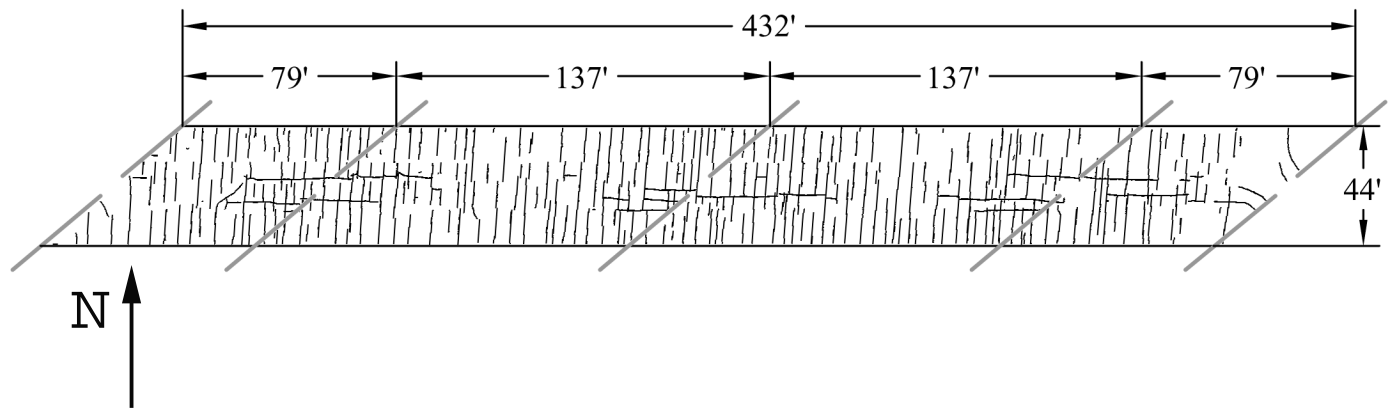


Fig. E.33 – Bridge Number 46-290 (Conventional Overlay). Scale 1" = 70'

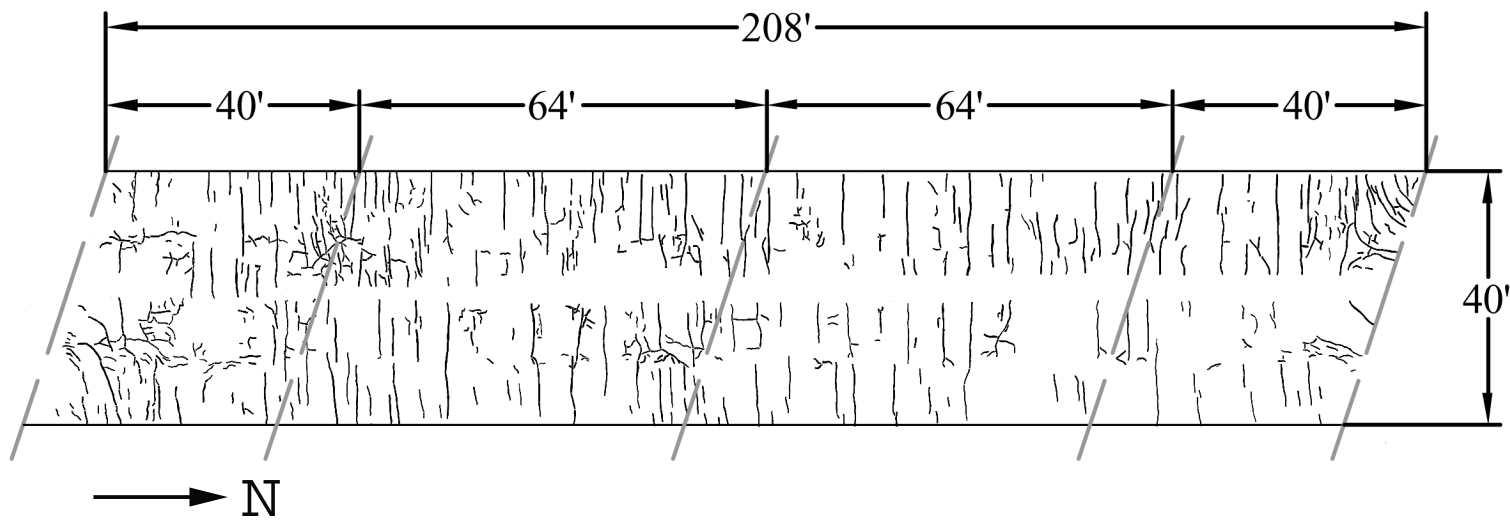


Fig. E.34 – Bridge Number 46-299 (Conventional Overlay). Scale 1" = 30'-0"

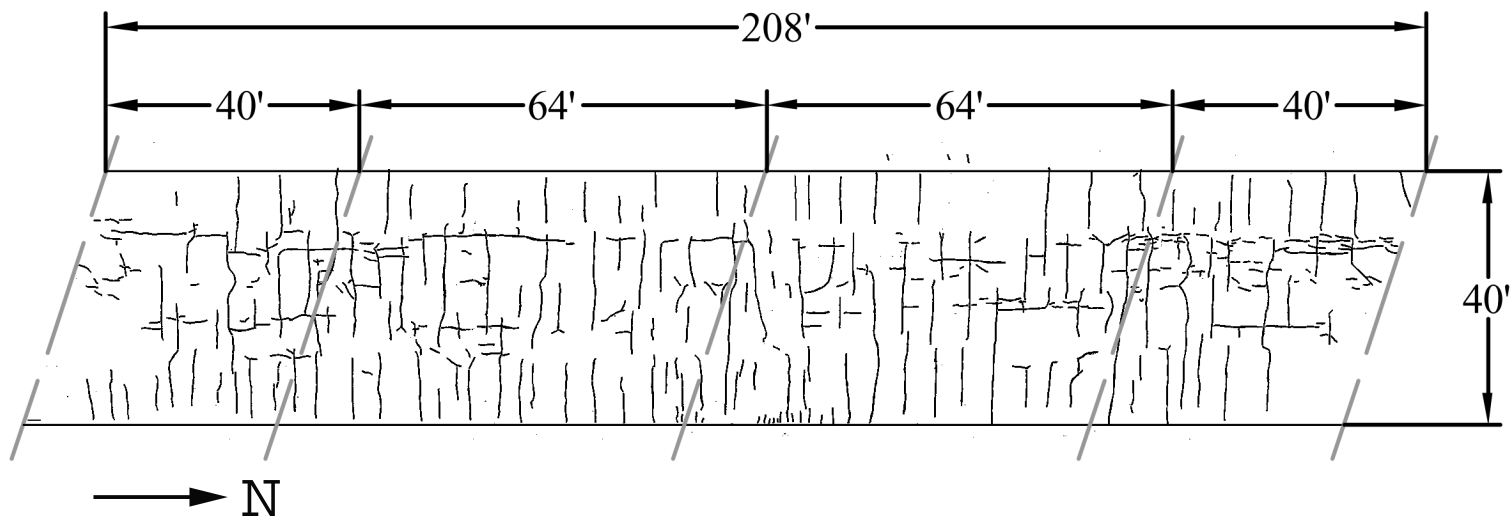


Fig. E.35 – Bridge Number 46-300 (Conventional Overlay). Scale 1" = 30'-0"

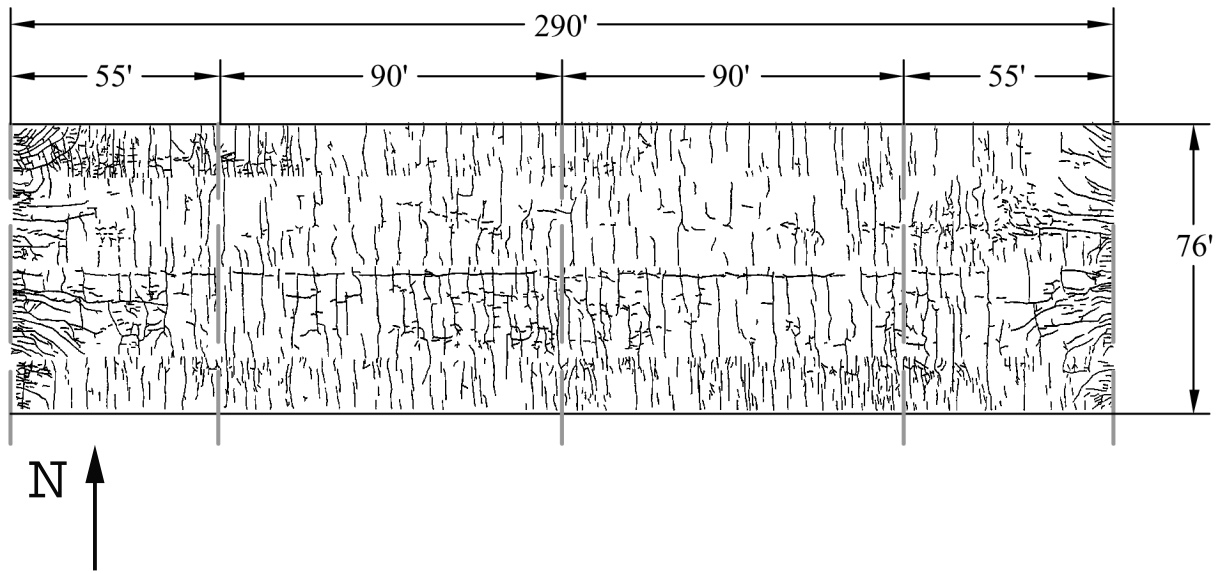


Fig. E.36 – Bridge Number 46-301 (Conventional Overlay). Scale 1" = 50'-0"

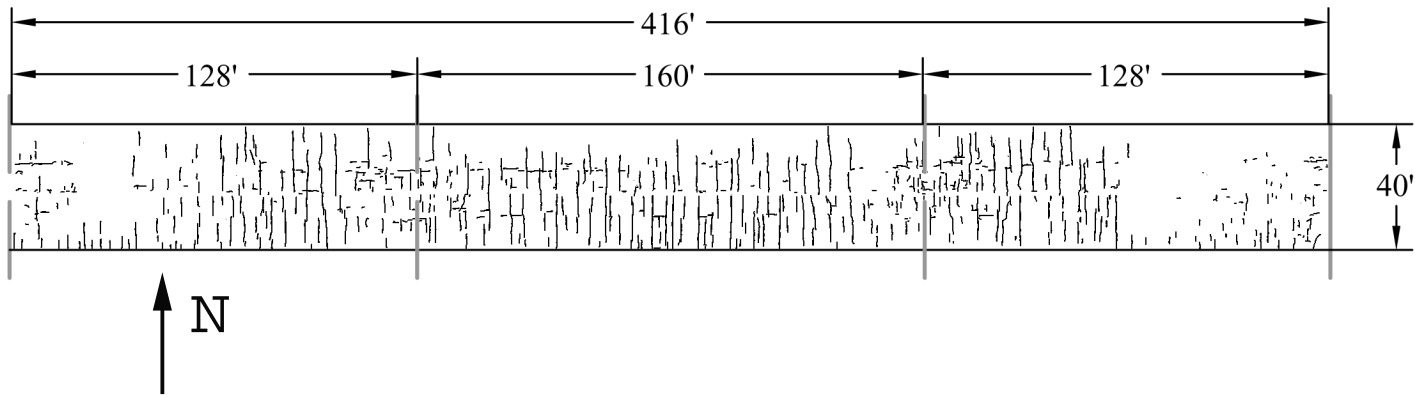


Fig. E.37 – Bridge Number 75-01 (Conventional Overlay). Scale 1" = 60'-0"

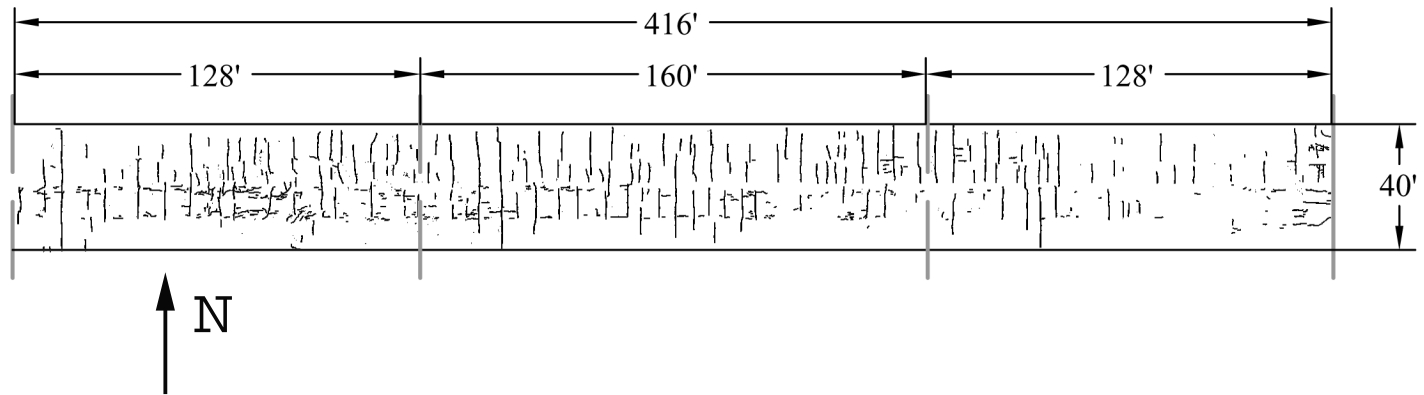


Fig. E.38 – Bridge Number 75-49 (Conventional Overlay). Scale 1" = 60'-0"

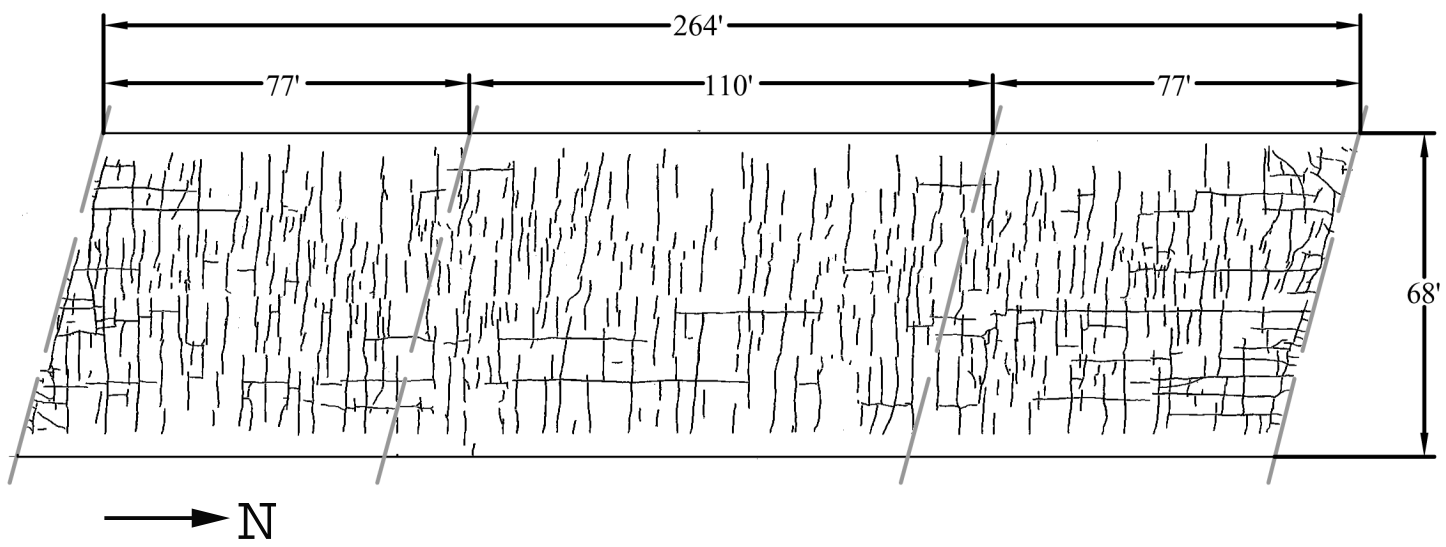


Fig. E.39 – Bridge Number 81-49 (Conventional Overlay). Scale 1" = 40'-0"

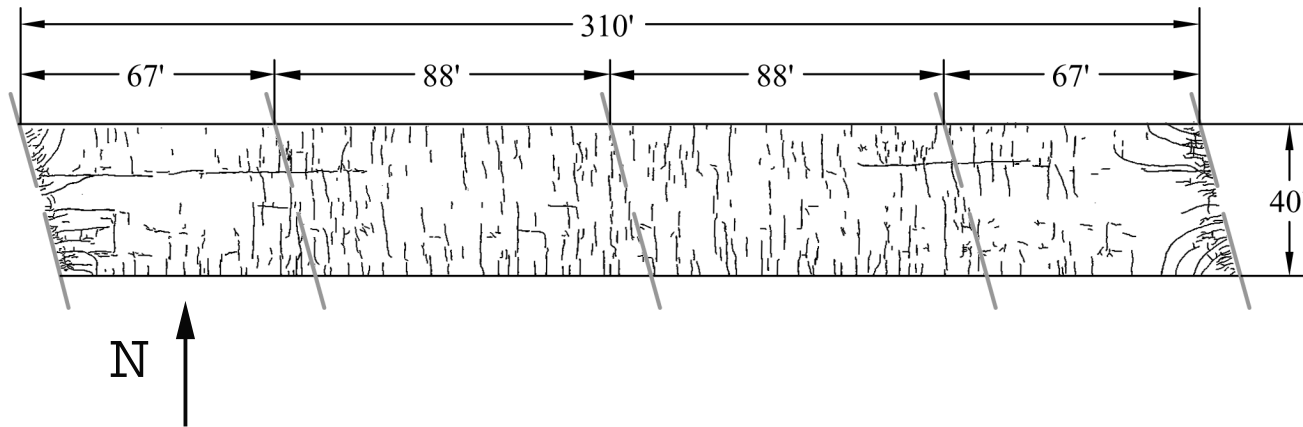


Fig. E.40 – Bridge Number 89-183 (Conventional Overlay). Scale 1" = 50'-0"

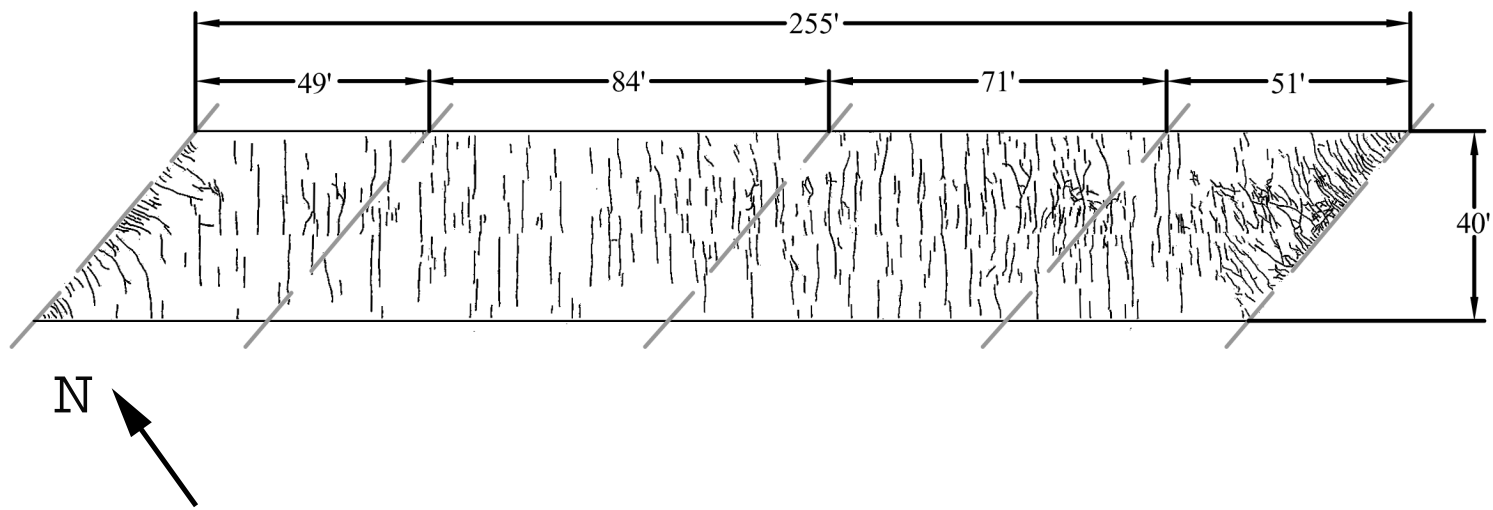


Fig. E.41 – Bridge Number 89-185 (Conventional Overlay). Scale 1" = 40'-0"

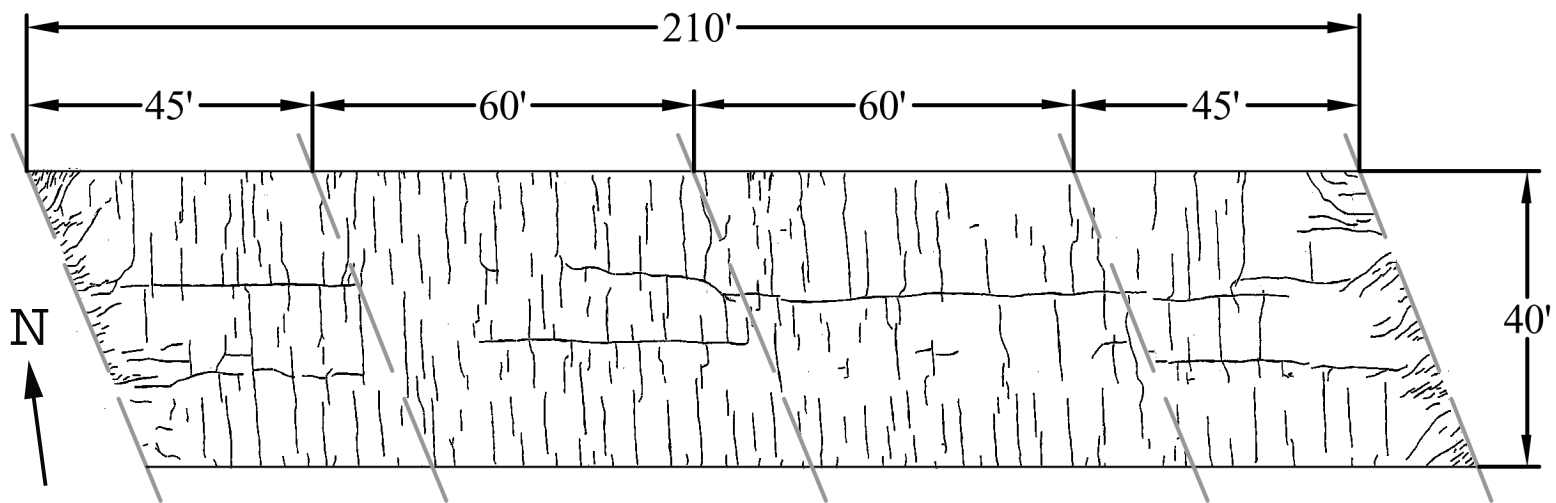


Fig. E.42 – Bridge Number 89-186 (Conventional Overlay). Scale 1" = 30'-0"

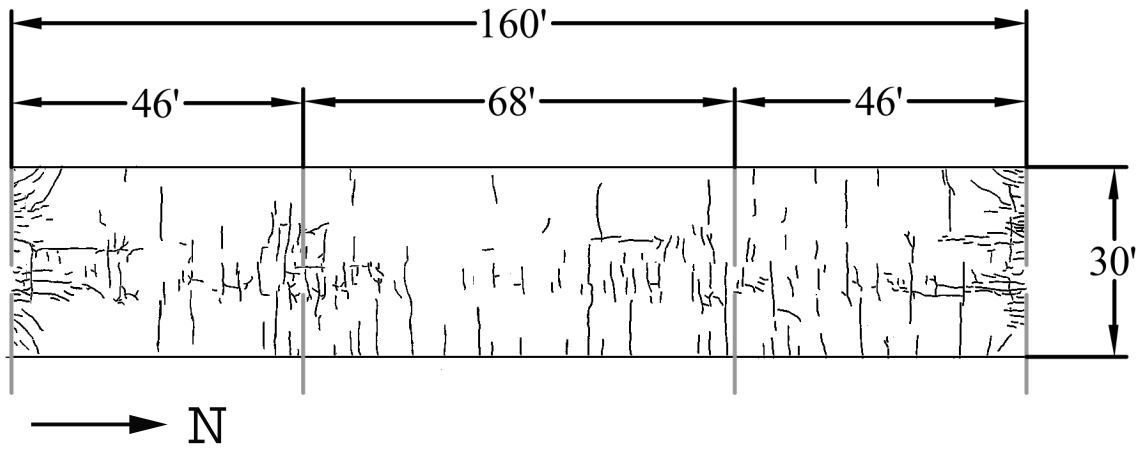


Fig. E.43 – Bridge Number 89-196 (Conventional Overlay). Scale 1" = 30'-0"

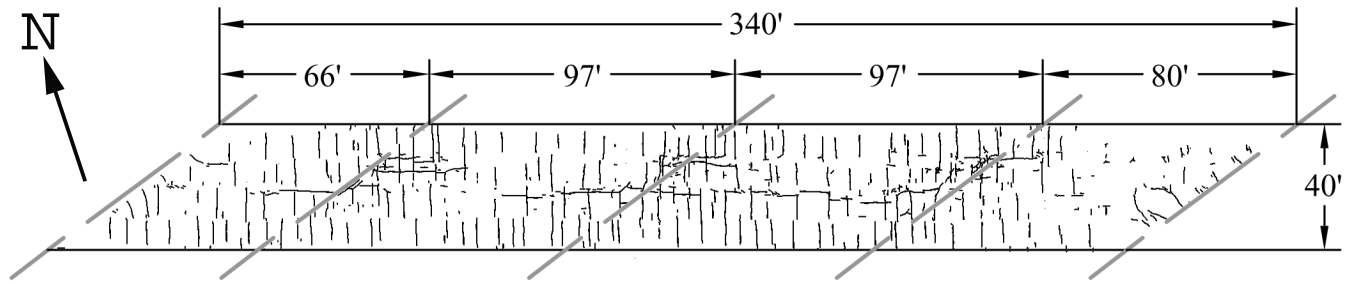


Fig. E.44 – Bridge Number 89-198 (Conventional Overlay). Scale 1" = 60'-0"

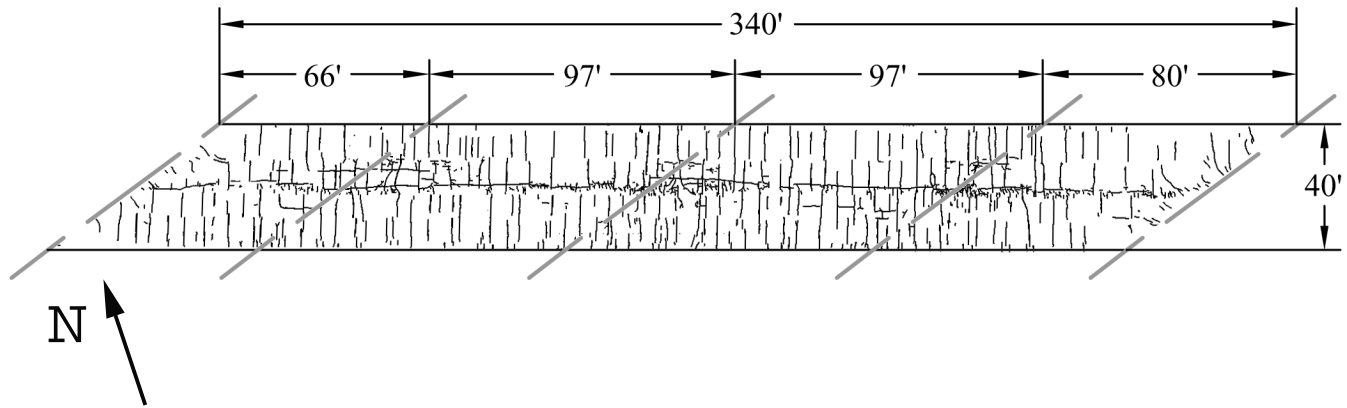


Fig. E.45 – Bridge Number 89-199 (Conventional Overlay). Scale 1" = 60'-0"

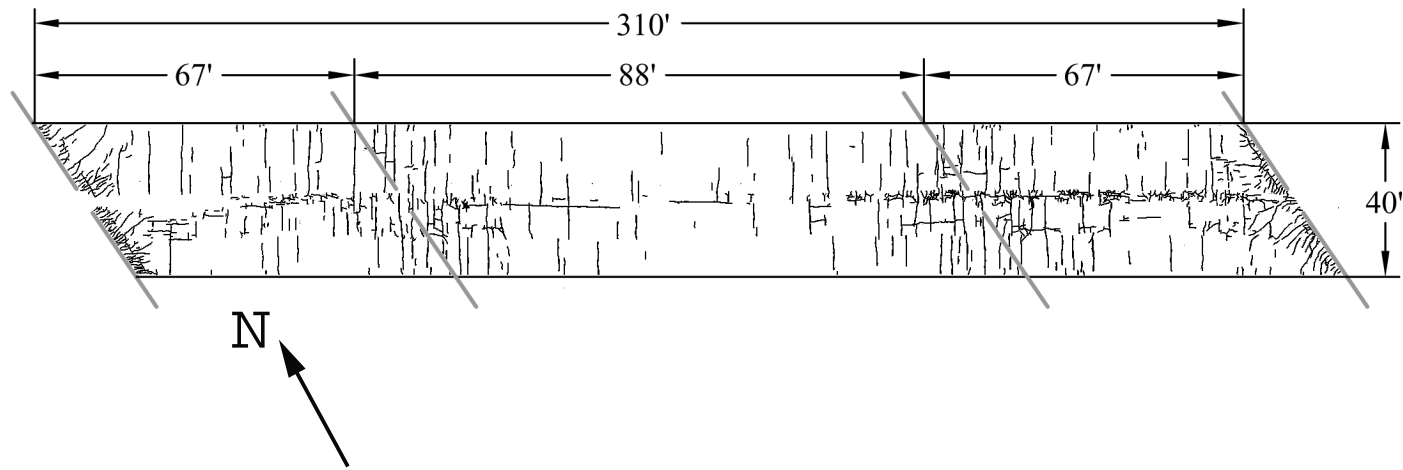


Fig. E.46 – Bridge Number 89-200 (Conventional Overlay). Scale 1" = 50'-0"

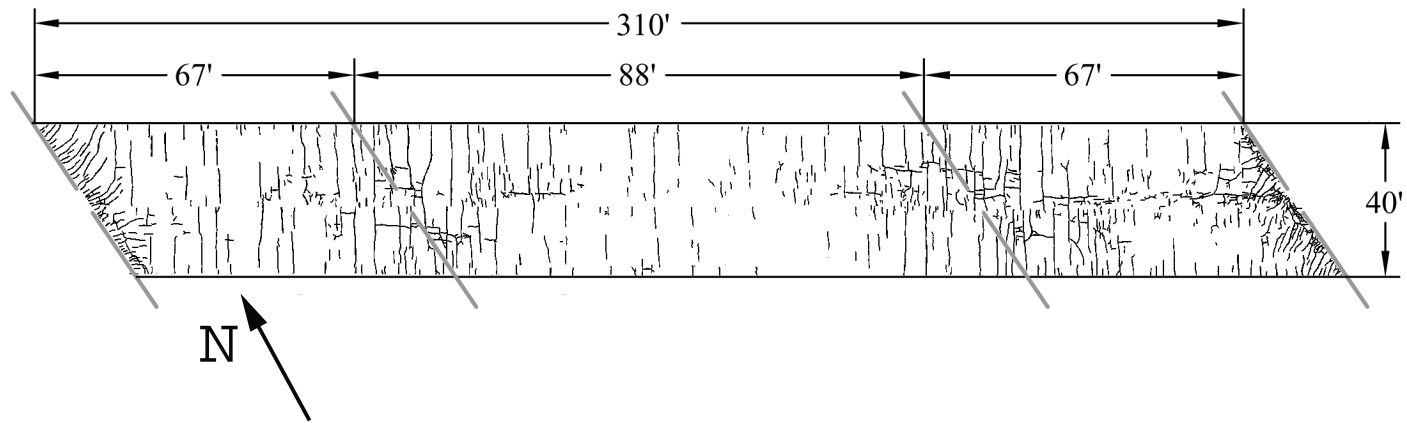


Fig. E.47 – Bridge Number 89-201 (Conventional Overlay). Scale 1" = 50'-0"

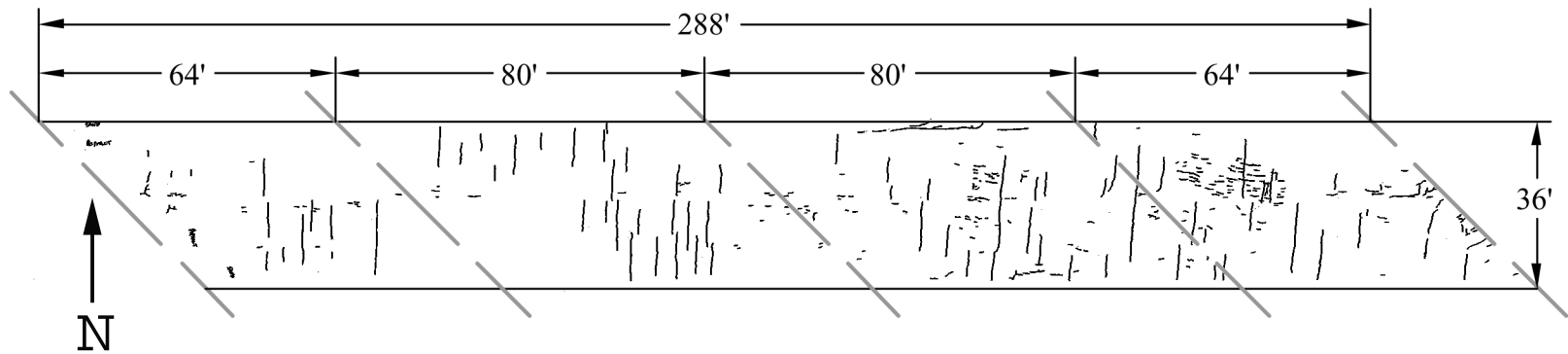


Fig. E.48 – Bridge Number 3-45 (Monolithic). Scale 1" = 40'-0"

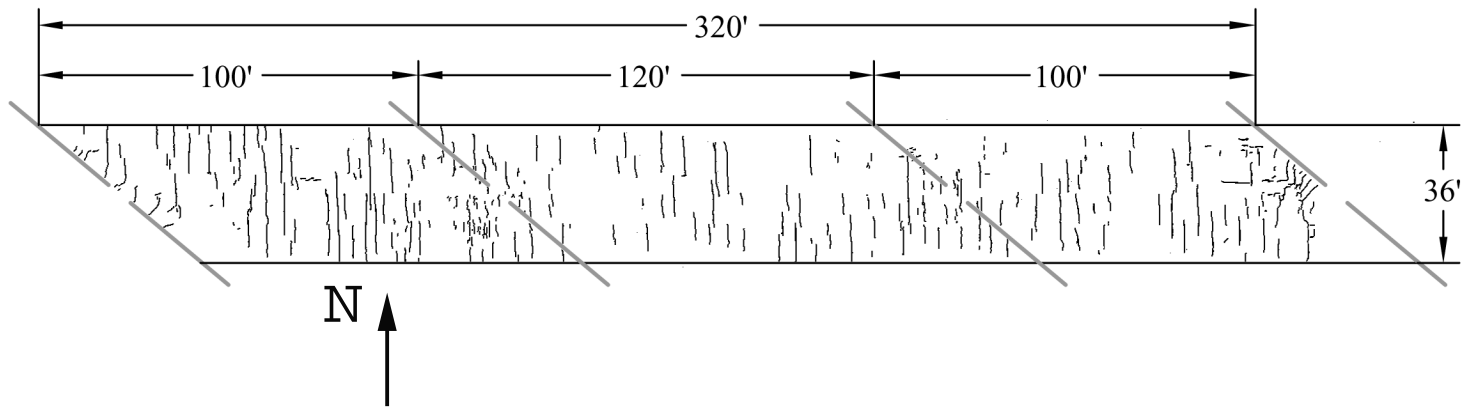


Fig. E.49 – Bridge Number 3-46 (Monolithic). Scale 1" = 50'-0"

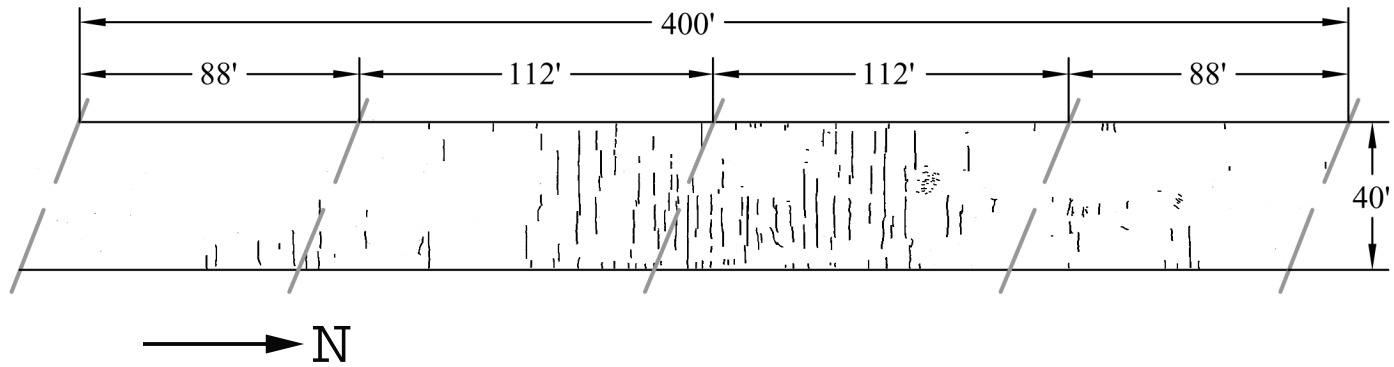


Fig. E.50 – Bridge Number 56-142 (Monolithic). Scale 1" = 60'-0"

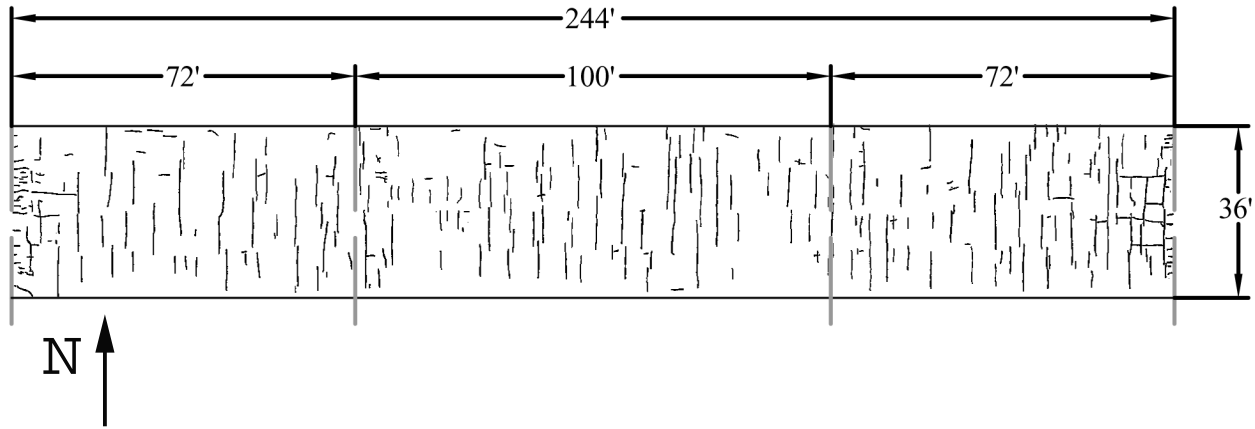
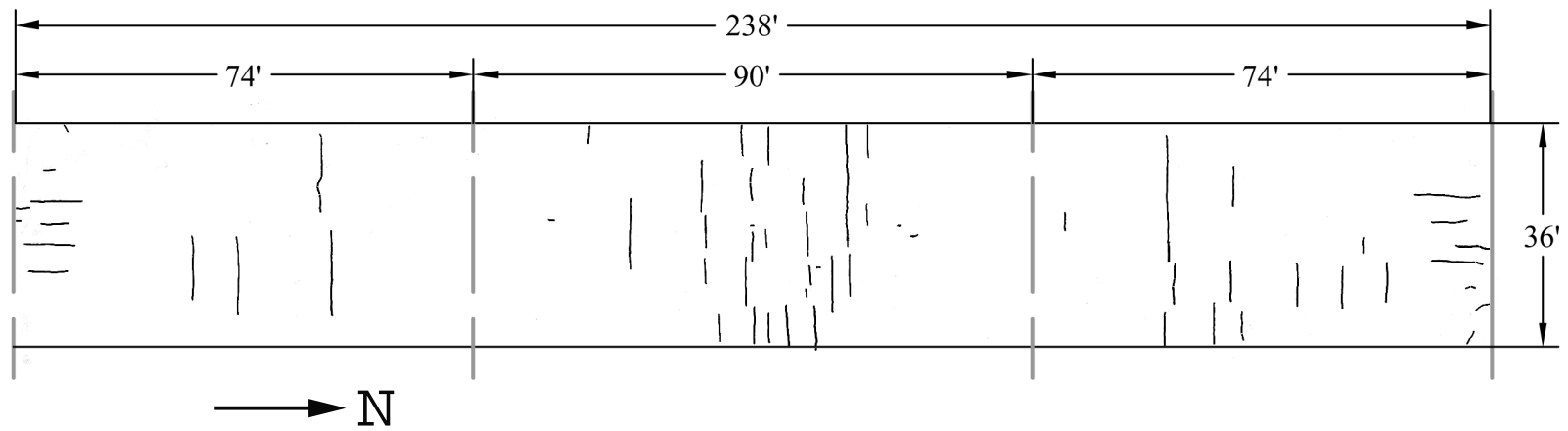


Fig. E.51 – Bridge Number 56-148 (Monolithic). Scale 1" = 30'-0"



445

Fig. E.52 – Bridge Number 70-95 (Monolithic). Scale 1" = 30'-0"

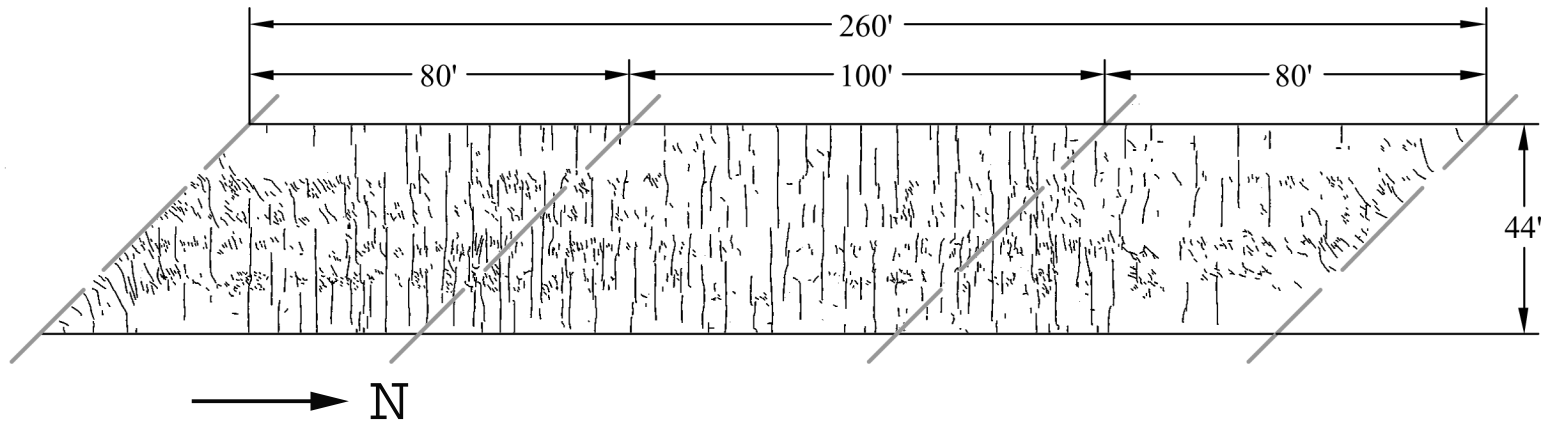


Fig. E.53 – Bridge Number 70-103 (Monolithic). Scale 1" = 40'-0"

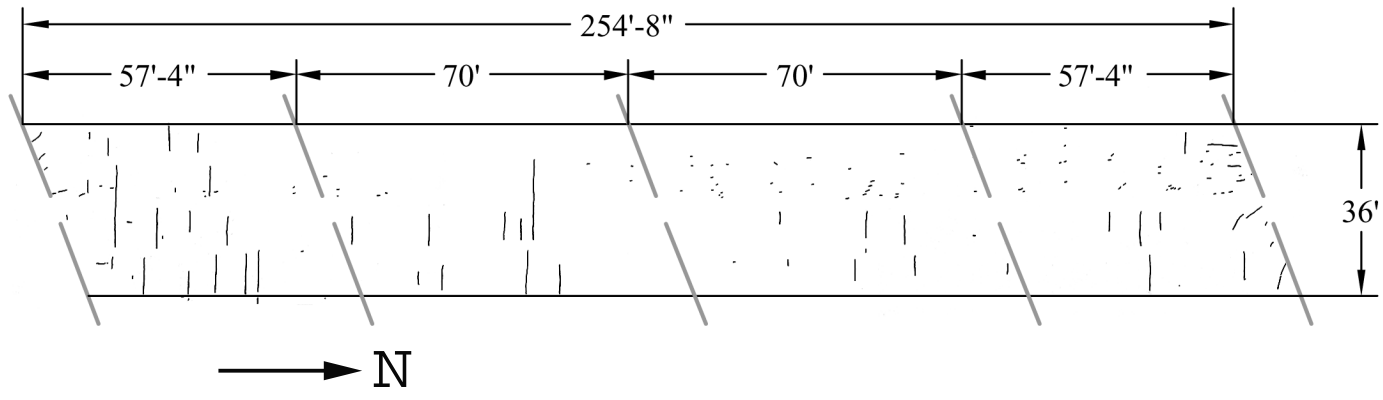


Fig. E.54 – Bridge Number 70-104 (Monolithic). Scale 1" = 40'-0"

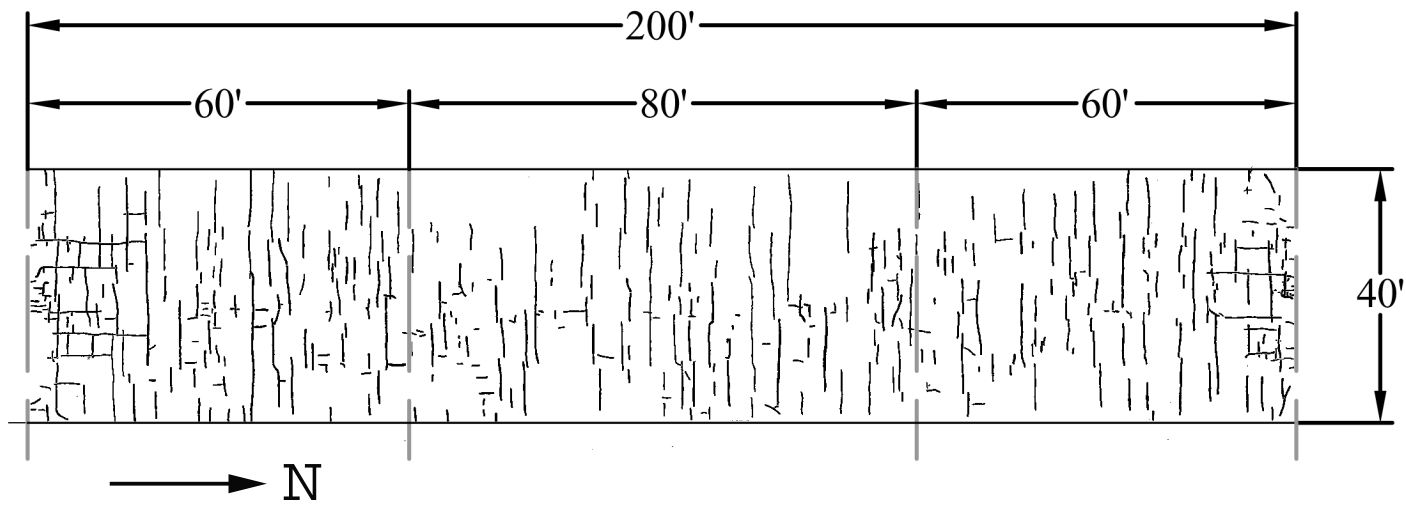


Fig. E.55 – Bridge Number 70-107 (Monolithic). Scale 1" = 30'-0"

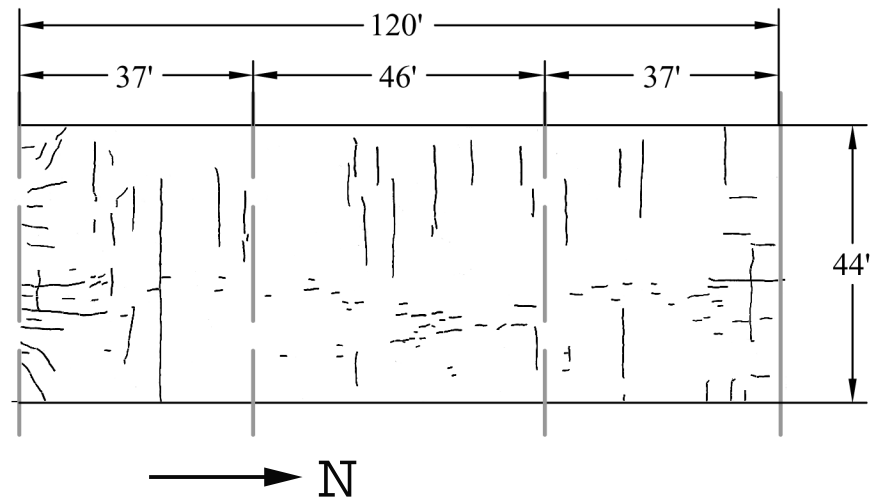
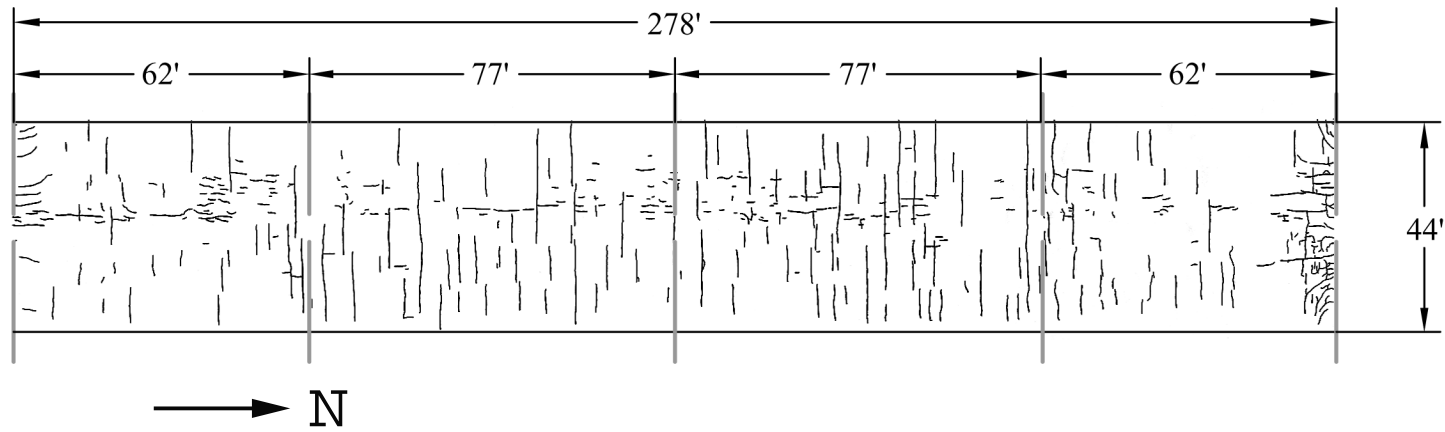


Fig. E.56 – Bridge Number 75-44 (Monolithic). Scale 1" = 30'-0"



450

Fig. E.57 – Bridge Number 75-45 (Monolithic). Scale 1" = 40'-0"

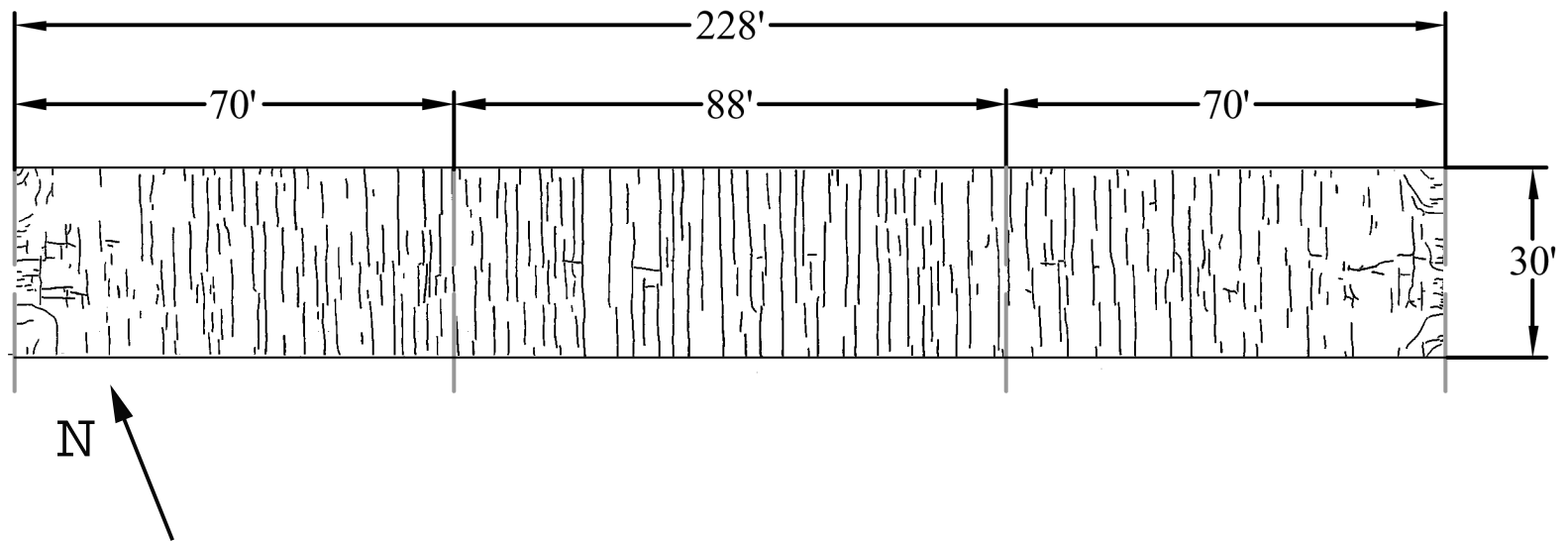


Fig. E.58 – Bridge Number 89-204 (Monolithic). Scale 1" = 30'-0"

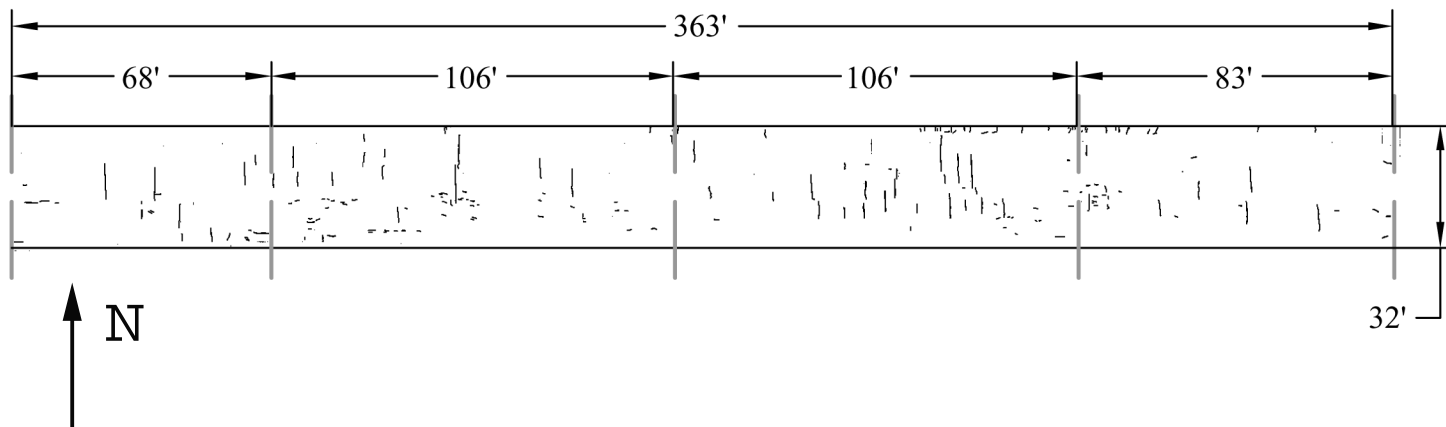


Fig. E.59 – Bridge Number 89-208 (Monolithic). Scale 1" = 50'-0"

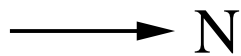
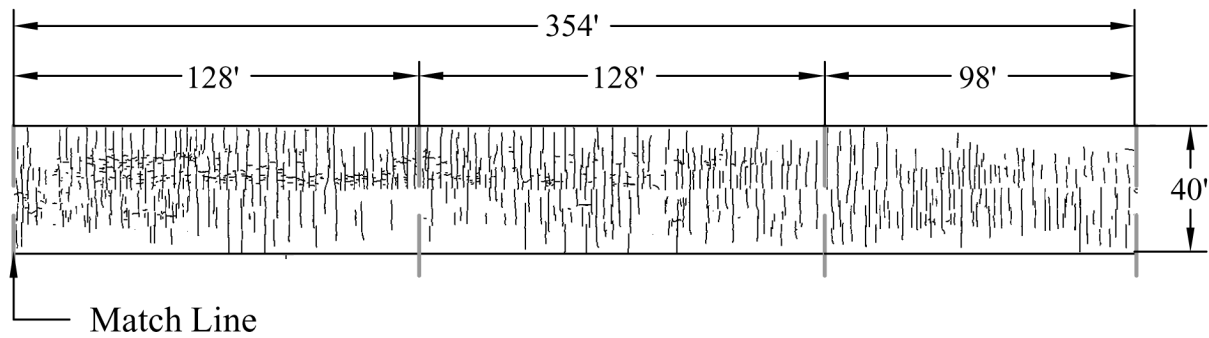
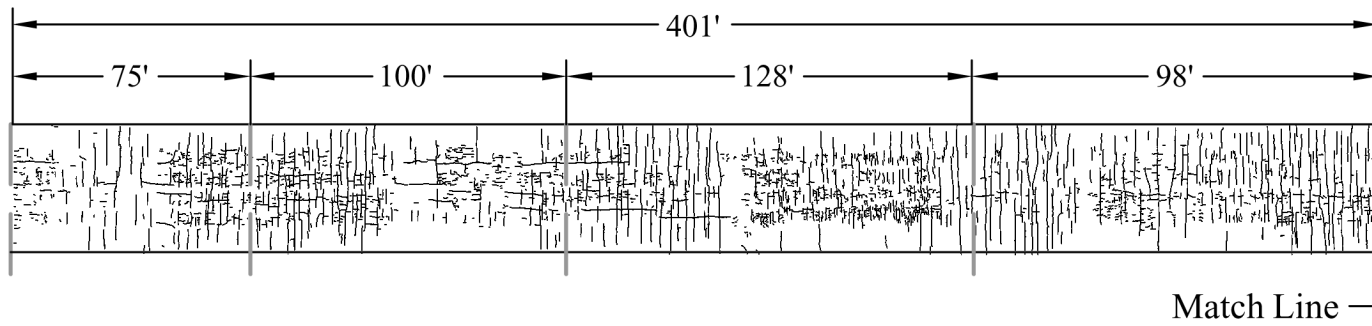


Fig. E.60 – Bridge Number 99-76 (Monolithic). Scale 1" = 50'-0"